ЖУРНАЛ
ЭКСПЕРИМЕНТАЛЬНОЙ И ТЕОРЕТИЧЕСКОЙ
ФИЗИКИ
АКАДЕМИЯ НАУК СССР

SOVIET PHYSICS

JETP

VOLUME 6(33) NUMBER 3

A Translation

of the

Journal of Experimental and Theoretical Physics

of the

Academy of Sciences of the USSR

Volume 33

MARCH, 1958

Published by the

AMERICAN INSTITUTE OF PHYSICS
INCORPORATED

SOVIET PHYSICS
JETP

A translation of the Journal of Experimental and Theoretical Physics of the USSR.

A publication of the

AMERICAN INSTITUTE OF PHYSICS

Governing Board

FREDERICK SEITZ, *Chairman*

Members:

WALTER S. BAIRD
JESSE W. BEAMS
RAYMOND T. BIRGE
R. H. BOLT
J. W. BUCHTA
J. H. DILLON
VERNET E. EATON
HERBERT A. ERF
IRVINE C. GARDNER
S. A. GOUDSMIT
C. KITTEL
WINSTON E. KOCK
R. BRUCE LINDSAY
WALTER C. MICHELS
G. E. PAKE
R. RONALD PALMER
JOSEPH B. PLATT
RALPH A. SAWYER
H. D. SMYTH
JOHN STRONG
GEORGE E. UHLENBECK

Administrative Staff

ELMER HUTCHISSON
Director

HENRY A. BARTON
Associate Director

WALLACE WATERFALL
Secretary and Treasurer

THEODORE VORBURGER
Advertising Manager

RUTH F. BRYANS
Publication Manager

ALICE MASTRO
Circulation Manager

KATHRYN SETZE
Assistant Treasurer

EUGENE H. KONE
Director of Public Relations

American Institute of Physics Advisory Board on Russian Translations

ROBERT T. BEYER, *Chairman*
FREEMAN J. DYSON, DWIGHT GRAY, DAVID HARKER,
MORTON HAMERMESH, VLADIMIR ROJANSKY

Editor of SOVIET PHYSICS—JETP

J. GEORGE ADASHKO, DEPARTMENT OF ELECTRICAL ENGINEERING,
THE CITY COLLEGE, CONVENT AVENUE AND 139TH STREET
NEW YORK 31, NEW YORK.

SOVIET PHYSICS is a monthly journal published by the American Institute of Physics for the purpose of making available in English reports of current Soviet research in physics as contained in the Journal of Experimental and Theoretical Physics of the Academy of Sciences of the USSR. The page size of SOVIET PHYSICS will be 8½" x 11", the same as other Institute journals.

Transliteration of the names of Russian authors follows the system employed by the Library of Congress.

This translating and publishing project was undertaken by the Institute in the conviction that dissemination of the results of researches everywhere in the world is invaluable to the advancement of science. The National Science Foundation of the United States encouraged the project initially and is supporting it in large part by a grant.

The American Institute of Physics and its translators propose to translate faithfully all the material in the Journal of EXPERIMENTAL AND THEORETICAL PHYSICS OF THE USSR appearing after January 1, 1955. The views expressed in the translated material, therefore, are intended to be those expressed by the original authors, and not those of the translators nor of the American Institute of Physics.

Two volumes are published annually, each of six issues. Each volume contains the translation of one volume of the Journal of EXPERIMENTAL AND THEORETICAL PHYSICS OF THE USSR.

Subscription Prices:

Per year (12 issues)

United States and Canada	$75.00
Elsewhere	79.00

Back Numbers

Single copies	$ 8.00

Subscriptions should be addressed to the American Institute of Physics, 335 East 45th Street, New York 17, New York.

Copyright by American Institute of Physics 1958

SOVIET PHYSICS

JETP

A translation of the Journal of Experimental and Theoretical Physics of the USSR.

SOVIET PHYSICS JETP VOL. 6 (33), No. 3, pp. 437-644 March, 1958

INVESTIGATION OF NUCLEAR DISINTEGRATIONS PRODUCED BY THE CHARGED COMPONENT OF COSMIC RADIATION

T. L. ASATIANI and G. V. KHRIMIAN

Physics Institute, Academy of Sciences, Armenian S.S.R.

Submitted to JETP editor March 4, 1957

J. Exptl. Theoret. Phys. (U.S.S.R.) **33**, 561-566 (September, 1957)

The momentum spectrum of negative π mesons from stars produced by charged cosmic ray particles of ~ 30 Bev has been measured. The power exponent of the spectrum is $\gamma = 1.46 \pm 0.2$. The ratio of positive to negative π mesons is $N_{\pi^+}/N_{\pi^-} = 1.67^{+0.81}_{-0.53}$ and the protons are found to constitute $\sim 30\%$ of all particles with momentum $p \geq 10^9$ ev/c.

THE products of nuclear disintegrations induced by fast charged particles of cosmic radiation in lead were investigated at 3200 m above sea level (Mt. Aragats) by means of the magnetic mass-spectrometer of Alikhanian and Alikhanov using a field of 6850 oersted. The schematic cross-sections of the instrument in two perpendicular planes are shown in Fig. 1.

The hodoscope placed above the spectrometer made it possible to select nuclear disintegrations produced by charged particles in the lead blocks ABCDEF, situated between the counter trays. Secondary products of the disintegrations were studied by means of the mass-spectrometer. The particle trajectory was determined in the plane of magnetic deviation by the coordinate trays 9, 12, 14, 16, 18, 20, 23, and in the plane perpendicular to it by the trays 5 — 8, 10, 11, 13, 15, 17, 19, 21, 22, 24 — 27. Each of the trays 6, 8, 10, 24 — 27 consisted of two layers of counters. The counters of the top layer covered the gaps between the coordinate counters and were connected in parallel. The side trays B_1, B_2, T_1, T_2 excluded particles entering the hodoscope from the sides and responded to particles produced in the stars.

The triggering system of the arrangement was so altered that all cases of star production were recorded, both when the secondary particles were stopped in the absorbers of the lower detecting array and when they succeeded in traversing them.

The mean square error of the momentum measurement amounted to 3, 13 and 65%, for particles of 2×10^9, 10^9, and 5×10^8 ev/c respectively.

Only the stars produced by a single charged particle entering the hodoscope at an angle smaller than 35° to the vertical in the plane perpendicular to the plane of magnetic deviation were selected. In order to exclude completely any cases of electromagnetic interaction of μ mesons with subsequent shower production we considered only the stars which had not less than five prongs, at least two of which penetrated the next absorber, i.e., produced discharges in the tray of counters below (cf. Fig. 1). From stars selected in the above manner only those were studied in which a secondary particle traversing the telescope satisfied the following conditions: (a) produced at least four discharges in the plane of magnetic deviation, the coordinates of which had to lie on a circle, and (b) produced at least three points laying on a straight line not passing through the pole pieces in the plane perpendicular to the plane of magnetic deviation.

The data were reduced by comparison of all actually observed events with master diagrams.

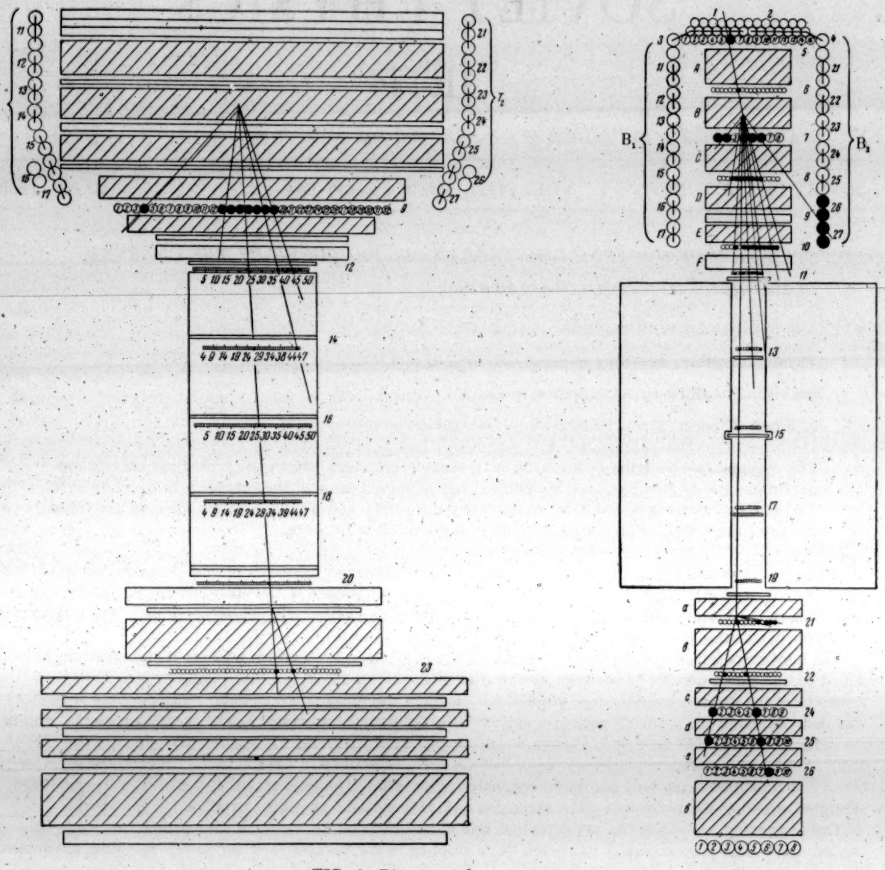

FIG. 1. Diagram of apparatus.

Series	Thickness of lead absorbers in the upper hodoscope (cm)						Thickness of absorbers in the lower detector (cm)					
	A	B	C	D	E	F	a	b	c	d	e	f
							Graphite					
1	0	7	6	5	4	3	4	9	4	3.6	3.6	1 Pb+9 Cu
2	0	7	6	0	0	0	4	9	4	2	2	1 Pb+9 Cu
3	8	7	6	5	4	3	Copper					
							3.6	8.26	4.26	3.1	2.66+1 Pb	9.25+1Pb

In the present article we report the results of three series of observations, which differed in the various disposition and thickness of the lead plates in which the stars were produced in the upper hodoscope and of the absorbers in the lower detecting arrangement (see table).

In the course of experiment we determined the momenta of 316 particles originating in stars. Of these, 231 were found to be positive and 85 negative. The differential momentum spectrum of these particles is shown in Fig. 2.

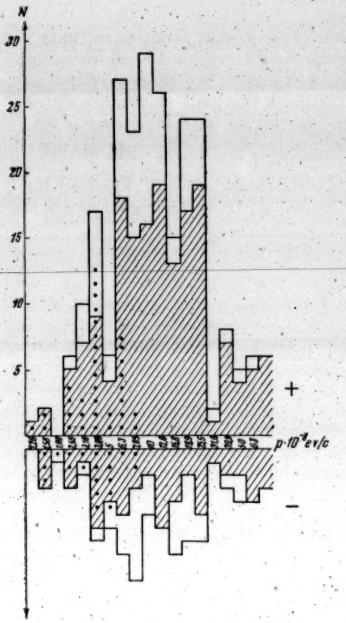

FIG. 2. Differential momentum spectrum of secondary particles: + — positive particles, - - — negative particles. Dashed region — first and third measurement series, undashed — second series.

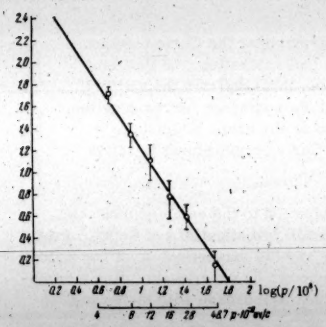

FIG. 3. Differential momentum spectrum of negative particles.

We sought to determine the ratio of positive to negative mesons $N^+_{\pi,K}/N^-_{\pi,K}$. The upper mass limit for particles in the momentum range $1.2-9 \times 10^9$ ev/c was found for this purpose from their momentum and their minimum range (cf. Ref. 1). The minimum range was taken as the absorber thickness traversed by the particle without apparent interaction.

The upper mass limit was taken as 1300 m_e to ensure a good differentiation between mesons and protons. This selection yielded 35 positive and 21 negative mesons (these particles are represented in Fig. 2 by dots).

The following value was obtained for the ratio of positive to negative mesons:

$$N^+/N^- = 1.67^{+0.81}_{-0.53}$$

Unfortunately, it was impossible to differentiate between π mesons and K particles. If we note, however, that the K mesons constitute only a few percent as compared with π mesons, one can regard the above ratio as N_{π^+}/N_{π^-}. It can be seen from Fig. 2 that, for $p \geq 10^9$ ev/c the ratio of the positive to negative particles is 110:40. If the ratio N_{π^+}/N_{π^-} does not vary considerably for $p > 10^9$ ev/c, then the number of protons with momentum $p > 10^9$ ev/c constitutes 0.3 of the number of star particles in lead. The results obtained are, within the limits of the errors, in agreement with the data of Refs. 2 – 6.

The momentum spectrum of secondary particles in the range $2 \times 10^8 - 10^9$ ev/c is considerably distorted due to ionization losses. The production spectrum of π mesons in this range can be obtained introducing corrections for ionization losses in lead. We have then the following value for the exponent of the momentum spectrum of negative particles (Fig. 3):

$$\gamma = 1.46 \pm 0.2.$$

We estimated the value of γ for the momentum spectrum of positive particles with $p \geq 10^9$ ev/c. This value, neglecting ionization corrections, was found to be of the order of 2.0 (Fig. 4).

In the third series of measurements, the interaction of secondary particles in the lower detecting arrangement, in which the observation conditions for stars were almost identical to the upper hodoscope, was studied for an estimate of the minimum energy of the star-producing primary particles. Not a single case, however, of a similar star was observed in the lower detector. It

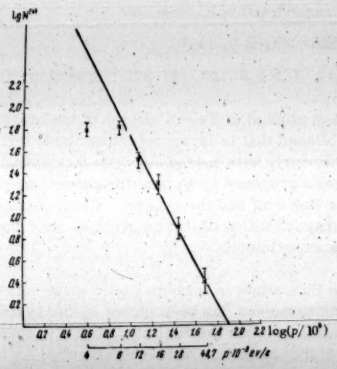

FIG. 4. Differential momentum spectrum of positive particles with momentum $p \geq 10^9$ ev/c (without ionization corrections).

follows that the energy of primary particles should be $> 6 \times 10^9$ ev.

By the method described in Ref. 7, using our data on the number of penetrating particles and their angular distribution, we obtained a value of the order of 30 Bev for the mean energy of the star-producing particles. The mean number of prongs was found to be 7.6, the mean number of secondary particles capable of penetrating 10 and 20 cm of lead is 5.6 and 2.7 respectively. The above results, however, are not very accurate because of the limitations of the hodoscope and the value obtained for the mean energy of the primary particles is only approximate. In addition, this value would be correct only for isotropic distribution of secondary particles in the center-of-mass system.

In conclusion, the authors wish to express their gratitude to A. I. Alikhanian and A. V. Khrimian for their help and discussion, to V. Sh. Kamalian and A. M. Gal'per for taking part in the measurements and to V. M. Krishchian for help in reducing data.

[1] A. V. Khrimian, Izv. Akad. Nauk SSSR, Ser Fiz. **19**, 700 (1955).
[2] Froehlich, Harth and Sitte, Phys. Rev. **87**, 504 (1952).
[3] R. L. Cool and O. Piccioni, Phys. Rev. **87**, 531 (1952).
[4] A. J. Hartzler, Phys. Rev. **82**, 359 (1951).
[5] Whetten, Preston, Adams, Walker and Kraybill, Phys. Rev. **93**, 1356 (1954).
[6] K. H. Barker and C. C. Butler, Proc. Phys. Soc. **A64**, 4 (1951).
[7] N. M. Duller and W. D. Walker, Phys. Rev. **93**, 215 (1954).

Translated by H. Kasha
114

SOVIET PHYSICS JETP VOLUME 6 (33), NUMBER 3 MARCH, 1958

ON THE HALL EFFECT IN FERROMAGNETICS

N. V. BAZHANOVA

Moscow Institute of Transportation Engineers

Submitted to JETP editor March 6, 1957

J. Exptl. Theoret. Phys. (U.S.S.R.) **33**, 567-570 (September, 1957)

The Hall effect has been studied in Fe—Ni alloys of the invar group near the Curie temperature. It has been established that in ferromagnetics above technical saturation, the Hall emf continues to increase linearly with increasing true magnetization; this confirms the validity of formula (2), which was proposed by Volkov for describing the Hall effect in ferromagnetics. A relation between the Hall emf and the magnetic field, obtained on the basis of Ginzburg's equation for the true magnetization of ferromagnetics near the Curie temperature, is satisfactorily confirmed by experiment.

NUMEROUS studies of the Hall effect in ferromagnetic materials have led to the establishment of a number of laws. Basic among these—as has been shown by the systematic investigations of Kundt,[1] Pugh,[2] and Kikoin[3]—is a linear relation between the Hall electromotive force and the magnetization of the material in the region of technical magnetization of ferromagnetics. As is shown by experiment, after a ferromagnetic has attained magnetic saturation, the Hall effect in it continues to increase with increase of the magnetic field.

On this basis, Pugh and his coworkers[2,4] proposed the following formula for describing the Hall effect in ferromagnetics:

$$E = R_0 H + R_t I_t, \tag{1}$$

where E is the Hall electromotive force for unit current density and for unit distance between the Hall electrodes, H is the magnetic field, I_t is the magnetization of the ferromagnetic, R_t is the constant of the so-called extraordinary Hall effect, and R_0 is the constant of the ordinary effect and is a measure of the number of conduction electrons per unit volume. The term $R_t T_t$ describes the Hall-effect behavior in weak fields; the term $R_0 H$ describes the behavior in strong fields, above technical saturation.

However, after analyzing the experimental material that led Pugh to formula (1) and after considering also the work of Kikoin,[5] Volkov[6] reached the conclusion that the increase of the Hall emf in ferromagnetics in strong fields (above technical saturation) is determined not by the magnetic field H but by the true magnetization I_i. Then for ferromagnetics the Hall emf should be expressed in the following form:

$$E = R_i I_i + R_t I_i, \tag{2}$$

where R_i is a constant of the material, which describes the Hall effect in those magnetic fields in which it is determined by the true magnetization. It must be expected that in general $R_i \neq R_t$. Experiment in fact confirms this expectation.

The aim of the present work was to study the Hall effect in the region of true magnetization of ferromagnetics (the region of the paraprocess). Chosen for study were iron-nickel alloys of the invar group; in these, as was shown by the systematic investigations of Belov,[7] the paraprocess is appreciable in comparatively weak magnetic fields.

The method that we used for measuring the Hall effect was similar to that used earlier by Pugh and by Kikoin. The specimens had the form of rectangular parallelopipeds, with dimensions 6 × 12 × 150 mm, with electrodes arranged on the middle part of the specimen. The magnetization of the ferromagnetic was measured by a ballistic method, with use of a remote coil mounted outside the solenoid and connected in series with the test coil. The remote coil was so arranged as to compensate the effect of the magnetic field of the solenoid on the test coil wound on the specimen. The measurements of the Hall emf and of the magnetization were made simultaneously.

As follows from formula (2), the dependence of the Hall emf on the magnetic field H above technical saturation will exhibit a linear character only when the true magnetization I_i increases linearly with the magnetic field intensity. For ferromagnetic materials this will be approximately the case far from the Curie point, where the paraprocess susceptibility is independent of the magnetic field H. Near the Curie temperature, however, this proportionality will not be observed, because at these temperatures the true magnetization I_i depends in a complicated way on the magnetic field H. The investigation of the Hall effect that we have conducted on the alloys mentioned has shown that at temperatures near the Curie tem-

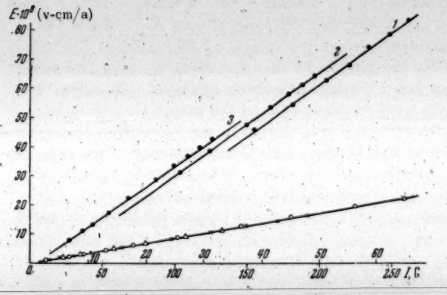

FIG. 1. Dependence of Hall emf on magnetization in the range of the paraprocess for an alloy containing 32% Ni, remainder Fe. The lower scale on the axis of abscissas corresponds to temperatures: Curve 1, 84°; 2, 100.5°; 3, 121°C. The upper scale corresponds to: ○, 150°C; ×, 159.5°C; Δ, 174°C.

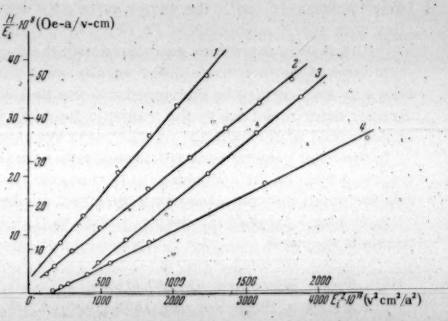

FIG. 2. Dependence of H/E_i on E_i^2 for alloys: 1, 30% Ni, 70% Fe, t = 71.5°C; 2, 32% Ni, 68% Fe, t = 121°C; 3, 34% Ni, 66% Fe, t = 178°C; 4, 37% Ni, 63% Fe, t = 235°C (1, 2, and 4, inner scale; 3, outer).

peratures, there actually is a nonlinear type of dependence of the Hall emf on magnetic field H above technical saturation in a ferromagnetic. Furthermore, in the region of the para-process—as is shown, for example, by Fig. 1—there indisputably exists a linear relation between the Hall emf and the true magnetization I_i of the ferromagnetic.

The establishment of a linear relation between the Hall emf and the magnetization in the paraprocess region makes it possible to obtain, in explicit form, the dependence of the Hall emf on the magnetic field H. By treating the Curie-point transition of the material from the ferromagnetic state to the paramagnetic as a phase transition of the second kind, Ginzburg[8] obtained the following equation for the true magnetization curve for ferromagnetics near the Curie temperature:

$$H = \alpha I_i + \beta I_i^3, \tag{3}$$

where α and β are constants, dependent on the temperature and on the pressure. Near the Curie temperature, the Hall effect due to technical magnetization, $E_S = R_I I_S$, is small in comparison with the size of the effect evoked by the paraprocess; clearly, therefore, we may expect that in this case the Hall effect will be described by the formula $E_i = R_i I_i$. Upon substituting the value of I_i from this formula in (3), we get the desired dependence of the Hall emf in the region of true magnetization upon the magnetic field:

$$H = aE_i + bE_i^3, \tag{4}$$

where

$$a = \alpha / R_i, \quad b = \beta / R_i^3. \tag{5}$$

Our experiments with the alloys mentioned show that near the Curie temperature the Hall effect satisfies the relation (4) over a wide range of values of H. This is evident, for example, from Fig. 2, which shows—in accordance with the relation (4)—the dependence of H/E_i on E_i^2 for a series of alloys of the invar group at temperatures in the immediate vicinity of the Curie point. The Curie points of these alloys were determined by the method suggested by Belov ($T = \Theta$ if $\alpha_T = 0$). The straight lines drawn in this figure have intercepts on the ordinate axis whose numerical values are evidently equal to the coefficients a in Eq. (4) for the corresponding alloys, and the slopes of the lines give the values of the coefficients b. It is possible to compare the graphically determined a and b with the values calculated from the known α, β, and R_i. The numerical values of α and β in Eq. (3) were determined from the graphs of H/I_i as a function of I_i^2 for the corresponding alloys; the coefficient R_i was determined, for example, from Fig. 1 for the alloy with 32% Ni and the rest Fe, and from similar figures for the other alloys. The comparison gives completely satisfactory results. For example, for the alloy with 32% Ni and the rest Fe ($t = 121°$), the values determined from Fig. 2 are $a = 1.3 \times 10^8$ (amp gauss/volt cm), $b = 2.7 \times 10^{22}$ (amp^3 gauss/volt^3 cm^2); the values calculated with formula (5) are $a = 0.9 \times 10^8$, $b = 2.75 \times 10^{22}$. For the alloy with 34% Ni and the rest Fe ($t = 178°C$), the values determined from Fig. 2 are $a = -4.3 \times 10^8$, $b = 10.16 \times 10^{21}$; the values calculated with the formula are $a = -6.7 \times 10^8$, $b = 9.68 \times 10^{21}$.

In view of the fact that similar results were found for the range of true magnetization in other Fe-Ni alloys as well, it may be concluded that the Hall effect in ferromagnetics above technical saturation is directly determined not by the magnetic field but by the true magnetization of the material, and should be described by formula (2).

In the most general case it is apparently necessary to take account also of the influence of the external magnetic field on the conduction electrons; but in ferromagnetics this effect, as is shown by experiment, is quite small in comparison with the effect produced by technical and true magnetization.

In closing I express my deep gratitude to D. I. Volkov, who proposed this problem, for his guidance of the work reported.

[1] A. Kundt, Wied. Ann. **49**, 257 (1893).
[2] E. M. Pugh, Phys. Rev. **36**, 1503 (1930); E. M. Pugh and T. W. Lippert, Phys. Rev. **42**, 709 (1932).
[3] I. K. Kikoin, Physik. Z. Sowjetunion **9**, 1 (1936).
[4] Pugh, Rostoker, and Schindler, Phys. Rev. **80**, 688 (1950).
[5] I. K. Kikoin, J. Exptl. Theoret. Phys. (U.S.S.R.) **10**, 11 and 1242 (1940).
[6] D. I. Volkov, Вестник Моск. ун-та (Bulletin of Moscow Univ.) **3**, 65 (1954).

[7] K. P. Belov, Упругие, тепловые и электрические явления в ферромагнитных металлах (Elastic, Thermal, and Electrical Phenomena in Ferromagnetic Metals), GITTL, 1951.

[8] V. L. Ginzburg, J. Exptl. Theoret. Phys. (U.S.S.R.) 17, 833 (1947).

Translated by W. F. Brown Jr.
115

SOVIET PHYSICS JETP VOLUME 6 (33), NUMBER 3 MARCH, 1958

INVESTIGATION OF THE CHARACTERISTIC ENERGY LOSSES OF ELECTRONS AND THE SECONDARY ELECTRON EMISSION FROM GeO_2

N. B. GORNYI and A. IU. REITSAKAS

Submitted to JETP editor March 1, 1957

J. Exptl. Theoret. Phys. (U.S.S.R.) 33, 571-575 (September, 1957)

The characteristic energy losses of electrons reflected from the surfaces of two germanium plates of the n and p types covered with GeO_2 are investigated. The spectra of the characteristic losses for both types of plates are similar. If the difference in the lattice constants is taken into account, the spectra of the characteristic energy losses for GeO_2 and MoO_2, which have identical (tetragonal) lattices, are found to be similar. Secondary electron emission has been investigated for the indicated GeO_2 samples. The secondary electron yield from GeO_2 is almost twice as large as the yield from germanium.

CHARACTERISTIC ENERGY LOSSES OF ELECTRONS

In an earlier work on the characteristic energy losses in reflection from a MoO_2 surface[1] one of the authors has showed that these losses can be determined by the formula

$$W = (h^2/8m)(n/d)^2.$$

For MoO_2 which crystallizes in a tetragonal lattice $(n/d)^2 + (h^2 + k^2)/a^2 = (l/c)^2$ where h, k, and l are the Miller indices, and a and c are the lattice constants. Thus, the spectra of the characteristic energy losses of electrons must depend on the structure and size of the crystal lattice of a given material. Therefore, different substances with the same crystal structure must have similar spectra. This conclusion was arrived at in one of the recent works of Marton and co-workers.[2]

To test the above conclusion we undertook to investigate the characteristic energy losses of electrons in GeO_2, which has the same crystal lattice as MoO_2. We treated two thin plates of germanium (thickness 0.5 mm), one type n and the other type p, with a solution of nitric acid; this, as is known, forms a layer of GeO_2 on the surface of germanium. After treating with nitric acid the sample was washed in distilled water, then treated in a solution of NaOH, and once again washed in distilled water and in pure alcohol. As a result there remained on the surface of the germanium a layer of GeO_2, "insoluble" in water, and crystallized in a tetragonal lattice.[3] The lattice constants of GeO_2 are a = 4.39 A and c = 2.859 A.

The method of electrical differentiation in a spherical capacitor[4,5] circuit was used to investigate the characteristic energy losses of electrons reflected from the surfaces of the above two GeO_2-coated germanium plates. The vacuum apparatus was as that used in Ref. 6. The two targets were arranged on a cylindrical table made of tantalum inside the spherical vacuum apparatus. By means of a magnet outside the vacuum it was possible to turn the table so that either one of the specimens could be placed in the beam. After long adjustment and degassing of the apparatus the pressure, measured with an ionization

gauge prior to firing the getter and unsoldering the apparatus, was less than 5×10^{-7} mm. The earth's magnetic field was compensated by two coils 1 m in diameter.

For both specimens there were obtained curves of the distribution of scattered electrons vs energy. The curves obtained for these two specimens at equal primary electron energy were very much the same. On Fig. 1 are shown the distribution curves obtained with GeO_2 layers on n-germanium for an emitter temperature of 400° C and for several values of incident electron energy. The table lists the values of energy loss calculated by the above formula for a series of values of h, k and l, and also the experimentally-obtained characteristic energy losses $V_p - V_k$. We first note the good agreement between the experimental and the calculated values. If we compare the curves of Fig. 1 and the table with Fig. 1 and the table of Ref. 1, we see that the fundamental inelastic-loss peaks obtained for MoO_2 for h, k and l equal to (111), (002) and (221) manifest themselves just as pronouncedly in the case of GeO_2. Further, by comparing the curves of Fig. 1 it is possible to note that, just as for MoO_2 (Ref. 1) and Cu_2O (Ref. 7), increasing of the incident electron energy increases the probability of characteristic losses of large energy (for $V_p - V_k$ equal to 7 and 9 ev), and decreases the losses at values of $V_p - V_k$ equal to 3.2 and 4.4 ev. The characteristic losses for $V_p - V_k = 2$ ev are clearly visible only for $V_p = 30$ v.

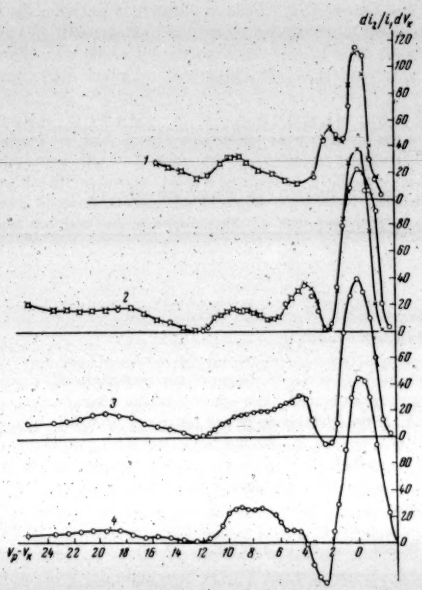

FIG. 1. (1) $V_p = 30$ v, (2) $V_p = 50$ v, (3) $V_p = 70$ v, (4) $V_p = 100$ v.

However, there are certain discrepancies between the results obtained for GeO_2 and for MoO_2. For GeO_2 we have two peaks of characteristic losses for h, k and l equal to (110) and (121) with values of energy W equal to 3.9 and 14.3 ev, respectively, which we do not find for MoO_2. The corresponding energies W for MoO_2 have the values 3.2 and 12.8 ev. Upon careful examination of the curves of inelastic loss for MoO_2 (Ref. 1) we may assume that the peak for $V_p - V_k = 4.5$ ev is the result of the superposition of two peaks, one with an energy loss W = 3.2 ev and the other with W = 4.8 ev, for h, k and l (110) and (001) respectively. Further, the 12.8 ev MoO_2 characteristic energy-loss peak coincides exactly with a minimum in all the curves of Fig. 1,[1] and the presence of this peak is therefore difficult to observe. However, the flattening of this minimum in the curves with increasing V_p (in particular in the curve for $V_p = 260$ volts) may be explained by the presence of a characteristic energy loss peak with W = 12.8 ev and by the increase in the probability of this loss with increasing energy of the incident electrons.

h	k	l	W, ev	$V_p - V_k$, v
1	0	0	1.96	2
0	0	1	3.1	3
1	1	0	3.9	4.4
1	0	1	6.6	7
1	1	1	8.6	9
1	2	1	14.3	14.5
0	0	2	18.5	19
2	2	1	20.3	

From the data obtained we may conclude: (1) that for GeO_2 the spectra of characteristic electron energy losses are determined by the structure of its crystalline lattice; (2) that the spectra of the electron characteristic energy losses are similar in GeO_2 and MoO_2, which have the same crystalline lattice, and the difference in the spectra depends only on the difference in their lattice constants.

SECONDARY ELECTRON EMISSION

As far as we know, the literature contains no information concerning the secondary electron emission

of GeO_2. We therefore present the results of our investigation of the secondary electron emission, obtained with the same apparatus and from the same two GeO_2 samples as used for the investigation of the characteristic electron energy losses.

The investigation of the secondary electron emission was in accordance with the usual scheme.[8] The dependence of the secondary electron coefficient δ on the energy of the primary electrons, $\delta = f(V_p)$, was obtained for both specimens (layer of GeO_2 formed on n-germanium and p-germanium). Figure 2 shows the curves of $\delta = f(V_p)$ obtained for GeO_2 on n-germanium. Curve 1, obtained at room temperature, gives the maximum value $\delta_{max} = 2.06$ for $V_p = 400$ volts. The curves obtained for the second specimen were identical.

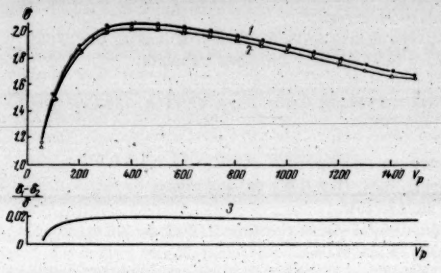

FIG. 2. (1) Room temperature, (2) t = 400° C, (3) Increased temperature.

The yield of secondary electrons from GeO_2 is approximately $1\frac{1}{2}-2$ times greater than the yield from Ge.[9-11] One cannot assume that the considerable increase of δ in the dioxide of Ge is due to the oxygen atoms, since in a number of cases the yield of secondary electrons not only did not increase for the oxidized substance, but actually decreased (for example, MoO_2 and Cu_2O). It is therefore necessary to assume that the variation of secondary emission characteristic of oxides is connected with the change in the crystal lattice, and consequently also in the energy levels.

From the curve of $\delta = f(V_p)$ obtained for for t = 400° C it is seen that the yield of secondary electrons is somewhat reduced with increased temperature. The character of the relative variation of δ for increased temperature, $(\delta_1-\delta_2)/\delta_1 = f(V_p)$, shows[8] that the decrease in δ is not caused by an increase in the work function but results from the change in thickness of the emitter. A similar character and an approximately equal reduction in δ with increasing temperature was observed for Ge;[10] in those investigations the same variation in δ was observed in samples differing in the free-electron concentration by more than three orders. It was therefore concluded that the energy loss of the secondary electrons is due not to the free electrons, but to the interaction between the electrons and the lattice. It is necessary to assume that also in the case of GeO_2 this same mechanism is responsible for the reduced yield of secondary electrons with increasing temperature.

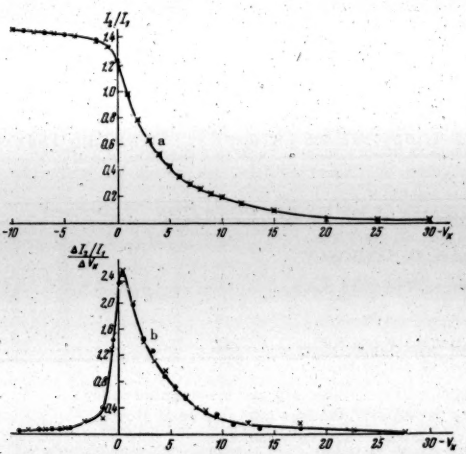

FIG. 3

The distribution of secondary electrons with respect to energy was investigated by the retarding field method. Figure 3a shows the retarding curve for GeO_2 on n-germanium obtained for V_p = 100 v and t = 400° C. Differentiation of the retarding curve gives the energy distribution of the secondary electrons (Fig. 3b). The curves are not corrected for contact potential difference between the GeO_2 and the aquadag on the collector since we do not know the work function of GeO_2. In the same way curves were obtained for 20° C, and also for V_p = 500 v at the above two temperatures. Analogous curves were obtained for GeO_2 on p-germanium. Curves obtained for the same value of V_p but for different

temperatures (20 and 400° C) were identical. The ordinate of the retarding curve I_2/I_1 obtained for V_p = 500 v becomes negative values starting with V_k = 11 v. The position of the peak of secondary electrons in the distribution curve was also obtained for V_p = 100 v (Fig. 3b), but the half-width of the peak of the distribution curves for V_p = 500 v is narrower (3 ev) than that of the curve obtained for V_p = 100 v (3.5 ev). The range of secondary-electron energies of the distribution curves for GeO_2, is characteristic of semiconductors.

The absence of saturation in the retarding curves in the region of positive values near zero, which leads to the appearance of electrons with "negative" energy, is explainable by tertiary electrons knocked out of the collector by the reflected primary or secondary electrons.[12]

In conclusion we regard it our agreeable duty to express thanks to V. P. Zhuze for making the germanium, and we also are thankful to B. F. Zhuravskii for his help with the measurements.

[1] N. B. Gornyi, J. Exptl. Theoret. Phys. (U.S.S.R.) 31, 132 (1956); Soviet Phys. JETP 4, 131 (1957).
[2] Leder, Mendlowitz, and Marton, Phys. Rev. 101, 1460 (1956).
[3] O. H. Johnson, Chem. Rev. 51, 431 (1952).
[4] N. B. Gornyi, J. Exptl. Theoret. Phys. (U.S.S.R.) 27, 171 (1954).
[5] N. B. Gornyi and L. M. Rachovich, J. Exptl. Theoret. Phys. (U.S.S.R.) 26, 454 (1954).
[6] N. B. Gornyi, J. Exptl. Theoret. Phys. (U.S.S.R.) 26, 88 (1954).
[7] N. B. Gornyi, J. Exptl. Theoret. Phys. (U.S.S.R.) 30, 160 (1956); Soviet Phys. JETP 3, 175 (1956).
[8] N. B. Gornyi, J. Exptl. Theoret. Phys. (U.S.S.R.) 26, 79 (1954).
[9] L. R. Koller and J. S. Burgess, Phys. Rev. 70, 571 (1948).
[10] J. B. Johnson and J. R. McKay, Phys. Rev. 93, 668 (1954).
[11] H. Gobrecht, F. Speer, Zeits. Phys. 135, 602 (1953).
[12] N. B. Gornyi, J. Tech. Phys. (U.S.S.R.) 26, 723 (1956), Soviet Phys. JTP 1, 702 (1956).

Translated by L. B. Leder
116

SOVIET PHYSICS JETP VOLUME 6 (33), NUMBER 3 MARCH, 1958

CHANGE IN THE ISOTOPIC COMPOSITION OF MERCURY BY EVAPORATION

V. N. GRIGOR'EV, IA. S. KAN, N. S. RUDENKO, and B. G. SAFRONOV

Physico-Technical Institute, Academy of Sciences, Ukranian S.S.R.

Submitted to JETP editor March 13, 1957

J. Exptl. Theoret. Phys. (U.S.S.R.) 33, 576-580 (September, 1957)

Evaporation-induced changes in the isotopic composition of mercury are investigated under various conditions. It is found that the kinetics of evaporation plays a large role at slow distillation rates. The upper limits of $\Delta p/p$ are evaluated for mercury isotopes.

INTRODUCTION

THE determination of the relative saturated vapor pressures for isotopes is important both for studying the influence of isotopic composition on the properties of matter and for isotope separation techniques. This measurement is often performed by evaporation of isotope mixtures at constant temperature. The change in the composition of a two-component mixture is then given by

$$\frac{c}{c_0} = \left(\frac{1-c_0}{1-c}\right)^{1/\alpha} \left(\frac{v_0}{v}\right)^{\frac{\alpha-1}{\alpha}}, \qquad (1)$$

where c_0 and c are the concentrations of the isotope in the liquid before and after evaporation, v_0 and v are the initial and final volumes of the liquid, and α is the separation coefficient.

Under equilibrium evaporation of an ideal mixture, α is equal to the vapor pressures of the components. Such experiments may give values of v_0/v of the order of several thousands, which makes it possible to determine α to within 0.03%. An expression similar to (1) can be obtained also for many-component ideal systems.[1]

This approach was used by many authors,[2-6] but when it was possible to compare the results so obtained with direct measurements of the vapor pressure ratio, it was found that the evaporation method gives $\Delta p/p$ values that are too high. In this connection it would seem interesting to study the mechanism of isotope separation by evaporation and to clarify the possibilities of determining the vapor pressure ratio by this method. We chose mercury as the object of our studies, since it is a liquid through a wide range convenient for experiment and can be very thoroughly cleaned of impurities.

A change in the isotopic composition of mercury by evaporation has been observed by many authors,[7-9] although the investigations were performed under conditions known to be nonequilibrium no attempt was made to explain the separation mechanism.

EXPERIMENTAL PART

Evaporation with small residues was performed in the apparatus shown in Fig. 1. Between 50 and 100 cm^3 of mercury was distilled into flask A, after which the apparatus was sealed off without breaking the vacuum. The vacuum was maintained by means of a carbon trap cooled by liquid nitrogen. The evaporated mercury condensed in the tube and flowed into flask C at room temperature. To avoid possible condensation of the vapors in the upper part of A, an additional heating coil was wound at the top. Evaporation continued until between 10^{-3} and 10^{-4} of the original quantity of mercury remained, after which the remainder was analyzed in a mass spectrometer. When the experiments were performed in the temperature interval from 60 to 270° C, it was always found that the residue was enriched in the heavy isotope. The large spread in the values of α obtained, however, made it difficult to interpret the results. A decrease of the distillation rate by the introduction of a diaphragm whose diameter lay between 1 and 2 mm into A led to a decrease in the separation coefficient. Experiments in which the vapor removal rate was varied through wide limits were performed at 200° C; the removal rate was varied by altering the resistance of the tube connecting A and C (Fig. 1). When the removal rate was reduced by a factor of about 50, the separation coefficient changed from 1.0050 to 1.0008.

In order to evaluate the vapor pressure ratio at low temperatures, one may make use of evaporation by molecular distillation, for which the mean free path λ of a vapor molecule is much greater than the distance d to the condenser. In this case $\alpha = (p_1/p_2)\sqrt{M_2/M_1}$, where p_1 and p_2 are the vapor pressures of the isotopes, and M_1 and M_2 are their atomic weights. Due to the very low evaporation rate, the Rayleigh distillation method cannot be used, and therefore the apparatus shown in Fig. 2 was used to remove a small quantity of the vapor.* The low-temperature kerosene bath A was cooled by means of heat conductor B immersed in liquid nitrogen. The vapor condensed on the inner wall of a Dewar flask cooled by liquid nitrogen. The amount of condensed vapor was no greater than 10^{-4} of the original mercury, so that the composition of the liquid could be assumed constant. Under such conditions the ratio of the concentrations in the distillate and residue gives the separation coefficient. Experiments were performed at temperatures of −20, −30, and −38° C. In all cases the separation coefficient was found to be equal to the square root of the isotope mass ratio within the experimental limits, regardless whether the mercury was stirred or not.

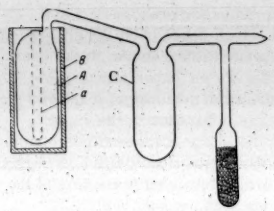

FIG. 1. Distillation apparatus. B — electric mercury heater; a — thermometer tube.

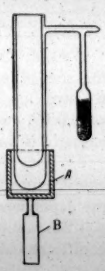

FIG. 2. Apparatus for removing the vapor at low temperatures.

*L. S. Kan took part in developing this method.

Distillations with small residues were performed at temperatures from 10 to 90°C under conditions close to molecular distillation. The separation coefficient decreased as the tmperature increased and as the distance to the condenser increased. Experiments on fractional distillation were performed under similar conditions in the apparatus shown in Fig. 3. Mercury on the outside wall 1 of the Dewar flask was heated by water vapor and condensed on the inner wall 2 which was cooled by liquid nitrogen. The evaporation continued until half the original mercury remained in the apparatus. The remainder (the so-called "heavy" fraction) was removed from the apparatus through the narrow rubber tube 3. After the nitrogen evaporated, the "light" fraction was removed. The "light" and "heavy" fractions thus obtained were subjected to further distillation. In this way we obtained fourteen fractions of "light" and twelve fractions of "heavy" mercury.

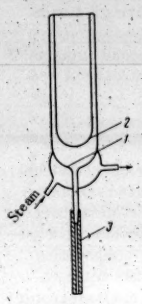

FIG. 3 Apparatus for fractional distillation.

MASS-SPECTROMETRIC ANALYSIS

A preliminary measurement established the fact that the change in the concentration of a given isotope in a sample is related linearly to the difference between the atomic weight of this isotope and the mean atomic weight of the mixture. We therefore performed an analysis to measure the change in the concentration ratio $a = c^{198}/c^{204}$ for the isotopes Hg^{198} and Hg^{204}. The measurements were performed on MS-2 and MS-4 mass spectrometers according to the following scheme: ordinary mercury — sample investigated — ordinary mercury. The background before the measurements on the sample of ordinary mercury was no greater than 3% of the operating intensity. No "memory" effect, (i.e., influence of the absorbed vapors on later measurements) was observed.

DISCUSSION OF RESULTS

The results of the experiments are shown in the tables and in Fig. 4. The tables give the temperatures at which the experiments were performed, the ratio v_0/v of the initial and final volumes, the ratio of the mean evaporation rate calculated by Langmuir's formula (G_{calc}) to the mean distillation rate as found from the time of evaporation (G_{exp}), the change of the concentration ratio of Hg^{198} and Hg^{204} of the residue as compared with ordinary mercury, and the calculated separation coefficient.

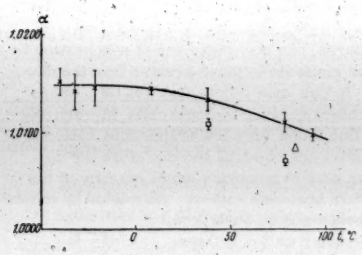

FIG. 4. The separation coefficient as a function of temperature for molecular distillation × — distillation in an apparatus with d = 2 cm, □ — d = 10 cm, Δ — mean value of α for fractional distillation.

It is known that isotope separation by evaporation can be due to two mechanisms: an equilibrium mechanism related to the difference in the vapor pressures, and a nonequilibrium mechanism which depends on the difference of the evaporation rates. As mentioned above, in the second case $\alpha = (p_1/p_2)\sqrt{M_2/M_1}$. From experiments performed with molecular distillation conditions, it follows that $\alpha \approx \sqrt{M_2/M_1}$, so that the difference in the vapor pressures does not exceed the error of these experiments. It is seen from Fig. 4 that the separation coefficient begins to decrease already at $\lambda \sim d$, which is an indication of the effect of molecular collisions in the vapor.

In the first experiments on evaporation with a small residue, the calculated evaporation rate exceeded the rate of vapor removal by a factor of several times ten. This would seem to assure conditions sufficiently close to equilibrium. The poor reproducibility of the results alone, however, makes it reasonable to suppose that the dependence of α on the distillation conditions is related to differences in the contributions from nonequilibrium processes. This point of view is supported by the experimental increase of the separation coefficient when the removal rate is changed, that is on approaching equilibrium. It is seen from Table III that the vapor removal rate is a very important parameter in the process of isotope separation by evaporation. In experiments performed at very low distillation rates, G_{calc}/G_{exp} was of the order of several thousands, yet in these cases one cannot assert that the separation is due only to the difference in the

TABLE I

t °C	$\frac{v_0}{v}$	$\frac{\sigma_{calc}}{\sigma_{exp}}$	$\frac{\Delta\alpha}{\alpha}$, %	α	$\Delta\alpha \cdot 10^4$	Remarks
70	2040		2.4	1.0031	6	
80	19000	40	2.6	1.0031	5	
100	5560	30	2.9	1.0033	5	
100	524		1.7	1.0030	4	Distillation with water vapor;
110	5880		2.2	1.0028	3	
120	2710	70	2.8	1.0036	3	
120	9000	100	1.6	1.0020	4	
140	2000		1.2	1.0017	5	
160	9700	150	2.9	1.0037	7	
160	183	170	1.7	1.0023	4	Distillation with a constant
200	7750	200	1.8	1.0022	5	mercury surface
250	532	3200	0.3	1.0004	2	

TABLE II

t °C	$\frac{v_0}{v}$	$\frac{\sigma_{calc}}{\sigma_{exp}}$	$\frac{\Delta\alpha}{\alpha}$, %	α	$\Delta\alpha \cdot 10^4$
100	2700	90	2.6	1.0033	4
160	8950	600	0.8	1.0007	2
200	15200	1000	1.9	1.0022	3
270	1960	3100	1.2	1.0013	3
270	10300	5000	0.5	1.0004	2

TABLE III

$t = 200°$ C

$\frac{\sigma_{calc}}{\sigma_{exp}}$	$\frac{v_0}{v}$	α	$\Delta\alpha \cdot 10^4$
100	5780	1.0051	4
800	2260	1.0019	4
1200	5380	1.0022	3
3000	209	1.0010	3
5000	256	1.0008	3

vapor pressures.

The influence of the evaporation kinetics is particularly important in the evaporation of small drops, which leads to anomalously large separation coefficients at v_0/v of the order of several times ten thousand and to a decrease of α for evaporation from a constant surface. It would seem that the evaporation kinetics plays an important role in distillation in the presence of an inert gas, since when the distillation is performed in the presence of water vapor the separation coefficient obtained is about the same as for ordinary distillation.

The literature cited in the introduction, unfortunately, does not contain data which can be used to evaluate the state of equilibrium of the evaporation. One can only suggest that the large values of the $C^{12}H_4$ and $C^{13}H_4$ vapor pressures obtained by several authors[5,6] may be explained in this way.

The experiments performed can be used to evaluate the upper limits of the relative vapor pressure difference of Hg^{198} and Hg^{204}. These are $\Delta p/p \leq 2 \times 10^{-3}$ at $t = -20°C$, and $\Delta p/p \leq 8 \times 10^{-4}$ at $t = 200°C$. These results do not contradict the $\Delta p/p$ value as calculated on the basis of the work of I. Lifshitz and Stepanova,[10] namely $\Delta p/p = 3 \times 10^{-4}$ at $t = 20°C$ and $\Delta p/p = 4 \times 10^{-5}$ at $t = 200°C$ for mercury vapor.

In conclusion we take this opportunity to thank B. G. Lazarev for discussions.

[1] I. A. Mirkin, J. Phys. Chem. (U.S.S.R.) **27**, 341 (1953).
[2] H. C. Urey and F. G. Brickwedde, G. M. Murphy, Phys. Rev. **40**, 1 (1932).
[3] H. C. Urey and A. H. W. Alten, Phys. Rev. **50**, 575 (1936).
[4] M. H. Wahl and H. C. Urey, J. Chem. Phys. **3**, 411 (1935).
[5] G. G. Deviatykh and A. D. Zorin, J. Phys. Chem. (U.S.S.R.) **30**, 1133 (1956).
[6] Iagodin, Uvarov, and Zhavoronkov, Dokl. Akad. Nauk SSSR **111**, 384 (1956).
[7] J. H. Bronsted and G. Hevesy, Phil. Mag. **6**, 60 (1922).
[8] W. D. Harkins and B. Mortimer, Phil. Mag. **6**, 601 (1928).
[9] A. K. Brewer and S. L. Madorsky, J. Research Natl. Bur. Standards **38**, 129 (1947).
[10] I. M. Lifshitz and G. I. Stepanov, J. Exptl. Theoret. Phys. (U.S.S.R.) **31**, 156 (1956), Soviet Phys. JETP **4**, 151 (1957).

Translated by E. J. Saletan
117

VARIATIONS IN THE ISOTOPIC COMPOSITION OF MERCURY IN A DC ELECTRIC FIELD

I. V. BOGOIAVLENSKII, V. N. GRIGOR'EV, N. S. RUDENKO, and D. G. DOLGOPOLOV

Physico-Technical Institute, Academy of Sciences, Ukrainian S.S.R.

Submitted to JETP editor March 13, 1957

J. Exptl. Theoret. Phys. (U.S.S.R.) **33**, 581-587 (September, 1957)

Direct current was passed through liquid mercury and the time variation of the isotopic composition of the mercury was studied. The experiments were carried out at two temperatures. We investigated the variation of isotope concentration along the electric field, and the relation between the isotopic composition at the cathode and the applied voltage. The experimental data are compared with some phenomenological calculations and possible causes for the effect are discussed.

THERE are many papers[1] devoted to the effect that direct current has on the constitution of binary metallic solutions. None of the theories which have been proposed to explain the effect has given satisfactory agreement with experiment, and the underlying mechanism remains obscure. The question is most conveniently considered if we take a mixture of metal isotopes as the object to be investigated.

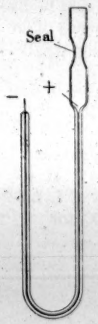

FIG. 1.

It has recently been observed that changes in isotopic constitution occur when direct current passes through mercury,[2,3] thallium,[4,5] potassium,[6] and indium.[7] In all these cases it has been found that the concentrations of the heavy isotopes increase near the cathode, and of the light ones near the anode. However, the work has not been carried out systematically, which makes comparison with theory difficult. It therefore appeared appropriate to measure some of the fundamental quantities connected with the effect.

EXPERIMENTAL PART

All the experiments were carried out in glass capillary tubes (Fig. 1) 28 cm long and of inner diameter 0.05 cm. Before being filled with mercury, the capillary tubes were evacuated by a diffusion pump and heated to a temperature of 300°C; mercury was then distilled into them. The volume of the reservoir was much greater than that of the capillary, so that the composition of the mercury at the anode was always the same. The experiments were carried out with temperatures of (41 ± 2)°C and (-10 ± 3)°C at the outer capillary wall. The temperature of (41 ± 2)°C was maintained by placing the capillary in a stirred-water bath. The temperature of (-10 ± 3)°C was maintained in a kerosene bath cooled by a copper rod with one end in liquid nitrogen. After a certain, definite time the current was turned off and the capillary quickly cut into pieces. The mercury in each piece was analyzed with a mass spectrometer. The method used to make the mass spectrometer measurements has been described before in detail.[8]

Fig. 2 shows how the variation of the concentrations of Hg^{198} and Hg^{204} with the time of current flow. The quantity plotted along the Y axis is $\Delta a/a_0$, where $\Delta a = a_0 - a$ and a_0, a are the ratios of the concentration of Hg^{198} to the concentration of Hg^{204} in normal mercury and that found near the cathode. The duration of current flow is plotted on the X axis. From the figure it is evident that the curves tend to saturate as the time increases, and for a fixed voltage the change in concentration is less at −10°C than it is at 41°C.

The curves of Fig. 3 show how the concentration varies along the length of the capillary. The value of $\Delta a/a_0$ from various parts of the capillary is plotted along the ordinate. Comparison of the curves shows that their curvature decreases as equilibrium is approached.

Fig. 4 shows how $\Delta a/a_0$ at the cathode depends on the voltage applied between the electrodes. The voltage across the electrodes is plotted along the X axis. The bath temperature was 41°C, the current was on for 1500 to 1800 hours.

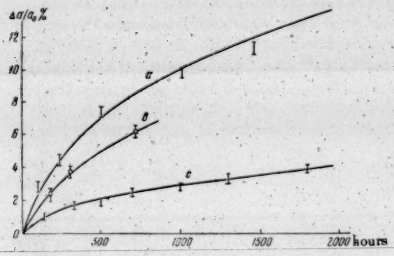

FIG. 2. Variation in the concentrations of Hg^{198} and Hg^{204} with duration of current flow. Curves a and c: bath temperature 41 ± 2°C, applied voltage 6 and 2 volts respectively; curve b: bath temperature — 10 ± 3°C, applied voltage 6.

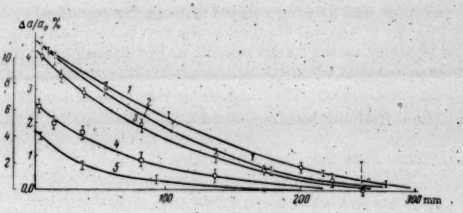

FIG. 3. The concentration of the mercury isotopes as a function of distance along the capillary. 1 — time t of current flow 1800 hrs, applied voltage U = 5.15 volts; 2 — t = 1460 hrs., U = 2.14 volts; 3 — t = 1800 hrs., U = 2 volts; 4 — t = 700 hrs., U = 2 volts; 5 — t = 340 hrs., U = 2 volts. The right-hand scale refers to curves 2 — 5, the left hand one to curve 1. Temperature 41°C.

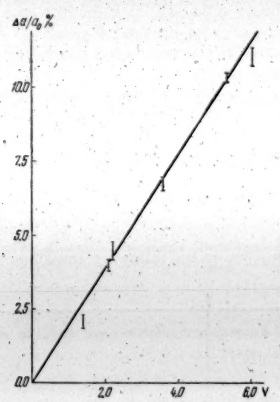

FIG. 4.

CALCULATION OF CONCENTRATION DISTRIBUTION

Bresler and Pikus[9] considered quantitatively the isotope separation induced by direct current. They studied a mixture of two isotopes and took the electric field to be constant along the length of the column. The electric field displaces both kinds of ions in the same direction; there is a backward hydrodynamic flow of the liquid as a whole because it is incompressible, and a backward diffusion flow because of the gradient in isotope concentration which is set up. The equations for the ion current show that the ions can be separated because they have different mobilities.

The boundary conditions used in the calculation above correspond to zero flux of matter at both ends of the capillary, a condition which did not obtain in our experiments. We therefore give a solution for different boundary conditions.

It is shown in Ref. 9 that if the diffusion coefficients of the two isotopes differ little, the equation for the concentration c can be put in the form [Eq. (6) of Ref. 9]

$$\frac{d}{dx}\left[\frac{\partial y}{\partial x}+y^2\right]=\frac{\partial y}{\partial \tau} \qquad (1)$$

where $\kappa = x/b$ is a dimensionless length, $\tau = tD/b^2$ is dimensionless time, $1/b = \Delta\mu\, E/D$, $\Delta\mu = \mu_2 - \mu_1$ is the difference between the mobilities of the second and first isotopes, D is the diffusion coefficient, E the applied voltage, and $y = {}^1/_2 - c$.

The condition that there be no flux of matter at the cathode can be written

$$[\partial y/\partial x + y^2 - 1/4]_{x=0} = 0. \qquad (2)$$

The second boundary condition, that the concentration be constant at the anode, is

$$y\,|_{x=L} = {}^1/_2 - c_0 = \alpha = \text{const}. \qquad (3)$$

The initial condition is:

$$y(x,\tau)\,|_{\tau=0} = \alpha.$$

Introducing, after Bresler and Pikus, a new variable $\varphi = \varphi^* \exp\left[-\int z(\tau)\,d\tau\right]$, we obtain Fourier's equation:

$$\partial^2\varphi/\partial x^2 = \partial\varphi/\partial\tau, \qquad (1a)$$

with y and φ being related through the equation

$$\varphi = \exp\left[\int_0^x y\,dx\right]. \tag{5}$$

The initial and boundary conditions then take the form

$$[\partial^2\varphi/\partial x^2 - {}^1/_4\varphi]_{x=0} = 0; \tag{2a}$$

$$[\partial\varphi/\partial x - \alpha\varphi]_{x=L} = 0; \tag{3a}$$

$$\varphi(x,\tau)|_{\tau=0} = \exp[\alpha x]. \tag{4a}$$

Upon taking Laplace transforms we obtain

$$\bar{\varphi}'' = p\bar{\varphi} - \exp[\alpha x]; \tag{1b}$$

$$[\bar{\varphi}'' - {}^1/_4\bar{\varphi}]_{x=0} = 0; \tag{2b}$$

$$[\bar{\varphi}' - \alpha\bar{\varphi}]_{x=L} = 0. \tag{3b}$$

A solution of (1b) satisfying (2b) and (3b) is

$$\bar{\varphi} = \frac{\alpha^2 - 1/4}{(p - 1/4)(\alpha^2 - p)}\,\frac{\sqrt{p}\cosh\sqrt{p}(x-l) + \alpha\sinh\sqrt{p}(x-l)}{\sqrt{p}\cosh\sqrt{p}\,L - \alpha\sinh\sqrt{p}\,L} + \frac{\exp[\alpha x]}{p - \alpha^2}. \tag{6}$$

Upon applying the inverse transform, we find that

$$\varphi = \frac{\cosh[(x-l)/2] + 2\alpha\sinh[(x-l)/2]}{\cosh(L/2) - 2\alpha\sinh(L/2)}\,e^{\tau/4} + \sum_{n=1}^{n=\infty} A_n \sin\lambda_n x \exp\{-\lambda_n^2\tau\}, \tag{7}$$

where

$$A_n = \left(\frac{L}{2} - \frac{\sin 2\lambda_n L}{4\lambda_n}\right)^{-1}\frac{\lambda_n(1/4 - \alpha^2)}{(\alpha^2 + \lambda_n^2)(\lambda_n^2 + 1/4)}, \tag{8}$$

and the λ_n are determined through the equations

$$\alpha\tan\lambda_n L = \lambda_n. \tag{9}$$

From (5) we can then conclude that the concentration is distributed according to the following equation:

$$c = \frac{1}{2}\left[1 - \frac{\sinh[(x-x_0)/2] + 2\cosh(x_0/2)\,e^{-\tau/4}\sum_{n=0}^{n=\infty} A_n\lambda_n\cos\lambda_n x\exp\{-\lambda_n^2\tau\}}{\cosh[(x-x_0)/2] + \cosh(x_0/2)\,e^{-\tau/4}\sum_{n=0}^{n=\infty} A_n\sin\lambda_n x\exp\{-\lambda_n^2\tau\}}\right], \tag{10}$$

κ_0 being determined by the condition that the concentration be a constant at κ = L:

$$\alpha = {}^1/_2\tanh[(L - x_0)/2]. \tag{11}$$

Equation (10) can conveniently be used for values of time causing the series to converge rapidly. A formula convenient for small times can be obtained by expanding the right hand side of (6) in powers of $\exp(-\sqrt{p})$ and using the inverse Laplace transformation on only the first few terms. However, formula (10) does not present any real computational difficulties for times down to 100 hrs.

DISCUSSION OF THE RESULTS

Equations (8) – (11) can be used to find the quantity L and the difference $\Delta\mu$ = DL/ℓE in ion mobilities from the experimental datax (ℓ is the length of the column). In the case that $\lambda_n^2 \gg 1$, $\alpha \ll 1$ and $\kappa_0/2 \ll 1$, which applies to all our experiments, the concentration at the cathode as a function of the time for which the current was on is given by the relation

$$\Delta c = \frac{L}{4}\left[1 - \sum_{n=0}^{n=\infty}\frac{8}{\pi^2(2n+1)^2}\exp\left[-\frac{\pi^2 D(2n+1)^2}{4l^2}t\right]\right] \tag{12}$$

The sum of the concentration changes in both isotopes, Δc is proportional to L, which agrees well with the experimental data shown in Fig. 4.

In order to find L, the mixture of mercury isotopes was considered to consist of two parts: the lighter one included the isotopes Hg^{196}, Hg^{198}, Hg^{199}, and Hg^{200} and was 50.14% of the whole, while the heavier part consisted of all the other isotopes. In this case, the changes in the concentrations of each component are the sum of the changes Δc_i in each isotope, and can be obtained from the mass spectrometer measurements, taking the Δc_i to be linear functions of the molecular weight of the isotope.

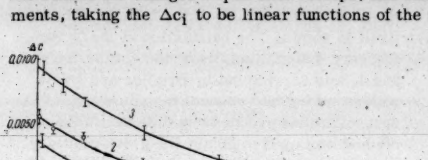

FIG. 5. Distribution of isotope concentration along the mercury column. 1 — t = 340; 2 — t = 700; 3 — t = 1800 hrs.

A value of L was calculated from each experimental value of $\Delta a/a_0$ whown in Fig. 2, and the average taken. The averages so obtained are: L = 0.24 ± 0.02 for 6 volts and 41° C and L = 0.08 ± 0.007 for 2 volts at the same bath temperature.

Using the Einstein relation $\mu = D\epsilon_0/kT$, where ϵ_0 is the charge on an electron, we obtain the relative difference in isotope mobilities as $\Delta\mu/\mu = (1.3 \pm 0.1) \times 10^{-3}$ when the temperature of the mercury column is 115° C, and $\Delta\mu/\mu = (1.1 \pm 0.1) \times 10^{-3}$ at 45° C, the temperatures inside the capillary being obtained by calculation. The average values of L so found were used to obtain $\Delta a/a_0$ as a function of time. The results are shown in Fig. 2 (curves a and c).

Using the calculated values of L the concentration along the mercury column was computed for a potential difference of 2 volts and for three values of time: t = 340, 700, and 1800 hours. The results are shown in Fig. 5, which also shows the experimental data. The sum of the changes in the concentrations of the light and heavy components is plotted on the Y axis, while the X axis shows the length of the capillary in millimeters. From Figs. 2 and 5 it is clear that the agreement between experiment and the results of the calculations is good.

For our experiments, the characteristic time

$$t_0 = \frac{4b^2}{D\left[1 + (2\lambda_n)^2\right]} = \frac{4l^2}{\pi^2 D}, \tag{13}$$

turns out to be about 5000 hours. From (13) it follows that t_0 does not depend on the magnitude of the applied electric field, and, what is more important, decreases as the square of the length of the isotope column, so that in order to decrease the time required for the experiment, one should use shorter capillaries.

For the stationary case, as $t \to \infty$, the distribution of concentration assumes the form

$$c = \frac{1}{2}\left[1 - \tanh\frac{x - x_0}{2}\right]. \tag{14}$$

It follows that the ratio of concentrations at the cathode is

$$\frac{c}{1-c} = \frac{c_0}{1-c_0}\exp\left[\frac{\Delta\mu}{\mu}\frac{\epsilon_0}{kT}El\right]. \tag{15}$$

In Ref. 10, thermodynamic arguments about the separation of isotopes in a dc electric field led to a similar equation, with $\Delta\mu/\mu$ being replaced by the relative difference in molar volumes of the isotopes, $\Delta V/V$, which leads to a difference in their specific charges. The difference in the mobility of the ions can be explained, as suggested by Bresler and Pikus, by a difference in their effective radii due to the different amplitudes of thermal motion in the two isotopes, and reduces essentially to a difference in molar volumes.

It is important to notice that, as follows both from Fig. 2 and Refs. 7 and 5, the isotope separation effect increases with increasing temperature. Hence we must presume that $\Delta V/V$ increases with temperature faster than the first power of T. However, it does not seem possible to explain such a temperature behavior. One must conclude, presumably, that the difference in molar volumes is not the only effect which plays an important role in the conentration changes induced by the flow of direct current.

The data available in the literature allow one to calculate $\Delta\mu/\mu$ for mercury, gallium, potassium, and

indium. The results of the calculation are presented in the table, together with the results obtained in the present experiments. In the table, β is defined to be $\Delta\mu/\mu \times m/\Delta m$. It is the relative difference in mobilities per unit relative difference in the isotope masses. The temperature shown is that of the bath, except for the experiments on potassium and those on mercury reported here. For these, the temperature of the column of isotopes itself is shown. The calculation of $\Delta\mu/\mu$ for mercury and gallium, using the data of Refs. 2 and 4, was carried out by Bresler and Pikus,[9] without taking into account the smoothing of the concentrations produced by diffusion. The same method was used to obtain $\Delta\mu/\mu$ for mercury from the results of Ref. 3; the boundary conditions in the other experiments were such that relation (12) could be used. From the table it is evident that the various values of $\Delta\mu/\mu$ for mercury are all of the same order of magnitude. The lack of complete agreement is presumably due to approximations in the calculations on the results of Haeffner,[2] and of Haeffner, Sjöborg and Lindhe.[3] In these calculations, it is difficult to take proper account of the volume of mercury at the end of the capillary opposite from the reservoir.

Material	$\Delta\mu/\mu$	β	T, °C	Literature
Hg	$1.1 \cdot 10^{-3}$	$0.73 \cdot 10^{-1}$	45	Present work
Hg	$1.3 \cdot 10^{-3}$	$0.86 \cdot 10^{-1}$	115	Present work
Hg	$0.7 \cdot 10^{-3}$	$0.5 \cdot 10^{-1}$	15	[2]
Hg	$2.0 \cdot 10^{-3}$	$1.3 \cdot 10^{-1}$	47	[3]
Ga	$3.6 \cdot 10^{-3}$	$1.3 \cdot 10^{-1}$	48	[4]
Ga	$1.4 \cdot 10^{-3}$	$0.5 \cdot 10^{-1}$	52	[5]
Ga	$3.6 \cdot 10^{-3}$	$1.3 \cdot 10^{-1}$	287	[5]
K	$0.5 \cdot 10^{-3}$	$0.1 \cdot 10^{-1}$	158	[6]
In	$0.14 \cdot 10^{-3}$	$0.8 \cdot 10^{-2}$	210	[7]
In	$0.9 \cdot 10^{-3}$	$5 \cdot 10^{-2}$	530	[7]

In conclusion we note (15) implies that when saturation has been reached, it is not necessary to know the coefficient of self diffusion in order to calculate $\Delta\mu/\mu$ (and hence L). If the size of the effect at saturation is known, the diffusion coefficient can then be obtained by comparing the experimental time dependence of Δc with (12).

The authors would like to express their deep gratitude to B. G. Lazarev for discussions.

[1] K. P. Romadin, Trudy, Zhukovskiy Academy, 167 (1947); K. E. Schwarz, Elektrolytische Wanderung in flüssigen und festen Körper, Leipzig, 1940.

[2] E. Haeffner, Nature 172, 775 (1953).

[3] Haeffner, Sjöborg, and Lindhe, Z. Naturforsch., 11a, 71 (1956).

[4] G. Nief and E. Roth, Compt. rend. 239, 162 (1954).

[5] Golman, Nief, and Roth, Compt. rend. 243, 1414 (1956).

[6] Lunden, Reuterswärd, and Lodding, Z. Naturforsch., 11a, 139 (1956).

[7] Lodding, Lunden, and Ubisch, Z. Naturforsch. 11a, 139 (1956).

[8] Grigor'ev, Kan, Rudenko, and Safronov, J. Exptl. Theoret. Phys. (U.S.S.R.) 33, 576 (1957); Soviet Phys. JETP, this issue p. 000.

[9] S. E. Bresler and G. E. Pikus, J. Tech. Phys. (U.S.S.R.) 26, 109 (1956); Soviet Phys. JETP 1, 102 (1956).

[10] Rudenko, Grigor'ev, Dolgopolov and Bogoiavlenskii, Sbornik (Collection) Session of the Academy of Sciences of the Ukrainian S.S.R. Devoted to the Peaceful Uses of Atomic Energy, Kiev, 1956.

Translated by R. Krotkov
118

AN INVESTIGATION OF CONVERSION LINES IN THE β SPECTRUM OF Ir^{192}

V. M. KEL'MAN, R. IA. METSKHVARISHVILI, V. A. ROMANOV, and V. V. TUCHKEVICH

Leningrad Physico-Technical Institute, Academy of Sciences, U.S.S.R.

Submitted to JETP editor March 18, 1957

J. Exptl. Theoret. Phys. (U.S.S.R.) 33 588-594 (September, 1957)

A prism β-spectrometer with a resolution of 0.04% was used to study the conversion electron spectrum of excited Pt^{192} and Os^{192} nuclei produced in the decay of Ir^{192}. The conversion coefficient ratios K/L and $L_I:L_{II}:L_{III}$ have been determined for the transition energies of 136.3, 201.3, 205.8, 295.9, 308.5, 316.5, 468.0 and 604.5 kev. For the most intense transitions the ratios K/M, $M_I:M_{II}:M_{III}$, K/N and K/O have also been determined. All the investigated transitions were found to be E2 or E2 + M1. The amount of M1 admixture has been determined.

THE radioactive isotope Ir^{192} has been investigated by many authors.[1-3] It was established that it decays by the following double process: it goes over to Pt^{192} by emitting β electrons and then to Os^{192} by K-capture. The γ-radiation of the excited Pt^{192} and Os^{192} comes from E2 and E2 + M1 transitions.[3] Thus these isotopes are well suited for the study of internal conversion involved in the above transitions. It is of interest to investigate their conversion electron spectrum by using a high-resolution β spectrometer able to resolve the conversion electrons from the L subshells and, if possible, from the M subshells. In order to complete the picture it is desirable also to find the total conversion coefficient ratios for the K, L, M, N, and O shells.

The above investigations have been performed on a prism β spectrometer.[4,5] The resolving power of the instrument corresponds to a line half-width of 0.04% (with respect to momenta), and its transmission is 0.02%. The source was a thin film of natural iridium deposited by cathode evaporation on a strip of aluminum film subjected to a neutron bombardment. The thickness of the aluminum foil was 5 μ. The following method was used to determine the thickness of iridium film deposited. The strip of aluminum foil 1 (Fig. 1) onto which the iridium is to be evaporated is placed on a glass plate 2 and covered by a thin metal plate 3 with a slot 4 cut out of it. In addition, this metal plate has several circular holes 5 which expose the glass close to the slot. The slot determines the area of the source, and the evaporated iridium is deposited simultaneously on the aluminum foil and the glass. The iridium deposited on the aluminum is assumed to be of the same thickness as that deposited on the glass, which is measured by an interferometer.[6] Even if these thicknesses are not the same, this method makes it possible to determine the relative thicknesses fo iridium films, thus simplifying the choice of a suitable source. Several samples were prepared in this way, and from them we choose one whose iridium film thickness was 0.48 mg/cm^2, making it possible to obtain sufficiently intense conversion lines with a half-width almost the same as that of the apparatus. The area of the iridium film was 1.6 by 11 mm^2.

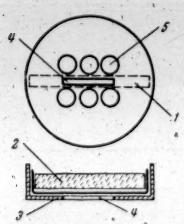

FIG. 1.

Within the limits of any given line group, a spectrum was obtained by applying a potential to the source. Since this method of measurement causes electrons of a given constant energy to pass through the spectrometer, it is unnecessary to correct for the width of an energy interval for any given group. Such a correction must be used on going from one group to another, when the magnetic system of the spectrometer is readjusted. The correction was applied according to the formula

$$n_{\text{true}} = k \frac{n_{\text{meas}}}{\epsilon (1 + 1/[1 + \epsilon/m_0c^2])},$$

where n_{true} is the number of electrons giving the true line intensity, n_{meas} is the number of counts of the recording system, k is a coefficient depending on the transmission of the instrument, and ϵ is the electron energy. Since ϵ is usually given in kev, the rest mass must be given in the same units, or $m_0c^2 = 511$ kev.

The window through which the β particles enter the counting chamber was covered by a 0.87 mg/cm^2 thick mica leaf. The electrons then passed through two aluminum foils covering neighboring counter windows, their total thickness being 1.1 mg/cm^2. Corrections for absorption in the mica were applied according to the data of Martin and Towsend.[7] The correction for adsorption in the aluminum foils was determined experimentally by comparing the number of counts of the first and second counters. Starting with energies of 300 kev these corrections produced no significant changes even in measuring the K/L ratio.

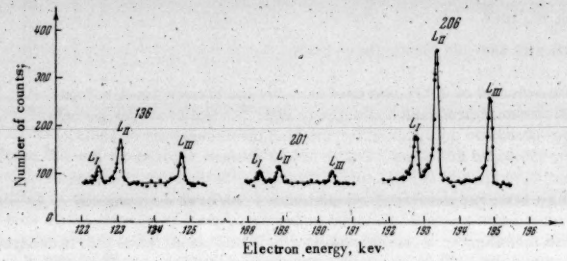

FIG. 2. Conversion lines of 136.3, 201.3, and 205.8 kev gammas on L subshells.

Conversion lines were observed for the 136.3, 295.9, 308.5, 316.5, 468.0, and 604.5 kev transitions in Pt and for the 201.3 and 205.8 kev transitions in Os. The transition energies which we give here are those of Baggerly and co-workers.[3] The measured separations between the lines of the L sublevels allowed us to verify the fact that they belong to the above transitions. Figures 2 – 5 show different sections of the β spectra (the background is subtracted). It is seen that the resolution of the instrument is sufficient to separate the conversion lines from the L subshells even for the 604.5-kev gamma quanta. For the most intense transitions, the data makes it possible to obtain the conversion coefficient ratios for the M subshells. Since the conversion lines from the M subshells were not entirely resolved, it was necessary to resolve them graphically. The conversion lines of the intense gammas on the N and O shells are clearly seen. In order to separate the overlapping lines due to conversion of 308.5 kev gammas on the L_{II} subshell and the 296 kev gammas on the N shell it was assumed that the N/L_{II} ratio for the 296 kev transitions was equal to the N/L_{II} ratio the 3.16.5 kev transitions, which was known from the experiment. Then knowing the area of the L_{II} peak for the 296 kev transition one can find the area of the N conversion

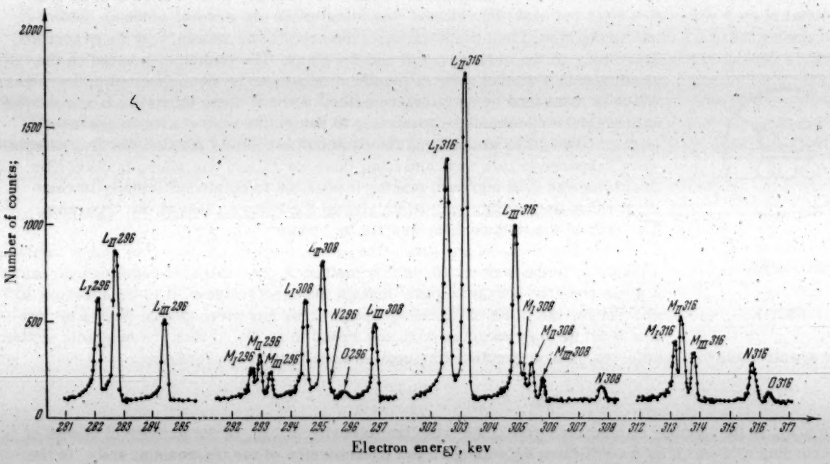

FIG. 3. Conversion lines of the 295.9, 308.5, and 316.5 kev gammas.

lines for this transition and thus separate from it the L_{II} line from the 308.5 kev transition. The separation of the electrons due to conversion of the 308.5 kev gammas on the M_I subshell from those due to conversion of the 316.5 kev gammas on the L_{III} subshell was performed graphically. In order to determine the conversion coefficient ratios, each line was measured five times, the mean value of the area ratios was obtained, and its probable error was found. The results for the K/L and L_I:L_{II}:L_{III} ratios are shown, after the necessary corrections, in Table I.

TABLE I

Transition energy, kev	Experimental conversion coefficient ratio; K/L	Experimental conversion coefficient ratio; $L_I : L_{II} : L_{III}$	Theoretical conversion coefficient ratio for E2 transitions; K/L	Theoretical conversion coefficient ratio for E2 transitions; $L_I : L_{II} : L_{III}$	Type of transition	Per cent of M1 admixture Determined from; L_{II}/L_I	Per cent of M1 admixture Determined from; L_{III}/L_I	Type of transition according to Ref. 3.
136.3	—	1:(2.1±0.1):(1.7±0.1)	0.62	1:6.7:5.0	E2+M1	21%	19%	E2
201.3	1.85±0.04	1:(1.42±0.06):(0.89±0.07)	1.5	1:2.9:1.7	E2+M1	16%	13%	E2+M1
205.8	1.83±0.04	1:(2.32±0.02):(1.41±0.02)	1.5	1:2.8:1.7	E2	—	—	E2
295.9	2.35±0.04	1:(1.39±0.03):(0.74±0.02)	2.0	1:1.7:0.8	E2	—	—	E2
308.5	2.38±0.02	1:(1.18±0.02):(0.67±0.01)	2.2	1:1.5:0.7	E2+M1	5%	1%	E2
316.5	2.22±0.02	1:(1.38±0.01):(0.73±0.01)	2.3	1:1.5:0.7	E2	—	—	E2
468.0	3.0 ±0.1	1:(0.68±0.01):(0.29±0.01)	3.1	1:0.77:0.30	E2	—	—	E2
604.5	4.7 ±0.1	1:(0.33±0.01):(0.13±0.01)	4.0	1:0.50:0.19	E2+M1	14%	10%	E2+(M1)

The multipole orders of the transitions were determined by comparing the measured conversion coefficient ratios on the L subshells and the K and L shells with the corresponding theoretical ratios for various multipole orders. The theoretical ratios of the conversion coefficients on the L subshells and the value of the total conversion coefficient on the L shell were obtain from the Rose tables[8] and the theoretical conversion coefficients for the K shell were obtained from the very detailed and accurate tables of Sliv and Band.[9] In agreement with Ref. 3 it was established that all the transitions investigated were either E2 or E2 + M1. The theoretical K/L and L_I:L_{II}:L_{III} ratios for E2 transitions are shown in Table I. The theoretical L_I:L_{II}:L_{III} ratio for magnetic dipole transitions hardly depend on energy, and for the transitions of interest remains practically constant at 1 : 0,088 : 0.006.

The per cent admixture p of magnetic dipole in the mixed transitions is

$$p = [\gamma_1/(\gamma_1+\gamma_2)]\cdot 100 = [\delta_{12}^2/(1+\delta_{12}^2)]\cdot 100,$$

where γ_1 and γ_2 are the intensities of magnetic dipole and electric quadrupole transitions, and $\delta_{12}^2 = \gamma_1/\gamma_2$ is the mixture ratio. The mixture ratio can be found if one knows the conversion coefficient ratio for any two shells or subshells for the mixed transition under consideration, as well as the conversion coefficient on these shells in the transition is purely of one kind:[10]

$$\delta_{12}^2 = \alpha_{2k}(R_0 - R_2)/\alpha_{1k}(R_1 - R_0),$$

where $R_i \equiv \alpha_{ij}/\alpha_{ik}$. Here α_{ij} and α_{ik} are the absolute conversion coefficients for γ-rays of the i-th kind on the shells or subshells j and k. They were found from the theoretical values given in the above-mentioned tables. The experimental conversion coefficient ratio is $R_0 \equiv \alpha_{0j}/\alpha_{0k}$. The values of L_{II}/L_I and L_{III}/L_I were used to find the mixture ratios. The ratio K/L is less sensitive to presence of some M1 admixture, and was therefore not used for this purpose. The percentage of M1 thus obtained is shown in the two next-to-last columns of Table 1, were it is indicated whether L_{II}/L_I or L_{III}/L_I was used to obtain the data. It should be noted that due to the small number of available theoretical conversion coefficients for the L subshells (L_{II} has been calculated for Z = 25, 55, and 85, and L_{III} for Z = 55 and 85), it is impossible to perform the necessary interpolation with sufficient accuracy. The per cent admixtures given in Table 1 may contain errors of several per cent. In particular, a per cent admixture of the order of 5 does not necessary indicate the actual presence of admixture, but may be due to error in interpolation. Therefore Table I shows admixtures whose percentage is greater than 5, and it is assumed otherwise that the transition is purely of one kind. The only exception is the 308.5 kev

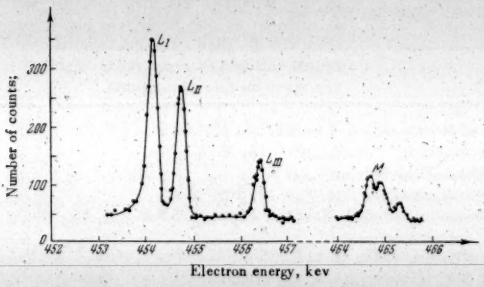

FIG. 4. Conversion lines of 468.0 kev gammas.

transition, for which the presence of M1 admixture can be deduced by comparing the experimental conversion coefficient ratio on the L subshells with this ratio for the neighboring 296 and 316.5 kev transitions. Lower amounts of admixture can be established only with the aid of more complete theoretical tables. The presence of some M1 in the 604.5 kev transition indicates that the spin and parity 3^+ should be assigned to the 920.9 kev level suggested[3] in the level scheme of Pt^{192}. The last column of the table gives the multipole orders as obtained in Ref. 3.

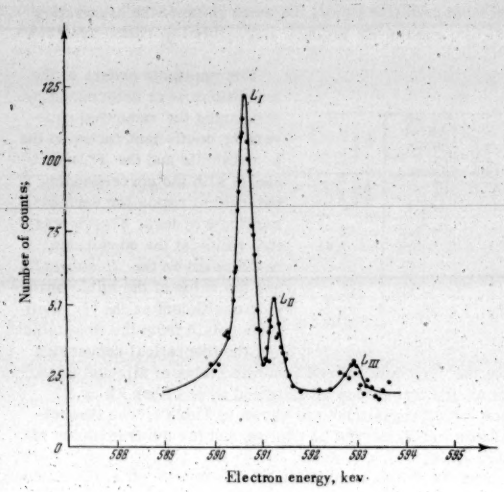

FIG. 5. Conversion lines of 604.5 kev gammas.

In Table II we present the K/M, $M_I : M_{II} : M_{III}$, K/N and K/O ratios for the most intense transitions. In no case were we able to observe conversion on the M_{IV} and M_V sublevels. We note that the $M_I : M_{II} : M_{III}$ ratios are quite close to the corresponding $L_I : L_{II} : L_{III}$ ratios. This latter situation has been noted also for M1 transitions.[11]

Measurement of the energy separation between the conversion lines denoted N and O in Fig. 3 and the corresponding M_{III} lines and their comparison with x-ray data shows that the N lines correspond to conversion on the N_I, N_{II}, and N_{III} subshells. Conversion electrons from the N_{IV} and N_V subshells, which lie between the N and O peaks, were not observed in the present work. Conversion electrons from the N_{VI} and N_{VII} subshells overlap with the electrons from the O shell, and thus form common lines indicated by the letters O in the figure.

Assuming that conversion on the N takes place primarily on the first three subshells, as is the case for conversion on the M shell, one may consider the O lines to be due mostly to electrons from the O shell. The conversion coefficient ratios K/N and K/O of Table 2 are given on this assumption.

TABLE II. Experimental conversion coefficient ratio.

Transition energy, kev	K/M	$M_I : M_{II} : M_{III}$	K/N	K/O
295.9	8.9±0.2	1 : (1.59±0.05) : (0.87±0.03)	—	(28±3)·10
308.5	9.5±0.2	1 : (1.69±0.05) : (0.87±0.04)	44±2	—
316.5	9.3±0.2	1 : (1.90±0.07) : (1.06±0.03)	38±1	255±7
468.0	10.2±0.2	—	—	—

[1] Cork, LeBlanc, Stoddard, Child, Branjan, and Martin, Phys. Rev. 82, 258 (1951).
[2] Bashilov, Anton'eva, and Dzhelepov, Izv. Akad. Nauk SSSR, Ser. Fiz. 16, 264 (1952).
[3] Baggerly, Marmier, Boehm, and DuMond, Phys. Rev. 100, 1364 (1955).
[4] Kel'man, Kaminskii, and Romanov, Izv. Akad. Nauk SSSR, Ser. Fiz. 18, 209 (1954).
[5] Kel'man Romanov, Metskhvarishvili, and Koliunov, J. Exptl. Theoret. Phys. (U.S.S.R.) 32, 39 (1957); Soviet Phys. JETP 5, 24 (1957).
[6] S. Tolansky, Multiple-Beam Interferometry (Oxford, 1948), p. 147.
[7] L. H. Martin and A. A. Towsend, Proc. Roy Soc. (London) A170, 190 (1939).
[8] K. Siegbahn, Beta- and Gamma-Ray Spectroscopy (Amsterdam, 1955), p. 905.
[9] L. A. Sliv and I. M. Band, Таблицы коэффициентов внутренней конверсии (Tables of Internal Conversion Coefficients) (M.-L., 1956).
[10] E. L. Church and J. E. Monahan, Phys. Rev. 98, 718 (1955).

[11] Ke'lman, Romanov, and Metskhvarishvili, Dokl. Akad. Nauk SSSR 103, 577 (1955).

Translated by E. J. Saletan
119

SOVIET PHYSICS JETP VOLUME 6 (33), NUMBER 3 MARCH, 1958

THE STRIPPING PROCESS IN THE INTERACTIONS OF ACCELERATED N^{14} IONS WITH THE NUCLEI OF SOME ELEMENTS

V. V. VOLKOV, A. S. PASIUK, and G. N. FLEROV

Academy of Sciences, U.S.S.R.

Submitted to JETP editor March 19, 1957

J. Exptl. Theoret. Phys. (U.S.S.R.) 33, 595-601 (September, 1957)

The formation of the radioactive isotope N^{13} was observed when Al, Ni, Cu, Ag, Cd and Sn foils were bombarded with N^{14} ions which had been accelerated to ~ 100 Mev in a cyclotron. Angular distribution measurements showed that the N^{13} was emitted in a relatively narrow angular range. The angle corresponding to maximum intensity increases with Z. When the energy of the bombarding particle exceeds the height of the Coulomb barrier the cross section for N^{13} production is only slightly dependent on the energy. The cross section is ~ 30 mb for Ni and ~ 12 mb for Al.

WHEN atomic nuclei are bombarded with multiply-charged ions stripping reactions can occur as well as the formation of compound nuclei. Such reactions for light nuclei at not very high energies have been studied in Refs. 1 — 7. At our Institute P. M. Morozov, B. N. Makov and M. S. Ioffe have devised a special ion source which furnishes monoenergetic beams of multiply-charged ions at considerably higher energies than those used in the investigations mentioned above. This had made it possible to study stripping reactions in heavier nuclei at higher energies.

The present work is a study of reactions involving several different elements to which N^{14} loses a neutron and is transformed into radioactive N^{13}.

EXPERIMENTAL METHOD

An internal cyclotron beam was used in all experiments. The bombarding particles were quintuply-charged N^{14} ions. Their range in nickel at the radius 66 cm was 48 μ, which corresponds to 115 Mev.[5] The energy spread of the particles did not exceed 5 to 7%.

The average beam intensity at the target was a few tenths of a microampere and was measured by a current integrator. The energy of the ions was varied by moving the target along the radius. The

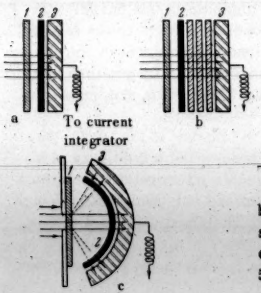

FIG. 1. Diagrams of the experiments: a — N^{13} production through bombardment of foils of different elements with nitrogen ions and the cross section measurement, b — Measurement of the angular distribution, c — Distribution of radioactivity in a stack of lead foils (there 7μ lead foils, 50μ collector). 1 — target; 2 — shield of Au or Pt foil; 3 — lead collector.

long range of the N^{13} particles was used to separate them. The experimental arrangement is shown in Fig. 1a. The accelerated N^{14} ions lost neutrons to the element of the thin target and as N^{13} were stopped in the collector made of 50μ lead foil. The 3.5μ gold foil between the collector and the target retarded particles which had been produced through a compound nucleus. A special experiment showed that reactions with the formation of beta-active nuclei in gold and lead began to occur only at ~ 70 — 80 Mev. The activity produced in the lead collectors was registered by an end-window Geiger counter. A magnetic analyzer was used to determine the sign of the beta particles.

For measurement of the N^{13} angular distribution the lead collector was put into the form of a cylindrical surface which included all angles from +60° to —60° (Fig. 1b). After irradiation the collector was cut into equal strips for measurement of the beta-activity decay curve.

Cross section measurements up to ~ 70 Mev were obtained with a thin target. Above 70 Mev the target thickness was increased with the energy in such a way that the bombarding particles struck the shielding foil with the previous energy. The yield-energy relation was calculated as follows. Let Q_1 be the yield of radioactive N^{13} from a thin target at 70 Mev. We increase the energy to 80 Mev and at the same time increase the target thickness to the point where the energy loss in the additional layer will be 10 Mev; there is thus no change in the conditions under which the original target is bombarded. If Q_2 is the N^{13} yield from the thicker target the difference $Q_2 - Q_1$ is the reaction yield in the 70 — 80 Mev interval. On a smooth cross section-energy curve this yield can be associated with an average energy of 75 Mev. With further increases of the bombarding energy and of the target thickness we similarly obtain the yield at 85 Mev, 95 Mev etc.

EXPERIMENTAL RESULTS

1. Production of N^{13} by Passage of a Beam of Accelerated N^{14} Ions through Foils of Various Elements

Previously published works report stripping studies for light elements only. It was therefore our first task to determine the possibility of this reaction in other elements. Targets made of Al, Ni, Cu, Ag, Cd, Sn, Pt, Au, and Pb were arranged as shown in Fig. 1a and were bombarded for a few minutes with a 100-Mev N^{14} beam. The target thickness was such that the particle energy after traversing the target did not exceed 70 Mev.

For the first six elements (from Al to Sn) 95 — 98% of all of the activity received by the collectors had a half-life of 10 minutes. By investigating the sign of the beta particles and of their maximum energy (through absorption in aluminum) it was shown that these are positrons with $E_{max} = 1.20 \pm 0.10$ Mev. Thus from our findings concerning the half-life, charge sign, and maximum energy of the beta particles we were able to conclude that when accelerated nitrogen ions interact with nuclei of the six elements mentioned the N^{14} loses a neutron in a highly efficient nuclear reaction and is transformed into N^{13}.

In the case of the heavy elements Pt, Au, and Pb there was no reliable indication of activity with a ten-minute half-life. Most of the activity, judging from the half-lives of 15 min, 70 min, and a few hours clearly belonged to fragments from gold fission.* The causes of the failure to observe the formation of N^{13} in the heavy elements became clear only after a study of the angular distribution and cross section.

A good illustration of the fact that N^{13} is produced by stripping when aluminum is bombarded with nitrogen ions is provided by the distribution of the ten-minute activity according to depth in the lead collector. The arrangement of this experiment is shown in Fig. 1c. The radioactive products of the nuclear reactions emerged from a 7μ aluminum foil which had been bombarded with 74-Mev nitrogen ions and were collected in a stack of lead foils for analysis of the beta decay period. The results are shown in Fig. 2.

The figure shows that all of the ten-minute activity is concentrated in the interior of the lead. This distribution could not be explained easily if it were assumed that the N^{13} results from the decay of a compound nucleus. But the stripping reaction provides a completely reasonable interpretation. When a bombarding N^{14} particle loses a neutron during a peripheral collision it suffers relatively little change of energy, so that the range of the N^{13} is comparable with that of the N^{14}. The short-lived activity

*Similar data will be found in a paper by N. I. Tarantin, Iu. B. Gerlit, L. I. Guseva, B. R. Miasoedov, K. V. Filippov and G. N. Flerov which is being prepared for publication.

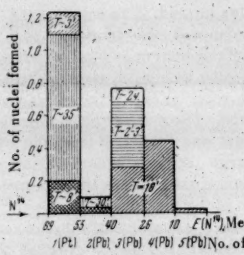

FIG. 2. Distribution of beta-active nuclei in a stack of lead foils. The numerals along the horizontal axis indicate the energy of the bombarding ions upon entering and leaving each foil; T is the half-life.

(2 — 3 min half-life) which is also appreciable in the interior of the lead is most likely due to the capture of protons from aluminum by the N^{14} nuclei. This must result in the formation of an O^{15} nucleus which decays with a 2-minute period. The activity in the platinum foil belongs to radioactive decay products of a compound nucleus.

2. Angular Distribution of N^{13}

The angular distribution of N^{13} was measured for aluminum, nickel, silver, tin and also for the heavy element platinum. Although in the first experiment we did not obtain a reliable separation of N^{13} from the bombardment of heavy elements, the geometry of the experiment for the angular distribution measurement (Fig. 1,b) led us to expect that at large angles it would be possible to separate N^{13} from the fragments. All of the lead strips of the collector except those which were struck directly by the beam showed only a 10-minute activity. The strips which were in the direct path of the beam (two or three out of twelve strips) yielded some additional activity which was due mainly to fission fragments from the shielding foils. The platinum shielding foil was increased to 8μ to stop fission fragments coming from the target.

The angular distribution in the center-of-mass system is shown in Fig. 3. The curves show the statistical errors and the angular spread due to the finite size of the strips. When aluminum was bombarded almost all of the ten-minute activity was concentrated in the two to four central strips. In this instance the angular resolution was inadequate for the plotting of curves such as those of the other elements. Therefore for aluminum Fig. 4 gives only a histogram of the ten-minute activity distribution in the strips compared with a histogram for nickel. From the histogram and the experimental geometry it is possible to determine the most probable N^{13} emission angle for aluminum; at 65 Mev the value is 23° ± 8° in the center-of-mass system.

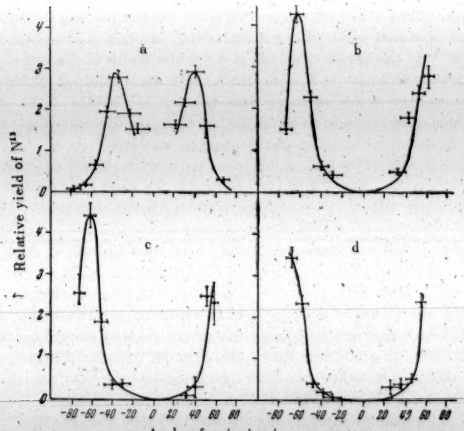

FIG. 3. Angular distribution of N^{13}: a — Ni, E(N^{14}) = 61 ± 6 Mev; b — Ag, E(N^{14}) = 72 ± 8 Mev; c — Sn, E(N^{14}) = 68 ± 7 Mev; d — Pt, E(N^{14}) = 91 ± 7 Mev.

3. Measurement of the Stripping Cross Section for Al and Ni

The stripping cross section was measured in the 28 — 105 Mev range for aluminum and in the 31 — 107 Mev range for nickel. The number of N^{13} nuclei produced by the reaction was determined by separation of the ten-minute activity in the lead collectors. The efficiency of the beta particle detection was determined by means of a radioactive source of known intensity. Since the N^{13} nuclei were stopped at some depth in the collector it was necessary to take into account the scattering

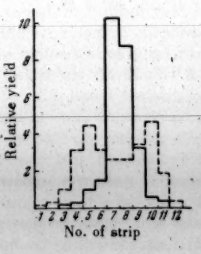

FIG. 4. Distribution of N^{13} in lead collector from nitrogen-bombarded Al and Ni. Solid line — Al, E(N^{14}) = 62 ± 6 Mev; dashed line — Ni, E(N^{14}) = 61 ± 6 Mev.

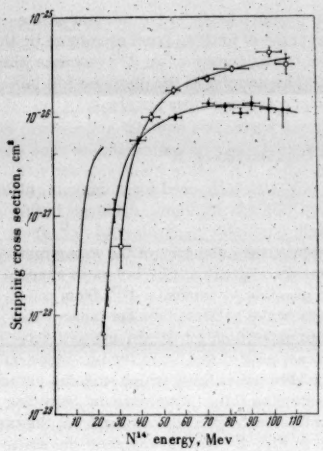

FIG. 5. Cross sections for N^{13} formation in Al and Ni. ● — our data for Al; □ — our data for Ni; Δ — data from Ref. 5 for Al; solid curve — data from Ref. 3 for N.

and absorption of the beta particles in lead. The appropriate corrections of 10 — 20% were determined experimentally. A source containing Na^{24}, whose beta spectrum is similar to that of N^{13}, was placed at different depths within the stack of lead foils of 50μ total thickness, and a relation was obtained between the count and position of the source. The number of bombarding particles passing through the target was computed from the collector current. We know that charge exchange causes variation of the average charge of an ion during its passage through matter. In our experiments, because of the high energies, the N^{14} ions lost all of their electrons while passing through the target, so that their average charge was seven. A small correction of 3 — 10% had to be introduced for only the very lowest energies.[8,9]

The results are shown in Fig. 5, where the data of Refs. 3 and 4 are given for comparison. The curves show the error of the relative measurements as well as the energy spread due to the finite target thickness. The error in determining the absolute value of the cross section was 30% and was caused principally by lack of accurate knowledge concerning the efficiency of detection of the beta particles.

EVALUATION OF RESULTS

As can be seen from Fig. 2, the character of the angular distribution of N^{13} is very different from the usual picture for the decay products of a compound nucleus. The distinguishing feature of this distribution is the fact that the particles are emitted in a relatively narrow angular range. The angle of maximum intensity increases with Z. This features of the angular distribution clearly show that N^{13} is actually formed as a result of stripping. For large impact parameters the probability of neutron loss by N^{14} is small; in nearly central collisions the two particles are fused to form a compound nucleus. Thus there exists an optimum impact parameter for which neutron loss is most probable. From the position and width of the maximum it is possible to obtain an approximate value for the closest approach of N^{14} to the target-nucleus and for the width of the geometric region around the nucleus within which stripping is most probable. Such estimates, without taking account of nuclear interactions, show that when the energy of the nitrogen ions exceeds the height of the Coulomb barrier the region in which stripping occurs corresponds to the distance between the colliding particles which is approximately equal to the sum of the radii of N^{14} and the target-nucleus.

The character of the relation between the angular distribution and Z enables us to understand why we could not distinguish a ten-minute activity from nitrogen-bombarded heavy elements. In such cases the angle of emission of the N^{13} particles is so much larger that they do not reach the collector but are stopped in the shielding foil or in the target itself.

We turn now to the energy dependence of the cross section. When a radioactive isotope is formed due to the decay of a compound nucleus the energy dependence of the cross section for its formation is a bell-shaped curve of ~ 10 Mev width.[10-13] In our case, as is seen in Fig. 5, this dependence is characterized by slight energy dependence of the cross section for N^{13} formation for energies considerably above the Coulomb barrier. At first glance it might seem that with increasing energy the cross section should decrease because the N^{14} is in the vicinity of the nucleus for a shorter time. But it must be remembered that the probability of neutron loss by N^{14} can be affected by other factors in addition to the transit time. For example, it may be expected that with variation of the acceleraged ion energy there will also be a variation of the neutron sticking probability as well as of the geometric region within which the reaction takes place.

The results contained in Refs. 2 — 5 show that a fast N^{14} ion which passes close to a nucleus may not only lose a neutron but is also able to capture a proton, neutron or even alpha particle. It was not our special purpose here to study other stripping reactions, but our results enable us to estimate the cross sections of other reactions. It will be useful to present such estimates here. In the experiment with a

lead foil stack (Fig. 3) it was found that nuclei with a half-life of 2 — 3 minutes have a long range, as well as the N^{13}. The two-minute activity was also distinguished during measurements of the cross section for N^{13} formation in Al and Ni, and the ratio of the two-minute activity yield to the N^{13} activity yield did not vary with energy. This indicates that the cross sections for the formation of both products have the same energy dependence. We believe that this two-minute activity can be assigned to O^{15}, which is formed when N^{14} captures a proton from the target nucleus, according to the scheme

$$A_Z(N^{14}, O^{15})\,A - 1_{Z-1}.$$

The cross section of this reaction is estimated to be for Al 40 ± 10% and for Ni 17 ± 5% of the cross section for loss of a neutron.

In conclusion we consider it our pleasant duty to thank Academician I. V. Kurchatov for several useful comments during discussions of this work. We also thank the cyclotron crew, directed by Iu. M. Pustovoit, for their excellent work and V. M. Strutinskii for theoretical calculations of several observed effects.

[1] K. F. Chackett and J. H. Fremlin, Phil. Mag. **45**, 735 (1954).
[2] Chackett, Chackett and Fremlin, Phil. Mag. **46**, 1 (1955).
[3] H. L. Reynolds and A. Zucker, Phys. Rev. **101**, 166 (1956).
[4] Reynolds, Scott and Zucker, Phys. Rev. **102**, 237 (1956).
[5] Webb, Reynolds and Zucker, Phys. Rev. **102**, 749 (1956).
[6] G. Breit and M. E. Ebel, Phys. Rev. **103**, 679 (1956).
[7] M. E. Ebel, Phys. Rev. **103**, 958 (1956).
[8] Reynolds, Scott and Zucker, Phys. Rev. **95**, 671 (1954).
[9] A. Papinean, Compt. rend. **242**, 2933 (1956).
[10] J. M. Blatt and V. F. Weisskopf, Theoretical Nuclear Physics (John Wiley and Sons, New York, 1952) Ch. IX.
[11] Baraboshkin, Karamian and Flerov, J. Exptl. Theoret. Phys. (U.S.S.R.) **32**, 1294 (1957), Soviet Phys. JETP **5**, 1055 (1957).
[12] R. E. Bell and H. M. Skarsgard, Can. J. Phys. **34**, 745 (1956).
[13] J. D. Jackson, Can. J. Phys. **34**, 767 (1956).

Translated by I. Emin
120

SOVIET PHYSICS JETP VOLUME 6 (33), NUMBER 3 MARCH, 1958

PRODUCTION OF NEGATIVE π MESONS BY 660-Mev PROTONS ON NUCLEI OF VARIOUS ELEMENTS

A. G. MESHKOVSKII, IA. IA. SHALAMOV, and V. A. SHEBANOV

Submitted to JETP editor March 25, 1957

J. Exptl. Theoret. Phys. (U.S.S.R.) **33**, 602-605 (1957)

The energy spectra and cross sections $d\sigma^-/d\Omega$ for π^--meson production have been measured at an angle of 45° with respect to the proton beam for Li, Be, Al and Cu. The differential cross sections $d^2\sigma^-/d\Omega dE$ for 157 Mev π^--mesons were measured for Ag and Pb. A conclusion is reached concerning the dependence of the cross section for π^--meson production on atomic weight for elements lying between Li and Pb. A comparison is made with similar results obtained for π^0 and π^+ mesons in other works.

THE dependence of π-meson yield on the number of nucleons in the nucleus has been investigated at various angles for neutral π mesons[1,2] and at an angle of 45° for positive π mesons,[3] the π mesons being produced by 660-Mev protons on nuclei of various elements. In the present work, carried out at the

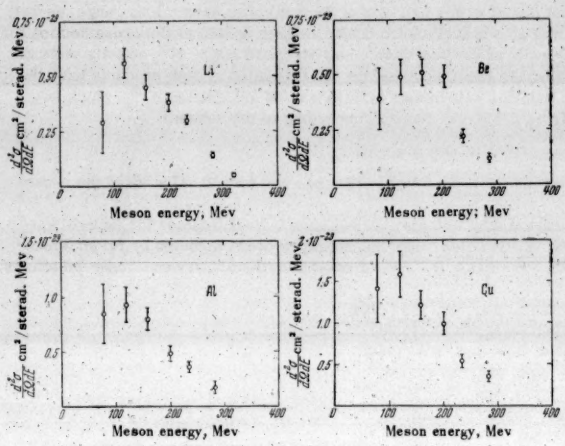

FIG. 1. Spectra of π^--meson production

synchrocyclotron of the Joint Institute for Nuclear Research, using methods described earlier,[3-5] we studied π-meson production at an angle of 45° with respect to the beam of 660 Mev protons on various elements.

The energy spectra of π^- mesons produced by targets of Li, Be, Al and Cu are shown in Fig. 1. Integration of the spectra, i.e., the differential cross sections $d\sigma^-/d\Omega$ in $cm^2\,sterad^{-1}$ for π^--meson production, calculated per nucleus, yielded the results given below. The quantity $d\sigma^-/d\Omega$ for carbon was measured earlier.[5] π^--meson yields from Ag and Pb were measured at only one meson energy, 157 ± 5 Mev. The quantity $d^2\sigma^-/d\Omega dE$ was (1.38 ± 0.22) $\times 10^{-29}\,cm^2\,sterad^{-1}\,mev^{-1}$ for Ag, and (2.01 ± 0.40) $\times 10^{-29}\,cm^2\,sterad^{-1}\,mev^{-1}$ for Pb.

Element	Li	Be	C	Al	Cu
$d\sigma^-/d\Omega \cdot 10^{27}$	0.93±0.14	1.00±0.15	1.00±0.13	1.64±0.26	2.82±0.43

As was shown earlier,[3] the spectra of π^+ mesons produced at an angle of 45° by 660-Mev protons on elements from Li to Cu are similar to one another. An approximate similarity of the spectra for π^- mesons was also observed in the present work, as may be seen if all the spectra shown in Fig. 1, as well as the spectrum for carbon,[5] are reduced to one scale. Using the apparent similarity of the π^- meson spectra, and the measured values of the quantity $d^2\sigma^-/d\Omega dE$ for Ag and Pg, we can calculate tentative values of the cross sections $d\sigma^-/d\Omega$ for these elements, if we assume that the form of the spectra does not change very much as we go to the heavier elements. In this connection, the cross section $d\sigma^-/d\Omega$ is (2.87 ± 0.88) $\times 10^{-27}\,cm^2\,sterad^{-1}$ for Ag, and (4.18 ± 1.16) $\times 10^{-27}\,cm^2\,sterad^{-1}$ for Pb.

The dependence of the π^--meson yield on the atomic weight is shown in Fig. 2. The abscissa represents $A^{2/3}$, and the ordinate represents the experimental values of $d\sigma^-/d\Omega$ in relative units. The differential cross sections for π^0- and π^+-meson production, measured at 33° and 45° respectively,[2,3] are also shown in the figure. All quantities are normalized to the values obtained for carbon. It is clear from Fig. 2 that the results obtained for π^- and π^0 mesons are very close to one another, but differ from the results for π^+ mesons. In particular, the relative yield of π^- and π^0 mesons is greater than that of π^+ mesons in the regions of small and large values of A.

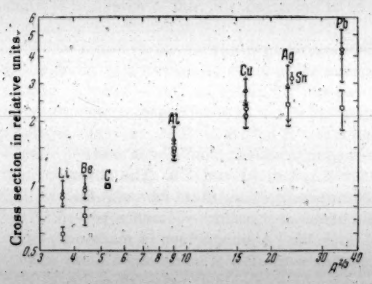

FIG. 2. Dependence of π-meson yield on atomic weight. ○ — π^0 mesons, △ — π^- mesons, □ — π^+ mesons.

To explain these experimental facts, it is necessary to take into account both the comparative effectiveness of π^+-, π^-- and π^0-meson creation on the nucleons of the nucleus, as well as the scattering of the produced π mesons by the nucleons. It can be shown, however, that in the region of π-meson energies investigated by us, the role of scattering is approximately the same for all π mesons, regardless of the sign of their charge.

A consequence of the hypothesis of isotopic invariance is that the cross sections of all possible reactions of the reactions of the interaction of π^+, π^-, and π^0 mesons with nucleons (without the production of other π mesons)

reduce to four independent cross sections, among which the relation[6]

$$\sigma_1(\pi^+p\to\pi^+p)+\sigma_2(\pi^-p\to\pi^-p)=\sigma_3(\pi^-p\to\pi^0n)+2\sigma_4(\pi^0p\to\pi^0p). \quad (1)$$

exists. Moreover, in the energy region in which the interaction of π mesons with nucleons occurs mainly in the state with isotopic spin $3/2$, we have the well known relation

$$\sigma_1:\sigma_3:\sigma_2=9:2:1. \quad (2)$$

Now, let λ^0, λ^+ and λ^- denote the mean interaction lengths of π^0, π^+, and π^- mesons with nuclear matter. Then, considering the scattering of π mesons on nucleons of a nucleus to be the same as on free nucleons, and using relations (1) and (2), it is easy to show that

$$\lambda^0/\lambda^\pm=1\mp(N-Z)/2(N+Z)\approx 1.$$

Numerous experimental data, in particular, confirm that $\lambda^+\approx\lambda^-$ in the energy region of 100 – 200 Mev.

Thus, to explain the dependence of the relative π-meson yield on atomic weight shown in Fig. 2, it is sufficient to consider only the comparative effectiveness of the creation of π^+, π^-, and π^0 mesons on nucleons of a nucleus, neglecting the possible insignificant difference in the cross sections of the interaction of π mesons of different signs with nuclear matter.

The production of π^- mesons by protons on nucleons occurs during single creation only in p-n collisions, according to the reaction $pn\to pp\pi^-$. The proximity of the results obtained for π^- and π^0 mesons may be explained by a preferred role for p-n collisions also in the case of π^0-meson production. In fact, experiment indicates[2] that $\sigma(pn\to\pi^0)/\sigma(pp\to\pi^0)\approx 2$ for collisions of 660-Mev protons with free nucleons. The significance of p-n collisions in the creation of π^0 mesons on the nucleons of a nucleus may become even stronger in the region of light nuclei (Li, Be) because of the relatively weak coupling of the neutrons in these nuclei. Finally, we must take into account the possible nonuniform distribution of neutrons and protons in the nucleus. Experiments on the scattering of high energy electrons lead to the extremely probable model of the nucleus in which there is a neutron excess on the surface of the nucleus.[7] On the other hand, because of the opacity of the nucleus, only some surface layer of the nucleus is effective for the creation of π mesons, which in connection with the above model of the nucleus must also strengthen the significance of p-n collisions. Thus, we are led to the conclusion that the identical character of the dependence of π^- and π^0 meson yield on atomic weight, established by the present experiments, may in fact be explained by the approximately identical role of p-n collisions in π^- and π^0 meson production.

In regard to π^+ mesons, we should note that they are produced preferentially in p-p collisions. This follows from the relation for the reactions on free nucleons $\sigma(pp\to\pi^+)/\sigma(pn\to\pi^+)\approx 3.5$, which may be evaluated from existing experimental data.[4,5] The excess of neutrons over protons in the regions of light and heavy nuclei may also explain the excess of the relative yields of π^- and π^0 mesons over the yield of π^+ mesons, which is observed in Fig. 2 for Li, Be, Cu, Ag and Pb.

[1] Tiapkin, Kozodaev, and Prokoshkin, Dokl. Akad. Nauk SSSR **100**, 689 (1955).

[2] Iu. D. Prokoshkin, CERN Symposium, 1956, Part 2, page 385.

[3] Meshkovskii, Pligin, Shalamov and Shebanov, J. Exptl. Theoret. Phys. (U.S.S.R.) **31**, 987 (1956), Soviet Phys. JETP **4**, 842 (1957).

[4] Meshkovskii, Pligin, Shalamov and Shebanov, J. Exptl. Theoret. Phys. (U.S.S.R.) **31**, 560 (1956), Soviet Phys. JETP **4**, 404 (1957).

[5] Meshkovskii, Pligin, Shalamov and Shebanov, J. Exptl. Theoret. Phys. (U.S.S.R.) **32**, 1328 (1957), Soviet Phys. JETP **5**, 1085 (1957).

[6] W. Heitler, Proc. Roy. Irish Acad. **51**, 33 (1946).

[7] M. H. Johnson and E. Teller, Phys. Rev. **93**, 357 (1954).

Translated by D. Lieberman
121

SOVIET PHYSICS JETP VOLUME 6 (33), NUMBER 3 MARCH, 1958

POLARIZATION OF PROTONS SCATTERED BY O^{16} SPIN AND PARITY OF THE 3.11-Mev LEVEL OF THE F^{17} NUCLEUS

P. V. SOROKIN, A. K. VAL'TER, B. V. GAVRILOVSKII, K. V. KARADZHEV, V. I. MAN'KO, and A. IA. TARANOV

Physico-Technical Institute, Academy of Sciences, Ukrainian S.S.R.

Submitted to the JETP editors March 26, 1957

J. Exptl. Theoret. Phys. (U.S.S.R.) 33, 606-609 (1957)

The polarization of protons scattered by O^{16} nuclei is investigated in the 2.6 – 2.8 Mev energy range. The measured value of the polarization, its resonance character, and its sign imply that the 3.11-Mev level of F^{17} has the characteristics $(1/2)^-$.

INTRODUCTION

THE levels of the F^{17} nucleus have been studied in investigations on the elastic scattering of protons by O^{16}. In the work of Ref. 1, carried out with an electrostatic generator, the p–O^{16} scattering was studied in the energy interval 0.6 – 4.5 Mev at a center-of-mass angle of 165°.

The determination of the characteristics of the levels of F^{17}, using the data of Ref. 1, are presented in Ref. 2 and are based on the resonance theory[3] with the help of the method of vector diagrams. As is shown in Ref. 2, the parameters of the low-lying levels of F^{17} are the most reliably determined: the 0.55-Mev $(1/2)^+$, 3.11-Mev $(1/2)^+$, and 3.88-Mev $(7/2)^-$ levels. References 4 and 5 are fairly short communications on experiments on p–O^{16} scattering, also carried out with electrostatic generators. In Ref. 4, the p–O^{16} scattering was investigated in the interval 0.28–4.6 Mev for nine values of the scattering angle, and in Ref. 5 in the interval 2.5–5.6 Mev for four values of the angle. The results of the measurements and their analysis in these investigations are not presented. Instead it is only indicated that, in disagreement with Ref. 2, the 3.11-Mev level of F^{17} is a $(1/2)^-$ state. The work of Ref. 6 was carried out with a cyclotron in the energy interval 3 – 7 Mev for eight values of the scattering angle.

The published information on the F^{17} levels is far from being complete and is not completely unambiguous. It appears expedient to use for the analysis of the levels of F^{17} information on the polarization of protons after p–O^{16} elastic scattering. The complete and unique phase analysis of the p–O^{16} scattering might be carried out if one could determine the angular dependence both for the effective scattering cross section and for polarization over a large interval of proton energies. However, even in the frame of resonance theory information on polarization is of value. The parameters of the levels of the compound nucleus, determined with the help of this theory, from the analysis of the energy dependence of the scattering cross section are related directly to the magnitudes of the phase shifts in scattering, and therefore, also with the values of the polarization.

We undertook the investigation of the polarization of protons upon p–O^{16} elastic scattering with the goal of the unambiguous solution of the question of the spin and parity of the 3.11-Mev level of the F^{17} nucleus.

1. RELATION BETWEEN THE POLARIZATION OF THE PROTONS AND THE CHARACTERISTICS OF THE 3.11-Mev LEVEL OF THE F^{17} NUCLEUS

According to Ref. 2, the resonance in the p–O^{16} scattering cross section at an energy of 2.66 Mev locates a 3.11-Mev level in the F^{17} nucleus, where this level is a $(1/2)^+$ state. The possibility of $(1/2)^-$, $(3/2)^-$, and $(3/2)^+$ states for this level are rejected by means of a comparison of the detailed form of the experimental curve with theoretical predictions. In Refs. 4 and 5 from measurements of the scattering cross section at an angle of 90° a deduction is made that this level has the characteristics $(1/2)^-$. However, it should be remarked that on the basis of the measurements at 90° one can eliminate the possibility $(3/2)^+$ but one cannot make an unambiguous choice between $(1/2)^-$ and $(3/2)^-$ states, since the energy

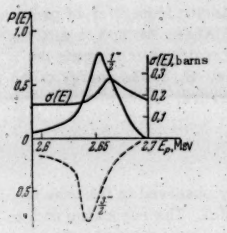

FIG. 1. $\theta = 60°$ in the center of mass system.

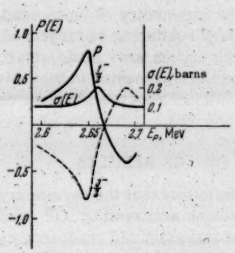

FIG. 2. $\theta = 90°$ in the center of mass system.

dependences of the cross section at this angle are exactly the same for the two possibilities indicated.

In order to identify nuclear levels, information on the analogous levels of mirror nuclei is often used. However information on the spin and parity of the 3.06-Mev level of the mirror nucleus O^{17} is not available.

We carried out calculations on the energy dependence of the polarization of the protons near the 2.66-Mev resonance for three assumptions of the spin and parity of the 3.11-Mev level. The calculations were carried out on the basis of the resonance theory for the following values of the parameters:[2] the radius of the potential scattering was taken to be 6.9×10^{-13} cm for S–waves, and 5.31×10^{-13} cm for P– and D-waves; for the lower $S_{1/2}$-resonance $E_\lambda = -0.436$ Mev; $\gamma_\lambda^2 = 7 \times 10^{-13}$ Mev-cm.

For the resonance studied $E_R = 2.66$ Mev, $\Gamma = 19.9$ kev. Figures 1 and 2 show the calculated energy dependence of the polarization for angles of 60° and 90° in the c.m.s. under the assumptions that the 3.11-Mev level is either a $(1/2)^-$ or a $(3/2)^-$ state. If the 3.11-Mev level has a $(1/2)^+$ character, the polarization must be equal to zero.

The weak effect of the levels located higher than 3.11 Mev was not taken into account in these calculations. It is possible that the influence of the higher levels will result in a deviation from zero polarization even in the case of a 3.11-Mev $(1/2)^+$ state. However, an estimate made by us shows that the magnitude of the polarization in this case will not be greater than 5 – 10%, and the dependence of the polarization on energy near 2.66 Mev will not have a resonance character. The form of the curves also changes little upon calculations (including) the upper levels.

One can make the deduction that in order to make a choice between the various values of the spin and parity of the 3.11-Mev level it is enough to carry out measurements of the polarization of the protons at some one angle of the $p–O^{16}$ scattering at energies near the 2.66 Mev resonance.

2. EXPERIMENTAL METHOD AND RESULTS

The measurements of the polarization of the protons were carried out with the aid of the equipment used in Ref. 7 for the investigation of the polarization of protons in scattering from C^{12}. The work was done with the electrostatic generator of the Physico-Technical Institute of the Academy of Sciences of the Ukrainian S.S.R.

The beam of protons from the electrostatic generator passed in a chamber where the scattering of the protons from an Al_2O_3 target took place. The protons, scattered through an angle of 60° in the center of mass system, passed into a helium analyzer with the aid of which the extent of the polarization of the scattered beam was determined. The 60° angle was chosen because the polarization at this angle does not change sign in the region of the resonance.

The Al_2O_3 target was prepared by anode oxidation of an aluminum foil in a weak solution of sulphuric acid. Non-oxidized aluminum was removed by dissolving it in concentrated hydrochloric acid. In this way a very clean and uniform film of Al_2O_3 was obtained. The thickness of the target used in the measurements was 0.47 mg/cm^2. The presence of aluminum in the Al_2O_3 target made it necessary to make a special investigation under the same conditions of the polarization of protons scattered elastically from aluminum. In these experiments an aluminum target of 0.27 mg/cm^2 thickness was used. The targets, over an appreciable period of time, were not destroyed for beam currents of 2 – 3 μa.

E_p, Mev	R for Al_2O_3	R for Al	R for O^{16}
2.500	—	0.94±0.03	—
2.600	1.01±0.03	0.96±0.03	—
2.650	1.17±0.03	0.96±0.03	—
2.675	1.14±0.03	0.93±0.03	1.32±0.03
2.700	1.12±0.03	1.01±0.03	—
2.725	1.13±0.03	1.01±0.03	—
2.750	1.05±0.03	1.10±0.03	—
2.800	1.03±0.03	1.07±0.03	1.35±0.03
3.060	—	1.00±0.03	—

Measurements were made on the magnitude of the asymmetry R upon scattering from He^4 of protons incident in the helium analyzer chamber after primary scattering on targets of Al_2O_3, Al and on a C^{12} film of 2 mg/cm² thickness. The measurements with carbon were made with the aim of calibrating the helium analyzer. The results of these measurements are presented in the table. E_p is the energy of the protons incident on the first target. The errors shown are root mean square errors.

3. DISCUSSION OF THE RESULTS

From the data presented in the table it follows definitely that the asymmetry observed in the case of the Al_2O_3 target is related to the polarization of protons scattered by O^{16} nuclei. The resonance character and the presence of this asymmetry show that the investigated resonance cannot be related to the excitation of a $(1/2)^+$ state of the F^{17} nucleus.

The value of $\overline{P}_{ox}$, the polarization in p–O^{16} scattering, averaged over the energy interval, corresponding to the ionization energy loss of the protons in the target, was calculated from the obtained values of R. The asymmetry observed in the case of the Al_2O_3 target is related to the polarization of the scattered beam according to the formula

$$R = (1 - \overline{P}P_{eff})/(1 + \overline{P}P_{eff}),$$

where P_{eff} is the effective value of the polarization of the protons scattered in the helium analyzer, $\overline{P}$ is the polarization of the proton beam scattered by the target. The value P_{eff} was determined in the experiments with the carbon target. The value of the polarization in proton scattering from C^{12} at an angle of 60° in the energy interval 2.6 – 2.8 Mev was taken from Ref. 8. The results of Ref. 7 were also used. The value P_{eff} is a constant in the 2.6 – 2.8 Mev interval and is equal to 0.80 ± 0.07.

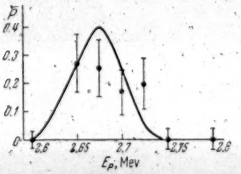

FIG. 3

The value of the polarization in p–O^{16}, $\overline{P}_{ox}$, is related to $\overline{P}$ by the formula

$$\overline{P}_{ox} = \left[\overline{P}\left(1 + \frac{3}{2}\frac{\sigma_{ox}}{\sigma_a}\right) - \overline{P}_a\right] \Big/ \left(3\sigma_{ox}/2\sigma_a\right),$$

where $\overline{P}_a$, the value of the polarization in proton scattering from aluminum nuclei in the Al_2O_3 target, was determined from the experiments with the pure Al; σ_{ox} is the scattering cross section of the protons on oxygen at an angle of 60°; σ_a is the same quantity for aluminum. The ratio σ_{ox}/σ_a was determined by us experimentally. The experimental values of $\overline{P}_{ox}$ are presented in Fig. 3. The full curve represents the theoretical dependence of $\overline{P}_{ox}$ with energy, computed with the aid of the $(1/2)^-$ curve of Fig. 1 and the data on the energy loss of protons in Al_2O_3.

The errors in the experimental points are determined from the errors in the determinations of R for the Al_2O_3 and Al targets and also the magnitudes of the errors in P_{eff} and σ_{ox}/σ_a. Because of the relatively large errors in the experimental values of $\overline{P}_{ox}$, a detailed comparison of the form of the theoretical curve for $\overline{P}_{ox}$ with the results of the investigation are not useful particularly since it is not required for an unambiguous conclusion on the character of the 3.11 Mev level.

The measurement of the magnitude of the polarization, its resonance character and its sign permit the conclusion that the 3.11-Mev level of the F^{17} nucleus can be neither a $(1/2)^+$ nor a $(3/2)^-$ state, and is a $(1/2)^-$ state.

We take this opportunity to thank A. I. Baz' and L. N. Rozentsveig for useful discussions, and A. A. Tsygikalo and the electrostatic generator crew for providing the cleanly working accelerator.

[1] Laubenstein, Laubenstein, Koester, and Mobley, Phys. Rev. **84**, 12 (1951).
[2] R. A. Laubenstein and M. J. W. Laubenstein, Phys. Rev. **84**, 18 (1951).
[3] E. P. Wigner and L. Eisenbud, Phys. Rev. **72**, 29 (1947).
[4] Eppling, Cameron, Davis, Divatia, Galonsky, Goldberg, and Hill, Phys. Rev. **91**, 438A (1953).
[5] Henry, Phillips, Reich, and Russell, Bull. Amer. Phys. Soc. **1**, 96 (1956).
[6] Sempert, Schneider, and Martin, Helv. Phys. Acta **27**, 313 (1954).

[7] P. V. Sorokin and A. Ia. Taranov, Dokl. Akad. Nauk SSSR **111**, 82 (1956), Soviet Phys. "Doklady" **1**, 637 (1956).

[8] I. T. Diatlov and L. N. Rozentsveig, Trudy, Khar'kov State Univ. **6**, 81 (1955).

Translated by Fay Ajzenberg-Selove
122

SOVIET PHYSICS JETP VOLUME 6 (33), NUMBER 3 MARCH, 1958

THE PHASE DIAGRAM FOR CERIUM

A. I. LIKHTER, IU. N. RIABININ, and L. F. VERESHCHAGIN

Very High Pressure Laboratory, Academy of Sciences, U.S.S.R.

Submitted to JETP editor March 26, 1957

J. Exptl. Theoret. Phys. (U.S.S.R.) **33**, 610-613 (September, 1957)

The p–T diagram of 99.8% pure cerium has been measured from − 150° to + 100°C over a pressure interval up to 12,000 kg/cm^2. In the p–T plane the phase equilibrium line is a straight line whose slope is 43 kg/cm^2–°C. It is shown that the transition at atmospheric pressure and low temperature is the same as that which occurs at room temperature and high pressure.

BRIDGMAN has observed a polymorphous transition in cerium at high pressure. His data on the transition pressure, however, is inconsistent. In 1927 he found[1] that the transition pressure was 7600 kg/cm^2 at 30°C and 9400 kg/cm^2 at 75°C. Later data[2] gave 12,430 kg/cm^2 at room temperature, which Bridgman explained in terms of the insufficient purity of his old sample. Later measurements of the electric resistance[3] showed, however, that the transition lies in the vicinity of 7000 kg/cm^2 at room temperature.

Lawson[4] has used x-ray methods to investigate the structure of cerium above the transition pressure, and found that on passing through the transition the lattice remains face-centered cubic. All that happens is that the lattice constant decreases by amount corresponding to the sum of the volume change in the transition and the compressibility of cerium. In addition, it is known that at atmospheric pressure cerium undergoes a transition with a volume change of the order of 10%; when the temperature is lowered, this transition takes place at − 164°C, and when it is raised, the transition occurs at − 98°C. All the data with respect to this transition has been collated by Trombe and Foëx.[5] X-ray investigations[6] have shown that the lattice again remains face-centered cubic and that only the lattice constant changes.

It is known that at room temperature cerium has two modifications, the face-centered cubic and the close-packed hexagonal. This latter modification is obtained by slow cooling from 400°C, and for it no low-temperature polymorphous transition is observed. Up to the present, however, the question of the relation between the low-temperature and the high-pressure transitions has remained unanswered. In order to clarify this subject we have measured the temperature dependence of the cerium transition pressure in the temperature range from − 185 to + 100°C on an instrument designed for measuring compressibility of solids.

This instrument (Fig. 1) is a multiplier whose low-pressure press has a piston 1 without packing, so that friction losses are reduced to a minimum. This piston is carefully ground to fit a cylinder 2 with a clearance of about 0.05 mm for a diameter of 192 mm. This high piston diameter makes it possible to operate at relatively low oil pressures in the cylinder (of the order of tenths of a kg/cm^2), so that with a highly viscous oil (in our case, castor oil) there is little leakage through the clearance. The leakage losses are compensated for by a fine regulation valve leading to a reservoir in which the oil pressure is maintained by an air cushion. In this way one may maintain a given constant pressure on the cylinder, or

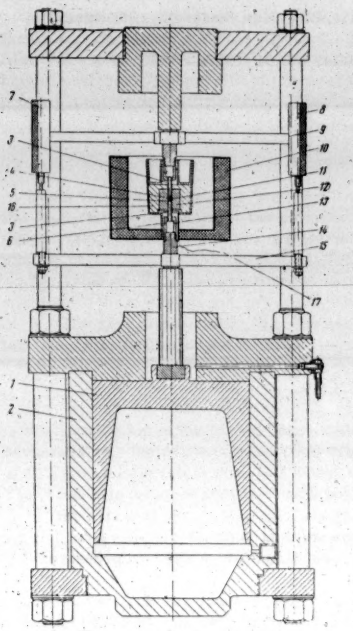

FIG. 1. Schematic diagram of the apparatus.

increase it smoothly to a given value. The high pressure is applied within a "pobedit"* piezometer 12 to the sample 4 which is surrounded by a lead casing 11; the low shear strength of lead makes it possible to apply a hydrostatic pressure distribution to the sample. For toughness the piezometer is conical with a vertex angle of 0.5° and pressed into a die 16 made of 45 KhMFA steel heat treated to a Rockwell hardness of 49. The inner opening of the piezometer has a diameter of 6 mm and is carefully ground by means of diamond powder. Two pobedit pistons 3, the upper and lower plunger, enter into it. The clearance between these pistons and the piezometer is no greater than 0.02 mm along the diameter. This small clearance is possible because Young's modulus of pobedit is three times greater than that of steel, and even at a pressure of 30,000 kg/cm^2 the lateral deformation of the pobedit pistons is less than 0.01 mm, so that the rods cannot be pressed against the walls of the piezometer. The rods were sectional, so that complicated pobedit parts could be avoided. Into the bearing 13 made of soft steel are pressed a pobedit plunger 3 of diameter 6 mm, a short rod 6 of diameter 9 mm, and a steel supporting part 14. The short rod 6 is necessary to keep 3 from cutting into the steel. Measuring levers 160 mm long are attached to 14. Attached to the lower level 15 are supports, and to the upper one 9 are dial indicators 7 and 8 with divisions indicating in microns. Two indicators are necessary to eliminate possible effects due to bending, and the actual displacement of the rods in the piezometer is determined from the average of the readings. The more accurately centered the plungers are in the press, the less is the difference in the indicator readings.

In order that the lead not flow through the clearance gap between the piezometer and rods, conical steel sealing rings 5 are placed on their ends. The piezometer is surrounded by a brass container 10 into which one may place a cooling mixture or boiling water. The container is wrapped with "mipor" thermal insulation. The temperature is measured outside the pobedit piezometer by a copper-constantan thermocouple. In view of the high mass of the piezometer, one may assume that the temperature in its interior, or that of the sample, hardly differs from the temperature measured by the thermocouple 17. A temperature difference even of 5°C would hardly alter the accuracy of the results, since the uncertainty in the pressure is ±300 kg/cm^2 and the slope of the line in the phase diagram (see Fig. 3) is about 43 kg/cm^2-°C.

A sample of height 5 mm and diameter 5 mm is pressed into a lead casing and placed between the rods in the piezometer. After preliminary compression to the maximum pressure, the cylinder pressure is slowly raised. The oil pressure is obtained from a standard manometer. When the manometer reading is integral, readings are taken on both displacement indicators.

When the maximum pressure is reached, the control valve is cracked so that the cylinder oil pressure drops at approximately the same rate as that at which it was raised. There then results a "hysteresis" loop in the rod displacement-pressure diagram; the two branches of this loop correspond to increasing and decreasing pressures. The difference between these two curves is explained by friction, which is the total of friction in the low-pressure cylinder and friction in the piezometer as the rods move in it. When the pressure is being raised, additional effort must be expended to overcome friction, and when the pressure is being lowered the friction force is subtracted. Therefore the distance between the two branches of the loop for a given value of the displacement corresponds to twice the friction, and in order to elimi-

* "Pobedit" is a solid powder alloy developed in the U.S.S.R. composed of tungsten carbide powder combined with cobalt under heat and pressure—Tr.

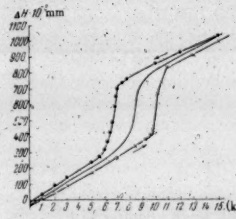

FIG. 2. The displacement H of the piezometer rods as a function of the pressure in the cylinder of the press, for increasing and decreasing pressure.

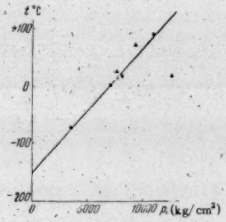

FIG. 3. Phase diagram of cerium. The pressure dependence of the polymorphous transtion temperature between phases I and II; ● — our data, ▲ — Bridgman's data.

inate this effect one need only draw an average line through this loop, thus obtaining the actual pressure dependence of the rod displacement. Now from this curve one can subtract the compressibility of the sample being investigated. If a polymorphous transition takes place in the sample, the start of this transition is observed by the rapid rate at which the readings change. When this occurs, the pressure is held constant or increased very slowly, in order that the whole transition take place in the smallest possible pressure interval. Figure 2 shows a characteristic hysteresis loop for cerium at 17°C. The beginning of the transition is very clearly seen, and a large part of the transition takes place in a sufficiently narrow pressure interval, but the end of the transition is somewhat spread out. The same pattern is observed as the pressure is decreased. The transition pressure as given by the average line, and the average of the transition pressures obtained by finding the beginning of the transition for increasing and decreasing pressures differ by a value less than the limits of experimental accuracy, which we take as ±300 kg/cm².

Figure 3 shows the p–T diagram obtained for cerium; it can be represented with sufficient accuracy by a straight line. The points obtained by Bridgman in 1927 (see above) lie in the vicinity of this line. The lowest point in Fig. 3 corresponds to the measurement at −71°C, for which the whole hysteresis loop was obtained. At −185°C, the transition started at 1000 kg/cm², but the opposite transition was not observed when the pressure was decreasing. The point at which the transition starts at −185°C lies on the same line as similar points for higher temperatures. It is therefore valid to extrapolate the p–T line to the temperature axis. The intersection is at T = −150°C, which corresponds to the transition observed in cerium at low temperatures and atmospheric pressure. The results of measurement are shown in the table.

The cerium was obtained from the Institute of Rare Metals, and contained 99.8% Ce.

From the rod-displacement-pressure curves obtained for each temperature, we can evaluate the volume change in the transition. An exact determination of this quantity is made difficult by the fact that the beginning and end of the transition are not very sharply indicated on the average line. We have therefore obtained only the average value $\Delta v \approx 8\%$ (Bridgman obtained 7.68%). We note that as the temperature increases, Δv clearly decreases. If the p–T diagram is known, the Clausius-Clapeyron equation can be used to find the heat of transition; we obtain 0.023 ev at 20°C. The question of why Bridgman obtained 12,430 kg/cm² for the transition pressure remains unanswered. One may suggest that this deviation can be explained by the different thermal histories of the samples and by different concentrations of the cubic and hexagonal phases. An answer to this question requires continuation of our investigations with cerium.

Points of the cerium p-T diagram

T (°C)	p (kg/cm²)
+94.5	11100
+20	8400
+17	7600
+4	7150
−71	3550
−150 (extrap.)	1

We consider it our duty to express our gratitude to I. V. Brandt for aid in the work.

[1] P. W. Bridgman, The Physics of High Pressures, G. Bell and Sons, Ltd., London, 1931, (Russ. Transl., ONTI, 1935).
[2] P. W. Bridgman, Proc. Am. Acad. Arts & Sci. **76**, 77 (1948).
[3] P. W. Bridgman, Proc. Am. Acad. Arts & Sci. **79**, 125 (1951); **81**, 165 (1952).
[4] A. W. Lawson, Ting-Huan Tang, Phys. Rev. **76**, 301 (1949).
[5] F. Tombe and M. Foëx, Changement de phases (1952), p. 308.
[6] A. F. Schuch and J. H. Stubdivant, J. Chem. Phys. **18**, 145 (1950).

Translated by E. J. Saletan
123

PHOTODISINTEGRATION OF DEUTERON AT ENERGIES FROM 50 TO 150 Mev

IU. A. ALEKSANDROV, N. B. DELONE, L. I. SLOVOKHOTOV, G. A. SOKOL, and L. N. SHTARKOV

P. N. Lebedev Physics Institute, Academy of Sciences, U.S.S.R.

Submitted to JETP editor March 27, 1957

J. Exptl. Theoret. Phys. (U.S.S.R.) **33**, 614-620 (September, 1957)

Photodisintegration of the deuteron was studied with the 265 Mev synchroton of the Physical Institute of the Academy of Sciences, using D_2O and H_2O targets. Protons were counted with a telescope of two proportional counters. The differential cross section was measured at angles of 22.5, 45, 67.5, 90, 112.5, 135 and 157.5° for γ-ray energies of 54, 70, 88, 110, 129 and 148 Mev in the laboratory system. The approximate angular distribution obtained is compared with results of the calculations of Marshall and Guth.

INTRODUCTION

THE reaction of photodisintegration of the deuteron by high-energy γ-rays has been studied in a series of experiments. The first work[1-5] already showed that the behavior of the total cross section diverged quantitatively from the results of theoretical calculations[6,7] for energies higher than ~ 50 Mev. In later work,[8-12] published in the period during which the present investigation was carried out, much more precise information has been obtained about the behavior with energy of the total cross section and angular distributions for the process, in the energy range from 20 to 450 Mev.

The results of the present work, which was carried out using proportional counters, are compared with theoretical calculations and with the results of Ref. 11, obtained by means of photo emulsions, in an analogous energy range and a somewhat narrower angular range.

1. EXPERIMENTAL ARRANGEMENT

The reaction of photodisintegration of the deuteron

$$\gamma + d \rightarrow p + n \qquad (1)$$

was studied for γ-ray energies from 50 to 150 Mev on the 265 Mev synchrotron of the Physics Institute of the Academy of Sciences with targets of heavy and ordinary water by counting the protons. Measurements of the energies of protons emerging at a given angle made it possible to determine the energies of the γ-rays producing the photodisintegration. The upper limit of the γ-ray spectrum in the main measurements was 264 Mev. Measurements at 22.5, 45, and 67.5° for γ-ray energies below 80 Mev were carried out for an upper limit of 170 Mev. The manner of measurement indicated separated the protons arising in the reaction (1) and the recoil protons arising in photo-production of mesons.

The separation of protons from other particles and measurement of their energies was carried out by a telescope of two proportional counters. In front of the counters there was an aluminum filter, the thickness of which was varied from 0.4 to 8.0 g/cm^2, depending on the energy of the protons being counted. The filter placed between the counters had a thickness of 0.13 g/cm^2. The angular resolution of the telescope was better than ±3°.

Pulses from the counters were transmitted after amplification to a threshold counter and then to a coincidence scheme with a resolving time ~ 1 μsec.

The track lengths of the counted protons were determined from the value of the threshold of the second counter and the total amount of material before it. The width of the track lengths constituted 0.2 g/cm^2 of aluminum, constituting an energy width of 4.0 to 1.0 Mev, depending on the mean energy of the registered protons. Protons were separated from mesons by the magnitude of specific ionization in the first counter. Deuterons could, in principle, be counted by the telescope; however, the energy of the recoil deuterons arising in production of neutral mesons, was insufficient for them to reach the second counter.

Cylindrical proportional counters were filled to a pressure of 200 mm Hg with argon containing an admixture of 1% CO_2. For absolute calibration, a collimated source of α-particles Po^{210} was inserted. In the process of measurement, the apparatus was periodically switched over to count α-particles; this permitted control of the stability of the counting interval.

The targets were in the form of flat thin-walled containers, filled with ordinary and heavy water. The target thicknesses were determined with a given energy resolution and constituted 0.2 to 0.9 cm in different measurements. Measurement of the proton yield at a given energy was carried out in the form of successive counts from D_2O and H_2O targets, placed in turn in the γ-ray beam; this made it possible to diminish the effect of instability in the working of the measuring apparatus and synchroton. All measurements were carried out with alternating filling of each of the containers with heavy and ordinary water.

Relative measurements of the γ-ray beam were carried out with a thin-walled monitoring ionization chamber placed in the beam. Absolute calibration of the thin-walled chamber was carried out using a thick-walled graphite chamber.

2. PROCESSING OF RESULTS

The differential cross section for photodisintegration of the deuteron was calculated from the experimental results by the formula

$$\frac{d\sigma}{d\Omega}(\overline{W}) = \frac{n_p}{\Omega_{\text{eff}} n_{\text{nuc}} n_\gamma} \eta_{\text{ms}} \eta_{\text{nuc}}. \qquad (2)$$

The number of protons n_p arising as a result of photodisintegration of deuterium nuclei, was determined by the difference in yields from the D_2O and H_2O targets. The contribution from the Compton effect on water was negligible. The standard statistical error in the number of protons constituted, on the average, 10%.

The effective solid angle for counting, Ω_{eff}, was calculated for the extended target taking into account edge effects in the counters. The accuracy of calculation was ~ 5%. Besides this, the error in measurement of the edge effects in the counters can lead to a systematic error of about 5%. The number of deuterium nuclei in one cm^2 of target, n_{nuc}, was determined to an accuracy of 3%.

The number of γ-rays n_γ incident on the whole area of the target and leading to the n_p protons, was calculated from the formula

$$n_\gamma = k \int_{W_1}^{W_2} f(W) \eta_i(W) dW.$$

The factor k is connected with the absolute calibration of the monitoring ionization chamber which was carried out to an accuracy of ~ 10%. The distribution of γ-rays with energy f(W) was calculated from the Bethe-Heitler formula with correction for the thickness of the target and it was averaged over the energies of the electrons incident on the synchrotron target. The energy resolution was determined by the ionization slowing of the protons in the target and the finite width of the telescope interval. The resolution function $\eta(W)$ was approximately an isoceles trapezium. The width at the base $(W_2 - W_1)$ was ~ 20 Mev and the width at half-maximum, approximately 15 Mev. The error in the determination of the value of n_γ, which was not connected with the systematic error in the quantity k, did not exceed 3%. The value of the differential cross section calculated by Eq. (2) was related to the mean γ-ray energy by $\overline{W} = \frac{1}{2}(W_1 + W_2)$.

Corrections taking into account multiple scattering and nuclear interaction of the protons in the filters of the telescope enter into Eq. (2). In the calculation of corrections for multiple scattering η_{ms}, the actual extended target was replaced by a point one. Results given in Refs. 13 and 14 were used in the calculation. The size of the correction grew with increasing energy of the protons counted and usually lay in the interval from 1 to 1.2. The restrictions introduced in the calculation cannot lead to an error in the value of η_{ms} exceeding 5%.

In calculating the influence of nuclear interactions, account was taken only of inelastic proton interactions, the cross section for which was taken equal to half the total cross section measured for neutrons of the corresponding energies. The value of this correction never exceeded 1.15. The error in evaluating η_{nuc} connected with the neglect of elastic interactions was less than 5%. An estimate of the number of

secondary protons created by the neutrons in the telescope filters showed that this effect could be neglected.

The error in the differential cross section, Eq. (2), was determined by the statistical error in the number of protons and the total random error from other quantities entering into Eq. (2), which did not exceed 10%. In addition, there was a systematic inaccuracy of about 15% connected with the absolute calibration of the monitor of the ionization chamber. In the future, only statistical errors will be taken into account.

3. RESULTS OF THE EXPERIMENT AND DISCUSSION

As a result of the experiment, values of the differential cross section were obtained for angles of 22.5, 45, 67.5, 90, 112.5, 135 and 157.5° in the laboratory system (l.s.). This data was split into six groups corresponding to mean γ-ray energies of 54, 70, 88, 110, 129 and 148 Mev. laboratory system. The spread of energy inside each group was substantially less than the width of the energy resolution, constituting, on the average, about ±7.5 Mev. Values of the differential cross section obtained by averaging within each group and converted to the c.m.s. are given in Fig. 1. The total cross section is given in Fig. 2.

TABLE I. Values of the parameters obtained in approximating the angular distributions by $d\sigma/d\Omega = (A + B \sin^2\theta)(1 + 2\beta \cos\theta)$.

W_{lab}, Mev	2β	A, $\frac{\mu barn}{sterad.}$	B, $\frac{\mu barn}{sterad.}$
54	0.30	3.9	8.6
70	0.40	3.4	6.7
88	0.36	4.7	4.1
110	0.40	4.4	2.5
129	0.40	5.0	0.0
148	0.36	5.0	0.7

For comparison of our data with the results of Ref. 11, which were obtained for the same energy range and somewhat smaller angular range by photo emulsions, we approximated the angular distribution in the form

$$\frac{d\sigma}{d\Omega}(A + B\sin^2\theta)(1 + 2\beta\cos\theta), \qquad (3)$$

connected with the choice of three parameters. The values of the parameters A, B, β (see Table I) and the value of the total cross section obtained by us agree, within the limits of error, with the results of Ref. 11.

Theoretical calculations of photodisintegration of the deuteron for energies of 20 to 150 Mev have been carried out by Schiff[6] and Marshall and Guth.[7] The total cross section and angular distribution were calculated under the assumption of a half-exchange, central force, acting between proton and neutron, for several potentials. The main term in the total cross section, according to Refs. 6 and 7, comes from electric dipole transitions. Corresponding to this, the angular distribution has a $\sin^2\theta$ character, with some asymmetry relative to 90°, caused by the interference of dipole (E1) and quadrupole (E2) electric transitions. The contribution of the magnetic quadrupole transitions (M2) calculated in Ref. 7 is small. In these articles the magnetic dipole transitions in the $^1S_0$-state leading to an isotropic yield of photo protons from deuterium are not calculated. Results of the calculations of Nagahara and Fujimura[15] for E1, E2 and M2 transitions differ little from Refs. 6 and 7; however, in Ref. 15 the M1 transition connected with the interaction with the exchange

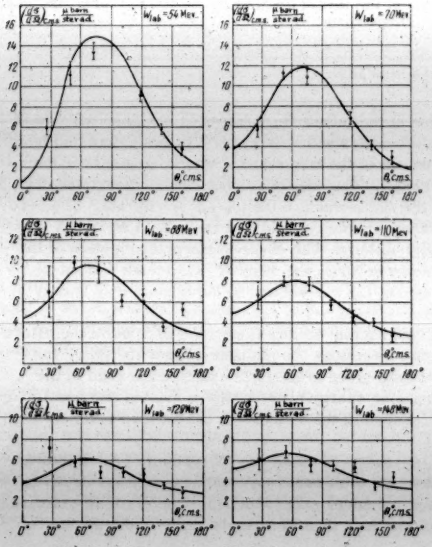

FIG. 1. Differential cross section vs. angle of the emitted proton in the c.m.s. for γ-rays of various energies (W_{lab} = 54, 70, 88, 110, 129 and 148 Mev, respectively). The solid curve corresponds to the approximate form $d\sigma/d\Omega = (d\sigma/d\Omega)_{M.G.} + P + Q\cos\theta$. Energy values have a definition of approximately 7.5 Mev. Errors of the experimental points are standard statistical errors.

magnetic moments, which are introduced phenomenologically, is also calculated.

In Fig. 2 we show our experimental points for the total cross section and curves of the total cross section calculated by Wilson[16] and Marshall and Guth.[7] Divergences from the results of Ref. 7 begin to become noticeable, apparently, at energies ~ 40 Mev, and at an energy of 150 Mev the experimental cross section exceeds that of Ref. 7 by a factor of about 5. The experimental angular distributions in this energy range also show differences, which increase with γ-ray energy, from the distributions of Ref. 7. They are characterized by a large isotropic component and a substantial asymmetry about 90°.

In view of the indicated difference between the experimental data and the results of Marshall and Guth, we approximated our angular distributions in the form

$$d\sigma/d\Omega = (d\sigma/d\Omega)_{M.G.} + P + Q\cos\theta, \qquad (4)$$

TABLE II. Values of the parameters, obtained in approximating the angular distributions by $d\sigma/d\Omega = (d\sigma/d\Omega)_{M.G.} + P + Q\cos\theta$. The uncertainty in the parameters correspond to the standard statistical error in the proton yield.

W_{lab}, Mev	P, $\frac{\mu barn}{sterad.}$	±ΔP	Q, $\frac{\mu barn}{sterad.}$	±ΔQ
54	1.30	0.41	−0.76	0.55
70	2.72	0.28	0.92	0.41
88	3.50	0.37	0.81	0.56
110	3.80	0.28	1.11	0.43
129	3.27	0.29	0.42	0.43
148	4.27	0.32	1.00	0.48

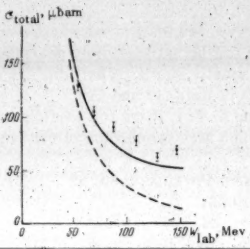

FIG. 2. Total cross section as a function of γ-ray energy W in the l.s. The solid curve is from the calculation of Wilson;[16] the dotted one, from the calculation of Marshall and Guth.[7] The errors in the experimental points are standard statistical ones.

where $(d\sigma/d\Omega)_{M.G.}$ is the differential cross section of Marshall and Guth and P and Q are parameters of the approximation. Curves of the form Eq. (4), obtained by the method of least squares, are given in Fig. 1, and the values of the parameters with their errors, in Table II. The total cross section, calculated as $\sigma_t = (\sigma_t)_{M.G.} + 4\pi P$, is shown on Fig. 2.

The angular distribution Eq. (4) describes well the experimental data in the energy region studied. We note that the approximation with the expression not containing the term with $\cos\theta$ is obviously unsatisfactory.

The result, Eq. (4), can be seen to be quite natural, if account is taken of the fact that, in addition to the processes calculated in Ref. 7 (E1, E2 and M2) for the energies considered, magnetic dipole M1 transitions not calculated there can be added. These transitions, beginning from the S-state, give an isotropic term in the angular distribution and their interference with M2 transitions gives a term proportional to $\cos\theta$. As noted in Ref. 6, there is no interference between magnetic and electric transitions. The total cross section for magnetic dipole transitions, equal to $4\pi P$, obtained in this interpretation, is compared in Fig. 3 with the theoretical calculations of Nagahara and Fujimura.[15] The experimental values are several times larger than the calculated result. This indicates that the particular interpretation in which magnetic dipole transitions are added to those calculated by Marshall and Guth, is, evidently, unsatisfactory.

Another possible explanation of the large isotropic component in the distribution, Eq. (4), is the supposition that, in the energy range considered, there is also the process of absorption of a dipole electric γ-ray, for which the transition into the $^3P_0$-state is large compared with transitions into $^3P_1$- and $^3P_2$-states. This process should give an isotropic yield of protons from deuterium.[17] In order to explain the forward peaking in this case, it is necessary to assume the existence of magnetic dipole transitions in the triplet state of the proton-neutron system, i.e.,

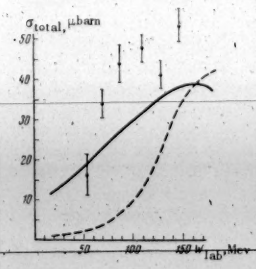

FIG. 3. Magnitude of $4\pi P$ as a function of γ-ray energy in the l.s. The experimental points are given with standard statistical errors. The solid curve comes from the results of Wilson's calculations[16] for photodisintegration by way of re-absorption of mesons. The dotted curve was calculated by Nagahara and Fujimura for magnetic dipole transitions caused by interaction of the γ-ray with the phenomenological exchange magnetic moment.

in the $^3S_1$–state. The interference of these transitions with transitions into the $^3P_0$–state gives a term proportional to $\cos\theta$.

A possible model for transitions into the $^3P_0$–state is photodisintegration of the deuteron connected with photo production of virtual mesons in an S–state on one of the nucleons of the deuteron and their successive absorption by the same deuteron. On Fig. 3 the total cross section for such processes calculated by Wilson[16,18] is compared with experimental data for the isotropic part of the cross section. The experimental points lie closer to this calculation than to the results of Ref. 15; however, the agreement is not complete.

As noted above, the model of re-absorption should be supplemented by magnetic dipole transitions into the $^3S_1$–state, which leads by itself to an isotropic distribution. Evaluation of the total cross section for magnetic dipole transitions, carried out with the experimental data using the cross section of Wilson, showed that the cross section of such transitions does not exceed 5 μbarn. We note that M1 transitions can also lead to the $^1S_0$–state; in this case they lead to an isotropic distribution, but do not interfere with the transitions into the $^3P_0$–state.

Thus, in the energy region considered, the total cross section and angular distributions for the process of photodisintegration of the deuteron can be satisfactorily described if, to the transitions calculated by Marshall and Guth, and by Wilson, magnetic dipole transitions are added, with a cross section lying within the limits of the theoretical estimates of Refs. 15 and 17.

The authors express their gratitude to V. I. Ritus for participation in the discussion of the results of the work, and also to the crew of the 265 Mev synchroton of the Physics Institute of the Academy of Sciences.

[1] T. S. Benedict and W. M. Woodward, Phys. Rev. **85**, 924 (1952).
[2] S. Kikuchi, Phys. Rev. **85**, 1062 (1952).
[3] R. Littauer and J. Keck, Phys. Rev. **86**, 1051 (1952).
[4] M. S. Gilbert and J. M. Rosengren, Phys. Rev. **88**, 901 (1952).
[5] Keck, Littauer, O'Neill, Perry and Woodward, Phys. Rev. **93**, 827 (1954).
[6] L. I. Schiff, Phys. Rev. **78**, 733 (1950).
[7] J. F. Marshall and E. Guth, Phys. Rev. **78**, 738 (1950).
[8] Yamagata, Barton, Hanson and Smith, Phys. Rev. **95**, 574 (1954).
[9] E. A. Whalin, Phys. Rev. **95**, 1362 (1954).
[10] Lew Allen, Jr., Phys. Rev. **98**, 705 (1955).
[11] Whalin, Schriever and Hanson, Phys. Rev. **101**, 377 (1956).
[12] J. C. Keck and A. V. Tollestrup, Phys. Rev. **101**, 371 (1956).
[13] R. Sternheimer, Rev. Sci. Instr. **25**, 1070 (1954).
[14] W. C. Dickinson and D. C. Dodder, Rev. Sci. Instr. **24**, 428 (1953).
[15] Y. Nagahara and J. Fujimura, Progr. Theoret. Phys. **8**, 49 (1952).
[16] R. R. Wilson, Phys. Rev. **104**, 218 (1956).
[17] N. Austern, Phys. Rev. **85**, 283 (1952).
[18] R. R. Wilson, Phys. Rev. **86**, 125 (1952).

Translated by G. E. Brown
124

ENERGY DEPENDENCE OF THE ANGULAR CORRELATION IN THE $\pi^+ - \mu^+ - e^+$ DECAY

A. O. VAISENBERG and V. A. SMIRNITSKII

Submitted to JETP editor June 10, 1957

J. Exptl. Théoret. Phys. (U.S.S.R.) 33, 621-624 (September, 1957)

The energy spectrum of positrons from $\pi^+ - \mu^+ - e^+$ decays in emulsions, and the energy dependence of the angular correlation in these decays are studied. It is shown that the coefficient A in the formula $1 + A \cos \vartheta$ for the angular correlation increases rapidly with increasing positron energy, in agreement with the two-component theory of the neutrino.

THE purpose of this work was the study of the dependence of the correlation between the directions of emission of the μ-meson and positron in $\pi^+ \to \mu^+ \to e^+$ decays on the energy of the positron. To obtain this we measured the energy of the positron and the angle between the direction in which it is emitted and that of the μ-meson for 580 decays in NIKFI-R and Ilford G-5 emulsions. Layers of the NIKFI-R emulsions of diameter 10 cm and thickness 400 μ were placed in a double magnetic screen, shielding the external magnetic field to a value less than 0.05 G, and were irradiated with a pulse of monochromatic π^+-mesons, slowed down by an absorber so that they would stop in the emulsion. Layers of Ilford G-5 emulsions of thickness 600 μ constituted part of a large emulsion camera, irradiated at a height of ~ 28 km. They were presented to us by C. Powell. Of 580 measured $\pi^+ - \mu^+ - e^+$ decays, 448 were found in the NIKFI-R emulsions and 132 in the Ilford G-5 ones. The analysis of the data for the first 120 decays in the Ilford G-5 emulsions were given in our preceding article.[1] Here we will consider the complete data, including 580 decays in all.

In the choice of the cases submitted to measurement out of the large number of $\pi^+ - \mu^+ - e^+$ decays, those were taken which satisfied the following criteria: (1) Both parts of the $\pi^+ - \mu^+ - e^+$ decay occurred in the same layer of emulsion. (2) The vertex of the $\mu^+ - e^+$ decay was at a distance greater than 100 μ from both surfaces of the emulsion. (3) The length of the positron track in the layer was not less than 1 mm.

Measurements of the positron energies were carried out by the multiple scattering method. The analysis showed that in both the NIKFI-R and Ilford G-5 emulsions there was substantial distortion, the influence of which strongly diminished in going from the second to the third and fourth differences. The spectra given below were constructed from the fourth differences. Scattering measurements were carried out for cells of 50, 100 or 200 μ, depending on the track length and on the signal-to-noise ratio. The distribution of positron tracks with length are given below:

Length of tracks in mm	1 – 2	2 – 3	3 – 4	4 – 5	5 – 6	>6
Number of tracks	313	126	78	34	23	6

The statistical error in the determination of energy (dispersion) in the measurements with 100 μ cells lay within the limits $\sim (30 - 10\%)$ at the beginning and end of the table, respectively.

For each decay, in addition to the energy of the positron, the angle ϑ in the plane of the emulsion between the directions of emission of the μ^+-meson and positron was measured. It should be noted that, thanks to the criteria employed in the choice, the tracks of the positrons and mesons made small angles with the plane of the emulsion; the half-width of the respective distributions was less than 7° for positron and 10° for meson tracks. Therefore, without introducing a considerable error, we may: (1) measure the projection of the volume angle ϑ on the plane of the emulsion instead of the angle itself, and (2) consider that the correlations for particles lying in the plane of the emulsion ("plane case") are investigated.

The measured positron decay spectra are given in Fig. 1 (positrons emitted forward $0° < \vartheta \leq 90°$) and in Fig. 2 (positrons emitted backward, $90° < \vartheta \leq 180°$), where the energy ϵ, expressed as a fraction of the maximum energy $E_{max} \approx 53$ mev, is plotted along the abscissa. The ordinate is the number of particles in an energy interval $\Delta\epsilon = 0.1$. These two spectra are distinctly different. The spectrum of particles emitted forward rises sharply for low energies and, going through a maximum lying between $\epsilon = 0.4 - 0.6$, smoothly drops with larger energies, whereas the spectrum of particles emitted backward grows noticeably more slowly to begin with, going through a maximum in the region $\epsilon = 0.7 - 1.0$ and sharply

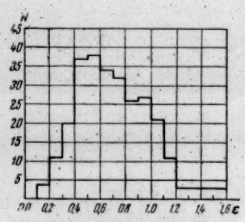

FIG. 1. Spectrum of positrons emitted forwards ($0° \leq \vartheta \leq 90°$).

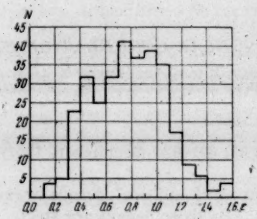

FIG. 2. Spectrum of positrons emitted backwards ($90° < \vartheta \leq 180°$).

drops with larger energies. Beginning with $\epsilon = 0.6$, there is a substantial excess of protons emitted backward, the relative magnitude of which grows with increasing energies. Thus, for example, the ratio of the number of particles emitted backwards to the number of particles emitted forwards is equal, respectively, to 219:163 for $\epsilon > 0.6$, 146:97 for $\epsilon > 0.8$, and 70:44 for $\epsilon > 1.0$.

For a quantitative analysis of the data obtained, we calculated mean values $\overline{\cos\vartheta}$ for each energy interval of the spectra Figs. 1 and 2. For a correlation of the type $1 + A\cos\vartheta$ measured in the plane as in our case the coefficient A is equal to twice the value of $\overline{\cos\vartheta}$. In the table the values are given of $\overline{\cos\vartheta}$ obtained for particles whose energy exceeds a given value.

Statistical errors given in the table were calculated as $0.79/\sqrt{N}$, where N is the number of particles of energy exceeding that given in the table. The data in the table show a monotonic growth in values of $\overline{\cos\vartheta}$ from ~ 0.05 to a value approximately four times larger.

Energy	$\overline{\cos\vartheta}_{>\epsilon} = A/2$	Energy	$\overline{\cos\vartheta}_{>\epsilon} = A/2$
0	$-(0.053 \pm 0.033)$	0.6	$-(0.118 \pm 0.040)$
0.1	$-(0.053 \pm 0.033)$	0.7	$-(0.148 \pm 0.04.)$
0.2	$-(0.052 \pm 0.033)$	0.8	$-(0.136 \pm 0.051)$
0.3	$-(0.064 \pm 0.034)$	0.9	$-(0.192 \pm 0.059)$
0.4	$-(0.060 \pm 0.035)$	1.0	$-(0.200 \pm 0.074)$
0.5	$-(0.083 \pm 0.037)$	1.1	$-(0.206 \pm 0.104)$

For comparison of the data obtained with the two-component theory of the neutrino, we turn to the formula describing the asymmetry in $\pi - \mu - e$-decay

$$dN = (a + b\alpha\lambda\cos\vartheta)\,dz\,d\cos\vartheta, \qquad (1)$$

where

$$a = 2z^2(3 - 2z); \quad b = 2z^2(2z - 1),$$

λ is a parameter of the theory and α is a coefficient equal to the relative proportion of μ^+-mesons which keep their original direction of spin until the moment of decay. This formula gives, for the "plane case," the following theoretical value of $\overline{\cos\vartheta}$ for particles of energy exceeding ϵ

$$\overline{\cos\vartheta}_{>\epsilon} = (\alpha\lambda/2)\left(\int_{\epsilon}^{1} b\,dz \Big/ \int_{\epsilon}^{1} a\,dz\right). \qquad (2)$$

Our data give the possibility of determining the quantity $\alpha\lambda$. However, a more precise determination of this quantity comes from the consideration of available work with emulsions, where the angular correlation, averaged over energy, was measured[2-6] (see also the private communication of Gurevich). In this case the coefficient A in the correlation formula $1 + A\cos\vartheta$ is equal to $1/3\alpha\lambda$, which is easy to obtain by integrating (1) over the energy. The data which have been available to us are given below:

Authors	Number of Particles	$A = \alpha\lambda/3$
Chadwick, Durrani *et al.*[2]	3021	$-(0.149 \pm 0.033)$
Bodlik *et al.*[3]	1562	$-(0.080 \pm 0.044)$
Biswas *et al.*[3]	2003	$-(0.095 \pm 0.039)$
Castaghnoli *et al.*[4]	1028	$-(0.222 \pm 0.054)$
Friedman and Telegdi[5]	1300	$-(0.120 \pm 0.048)$
Gurevich *et al.* (private communication)	2000	$-(0.120 \pm 0.039)$

The statistical errors indicated here were calculated according to the formula $1.73/\sqrt{N}$, where N is the total number of particles.

The mean weighted value of the coefficient A from these data is $A = -0.127 \pm 0.017$, corresponding to $\alpha\lambda = -0.380 \pm 0.050$. We used this value of $\alpha\lambda$ for comparison of the experimental values of $\overline{\cos\vartheta}$ in the table with the theory.

Curve 1 on Fig. 3 gives the theoretical values of $\cos\vartheta/\alpha\lambda$; they vary from 0.167 for $\epsilon = 0$ to 0.500 for $\epsilon = 1$. A direct comparison of the experimental data with this curve is difficult, because our spectra (see Figs. 1 and 2) are smeared out by the dispersion in energy measurements and bremsstrahlung. We neglected the bremsstrahlung and calculated the smearing out in curve 1, starting from dispersions in the

energy measurements of 15 and 30%; almost all of our measurements are confined to the region between these values of the dispersion. The results obtained are given in curves 2 and 3 which differ only slightly from each other. These curves whould be used for comparison with the experimental data. The experimental points on Fig. 3 correspond to values of $\overline{\cos\vartheta}$ from the table, divided by $\alpha\lambda = -0.38$. The encircled point at the beginning of the curve corresponds to the normalized value $\alpha\lambda = -0.380 \pm 0.050$. The experimental data show the sharp rise in the mean value of $\overline{\cos\vartheta}$ with energy predicted by the two-component theory of the neutrino. From Fig. 3 it can be seen that the experimentally observed increase somewhat exceeds the theoretical values. The accuracy of the experiment was, however, insufficient to make this significant.

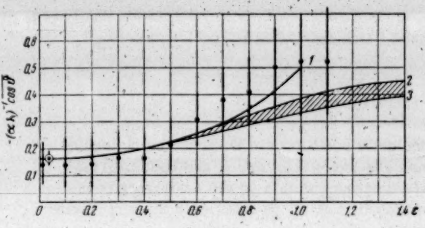

FIG. 3

We consider separately the data in the region of small energies. Because of the dispersion of the measurements, the change in sign of the correlation predicted by the theory is displaced from $\epsilon = 0.5$ in the direction of an ϵ lying in the region $0.3 - 0.4$, depending on the magnitude of the dispersion. In the range $\epsilon < 0.4$, 34 positrons emitted forwards, 32 backwards were observed, which agrees with the strong decrease in correlation and change in sign predicted by the theory.

A detailed description of the work and a through statistical analysis will be given in the near future.

The authors thank A. I. Alikhanov for help and interest in the work and D. M. Samoilovich, in whose laboratory the NIKFI-R emulsions were processed. A large part of the difficult scattering measurements and scanning of the emulsions was carried out by E. D. Kolganova, N. V. Rabin, E. V. Minervina, E. A. Pesotskaia, V. F. Kuzichev, A. G. Avalishvili, V. V. Titova, V. N. Kuznetsova, and V. A. Savel'ev to whom the authors express their gratitude. The authors thank I. L. Il'in and A. S. Kronrod for calculation of the smearing out of the theoretical spectra owing to the dispersion, and to P. S. Bruk for permission to use the LUMS computer of the Academy of Science of the U.S.S.R.

[1] A. O. Vaisenberg and V. A. Smirnitskii, J. Exptl. Theoret. Phys. (U.S.S.R.) 32, 1340 (1957); Soviet Phys. JETP 5, 1093 (1957).

[2] G. B. Chadwick et al. (preprint).

[3] Biswas, Ceccarelli, and Crussard, Nuovo cimento 5, 756 (1957).

[4] Castaghnoli, Franzinetti, and Manfredini, Nuovo cimento 5, 684 (1957).

[5] J. Friedman and B. L. Telegdi, Phys. Rev. 105, 1681 (1957).

Translated by G. E. Brown
125

SCATTERING OF SLOW NEUTRONS BY DIATOMIC MOLECULES

A. A. ANSEL'M

Leningrad Physico-Technical Institute, Academy of Sciences, U.S.S.R.

Submitted to JETP editor January 4, 1957

J. Exptl. Theoret. Phys. (U.S.S.R.) 33, 625-633 (September, 1957)

We compute the cross sections for elastic and inelastic scattering of neutrons by molecules consisting of two identical or two different atoms. The general formulas are used to treat the scattering by T_2, HT and DT. Comparison of experimental data on the scattering cross sections of these molecules with our formulas makes it possible to determine the amplitudes for scattering of neutrons by tritium.

1. SCATTERING OF NEUTRONS BY MOLECULES CONSISTING OF TWO IDENTICAL ATOMS.

SCHWINGER and Teller[1] and Hamermesh and Schwinger[2] developed the theory of slow neutron scattering by molecules of ortho- and parahydrogen and deuterium. Using the Fermi quasipotential,[3] they expressed the neutron scattering cross sections of these molecules in terms of the amplitudes for neutron scattering by H and D nuclei.

In this section we shall treat molecules consisting of two arbitrary but identical atoms. (We shall refer to such molecules as "symmetric" molecules in contrast to "unsymmetric" molecules which contain different atoms.)

The interaction energy of the neutron and the symmetric diatomic molecule can be written as:[2]

$$\hat{U} = -\frac{2\pi\hbar^2}{M}\frac{A+1}{A}\frac{1}{2s_1+1}[(s_1+1)\,a_{s_1+1/2}+s_1a_{s_1-1/2}+(\sigma\cdot\mathbf{s}_1)(a_{s_1+1/2}-a_{s_1-1/2})]\,\delta^3(\mathbf{r}-\mathbf{r}_1)+\text{ similar terms with } 1\to 2$$

$$=-\frac{2\pi\hbar^2}{M}\frac{A+1}{A}\frac{1}{2s_1+1}\left\{\left[(s_1+1)\,a_{s_1+1/2}+s_1a_{s_1-1/2}+\frac{1}{2}(\sigma\cdot\mathbf{s})(a_{s_1+1/2}-a_{s_1-1/2})\right][\delta^3(\mathbf{r}-\mathbf{r}_1)+\delta^3(\mathbf{r}-\mathbf{r}_2)]\right.$$
$$\left.+\frac{1}{2}[\sigma\cdot(\mathbf{s}_1-\mathbf{s}_2)](a_{s_1+1/2}-a_{s_1-1/2})\,[\delta^3(\mathbf{r}-\mathbf{r}_1)-\delta^3(\mathbf{r}-\mathbf{r}_2)]\right\}\qquad(\mathbf{s}=\mathbf{s}_1+\mathbf{s}_2). \tag{1}$$

The quantities $a_{s_1+1/2}$ and $a_{s_1-1/2}$ are the neutron scattering amplitudes for an atom with total spin $s_1+1/2$ and $s_1-1/2$, respectively; $1/2\ \sigma$, $\mathbf{s}_1$, $\mathbf{s}_2$ are the spin operators for the neutron, the first atom and the second atom; $\mathbf{r}$, $\mathbf{r}_1$, $\mathbf{r}_2$ are the respective radius vectors; A and $\mathbf{s}_1$ are the atomic weight and spin of each of the atoms, and M is the mass of the nucleon.

The wave functions of the initial and final state of the system (if we treat the molecule as rigid rotator are

$$\Psi_1=\exp\{i\mathbf{k}_0\cdot\mathbf{r}-i\mathbf{k}_0(\mathbf{r}_1+\mathbf{r}_2)/2\}\,Y_{j\mu}\left(\frac{1}{l}\right)\frac{V\delta(l-r_0)}{r_0}\,\chi_\sigma\chi_{sM_s},$$

$$\Psi_2=\exp\{i\mathbf{k}\mathbf{r}-i\mathbf{k}\cdot(\mathbf{r}_1+\mathbf{r}_2)/2\}\,Y_{j'\mu'}\left(\frac{1}{l}\right)\frac{V\delta(l-r_0)}{r_0}\,\chi_{\sigma'}\chi_{s'M_s'}\qquad(\mathbf{l}=\mathbf{r}_1-\mathbf{r}_2). \tag{2}$$

The factor $e^{i\mathbf{k}_0\cdot\mathbf{r}}$ describes the neutron incident on the molecule in the center of mass system; $e^{-i\mathbf{k}_0\cdot(\mathbf{r}_1+\mathbf{r}_2)/2}$ describes the motion of the center of mass of the molecule with momentum $-\mathbf{k}_0$; $Y_{j\mu}$ is the angular part of the wave function for a molecule with total angular momentum j and projection μ; $\sqrt{\delta(l-r_0)}/r_0$ is the radial part of the wave function, corresponding to internuclear distance r_0; χ_σ, χ_{sM_S} are the spin functions of the neutron (spin 1/2, projection σ), and the molecule (spin s, projection M_S). The notation for Ψ_2 is similar.

We first treat scattering processes in which $Y_{j\mu}$ and $Y_{j'\mu'}$ have the same parity. In this case the parities of χ_{sM_S} and $\chi_{s'M_S'}$ also coincide. We may therefore limit ourselves to terms in (1) whose spin parts are 1 or $\sigma\cdot\mathbf{s}$. Since both these operators commute with $\mathbf{s}^2$, $s=s'$.

For this case the space integral which occurs when we calculate the matrix element of $\hat{U}$ between

Ψ_2 and Ψ_1 is

$$I^{(1)}_{\mu\mu'} = 2\int Y^*_{l'\mu'}\left(\frac{\mathbf{l}}{l}\right) Y_{l\mu}\left(\frac{\mathbf{l}}{l}\right)\frac{\delta(l-r_0)}{r_0^2}\cos\left(\frac{\mathbf{q}\cdot\mathbf{l}}{2}\right)d\mathbf{r}_1 d\mathbf{r}_2 \quad (\mathbf{q}=\mathbf{k}_0-\mathbf{k}).$$

Expanding the product of the spherical harmonics in a Clebsch—Gordan series and writing cos $(\mathbf{q}\cdot\boldsymbol{\ell}/2)$ as a sum of Legendre polynomials, we easily find

$$I^{(1)}_{\mu\mu'} = 2\sqrt{(2j+1)(2j'+1)}\sum_{\text{even } l}(-1)^{\mu'} C^{l0}_{j0j'0}\, i^l f_l\left(\frac{qr_0}{2}\right) C^{l\mu-\mu'}_{j\mu j'\mu'} P_{l\mu-\mu'}\left(\frac{\mathbf{q}}{q}\right)$$

($C^{\ell_0}_{j_0 j'_0}$ and $C^{\ell\mu-\mu'}_{j\mu j'\mu'}$ are Clebsch—Gordan coefficients, $P_{\ell\mu-\mu'}$ are spherical harmonics normalized to the value $4\pi/(2\ell+1)$, $f_\ell(qr_0/2)$ are spherical Bessel functions).

We want the square modulus of this expression, summed over μ' and averaged over μ:

$$\frac{1}{(2j+1)}\sum_{\mu'\mu}|I^{(1)}_{j\mu j'\mu'}|^2 = 4(2j'+1)\sum_{\text{even } l}(C^{l0}_{j0j'0})^2 f_l^2\left(\frac{qr_0}{2}\right).$$

The calculation of the various spin sums and the summation over σ, σ', M_s and M'_s is done by the standard methods; we give the final result for the differential cross section for scattering with $j \to j'$ (where j and j' have the same parity)

$$\frac{d\sigma^{(1)}_{jj'}}{d\Omega} = \frac{k}{k_0}\frac{(A+1)^2}{(2A+1)^2}\frac{16}{(2s_1+1)^2}\left[((s_1+1)a_{s_1+1/2}+s_1 a_{s_1-1/2})^2 + \frac{s(s+1)}{4}(a_{s_1+1/2}-a_{s_1-1/2})^2\right](2j'+1)\sum_{\text{even } l}(C^{l0}_{j0j'0})^2 f_l^2\left(\frac{qr_0}{2}\right). \quad (3)$$

For transitions $j \to j'$ with change of parity, we must use only the term proportional to $\sigma\cdot(\mathbf{s}_1-\mathbf{s}_2)$ in (1). In this case, the expression for the cross section will depend on the spin s' of the final state. Obviously, we want to sum the cross section over those values of s' for which the given j' can occur (for even j' and half-integer s_1, these are $s' = 0, 2, \ldots 2s_1-1$; for odd j' and half-integer s_1, $s' = 1, 3, \ldots 2s_1$; etc.). In carrying out the summation, we can formally sum over all s', since the values of s' which don't match give null terms.

This remark enables us to simplify the calculation of the spin sum

$$\frac{1}{2(2s+1)}\sum_{\sigma\sigma' M_s M'_s}|\chi^*_{\sigma'}\chi^*_{s'M'_s}[\sigma\cdot(\mathbf{s}_1-\mathbf{s}_2)]\chi_{\sigma}\chi_{sM_s}|^2$$

$$= \frac{1}{2(2s+1)}\sum_{\sigma M_s}(\chi^*_{\sigma}\chi^*_{sMs}[\sigma\cdot(\mathbf{s}_1-\mathbf{s}_2)]^2\chi_{\sigma}\chi_{sM_s}) = 4s_1(s_1+1)-s(s+1).$$

The calculation of the space integral is just like the one done previously, and the final result for the scattering cross section with $j \to j'$ and change of parity is

$$\frac{d\sigma^{(2)}_{jj'}}{d\Omega} = \frac{k}{k_0}\frac{(A+1)^2}{(2A+1)^2}\frac{16}{(2s_1+1)^2}\left[s_1(s_1+1)-\frac{s(s+1)}{4}\right](a_{s_1+1/2}-a_{s_1-1/2})^2(2j'+1)\sum_{\text{odd } l}(C^{l0}_{j0j'0})^2 f_l^2\left(\frac{qr_0}{2}\right). \quad (4)$$

To get the total cross sections, (3) and (4) must be integrated over all solid angle. The procedure is the same as that of Hamermesh and Schwinger.[2] The result is

$$\sigma^{(1)}_{jj'} = \frac{(A+1)^2}{(2A+1)^2}\frac{1}{(2s_1+1)^2}\frac{64\pi}{(k_0r_0)^2}\left[((s_1+1)a_{s_1+1/2}+s_1a_{s_1-1/2})^2+\frac{s(s+1)}{4}(a_{s_1+1/2}-a_{s_1-1/2})^2\right](2j'+1)A_{jj'};$$

$$\sigma^{(2)}_{jj'} = \frac{(A+1)^2}{(2A+1)^2}\frac{1}{(2s_1+1)^2}\frac{64\pi}{(k_0r_0)^2}\left[\left(s_1(s_1+1)-\frac{s(s+1)}{4}\right)(a_{s_1+1/2}-a_{s_1-1/2})^2\right](2j'+1)A_{jj'};\quad A_{jj'} = \left[\mathrm{Cin}\,2x-\sum_l(C^{l0}_{j0j'0})^2 F_l(x)\right]_{x_1}^{x_2};$$

$$x_1 = \frac{|k-k_0|r_0}{2};\qquad x_2 = \frac{(k+k_0)r_0}{2};\qquad F_l(x) = 0,\quad l=0;\qquad F_l(x) = x^2(f_0^2+f_1^2),\quad l=1;$$

$$F_l(x) = x^2\left(f_0^2+\frac{1}{l}f_1^2+\sum_{k=1}^{l-1}\frac{2k+1}{k(k+1)}f_k^2\right),\quad l>1;\quad \mathrm{Cin}\,x = \ln x + C - \mathrm{Ci}\,x; \quad (5)$$

where Ci is the integral cosine, and C the Euler constant.

The next problem is the averaging of the cross sections $\sigma^{(1)}_{jj'}$ and $\sigma^{(2)}_{jj'}$ over those values of s which are present in a gas for a given value of j. For example, for half integer s_1 and even j the gas is a mixture of molecules with $s = 0, 2, \ldots, 2s_1-1$. Then the total number of initial states is

$$1+(2\cdot 2+1)+\ldots+[2(2s_1-1)+1]=s_1(2s_1+1).$$

The statistical weights of the individual states are

$$\begin{array}{llll} s=0, & 2, & \ldots & 2s_1-1 \\ g=1/s_1(2s_1+1), & (2\cdot 2+1)/s_1(2s_1+1), & \ldots, & (4s_1-1)/s_1(2s_1+1). \end{array}$$

In this case, after averaging, $s(s+1)$ should be replaced by

$$s(s+1)\to\sum_{(\text{even})}^{2s_1-1}\sum_{s=0}s(s+1)\frac{2s+1}{s_1(2s_1+1)}=(s_1+1)(2s_1-1).$$

If s_1 is integral and j odd, the replacement is

$$s(s+1)\to(s_1+1)(2s_1-1).$$

Similarly, for s_1 half integral, j odd, or s_1 integral and j even,

$$s(s+1)\to(s_1+1)(2s_1+3).$$

We give the cross sections for the following three processes: (1) elastic scattering, $j=0\to j'=0$; (2) elastic scattering, $j=1\to j'=1$; and (3) collision of the second kind, $j=1\to j'=0$. We assume that the incident neutron energy E is below the threshold E_1 for excitation of the first rotational level of the molecule (cf. Refs. 1, 2).

$$\sigma_{\substack{0\to 0\\1\to 1}}(E)=\left[((s_1+1)a_{s_1+1/2}+s_1a_{s_1-1/2})^2+\left\{\begin{array}{c}(s_1+1)(2s_1-1)/4\\ s_1(2s_1+3)/4\end{array}\right\}(a_{s_1+1/2}-a_{s_1-1/2})^2\right]F_{\substack{0\to 0\\1\to 1}}(E),$$

$$\sigma_{0\to 1}(E)=(a_{s_1+1/2}-a_{s_1-1/2})^2F_{0\to 1}(E);\quad F_{0\to 0}(E)=\frac{64\pi}{(2s_1+1)^2}\cdot\frac{(A+1)^2}{(2A+1)^2}\cdot\frac{1}{\xi^2}\operatorname{Cin}2\xi, \tag{6}$$

$$F_{1\to 1}(E)=\frac{64\pi}{(2s_1+1)^2}\frac{(A+1)^2}{(2A+1)^2}\cdot\frac{3}{\xi^2}\left[\operatorname{Cin}2\xi-\xi^2\left(\frac{2}{3}f_0^2(\xi)+f_1^2(\xi)+\frac{1}{3}f_2^2(\xi)\right)\right],$$

$$F_{0\to 1}(E)=\frac{64\pi}{(2s_1+1)^2}\frac{(A+1)^2}{(2A+1)^2}\left\{\begin{array}{c}s_1(2s_1+1)/4\\ (s_1+1)(2s_1+1)/4\end{array}\right\}\frac{1}{\xi^2}[\operatorname{Cin}2x-x^2(f_0^2+f_1^2)]_{\xi_1}^{\xi_2} \tag{7}$$

$$\xi=k_0r_0,\quad \xi_{1,2}=1/2(kr_0\mp k_0r_0).$$

In the formula for $\sigma_{\substack{0\to 0\\1\to 0}}$, the upper expression in the curly brackets is taken for half integral s_1 in $\sigma_{0\to 0}$ and for integral s_1 in $\sigma_{1\to 1}$; the lower expression applies when s_1 is half integral in $\sigma_{1\to 1}$ and when s_1 is integral in $\sigma_{0\to 0}$.

In $F_{0\to 1}(E)$, the upper expression should be used for half integral s_1 and the lower for integral S_1. Following the procedure of Ref. 2, we express ξ, ξ_1 and ξ_2 in terms of E and E_1

$$\xi=\frac{4}{2A+1}\sqrt{\frac{AE}{E_1}};\quad \xi_{1,2}=\frac{1}{2}\left[\sqrt{\xi^2+\frac{8}{2A+1}}\mp\xi\right]. \tag{8}$$

We give the expressions for $\sigma_{0\to 0}$, $\sigma_{1\to 1}$ and $\sigma_{0\to 1}$, which are obtained when $F_{0\to 0}(E)$, $F_{1\to 1}(E)$ and $F_{0\to 1}(E)$ are expanded in powers of E/E_1 up to first order terms, for the T_2 molecule:

$$\sigma_{0\to 0}=1/4(3a_1+a_0)^2F_{0\to 0}(E),\quad \sigma_{1\to 1}=1/4[(3a_1+a_0)^2+2(a_1-a_0)^2]F_{1\to 1}(E),\quad \sigma_{0\to 1}=(a_1-a_0)^2F_{0\to 1}(E),$$

$$F_{0\to 0}(E)\approx F_{1\to 1}(E)\approx\frac{256\pi}{49}\left(1-\frac{8}{49}\frac{E}{E_1}\right),\quad F_{0\to 1}(E)\approx\frac{64\pi}{49}\left(0.03201\sqrt{\frac{E_1}{E}}+0.06413\sqrt{\frac{E}{E_1}}\right). \tag{9}$$

The results for H_2 and D_2 were given in Refs. 1 and 2.

Finally, we can tackle the problem of averaging the cross section over the thermal motion of the gas molecules. The calculations are exactly like those of Hamermesh and Schwinger.[2] For the case of T_2, the functions $F_{0\to 0}$, $F_{1\to 1}$ and $F_{0\to 1}$ are replaced by $G_{0\to 0}$, $G_{1\to 1}$ and $G_{0\to 1}$. For $kT<6E$,

$$G_{0\to 0}(E)\approx G_{1\to 1}(E)\approx\frac{256\pi}{49}\left[1+\frac{1}{12}\frac{kT}{E}-\frac{8}{49}\frac{E}{E_1}\left(1+\frac{1}{2}\frac{kT}{E}+\frac{1}{48}\left(\frac{kT}{E}\right)^2\right)\right],$$

$$G_{0\to 1}(E)\approx\frac{64\pi}{49}\left[0.03201\sqrt{\frac{E_1}{E}}+0.06413\sqrt{\frac{E}{E_1}}\left(1+\frac{1}{4}\frac{kT}{E}\right)\right]. \tag{10}$$

2. SCATTERING OF NEUTRONS BY MOLECULES CONSISTING OF TWO DIFFERENT ATOMS

In this section, we treat neutron scattering by non-symmetric molecules. The ground state of a non-symmetric molecule always has rotational quantum number j = 0, so that when the energy E of the incident neutron is insufficient for excitation of rotation, of three processes treated above the only one which remains is the elastic scattering with j = 0 → j′ = 0.

In addition, since the assignment of j now imposes no limitations on the molecular spin s, the averaging of the cross section over s and s′ can be done very simply. In fact, in the present case we need only calculate the sum

$$\frac{1}{(2j+1)\,2\,(2s_1+1)\,(2s_2+1)}\sum_{(ss'M_sM'_s\sigma\sigma'\mu\mu')}\sigma_{jj'}(ss'M_sM'_s\sigma\sigma'\mu\mu')$$

over all values of $ss'\,M_S M'_S\sigma\sigma'\mu\mu'$ ($\sigma_{jj'}$ is the cross section for the transition from $j\mu s M_S\sigma$ to $j'\mu' s' M'_S\sigma'$.

The interaction energy of the neutron and molecule is now

$$\hat{U}=-\frac{2\pi\hbar^2}{M_c}\Big\{\frac{A_1+1}{A_1}\frac{1}{2s_1+1}\left[(s_1+1)\,a_{s_1+1/2}+s_1a_{s_1-1/2}\right]\delta^3(\mathbf{r}-\mathbf{r}_1)+\frac{A_2+1}{A_2}\frac{1}{2s_2+1}\left[(s_2+1)\,a_{s_2+1/2}+s_2a_{s_2-1/2}\right]\delta^3(\mathbf{r}-\mathbf{r}_2)$$

$$+\frac{1}{2}(\boldsymbol{\sigma}\cdot\mathbf{s})\Big[\frac{A_1+1}{A_1}\frac{1}{2s_1+1}(a_{s_1+1/2}-a_{s_1-1/2})\,\delta^3(\mathbf{r}-\mathbf{r}_1)+\frac{A_2+1}{A_2}\frac{1}{2s_2+1}(a_{s_2+1/2}-a_{s_2-1/2})\,\delta^3(\mathbf{r}-\mathbf{r}_2)\Big]$$

$$+\frac{1}{2}[\boldsymbol{\sigma}\cdot(\mathbf{s}_1-\mathbf{s}_2)]\Big[\frac{A_1+1}{A_1}\frac{1}{2s_1+1}(a_{s_1+1/2}-a_{s_1-1/2})\,\delta^3(\mathbf{r}-\mathbf{r}_1)-\frac{A_2+1}{A_2}\frac{1}{2s_2+1}(a_{s_2+1/2}-a_{s_2-1/2})\,\delta^3(\mathbf{r}-\mathbf{r}_2)\Big]\Big\} \qquad (11)$$

[the notation is the same as in Eq. (1)]. The wave functions of the initial and final states are:

$$\Psi_1=\exp\{i\mathbf{k}_0(\mathbf{r}-\mathbf{r}_c)\}\,Y_{j\mu}\Big(\frac{1}{l}\Big)\frac{\sqrt{\delta(l-r_0)}}{r_0}\chi_\sigma\chi_{sM_s},\quad \Psi_2=\exp\{i\mathbf{k}_1(\mathbf{r}-\mathbf{r}_c)\}\,Y_{j'\mu'}\Big(\frac{1}{l}\Big)\frac{\sqrt{\delta(l-r_0)}}{r_0}\chi_{\sigma'}\chi_{s'M'_s}, \qquad (12)$$

where now

$$\mathbf{r}_c=(A_1\mathbf{r}_1+A_2\mathbf{r}_2)/(A_1+A_2).$$

The calculation of the spin sums is somewhat lengthy, but entirely trivial. The expression for the j → j′ cross section now does not depend on the relative parity of j and j′, and has the form

$$\frac{d\sigma_{jj'}}{d\Omega}=\frac{k}{k_0}\frac{(A_1+A_2)^2}{(A_1+A_2+1)^2}\sum_{\mu\mu'}\frac{1}{(2j+1)}\{|B|^2+(|C|^2+|D|^2)\,[s_1(s_1+1)+s_2(s_2+1)]$$

$$+(C^*D+CD^*)\,[s_1(s_1+1)-s_2(s_2+1)]\},\quad B=\alpha_1I_1+\alpha_2I_2,\quad \alpha_i=\frac{A_i+1}{A_i}\frac{1}{2s_i+1}\left[(s_i+1)\,a_{s_i+1/2}+s_ia_{s_i-1/2}\right],$$

$$C=\frac{1}{2}(\beta_1I_1+\beta_2I_2),\quad \beta_i=\frac{A_i+1}{A_i}\frac{1}{2s_i+1}\left[a_{s_i+1/2}-a_{s_i-1/2}\right],\quad D=\frac{1}{2}(\beta_1I_1-\beta_2I_2),\quad I_i=\int\varphi_2^*\delta^3(\mathbf{r}-\mathbf{r}_i)\,\varphi_1 d\mathbf{r}d\mathbf{r}_1d\mathbf{r}_2,$$

where φ_1 and φ_2 are the coordinate parts of the wave functions (12).

The calculation of the integrals is completely analogous to those in the first section. The result is

$$\frac{1}{(2j+1)}\sum_{\mu\mu'}|I_1|^2=(2j'+1)\sum_l(C^{l0}_{j0j'0})^2f_l^2\Big(\frac{q_1r_0}{2}\Big),\quad \frac{1}{(2j+1)}\sum_{\mu\mu'}|I_2|^2=(2j'+1)\sum_l(C^{l0}_{j0j'0})^2f_l^2\Big(\frac{q_2r_0}{2}\Big),$$

$$\frac{1}{(2j+1)}\sum_{\mu\mu'}I_1I_2=\frac{1}{(2j+1)}\sum_{\mu\mu'}I_1I_2^*=(2j'+1)\sum_l(-1)^l(C^{l0}_{j0j'0})^2f_l\Big(\frac{q_1r_0}{2}\Big)f_l\Big(\frac{q_2r_0}{2}\Big),\quad q_1=\frac{2A_2}{A_1+A_2}(\mathbf{k}_0-\mathbf{k}),$$

$$q_2=\frac{2A_1}{A_1+A_2}(\mathbf{k}_0-\mathbf{k}).$$

The expression for the differential cross section is

$$\frac{d\sigma_{jj'}}{d\Omega}=\frac{k}{k_0}\frac{(A_1+A_2)^2}{(A_1+A_2+1)^2}\left[G_{jj'}+s_1(s_1+1)\,Q^{(1)}_{jj'}+s_2(s_2+1)\,Q^{(2)}_{jj'}\right],$$

$$G_{jj'}=(2j'+1)\sum_l(C^{l0}_{j0j'0})^2\left[\alpha_1f_l\Big(\frac{q_1r_0}{2}\Big)+(-1)^l\alpha_2f_l\Big(\frac{q_2r_0}{2}\Big)\right]^2,\quad Q^{(i)}_{jj'}=(2j'+1)\sum_l(C^{l0}_{j0j'0})^2\beta_i^2f_l^2\Big(\frac{q_ir_0}{2}\Big)\quad (i=1,2). \qquad (15)$$

The total cross section for elastic scattering, j = 0 → j′ = 0, is

$$\sigma = \pi \frac{(A_1+A_2)^4}{A_1^2A_2^2(A_1+A_2+1)^2} \left\{\frac{(A_1+1)^2}{(2s_1+1)^2}\left[((s_1+1)a_{s_1+1/2}+s_1a_{s_1-1/2})^2+s_1(s_1+1)(a_{s_1+1/2}-a_{s_1-1/2})^2\right]\frac{1}{\xi^2}\operatorname{Cin}2\lambda_1\xi\right. \quad (16)$$

$$+ \text{ similar terms with } 1\to 2 + 4\frac{(A_1+1)(A_2+1)}{(2s_1+1)(2s_2+1)}((s_1+1)a_{s_1+1/2}+s_1a_{s_1-1/2})((s_2+1)a_{s_2+1/2}+s_2a_{s_2-1/2})\frac{1}{\xi^2}R(\xi,\lambda_1,\lambda_2),$$

where

$$\lambda_1 = \frac{2A_2}{A_1+A_2}, \quad \lambda_2 = \frac{2A_1}{A_1+A_2}, \quad \xi = k_0r_0 = \frac{A_1+A_2}{A_1+A_2+1}\sqrt{\frac{2(A_1+A_2)}{A_1A_1}}\sqrt{\frac{E}{E_1}}; \quad R(\xi,\lambda_1,\lambda_2) = \int_0^\xi \frac{\sin\lambda_1 t\sin\lambda_2 t}{t}\,dt$$

$$= \frac{1}{2}\left[\ln\frac{\lambda_1+\lambda_2}{|\lambda_1-\lambda_2|} + \operatorname{Ci}[|\lambda_1-\lambda_2|\xi] - \operatorname{Ci}[(\lambda_1+\lambda_2)\xi]\right].$$

Using the well-known expansion of the integral cosine, we find, for $E \ll E_1$, to terms of order $\sim E/E_1$:

$$\sigma = \frac{(A_1+A_2)^2}{(A_1+A_2+1)^2}\left\{\sigma_1\left(\frac{A_1+1}{A_1}\right)^2\left[1-\frac{4}{3}\frac{A_2}{A_1}\frac{A_1+A_2}{(A_1+A_2+1)^2}\frac{E}{E_1}\right]+\sigma_2\left(\frac{A_2+1}{A_2}\right)^2\left[1-\frac{4}{3}\frac{A_1}{A_2}\frac{A_1+A_2}{(A_1+A_2+1)^2}\frac{E}{E_1}\right]\right. \quad (17)$$

$$\left. + 8\pi\frac{A_1+1}{A_1}\frac{A_2+1}{A_2}\left[\frac{s_1+1}{2s_1+1}a_{s_1+1/2}+\frac{s_1}{2s_1+1}a_{s_1-1/2}\right]\left[\frac{s_2+1}{2s_2+1}a_{s_2+1/2}+\frac{s_2}{2s_2+1}a_{s_2-1/2}\right]\left[1-\frac{2}{3}\frac{A_1^2+A_2^2}{A_1A_2}\frac{A_1+A_2}{(A_1+A_2+1)^2}\frac{E}{E_1}\right]\right\}$$

We have introduced the scattering cross section for the i-th atom

$$\frac{1}{4\pi}\sigma_i = \frac{s_i+1}{2s_i+1}|a_{s_i+1/2}|^2+\frac{s_i}{2s_i+1}|a_{s_i-1/2}|^2 \quad (i=1,2). \quad (18)$$

We apply formula (17) to HD, HT, and DT. (We give the cross sections averaged over the thermal motion of the molecules.)

For the HD molecule (a_0 and a_1 are the scattering amplitudes for H, $a_{1/2}$ and $a_{3/2}$ are the amplitudes for D)

$$\sigma_{HD} = \left[\frac{9}{4}\sigma_H+\frac{81}{64}\sigma_D+\frac{9\pi}{8}(3a_1+a_0)(2a_{3/2}+a_{1/2})\right]\left(1+\frac{1}{6}\frac{kT}{E}\right)$$
$$-\left[\frac{9}{8}\sigma_H+\frac{81}{512}\sigma_D+\frac{45\pi}{128}(3a_1+a_0)(2a_{3/2}+a_{1/2})\right]\frac{E}{E_1}\left(1+\frac{kT}{E}+\frac{1}{12}\left(\frac{kT}{E}\right)^2\right) \quad (19)$$

For the HT molecule (a_0 and a_1 are the H scattering amplitudes, b_0 and b_1 are the T scattering amplitudes)

$$\sigma_{HT} = \left[\frac{64}{25}\sigma_H+\frac{256}{225}\sigma_T+\frac{64\pi}{75}(3a_1+a_0)(3b_1+b_0)\right]\left(1+\frac{1}{8}\frac{kT}{E}\right)-\left[\frac{1024}{625}\sigma_H+\frac{4096}{50625}\sigma_T+\frac{1024\pi}{3375}(3a_1+a_0)(3b_1+b_0)\right]$$
$$\times\frac{E}{E_1}\left(1+\frac{3}{4}\frac{kT}{E}+\frac{3}{64}\left(\frac{kT}{E}\right)^2\right). \quad (19')$$

For the DT molecule

$$\sigma_{DT} = \left[\frac{25}{16}\sigma_D+\frac{1100}{81}\sigma_T+\frac{25\pi}{27}(2a_{3/2}+a_{1/2})(3b_1+b_0)\right]\left(1+\frac{1}{10}\frac{kT}{E}\right)-\left[\frac{125}{288}\sigma_D+\frac{1000}{6561}\sigma_T+\frac{1625\pi}{8748}(2a_{3/2}+a_{1/2})(3b_1+b_0)\right]$$
$$\times\frac{E}{E_1}\left(1+\frac{3}{5}\frac{kT}{E}+\frac{3}{100}\left(\frac{kT}{E}\right)^2\right). \quad (19'')$$

3. INCLUSION OF ZERO-POINT VIBRATIONS OF THE MOLECULE

All the computations done in the previous sections were based on the rigid rotator model for the molecule, i.e., on a molecule having a fixed internuclear distance r_0. This was expressed mathematically in the use of $\sqrt{\delta(l-r_0)}/r_0$ as the radial part of the wave function, in place of the appropriate oscillator functions. Our next problem is to examine the validity of this approximation, and to include the normal vibrations of the molecule at least to first approximation. The analogous problem for the hydrogen molecule was considered recently by Drozdov.[4]

We shall restrict ourselves to treating the zero point vibrations, since the excitation of higher vibrational levels is much more difficult than rotational excitation. In addition, we shall treat only elastic scattering with $j = 0 \to j' = 0$ and $j = 1 \to j' = 1$ for symmetric molecules.

Carrying out the calculations, which are exactly the same as those in Sec. 1, we easily verify that the only change from our previous results is that, in formulas (3) and (4), the quantities $f_l^2(qr_0/2)$ are replaced by the integral:

$$I_l = \sqrt{\frac{\alpha}{\pi}} \int_0^\infty f_l\left(\frac{ql}{2}\right) e^{-\alpha(l-r_0)^2} dl \approx \sqrt{\frac{\alpha}{\pi}} \int_{-\infty}^{+\infty} f_l\left(\frac{q}{2}(r_0+r)\right) e^{-\alpha r^2} dr,$$

where $\alpha = 1/x_0^2 = \mu\omega/\hbar$, μ is the reduced mass of the molecule, and ω the frequency of zero point vibration of the molecule.

To calculate the integral I_l approximately, we expand the slowly varying Bessel function f_l in series around the point $qr_0/2$, and integrate term by term. Then $A_{jj'}$ in formula (5) is changed to

$$A_{jj'} = \sum_l (C_{j0l'0}^{l0})^2 \left[2 \int_{x_1}^{x_2} f_l^2(x)\, x\, dx + \left(\frac{x_0}{r_0}\right)^2 \int_{x_1}^{x_2} f_l(x) f_l''(x)\, x^2 dx \right].$$

We note that $x_0 = (\hbar/\mu\omega)^{1/2} = (2\hbar/AM\omega)^{1/2}$, $r_0 = (2\hbar^2/AME_1)^{1/2}$, so that

$$(x_0/r_0)^2 = E_1/\hbar\omega.$$

Our computation corresponds to the first approximation with respect to $E/\hbar\omega$; in order to avoid dropping terms of this same order, we must also keep quadratic terms in E/E_1.

After expanding in series, we get the following final result for T_2 [cf. Eq. (19)]:

$$F_{0\to 0}(E) = \frac{256\pi}{49}\left[1 - \frac{8}{49}\left(\frac{E}{E_1} + \frac{E}{2\hbar\omega}\right) + \frac{512}{15\cdot 7^4}\left(\frac{E}{E_1}\right)^2\right], \quad F_{1\to 1}(E) = \frac{256\pi}{49}\left[1 - \frac{8}{49}\left(\frac{E}{E_1} + \frac{E}{2\hbar\omega}\right) + \frac{1024}{25\cdot 7^4}\left(\frac{E}{E_1}\right)^2\right].$$

The correction may be $2-3\%$ of the leading term which gives the dependence on the energy E/E_1.

DISCUSSION OF RESULTS

The results obtained can be used for the solution of an important experimental problem: the determination of the amplitudes a_0 and a_1 for scattering of slow neutrons by tritium.

According to formulas (9) and (10), if we know the elastic scattering cross section for paratritium ($\sigma_{0\to 0}$), orthotritium ($\sigma_{1\to 1}$) or the cross section for scattering with transition of the molecule from the ortho to the para state ($\sigma_{0\to 1}$), we can determine the absolute values and relative sign of the amplitudes a_0 and a_1. The common sign of the amplitudes cannot be determined from the values of these cross sections. (A change in sign of both amplitudes produces no change in the values of $\sigma_{0\to 0}$, $\sigma_{1\to 1}$ and $\sigma_{0\to 1}$.)

One possibility for determining this common sign is to investigate the scattering of neutrons by molecules consisting of T and any other atom whose neutron scattering amplitudes are known. The formulas (19) show how the interference term depends on the common sign of the amplitudes. Unfortunately, this term is usually smaller than the other terms appearing in the formula.

A final decision on the question of determining the common sign of the amplitudes can be made only by examining the experimental accuracy attainable.

In conclusion, I express my profound gratitude to K. A. Ter-Martirosian for proposing this topic and for continual interest in the work.

[1] J. Schwinger and E. Teller, Phys. Rev. 52, 286 (1937).
[2] M. Hamermesh and J. Schwinger, Phys. Rev. 69, 145 (1946).
[3] E. Fermi, Ricerca Sci. 7, 13 (1936).
[4] S. I. Drozdov, Атомная энергия (Atomic Energy) 3, 50 (1956).

Translated by M. Hamermesh
126

ON THE SCATTERING OF LIGHT IN $He^3 - He^4$ *MIXTURES*

L. P. GOR'KOV and L. P. PITAEVSKII

Institute of Physical Problems, Academy of Sciences, U.S.S.R.

Submitted to JETP editor March 25, 1957

J. Exptl. Theoret. Phys. (U.S.S.R.) **33**, 634-636 (September, 1957)

The scattering of light in $He^3 - He^4$ mixtures below the λ-point is considered. It is shown that the spectrum of the scattered light will contain five lines. Formulas are presented for the intensities of these lines, and the question of their width is discussed briefly.

THE scattering of light in $He^3 - He^4$ mixtures has certain peculiarities as compared with the scattering in pure He^4. In He^4, as Ginzburg[1] has shown, two doublets should be observed, corresponding to scattering by first and second sound; the undisplaced line is absent. Unfortunately, the small amount of separation in the inner doublet, and, in particular, its low intensity, make it difficult to observe this effect experimentally. In $He^3 - He^4$ mixtures there would appear to be greater opportunities for observing peculiarities in the scattering of light resulting from superfluid motion. The recent results of Walters and Fairbank,[2] moreover, show that at temperatures below 0.8° a given $He^3 - He^4$ mixture separates into phases of differing concentration, in connection with which there evidently occurs in the diagram of state a critical point situated in the region in which the two superfluid mixtures exist in equilibrium. In the vicinity of this point the phenomenon of critical opalescence should be observed in the scattering of light. The spectrum of the scattered light should contain five lines, of which four compose the two doublets corresponding to scattering by the fluctuations of first and second sound, while the fifth line represents scattering by stationary (if we neglect thermal conductivity and diffusion) fluctuations in concentration and entropy of a special type.

In computing the fluctuations we shall start with the following expression for the probability for thermodynamic fluctuations in the temperature T, the pressure p, and the mass concentration c

$$W \sim \exp\left\{-\frac{1}{2kT}\left[\rho\frac{\partial\sigma}{\partial T}\Delta T^2 + \frac{2}{\rho}\frac{\partial\rho}{\partial T}\Delta T\Delta p + \frac{1}{\rho}\frac{\partial\rho}{\partial c}\Delta\rho^2 + \rho\frac{\partial(Z/\rho)}{\partial c}\Delta c^2\right]\right\}. \quad (1)$$

Here and below we employ the notation used in the work of Khalatnikov:[3] ρ is the density; σ is the entropy per unit mass; $Z = \rho(\mu_3 - \mu_4)$, where μ_3 and μ_4 are the chemical potentials per unit mass, respectively, for He^3 and He^4. In what follows we shall everywhere neglect terms containing $\partial\rho/\partial T$, considering them to be small. With this approximation all of the fluctuations prove to be independent.

The extinction coefficient for total scattering turns out to be

$$h = \frac{\omega^4 kT}{6\pi c^4}\left[\rho\frac{\partial\rho}{\partial p}\left(\frac{\partial\varepsilon}{\partial p}\right)^2 + \left(\frac{\partial\varepsilon}{\partial T}\right)^2\frac{T}{\rho c_p} + \left(\frac{\partial\varepsilon}{\partial c}\right)^2\left(\rho\frac{\partial(Z/\rho)}{\partial c}\right)^{-1}\right], \quad (2)$$

where ε is the dielectric constant and c_p is the specific heat at constant pressure. In this expression the third term is the principal one; at the critical point $\partial(Z/\rho)/\partial c$ falls to zero and the intensity of the scattered light rises sharply. Experimental data are completely lacking for nearly all of the quantities entering into the theory, for mixtures in the concentration range (~ 50%) in which we are interested. Rough estimates show that we may regard all terms containing $\partial\varepsilon/\partial T$ as small.*

The lines of the doublets corresponding to scattering by the fluctuations of first and second sound are displaced relative to the primary frequency ω by an amount

$$\Delta\omega = \pm 2\omega(u/c)\sin(\theta/2),$$

where θ is the angle between the directions of the incident and scattered waves.

The velocities of first and second sound are[3]

*It is also obvious that the quantities $\rho(\partial\varepsilon/\partial\rho)$ and $c(\partial\varepsilon/\partial c)$ are of the same order.

$$u_1^2=\left(\frac{\partial p}{\partial \rho}\right)_{c,T}\left[1+\frac{\rho_s}{\rho_n}\left(\frac{c}{\rho}\frac{\partial \rho}{\partial c}\right)^2\right],\quad u_2^2=\left(\frac{\partial p}{\partial \rho}\right)_{c,T}\frac{\rho_s}{\rho_n u_1^2}\left[\bar{\sigma}^2\left(\frac{\partial T}{\partial \sigma}\right)_{c\rho}+c^2\frac{\partial (Z/\rho)}{\partial c}\right]$$

($\bar{\sigma}=\sigma-c\partial\sigma/\partial c$). As is well known, $u_1^2 \gg u_2^2$; the separation of the inner doublet is therefore extremely small ($\Delta\omega/\omega \sim 10^{-7}$). In the sound wave, the relations between the deviations of the various quantities from their equilibrium values have the following form:

$$\delta c=-\left[\frac{\partial p}{\partial p}u^2-1\right]\delta p\Big/\frac{\partial p}{\partial c}u^2,$$

where u is the corresponding sound velocity. Computing the value of the fluctuations $\overline{(\delta\epsilon)^2}$ from Eq. (1), using these relations, we obtain for the intensities of the first and second sound doublets:

$$h_I=\frac{\omega^4}{6\pi c^4}\frac{\rho kT}{(\partial p/\partial\rho)_{T,c}}\left[\frac{\partial \varepsilon}{\partial \rho}-\left(\frac{c}{\rho}\frac{\partial \varepsilon}{\partial c}\right)\left(\frac{\rho_s}{\rho_n}\right)\frac{(\partial p/\partial\rho)_{T,c}}{u_1^2}\left(\frac{c}{\rho}\frac{\partial \rho}{\partial c}\right)\right]^2,\quad h_{II}=\frac{\omega^4}{6\pi c^4}\frac{\rho kT}{(\partial p/\partial\rho)_{T,c}}\left[\left(\frac{\rho_s}{\rho_n}\right)\left(\frac{c}{\rho}\frac{\partial \varepsilon}{\partial c}\right)^2\frac{(\partial p/\partial\rho)^2_{T,c}}{u_1^2u_2^2}\right].$$

It follows from this that the intensity of the second doublet is $\sim (u_1/u_2)^2$ ($\sim 10^2$) times that of the first sound doublet, in contrast with the situation for pure helium. The intensity of the first doublet will evidently differ only slightly from its value for the case of pure He^4 ($\sim 10^{-8}$). The fifth line in the spectrum of the scattered light arises as a consequence of the possibility for existence in the mixture of fluctuations of a third type, described by the conditions:[3]

$$p=\text{const},\quad \mu_4=\text{const}.$$

By virtue of these conditions the variations in the thermodynamic quantities are interrelated in the following manner:

$$\delta p=0,\quad \delta T=-\frac{c}{\bar{\sigma}}\frac{\partial (Z/\rho)}{\partial c}\delta c.$$

Computing with the aid of these relations the intensity of the undisplaced line, we obtain

$$h_0=\frac{\omega^4}{6\pi c^4}\frac{\rho kT}{(\partial p/\partial\rho)_{T,c}}\left[\left(\frac{\rho_s}{\rho_n}\right)\left(\frac{c}{\rho}\frac{\partial \varepsilon}{\partial c}\right)^2\frac{\bar{\sigma}^2(\partial T/\partial\sigma)(\partial p/\partial\rho)^2_{T,c}}{c^2(\partial (Z/\rho)/\partial c)u_1^2u_2^2}\right].\qquad(3)$$

Away from the critical point for the mixture the intensity of the central line has approximately the same order of magnitude as the intensity of the inner doublet. For the order-of-magnitude estimation it is convenient to use the relation between the derivatives[3]

$$\left(\frac{\rho_s}{\rho_n}\right)\left[\bar{\sigma}^2\frac{\partial T}{\partial \sigma}+c^2\frac{\partial (Z/\rho)}{\partial c}\right]=u_1^2u_2^2(\partial\rho/\partial p)_{T,c}.$$

At the critical point, where $\partial(Z/\rho)/\partial c = 0$, the coefficient h_0 calculated from (3) goes to infinity. In order to treat the scattering in the immediate vicinity of the critical point, therefore, it is necessary to allow for the correlation of fluctuations in the concentration, adding into the exponential of Eq. (1) a term of the form $(b/2)(\nabla c)^2$, where b is some constant. We shall omit presentation of the formulas for the intensity of the scattered light and its angular distribution, which may be obtained from this expression in the usual manner.

We shall consider briefly the question of the width of the lines. The width of the lines in the first and second doublets is determined in the usual manner, using the attenuation coefficients for first and second sound, respectively.

The width of the undisplaced line is determined from the rate of resorption of the corresponding fluctuations, and is expressed in terms of the diffusion and thermal conductivity coefficients. Calculations yield for the width the value

$$\gamma=\frac{2\omega^2}{c^2}(1-\cos\theta)\frac{\frac{\partial (Z/\rho)}{\partial c}\left\{\varkappa+\frac{\rho DT}{\partial (Z/\rho)/\partial c}\left[c\frac{\partial \sigma/c}{\partial c}+\frac{k_T\partial (Z/\rho)}{T\ \partial c}\right]^2\right\}}{\rho\left[T\left(c\frac{\partial \sigma/c}{\partial c}\right)^2+c_p\frac{\partial (Z/\rho)}{\partial c}\right]},$$

where κ, k_T, and D are the thermal conductivity, thermodiffusion, and diffusion coefficients for the mixture. At the critical point γ is determined by the diffusion coefficient. From unpublished measurements by Zinov'eva the viscosity coefficient for He^3 is of the same magnitude as for He^4, and is on the order of

10^{-4} cm^2/sec. Taking D to be of the same order as the kinematic viscosity, we obtain near the critical point the rough estimate $\gamma/\omega \sim 10^{-9}$, which is less than the separation of the lines of the inner doublet.

In conclusion, the authors wish to express their gratitude to I. E. Dzialoshinskii for his helpful discussions, and K. N. Zinov'eva for communication of results of her measurements prior to their publication.

[1] V. L. Ginzburg, J. Exptl. Theoret. Phys. (U.S.S.R.) **13**, 243 (1943).
[2] G. K. Walters and W. M. Fairbank, Phys. Rev. **103**, 262 (1956).
[3] I. M. Khalatnikov, Usp. Fiz. Nauk **59**, 673 (1956); **60**, 70 (1956).

Translated by S. D. Elliott
127

SOVIET PHYSICS JETP VOLUME 6 (33), NUMBER 3 MARCH, 1958

SOLUTION OF THE KINETIC EQUATIONS FOR HIGH-ENERGY NUCLEAR CASCADE PROCESSES

N. M. GERASIMOVA

P. N. Lebedev Physics Institute, Academy of Sciences, U.S.S.R.

Submitted to JETP editor February 4, 1957

J. Exptl. Theoret. Phys. (U.S.S.R.) **33**, 637-644 (September, 1957)

The altitude dependence of high-energy nuclear-active particles and the spectrum of the μ mesons produced by the decay of π mesons are investigated. The elementary act is described hydrodynamically; the energy distribution function used for the particles produced is that of Landau, corrected to take account of the traveling wave in the hydrodynamical solution.

LANDAU'S hydrodynamic theory of the multiple production of particles[1] gives agreement with experiment as to the multiplicity and angular distribution of the secondary particles.[2] But the energy distribution obtained by Landau gives more fractionation of the energy among the particles produced than is observed experimentally. According to Grigorov's data,[3] in high energy nuclear interactions (at about $10^{10} - 10^{12}$ ev) a larger part of the energy remains with one of the particles produced. In this connection Zatsepin and Guzhavin[4] have made numerical calculations of the altitude dependence of the density spectrum of showers, using a phenomenological introduction of such a particle into the description of the elementary act. The results were found to be in good agreement with experiment. In a paper by Chernavskii and the writer[5] it was shown that the inclusion of a traveling wave in the hydrodynamical equation leads to the necessity of introducing a fast particle into the Landau distribution. At present the fraction α of the energy carried away by the fastest of the secondary particles produced cannot be precisely determined theoretically and must be regarded as a parameter.

The disintegration temperature T_k of the hydrodynamical system also appears as a parameter in the theory. In view of the absence of precise data on the index of the energy spectrum of the primary particles and on the interaction distance of particles at high energies, it is also particularly desirable to obtain explicity relations characterizing the passage of high-energy particles through the atmosphere. By the method of successive generations Rozental' has determined the number of particles in an individual shower as a function of α and the fraction of the energy transferred to the soft component. In the present paper we find the solution of the kinetic equations for high-energy ($E \gtrsim 10^{12}$ ev) nuclear cascade processes in the atmosphere and use it to determine the absorption coefficient of particles interacting strongly with nuclei and the spectrum of the μ mesons produced from the decay of π mesons.

The experimental data indicate the production in stars of heavy mesons, hyperons, and nucleons, in addition to π mesons. The most important contribution for a nuclear cascade process is that of the nucleons, since initial nucleons also take part in the development of the cascades. Therefore we shall assume that π mesons and nucleons are produced in the elementary act. Then the numbers of π mesons and of nucleons produced in the energy range (E, E + dE) as the result of the collision of a particle of energy E′ with a nucleus of air are written

$$dN^{\pi}(E, E') = \pi_1(E')\,\delta(E - \alpha E')\,dE + dN_L^{\pi}[E, (1-\alpha)E'], \quad dN^{N}(E, E') = H_1(E')\,\delta(E - \alpha E')\,dE + dN_L^{N}[E, (1-\alpha)E']. \quad (1)$$

The first terms in Eq. (1) give the probability of formation of one particle with energy $\alpha E'$, and the second terms correspond to the distribution for the other particles: dN_L and dN_L^N are the Landau distributions, in which, as also in the first terms, we introduce coefficients corresponding to the ratios of the numbers of particles of different kinds and their energies as calculated by Belen'kii,[6,7] and satisfying the basic relations

$$N = N^{\pi} + N^{N}; \quad \int E^{\pi} dN_L^{\pi} + \int E^{N} dN_L^{N} = (1-\alpha)E'.$$

The second relation is related to the parametric statement of the Landau formulas and leads to the appearance in the energy distributions for E^{π} and E^{N} of the factors $\pi_2(E')(1-\alpha)$ and $H_2(E')(1-\alpha)$, respectively, instead of the factors $\pi_1(E')$ and $N_1(E')$ of the distributions of the numbers of particles (cf. Ref. 8).

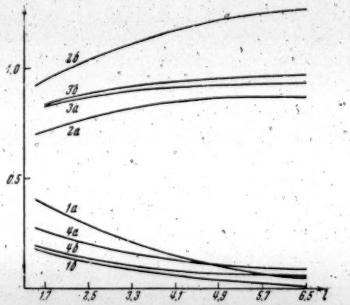

The curves show the various coefficients as functions of ℓ, as follows: $1 - H_1$, $2 - \ln H_2$, $3 - \pi_1$, $4 - \ln \pi_2$; curves a are for $kT_k = M_{\pi}c^2$, and curves b for $kT_k = 1/2 M_{\pi}c^2$.

The diagram shows the energy dependences of π_1, H_1, $\ln\pi_2$, and $\ln H_2$, expressed on a logarithmic scale [$\ell = \frac{1}{2}(\ln E - 24.2)$], with the same notations as in Ref. 8, here and in what follows.

With the distributions (1) one solves the system of kinetic equations for the numbers of nucleons, $\mathcal{F}^{N}(E, t)$, and of π mesons, $\mathcal{F}(E, t)$, present at the given depth t and with energies between E and E + dE:

$$\frac{\partial \mathcal{F}^{N}(E,t)}{\partial t} = -\mathcal{F}^{N}(E,t) + \int_E^{\infty} \frac{dN^{N}(E',E)}{dE}\,\mathcal{F}^{N}(E',t)\,dE' + \int \frac{dN^{N}(E',E)}{dE}\,\mathcal{F}^{\pi}(E',t)\,dE';$$

$$\frac{\partial \mathcal{F}^{\pi}(E,t)}{\partial t} = -\mathcal{F}^{\pi}(E,t) + \frac{2}{3}\int_E^{\infty} \frac{dN^{\pi}(E'E)}{dE}\,\mathcal{F}^{\pi}(E',t)\,dE' + \frac{2}{3}\int_E^{\infty} \frac{dN^{\pi}(E',E)}{dE}\,\mathcal{F}^{N}(E',t)\,dE'. \quad (2)$$

Here the depth t is measured in units t_0; the factor 2/3 allows for the fact that neutral π mesons play no part in the development of the nuclear-active component. We neglect the decay of the π mesons. As boundary condition for the equations (2) one assumes a power-law spectrum of the primary nucleons:

$$\mathcal{F}^{N}(E, 0) = BE^{-\gamma+1}; \quad \mathcal{F}^{\pi}(E, 0) = 0.$$

Substituting the distributions (1) into Eq. (2) and making the substitution

$$\mathcal{F}^{N}(E,t) = e^{-t}P^{N}(E,t), \quad \mathcal{F}^{\pi}(E,t) = e^{-t}P^{\pi}(E,t),$$

we get

$$\frac{\partial P^{N}(E,t)}{\partial t} = \frac{1}{\alpha}H_1\left(\frac{E}{\alpha}\right)P^{N}\left(\frac{E}{\alpha}, t\right) + \frac{1}{\alpha}H_1\left(\frac{E}{\alpha}\right)P^{\pi}\left(\frac{E}{\alpha}, t\right) + \int_E^{\infty}\frac{dN_L^{N}}{dE}P^{N}(E',t)\,dE' + \int_E^{\infty}\frac{dN_L^{N}}{dE}P^{\pi}(E',t)\,dE',$$

$$\frac{\partial P^{\pi}(E,t)}{\partial t} = \frac{1}{\alpha}\pi_1\left(\frac{E}{\alpha}\right)P^{\pi}\left(\frac{E}{\alpha}, t\right) + \frac{1}{\alpha}\pi_1\left(\frac{E}{\alpha}\right)P^{N}\left(\frac{E}{\alpha}, t\right) + \int_E^{\infty}\frac{dN_L^{\pi}}{dE}P^{\pi}(E',t)\,dE' + \int_E^{\infty}\frac{dN_L^{\pi}}{dE}P^{N}(E',t)\,dE'. \quad (3)$$

We seek the solution of the equations (3) in the form

$$P^{N}(E,t)=\frac{B}{E^{\gamma+1}}\exp\left\{\omega\left(\frac{E}{\alpha}\right)\alpha^{\gamma}t\right\}[1+\chi_{1}^{N}(E,t)+\cdots],\quad P^{\pi}(E,t)=\frac{B}{E^{\gamma+1}}\exp\left\{\omega\left(\frac{E}{\alpha}\right)\alpha^{\gamma}t\right\}[\chi_{1}^{\pi}(E,t)+\cdots],$$
$$\omega\left(\frac{E}{\alpha}\right)\equiv H_{1}\left(\frac{E}{\alpha}\right)+\frac{2}{3}\pi_{1}\left(\frac{E}{\alpha}\right). \tag{4}$$

The choice of the zeroth approximation

$$P_{0}^{N}(E,t)=\frac{B}{E^{\gamma+1}}\exp\left[\omega\left(\frac{E}{\alpha}\right)\alpha^{\gamma}t\right]$$

is due to the assumption that the fraction α is large and that the main terms in Eq. (1) are those containing the δ-function. In the determination of the equations for $\chi_1^N(E,t)$ and $\chi_1^\pi(E,t)$ the integrals obtained by substituting $P_0^N(E,t)$ into the right members of the equations (3) are calculated by the method of steepest descents:[8]

$$\int_{E}^{\infty}\frac{dN_{L}^{N}(E',E)}{dE}\,P_{0}^{N}(E',t)\,dE'=P_{0}^{N}(E_{1}^{\alpha N},t)\,\Delta^{\alpha N}(E); \tag{5a}$$

$$\int_{E}^{\infty}\frac{dN_{L}^{\pi}(E',E)}{dE}\,P_{0}^{N}(E',t)\,dE'=P_{0}^{N}(E_{1}^{\alpha\pi},t)\,\Delta^{\alpha\pi}(E), \tag{5b}$$

where[8]

$$\Delta^{\alpha N}(E)=H_{1}(E_{1}^{\alpha N})\,S(\gamma)\,[H_{2}(E_{1}^{\alpha N})]^{\gamma+\delta(\gamma)}(1-\alpha)^{\gamma+\delta(\gamma)}E^{-\delta(\gamma)};\quad \Delta^{\alpha\pi}(E)=\pi_{1}(E_{1}^{\alpha\pi})\,S(\gamma)\,[\pi_{2}(E_{1}^{\alpha\pi})]^{\gamma+\delta(\gamma)}(1-\alpha)^{\gamma+\delta(\gamma)}E^{-\delta(\gamma)}.$$

The saddle points $E_1^{\alpha N}$ and $E_1^{\alpha\pi}$ are found from the equations

$$\ln E_{1}^{\alpha N}-24.2=2d(\gamma)\,[\ln E-\ln(C_{2}(1-\alpha)\,H_{2}(E_{1}^{\alpha N}))],\quad \ln E_{1}^{\alpha\pi}-24.2=2d(\gamma)\,[\ln E-\ln(C_{2}(1-\alpha)\,\pi_{2}(E_{1}^{\alpha\pi}))]. \tag{6}$$

Regarding $\chi_1^N(E,t)$ and $\chi_1^\pi(E,t)$ as slowly varying functions of the energy and neglecting the weak energy dependence of the coefficients and inhomogeneous terms in the equations for χ_1^N and χ_1^π (it can be verified that the error thus admitted is $\lesssim 10\%$ for $E\gtrsim 10^{12}$ ev), we find the solutions:

$$\chi_{1}^{\pi}(E,t)=\frac{2\pi_{1}(E/\alpha)}{3\omega(E/\alpha)}\left[\exp\left\{-\alpha^{\gamma}\omega\left(\frac{E}{\alpha}\right)t\right\}-1\right]+\frac{2\pi_{1}(E/\alpha)}{3\omega(E/\alpha)}\left\{\frac{\Delta^{\alpha\pi}(E)\left[\exp\left\{-\alpha^{\gamma}\Delta\omega\left(\frac{E_{1}^{\alpha\pi}}{\alpha}\right)t\right\}-1\right]}{\alpha^{\gamma}[\omega(E_{1}^{\alpha\pi}/\alpha)-\omega(E/\alpha)]}\right.$$
$$\left.+\frac{\Delta^{\alpha N}(E)\left[\exp\left\{-\alpha^{\gamma}\Delta\omega\left(\frac{E_{1}^{\alpha N}}{\alpha}\right)t\right\}-1\right]}{\alpha^{\gamma}[\omega(E_{1}^{\alpha N}/\alpha)-\omega(E/\alpha)]}\right\}+\frac{2\pi_{1}(E/\alpha)\,\Delta^{\alpha N}(E)}{3\omega(E/\alpha)\,\alpha^{\gamma}\omega(E_{1}^{\alpha N}/\alpha)}\left[\exp\left\{-\alpha^{\gamma}\omega\left(\frac{E}{\alpha}\right)t\right\}-\exp\left\{-\alpha^{\gamma}\Delta\omega\left(\frac{E_{1}^{\alpha N}}{\alpha}\right)t\right\}\right]$$
$$-\frac{H_{1}(E/\alpha)\,\Delta^{\alpha\pi}(E)}{\omega(E/\alpha)\,\alpha^{\gamma}\omega(E_{1}^{\alpha\pi}/\alpha)}\left[\exp\left\{-\alpha^{\gamma}\omega\left(\frac{E}{\alpha}\right)t\right\}-\exp\left\{-\alpha^{\gamma}\Delta\omega\left(\frac{E_{1}^{\alpha\pi}}{\alpha}\right)t\right\}\right];\quad \Delta\omega\left(\frac{E_{1}^{\alpha N}}{\alpha}\right)=\omega\left(\frac{E}{\alpha}\right)-\omega\left(\frac{E_{1}^{\alpha N}}{\alpha}\right), \tag{7}$$
$$\Delta\omega\left(\frac{E_{1}^{\alpha\pi}}{\alpha}\right)=\omega\left(\frac{E}{\alpha}\right)-\omega\left(\frac{E_{1}^{\alpha\pi}}{\alpha}\right),$$

χ_1^N is similar in form.

In just the same way one determines $\chi_2^N(E,t)$ and $\chi_2^\pi(E,t)$, and so on (with the successive saddle points being also found from Eq. (6), where one substitutes for E the values of the preceding saddle points). The series (4) converge rapidly. We shall not write out the solutions in general form, however, since it is not convenient to use them in practice. The total number of nuclear-active particles $\mathcal{F}=\mathcal{F}^N+\mathcal{F}^\pi$ can be represented in the form of a double sum with respect to t (the expansion of $\chi_1(E,t)=\chi_1^\pi(E,t)+\chi_1^N(E,t)$ begins with the first power of t, that of $\chi_2(E,t)+\chi_2^\pi(E,t)+\chi_2^N(E,t)$ with the second, and so on). To accuracy about 10% for the energies in which we are interested, we can confine ourselves to terms in the expansion up to the second order inclusive. Therefore we get finally

$$\mathcal{F}(E,t)=\frac{B}{E^{\gamma+1}}\exp\left\{-\left[1-\alpha^{\gamma}\omega\left(\frac{E}{\alpha}\right)\right]t\right\}[1+\bar{\chi}_{1}+\bar{\chi}_{2}]=\frac{B}{E^{\gamma+1}}\exp\left\{-\left[1-\alpha^{\gamma}\omega\left(\frac{E}{\alpha}\right)\right]t\right\}\left\{1+\left[\Delta^{\alpha N}(E)+\Delta^{\alpha\pi}(E)\right]t\right.$$
$$\left.-\alpha^{\gamma}\left[\Delta^{\alpha N}(E)\,\Delta\omega\left(\frac{E_{1}^{\alpha N}}{\alpha}\right)+\Delta^{\alpha\pi}(E)\,\Delta\omega\left(\frac{E_{1}^{\alpha\pi}}{\alpha}\right)\right]\frac{t^{2}}{2}+[\Delta^{\alpha N}(E)\,(\Delta^{\alpha N}(E_{1}^{\alpha N})+\Delta^{\alpha\pi}(E_{1}^{\alpha N}))+\Delta^{\alpha\pi}(E)\,(\Delta^{\alpha\pi}(E_{1}^{\alpha\pi})+\Delta^{\alpha\pi}(E_{1}^{\alpha\pi}))]\frac{t^{2}}{2}\right\}. \tag{8}$$

The distribution that has been found for the nuclear-active particles in the atmosphere makes it possible to obtain the characteristics of the nuclear cascade process in explicit form and to analyze their dependence on the theoretical parameters α and T_k and also on the index γ of the primary spectrum and the interaction path length t_0.

The form of the energy spectrum of the particles produced in the nuclear interactions has the strongest effect on the altitude distribution of the particles in the atmosphere. By the use of the expression we have determined for $\mathcal{F}(E, t)$ the absorption coefficient of the nuclear-active particles,

$$\eta = -(1/\mathcal{F}(E, t))\,\partial\mathcal{F}(E, t)/\partial t$$

can be written in the following way:

$$\eta = \frac{1-D}{t_0}; \quad D = \alpha^{\gamma}\omega\left(\frac{E}{\alpha}\right) + \frac{1}{t}\ln\left[1+\bar{\gamma}_1(E, t)+\bar{\gamma}_2(E, t)\right]. \tag{9}$$

TABLE I. Absorption Path Length of Nuclear-Active Particles, $1/m$ (in g/cm^2)

t \ E (ev)	10^{12}	10^{13}	α \ kT_k	$M_\pi c^2$	$0.5\,M_\pi c^2$
$\alpha=0.7$;		$kT_k=M_\pi c^2$	$E=10^{12}$ ev;		$t^*=10$
		$\gamma=1.5$;	$t_0=65$ g/cm^2		
10	119.3	100.5	0.6	104.4	104.8
15.9	119	99.9	0.7	119.3	119.5
		$\gamma=1.7$;	$t_0=65$ g/cm^2		
10	110.1	93.8	0.6	96.8	97
15.9	110.1	93.7	0.7	110.1	110.5
$\alpha=0.5$;		$kT_k=M_\pi c^2$	$E=10^{13}$ ev;		$t=8.7$
		$\gamma=1.7$;	$t_0=75$ g/cm^2		
8.7	100.8	93	0.5	100.8	101.5
13.8	100.5	92.8	0.6	111.9	112.5

* The values of t, expressed in units of t_0, correspond to the altitudes at Pamir and at Moscow.

The first term in D is due to the fastest particle produced in the elementary act. For $\alpha \sim 0.6$—0.7 it amounts to 90 to 95 percent of D, i.e., the absorption of the cascade is almost entirely determined by the value of the fraction of the total energy carried by this particle. The dependence of the main term of D on α is in agreement with that found by Zatsepin.[9] The factor $\omega(E/\alpha)$ makes a statistical allowance for the fact that this particle may be either a nucleon or a π meson.

With increase of the energy the role played by the nucleons decreases and $\omega(E/\alpha)$ becomes smaller, approaching the value $2/3$. Values of m computed by Eq. (9) are given in Table I.* According to the data of Kaplon and others,[10] for heights in the range less than 700 g/cm^2 one has $m \sim 1/120$ g/cm^2; for about this same energy value Ryzhkova and Sarycheva[11] found $m = 1/(112 \pm 6)$ g/cm^2 as an average value from Pamir ($t \sim 650$ g/cm^2) to Moscow ($t \sim 1020$ g/cm^2). From Table I it follows that with reasonable assumptions as to γ[12] and t_0[13] values of α between 0.6 and 0.7 give satisfactory agreement with experiment; variation of T_k has practically no effect on the results.

We shall now determine the spectrum of the μ mesons produced by the decay of the π mesons. The main contribution to the intensity of the μ mesons with energies $\gtrsim 10^{12}$ ev is made by the μ mesons from the decay of the π mesons with spectrum given by the first term of the series for $\mathcal{F}^{\pi}(E, t)$:

$$\mathcal{F}_1^{\pi}(E, t) = \exp\left\{-\left[1-\alpha^{\gamma}\omega\left(\frac{E}{\alpha}\right)\right]t\right\}\chi_1^{\pi}(E, t), \tag{10}$$

(here in expanding the curly brackets in $\chi_1^{\pi}(E, t)$ in terms of t we can confine ourselves to the first power of t).

The number of μ mesons with energies greater than E at the depth t is calculated in the following way:[14]

$$\mathcal{F}^{\mu}(>E, t) = \int_0^t e^{-t'}\,t'^{-1}\,dt' \int_E^{\infty} dE' \int_{E'}^{E'(M_\pi/M_\mu)^2} P^{\pi}(E^*, t')\,k_\pi(E^*)\,D_\mu^{\pi}(E^*, E')\,dE^*. \tag{11}$$

Here $k_\pi(E)$ is a coefficient characterizing the probability of decay of a π meson with energy E. Following Ref. 15, we take

$$k_\pi \equiv E_\pi/E = (t_0/65\ \text{g/cm}^2)\ 1.17\cdot 10^{11}\ \text{ev}/E,$$

* The writer is grateful to Z. S. Maksimova for aid with the numerical calculations.

$D_\mu^\pi(E'', E')\,dE'$ is the probability for formation of a μ meson with its energy in the range dE' from the decay of a π meson with energy E''. If we assume that the μ mesons are distributed isotropically in the reference system of the π meson, then

$$D_\mu^\pi\,dE' = dE' / [1 - (M_\pi / M_\mu)^2]\,E'$$

(M_μ and M_π are the masses of the μ meson and the π meson). The limits of integration in the integral with respect to E'' correspond to the π-meson energies necessary for the production of a μ meson of energy E' when it is emitted forward and backward, respectively, with maximum energy in the system of the π meson. In calculating by Eq. (11) we take advantage of the weak dependence on the energy of the quantities π_1, H_1, ω, $\Delta^{\alpha\pi}(E)$, and $\Delta^{\alpha N}(E)$, and also of the closeness of the limits of the integration, bring these factors outside the sign of integration with respect to E''. Using the fact that

$$\int_0^t [e^{-xt'} - e^{-t'}]\frac{dt'}{t'} \approx \ln x$$

for sufficiently large t, we get:

$$\mathcal{F}^\mu(>E, t) = \frac{BE_\pi [1 - (M_\mu / M_\pi)^{2(\gamma+2)}}{(\gamma+2)(\gamma+1)E^{\gamma+1}[1 - (M_\mu / M_\pi)^2]} \left\{ \frac{2\pi_1(E/\alpha)}{3\omega(E/\alpha)} \times \ln \frac{1}{[1 - \alpha^\gamma \omega(E/\alpha)]} + \frac{2\pi_1(E/\alpha)[\Delta^{\alpha\pi}(E) + \Delta^{\alpha N}(E)]\left[1 - \exp\left\{-\left[1 - \alpha^\gamma \omega\left(\frac{E}{\alpha}\right)\right]t\right\}\right.}{3\omega(E/\alpha) - \alpha^\gamma \omega(E/\alpha)]} - \frac{2\pi_1(E/\alpha)\Delta^{2N}E}{3\omega(E/\alpha)\alpha^\gamma \omega(E_1^{2N}/\alpha)} \ln \frac{1}{[1 - \alpha^\gamma \omega(E_1^{2N}/\alpha)]} + \frac{H_1(E/\alpha)\Delta^{\alpha\pi}(E)}{\omega(E/\alpha)\alpha^\gamma \omega(E_1^{\alpha\pi}/\alpha)} \ln \frac{1}{[1 - \alpha^\gamma \omega(E_1^{\alpha\pi}/\alpha)]} \left.\right\}$$

(the contribution to the total number of μ mesons from the decay of the π mesons from the part of the spectrum given by the remaining terms of the series for $\mathcal{F}^\pi(E, t)$ can be neglected).

TABLE II. Intensity of μ Mesons at Sea Level (particles $cm^{-2}\,sec^{-1}\,sterad^{-1}$)

$kT_k = M_\pi c^2$, $\gamma = 1.7$.

$t_0 = 65$ g/cm²			$\alpha = 0.7$		
E, ev \ γ	1.5	1.7	E, ev \ kT_k	$M_\pi c^2$	$0.5\,M_\pi c^2$
10^{12}	$4.8 \cdot 10^{-7}$	10^{12}	10^{12}	$4.8 \cdot 10^{-7}$	$4.8 \cdot 10^{-7}$
$3 \cdot 10^{12}$	$3.8 \cdot 10^{-8}$	$2.5 \cdot 10^{-8}$	$3 \cdot 10^{12}$	$2.5 \cdot 10^{-8}$	$2.6 \cdot 10^{-8}$

$t_0 = 75$ g/cm²			$\alpha = 0.6$		
E, ev \ α	0.6	0.5	E, ev \ t_0	65 g/cm²	75 g/cm²
10^{12}	$4 \cdot 10^{-7}$	$2.9 \cdot 10^{-7}$	10^{12}	$3.5 \cdot 10^{-7}$	$4 \cdot 10^{-7}$
$3 \cdot 10^{12}$	$2.1 \cdot 10^{-8}$	$1.5 \cdot 10^{-8}$	$3 \cdot 10^{12}$	$1.8 \cdot 10^{-8}$	$2.1 \cdot 10^{-8}$

In the formula (12), just as in Eq. (9), the main term is that caused by the fastest particle [it gives ~ 90–95% of $\mathcal{F}^\mu(>E, t)$ for $\alpha \sim 0.6$–0.7]. Here the coefficient $2\pi_1(E/\alpha)/3\omega(E/\alpha)$ is a manifestation of the fact that the presence of nucleons reduces $\mathcal{F}^\mu$. Values calculated by Eq. (12) for the numbers of μ mesons* at sea level with energies 10^{12} ev and 3×10^{12} ev for various values of α, T_k, γ, and t_0 are shown in Table II; the coefficient B is determined for the various values of γ from the normalization of the spectrum used to the intensity[4] of the primary particles at $E = 10^{12}$ ev. Gorchakov[16] has made numerical calculations of $\mathcal{F}^\mu(10^{12}\,ev)$ for several values of α, T_k, γ, and t_0; his results agree with ours.

Comparing the values of $\mathcal{F}^\mu$ from Table II with the experimental values obtained on the basis of the work of George,[17]

$$\mathcal{F}^\mu(>10^{12}\,ev) \approx 2 \cdot 10^{-7};\ \mathcal{F}^\mu(>3 \cdot 10^{12}\,ev) \approx 10^{-8}\ \frac{\text{particles}}{\text{cm}^2\,\text{sec steradian}}$$

we see that the theoretical values of the intensity of the μ mesons have turned out too high. But no great significance is to be attached to this discrepancy, since the data on μ mesons of such high energies are

*In the derivation of Eqs. (9) and (12) α was assumed not to depend on the energy. In actual fact[5] $\alpha \sim E^{-(2c_0 - c)/4c_0} = E^{-0.065}$, i.e., it decreases slowly with increasing energy. In the computations for Tables I and II we have used this dependence directly in Eqs. (9) and (12) [the values indicated in Tables I and II are for $\alpha \equiv \alpha(10^{12}\,ev)$].

extremely rough. The attempt to diminish $\mathcal{P}^{\mu}$ by assuming that the fastest particle is always a nucleon leads to a decided lowering of the absorption coefficient. At the same time the data on the absorption coefficient, which can be accounted for without additional assumptions, appear more reliable than those on the μ mesons. Because of the strong dependence of both characteristics on γ and t_0 and the uncertainties in these quantities we cannot establish strict limits on the variation of α. From Table I it follows that satisfactory agreement with experiment is given by $\alpha \sim 0.6-0.7$, but we cannot exclude also 0.5 and 0.8. From the estimates for the traveling wave[8] one found $\alpha \sim 0.5$. Thus the hydrodynamic theory of multiple production of particles is not in contradiction with the existing experimental data on nuclear cascade processes in the atmosphere.

The present work was inspired by the late S. Z. Belen'kii, whose advice was especially valuable to me. I am extremely grateful to I. L. Rozental' and G. T. Zatsepin for helpful discussions.

[1] L. D. Landau, Izv. Akad. Nauk SSSR, Ser. Fiz., **17**, 51 (1953).
[2] I. L. Rozental' and D. S. Chernavskii, Usp. Fiz. Nauk **52**, 185 (1954).
[3] N. L. Grigorov, Dissertation, Moscow State University, 1955.
[4] V. V. Gurzhavin and G. T. Zatsepin, J. Exptl. Theoret. Phys. (U.S.S.R.) **32**, 365 (1957), Soviet Phys. JETP **5**, 312 (1957).
[5] N. M. Gerasimova and D. S. Chernavskii, J. Exptl. Theoret. Phys. (U.S.S.R.) **29**, 372 (1955), Soviet Phys. JETP **2**, 344 (1956).
[6] S. Z. Belen'kii, Dokl. Akad. Nauk SSSR **99**, 523 (1954).
[7] S. Z. Belen'kii, J. Exptl. Theoret. Phys. (U.S.S.R.) **28**, 111 (1955), Soviet Phys. JETP **1**, 161 (1955).
[8] S. Z. Belen'kii, and N. M. Gerasimova, J. Exptl. Theoret. Phys. (U.S.S.R.) **32**, 547 (1957), Soviet Phys. JETP **5**, 456 (1957).
[9] G. T. Zatsepin, J. Exptl. Theoret. Phys. (U.S.S.R.) **19**, 1104 (1949).
[10] Kaplon, Klose, Ritson, and Walker, Phys. Rev. **91**, 1573 (1953).
[11] L. I. Sarycheva and K. P. Ryzhkova, J. Exptl. Theoret. Phys. (U.S.S.R.) **28**, 618 (1955), Soviet Phys. JETP **1**, 572 (1955).
[12] Barrett, Bollinger, Cocconi, Eisenberg, and Greisen, Revs. Mod. Phys. **24**, 133 (1952).
[13] Vernov, Grigorov, Zatsepin, and Chudakov, Izv. Akad. Nauk SSSR, Ser. Fiz., **19**, 493 (1955).
[14] G. T. Zatsepin and I. L. Rozental', Dokl. Akad. Nauk SSSR **99**, 369 (1954).
[15] Guzhavina, Guzhavin, and Zatsepin, J. Exptl. Theoret. Phys. (U.S.S.R.) **31**, 819 (1956), Soviet Phys. JETP **4**, 690 (1957).
[16] E. V. Gorchakov, Degree research, Moscow State University, 1955.
[17] E. George, Progress in Cosmic Ray Physics, Amsterdam, 1952; E. George, Russ. Transl. (Physics of Cosmic Rays) **1**, 328 (1954).

Translated by W. H. Furry
128

THE BEHAVIOR OF A COMPLETELY IONIZED PLASMA IN A STRONG MAGNETIC FIELD*

S. I. BRAGINSKII

Academy of Sciences, U.S.S.R.

Submitted to JETP editor February 13, 1957

J. Exptl. Theoret. Phys. (U.S.S.R.) **33**, 645-654 (September, 1957)

In the first part of this work certain paradoxes are considered which arise when the transfer equations are applied to a quasi-stationary, completely ionized plasma in the case in which the frequency of collisions between particles is much smaller than their frequency of rotation in the magnetic field. In the second part a cylindrical pinched plasma is considered in which the plasma pressure is balanced by the electrodynamic forces produced by the current which flows through the pinched plasma. Several solutions of the plasma equations are found for stationary and non-stationary cases.

1. CERTAIN PARADOXES

THE nature of the particle motion in a plasma depends critically on the ratio between the collision frequency $1/\tau$ and the frequency of rotation in the magnetic field ω. When $\omega\tau \ll 1$ the particles move in virtually straight lines between collisions and the influence of the magnetic field on kinetic effect (diffusion coefficient, heat conductivity, etc.) is small. In the second case, when $\omega\tau \gg 1$, the magnetic field has a strong effect on the plasma kinetics. In this case, if one compares the results obtained by a direct application of the transfer equations with those which are to be expected on the basis of the motion of individual particles in a magnetic field, there are seeming contradictions and paradoxes. Certain of these paradoxical situations have been considered by Alfvén and Spitzer;[1,2] a number of paradoxes are considered by us below.

We shall limit ourselves to the case in which the gradients of all quantities and the electric field are perpendicular to the magnetic field. The transfer equations from Ref. 3 will be used. We will assume that the processes involved are so slow that all quantities change only slightly in the time between collisions. It is easy to show that in this case, we can neglect the terms $d\mathbf{v}/dt$ and div σ (inertia and viscosity) in the projections of the transfer equations on the plane perpendicular to the magnetic field. Using these equations it is possible to obtain explicit expressions for the components of electron velocity $\mathbf{v}_e$ and ion velocity $\mathbf{v}_i$ perpendicular to the magnetic field in terms of the gradients

$$\begin{aligned}\mathbf{v}_e &= \frac{c}{H^2}[\mathbf{E}\times\mathbf{H}] - \frac{c}{eH^3 n}[\mathbf{H}\times\nabla nT_e] - \frac{mc^2}{e^2H^2\tau}\left\{(T_e+T_i)\frac{\nabla n}{n} + \nabla T_i - \frac{1}{2}\Delta T_e\right\},\\ \mathbf{v}_i &= \frac{c}{H^2}[\mathbf{E}\times\mathbf{H}] + \frac{c}{eH^3 n}[\mathbf{H}\times\nabla nT_i] - \frac{mc^2}{e^2H^2\tau}\left\{(T_e+T_i)\frac{\nabla n}{n} + \nabla T_i - \frac{1}{2}\nabla T_e\right\}.\end{aligned} \tag{1}$$

where m is the mass of the electron, c is the velocity of light, $1/\tau$ is the frequency of electron collisions with ions, T_e and T_i are the electron and ion temperatures. Here we carry out an expansion in powers of $1/H$ and discard terms of order higher than $1/H^2$. The plasma is assumed to be comprised of electrons and singly-charged ions with charge e. The number of particles of each type, as is generally assumed for a plasma, is taken to be the same, $n_i = n_e = n$. The velocity components along the magnetic field cannot be expressed directly in terms of the gradients; we will assume that these are all zero. Using Eq. (1) we find that the electric current depends only on the pressure gradient $p = n(T_e + T_i)$ and is perpendicular to this quantity

$$\mathbf{j} = en(\mathbf{v}_i - \mathbf{v}_e) = cH^{-2}[\mathbf{H}\times\nabla p]. \tag{2}$$

It is of interest to compare Eq. (1) with the picture based on the motion of individual particles in the magnetic field in order to interpret conveniently the various terms in these expressions.

*This work was performed in 1952.

As is well known, in a strong magnetic field a particle moves along the magnetic field lines, rotating about these lines with a frequency $\omega = eH/mc$. The presence of the electric field and a small inhomogeneity in the magnetic field means that the center of the circle moves across the magnetic field with a velocity $\mathbf{V}$

$$\mathbf{V} = \frac{c}{H}[\mathbf{E}\times\mathbf{h}] - \frac{v_\perp^2}{2\omega}\left[\frac{\nabla H}{H}\times\mathbf{h}\right] - \frac{v_\parallel^2}{\omega}[(\mathbf{h}\cdot\nabla)\,\mathbf{h}\times\mathbf{h}]. \tag{3}$$

Here $\mathbf{h} = \mathbf{H}/H$ is a unit vector in the direction of the magnetic field. The first term in Eq. (3) is usually called the electric-drift term, the second the magnetic-drift term and the third the centrifugal-drift term. If we average Eq. (3) over a Maxwellian distribution we find an expression for the flow of circle centers (the charge of the particles is assumed to be positive)

$$\bar{\mathbf{V}} = \frac{c}{H}[\mathbf{E}\times\mathbf{h}] - \frac{cT}{e}\left[\frac{\nabla H}{H} + (\mathbf{h}\cdot\nabla)\,\mathbf{h}\times\mathbf{h}\right]. \tag{4}$$

Using the condition $\mathbf{H}\cdot\operatorname{curl}\mathbf{H} = 0$ we can transform this expression to the form

$$\bar{\mathbf{V}} = \frac{c}{H}[\mathbf{E}\times\mathbf{h}] + \frac{cT}{e}\operatorname{curl}\frac{\mathbf{h}}{H}. \tag{4'}$$

Thus, the first term in Eq. (1) may be interpreted easily—it is the electric-drift term.

The second term in Eq. (1), which we will call the Larmor flux, is related to the fact that particles which intersect any area, moving from right to left and from left to right, move between regions with different densities and temperatures, as a result of which the fluxes do not cancel. The particles travel a distance of order $\rho = mvc/eH$ and "carry" a flux nv, hence, the resultant flux is proportional to $\nabla n\bar{v}^2 \sim \nabla nT$.

At first glance, it seems to be paradoxical that there are no terms in Eq. (1) which correspond to the magnetic and centrifugal drift terms and which contain explicitly spatial derivatives of the magnetic field. Actually, however, the absence of these terms is completely reasonable since the magnetic field, whether uniform or not, does not disturb the Maxwellian distribution. Hence, if the density and temperature of the particles are independent of coordinates, the particle flux should not be coordinate-dependent (cf. for example, Ref. 2). Under these conditions the magnetic and centrifugal drift terms appear as edge effects, giving rise to "by-pass" currents at the boundaries of the region characterized by constant density and temperature. One is easily convinced of this by a simple example. If we re-write the terms in Eq. (1) of order $1/H$ in the form

$$n\mathbf{v} = \frac{cn}{H}[\mathbf{E}\times\mathbf{h}] + \frac{cnT}{e}\operatorname{curl}\frac{\mathbf{h}}{H} - \operatorname{curl}\left(\frac{cnT}{eH}\mathbf{h}\right) = n\bar{\mathbf{V}} - \operatorname{curl}\left(\frac{cnT}{eH}\mathbf{h}\right),$$

it becomes immediately obvious that the difference between the flux of "centers" and the flux of particles through any area is completely determined by the values of the quantities at the boundaries of this area. This difference is due to the fact that some particles pass close to the edges of the area and the "centers" of the circles associated with these do not pass through the area. The flux created by these particles is cnT/eH (per unit length of edge along $\mathbf{h}$) where the opposite edges of the area are traversed in opposite directions.

The last terms in Eq. (1) (these are enclosed in curly brackets), in contrast with the first terms, depend on particle collisions, in particular, collisions of electrons with ions. These terms may provisionally be called diffusion terms. They are the same for ions and electrons and depend only on the density gradient and temperature gradient but are independent of the electric field. At first glance both of these results seem paradoxical. Actually, the factor which characterizes the diffusion of particles across the magnetid field is of order $D \sim \rho^2/\tau$ because a particle which does not experience collisions circles about one point and, as a result of collisions, is displaced randomly by an amount of the order of the Larmor radius ρ during the time between impulses τ. In an ion of mass M, both ρ and τ are larger by a factor of $\sqrt{M/m}$ than for electrons, hence it is to be expected that the ion diffusion coefficient should be $\sqrt{M/m}$ times larger than the electron diffusion coefficient. In actuality, however, this is not the case. Suppose, for example, there is an ion-density gradient along the x-axis and the magnetic field is along the z-axis; under these conditions there will be produced a Larmor ion flow along the y-axis with a velocity $v_y = (cT/eHn)\,dn/dx$. In this case it is impossible to apply the formula for ρ^2/τ directly in estimating

the diffusion coefficient because the diffusion takes place in a moving medium and in collisions an ion will receive, on the average, some momentum along the y-axis. We now go over to a system of coordinates in which $v_y = 0$. In this system there is an electric field $E_x = (v_y/C)H = (T/e)\,d \ln x/dx$ in which the ions have a Boltzmann distribution and the ion flux vanishes because the motion cancels the diffusion. Thus collisions between identical particles do not result in diffusion of these particles across the magnetic field. Collisions between electrons and ions, however, lead to "diffusion" because the Larmor flows of ions and electrons are in opposite directions. The resultant flux along the x-axis may be considered as the result of drift produced by the effect of the friction force between electrons and ions R directed along the y-axis. Inasmuch as $R_{ion} = -R_{elec}$, the velocities of both kinds of particles are identical.

We now consider the role of the electric field. Suppose there is an electric field along the z-axis. It produces drift of particles of both signs along the y-axis with a velocity $v_y = -cE/H$. In the system of coordinates in which $v_y = 0$ the electric field $E_x' = 0$ so that no flux due to an electric field is produced along the y-axis.

It is well known that when a magnetic field changes slowly in time the energy associated with the transverse motion of particles $\epsilon_\perp = mv_\perp^2/2$ changes in proportion to the field — the betatron effect. The heat transfer equation does not contain a term proportional to $\partial H/\partial t$. However, it is easy to show from a simple example that the betatron effect is taken into account.

Suppose, for example, that a uniform magnetic field is directed along the z-axis and increases with time. Let the plasma occupy a cylindrical volume which is infinite along the z-axis. We will assume that the temperature and density of the plasma are constant over the volume (thus there will be no heat flow) and, for simplicity, we neglect collisions between electrons and ions. We also neglect the shielding of the external magnetic field by currents in the plasma. Then the induction electrical field is $E = E_\varphi = -\dot{H}r/2c$. The electrical drift leads to a contraction of the plasma with velocity $v_r = -\dot{H}r/2H$. The heat-transfer equation assumes the form

$$\frac{3}{2} n \frac{dT}{dt} = -nT \operatorname{div} \mathbf{v} = -nT(\dot{H}/H).$$

This expression is precisely the betatron effect. Actually, in betatron heating only the energy associated with the transverse motion $d\epsilon = \epsilon_\perp dH/H$ is increased directly. Collisions establish an equal distribution over the various degrees of freedom so that $\epsilon_\perp = (2/3)\,\epsilon$ and $(3/2)\,d\epsilon/dt = (\epsilon/H)\,dH/dt$. In this case the betatron effect appears as heating due to the adiabatic contraction of the plasma.

We now consider the case in which the ion-electron collisions exactly "balance" the electric drift so that the plasma is at rest. In this case heat fluxes are produced in the plasma, hence, we shall consider the total increase in the energy of the plasma. If the heat-transfer equations for the ions and electrons are added and integrated over the volume of the plasma cylinder (unit height along the z-axis), we obtain

$$\frac{3}{2} \frac{d}{dt} \int n(T_e + T_i)\, 2\pi r\, dr = \int Ej 2\pi r dr.$$

Substituting everywhere $E = -\dot{H}r/2c$, $j = (cH)\,\partial p/\partial r$ and integrating by parts we again find $(3/2)\,d\epsilon/dt = (\epsilon/H)\,dH/dt$. In this case the betatron effect is manifest in the evolution of Joule heat.

The two cases which have been considered differ in one respect. In the first case the ions and electrons are heated in the same way by the contraction. In the second case the heat is generated directly in the electron gas and only then, by collisions, is it transferred to the ions, although it would appear that in betatron heating the ions should obtain as much heat as the electrons. The point is, however, that in the absence of an ion current in the plasma a radial electric field is produced; the magnitude of this field is determined by the ion balance condition $enE_r = -\partial n T_i/\partial r$. This field causes an ion drift in the azimuthal direction against the vortex electric field. It is easy to show that its work (negative) on this drift exactly compensates for the betatron heating of the ions. The electrons also drift in the radial field and acquire as much energy as is lost by the ions.

2. CONTRACTION OF THE PLASMA DUE TO HIGH SELF-CURRENT

1. Basic Equations

The magnetic field produced by a large current flowing through the plasma has a very strong effect on the motion of particles in the plasma and on the configuration of the plasma as a whole. The joint effect of the electric field which gives rise to the current and the magnetic field produced by this current is a

"drift" of charged particles of both signs within the current-carrying channel; as a result the plasma contracts into a more or less narrow filament. Considering this picture phenomenologically, we can attribute the contraction of the plasma to the mutual attraction between the elementary "filamentary currents" which make up the total current.

As has already been shown in a number of papers (cf. for example, Ref. 6), such a filament is unstable against various deformations; nonetheless it is of interest to study the problem, even if only from the point of view of methodology. The stationary filament has already been considered by Schlüter.[5]

We will consider a plasma filament with cylindrical symmetry, neglecting end effects (electrode effects). The gradients of all quantities are directed along the radius r and the electric current flows along the z-axis while the magnetic field is azimuthal.

It will be assumed that all changes in the plasma occur so slowly that we can neglect "inertia" effects, in which case the momentum balance equations assume the form of equilibrium equations. The magnetic field is assumed large so that $\omega\tau \gg 1$ both for electrons and ions (ω is the Larmor frequency, $1/\tau$ is the collision frequency). The expressions for the kinetic coefficients are expanded in powers of $1/\omega\tau$ and small terms are neglected. It will be assumed that the density of electrons and ions (singly charged) is virtually the same $n_i = n_e = n$. A sufficiently dense plasma is always characterized by this so-called quasi-neutral property. It will also be assumed that the ion and electron temperatures are the same $T_e = T_i = T$.

Under these assumptions the system of basic equations is of the form (cf. Ref. 3):

$$\frac{\partial E}{\partial r} = \frac{1}{c}\frac{\partial H}{\partial t}; \tag{1a}$$

$$\frac{\partial rH}{r\partial r} = \frac{4\pi}{c} j; \tag{1b}$$

$$\frac{\partial n}{\partial t} + \frac{\partial rnv}{r\partial r} = 0; \tag{1c}$$

$$j = \sigma\left(E + \frac{v}{c} H\right) - \frac{3}{2}\frac{cn}{H}\frac{\partial T}{\partial r}; \tag{1d}$$

$$-\frac{\partial P}{\partial r} = -2\frac{\partial n T}{\partial r} = \frac{1}{c} jH; \tag{1e}$$

$$3n\left(\frac{\partial T}{\partial t} - v\frac{\partial T}{\partial r}\right) + 2nT\frac{\partial rv}{r\partial r} + \frac{\partial rq}{r\partial r} = \left(E + \frac{v}{c} H\right) j - \beta n^2\sqrt{T}. \tag{1f}$$

Here Eqs. (1a) and (1b) are Maxwell's equations, E is the axial component of the electric field and H is the magnetic field. Eq. (1c) is the equation of continuity and v is the radial velocity both for ions and electrons. The expression for the current density (1d) is obtained from the electron equilibrium equation if it is projected on the z-axis: $en(E + vH/c) = R$. The force R is made up of friction forces, which depend on the relative velocities between the electrons and ions $(m/e\tau)j$ and on thermal forces which depend on the electron temperature gradient $(3/2)(n/\omega\tau)\partial T/\partial r$. The time between ion-electron collisions τ and the coefficient of electrical conductivity σ are expressed as follows: ("the Coulomb logarithm" $\lambda \approx 10$):

$$\tau = 3\sqrt{m}\,T^{3/2}/4\sqrt{2\pi}\lambda e^4 n \approx 3.5\cdot 10^4 T_{ev}^{3/2}/n_{cm^{-3}}\ (\text{sec}), \tag{2}$$

$$\sigma = e^2 n\tau/m = \sigma_1 T^{3/2}, \quad \sigma_1 = 0.9\cdot 10^{13}\,\text{sec}^{-1}\,(\text{ev})^{-3/2}. \tag{3}$$

We may note that the electrical conductivity depends only on the temperature. Eq. (1e) is the plasma equilibrium equation projected on the radius; Eq. (1f) is the total heat balance equation. The main role in the transfer of heat across the strong magnetic field is played by ions as a consequence of the fact that the Larmor radius for the ions is so much larger than that for the electrons. In Eq. (1f) we will assume only an ionic flow; hence we have the following expression for the heat conductivity

$$q = -\varkappa\partial T/\partial r, \quad \varkappa = \sqrt{2M/m}\,mc^2 nT/e^2\tau H^2 \tag{4}$$

(M is the mass of the ion, m is the mass of the electron).

The first term on the right side of Eq. (1f) is to be associated with the generation of Joule heat while the second term is the heat loss produced as a consequence of electron bremsstrahlung. The coefficient β can be obtained using the results given by Heitler.[4] Averaging over the Maxwellian electron distribution we have

$$\beta = 32\sqrt{2}\,e^2/3\sqrt{\pi}\cdot 137\,m^{1/2}c^2. \tag{5}$$

If inertia effects are taken account in the equation for the radial motion of the plasma, in place of Eq. (1e) we obtain

$$Mn(\partial v/\partial t + v\partial v/\partial r) = -\partial p/\partial r - jH/c. \tag{1e'}$$

We now compare the inertia term in (1e') with the pressure force. The first quantity is of order Mnv/t, where t is the characteristic time for radial motion. In the case of uniform motion we may set $t \sim a/v$ where a is the radius of the plasma cylinder. The second term is of order p/a. Thus the ratio of the inertia term to the pressure term is of order Mv^2/T and if the radial velocity is small compared with the thermal velocities of the ions the inertia effects can be neglected. Suppose for example, $a \sim 10$ cm, $t \sim 10^{-5}$ sec; then $Mv^2 \sim 1$ Mev which, in cases of practical interest, is always much smaller than the energy associated with thermal motion.

If, at the starting time, the radial distribution of current density and pressure is such that the pressure and magnetic attraction are not balanced at each point, or if there is a sudden change in the current strength, a rapid redistribution of matter takes place in the plasma; this effect can be accompanied by the production of intense shock waves. In this case the velocities associated with the motion may become "supersonic" and the inertia effect can play an important role (cf. for example, Ref. 7). Below we shall consider only the "continuous" cases in which inertia effects can be neglected.

Substituting the expression for the current from (1d) in (1e) we find that the radial velocity is composed of an electric particle drift toward the axis and a diffusion outwards, resulting from collisions

$$v = -\frac{cE}{H} - \frac{2mc^2T}{e^2\pi H^3}\left(\frac{1}{n}\frac{\partial n}{\partial r} + \frac{1}{4T}\frac{\partial T}{\partial r}\right). \tag{6}$$

The filament is considered in the coordinate system ("laboratory") in which the ion velocity along the axis is equal to zero. Under these conditions, the equilibrium equations, written separately for ions and electrons, assume the form

$$-\partial(nT)/\partial r + enE_r = 0; \tag{7}$$

$$-\partial(nT)/\partial r - enE_r = jH/c. \tag{8}$$

The ions are constrained in the plasma column by the radial electric field E_r which transfers the pressure of the ion to the electrons. If $\partial T/\partial r = 0$, the ions have a Boltzmann distribution in this field.

Determining the current density from (8) and integrating over radius, we have

$$J = \int j2\pi r dr = -e\int n\left\{\frac{cE_r}{H} + \frac{cnT}{eH}\left(\frac{1}{H}\frac{\partial H}{\partial r} - \frac{1}{r}\right)\right\}2\pi r dr.$$

This expression shows graphically the mechanism which makes it possible for the electrons to carry current across the magnetic field — the drift of electrons under the effect of the radial electric field and the inhomogeneous magnetic field.

Neglecting inertia effects it is possible to obtain a simple relation between the total current flowing in the plasma and the mean particle temperatures. If the expression for the current (1e) is substituted in (1b), multiplied by $c^2Hr^2/2$, and integrated from $r = 0$ to the edge of the plasma cylinder $r = a$ and if it is assumed that $H(a) = 2J/ca$, where J is the total current, we find

$$J^2 = -2\pi c^2\int_0^a r^2\frac{\partial p}{\partial r}dr = 2c^2\left(\int_0^a p2\pi r dr - \pi a^2 p(a)\right).$$

When the pressure at the edge can be neglected as compared with the internal pressure, it follows that

$$J^2 = 4c^2NT,\quad N = \int_0^a n2\pi r dr,\quad \overline{T} = N^{-1}\int_0^a nT2\pi r dr. \tag{9}$$

Here N is the number of particles per unit length of filament, $\overline{T}$ is the mean value of the temperature. The relation given in (9) has already been obtained by Schlüter[9] for the case in which the current density and temperature are constant over the radius.

We consider a numerical example. If $N = 10^{18}$, the plasma temperature is $T = 1$ kev at a current of $J = 800$ kiloamperes.

We now estimate the difference between the ion temperature and the electron temperature. For this

purpose we compare the Joule heat which has been obtained j^2/σ with the heat transfer due to collisions between electrons and ions. $\Delta Q = (3mn/M\tau)(T_e - T_i)$. If we take Eq. (9) into account the comparison yields $\Delta Q/j^2/\sigma \sim \Pi(T_e - T_i)/T$ where

$$\Pi = e^2N/Mc^2. \tag{10}$$

If $\Pi \gg 1$, the assumption made above that $T_e = T_i = T$ is valid. This dimensionless criterion implies that the ion Larmor radius ρ_i is small compared with the radius of the filament. A simple estimate, taking Eq. (9) into account, yields $\rho_i/a \sim \Pi^{-1/2}$. The dimensionless quantity Π is an important similitude criterion in plasma theory, particularly, in pinched plasmas. A high numerical value of Π is a necessary condition for the applicability of the system of magneto-hydrodynamic equations used above. We shall assume that this condition is satisfied.

2. Stationary Mode

The system of equations given in (1) becomes considerably simpler if all the quantities are time independent. In this case Eq. (1a) and (1c) yield $E = \text{const}$ and $v = 0$.

The temperature change over the radius may be assumed small. If we compare the order of magnitude of the Joule heat j^2/σ with the divergence of the heat flux, which is of order $\kappa(dT/dr)/a$ we find $(a/T)\,dT/dr \sim \sqrt{m/M}$. We can obtain an approximate solution by assuming the temperature constant. In this case the thermal forces vanish and the electric conductivity is constant. Hence, the current density is constant, and the remaining quantities are easily determined

$$H = (2J/ca)\,r/a,\quad n = (2N/\pi a^2)(1 - r^2/a^2),\quad T = \text{const}. \tag{11}$$

This solution has already been obtained by Schlüter.[5] In accordance with Eq. (9), the temperature is completely determined by the total current which flows through the filament. The electric field decreases with increasing current

$$E = J/\sigma\pi a^2 = 8c^3N^{1/2}/\sigma_1\pi a^2J^2. \tag{12}$$

Naturally, the stationary mode can be realized only if the heat generated in the filament is removed. For example, the plasma filament could have its outer surface in contact with the walls of a cylindrical discharge chamber, thereby transferring heat to the walls by conduction. Another possibility is the energy loss from the filament via radiation. In the first case the radius of the filament must be equal to the radius of the discharge chamber a_0; in the second case the radius of the filament can be arbitrary (but must be smaller than the radius of the chamber).

Strictly speaking, in a filament which is in contact with the walls the temperature cannot be constant over the entire cross section since there must be a drop in the region of the walls. Nonetheless, the solution given in (11) is still a good approximation. Numerical integration of the system given in (1) in conjunction with (3), (4) (for $\partial/\partial t = 0$ and without radiation) indicates that the behavior of all quantities over the larger portion of the radius is approximately the same as that given in (11) while close to the edge, where the density and heat conductivity are much lower, the temperature falls off sharply and then rapidly approaches zero.

There is another remark which must be made concerning the central portion of the filament. A detailed investigation shows that close to the axis of the filament, over a region of width of order $a\Pi^{1/4}$, the difference between the ion temperature and electron temperature is of order $\Pi^{-1/2}$ (not Π^{-1}). In this central region the thermal force is of importance; as a consequence the current density is larger than in the remaining portion of the filament. Calculations carried out using a separate heat balance equation for electrons (assuming that $\omega\tau \gg 1$) indicate that the ratio of the current density at the axis to that outside the central region is 1.93.

The energy balance relation in the filament (per unit length) is of the form

$$EJ = Q_{heat} + Q_{rad},\quad Q_{heat} = 2\pi aq(a),\quad Q_{rad} = \beta n^{-2}T^{1/2} = \frac{4}{3}\beta T^{1/2}\frac{N^2}{\pi a^2},$$

where the first term is the flux to the wall while the second is the energy loss due to bremsstrahlung. Using Eqs. (9) and (12) it is easy to show that the ratio of radiation to Joule heat depends only on the magnitude of the current in the filament $Q_{rad}/EJ = J^2/J^2_{rad}$, where

$$J_{rad} = (12\,c^4/\beta\sigma_1)^{1/2} = (3\pi\cdot 137\hbar/2)^{1/2}mc^3/e \approx 1{,}4\cdot 10^6\ \text{A}. \tag{13}$$

If the current is smaller then J_{rad}, part of the Joule heat is radiated and the remaining part is removed by conductivity. When $J = J_{rad}$ (9) and (12) yield

$$T = J_{rad}^2/4c^2N \approx 3\cdot 10^{21}/N\ \text{ev};\quad a = (2\beta/3\pi c)^{1/2}N^{3/4}/E^{1/2}. \tag{14}$$

It is impossible to have a current larger than that given in (13) in the stationary mode since the filament cannot be heated beyond the temperature given in (14).* An increase in the electric field in the filament leads to further compression and increased radiation because the temperature and current do not change. The volt-ampere characteristic of the stationary plasma filament thus consists of two parts: a branch with negative slope (12) and the vertical line $J = J_{rad}$. Finally, the value of the current given in (13) is the limiting value for the stationary mode only. In the non-stationary mode the current can exceed the value given in (13).

3. Non-Stationary Modes

In the non-stationary case (1) becomes a system of nonlinear partial differential equations, the solution of which is, in general, extremely difficult. We shall consider only a certain class of solutions in which all quantities change with time in such a way that the distribution over cross section maintains similitude as a function of time. Solutions of this type are usually called "self-similar" solutions. The idea of looking for self-similar solutions was suggested by A. D. Sakharov.

In place of the radius we introduce the variable $x = r/a(t)$. The variables t and x are separable and we perform the integration of usual equations. The equation of continuity indicates that the velocity in the self-similar solution changes in accordance with the relation $v = \dot{a}x$. As in the stationary mode, it may be assumed with reasonable accuracy that the temperature is constant over the radius. In the self-similar solution the magnetic field is expressed in the form $H = (2J/ca)h(x)$ where $h(0) = 0$ and $h(1) = 1$. Using Eqs. (1a) (1b) and (1d) we obtain the following equation for h(x)

$$\frac{d}{dx}\left(\frac{1}{x}\frac{dxh}{dx}\right) = k^2h, \tag{15}$$

where

$$k^2 = (4\pi a^2\sigma/c^2J)\,dJ/dt = (\sigma_1\pi a^2J^2/2c^6N^{3/2})\,dJ/dt. \tag{16}$$

In what follows we shall consider for simplicity only the case in which $dJ/dt > 0$. The solution of Eq. (15), and then all the remaining quantities, are easily expressed in terms of Bessel functions of imaginary argument

$$H = (2J/ca)\,I_1(kx)/I_1(k); \tag{17a}$$

$$n = (N/\pi a^2)\,[I_0^2(k) - I_0^2(kx)]/I_1^2(k); \tag{17b}$$

$$E + \frac{v}{c}H = \frac{2}{c^2}\frac{\partial J}{\partial t}\frac{I_0(kx)}{kI_1(k)}. \tag{17c}$$

This solution applies if the quantity k remains constant in time. The quantity k gives the ratio of the filament radius to the thickness of the skin-layer and characterize the degree of non-stationarity of the process.

When $k \ll 1$ there is no skin effect and the distribution of all quantities over the cross section of the filament is very similar to that which obtains in the stationary mode.

When $k \gg 1$ the skin effect is pronounced and the plasma density is constant almost over the entire cross section; at the edge the density falls off sharply and the current and magnetic field penetrate the filament to a small depth. At the edge the magnetic field forms a sort of magnetic wall; at this wall the electrons experience a sharp deflection, being reflected in a way similar to that in which molecules of a gas are reflected at an ordinary solid wall. The ions in the filament are constrained by the radial electric field which is formed close to the edge of the analogous "electric wall." The "magnetic wall" acts

*A similar result has been obtained by R. S. Pease [Proc. Phys. Soc. B70, 445 (1957)].

something like a piston, compressing the ionized gas and heating it. If the compression takes place slowly so that the energy of the particles can become equalized over all three degrees of freedom by collisions, this heating obeys the usual adiabatic relation $T^{3/2}/n = \text{const}$. Writing Eq. (16) in the form $k^2 = (4\dot{J}\tau/J)\Pi$ it is easy to show that the current can change slightly during the time between collisions for $k^2 \gg 1$, if Π is sufficiently large.

Equations (17) contain J(t) and a(t). The time dependence of the current is determined by the properties of the electrical circuit of which the plasma filament is a part. The time change of the filament radius is determined by the energy balance condition: the heating (cooling) due to compression (expansion) of the filament must be such that at each moment the condition which relates the temperature and current is satisfied. Integrating Eq. (1f) over the cross section we find, assuming that the filament is not in contact with the wall, q(a) = 0

$$\frac{3}{T}\frac{dT}{dt} + \frac{4}{a}\frac{da}{dt} = \frac{J^2}{NT\sigma\pi a^2}\frac{k^2}{4}\left(\frac{I_0^2(k)}{I_1^2(k)} - 1\right) - \frac{Q_{rad}}{NT}, \tag{18}$$

where Q_{rad} differs from $(J^2/\sigma\pi a^2)$ (J^2/J_{rad}) by only a factor on the order of unity. If radiation is neglected, as may be done when $J \ll J_{rad}$, and the relation between the current and temperature and Eq. (16) are used, we find

$$\frac{1}{a}\frac{da}{dt} = -\left(\frac{5}{2} - \frac{I_0^2(k)}{I_1^2(k)}\right)\frac{1}{J}\frac{dJ}{dt}. \tag{19}$$

This equation is easily integrated and, in conjunction with the condition $k^2 = \text{const}$, indicates that the self-similar solution corresponds to the case in which the current in the filament increases in accordance with a power law. Thus, for example, if $k = 1.65$, $I_0^2(k)/I_1^2(k) = 5/2$ so that the radius of the filament does not change in time and the current must increase in proportion to $t^{1/3}$. A linear current increase with time corresponds to $k = 3.08$, in which case $I_0^2(k)/I_1^2(k) = 3/2$ and the radius of the filament is inversely proportional to the time. If the current increases so slowly that $k < 1.65$, the filament expands in the course of time. In the limiting cases $k \ll 1$ and $k \gg 1$ the condition that k is constant no longer obtains. When $k \gg 1$, $I_0^2(k)/I_1^2(k) \approx 1$ this means that we can neglet the Joule heat and Eq. (19) gives $aJ^{3/2} = \text{const}$ or $T^{3/2}/n = \text{const}$, i.e., the adiabatic equation. When $k \ll 1$ the skin effect is small. If we neglect the skin effect the change of radius with time is determined by the equation (taking radiation into account)

$$\frac{1}{a}\frac{da}{dt} + \frac{3}{2J}\frac{dJ}{dt} = \frac{c^2}{\pi a^2\sigma}\left(1 - \frac{J^2}{J_{rad}^2}\right) = \frac{8c^2N^{3/2}}{\pi\sigma_1 a^2 J^2}\left(1 - \frac{J^2}{J_{rad}^2}\right). \tag{20}$$

Suppose, for example, that $dJ/dt = 0$, $T = 10^3$ ev, and $a = 10$ cm; in this case the filament radius is doubled in a time of the order of 0.05 sec.

The author wishes to express his gratitude to B. I. Davydov, M. A. Leontovich, and G. I. Butker for many illuminating discussions.

[1] H. Alfven, Cosmical Electrodynamics, Oxford 1952 (Russ. Transl.).
[2] L. Spitzer Jr., Astrophys. J. **116**, 299 (1952).
[3] S. Braginskii, J. Exptl. Theoret. Phys. (U.S.S.R) **33**, 459 (1957); Soviet Phys. JETP **6**, 358 (1958).
[4] W. Heitler, The Quantum Theory of Radiation, Oxford, Clarendon Press, 1936 (Russ. Transl.).
[5] A. Schlüter, Z. Naturforsch. **5A**, 72 (1950).
[6] M. Kruskal and M. Schwarzschild, Proc. Roy. Soc., (London) **A223**, 348 (1954).
[7] M. Leontovich and S. Osovets, Атомная энергия (Atomic energy) **3**, 81 (1956).

Translated by H. Lashinsky
129

RESONANCE SCATTERING OF γ-RAYS

N. A. BURGOV

Submitted to JETP editor February 15, 1957

J. Exptl. Theoret. Phys. (U.S.S.R.) **33**, 655-659 (September, 1957)

Some experiments are suggested which may be used to determine the width of excited levels as well as to determine the correlation constant λ between the electron and the neutrino (if the experiments are of sufficent duration). The experiments consequently can be used to ascertain the choice of type of forces in β-decay.

1. The observation of nuclear resonance scattering is made difficult by the Doppler shift which the γ-rays experience due to nuclear recoil both in emission and absorption, while at the same time the nuclear levels are very narrow. However, in radioactive substances the emission of a γ-ray in a ground state transition is usually preceded by a β-decay and, sometimes, by another γ-quantum. The nuclear recoil due to this proceding radiation can be utilized to compensate for the Doppler shift. In Refs. 1 and 2 the conditions necessary for such a compensation have been treated if the preceding radiation is a γ-ray. The present paper is devoted to the case when the preceding radiation is a β-decay, or a β-decay with a γ-ray cascade.

2. We analyze the following experimental setup (Fig. 1). The source S emits β-particles and γ-quanta. The decay of the source material takes place according to Fig. 2. We assume

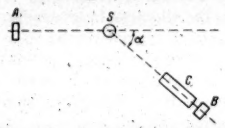

FIG. 1

$$E_{k\beta\,\max} \geqslant \sqrt{E_\gamma^2 + m_0^2c^4} - m_0c^2. \tag{1}$$

Here $E_{k\beta\,max}$ is the maximum kinetic energy of the electron in the β-decay, E_γ — the energy of the photon and m_0c^2 — the rest energy of the electron. In Fig. 1, A detects β-particles of a given energy and B is a γ-ray counter. The scatterer C is placed in the path of the γ-rays and comprises the nuclei obtained after the β-decay. The transparency of the specimen C to gamma rays from the source is determined, also as a function of the angle α.

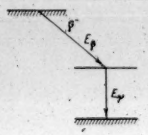

FIG. 2

Resonance scattering will lead to increased γ-ray absorption in the scatterer C. We shall now determine the cross section of resonance scattering in terms of the above experiment. We shall assume that the radioactive source material is given in gaseous form so that one can assume the recoil nucleus to be free.

3. We start from Eq. (10) of Ref. 2. The cross section for resonance scattering of γ-rays is

$$\sigma = \sigma_0 (\sqrt{\pi}\,\Gamma / 2\Delta) \exp\{-(E_{\gamma 1} - E_r)^2 / \Delta^2\}. \tag{2}$$

with the following abbreviations:

$$\sigma_0 = 4\pi\lambda\!\!\!^{-2}(2j+1)/(2i+1) \tag{3}$$

i.e., the peak resonance scattering cross section (see, for example, Ref. 3); j is the angular momentum of the excited state of the daughter nucleus, i is angular momentum of the ground state of the daughter nucleus $\lambda\!\!\!^{-} = c\hbar/E_{\gamma_1}$; Γ — intrinsic width of the excited level Δ — Doppler width, due to the thermal motion of the nuclei both in the source and in the scatterer, given by (see, for example, Ref. 4)

$$\Delta = E_\gamma \sqrt{2k(T_1 + T_2)/m_1c^2}, \tag{4}$$

where T_1 is the absolute temperature of the source, T_2 the absolute temperature of the scatterer, k is Boltzmann's constant, m_1 the nuclear mass, and E_r the energy required to excite the nucleus:

$$E_r = E_{\gamma 1}(1 + E_{\gamma 1}/m_1c^2); \tag{5}$$

E_{γ_1} is energy of the γ-quantum emitted in the direction of the γ-counter after emission of the β-particle. The energy E_{γ_1} depends on the angle α between the directions of the electron and the γ-quantum, and also on the direction of emission of the neutrino if the momentum of the electron is not close to the maximum. Since one cannot observe the neutrino, one has to average (2) over all directions of the outgoing neutrinos.

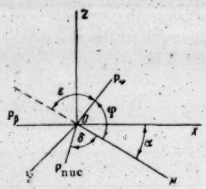

FIG. 3

4. We introduce the coordinate system shown in Fig. 3. The source is placed at the origin of the coordinate system. The electron is emitted in the direction of the negative X axis, and OM is the direction of the γ-ray counter. We denote the angles between OM and the momentum $\mathbf{p}_{nuc}$ of the nucleus by δ, between the momenta of the β-particle $\mathbf{p}_\beta$ and of the neutrino $\mathbf{p}_\nu$ by β, and between OM and $\mathbf{p}_\nu$ by φ; $\epsilon = \pi - \varphi$. Then

$$E_{\gamma 1} = E_\gamma (1 - E_\gamma / 2m_1c^2 + p_{nuc} \cos\delta / m_1 c). \tag{6}$$

The mean value of the cross section is

$$\bar{\sigma} = \frac{1}{4\pi} \int \sigma \left(1 + \lambda \frac{v_\beta}{c} \cos\beta\right) d\Omega. \tag{7}$$

Here σ is given by (2), $v\beta$ is the velocity of the electron λ the electron-neutrino correlation constant for β-decay (see, for example, Ref. 5). Utilizing the conservation laws

$$E_\beta + E_\nu = E_{\beta\,max},\quad \mathbf{p}_\beta + \mathbf{p}_\nu + \mathbf{p}_{nuc} = 0, \tag{8}$$

where $E\beta$ is the energy of the detected electron, E_ν the energy of the neutrino, $E_{\beta max}$ the energy of the β-decay, and taking into account

$$p_{nuc} \cos\delta = p_\beta \cos\alpha + p_\nu \cos\varepsilon,\quad \cos\beta = \cos\varepsilon\cos\alpha + \sin\varepsilon\sin\alpha\cos\psi, \tag{9}$$

and that $d\Omega = \sin\epsilon\, d\epsilon\, d\psi$ (ψ — azimuthal angle in a plane perpendicular to OM), one can evaluate the integral (7).

The mean cross section σ depends not only on Γ and Δ but also on the quantity λ which characterizes the interaction of the β-decay. Defining

$$\rho = \Delta m_1 c / p_\nu E_\nu,\quad \tau = \Delta m_1 c / E_\nu p_\beta,\quad \omega = \Delta m_1 c^2 / E_{\gamma_1}, \tag{10}$$

we have

$$\bar{\sigma}(\alpha, p_\beta, \lambda) = \sigma_0 \frac{\sqrt{\pi}}{2} \frac{\Gamma}{\Delta} \frac{1}{2} \left\{ \left(1 + \lambda \frac{cp_\beta}{E_\beta} \frac{\rho}{\omega} \cos\alpha - \lambda \frac{cp_\beta}{E_\beta} \frac{\rho}{\tau} \cos^2\alpha\right) \frac{\sqrt{\pi}}{2} \rho \left[\operatorname{erf}\left(\frac{1}{\rho} + \frac{\cos\alpha}{\tau} - \frac{1}{\omega}\right) + \operatorname{erf}\left(\frac{1}{\rho} - \frac{\cos\alpha}{\tau} + \frac{1}{\omega}\right)\right] \right.$$
$$\left. + \lambda \frac{cp_\beta}{E_\beta} \frac{\rho^2}{2} \cos\alpha \left[\exp\left\{-\left(\frac{\cos\alpha}{\tau} - \frac{1}{\omega} - \frac{1}{\rho}\right)^2\right\} - \exp\left\{-\left(\frac{\cos\alpha}{\tau} - \frac{1}{\omega} + \frac{1}{\rho}\right)^2\right\}\right] \right\}. \tag{11}$$

The cross sections for the β^+ decay of As^{74} are plotted in Fig. 4. The following values have been used: $E_{k\beta\,max}$ = 0.92 Mev, E_γ = 0.596 Mev, E_β = 0.8 $E_{\beta\,max}$. The shapes of the curves depend markedly on λ. The position of the maximum for λ = − 1 and λ = 1/3 differs by 28°. In order to calculate the absolute value of the maximum one needs to know the width of the excited state of Ge^{74}. The mean life of this state has been determined by Metzger[6] by the method of resonance scattering and was found to be $(1.9 \pm 0.3) \times 10^{-11}$ sec.

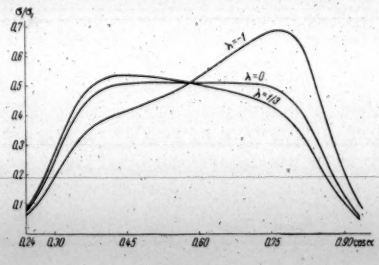

FIG. 4

The cross section at the maximum then turns out to be 6.9×10^{-24} cm^2. Such a cross section can be measured (it is ~ 80% of the cross section of the Compton effect and the photo effect).

5. We now turn to the case where the decay scheme is given by Fig. 5. In the experimental arrangement of Fig. 1 counter A now detects γ-rays of energy E_{γ_1} and counter B γ-rays of energy E_{γ_2}. C is a scatterer consisting of nuclei with atomic number Z + 1. In Ref. 2

this case was treated neglecting the influence of the preceding β-decay. We shall here again consider the recoiling nuclei to be free (gas source). We now shall determine the cross section for resonance scattering of γ-quanta with energy E_{γ_2} on nuclei of the scatterer C if γ-coincidences are counted.

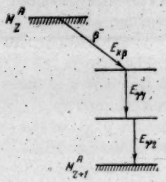

FIG. 5

6. Let the β-decay-induced momentum of the nucleus prior to the emission of the first γ-quantum be p_{nuc}, making an angle θ with the direction of the second γ-quantum. Then the energy E_{γ_2} of the second γ-quantum will be

$$E_{\gamma 2} = E^0_{\gamma 2}\left(1 - \frac{E^0_{\gamma 2}}{2m_1c^2}\right)\left(1 + \frac{p_{nuc}}{m_1 c}\cos\vartheta + \frac{E_{\gamma 1}}{m_1c^2}\cos\alpha\right). \tag{12}$$

The energy needed to excite the scattering nucleus is, as before,

$$E_r = E^0_{\gamma 2}(1 + E^0_{\gamma 2}/2m_1c^2), \tag{13}$$

and the cross section will be given by (2) where one has to replace $E_{\gamma_1} - E_r$ by

$$E_{\gamma 2} - E_r = E^0_{\gamma 2}\left(\frac{E_{\gamma 1}}{m_1c^2}\cos\alpha - \frac{E_{\gamma 2}}{m_1c^2} + \frac{p_{nuc}}{m_1 c}\cos\vartheta\right). \tag{14}$$

Since the β-decay is no longer recorded one has now to average over the angle θ and over all momenta of the recoil nuclei. We shall assume an allowed β-decay so that there are no $\beta - \gamma -$ correlations. Denoting by $f(p_{nuc})\,dp_{nuc}$ the distribution of recoil momenta normalized to unity we have

$$\bar{\sigma} = \sigma_0 \frac{\sqrt{\pi}}{2}\frac{\Gamma}{\Delta}\frac{1}{2}\int_0^{p_{nuc\,lim}} f(p_{nuc})\,dp_{nuc}\int_0^{\pi}\exp\left\{-\frac{E^2_{\gamma 2}}{\Delta^2}\left(\frac{E_{\gamma 1}}{m_1c^2}\cos\alpha - \frac{E_{\gamma 2}}{m_1c^2} + \frac{p_{nuc}}{m_1c}\cos\vartheta\right)^2\right\}\sin\vartheta\,d\vartheta.$$

Since $E_{\gamma_2}p_{nuc}/\Delta m_1 c \gg 1$ one can evaluate the integral over θ by approximating its argument by a δ-function. Thus we obtain

$$\bar{\sigma} = \sigma_0 \frac{\pi}{4}\frac{\Gamma}{E_{\gamma 2}}\int_{|E_{\gamma 1}\cos\alpha - E_{\gamma 2}|}^{p_{nuc\,lim}} \frac{m_1c}{p_{nuc}} f(p_{nuc})\,dp_{nuc}. \tag{15}$$

7. The recoil-nuclei distribution function can be obtained numerically for each concrete case. From (8) follows

$$p^2_{nuc} = p^2_\beta + p^2_\nu + 2p_\beta p_\nu \cos\beta, \tag{16}$$

where β is as above the angle between the electron and neutrino directions. The number of decays with this angle between β and $\beta + d\beta$ is given by

$$\frac{1}{2}\left(1 + \lambda\frac{cp_\beta}{E_\beta}\cos\beta\right)\sin\beta\,d\beta.$$

For a given momentum p_β the distribution function of the recoil nuclei is thus

$$\frac{1}{2}\left(1 + \lambda\frac{cp_\beta}{E_\beta}\frac{p^2_{nuc} - p^2_\beta - p^2_\nu}{2p_\beta p_\nu}\right)\frac{p_{nuc}\,dp_{nuc}}{p_\beta p_\nu}, \tag{17}$$

if

$$p_\beta + p_\nu > p_{nuc} > |p_\beta - p_\nu|, \tag{18}$$

and equal to zero if (18) is not satisfied. By virtue of (18) the momentum p_β for a given p_{nuc} has to lie between $A_2(p_{nuc}) > p_\beta > A_1(p_{nuc})$, where

$$A_1(p_{nuc}) = \frac{1}{c}\left|\frac{(E_{\beta\,max} - cp_{nuc})^2 - m^2_0c^4}{2(E_{\beta\,max} - cp_{nuc})}\right|;\quad A_2(p_{nuc}) = \frac{1}{c}\frac{(E_{\beta\,max} + cp_{nuc})^2 + m^2_0c^4}{2(E_{\beta\,max} + cp_{nuc})}. \tag{19}$$

Assuming an allowed β-spectrum, the momentum distribution function of the recoil nuclei will have the form

$$f(p_{nuc}) = cp_{nuc}\int_{A_1}^{A_2}\left(1+\lambda\frac{cp_\beta}{E_\beta}\frac{p^2_{nuc}-p^2_\beta-p^2_\nu}{2p_\beta p_\nu}\right)F(Z,E_\beta)\,p_\beta p_\nu\,dp_\beta. \qquad (20)$$

Here $F(Z, E_\beta)$ is the well known Fermi function describing the influence of the nuclear Coulomb field on the β-decay. The integral (20) can be evaluated numerically. The distribution function depends on λ.

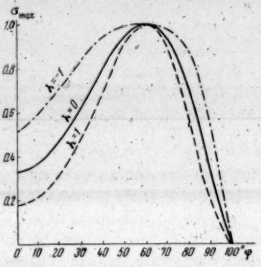

FIG. 6

8. The numerical integration was performed for the decay of Na^{24} which has a decay scheme similar to that of Fig. 5. The following values have been assumed:

$$E_{\beta\,max} = 1.911, \quad E_{\gamma 1} = 2.76, \quad E_\gamma = 1.38\ \text{Mev}.$$

One sees easily that the maximum of the cross section occurs when

$$\cos\alpha = E_{\gamma 2}/E_{\gamma 1}.$$

The integral in (15) which determines the cross section equals 0.448 m_1/m_0 for $\lambda = 0$, 0.378 m_1/m_0 for $\lambda = +1$, and 0.530 m_1/m_0 for $\lambda = -1$ (m_1 — mass of the nucleus, m_0 — electron mass).

The dependence of the cross section on the angle α has been plotted in Fig. 6. All curves have been normalized at the point $\bar{\sigma} = \sigma_{max}$. The maximum cross section (assuming $\Gamma = 3.4 \times 10^{-3}$ ev, lifetime 2×10^{-12} sec) will be 3×10^{-25} cm^2, 2.4×10^{-25} cm^2, and 2×10^{-25} cm^2 for $\lambda = -1.0$, and $+1$ respectively. The variation of the cross section with the angle is quite dependent on λ.

[1] E. Pollard and D. E. Altburger, Phys. Rev. 74, 926 (1948).
[2] N. A. Burgov and Iu. V. Terekhov, Атомная энергия (Atomic Energy) (in press).
[3] K. Siegbahn, Beta- and Gamma-Ray Spectroscopy, Amsterdam (1955), p. 521.
[4] H. A. Bethe, Nuclear Physics (Russ. transl.) Goshekhteorizdat (1950), Part II, p. 139.
[5] J. M. Blatt and V. F. Weisskopf, Theoretical Nuclear Physics (Russ. trans.) IIL (1954) p. 559.
[6] F. R. Metzger, Phys. Rev. 101, 286 (1956).

Translated by M. Danos
130

ON THE THEORY OF THE INFRARED ABSORPTIVITY OF METALS

R. N. GURZHI

P. N. Lebedev Physics Institute, Academy of Sciences, U.S.S.R.

Submitted to JETP editor February 16, 1957

J. Exptl. Theoret. Phys. (U.S.S.R.) **33**, 660-668 (September, 1957)

The infrared absorptivity of metals is studied by means of the quantum kinetic equation. The quantum properties of the electromagnetic field and the anomalous character of the skin effect are taken into account.

1. In the infrared region the energy $\hbar\omega$ of a photon is usually comparable with or greater than the imprecision kT of the Fermi level for electrons in a metal, so that a quantum method of study is required.[1-3] We shall first endeavor to carry through a qualitative analysis of the light absorption mechanism of a metal. In an electromagnetic field the equilibrium electron distribution function $f_0(E_p)$ is modified by an additional small term which is proportional to the field amplitude. If the electromagnetic field is regarded as classical (unquantized) the electrons cannot rise appreciably above the breadth kT of the Fermi level, because the energy acquired by an electron in a mean free path is always small compared with this quantity.

At high temperatures ($T \gg \Theta$) electrons are obviously able to absorb and emit phonos of all momenta up to the limit. This results in relatively high absorptivity which is proportional to the temperature.

At low temperatures ($T \ll \Theta$) momentum exchange is difficult. Indeed, there are almost no "large" phonons, so that they are seldom absorbed. On the other hand the majority of the electrons do not possess sufficient energy for the emission of "large" phonons, since the average electron energy above the Fermi level is of the order kT, which is small compared with $k\Theta$. As a result there is weak absorption which decreases rapidly with temperature ($\sim T^5$). When we take into account the quantum properties of the field an especially important difference appears in the limiting case of low temperatures and large electromagnetic quanta, when

$$\hbar\omega \gg k\Theta \gg kT. \tag{1}$$

Indeed, electrons which absorb quanta rise far above the region of the Fermi level. To be sure, they are, as previously, unable to absorb "large" phonons, but because of their high energy they can emit phonons over the entire spectrum. In this respect the quantum absorption mechanism in the limiting case (1) is similar to the classical absorption mechanism at high temperatures.

We shall here discuss the near infrared region for which

$$\omega \gg 1/\tau, \quad v_0/\omega \ll \delta, \quad \delta = (4\pi Ne^2/mc^2)^{-1/2}, \tag{2}$$

where τ is the mean free time, δ is the skin depth v_0/ω is the distance traversed by an electron during one period of vibration of the electromagnetic field and v_0 is the velocity of an electron at the Fermi level. It will also be assumed that the photoconductive threshold has not been reached. For most metals (2) is satisfied when $\lambda \ll 100\mu$.

Except at very high temperatures, the skin effect in the infrared region is anomalous, i.e.,

$$l = v_0\tau \gg \delta. \tag{3}$$

If, however, it is assumed that the electromagnetic field and the electron distribution vary little in a mean free path l, for the purpose of calculating the volume absorptivity of a metal it is possible to employ perturbation theory, as was done by Holstein.[2] As Holstein gave a result only for the limiting case (1) and did not show his calculation, we began with a similar calculation.

In calculating the probability of photon absorption it is necessary to take into account all second-order processes with simultaneous participation of a photon and a phonon; there are 8 such processes in all. By simple calculation the expression for the volume absorptivity A_V ($A = 1-r$, r is the reflection

coefficient) assumes the general form

$$A_\omega = 2\delta / c\tau(T), \tag{4}$$

after introduction of the effective mean free time

$$\tau(T) = \tau^{(cl)}(T) / \varphi(T), \tag{5}$$

where $\tau^{(cl)}(T) \sim 1/T$ is the usual high-temperature mean free time and*

$$\varphi(T) = \frac{2}{\alpha}\left(\frac{T}{\Theta}\right)^4 \int_0^{\Theta/T} dv\, v^4 \left(\frac{2\alpha}{e^v - 1} + \frac{v-\alpha}{e^{v-\alpha}-1} - \frac{v+\alpha}{e^{v+\alpha}-1}\right), \quad \alpha = \frac{\hbar\omega}{kT}. \tag{6}$$

When $kT \gg k\vartheta \gg \hbar\omega$ we necessarily have $\varphi \approx 1$, whereas in the other limiting case (1) $\varphi \approx 2\Theta/5T$ and consequently,

$$\tau(T) \approx (5T/2\Theta)\tau^{(cl)}(T) = {}^5/_2\tau^{(cl)}(\Theta),$$

which is in agreement with Holstein's results.[2]

We note that (5) and (6) are obtained simply from the quantum kinetic equation derived in Ref. 1.

For convenience we introduce the notation

$$\psi(E_p) = m\tau(T)D(p),$$

where $\tau(T)$ is given by (5) and it can easily be shown that

$$\int_0^\infty dE\psi(E) = -1.$$

Then the kinetic equation (17) of Ref. 1 becomes

$$i\omega f_1 + \frac{\mathbf{p}}{m}\frac{\partial f_1}{\partial \mathbf{r}} + \tau^{-1} f_1 = e\mathbf{E}\left[\frac{\partial f_0}{\partial p} + \frac{1}{i\omega\tau}\frac{\partial f_0}{\partial p} - \frac{\mathbf{p}}{i\omega m\tau(T)}\psi(E_p)\right]. \tag{7}$$

The term $(\mathbf{p}/m)\,\partial f_1/\partial \mathbf{r}$ drops out of a spatially uniform distribution, after which, in virtue of $\omega \gg 1/\tau(T)$, the kinetic equation is solved simply by successive approximations:

$$f_1^{(I)}(\mathbf{p}) = \frac{e}{i\omega}\left(\mathbf{E}\frac{\partial f_0}{\partial \mathbf{p}}\right), \quad f_1^{(II)}(\mathbf{p}) = \frac{e}{\omega^2 m\tau(T)}(\mathbf{E}\mathbf{p})\psi(E_p), \ldots$$

The first approximation naturally yields the dielectric constant

$$\varepsilon = 1 - 4\pi Ne^2/m\omega^2, \quad N = (8\pi/3)(p_0/2\pi\hbar)^3$$

(where N is the electron density), and the second approximation gives the conductivity

$$\sigma = Ne^2/m\omega^2\tau(T),$$

where, as expected, $\tau(T)$ is given by (5). A free electron cannot absorb an electromagnetic quantum; therefore losses occur only through electron collisions with phonons (or impurities) or with the metal boundary. Since, according to (2) and (3), in the infrared region the path v_0/ω of an electron during a period of the field vibration is small compared with the mean free path l, for calculation of the surface loss it is possible to neglect collisions with the lattice in first approximation. For diffuse electron reflection from the boundary the surface absorption is given by[3]

$$A_d = 3v_0/4c. \tag{8}$$

However, one must first be certain that even for very high frequencies it is possible as in Ref. 2 to simply add volume and surface losses in first approximation.

2. We now proceed to a rigorous examination of the problem with allowance for the anomalous nature of the skin effect. We first note that in the infrared region $|\epsilon| \gg 1$, so that it is sufficient for us to confine ourselves to normal incidence of electromagnetic waves on the surface of the metal.[3] Then all quantities will depend only on the distance z between any point and the metal surface.

*In all calculations it is assumed that kT, $k\Theta$ and $\hbar\omega$ are small compared with the electron energy limit E_0.

In momentum space we select spherical coordinates (p, ϑ, φ) with the axis directed into the metal and perpendicular to its boundary, while the angle φ is measured from the direction of the electric field **E**.

It is known that in the case of the anomalous skin effect the electron distribution function must be subject to boundary conditions whose form depends essentially on the character of electron reflection from the metal surface. Certain theoretical considerations,[3] as well apparently as experiments, would indicate diffuse reflection.

We denote by $f_1^{(1)}$ and $f_1^{(2)}$ the respective values of $f_1(\mathbf{p}, z)$ for electrons reflected from $(p_z > 0)$ and approaching $(p_z < 0)$ the metal boundary. Then the condition for diffuse reflection is

$$f_1^{(1)}(\mathbf{p}, 0) = 0. \tag{9}$$

In addition, we must impose the condition for vanishing of $f_1^{(2)}$ within the metal:

$$f_1^{(2)}(\mathbf{p}, \infty) = 0. \tag{10}$$

We introduce the dimensionless coordinate $x = \omega z / v_0$ and the dimensionless quantities:

$$\eta = v_0 / \omega\delta, \quad \varkappa = l / \omega\tau(T), \quad \hat{s} = \tau(T)/\hat{\tau}, \quad \hat{L}^{-1} = (i + \varkappa\hat{s}) / \cos\vartheta.$$

With this notation the kinetic equation (7) becomes

$$\hat{L}^{-1} f_1 + \partial f_1 / \partial x = (ev_0 / \omega) E(x) \chi(\mathbf{p}),$$

where

$$\chi(\mathbf{p}) = -i\hat{L}^{-1} \sin\vartheta \cos\varphi \, \partial f_0 / \partial E_p + i\varkappa \tan\vartheta \cos\varphi \cdot \psi(E_p).$$

The general solution of this equation can be written as

$$f_1(\mathbf{p}, x) = e\frac{v_0}{\omega}\int_0^x dx' E(x') \exp\{(x' - x)\hat{L}^{-1}\} \chi(\mathbf{p}).$$

Determining the lower limit of integration from the boundary conditions (9) and (10), we obtain

$$f_1^{(1)}(\mathbf{p}, x) = e\frac{v_0}{\omega}\int_0^x dx' E(x') \exp\{(x' - x)\hat{L}^{-1}\} \chi(\mathbf{p}), \quad f_1^{(2)}(\mathbf{p}, x) = -e\frac{v_0}{\omega}\int_x^\infty dx' E(x') \exp\{(x' - x)\hat{L}^{-1}\} \chi(\mathbf{p}).$$

The corresponding current density

$$j(x) = -\frac{2e}{(2\pi\hbar)^3}\left\{\int_{p_z>0} d\mathbf{p} \cdot \sin\vartheta \cos\varphi \frac{p}{m} f_1^{(1)}(\mathbf{p}, x) + \int_{p_z<0} d\mathbf{p} \cdot \sin\vartheta \cos\varphi \frac{p}{m} f_1^{(2)}(\mathbf{p}, x)\right\}$$

after some transformations becomes

$$j(x) = -\frac{3Ne^2}{4\pi\omega m}\int_0^\infty dx' E(x') \int_0^\infty dE_p \int_0^{2\pi} d\varphi \int_0^{\frac{\pi}{2}} d\vartheta \cdot \sin^2\vartheta \cos\varphi \exp\{-|x - x'| \hat{L}^{-1}\} \chi(\mathbf{p}).$$

Inserting this expression into the equation for the electric field we obtain, since the term $(\omega/c)^2 E$ associated with the vacuum displacement current is small in the infrared region:

$$E''(x) = \zeta\int_0^\infty dx' E(x') K(x - x'), \tag{11}$$

where

$$K(x) = -\frac{1}{\pi}\int_0^\infty dE_p \int_0^{2\pi} d\varphi \int_0^{\frac{\pi}{2}} d\vartheta \cdot \sin^2\vartheta \cos\varphi e^{-|x|\hat{L}^{-1}} \chi(\mathbf{p}), \quad \zeta = i\frac{3}{4}\eta^2.$$

An equation such as (11) is basic in the theory of the anomalous skin effect and has been thoroughly studied by Reuter and Sondheimer.[4]

Specifically, for the surface impedance

$$Z = R + iX = -i\,(4\pi v_0/c^2)\,E(0)/E'(0)$$

Reuter and Sondheimer's results easily yield the expression

$$Z = i\,\frac{4\pi v_0}{c^2}\,[I(\zeta)]^{-1},$$

where

$$I(\zeta) = \frac{1}{\pi}\int_0^\infty dt\cdot \ln\left(1+\zeta\,\frac{k(t)}{t^2}\right); \tag{12}$$

$$k(t) = \int_{-\infty}^{+\infty} dx K(x)\, e^{-itx} = -\frac{2}{\pi}\int_0^\infty dE_p \int_0^{2\pi} d\varphi \int_0^{\frac{\pi}{2}} d\vartheta\, \sin^2\vartheta\cos\varphi\,\frac{\hat{L}}{1+\hat{L}^2 t^2}\,\chi(\mathbf{p}). \tag{13}$$

In virtue of (2) we have for the infrared region $|\zeta| \ll 1$. It is therefore reasonable to attempt a representation of the surface impedance by a power series in ζ. However, when the integrand of (12) is directly expanded in ζ divergent expressions appear. As will be seen below, this follows particularly from the fact that the expansion does not take place in whole powers of ζ.

For the purpose of obtaining a suitable expansion we can follow Dingle[5] and use the Mellin transform of $I(\zeta)$, which is given by

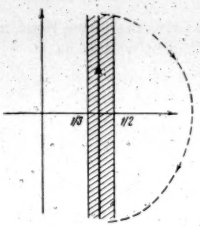

$$M(z) = \int_0^\infty d\zeta I(\zeta)\,\zeta^{z-1}. \tag{14}$$

(See Ref. 6, for example). Let the integral be bounded as follows in the region $z_1 < \mathrm{Re}\, z < z_2$:

$$\int_0^\infty d\zeta\,|I(\zeta)|\,\zeta^{z-1} < \mathrm{const}, \tag{15}$$

then the inverse transformation is given by

$$I(\zeta) = \frac{1}{2\pi i}\int_{c-i\infty}^{c+i\infty} M(z)\,\zeta^{-z}\,dz \tag{16}$$

and exists for $z_1 < c < z_2$.

In our case we easily obtain from (14) and (12)

$$M(z) = \frac{1}{z\sin\pi z}\int_0^\infty dt k^{-z}(t)\,t^{2z}.$$

Substituting this expression into (16), we obtain after changing the sign of the integration variable

$$I(\zeta) = \frac{1}{2\pi i}\int_{c-i\infty}^{c+i\infty} dz\,\frac{\zeta^z}{z\sin\pi z}\int_0^\infty dt k^z(t)\,t^{-2z}, \tag{17}$$

with the condition (15) satisfied when

$$1/3 < \mathrm{Re}\, z < 1/2. \tag{18}$$

In order to obtain an expansion in increasing powers of ζ we naturally close the integration contour at infinity in the right-hand half-plane and use the theory of residues (see the figure). However, for all z outside of the limits given by (18) the integral

$$\int_0^\infty dt k^z(t)\,t^{-2z}. \tag{19}$$

diverges. This difficulty can be overcome if we succeed in constructing an analytic continuation of (19), as was done in Ref. 5.

For this purpose we assume now that z lies in the zone given by (18) and write (19) in the form

$$\int_0^\infty dt k^z(t)\,t^{-2z} = \int_0^1 dt\,k^z(t)\,t^{-2z} + \int_1^\infty dt\,k^z(t)\,t^{-2z}. \tag{20}$$

We shall also assume that we have obtained the expansion

$$k(t \leqslant 1) = a \sum_{n=0}^{\infty} a_n t^{2n}, \qquad k(t \geqslant 1) = t^{-1} b \sum_{n=0}^{\infty} b_n t^{-n}, \quad a_0 = b_0 = 1$$

and hence

$$k^z(t \leqslant 1) = a^z \sum_{n=0}^{\infty} A_n(z)\, t^{2n}, \qquad k^z(t \geqslant 1) = t^{-z} b^z \sum_{n=0}^{\infty} B_n(z)\, t^{-n}. \tag{21}$$

The coefficients A_n and B_n can be expressed simply in terms of a_n and b_n; specifically,

$$A_0 = 1, \quad A_1 = a_1 z, \quad A_2 = a_2 z + {}^1/_2 z(z+1) a_1^2, \ldots \tag{22}$$

Substituting the expansions (21) into the first and second integrals of (20), respectively, we obtain after integrating

$$\int_0^{\infty} dt\, k^z(t)\, t^{-2z} = \sum_{n=0}^{\infty} \left(\frac{a^z A_n(z)}{2n^2 - 2z + 1} + \frac{b^z B_n(z)}{3z + n - 1} \right). \tag{23}$$

For the integration it was assumed that (18) is fulfilled, although the final result, unlike the integral on the left, is analytic over the entire z plane.

This analytic continuation can be written in a somewhat different form. We note that the lower limit 0 did not contribute to the integral in (20). Therefore the analytic continuation (23) can be written as

$$\int_{\infty}^{\infty} dt\, k^z(t)\, t^{-2z}. \tag{24}$$

The arbitrary constant in the original function

$$\Psi(x, z) = \int_{x}^{\infty} dt\, k^z(t)\, t^{-2z}$$

is derived from the condition that $\Psi(0, z)$ vanish in the region (18), since otherwise (24) obviously is meaningless.

Substituting (23) into (17) we have

$$I(\zeta) = \frac{1}{2\pi i} \int_{c-i\infty}^{c+i\infty} dz \frac{a^z \zeta^z}{z \sin \pi z} \sum_{n=0}^{\infty} \frac{A_n(z)}{2n - 2z + 1} + \frac{1}{2\pi i} \int_{c-i\infty}^{c+i\infty} dz \frac{b^z \zeta^z}{z \sin \pi z} \sum_{n=0}^{\infty} \frac{B_n(z)}{3z + n - 1}.$$

When the integration contour is closed on the right-hand side (see figure) it encloses the zones for $\sin \pi z$ at $z = 1, 2, 3 \ldots$ and, for the first term, the zones $z = (2n+1)/2$ $(n = 0, 1, 2 \ldots)$. A complication appears in the fact that, whereas the coefficients A_n are easily obtained, the coefficients B_n cannot be given in explicit form. Indeed, according to (2) $\kappa \ll 1$, and thus $\hat{L} = (i + \kappa\hat{s})^{-1} \cos\vartheta \approx -i \cos\vartheta$ is a bounded quantity. Therefore in (13) an expansion in $\hat{L}t$ is possible for small t. On the other hand, when $t \gg 1$ $\hat{L}t$ cannot be regarded as large, so that an expansion in $(\hat{L}t)^{-1}$ is not permissible. In Dingle's classical treatment[5] a number replaced the operator $\hat{L}$, so that it was possible to integrate in (13) and then expand the result in reciprocal powers of t.

We shall first take the residues at the poles $z = (2n+1)/2$, and in calculating the residues due to $\sin \pi z$ we shall use Eq. (24) for the analytic continuation. The result is

$$I(\zeta) = (a\zeta)^{1/2} \sum_{n=0}^{\infty} \frac{(-1)^n}{2n+1} (a\zeta)^n A_n\left(n + \frac{1}{2}\right) - \frac{1}{\pi} \sum_{n=1}^{\infty} \frac{(-1)^n}{n} \zeta^n \int_{\infty}^{\infty} dt\, k^n(t)\, t^{-2n}.$$

If the integration contour were closed in the left-hand half-plane it would be possible in exactly the same way to obtain an expansion in reciprocal powers of ζ, which would correspond to the radio frequency range. But it would be necessary to know an explicit form of the B_n.

Expanding (13) in powers of $(\hat{L}t)^2$, we obtain

$$a = -\frac{2}{\pi}\int_0^\infty dE \int_0^{2\pi} d\varphi \int_0^{\frac{\pi}{2}} d\vartheta \sin^2\vartheta \cos\varphi \hat{L}\chi(\mathbf{p}), \quad a_n = -\frac{(-1)^n}{a}\frac{2}{\pi}\int_0^\infty dE \int_0^{2\pi} d\varphi \int_0^{\frac{\pi}{2}} d\vartheta \sin^2\vartheta \cos\varphi \hat{L}^{2n+1}\chi(\mathbf{p}).$$

The values of A_n can be obtained from (22). Furthermore, according to (13)

$$\int_0^\infty k^n(t)\, t^{-2n}\, dt = (-1)^n\left(\frac{2}{\pi}\right)^n \prod_{k=1}^n \int_0^\infty dE_k \int_0^{2\pi} d\varphi_k \int_0^{\frac{\pi}{2}} d\vartheta_k \sin^2\vartheta_k \cos\varphi_k \int_0^\infty dt \cdot t^{-2n} \frac{\hat{L}_k^{-1}}{t^2 + \hat{L}_k^{-2}}\chi(\mathbf{p}_k)$$

$$= \left(\frac{2}{\pi}\right)^n \prod_{k=1}^n \int_0^\infty dE_k \int_0^{2\pi} d\varphi_k \int_0^{\frac{\pi}{2}} d\vartheta_k \sin^2\vartheta_k \cos\varphi_k \hat{L}_k^{-1} \sum_{m=1}^n \int_0^\infty dt \left[\frac{\hat{\alpha}_{mn}}{t^2 + \hat{L}_m^{-2}} + \hat{\beta}_{mn} t^{-2m}\right]\chi(\mathbf{p}_k),$$

where

$$\hat{\alpha}_{mn} = \hat{L}_m^{2n} \prod_{i=1}^{n\,\prime} (\hat{L}_i^{-2} - \hat{L}_m^{-2})^{-1};$$

the prime denotes that the product includes no factor with $i = m$. From our definition of the original function

$$\int_0^\infty dt \cdot t^{-2m} = \frac{t^{1-2m}}{1-2m}\Big|_0^\infty = 0; \qquad \int_0^\infty \frac{dt}{t^2 + \hat{L}^{-2}} = \frac{\pi}{2}\hat{L}.$$

Thus

$$\int_0^\infty dt \cdot k^n(t)\, t^{-2n} = +\left(\frac{2}{\pi}\right)^{n-1} \prod_{k=1}^n \int_0^\infty dE_k \int_0^{2\pi} d\varphi_k \int_0^{\frac{\pi}{2}} d\vartheta_k \sin^2\vartheta \cos\varphi_k \hat{L}_k^{-1} \sum_{m=1}^n \hat{L}_m^{2n+1} \prod_{i=1}^n (\hat{L}_i^{-2} - \hat{L}_m^{-2})^{-1}\chi(\mathbf{p}_k).$$

When $\hat{L} = (1 + \kappa\hat{s})^{-1}\cos\vartheta$ and $\zeta = i3\eta^2/4$ are substituted in these expressions $I(\zeta)$ can easily be represented as a series in the small dimensionless parameters η and κ. Limiting ourselves to quadratic terms in η and κ, we obtain after some tedious calculations

$$A \approx \frac{c}{\pi}R = \frac{3}{4}\beta + 2\beta\eta_l^{-1}\varkappa - \frac{1}{4}\beta\eta_l^2\left(\frac{16}{35}\ln 2 + \frac{8723}{26880}\right) - 3\beta\eta_l\varkappa\left[\frac{83}{1720} + \Phi\left(\frac{3}{8}\hat{s}\cos\vartheta - \hat{s}\cos^2\vartheta - \cos\vartheta\,\hat{s}\cos\vartheta,\ \frac{\partial f_0}{\partial E}\right)\right]$$

$$+ 3\beta\varkappa^2\left[\Phi\left(\hat{s}^2\cos\vartheta - \hat{s}\cos\vartheta,\ \frac{\partial f_0}{\partial E}\right) + \Phi\left(\hat{s}\cos\vartheta + \cos\vartheta\,\hat{s} - \frac{3}{8}\hat{s},\ \psi\right)\right] - 3\beta\eta_l^{-1}\varkappa^3\left[\frac{5}{12} + \Phi\left(\frac{3}{2}\hat{s} - \hat{s}^2, \psi\right)\right], \tag{25}$$

$$\frac{c}{\pi}X = 4\beta\eta_l^{-1} + \frac{83}{320}\beta\eta_l - 3\beta\varkappa\Phi\left(\hat{s}\cos\vartheta, \frac{\partial f_0}{\partial E}\right) - \frac{3}{2}\beta\eta_l^{-1}\varkappa^2[1 + 2\Phi(\hat{s}, \psi)]. \tag{26}$$

Here $\beta = v_0/c$, $\eta = v_0/\omega\delta$, $\kappa = 1/\omega\tau(T)$ and Φ denotes integrals of the form

$$\Phi(\hat{s}, \psi) = \frac{1}{\pi}\int_0^\infty dE \int_0^{2\pi} d\varphi \int_0^{\frac{\pi}{2}} d\vartheta \sin^2\vartheta \cdot \cos\varphi \cdot \hat{s}\sin\vartheta \cdot \cos\varphi \cdot \psi(E_p).$$

It is easily seen that when the operator $\hat{s}$ is replaced by unity (25) and (26) go over into the corresponding expressions which were obtained in a classical treatment by Dingle.[1] The first term in (25) coincides with (8) and thus gives the loss associated with electron reflection from the metal boundary, whereas the second term coincides with (4) and thus gives the exchange loss. Thus in first approximation we actually have a simple addition of exchange and surface losses.

All of the integrals Φ are of the order of unity and can be calculated without great difficulty. However, the corresponding expressions cannot be written in compact form. We note that the ratio $(\eta/\kappa)^2 = (l/\delta)^2$ for most good conductors is large compared with unity.* Therefore in (25) the first two corrections, which are proportional to η^2 and $\eta\kappa$, are usually most important. A calculation shows that

*For example, for Cu, Ag and Au $(l/\delta)^2 \sim 10$ even at room temperature.

$$\Phi\left(\frac{3}{8}\hat{s}\cos\vartheta-\hat{s}\cos^2\vartheta-\cos\vartheta\,\hat{s}\cos\vartheta,\ \frac{\partial f_0}{\partial E}\right)=\frac{1}{\varphi(T)}\left(\frac{T}{\Theta}\right)^4\int_0^{\Theta/T}dv\cdot v^4\frac{1}{1920}\left[484-569v^2\left(\frac{kT}{up_0}\right)^2\right]$$

$$\times\left[2\coth\frac{v}{2}-\coth\frac{\alpha+v}{2}+\coth\frac{\alpha-v}{2}+\frac{2(\alpha+v)e^{\alpha+v}}{(e^{\alpha+v}-1)^2}-\frac{2(\alpha-v)e^{\alpha-v}}{(e^{\alpha-v}-1)^2}\right]. \tag{27}$$

It has already been mentioned that in the infrared region we usually have $\hbar\omega > kT$. We therefore assume that

$$e^{\hbar\omega/kT}\gg 1,\quad e^{\hbar\omega/kT}\gg e^{\Theta/T}. \tag{28}$$

Then when terms of the order of $e^{-\hbar\omega/kT}$ are neglected the integral in (27) is greatly simplified and in our approximation $(\eta^2 \gg \varkappa^2)$ the absorption becomes

$$A\approx\frac{3}{4}\beta+2\beta\gamma_l^{-1}\varkappa-\frac{1}{4}\beta\gamma_l^2\left(\frac{16}{35}\ln 2+\frac{8723}{26880}\right)-\beta\gamma_l\varkappa\left[\frac{82}{640}+\frac{1}{\varphi(T)}\left(\frac{T}{\Theta}\right)^4\int_0^{\Theta/T}dv\cdot v^4\coth\frac{v}{2}\cdot\frac{1}{320}\left[484-569\cdot v^2\left(\frac{kT}{up_0}\right)^2\right]\right].$$

On the basis of (27) in the classical limit $(\hbar\omega \ll k\Theta \ll kT)$ we easily obtain the following expression for the second absorption correction:

$$-\beta\gamma_l\varkappa\frac{1}{640}\left[567-\frac{2}{3}\,569\left(\frac{k\Theta}{up_0}\right)^2\right].$$

If we immediately set $\hat{s} = 1$ in (25) the result is $-\beta\eta\kappa 83/12$, which agrees with the corresponding term in Ref. 7. It appears that in Ref. 7 all corrections beginning with the second were calculated incorrectly, because even when $\hbar\omega \ll kT$ it is not always correct in the case of the anomalous skin effect to approximate the collision integral by means of an expression of the form f_1/τ (see the comment at the end of Ref. 8).

When the inequalities (28) are fulfilled it follows from (6) that

$$\varphi(T)\approx 2\left(\frac{T}{\Theta}\right)^4\int_0^{\Theta/T}dv\,v^4\coth\frac{v}{2}-\frac{\Theta}{3T}\frac{k\Theta}{\hbar\omega}, \tag{29}$$

An investigation of this expression shows that from room temperature down to the temperature of liquid helium the mean free time $\tau(T) = \tau^{(cl)}(T)/\varphi(T)$ is relatively independent of temperature and changes smoothly from $\tau^{(cl)}(T)$ at high temperatures to $\frac{5}{2}\tau^{(cl)}(\Theta)$ at low temperatures. Classically, as we know, $\tau(T)$ increases very rapidly as the temperature is reduced (at low temperatures it is inversely proportional to T^5). It is significant that (29) was derived subject to the relatively mild limitations of (28); therefore quantum effects play an important part at least when $\hbar\omega \sim (2-3)kT$.

It must be remembered that the results obtained here are based on the assumption of a spherical Fermi surface for the electrons of a metal and can apparently be applied only to polycrystalline specimens. Of course, m and v_0 mean averaged quantities. In addition, and especially at low temperatures, interelectronic collisions may play a large role. This question will be discussed at a later date.

The author is profoundly grateful to V. L. Ginzburg and V. P. Silin for their continued interest and valuable comments.

[1] R. N. Gurzhi, J. Exptl. Theoret. Phys. (U.S.S.R.) **33**, 451 (1957), Soviet Phys. JETP **6**, 352 (1958).
[2] T. Holstein, Phys. Rev. **96**, 535 (1954).
[3] V. L. Ginzburg and G. P. Motulevich, Usp. Fiz. Nauk **55**, 469 (1955).
[4] G. E. Reuter and E. H. Sondheimer, Proc. Roy. Soc. (London) **A195**, 336 (1948).
[5] R. B. Dingle, Appl. Scient. Res., Sec. B, **3**, 69 (1953).
[6] E. C. Titchmarsh, Introduction to the Theory of Fourier Integrals (Oxford, 1937).
[7] R. B. Dingle, Physica **19**, 311, 729 (1953).
[8] V. L. Ginzburg and V. P. Silin, J. Exptl. Theoret. Phys. (U.S.S.R.) **29**, 64 (1955); Soviet Phys. JETP **2**, 46 (1956).

Translated by I. Emin
131

CORRELATION THEORY FOR RAYLEIGH SCATTERING OF LIGHT. II

S. M. RYTOV

P. N. Lebedev Physics Institute, Academy of Sciences, U.S.S.R.

Submitted to JETP editor March 2, 1957

J. Exptl. Theoret. Phys. (U.S.S.R.) **33**, 671-682 (September, 1957)

A number of further consequences which follow from the general formulas obtained in Ref. 1 for the spectral intensities of scattered light are considered. The integrated intensities of the fine structure components of the isotropic part of the scattered light are obtained for a medium with small viscous losses and small heat losses using specific dispersion relations. The dispersion corrections for the Landau-Placzek relation are considered in greater detail for a low-viscosity liquid. The results of the general theory which concern anisotropic scattering are discussed and simple dispersion relations are indicated which yield a satisfactory approximation to the observed intensity distribution in the wing of the Rayleigh line for a low-viscosity liquid. Using these relations the integrated intensities are obtained and an approximation formula is derived for the depolarization coefficient in Rayleigh scattering.

IN an earlier paper[1] (referred to hereafter as I) we have developed a spectral theory for Rayleigh scattering, based on correlation theory as applied to the thermal fluctuations in an isotropic medium.[2] General formulas were obtained for observation at right angles to the primary wave and four combinations of the polarization of the primary and scattered light [Eqs. (3.1) of I]. These general formulas apply for any dispersion relation between the parameters which is consistent with the dissipation requirements of the medium. As a first result we have obtained the integrated intensity of the isotropic part of the scattered light and, using certain assumptions, have found the dispersion correction to the Einstein formula for liquids.

In the present part of the work we consider further consequences which follow from the general formulas; first of all, we consider the problem of the integrated intensities of the components of the isotropic part of the scattered light – the central line of the Mandel'shtam-Brillouin doublet and the background. Although the background due to dispersion in the compression modulus $\overline{K}$ and the shear modulus $\overline{\mu}$ is present in isotropic scattering, in low-viscosity liquids it turns out to be extremely weak. In practice, the isotropic part of the scattered light tends to be characterized by the usual triplet in this case. The intensity of the triplet components is calculated in the approximation that there is dispersion only in the elastic moduli; the simplest dispersion relations are assumed – with a single relaxation time for each modulus (τ' for $\overline{K}$ and τ for μ). The neglect of the dispersion background is manifest only in the correction to the intensity I_{MB} of the Mandel'shtam-Brillouin doublet. This correction, due to the dispersion in $\overline{K}$ leads specifically to the intensity ratio for the non-displaced line I_{cent} and the doublet which was obtained earlier by I. L. Fabelinskii[3,4] in an analysis of the doublet based on diffraction by Debye waves.

Essentially new results are obtained in an analysis of the anisotropic scattering (Secs. 3 – 5). The spectral intensities are given by formulas which contain the results of the wing analysis for liquids developed by Leontovich[5] as a particular case corresponding to the assumption that the mechanical-optical coefficient X is directly proportional to the compression modulus $\overline{\mu}$. A departure from this assumption allows a good approximation for the distribution of intensity in the wing, including the intense center part even when the simplest dispersion relations for X and $\overline{\mu}$ are assumed. In this case it is sufficient to assume two relaxation times for X, τ_1 and $\tau_2 \gg \tau_1$, the values of which may be obtained from the spectral intensity distribution. A calculation of the integrated intensities for the dispersion laws which have been indicated leads to an approximation formula (5.9) for the Kabanovsky depolarization factor Δ. An estimate of Δ in benzol based on this formula turns out to be in good agreement with the experimental value.

1. INTEGRATED INTENSITIES OF THE I_{iso} COMPONENT (FORMULATION OF THE PROBLEM)

The spectral intensity of the isotropic part of the light which is scattered by fluctuations in the density and temperature of the medium is given by the following general expression [Eq. (4.1) of I; all notation is the same as in I]:

$$J_{iso} = \frac{\theta}{2\pi i\Omega}\left\{\frac{1}{\Delta}\left[|Y|^2\left(\frac{d_1A_3}{\overline{K}^*} - CC^*\overline{K}q^2\right) - YZ^*C\overline{K}q^2 + Y^*Z\left(C^*A_1 - C\frac{\overline{K}}{\overline{K}^*}A_3\right) + |Z|^2A_1\right] - \text{comp. conj.}\right\} \qquad (1.1)$$

In calculating the total integrated intensity in I

$$I_{iso} = \int_{-\infty}^{+\infty} J_{iso}\, d\Omega, \qquad (1.2)$$

we have made use of general theorems[2] which make it possible to obtain a definite result by simplifying the dispersion relations for some of the parameters which appear in (1.1); in particular, Y, Z, C and $\overline{K}$. This approach is not adequate in problems in which loss must be taken into account since separating I_{iso} into component intensities means that we must find the residues of the integral (1.2) at separate poles of the integrand; consequently this procedure requires a complete knowledge of the function.

As in I, we shall make the following assumptions with respect to the parameters Y, Z, C and $\overline{K}$: (a) the coefficients Y and Z are independent of Ω, (b) the thermal parameters C, D, and κ are independent of Ω, (c) the elastic moduli $\overline{K}$ and $\overline{\mu}$ are characterized by the simplest dispersion relation with a single relaxation time for each (τ' and τ respectively)

$$\overline{K} = \frac{K_\infty z + K_0/\tau'}{z + 1/\tau'}, \quad \overline{\mu} = \frac{\mu_\infty z + \mu_0/\tau}{z + 1/\tau} \qquad (z = i\Omega). \qquad (1.3)$$

We note that by virtue of the assumptions in (a) and (b) the corresponding parameters are given by the real thermodynamic values

$$Y = -\rho_0(\partial\varepsilon/\partial\rho)_T, \quad Z = T_0(\partial\varepsilon/\partial T)_\rho, \quad C = \alpha T_0, \quad D = \rho_0 T_0 c_p. \qquad (1.4)$$

Using these assumptions the determinant Δ which appears in the denominator of Eq. (1.1) has the form

$$\Delta = \left(D_1 + \frac{\varkappa T_0 q^2}{i\Omega}\right)\left(\rho_0\Omega^2 - \frac{4}{3}\overline{\mu}q^2\right) - \left(D + \frac{\varkappa T_0 q^2}{i\Omega}\right)\overline{K}q^2 = -\frac{\rho_0 D}{z(z+1/\tau')(z+1/\tau)}\left\{v(z)\,u(z) + \frac{K_\infty q^2}{\rho_0}(z+\chi q^2)\left(z+\frac{1}{\tau}\right)(z+a)\right\} = -\frac{\rho_0 D_{1\infty}}{z(z+1/\tau')(z+1/\tau)}(z-z_1)(z-z_2)(z-z_3)(z-z_4)(z-z_5), \qquad (1.5)$$

where

$$u(z) = z^2(z+1/\tau) + (M_\infty q^2/\rho_0)(z+b), \quad v(z) = (z+\chi q^2)(z+1/\tau') - \frac{\gamma-1}{\gamma}\frac{K_\infty}{K_0}z(z+a),$$
$$a = K_0/K_\infty\tau', \quad b = \mu_0/\mu_\infty\tau, \quad \overline{M} = {}^4/_3\,\overline{\mu}, \quad D_1 = D - c^2\overline{K} = D\left(1 - \frac{\gamma-1}{\gamma}\frac{\overline{K}}{K_0}\right). \qquad (1.6)$$

$\chi = \varkappa/\rho_0 c_p$ is the heat conductivity of the medium, $\gamma = c_p/c_v$. Thus, the numerator of Δ contains a polynomial of the fifth degree in z in which all the roots z_j must, in accordance with the dissipation requirements of the system, lie in the left half-plane of z. All dispersion laws for the parameters must satisfy this criterion.

Substituting Eqs. (1.1) and (1.5) in Eq. (1.2) and using the notation of (1.6) it is easy to reduce the expression for the integrated intensity of the isotropic scattering to the form

$$I_{iso} = \frac{\theta}{2\pi i D_{1\infty}}\oint_\Gamma \left\{\frac{g(z)}{f(z)} - \frac{g(-z)}{f(-z)}\right\}\frac{dz}{z}, \quad f(z) = (z-z_1)(z-z_2)(z-z_3)(z-z_4)(z-z_5), \qquad (1.7)$$

where the path of integration Γ goes along the imaginary z-axis and is closed at infinity, encompassing the left half-plane, and where

$$g(z) = \frac{DY^2}{K_\infty}\cdot\frac{(z+\chi q^2)(z^2-1/\tau'^2)\,u(z)}{z-a} - 2YZ_1C\frac{z(z^2-a/\tau')\,u(z)}{z-a} + Z_1^2 z\,[u(z)(z+1/\tau') + (K_\infty q^2/\rho_0)(z+a)(z+1/\tau)]. \qquad (1.8)$$

Here, in place of Z we introduce the quantity

$$Z_1 = Z + CY, \tag{1.9}$$

by virtue of which the expression for g(z) can be written in shorter form. The thermodynamic significance of Z_1, in accordance with Eqs. (1.4) and (1.9), is the following:

$$Z_1 = T_0(\partial\varepsilon/\partial T)_p - \alpha T_0(\partial\varepsilon/\partial p)_T = T_0(\partial\varepsilon/\partial T)_p, \tag{1.10}$$

where p is the pressure.

The path of integration Γ chosen in (1.7) encloses all the poles z_j (j = 1, ..., 5) and, in addition, the pole z = −a of the function g(−z).* Now we find explicit expressions for the roots z_j in order to establish with which roots the specific individual components of I_{iso} are to be associated.

From eqs. (1.5) and (1.6) it is easy to show that one of the roots z_j (suppose this is z_1) becomes zero along with the heat conductivity χ. Actually — at least for liquids — the root z_1 is extremely small in absolute value as compared with the other roots. This allows us to consider values of z_1, calculated only to second order in χq^2, while the values of the other roots are taken for χ = 0, that is, without taking the effect of heat conductivity into account. Thus

$$z_1 = \chi q^2 \gamma (M_0 + K_0)/(M_0 + \gamma K_0) \tag{1.11}$$

and

$$D_{1\infty}(z - z_2)(z - z_3)(z - z_4)(z - z_5) = D\left\{\left[z + \frac{1}{\tau} - \frac{\gamma - 1}{\gamma}\frac{K_\infty}{K_0}(z + a)\right]u(z) + \frac{K_\infty q^2}{\rho_0}\left(z + \frac{1}{\tau}\right)(z + a)\right\}. \tag{1.12}$$

In what follows we shall limit ourselves to the case of a medium with rather small viscous losses or [in accordance with (1.3)] what is the same thing, a medium with rather small dispersion differentials $\Delta K = K_\infty - K_0$ and $\Delta M = M_\infty - M_0$. Under these conditions we can use the values of the roots z_j, calculated from Eq. (1.12) with accuracy up to first order in ΔK and ΔM. These values are as follows:

$$z_2 = i\Omega_{MB} + h,\ z_3 = z_2^*,\ z_4 = -\frac{1}{\tau'}(1 - \zeta'),\ z_5 = -\frac{1}{\tau}(1 - \zeta), \tag{1.13}$$

where

$$\Omega_{MB}^2 = (M_0 + \gamma K_0)\frac{q^2}{\rho_0} = \frac{K_0 q^2}{\rho_0}\left(\gamma + \frac{4}{3}\beta_T\mu_0\right),\quad h = -\frac{\gamma^2\tau' q^2 \Delta K}{2\rho_0(1 + i\Omega_{MB}\tau')} - \frac{\tau q^2 \Delta M}{2\rho_0(1 + i\Omega_{MB}\tau)},$$

$$\zeta' = \frac{\Delta K}{K_0}\left(1 - \gamma\frac{1 + \tau'^2 M_0 q^2/\rho_0}{1 + \Omega_{MB}^2\tau'^2}\right),\quad \zeta = \frac{\tau^2 q^2 \Delta M}{\rho_0(1 + \Omega_{MB}^2\tau^2)}.$$

It is apparent from Eqs. (1.11) and (1.13) that the residue at $z = z_1$ yields the integrated intensity of the central maximum (the undisplaced line). The residues at $z = z_2$ and $z = z_3$ determine the total intensity of the Mandel'shtam—Brillouin doublet, the maxima of which (with an accuracy up to the first-order dispersion corrections) lie at the frequencies $\Omega \pm \Omega_{MB}$. The residues at the poles $z = z_4 \approx -1/\tau'$ and $z = a \approx -1/\tau'$ yield the integrated intensity of that part of the background which is due to dispersion in the compression modulus K. For brevity we will call this part of the background the "compression wing" to distinguish it from the "shear wing" or, in accordance with established terminology, simply the wing. This latter is the other part of the background, which is caused by dispersion in the shear modulus $\overline{\mu}$; the integrated intensity of this component is determined by the residue at the pole $z = z_5 \approx -1/\tau$. In low-viscosity liquids the extent of the two background components turns out to be considerably different because of the large difference in the relaxation times τ′ and τ ($\tau'/\tau \sim 10^3$).

2. INTEGRATED INTENSITIES OF THE COMPONENTS OF I_{iso} (RESULTS)

Taking the residues at the poles or groups of poles indicated above and using the values of the roots (1.11) and (1.13), from Eq. (1.7) we find the following expressions for the integrated intensities.†

*It is easily shown that z = 0 is not a singular point.

†In computing the residues we keep only those terms of order lower than the dispersion corrections in the expressions for the corresponding roots. Thus, taking the residue at $z = z_1$, everywhere, aside from the factor $z + \chi q^2$ we can substitute z = 0 in (1.8). In the remaining residues we can assume at the outset that χ = 0 and z_1 = 0, keeping terms only of first order in ΔK and ΔM.

The undisplaced line:

$$I_{\text{cent}} = \frac{\Theta(\gamma-1)q^2}{\Omega_{\text{MB}}^2\rho_0(1+4\beta_T\mu_0/3)}\left(Y+\frac{1+4\beta_T\mu_0/3}{\alpha T_0}Z\right)^2; \tag{2.1}$$

the Mandel'shtam—Brillouin doublet:

$$I_{\text{MB}} = \frac{\Theta q^2}{\rho_0}\left\{\frac{Y_1^2}{\Omega_{\text{MB}}^2} - \frac{\Delta K}{K_0}\cdot\frac{\gamma\tau^{-2}Y_1}{1+\Omega_{\text{MB}}^2\tau^{-2}}\left[\frac{q^2\gamma\tau^{-2}Y_1}{\beta_T\rho_0(1+\Omega_{\text{MB}}^2\tau^{-2})} + 2\,\frac{\gamma-1}{\alpha T_0}Z\right] - \frac{\tau^4q^2\Delta M}{\rho_0(1+\Omega_{\text{MB}}^2\tau^2)^2}Y_1^2\right\}; \tag{2.2}$$

the compression wing:

$$I_{\text{comp.wing}} = \Theta\beta_T\frac{\Delta K}{K_0}\left(\frac{1+4\mu_0q^2\tau^2/3\rho_0}{1+\Omega_{\text{MB}}^2\tau^2}\right)^2; \tag{2.3}$$

the shear wing:

$$I_{\text{wing}} = \Theta Y_1^2\tau^4q^2\Delta M/\rho_0(1+\Omega_{\text{MB}}^2\tau^2)^2. \tag{2.4}$$

In these formulas we use the thermodynamic expressions (1.4) for the parameters C and d (in accordance with the assumption that they do not exhibit dispersion) and the fact that $K_0 = 1/\beta_T$, where β_T is the isothermal compressibility. In addition, we take account of the well-known thermodynamic relations:

$$\alpha^2T_0 = \rho_0c_p(\beta_T-\beta_S),\quad \gamma = c_p/c_v = \beta_T/\beta_S, \tag{2.5}$$

where β_S is the adiabatic compressibility. Finally, we use the symbol Y_1 to denote the quantity $Y_1 = Y - ZCK_0/D_1$, the thermodynamic significance of which is easily established by means of (1.4) and (2.5):

$$Y_1 = -\rho_0\left(\frac{\partial\varepsilon}{\partial\rho}\right)_T - \frac{\gamma-1}{\alpha}\left(\frac{\partial\varepsilon}{\partial T}\right)_\rho = -\rho_0\left(\frac{\partial\varepsilon}{\partial\rho}\right)_S. \tag{2.6}$$

Before proceeding to a discussion of Eqs. (2.1) — (2.4) we point out that the sum of these expressions coincides with the intensity I_{iso} obtained earlier by more general methods [Eq. (4.3) in I] if, in the latter, we make the same additional assumptions as to which terms can be neglected in calculating the density of the component (specifically, that D is dispersionless, that the heat conductivity can be neglected and that only first-order terms in the dispersion corrections are needed). Eq. (4.3) of I then assumes the form

$$I_{\text{iso}} = \Theta\left\{\frac{Y^2}{K_0+M_0} + \frac{Z^2}{D_{10}} + \frac{\Delta K}{K_0^2}Y_1\left[2\,\frac{1+(4\mu_0q^2/3\rho_0)\tau^2}{1+\Omega_{\text{MB}}^2\tau^2}Y - \left(Y+\frac{CK_0}{D_{10}}Z\right)^2\right]\right\},$$

which coincides with the sum of the intensities given by (2.1) — (2.4).

It is apparent from Eqs. (2.2) and (2.4) that the intensity of the shear wing compensates for the correction due to the dispersion in the shear modulus which is contained in the intensity expression for the doublet. Hence, I_{iso} is independent of ΔM as should be the case for the explicit dispersion relation given for $\bar{\mu}$, in accordance with the more general Eq. (4.3) given in I.

In what follows we shall limit ourselves to the case of a liquid ($\mu_0 = 0$). If we introduce the parameter

$$s = 1/\Omega_{\text{MB}}^2\tau^2, \tag{2.7}$$

already used in I [Eq. (5.2)], Eqs. (2.1) — (2.3) assume the form

$$I_{\text{cent}} = \Theta\beta_T\left(\frac{Z_1}{\alpha T_0}\right)^2\cdot\frac{\gamma-1}{\gamma} = \Theta\frac{Z_1^2}{\rho_1T_0c_p}, \tag{2.8}$$

$$I_{\text{MB}} = \Theta\beta_TY_1^2\left\{\frac{1}{\gamma} - \frac{\Delta K}{K_0(1+s)}\left[\frac{1}{1+s} + 2\,\frac{(\gamma-1)Z}{\alpha T_0Y_1}\right]\right\} - I_s; \tag{2.9}$$

$$I_{\text{comp.wing}} = \Theta\beta_TY_1^2\frac{\Delta K}{K_0}\left(\frac{s}{1+s}\right)^2. \tag{2.10}$$

In the isotropic part of the scattering, which is due to fluctuations in density and temperature only, the intensity of the shear wing (2.4) is extremely small. It is sufficient to compare I_{wing} with the first dispersion correction in the doublet intensity (2.9), i.e., the quantity

$$\Delta I_{\text{MB}} = \Theta\beta_TY_1^2\Delta K/K_0(1+s)^2.$$

Taking the ratio I_{wing}/I_{MB} and keeping in mind the fact that $\gamma K_0 q^2/\rho_0 = \Omega_{MB}^2$, we have

$$\frac{I_{wing}}{\Delta I_{MB}} = \frac{\Omega_{MB}^2\tau^2 (q^2\tau^2\Delta M/\rho_0)(1+s)^2}{(\gamma\Delta K/K_0)(1+\Omega_{MB}^2\tau^2)^2}$$

But for liquids the values of the quantities $\Omega_{MB}^2\tau^2$ and $q^2\tau^2\Delta M/\rho_0 = 4\mu_\infty q^2\tau^2/3\rho_0 = 4q^2\eta_0\tau/3\rho_0$ are of the order of 10^{-4} so that

$$I_{wing}/\Delta I_{MB} \sim (K_0/\gamma\Delta K)\ 10^{-8},$$

i.e., these are vanishingly small quantities even in the case in which $\Delta K/K_0$ amounts to a fraction of a per cent. Hence, we may neglect both the intensity of the shear wing and the corresponding correction in the doublet intensity (2.9).

The intensity of the compression doublet (2.10) is also small as compared with ΔI_{MB}

$$I_{comp.wing}/\Delta I_{MB} = s^2.$$

For the highest value of s which is at our disposal (s = 0.52 in carbon bisulfide) $I_{comp.wing}$ amounts to approximately one-quarter of ΔI_{MB}. Consequently, in comparing the intensities of the doublet and the undisplaced line we need not add $I_{comp.wing}$ to the latter.

Taking the ratio of the intensities (2.8) and (2.9) with the accuracy given above (to first order in ΔK) we find

$$\frac{I_{center}}{I_{MB}} = \left(\frac{Z_1}{\alpha T_0\gamma_1}\right)^2 (\gamma - 1)\left\{1 + \frac{\gamma\Delta K}{K_0(1+s)}\left[\frac{1}{1+s} + 2\frac{(\gamma-1)Z}{\alpha T_0\gamma_1}\right]\right\}. \qquad (2.11)$$

or, neglecting the quantities s and Z in the dispersion correction and making use of (1.10), (2.5), and (2.6)

$$\frac{I_{center}}{I_{MB}} = \left[\frac{1}{\alpha}\left(\frac{\partial\varepsilon}{\partial T}\right)_\rho \Big/ \rho_0\left(\frac{\partial\varepsilon}{\partial\rho}\right)_S\right]^2 \frac{\alpha^2 T_0}{\rho_0 c_p \beta_S}\left\{1 + \gamma\frac{\Delta K}{K_0}\right\}. \qquad (2.12)$$

If we disregard the dispersion correction $\gamma\Delta K/K$ and set $Z = T_0(\partial\varepsilon/\partial T)_\rho = 0$ in accordance with (1.10) and (2.6), the first factor in (2.12) becomes unity, i.e., we obtain the Landau—Placzek formula[6]

$$I_{center}/I_{MB} = \alpha^2 T_0/\rho_0 c_p \beta_S = \gamma - 1.$$

As has already been noted by Fabelinskii,[3,7] without taking dispersion into account, that is, even in the framework of the thermodynamic theory, the first factor in Eq. (2.12) is considerably different from unity if we do not neglect $(\partial\varepsilon/\partial T)_\rho$. We can neglect this quantity without introducing a noticeable error in the value of integrated intensity of the isotropic scattering; however, it turns out that we cannot neglect it in the formula for the ratio of the intensities of the fine-structure components.

It can be shown that the dispersion correction can be taken into account in the ratio I_{cent}/I_{MB} using a formula of the usual "thermodynamic" form if for the adiabatic compressibility we take the quantity

$$\tilde{\beta}_S = \beta_S(1 - \gamma\Delta K/K_0),$$

i.e., the reciprocal of the "adiabatic" compression modulus [cf. Eq. (5.5) of I].

$$\tilde{K}_{ad} = KD/D_1 = D\tilde{K}/(D - C^2\tilde{K})$$

for $\Omega \to \infty$ or, more precisely, for $\Omega\tau' \gg 1$. The more complete expression for the dispersion correction contained in (2.11) corresponds to the case in which the compression modulus has not completely relaxed at the frequency of the doublet so that it is not very small as compared with unity.

The formula for I_{cent}/I_{MB} which contains the value of the compressibility at the doublet frequency was obtained earlier by Fabelinskii[3,4] from an analysis of the doublet on the basis of the diffraction of light by the Debye waves. He also allows for dispersion in the coefficient $(\partial\varepsilon/\partial\rho)_S$ so that we must also introduce the value of this parameter which corresponds to the doublet frequency in the ratio I_{cent}/I_{MB}. This is certainly proper (cf. below) if we depart from the purely terminological moment: if there is a frequency dependence in $Y_1(i\Omega)$ the use of the thermodynamic notation $(\partial\varepsilon/\partial\rho)_S = -Y_1(0)/\rho_0$ has significance only at sufficiently low frequencies. In concluding this section we consider the problem of how to introduce dispersion in Y and Z into the results of the calculation of the integrated intensities of the fine-structure components.

The derivation of Eqs. (2.1) – (2.4) indicates that the dispersion in Y and Z may appear in two ways. Firstly, in the component intensity we introduce the values Y(z) and Z(z) at the appropriate poles – at $z = z_1$ for the undisplaced line (i.e., the quasi-static values), at $z = z_2$ and $z = z_3$ for the doublet (i.e., the values of Y and Z at the frequency Ω_{MB}), and at $z = z_4 \approx -1/\tau'$ and $z = z_5 \approx -1/\tau$ respectively for the compression wing and the shear wing. Secondly, additional background components appear, given by the residues at the poles $z = \tilde{z}_w$ of the functions Y(z) and Z(z). If, however, the dispersion in Y and Z is small, wherever the intensity $J_{iso}(z)$ is still noticeable, these additional terms will be small and, in practice, we need consider only the first of the indicated effects. In other words, the additional terms do not play an important role in the case in which the characteristic frequencies of the coefficients Y and Z lie beyond the limits of the observed spectrum, i.e., $|\tilde{z}_w| \gg |z_j|$. This is the case even for the root $z_5 \approx -1/\tau$ of the dispersion equation ($|z_5| \gg |z_j|$, $j = 1, \ldots 4$) as a result of which it turns out that the shear wing is absent in practice and the observed region in the spectrum of J_{iso} is limited to the doublet components.

3. ANISOTROPIC SCATTERING. REMARKS ON THE ANALYSIS GIVEN BY M. A. LEONTOVICH[5]

Turning now to scattering by anisotropic fluctuations, which are responsible for the wing of the Rayleigh line (i.e., the shear wing), we may note, first of all, that the results of the well-known analysis by Leontovich[5] can be obtained from Eq. (3.1) of I as a particular case for the following assumptions as to the parameters. In Eq. (2.1) of I, which relates fluctuations of the dielectric constant to fluctuations in deformation and temperature

$$\varepsilon_{\alpha\beta} = Xu'_{\alpha\beta} + Yu\delta_{\alpha\beta} + Z\vartheta\delta_{\alpha\beta} \quad (u'_{\alpha\beta} = u_{\alpha\beta} - {}^1/_3 u\delta_{\alpha\beta}) \tag{3.1}$$

it is assumed that

(a) the coefficient X is proportional to the complex shear modulus

$$X(i\Omega) = B\mu(i\Omega), \quad B = \text{const}; \tag{3.2}$$

(b) the coefficient Y is dispersionless and is given by the real thermodynamic value (1.4);

(c) the quantity $\epsilon_{\alpha\beta}$ is independent of temperature (for fixed density) i.e. $z = 0$.

With respect to the mechanical and thermal parameters of the medium it is assumed that

(d) there is no thermal expansion ($C = 0$);

(e) there is no dispersion in the compression modulus ($\overline{K} = K_0 = 1/\beta_T$, $\zeta = 0$);

(f) the shear modulus obeys the simplest dispersion law with a single relaxation time τ and $\mu_0 = 0$ (liquid)

$$\overline{\mu} = \mu + i\Omega\eta = \mu_\infty i\Omega/(i\Omega + 1/\tau). \tag{3.3}$$

It should be emphasized that some of these assumptions [(c), (d) and (e)] were made only to simplify the basic problem – the explanation of the wing in the case of liquids – thus dispensing beforehand with descriptions of the undisplaced line and the doublet.

Using the assumptions enumerated above and the notation

$$B = A/\mu_\infty, \quad \Omega_T^2 = \mu_\infty q^2/\rho_0, \quad \Omega_L^2 = K_0 q^2/\rho_0, \quad \Omega_S^2 = \Omega_L^2 + \frac{4}{3}\Omega_T^2, \quad \Delta_L = \Omega^2 - \Omega_L^2 + i\Omega\tau(\Omega^2 - \Omega_S^2), \quad \Delta_T = i\Omega + \tau(\Omega^2 - \Omega_T^2),$$

after several transformations Eq. (3.1) of I leads to the same expression which was obtained in the cited work of Leontovich, namely,

$$J_x^1 = \frac{\theta A^2\tau}{16\pi\mu_\infty}\left\{\frac{3(\Omega^2 - \Omega_T^2)^2}{|\Delta_L|^2} + \frac{1}{1 + \Omega^2\tau^2}\right\}, \quad J_z^1 = J_x^1 = \frac{\theta A^2\tau}{8\pi\mu_\infty}\left\{\frac{\Omega^2}{|\Delta_T|^2} + \frac{1}{1 + \Omega^2\tau^2}\right\},$$

$$J_z^1 = \frac{\theta\tau}{2\pi\mu_\infty}\left\{\frac{A^2}{2}\left[\frac{(\Omega^2 - \Omega_L^2)^2}{3|\Delta_L|^2} + \frac{1}{1 + \Omega^2\tau_2}\right] - \frac{4AY\Omega_T^2(\Omega^2 - \Omega_L^2)}{3|\Delta_L|^2} + \frac{8Y^2\Omega_T^4}{3|\Delta_L|^2}\right\}.$$

We note that because of assumptions (d) and (e) the frequency dependence of the isotropic part of J_z^1, i.e. of the quantity

$$J_{iso} = (\theta\tau/2\pi\mu_\infty)\cdot 8Y^2\Omega_T^4/3|\Delta_L|^2,$$

cannot give the intensity distribution in the region of the doublet and the undisplaced line; nevertheless,

the integral of J_{iso} over Ω yields the Einstein formula, as can be shown by direct computation. In accordance with the general expression for the integrated intensity I_{iso} [cf. Eq. (4.3) I] this should be the case since a liquid is being considered ($\mu_0 = 0$) and (c) and (e) are assumed.

In that region of the wing which lies beyond the limits of the doublet, i.e., for $\Omega^2 > \Omega_s \approx \Omega_{MB}$, Eq. (3.4) yields*

$$J_x^- = J_z^- = J_x^+ = \frac{3}{4} J_z^+ = (\Theta A^2 \tau / 4\pi\mu_\infty) / (1 + \Omega^2\tau^2),$$

so that the degree of depolarization in the wing is

$$J_x / J_z = (J_x^- + J_x^+) / (J_z^- + J_z^+) = 6/7,$$

and the reciprocal intensities are proportional to $1 + \Omega^2\tau^2$. The slope of the line in the curve which shows the dependence of $1/J$ on Ω^2 obviously allows us to determine the relaxation time τ. This determination has been carried out by Fabelinskii[3,8] whose measurements have shown that in a number of liquids there is actually a wide region ($40 - 60$ cm^{-1}) in which the dependence of $1/J$ on Ω^2 is linear. The deviations from linearity occur in the region of Ω smaller than $15 - 25$ cm^{-1} and larger than 70 cm^{-1}. In this connection special attention is merited by the assumption in (3.2) which is important in the Leontovich analysis.

Generally speaking, it is difficult to find any basis for the fact that the frequency behavior of the mechanical-optical parameter $X(i\Omega)$ is completely determined by the dispersion of the purely mechanical quantity — the shear modulus $\bar{\mu}$. In Ref. 5, Leontovich starts with the assumption that

$$\varepsilon_{\alpha\beta}^{aniso} = A\zeta_{\alpha\beta} \quad (A = \text{const}),$$

where $\zeta_{\alpha\beta}$ is the so-called anisotropy tensor which is related to the pure shear deformations $u'_{\alpha\beta}$ by the relaxation equation

$$\dot{\zeta}_{\alpha\beta} + \zeta_{\alpha\beta}/\tau = \dot{u}'_{\alpha\beta},$$

or spectrally by

$$\zeta_{\alpha\beta} = i\Omega u'_{\alpha\beta} / (i\Omega + 1/\tau). \tag{3.4}$$

Consequently, $\epsilon_{\alpha\beta}^{aniso} = X u'_{\alpha\beta}$, where

$$X = Ai\Omega / (i\Omega + 1/\tau),$$

On the other hand, Leontovich has assumed that in the equations of motion of the liquid the pure shear stresses are also determined by the tensor $\zeta_{\alpha\beta}$, specifically, $\sigma'_{\alpha\beta} = 2\mu_\infty \zeta_{\alpha\beta}$. According to Eq. (3.4) this relation means that the complex shear modulus $\bar{\mu}$ obeys the dispersion law in (3.3). As a result X is expressed by Eq. (3.2) where $B = A/\mu_\infty$.

The fact that the observed dependence of the reciprocal intensity of the wing on Ω^2 departs from a linear relation may indicate both a more complicated dispersion for $\bar{\mu}$ if the assumption in (3.2) is to be retained and/or the inapplicability of (3.2), i.e., in the final analysis it may not be valid to assume that $\epsilon_{\alpha\beta}^{aniso}$ and $\sigma'_{\alpha\beta}$ depend on the same internal parameter in the same way. It is reasonable, at sufficiently low frequencies when

$$X(i\Omega) \approx X_0 + (\partial X / i\partial\Omega)_0 i\Omega, \quad \bar{\mu}(i\Omega) \approx \mu_0 + i\Omega\eta_0,$$

to assume for solid bodies that X_0 is proportional to μ_0 while for liquids ($X_0 = 0$, $\mu_0 = 0$) $(\partial X/i\partial\Omega)_0$ is proportional to η_0. Formally both cases are connected by the relation in (3.2).

The optical anisotropy in a solid body, which arises as a result of the static (or sufficiently low-frequency) stresses, is expressed by the following empirical formula[9] which we do not write in the usual way (in terms of the stresses) but in terms of the shear deformations

$$\varepsilon_{\alpha\beta}^{aniso} = 4\sqrt{\varepsilon_0} c\mu_0 u'_{\alpha\beta}.$$

Here c is the so-called relative optical stress coefficient, measured in Brewsters (1 Brewster = 10^{-13} cm^2/dyne). An empirical formula for the anisotropy due to flow in the liquid (the Maxwell effect) is of the form[10]

$$\varepsilon_{\alpha\beta}^{aniso} = 2i\Omega\varepsilon_0\eta_0 M u'_{\alpha\beta}, \tag{3.5}$$

*It is sufficient if Ω exceeds Ω_{MB} by several line-widths of the doublet.

where M is the Maxwell constant. According to (3.2) at low frequencies we should have $B = \sqrt{\epsilon_0 c} = 2\epsilon_0 M$, i.e., the following relation between the photo-elastic constant for solid bodies c and the Maxwell constant for liquids M:

$$c = {}^1/_2 \sqrt{\epsilon_0} M. \tag{3.6}$$

It is possible to establish the validity of this relation only in bodies which, in the low frequency region being considered, behave as "intermediate cases" between solids and liquds, i.e., bodies which allow measurement of both anisotropic effects. In typical liquids and typical bodies in which the comparison indicated above cannot be made, (3.6) is essentially meaningless. Without going any further into this problem we wish to emphasize once again that even if there is an actual relation like (3.6) at low frequencies there is no reason to expect that this relationship is maintained at frequencies of the order of 10^{11} and that the relation in (3.2) is satisfied.

4. SPECTRAL INTENSITIES IN THE SHEAR WING

We now turn to a consideration of the shear wing and certain consequences which follow from the general formulas (3.1) in I. We are interested in frequencies Ω which exceed both the doublet frequency Ω_{MB} as well as the characteristic frequency of the compression modulus $1/\tau'$. In this case, from Eq. (3.2) in I we have

$$d \approx D_\infty, \quad d_1 \approx D_{1\infty} = D_\infty - C_\infty^2 K_\infty, \quad \Delta \approx D_{1\infty}\rho_0\Omega^2, \quad A_1 \approx A_3 \approx A_4 \approx \rho_0\Omega^2,$$

as a result of which the general expressions for the intensities (3.1) from I are reduced to the following:

$$J_x^- = J_z^- = J_x^+ = \frac{3}{4} J_z^+ = \frac{\Theta}{8\pi i\Omega} |X|^2 \left(\frac{1}{\mu^*} - \frac{1}{\mu}\right) = \frac{\Theta}{4\pi} \left|\frac{X}{\mu}\right|^2 \gamma_i. \tag{4.1}$$

Thus, the degree of polarization J_X/J_Z is ${}^6/_7$ in the wing regardless of the frequency behavior of X and $\overline{\mu}$.

According to Eq. (4.1), a graph on which is plotted the reciprocal value of any of the intensities as a function of Ω^2 represents the quantity $|\overline{\mu}/X|^2/\eta$ as a function of Ω^2. If we grant the validity of the relation given in (3.2), i.e., $X = B\overline{\mu}$, this quantity is simply const/η which indicates a linear dependence of $1/\eta$ on Ω^2 if the dispersion relation given in (3.3) for μ is assumed. Since, as was indicated above, the relation given in (3.2) is open to doubt, it is reasonable to interest ourselves in those relations which give simple dispersion laws for X and $\overline{\mu}$ in the event that (3.2) is inapplicable.

Using the dispersion relation for $\overline{\mu}$ given in (3.3) we assume that

$$X(i\Omega) = (X_\infty i\Omega + X_0/\tau_1)/(i\Omega + 1/\tau_1). \tag{4.2}$$

Then, as can easily be shown, each of the intensities (4.1) has a frequency dependence given by the expression

$$\frac{1}{J} \sim \left|\frac{\overline{\mu}}{X}\right|^2 \frac{1}{\gamma_i} \sim x\frac{x+1}{x+\beta}, \quad x = \Omega^2\tau_1^2, \quad \beta = \frac{X_0^2}{X_\infty^2}. \tag{4.3}$$

FIG. 1

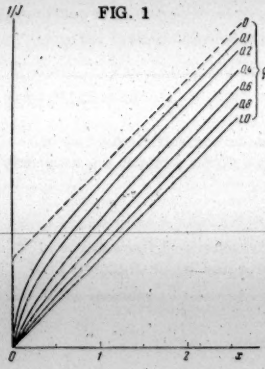

For different values of $\beta < 1$ the relation in (4.3) is shown by the solid curves in Fig. 1. The dashed line corresponds to the value $\beta = 0$ and is inclined at the same angle as the asymptotes of the other curves for increasing x. This dashed line corresponds, in particular, to the Leontovich theory, since it is assumed that X is proportional to $\overline{\mu}$ and consequently that $\tau_1 = \tau$, $\beta = \mu_0^2/\mu_\infty^2 = 0$. However, the departure of the experimental curves in the low frequency region from the linear behavior is precisely that which is to be expected from (4.3) for $\beta \neq 0$. Assuming the relation in (4.2), we have the possibility of determining from the experimental curves not only τ_1 but also the value of the parameter β. Thus, for example, the curve for carbon bisulfide given in Fig. 2 of Ref. 8, which is incorrect according to Eq. (4.30), gives $\tau_1 \approx 1.5 \times 10^{-13}$ sec from the slope of the asymptote whereas the fourth point in the region in which the curve slopes downward gives a value of $\beta \approx 0.09$ with a spread of not more than 10 per

cent. From the data of Weiler,[11] we obtain in benzol a value of $\tau_1 \approx 2.16 \times 10^{-13}$ sec and $\beta \approx 0.385$.

It is clear, however, that in the liquid case being considered the dispersion law for X given in (4.2) cannot remain effective to any arbitrarily low frequency because when $\Omega \to 0$, this relation gives a value $X = X_0$ different from zero. According to Eq. (3.1) this would denote a photo-elastic anisotropy, which is possible only in a solid body. Assuming that the relation given in (4.2) applies only at sufficiently high values of x we may assume that deviations from this relation are due to the existence of other relaxation times $\tau_2 \gg \tau_1$ in X. The simplest dependence, for which we introduce only one other additional relaxation time τ_2 and which by giving $X \to 0$ as $\Omega \to 0$ maintains (4.2) for $\Omega \gg 1/\tau_2$, is of the form

$$X(i\Omega) = \frac{i\Omega\tau_1}{i\Omega + 1/\tau_2} \cdot \frac{X_\infty i\Omega + X_0/\tau_1}{i\Omega + 1/\tau_1}. \qquad (4.4)$$

Then, in place of (4.3) the reciprocal intensity is given by the expression

$$\frac{1}{J} \sim \left(\frac{\tau_1^2}{\tau_2^2} + x\right)\frac{x+1}{x+\beta}, \qquad (4.5)$$

which gives the former behavior of the curve (Fig. 1) at $x \gg \tau_1^2/\tau_2^2$ but a value of $1/J$ different from zero as $x \to 0$.

The first factor in (4.5) determines the behavior of $1/J$ in the narrow and most intense central part in which both the width of the central part as well as the maximum value of the intensity depend on τ_2 for $x = 0$. The value of τ_2 can be estimated from any of these parameters; however, in view of the difficulty in measuring the intensity of the wing at zero, more reliable results can be obtained by estimating the width of the central part of the wing.

At low frequencies ($\Omega \ll 1/\tau_2$), in accordance with (4.4) we have $X = i\Omega\tau_2 X_0$ so that the anisotropic part of $\epsilon_{\alpha\beta}$ is found to be equal to $\epsilon_{\alpha\beta}^{\text{aniso}} = i\Omega\tau_2 X_0 u'_{\alpha\beta}$. Comparison with Eq. (3.5) indicates that in the relation given in (4.4)

$$X_0 = 2z_0\gamma_{i0}M/\tau_2. \qquad (4.6)$$

In evaluating the applicability of Eq. (4.4) at low frequencies special interest attaches to the observation of the diffraction of linear polarized light on ultrasonic waves, propagating at an angle (say, 45°) to the direction of the crossed axes of the analyzer and polarizer. An experiment of this type may give some idea of the frequency dependence of $|X|^2$ up to $\Omega \sim 10^8$.

As has already been noted, the experimental curves which show the dependence of $1/J$ on Ω^2 also exhibit a departure from a linear dependence in the high-frequency region. This result also indicates a departure in the dispersion relations for and/or $\bar{\mu}$ from the simple forms taken above but we will not dwell on this problem at this point.

5. INTEGRATED INTENSITIES OF THE ANISOTROPIC SCATTERING

Since the dispersion relations given in (3.3) for $\bar{\mu}$ and in (4.4) for X permit a good approximation to the behavior of the intensity over the entire extent of the wing, with the exclusion of the high-frequency part, where the intensity is small,* it is of interest to calculate the integrated intensities of the anisotropic scattering using (3.3) and (4.4). For this purpose we turn to Eq. (3.1) of I noting, first of all, that in the case of a low-viscosity liquid, to which we are limiting ourselves, the quantity $\Omega_T^2 \tau^2 = q^2\eta_0\tau/\rho_0$ is of the order of 10^{-4} thus making it possible to neglect certain terms and to simplify considerably the expression for the spectral intensities.† In particular, in the expression for $J_{\vec{X}}^{\rightarrow}$ we can neglect terms which contain the determinant Δ in the denominator while in the expression for $J_{\vec{Z}}^{\rightarrow} = J_X^{\uparrow}$ it may be assumed that $A_4 = \rho_0\Omega^2 - \bar{\mu}q^2 \approx \rho_0\Omega^2$. Then Eq. (3.1) of I assumes the form

$$J_x^{\rightarrow} = J_{z'}^{\rightarrow} = J_x^{\uparrow} = \frac{\theta|X|^2}{8\pi i\Omega} \cdot \left(\frac{1}{\bar{\mu}^*} - \frac{1}{\bar{\mu}}\right), \qquad J_z^{\uparrow} = {}^4/_3 J_x^{\rightarrow} + J_{\text{cross}} + J_{\text{iso}},$$

*Actually, this intensity falls off more rapidly than as given by (4.5), i.e., more rapidly than $1/\Omega^2$.

†The validity of neglecting these terms was verified in calculations of the integrated intensities which were carried out without eliminating small terms.

where J_{cross} denotes "cross" terms of I_z^+ which contain products of X and Y or Z and where I_{iso} is given by Eq. (1.1).

To compute the integral of J_{cross} over Ω we neglect terms with Z and assume that Y, C and $\overline{K}$ are dispersionless. Then the integrated intensities are

$$I_x^+ = I_z^+ = I_x^- = \frac{\Theta}{4}\frac{1}{2\pi i}\oint_\Gamma |X|^2\left(\frac{1}{\mu^*}-\frac{1}{\mu}\right)\frac{dz}{z}, \quad I_z^- = {}^4/_3 I_x^- + I_{cross} + I_{iso}, \tag{5.1}$$

$$I_{cross} = \frac{\Theta Y q^2}{3}\frac{1}{2\pi i}\oint_\Gamma \left\{\left(X + X^*\frac{\overline{\varkappa}}{\mu^*}\right)\frac{d_1}{\Delta} - \text{comp. conj.}\right\}\frac{dz}{z}.$$

Here $z = i\Omega$ while the path of integration Γ goes along the imaginary z axis and is closed at infinity, enclosing the left-hand plane. The expression for I_{iso} has been found in I [Eqs. (5.1) or (5.3)] but for the following estimates we will simply use the Einstein formula

$$I_{iso} = \Theta Y^2 \beta_T. \tag{5.2}$$

Substituting Eqs. (3.3) and (4.4) in the top formula in Eq. (5.1) we find

$$I_x^- = \frac{\Theta X_\infty^2}{4\mu_\infty}\frac{1}{2\pi i}\oint_\Gamma\left\{\frac{g(z)(z-\alpha)(z-\alpha')}{f(z)(z-a)(z-a')} - \frac{g(-z)(z+\alpha)(z+\alpha')}{f(-z)(z+a)(z+a')}\right\}\frac{dz}{z} \tag{5.3}$$

where we have introduced the notation

$$\frac{g(z)}{f(z)} = \frac{(z+\alpha)z}{(z+a)(z+a')}, \quad \alpha = \frac{\sqrt{3}}{\tau_1}, \quad \alpha' = \frac{1}{\tau}, \quad a = \frac{1}{\tau_1}, \quad a' = \frac{1}{\tau_2}. \tag{5.4}$$

As to I_{cross}, the integral of $(Xd_1/\Delta - \text{comp. conj.})$ is obtained by the theorem given in (7.5) of Ref. 2 and is X_0/K_0q^2 while the integral of $((\varkappa^*\mu d_1/\mu^*\Delta) - \text{comp. conj.})$, after substitution of (3.3) and (4.4), assumes the same form as the integral in (5.3) except that

$$g(z)/f(z) = X_\infty z d_1/(z+\alpha')\Delta.$$

Thus, all the calculations lead to computation of an integral of the type given in (5.3) where all the roots of f(z) are in the left half-plane while the poles z = a and z = a′ are in the right half-plane. An appropriate extension of the theorem given in (7.4) of Ref. 2 (which provides for only the existence of one root on the right) is not difficult; specifically:

$$\frac{1}{2\pi i}\oint_\Gamma\left\{\frac{g(z)(z-\alpha)(z-\alpha')}{f(z)(z-a)(z-a')} - \frac{g(-z)(z+\alpha)(z+\alpha')}{f(-z)(z+a)(z+a')}\right\}\frac{dz}{z}$$
$$= \frac{g(\infty)}{f(\infty)} - 2\frac{g(a)}{f(a)}\left(1-\frac{\alpha}{a}\right)\frac{a-\alpha'}{a-a'} - 2\frac{g(a')}{f(a')}\left(1-\frac{\alpha'}{a'}\right)\frac{a'-\alpha}{a'-a} - \frac{g(0)}{f(0)}\frac{\alpha\alpha'}{aa'}. \tag{5.5}$$

Using this formula, from (5.3) we have

$$I_x^- = (\Theta X_\infty^2/4\mu_\infty)\alpha'(\alpha^2 + a\alpha')/aa'(a+a'), \tag{5.6}$$

while for I_{iso}, calculating the values of Δ and $d_1 = D_1 + \varkappa T_0 q^2/z$ for $z \to \infty$, z = a and z = a′ by means of Eqs. (1.5), (1.6) and (3.3), we find

$$I_{cross} = -\frac{\Theta X_0 Y}{3K_0}\left\{1 - \frac{2\Omega_{MB}^2 X_\infty}{(a-a')X_0}\left[\frac{(a-\alpha')(a-\alpha)}{(a^2+\Omega_{MB}^2)(a+\alpha')+\frac{4}{3}\Omega_T^2 a} - \frac{(a'-\alpha')(a'-\alpha)}{(a'^2+\Omega_{MB}^2)(a'+\alpha')+\frac{4}{3}\Omega_T^2 a'}\right]\right\},$$

where, as before, $\Omega_{MB}^2 = \gamma K_0 q^2/\rho_0$, $\Omega_T^2 = \mu_\infty q^2/\rho_0 = \eta_0 q^2/\rho_0\tau$. If we now take account of the fact that the quantity $a \sim \alpha \sim \alpha'$ is much larger than $\Omega_{MB} \sim \Omega_T$, the first correction term in I_{iso} turns out to be very small (smaller than $\Omega_{MB}^2\tau_1^2 \sim 10^{-4}$) and may be disregarded while the second term can be simplified considerably

$$I_{cross} = -\frac{\Theta X_0 Y}{3}\beta_T\left\{1 - \frac{2X_\infty\Omega_{MB}^2\alpha}{X_0 a(a'^2+\Omega_{MB}^2)}\right\}. \tag{5.7}$$

In Eqs. (5.6) and (5.7), returning to the original notation, using (5.4) and replacing X_∞ by $\sqrt{\beta}X_0$, from Eqs. (5.1) and (5.2) we have the following final result:

$$I_x^{\prime} = I_x^{\uparrow} = I_z^{\leftrightarrow} = \frac{\Theta X_0^2}{4\gamma_0} \frac{\tau_2(\tau_2+\tau_1/\beta)}{\tau_2+\tau_1}, \quad I_z^{\uparrow} = \frac{4}{3} I_x^{\leftrightarrow} - \frac{\Theta X_0 Y}{3} \beta_T \frac{1-\Omega_{MB}^2\tau_2^2}{1+\Omega_{MB}^2\tau_2^2} + \Theta Y^2 \beta_T. \tag{5.8}$$

The increase in the anisotropic intensities with increasing τ_2 is completely understandable since the finite value of τ_2 specifically limits the intensity of the brightest central part of the curve. The intensity I_{cross} can take on different values between $\pm\Theta X_0 Y\beta_T/3$ depending on the magnitude of $\Omega_{MB}\tau_2$, i.e., on the ratio between the width of the central part of the wing and the frequency of the doublet. In low-viscosity liquids $\Omega_{MB}^2\tau_2^2 \ll 1$ so that the correction to $I_{cross} = -\Theta X_0 Y\beta_T/3$ can, in general, be discarded.

Finally, we have the following expression for the depolarization coefficient in Rayleigh scattering in low-viscosity liquids:

$$\Delta = \frac{I_x^{\leftrightarrow} + I_x^{\uparrow}}{I_z^{\leftrightarrow} + I_z^{\uparrow}} = \frac{6}{7}\left[1 + \frac{12}{7}\beta_T\gamma_0 k \frac{\tau_2+\tau_1}{\tau_2+\tau_1/\beta}\left(k\tau_2 + \frac{1}{3}\right)\right]^{-1}, \tag{5.9}$$

where [cf. Eq. (4.6)]

$$k = |Y|/X_0\tau_2 = \rho_0(\partial\varepsilon/\partial\rho)_T/2\tau_0\gamma_0 M. \tag{5.10}$$

We estimate the value of Δ for benzol, assuming that* $\beta_T = 9.36 \times 10^{-11}$, $\eta_0 = 6.5 \times 10^{-3}$, $\epsilon_0 = 2.32$, $\rho_0(\partial\epsilon/\partial\rho)_T = 1.62$, $M = 9 \times 10^{-11}$, $\tau_1 = 2.16 \times 10^{-13}$, $\beta = 0.385$, $\tau_2 = 3 \times 10^{-12}$. The condition that $\Omega_{MB}^2\tau_2^2$ be small is thus satisfied (this quantity is approximately 7×10^{-3}). Eq. (5.10) gives $k = 5.97 \times 10^{11}$. From Eq. (5.9) we find $\Delta = 0.39$ while the experimental value is $\Delta = 0.43$. The latter is obtained from Eq. (5.9) if, maintaining all the other parameters fixed we set $\tau_2 = 2.5 \times 10^{-12}$. Considering the inaccuracy of the determination of τ_2† and the presence of a number of (apparently less important) assumptions which were made in deriving Eq. (5.9),‡ the result which has been obtained is completely satisfactory. In the present paper we are concerned with only approximate values. A more complete comparison of the available experimental data for low-viscosity liquids with the formulas which have been obtained as well as the consideration of high-viscosity liquids and solid bodies will be carried out in a separate paper.

[1] S. M. Rytov, J. Exptl. Theoret. Phys. (U.S.S.R.) **33**, 514 (1957); Soviet Phys. JETP 401 (1958).

[2] S. M. Rytov, J. Exptl. Theoret. Phys. (U.S.S.R.) **33**, 166 (1957); Soviet Phys. JETP 130 (1958).

[3] I. L. Fabelinskii, Molecular Scattering of Light in Liquids, Dissertation, Physics Institute, Academy of Sciences, U.S.S.R., 1955.

[4] I. L. Fabelinskii, Dokl. Adad. Nauk SSSR **106**, 822 (1956), Soviet Phys. "Doklady" **1**, 115 (1956).

[5] M. A. Leontovich, Izv. Akad. Nauk SSSR, Ser. Fiz. **5**, 148 (1941); J. Physics (U.S.S.R.) **4**, 499 (1941).

[6] L. D. Landau and G. Placzek, Sow. Phys. **5**, 172 (1934).

[7] I. L. Fabelinskii, Izv. Akad. Nauk SSSR, Ser. Fiz. **17**, 538 (1953).

[8] I. L. Fabelinskii, Izv. Akad. Nauk SSSR, Ser. Fiz. **9**, 186 (1945).

[9] R. Mindlin, J. Appl. Phys. **10**, 229 (1939); Russ. Transl. in Usp. Fiz. Nauk **23**, 16 (1940).

[10] J. C. Maxwell, Proc. Roy. Soc. (London) **A22**, 46 (1873).

[11] J. Weiler, Z. Physik **68**, 782 (1931).

[12] E. Winkler, Z. Physik **118**, 232 (1941).

Translated by H. Lashinsky
132

*The values of the quantities written in the upper line are taken from Ref. 3 where the statistical value was used for $\rho_0(\partial\epsilon/\partial\rho)_T$, in accordance with the neglect of dispersion assumed above in estimating I_{cross} and I_{iso}. The values for τ_1 and β were obtained in Section 4 from the data of Weiler.[11] The Maxwell constant M is taken from Ref. 12 (for 20°C).

†We assume the value of τ_2, calculated from the results of the measurements made by Fabelinskii[3] from the width of the central part of the plane (at the half-intensity level). In this procedure the frequency interval from 0 to 20 cm^{-1} alone is used. The estimate of τ_2 made by Fabelinskii considering the region from 0 to 8 cm^{-1} gives a close value 3.3×10^{-12}. According to the data of Ref. 11, using the slope of the tangent to the curve $1/J(\Omega^2)$ at the point $\Omega = 0$ we find $\tau_2 = 2 \times 10^{-12}$.

‡The neglect of dispersion in Y and K and the fact that the anisotropic intensities fall off faster than $1/\Omega^2$ in the high-frequency part of the wing.

ON THE GREEN'S FUNCTION OF THE KINETIC EQUATIONS OF A CASCADE

KH. IA. KHRISTOV

Moscow State University

Submitted to JETP editor March 1, 1957

J. Exptl. Theoret. Phys. (U.S.S.R.) 33, 683-695 (September, 1957)

The cascade considered consists of several types of particles which, moving in an inhomogeneous medium which may also vary with the time, collide with the particles of the medium and may be scattered or absorbed, and can also produce new cascade particles. Functions are introduced to characterize the distributions of the particles of each type in coordinate space and velocity space at any instant of time. Integral equations are obtained for these functions. For the case of a homogeneous medium not changing with time approximate solutions of these equations which are good for large values of the time, are obtained. Better approximations are obtained by iteration.

We consider a cascade consisting of n types A_j ($j = 1, 2, \ldots, n$) of particles K which move in a given medium and collide with its particles, so that there are scatterings, absorptions, and productions of new particles of the various types. We suppose that the properties of the medium in which the cascade develops are functions of the coordinates and the time. We also assume that the density of the cascade is small, so that its particles have practically no collisions with each other, and so that motion of each particle between collisions, and also its acts of collision with the particles of the medium, are not affected by the motion of the other particles of the cascade. It is further assumed that the motion of the particles between collisions takes place according to the laws of dynamics, being determinate for given initial positions and velocities, and that distributions as to type and velocities of the particles emerging from collisions is a stochastic one. Examples of such cascades are first of all electron-photon cosmic-ray showers, and also nucleon-meson and nucleon-photon cascades.[1-5] Cascades of this type are also studied in the theory of the multiple scattering of particles,[6,7] in the theory of chemical chain reactions,[8,9] in the theory of gas discharges, and so on.

In the theory of cosmic-ray showers one usually considers only the energy distribution of the particles of the different types as function of the depth, and their scattering and distribution as to direction are found separately.[1] Sometimes also all these quantities are considered simultaneously, but the time is still not introduced into the discussion. But in such treatments the postulate that the process be of the Markov type, which is necessary for the setting up of equations for the distribution function, is only approximately fulfilled.[10] In the researches of Janossy[3] the development of a shower is traced through in great detail. The particles are characterized not only by the magnitude, but also by the direction of the velocity, so that the Markov property of the process is assured. The results obtained make it possible to follow the motion of each particle, but with the development of the cascade the number of variables increases without limit, and the expressions become complicated. In general the discussion of cascade processes is always carried out under strong simplifying assumptions regarding the form of the functions giving the distribution of the particles in the cascade, and also of the form of the functions characterizing the elementary processes of scattering, of absorption, and of production of new particles. Therefore it has seemed to us worth while to find equations for the functions that characterize at each given moment the distribution of the particles as to type, position, and velocity, without interesting ourselves in the history of each individual particle. This seems expedient because, on one hand, in such a treatment the Markov character of the process is assured, and on the other hand the number of variables does not increase with the development of the cascade, so that the equations are not very complicated. By the use of suitable substitutions one can solve these equations, though indeed only approximately, under very general assumptions about the functions characterizing the elementary processes of motion and transmutation of the particles, and, as we shall see in two subsequent papers, by means of the resulting distribution functions one can solve a number of more complicated problems.

Let A_j, $\mathbf{r}$, and $\mathbf{v}$ be the type, radius vector, and velocity of a single cascade particle. We assume that between collisions this particle moves according to the law

$$d\mathbf{r}/dt = \mathbf{v}, \quad d\mathbf{v}/dt = \mathbf{F}_j(t, \mathbf{r}, \mathbf{v}), \tag{1}$$

where $\mathbf{F}_j$ is the force acting on the particle divided by its mass. We denote by

$$\varphi_j^s = \varphi_j(t, \mathbf{r}, \mathbf{v}, s), \qquad \psi_j^s = \psi_j(t, \mathbf{r}, \mathbf{v}, s) \tag{2}$$

the solution of the system (1), i.e., the values of the radius vector and the velocity of the particle at the time s, if at the time t it has the radius vector $\mathbf{r}$ and the velocity $\mathbf{v}$.

In a given collision the incident particle may be scattered or absorbed. In either case new particles may be produced. Since we are interested not in the individual paths of the separate particles, but only in their distribution as to type, position, and velocity, for the sake of unifying the notation we shall regard scattering as absorption of the incident particle and production of a new particle of the same type at the same position, but with a different velocity. We shall also regard processes of spontaneous decay and production of new particles conventionally as collisions, since both kinds of processes are characterized by transition probabilities of the same type, and we shall not concern ourselves with the mechanisms of elementary processes.

$$Q_{jk_i}^m(t, \mathbf{r}, \mathbf{v}, \mathbf{w}_i)\, dt\, d\mathbf{w}_i \qquad (i = 1, 2, \ldots m) \tag{3}$$

denote the probability that the particle of type A_j with radius vector $\mathbf{r}$ and velocity $\mathbf{v}$ undergoes a collision in the time interval t, t + dt and that among the particles obtained from this process there are m particles (m = 0, 1, ...) of type A_{k_i} with velocities between $\mathbf{w}_i$ and $\mathbf{w}_i + d\mathbf{w}_i$. Here $d\mathbf{w}_i$ means the product $d\mathbf{w}_1 d\mathbf{w}_2 \ldots d\mathbf{w}_m$, k_i (i = 1, 2, ...) and m are integers between 1 and m, and the $\mathbf{w}_i$ are m arbitrary velocities. We shall take the probabilities (3) to be given.

The value of (3) for m = 0

$$p_j(t, \mathbf{r}, \mathbf{v})\, dt = Q_j^0(t, \mathbf{r}, \mathbf{v})\, dt \tag{4}$$

gives the probability that the particle K undergoes a collision of arbitrary type in the time interval dt, and the value of (3) for m = 1

$$Q_{jk}^1(t, \mathbf{r}, \mathbf{v}, \mathbf{w})\, dt\, d\mathbf{w} \tag{5}$$

gives the probability that this particle undergoes a collision in the time interval dt and among the particles produced there is a particle A_k with velocity between $\mathbf{w}$ and $\mathbf{w} + d\mathbf{w}$.

Out of all possible collisions we single out a certain class of collisions — let us call it the class C — by using any chosen criterion as to the time and place of the collision, and also as to the types and velocities of the incident particle and the emerging particles. For example, we can include in the class C all collisions in which the incident particle has an energy larger than a given value E and the sum of the energies of the particles emerging is less than another given value E′. The class C can be empty, and also can include all collisions. But by the definition given we cannot assign to the class C those collisions, for example, in which the incident particle has appeared as the result of another collision with a given number of emerging particles. In particular, we can take as the class C those collisions in which the incident particle is absorbed without producing any other particles — the class C_1 — or those collisions in which there are particles of the type of the incident particle among those emerging — the class C_2. We designate all the particles of the same type as the particle K produced from it in collisions of the class C as the swarm of particle K. If the particle K itself does not belong to the swarm of another particle, we call it the primary particle of the swarm.

In the following arguments the concept of the class C is not necessary. It is very suitable, however, in obtaining greater precision in finding the desired functions that give the distribution of the cascade particles. As we shall see, this classification makes it possible to consider collisions that lead only to scattering of the particles separately from those that lead to the production of new particles; the latter collisions may be small in number in comparison with the former, but are quite essential for the development of the cascade. For similar reasons the classification is useful in cases in which the processes causing the development of the cascade at high and low energies are different. This case occurs, for example, in cosmic rays, for which ionization, Compton scattering, and pair production become prominent at different energies.

The quantities (3) – (5) which we have defined on the basis of all possible collisions can also be defined with the restriction to collisions of class C only. We denote the quantity (5) for k = j, calculated only for collisions of class C, by

$$P_j(t, \mathbf{r}, \mathbf{v}, \mathbf{w})\, dt\, d\mathbf{w}. \tag{6}$$

Obviously this is the probability for a collision of class C of one particle of type A_j during the time dt, accompanied by the emission of a particle of its swarm with velocity between $\mathbf{w}$ and $\mathbf{w} + d\mathbf{w}$. Furthermore we denote by

$$P_{jk}\, dt\, d\mathbf{w} = (Q'_{jk} - \delta_{jk} P_k)\, dt\, d\mathbf{w} \tag{7}$$

the probability of a collision of the particle K in the time dt accompanied by the emission of one primary particle of type A_k with velocity between $\mathbf{w}$ and $\mathbf{w} + d\mathbf{w}$.

Suppose that at the time s there is a particle K_0 of type A_i with radius vector $\mathbf{q}$ and with velocity $\mathbf{u}$. We call it the initial particle of the cascade. We denote by

$$W_i(s, \mathbf{q}, \mathbf{u}, t, \mathbf{r}, \mathbf{v})\, d\mathbf{r}\, d\mathbf{v} \tag{8}$$

the probability that at the time t a particle belonging to the swarm of K_0 has radius vector between $\mathbf{r}$ and $\mathbf{r} + d\mathbf{r}$ and velocity between $\mathbf{v}$ and $\mathbf{v} + d\mathbf{v}$. Since according to the assumptions that have been made the development of the cascade is caused by the action of the medium, and the state of the medium does not depend on the propagation of the cascade, it is clear that the development of the cascade will have the Markov property.[10] Because of this the functions W_i will satisfy the equation[11] (integration with respect to vector quantities is always taken over the entire space):

$$\begin{aligned} W_i(s, \mathbf{q}, \mathbf{u}, t, \mathbf{r}, \mathbf{v}) &= \delta(\boldsymbol{\varphi}_i^s - \mathbf{q})\, \delta(\boldsymbol{\psi}_i^s - \mathbf{u})\, \partial(\boldsymbol{\varphi}_i^s, \boldsymbol{\psi}_i^s) / \partial(\mathbf{r}, \mathbf{v}) \\ &+ \int_s^t \iint W_i(s, \mathbf{q}, \mathbf{u}, \tau, \boldsymbol{\varphi}_i^\tau, \mathbf{w})\, P_i(\tau, \boldsymbol{\varphi}_i^\tau, \mathbf{w}, \boldsymbol{\psi}_i^\tau)\, M_i(t, \mathbf{r}, \mathbf{v}, \tau)\, [\partial(\boldsymbol{\varphi}_i^\tau, \boldsymbol{\psi}_i^\tau) / \partial(\mathbf{r}, \mathbf{v})]\, d\tau\, d\mathbf{w}. \end{aligned} \tag{9}$$

Here the functions $\boldsymbol{\varphi}_1^s$ and $\boldsymbol{\psi}_1^s$ are given by Eq. (2), and

$$M_i(t, \mathbf{r}, \mathbf{v}, s) = \exp\left(-\int_{\tau=s}^{t} p_i(\tau, \boldsymbol{\varphi}_i^\tau, \boldsymbol{\psi}_i^\tau)\, d\tau\right) \tag{10}$$

gives the probability that a particle of type A_i that at the time t has radius vector $\mathbf{r}$ and velocity $\mathbf{v}$ has not undergone any collisions in the time interval s, t.[11]

Let $V_j(t, \mathbf{r}, \mathbf{v})\, d\mathbf{r}\, d\mathbf{v}$ be the probability for finding at the time t a cascade particle of type A_j with radius vector between $\mathbf{r}$ and $\mathbf{r} + d\mathbf{r}$ and velocity between $\mathbf{v}$ and $\mathbf{v} + d\mathbf{v}$, and let $U_j(t, \mathbf{r}, \mathbf{v})$ be the probability for production of one primary particle in the time interval dt with radius vector between $\mathbf{r}$ and $\mathbf{r} + d\mathbf{r}$ and velocity between $\mathbf{v}$ and $\mathbf{v} + d\mathbf{v}$. Let

$$V_{ij}(s, \mathbf{q}, \mathbf{u}, t, \mathbf{r}, \mathbf{v})\, d\mathbf{r}\, d\mathbf{v} \text{ and } U_{ij}(s, \mathbf{q}, \mathbf{u}, t, \mathbf{r}, \mathbf{v})\, dt\, d\mathbf{r}\, d\mathbf{v} \tag{11}$$

be these same probabilities, but on the hypothesis that the cascade is produced from a single particle K_0 of type A_i that has appeared at the time s at the point $\mathbf{q}$ with the velocity $\mathbf{u}$.

Making use of the Markov property of the process, we find that the functions U_j and V_j are connected by the relations

$$V_j(t, \mathbf{r}, \mathbf{v}) = \int_{-\infty}^{t} \iiint U_j(s, \mathbf{q}, \mathbf{u})\, W_j(s, \mathbf{q}, \mathbf{u}, t, \mathbf{r}, \mathbf{v})\, ds\, d\mathbf{q}\, d\mathbf{u}, \tag{12}$$

$$U_j(t, \mathbf{r}, \mathbf{v}) = U_j^0(t, \mathbf{r}, \mathbf{v}) + \sum_i \int V_i(t, \mathbf{r}, \mathbf{w})\, P_{ij}(t, \mathbf{r}, \mathbf{w}, \mathbf{v})\, d\mathbf{w}, \tag{13}$$

where U_j^0 is the density of sources of initial particles that occur not as the result of collisions of the cascade particles, but as the consequence of external processes.

By elimination of U_j we get

$$V_j(t, \mathbf{r}, \mathbf{v}) = V_j^0(t, \mathbf{r}, \mathbf{v}) + \sum_i \int_{-\infty}^{t} \iiint V_i(s, \mathbf{q}, \mathbf{u}) P_{ij}(s, \mathbf{q}, \mathbf{u}, \mathbf{w}) W_j(s, \mathbf{q}, \mathbf{w}, t, \mathbf{r}, \mathbf{v})\, ds\, d\mathbf{q}\, d\mathbf{u}\, d\mathbf{w}. \quad (14)$$

Here for brevity we have denoted by

$$V_j^0(t, \mathbf{r}, \mathbf{v}) = \int_{-\infty}^{t} \iint U_j^0(s, \mathbf{q}, \mathbf{u}) W_j(s, \mathbf{q}, \mathbf{u}, t, \mathbf{r}, \mathbf{v})\, ds\, d\mathbf{q}\, d\mathbf{u}$$

the density of particles of type A_j belonging to the swarms of the particles produced by the external sources.

Suppose that the cascade is produced by a single particle of type A_i with velocity $\mathbf{u}$ which has appeared at the time t at the point $\mathbf{q}$:

$$U_j^0 = \delta_{ij}\delta(t - s)\,\delta(\mathbf{r} - \mathbf{q})\,\delta(\mathbf{v} - \mathbf{u}), \quad V_j^0 = \delta_{ij} W_j(s, \mathbf{q}, \mathbf{u}, t, \mathbf{r}, \mathbf{v}).$$

The corresponding solution $V_{ij}(\mathbf{s}, \mathbf{q}, \mathbf{u}, \mathbf{t}, \mathbf{r}, \mathbf{v})$ of Eq. (14) is to be regarded as the Green's function of these equations. For it we get the equations

$$V_{ij}(s, \mathbf{q}, \mathbf{u}, t, \mathbf{r}, \mathbf{v}) = \delta_{ij} W_j(s, \mathbf{q}, \mathbf{u}, t, \mathbf{r}, \mathbf{v}) + \sum_k \int_s^t \iiint V_{ik}(s, \mathbf{q}, \mathbf{u}, \tau, \rho, \nu) P_{kj}(\tau, \rho, \nu, \mathbf{w})\; W_j(\tau, \rho, \mathbf{w}, t, \mathbf{r}, \mathbf{v})\, d\tau\, d\rho\, d\nu\, d\mathbf{w}. \quad (15)$$

The functions p_i, P_i, P_{ij}, $\mathbf{F}_i$, and consequently also φ_i^s and ψ_i^s, are known. Then the functions W_i are determined by Eq. (9), and V_{ij} by (15).

Let us suppose that $C \equiv C_1$, and consequently $P_i = 0$. Then from Eq. (9) we get

$$W_i(s, \mathbf{q}, \mathbf{u}, t, \mathbf{r}, \mathbf{v}) = \delta(\boldsymbol{\varphi}_i^s - \mathbf{q})\,\delta(\boldsymbol{\psi}_i^s - \mathbf{u})\, M_i(t, \mathbf{r}, \mathbf{v}, s)\, \partial(\boldsymbol{\varphi}_i^s, \boldsymbol{\psi}_i^s) / \partial(\mathbf{r}, \mathbf{v}), \quad (16)$$

and Eq. (15) takes the form

$$V_{ij}(s, \mathbf{q}, \mathbf{u}, t, \mathbf{r}, \mathbf{v}) = \delta_{ij}\delta(\boldsymbol{\varphi}_i^s - \mathbf{q})\,\delta(\boldsymbol{\psi}_i^s - \mathbf{u})\, M_j(t, \mathbf{r}, \mathbf{v}, s)\, \partial(\boldsymbol{\varphi}_i^s, \boldsymbol{\psi}_i^s) / \partial(\mathbf{r}, \mathbf{v})$$
$$+ \sum_k \int_s^t V_{ik}(s, \mathbf{q}, \mathbf{u}, \tau, \boldsymbol{\varphi}_i^\tau, \mathbf{w}) P_{kj}(\tau, \boldsymbol{\varphi}_i^\tau, \mathbf{w}, \boldsymbol{\psi}_i^\tau)\, M_j(t, \mathbf{r}, \mathbf{v}, \tau)\, [\partial(\boldsymbol{\varphi}_i^\tau, \boldsymbol{\psi}_i^\tau) / \partial(\mathbf{r}, \mathbf{v})] d\tau\, d\mathbf{w}. \quad (17)$$

If the properties of the medium are independent of the coordinates and the time and the forces $\mathbf{F}_i$ acting on the particles are equal to zero, we get

$$W_i(s, \mathbf{q}, \mathbf{u}, t, \mathbf{r}, \mathbf{v}) = W_i(t - s, \mathbf{r} - \mathbf{q}, \mathbf{u}, \mathbf{v}), \quad V_{ij}(s, \mathbf{q}, \mathbf{u}, t, \mathbf{r}, \mathbf{v}) = V_{ij}(t - s, \mathbf{r} - \mathbf{q}, \mathbf{u}, \mathbf{v}), \quad P_i(t, \mathbf{r}, \mathbf{v}, \mathbf{w}) = P_i(\mathbf{v}, \mathbf{w}),$$
$$P_{ij}(t, \mathbf{r}, \mathbf{v}, \mathbf{w}) = P_{ij}(\mathbf{v}, \mathbf{w}), \quad p_i(t, \mathbf{r}, \mathbf{v}) = p_i(v), M_i(t, \mathbf{r}, \mathbf{v}, s) = e^{-p_i(v)|t-s|}, \quad \boldsymbol{\varphi}_i^s = \mathbf{r} - \mathbf{v}(t - s), \quad \boldsymbol{\psi}_i^s = \mathbf{v}. \quad (18)$$

Then, without loss of generality, we can set $s = 0$, $\mathbf{q} = 0$, and from Eqs. (9), (11), (17), (18) we find for W_i and V_{ij} with $C \equiv C_1$:

$$W_i(t, \mathbf{r}, \mathbf{u}, \mathbf{v}) = \delta(\mathbf{r} - \mathbf{u}t)\,\delta(\mathbf{v} - \mathbf{u})\, e^{-p_i(v)t}, \quad (19)$$

$$V_{ij}(t, \mathbf{r}, \mathbf{u}, \mathbf{v}) = \delta_{ij}\delta(\mathbf{r} - \mathbf{u}t)\,\delta(\mathbf{v} - \mathbf{u})\, e^{-p_j(v)t} + \sum_k \int_0^t \iint V_{ik}(t - \tau, \mathbf{r} - \mathbf{v}\tau, \mathbf{u}, \mathbf{w})\; P_{kj}(\mathbf{w}, \mathbf{v})\, e^{-p_j(v)\tau} d\tau\, d\mathbf{w}, \quad (20)$$

and with $C \equiv C_2$ we get

$$W_i(t, \mathbf{r}, \mathbf{u}, \mathbf{v}) = \delta(\mathbf{r} - \mathbf{u}t)\,\delta(\mathbf{v} - \mathbf{u})\, e^{-p_i(v)\tau} + \int_0^t \iint W_i(t - \tau, \mathbf{r} - \mathbf{v}\tau, \mathbf{u}, \mathbf{w})\, P_i(\mathbf{w}, \mathbf{v})\, e^{-p_i(v)\tau} d\tau\, d\mathbf{w}, \quad (21)$$

$$V_{ij}(t, \mathbf{r}, \mathbf{u}, \mathbf{v}) = \delta_{ij} W_j(t, \mathbf{r}, \mathbf{u}, \mathbf{v}) + \sum_k \int_0^t \iiint V_{ik}(t - \tau, \mathbf{r} - \rho, \mathbf{u}, \nu) P_{kj}(\nu, \mathbf{w})\, W_j(\tau, \rho, \mathbf{w}, \nu)\, d\tau\, d\rho\, d\nu\, d\mathbf{w}. \quad (22)$$

All the equations (9), (15), (17), (20) — (22) we have obtained for W_i and V_{ij} are integral equations,[12] and not integro-differential equations such as are usually found in the theory of cosmic-ray

showers.[1,4] To each of them three corresponds another integral equation adjoint to it.[12,13]

By well known methods[14,15] one can get from each of these equations two systems of mutually adjoint differential equations for the unknowns W_i and V_{ij}. They are equations of first order with respect to t, but of infinite order with respect to u, or to v, respectively, and therefore are of no great practical interest.

All the equations (14), (15), (17), (20), and (22) are equations of the type

$$V = A + \Phi V,$$

where A is the inhomogeneous terms and Φ is a corresponding integral operator. By the iteration method an m-th order approximate solution is obtained in the form

$$V^m = A + \Phi A + \Phi^2 A + \ldots + \Phi^{m-1} A + \Phi^m V^0, \tag{23}$$

where V^0 is the initial approximation for V. Whatever V^0 may be, the iteration process converges. If, as is usually done, we take $V^0 = A$, it is not hard to verify[16] that V^m gives a good approximation only for $t - s < m\bar{\tau}$, where $\bar{\tau}$ is the average time of free flight of a particle. In order to find a solution giving a good approximation for arbitrary t, we use Eq. (23), but as V^0 we take a function giving a good approximation for V for large t.

Let us consider Eq. (20). As the initial approximation we set

$$V^0_{ij}(t, \mathbf{r}, \mathbf{u}, \mathbf{v}) = \{(1 + \varepsilon' e^{-\delta' t} + \varepsilon'' e^{-\delta'' t} + \ldots)\, \varepsilon_{ij} \gamma_i^3 / \pi^3 \alpha_i^3 \beta_i^3\, (1 - \varkappa_j^2)^{3/2} \times (\gamma_j t - 2\lambda_j)^{3/2}\} \exp\left\{ -\delta_j t - \frac{(\mathbf{v} - \varkappa_j \mathbf{u})^2}{\alpha_j^2 (1 - \varkappa_j^2)} - \frac{(\gamma_j \mathbf{r} - \lambda_j (\mathbf{u} + \mathbf{v}))^2}{\beta_j^2 (\gamma_j t - 2\lambda_j)} \right\}, \tag{24}$$

where

$$\varkappa_j = \exp\{-\gamma_j t\}, \quad \lambda_j = (1 - \exp\{-\gamma_j t\}) / (1 + \exp\{-\gamma_j t\}). \tag{25}$$

Here the quantities

$$\alpha_j, \beta_j, \gamma_j, \delta_j, \varepsilon_j, \delta', \varepsilon', \delta'', \varepsilon'' \ldots \tag{26}$$

depend on the variables i and u that characterize the initial particle. For brevity we have not written the arguments i and u. Without loss of genrality we shall suppose that

$$0 < \delta' < \delta'' < \ldots. \tag{27}$$

The quantities (26) must be determined in such a way that the function (24) approximate V_{ij} as well as possible for large t. The expression (24) represents a certain generalization of the Chandrasekhar function that gives the analogous probability in the diffusion of particles in Brownian motion. This function is obtained from (24) for n = 1 if

$$\alpha = \beta / \sqrt{2} = c, \quad \gamma = 6\pi a \eta / m, \quad \delta = 0, \quad \varepsilon = 1, \quad \varepsilon' = \varepsilon'' = \ldots = 0, \tag{28}$$

where m, a, and c are respectively the mass, radius, and most probable speed of the particle, and η is the viscosity of the medium.[13] We shall not use the relations (28), since the cascade particles, unlike particles in Brownian motion, are produced and absorbed and do not come into thermal equilibrium with the medium. The formula (24) is a generalization of the expression that we used in Ref. 16 in the solution of an analogous problem of the diffusion of neutrons.

To determine the constants (26), we substitute Eq. (24) into Eq. (20). We find that the error to within which V^0_{ij} satisfies Eq. (20) can be written in the form $V^0_{ij} R^0_{ij}$, where

$$R_{ij}(t, \mathbf{r}, \mathbf{u}, \mathbf{v}) = 1 - \delta_{ij} \delta(\mathbf{r} - \mathbf{u}t)\, \delta(\mathbf{v} - \mathbf{u})\, e^{-p_j(v)t} / V^0_{ij}(t, \mathbf{r}, \mathbf{u}, \mathbf{v})$$
$$- \sum_k \int_0^t \int [V^0_{ik}(t - \tau, \mathbf{r} - \mathbf{v}\tau, \mathbf{u}, \mathbf{w}) / V^0_{ij}(t, \mathbf{r}, \mathbf{u}, \mathbf{v})]\, P_{kj}(\mathbf{w}, \mathbf{v})\, e^{-p_j(v)\tau} d\tau\, d\mathbf{w} \tag{29}$$

is the fractional error. We try to determine the quantities (26) in such a way that the error R_{ij} goes to zero as rapidly as possible with increasing t. From Eq. (24) it is clear that the terms of highest order for large t will be of the type $c \exp\{-(\delta_k - \delta_j)t\}$, so that for $\delta_j \neq \delta_k$ in Eq. (24) terms appear that

increase exponentially as t increases. Consequently, in order to make the error a minimum, we must set

$$\delta_j = \delta. \tag{30}$$

Let us expand R_{ij} in powers of t^{-1} (and $\exp\{-\gamma_j t\}$, but these latter go to zero faster than any power of t^{-1}, so that they can be neglected) and try to determine the quantities (26) in such a way that as many as possible of the coefficients of this expansion are zero. In the calculation of R_{ij} we can take $\kappa_j = 0$, $\lambda_j = 1$, $\epsilon' = \epsilon'' = \ldots = 0$, drop the second term in Eq. (29), and take the upper limit in the integration over τ to be ∞, since all these steps lead to errors that decrease exponentially. We find

$$\varepsilon_i R_{ij} = \varepsilon_j - \sum_k \varepsilon_k \frac{\alpha_j^3 \beta_j^3}{\alpha_k^3 \beta_k^3} \int\limits_0^\infty \int\limits_0^\infty \frac{(\gamma_j t - 2)^{3/2}}{(\gamma_k (t-\tau) - 2)^{3/2}} e^{-(\rho_j(v) - \delta_j)\tau} P_{hj}(\mathbf{w}, \mathbf{v})$$
$$\times \exp\left\{ \frac{v^2}{\alpha_j^2} - \frac{w^2}{\alpha_k^2} + \frac{(\gamma_j \mathbf{r} - \mathbf{u} - \mathbf{v})^2}{\beta_j^2 (\gamma_j t - 2)} - \frac{(\gamma_k \mathbf{r} - \mathbf{u} - \mathbf{w})^2}{\beta_k^2 (\gamma_k (t-\tau) - 2)} \right\} d\tau\, d\mathbf{w}. \tag{31}$$

As can be seen, we cannot make more than two coefficients in the expansion of R_{ij} equal to zero, so that we confine ourselves to terms of order t^{-1}. We get:

$$\varepsilon_i R_{ij} = \varepsilon_j - \sum_k \varepsilon_k \frac{\alpha_j^3 \beta_j^3}{\alpha_k^3 \beta_k^3} \int\limits_0^\infty \int \left\{ \exp\left\{ \frac{v^2}{\alpha_j^2} - \frac{w^2}{\alpha_k^2} - (\rho_j(v) - \delta)\tau \right\} \right.$$
$$\left. \times P_{hj}(\mathbf{w}, \mathbf{v}) \left\{ 1 + \frac{1}{t} \left[\frac{3}{2}\tau + \frac{(\gamma_j \mathbf{r} - \mathbf{u} - \mathbf{v})^2}{\beta_j^2 \gamma_j} - \frac{(\gamma_k \mathbf{r} - \mathbf{u} - \mathbf{w})^2}{\beta_k^2 \gamma_k} \right] \right\} d\tau d\mathbf{w}.$$

From Eq. (24) it is clear that, at least for large t,

$$m_j(v)\, d\mathbf{v} = \frac{1}{\pi^{3/2} \alpha_j^3} \exp\{-v^2/\alpha_j^2\}\, d\mathbf{v} \tag{32}$$

will be the probability that a cascade particle of type A_j has its velocity between $\mathbf{v}$ and $\mathbf{v} + d\mathbf{v}$. If we set

$$\int m_k(w) P_{hj}(\mathbf{w}, \mathbf{v})\, d\mathbf{w} = a_{hj}(v), \qquad \int \mathbf{w} m_k(w) P_{hj}(\mathbf{w}, \mathbf{v})\, d\mathbf{w} = \mathbf{v} b_{hj}(v), \qquad \int w^2 m_k(w) P_{hj}(\mathbf{w}, \mathbf{v})\, d\mathbf{w} = v^2 c_{hj}(v), \tag{33}$$

the integration over $\mathbf{w}$ and then over τ can be carried out simply. We find

$$\varepsilon_i R_{ij} = \varepsilon_j - \sum_k \varepsilon_k \pi^{3/2} \alpha_j^3 \frac{\beta_j^3}{\beta_k^3} \exp\{v^2/\alpha_j^2\} \left\{ \frac{a_{hj}(v)}{\rho_j(v) - \delta} + \frac{1}{t} \left[\frac{3}{2} \frac{1}{(\rho_j(v) - \delta)^2} + \frac{\gamma_j \mathbf{r} - \mathbf{u} - \mathbf{v})^2 a_{hj}(v)}{\beta_j^2 \gamma_j (\rho_j(v) - \delta)} \right. \right.$$
$$\left. \left. - \frac{(\gamma_k \mathbf{r} - \mathbf{u})^2 a_{hj}(v) - 2(\gamma_k \mathbf{r} - \mathbf{u}) \mathbf{v} b_{hj}(v) + v^2 c_{hj}(v)}{\beta_k^2 \gamma_k (\rho_j(v) - \delta)} \right] \right\}.$$

We cannot equate to zero the constant term and the coefficient of t^{-1} in this expression, since they involve the variables $\mathbf{r}$ and $\mathbf{v}$, on which the quantities (26) cannot depend. Therefore, as in Ref. 13, we confine ourselves to setting their average values with respect to $\mathbf{v}$ equal to zero. Multiplying by (32), integrating with respect to $\mathbf{v}$, and using certain considerations of symmetry, we get

$$\varepsilon_j - \sum_k \varepsilon_k \frac{\beta_j^3}{\beta_k^3} \int \left\{ \frac{a_{hj}(v)}{\rho_j(v) - \delta} + \frac{1}{t} \left[\frac{3}{2} \frac{a_{hj}(v)}{(\rho_j(v) - \delta)^2} + \frac{(\gamma_j \mathbf{r} - \mathbf{u})^2 a_{hj}(v) + v^2 a_{hj}(v)}{\beta_j^2 \gamma_j (\rho_j(v) - \delta)} - \frac{(\gamma_k \mathbf{r} - \mathbf{u})^2 a_{hj}(v) + w^2 c_{hj}(v)}{\beta_k^2 \gamma_k (\rho_j(v) - \delta)} \right] \right\} d\mathbf{v} = 0. \tag{34}$$

This equation must hold for all $\mathbf{r}$ and t. Therefore it falls apart into five, or more precisely into $5n^2$, equations, since it must be satisfied for all values of the index j and of the omitted index i. Thus we get a number of equations that exceeds by n^2 the number of unknowns involved in Eq. (34). But all of these equations are satisfied if we set

$$\beta_j = \beta, \qquad \gamma_j = \gamma. \tag{35}$$

Then Eq. (34) separates into

$$\varepsilon_j - \sum_k \varepsilon_k \int \frac{a_{hj}(v)}{\rho_j(v) - \delta}\, d\mathbf{v} = 0, \tag{36}$$

$$\sum_k \varepsilon_k \int \left[\frac{3}{2} \frac{a_{hj}(v)}{(\rho_j(v) - \delta)^2} + \frac{v^2}{\beta^2 \gamma} \frac{a_{hj}(v) - c_{hj}(v)}{\rho_j(v) - \delta} \right] d\mathbf{v} = 0. \tag{37}$$

From Eq. (36) it can be seen that ϵ_j is determined apart from a certain factor,

$$\varepsilon_j = \varepsilon e_j, \tag{38}$$

where ϵ is a function of i and u still to be determined, and the quantities e_j are normalized by

$$\sum e_j = 1. \tag{39}$$

We cannot find the equations that are still lacking in order to determine all the unknowns (26) by equating to zero the successive coefficients in the expansion of R_{ij} as averaged over v because, as can easily be verified, this gives an infinite set of new equations. Therefore we must bring in new considerations in order to get the required equations.

From Eqs. (32), (33), and (39) we find that, at least for large t,

$$n_j(v)\,dv = \sum_i e_i a_{ij}(v)\,dv \Big/ \sum_{ij} e_i \int a_{ij}(v)\,dv \tag{40}$$

will be the probability for the production of a primary particle of type A_j with velocity between v and v + dv.

Let $\bar{r}_i(u)$ be the average radius vector of all particles for large t, if the initial particle of the cascade was of type A_i and had velocity u; then

$$R = \sum_i \int n_i(u)\,\bar{r}_i(u)\,du \tag{41}$$

is the absolute value of this radius vector, averaged over i and u according to Eq. (40). Let $\bar{r}^2(t)$ be the dispersion of the displacements of the particles at the time t, averaged over the type and the velocity of the initial particle, so that the quantity

$$D = \lim_{t\to\infty} \frac{1}{6t}\,\bar{r}^2(t) \tag{42}$$

can be called the diffusion coefficient of the cascade particles. The quantities R and D can be found by two methods — from Eq. (24), or by statistical calculations, for example by the method of Yang.[18] As in Ref. 13, by equating these values we find two more equations.

From Eqs. (24), (41), and (42) we find

$$R = \frac{1}{\gamma} \sum_i \int n_i(u)\,u\,du, \quad D = \frac{1}{4}\,\frac{3^2}{\gamma}. \tag{43}$$

Let us introduce the concept of the chain C of a given particle K at the time t. This is the succession of particles, each converted into the next, by which K is obtained from K_0. We call the particle K a particle of the m-th generation if its chain consists of m particles. Let $V_{ij}^m(u, v)\,dv$ be the probability that one particle among the particles of the m-th generation produced from a single particle of type A_i with velocity u is a particle of type A_j with velocity between v and v + dv.

Following Ref. 13, we find

$$V_{ij}^1(u, v) = \delta_{ij}\,\delta(v - u), \quad V_{ij}^{m+1}(u, v) = \sum_k \int V_{ik}^m(u, w)\,\frac{P_{kj}(w, v)}{\sum_j \int P_{kj}(w, v)\,dv}\,dw. \tag{44}$$

Let $\bar{r}_i^m(u)$ be the average displacement of the particles of the m-th generation, if the particle that produced the cascade was of type A_i and had velocity u. We get

$$\bar{r}_i^m(u) = \sum_j \int V_{ij}^m(u, v)\,\frac{v}{p_j(v)}\,dv, \tag{45}$$

$$\bar{r}_i(u) = \sum_{m=1}^{\infty} \bar{r}_i^m(u). \tag{46}$$

Then from Eqs. (41), (45), and (46) we find a second expression for R and, equating it to the expression (43), we get

$$\sum_i \int n_i(u)\,u\,du = \gamma \sum_i \int n_i(u) \left| \sum_{m=} \bar{r}_i^m(u) \right| du. \tag{47}$$

Let $\bar{t}_N$ and $\overline{r_N^2}$ be the mean lifetime and the dispersion of the displacements of all the particles of the N-th generation, so that we can set[13,18]

$$D \approx \lim_{N\to\infty} \frac{1}{6\bar{t}_N}\,\overline{r_N^2}. \tag{48}$$

Here, following (18), we have

$$\bar{t}_N = N\bar{t},\ \overline{r_N^2} = \sum_{m,n=1}^{N} \overline{\mathbf{r}^m\mathbf{r}^n} = N\overline{r'^2} + 2(N-1)\,\overline{\mathbf{r}'\cdot\mathbf{r}^2} + 2(N-2)\,\overline{\mathbf{r}'\cdot\mathbf{r}^3} + \ldots, \tag{49}$$

where $\bar{t}$ is the mean lifetime of one particle, and $\mathbf{r}^m$ is the displacement of one particle of the m-th generation. We find that

$$\bar{t} = \sum_i \int \frac{n_i(u)}{p_i(u)}\,d\mathbf{u}, \tag{50}$$

$$\overline{r'^2} = 2\sum_i \int \frac{n_i(u)}{p_i^3(u)}\,u^2 d\mathbf{u}, \tag{51}$$

$$\overline{\mathbf{r}'\cdot\mathbf{r}^m} = \sum_{ij} \iint n_i(u)\,V_{ij}^m(\mathbf{u},\mathbf{v})\,\frac{\mathbf{u}\cdot\mathbf{v}}{p_i(u)\,p_j(v)}\,d\mathbf{u}\,d\mathbf{v}. \tag{52}$$

From Eqs. (48) and (49) we find a second expression for D and, equating to Eq. (43), we get finally

$$\frac{3}{4}\,\frac{\beta^2}{\gamma}\,\bar{t} = \frac{1}{2}\,\overline{r'^2} + \sum_{m=2}^{\infty} \overline{\mathbf{r}'\cdot\mathbf{r}^m}, \tag{53}$$

where $\bar{t}$, $\overline{r'^2}$, and $\overline{\mathbf{r}'\cdot\mathbf{r}^m}$ are given by Eqs. (50) – (52).

Equations (30), (35) – (37), (39), (47), and (53) are sufficient for the determination of the quantities α_j, β_j, γ_j, δ_j, and e_j. In this connection it must be noted that in all these equations i and u do not occur. Consequently, all these quantities, which we had taken dependent on i and u, without indicating this only for the sake of brevity, turn out to be independent of i and u, and β_j, γ_j, δ_j are even independent of j.

In order to find the remaining unknowns

$$\delta_i'(u),\ \delta_i''(u),\ \ldots\ \varepsilon_i(u),\ \varepsilon_i'(u),\ \varepsilon_i''(u),\ \ldots \tag{54}$$

we integrate (24) with respect to r and v and sum with respect to j. Using Eqs. (38) and (39), we find

$$\varepsilon_i e^{-\delta t} + \varepsilon_i\varepsilon_i' e^{-(\delta+\delta_i')t} + \varepsilon_i\varepsilon_i'' e^{-(\delta+\delta_i'')t} + \cdots = N_i(t,u), \tag{55}$$

where $N_i(t,u)$ is the total number of particles at the time t. From the definition of the functions V_{ij} it is clear that $N_i(0,u) = 1$. We denote by N_i', N_i'', ... the derivatives of the functions N_i with respect to t for t = 0. Differentiating Eq. (55) and setting t = 0, we find

$$\begin{aligned} &\varepsilon_i + \varepsilon_i\varepsilon_i' + \varepsilon_i\varepsilon_i'' + \cdots = 1, \quad -\delta\varepsilon_i - (\delta+\delta_i')\,\varepsilon_i\varepsilon_i' - (\delta+\delta_i'')\,\varepsilon_i\varepsilon_i'' - \cdots = N_i', \\ &\delta^2\varepsilon_i + (\delta+\delta_i')^2\,\varepsilon_i\varepsilon_i' + (\delta+\delta_i'')^2\,\varepsilon_i\varepsilon_i'' + \cdots = N_i'', \quad \ldots\ldots\ldots\ldots\ldots\ldots\ldots \end{aligned} \tag{56}$$

We calculate the quantities N_i', N_i'' from Eq. (23) with $V^0 = A$. Then, using the fact that the operator Φ is of the order of t, we see that in the calculation of N_i^k we can without loss of accuracy use Eq. (23) with m = k. Breaking off the series $1 + \epsilon' e^{-\delta' t} \ldots$ in Eq. (24) at a certain term, we can write a sufficient number of equations of the type of Eq. (56) to determine all the quantities (54). In particular, if we use two terms we get for ϵ_i', ϵ_i'' and δ_i'

$$\varepsilon_i = \frac{N_i'' - N_i'^2}{N_i'' + 2\delta N_i' + \delta^2}, \quad \varepsilon_i' = \frac{(N_i' + \delta)^2}{N_i'' - N_i'^2}, \quad \delta_i' = -\frac{N_i'' + 2\delta N_i' + \delta^2}{N_i' + \delta}. \tag{57}$$

From Eq. (23), with $V^0 = A$ and m = 2, in virtue of Eq. (20), we get for N_i' and N_i'', after some calculation,

$$\begin{aligned} N_i'(u) &= -p_i(u) + \sum_j \int P_{ij}(\mathbf{u},\mathbf{v})\,d\mathbf{v}, \\ N_i''(u) &= \frac{1}{2}\,p_i^2(u) + \frac{1}{2}\sum_{jk} \iint P_{ik}(\mathbf{u},\mathbf{w})\,P_{kj}(\mathbf{w},\mathbf{v})\,d\mathbf{w}\,d\mathbf{v} - \frac{1}{2}\sum_j \int (p_i(u) + p_j(v))\,P_{ij}(\mathbf{u},\mathbf{v})\,d\mathbf{v}. \end{aligned} \tag{58}$$

The expressions (57) and (58) determine the quantities (54). It is clear that the values obtained for them depend on i and u. They must satisfy the inequality (27).

Consequently, V_{ij}^0 finally takes the form

$$V_{ij}^0(t, \mathbf{r}, \mathbf{u}, \mathbf{v}) = \varepsilon_i e_j \pi^{3} [(1+\varepsilon_j' e^{-\delta_j' t} + \varepsilon_j'' e^{-\delta_j'' t} + \ldots)/\pi^3 \alpha_j^3 \beta^3 (1-\varkappa^2)^{3/2} (\gamma t - 2\lambda)^{3/2}]$$
$$\times \exp\left\{-\delta t - \frac{(\mathbf{v}-\varkappa \mathbf{u})^2}{\alpha_j^2(1-\varkappa^2)} - \frac{(\gamma \mathbf{r} - \lambda(\mathbf{u}+\mathbf{v}))^2}{\beta^2(\gamma t - 2\lambda)}\right\} (\varkappa = e^{-\gamma t},\ \lambda = (1-e^{-\gamma t})/(1+e^{-\gamma t})). \tag{59}$$

The constants α_j, β, γ, δ, and e_j are determined from Eqs. (36), (37), (39), (47), and (53). In the solution of these equations it is expedient first to eliminate β, γ, and e_j and determine δ and α_j. Since the functions (54) are not involved in these equations, they are determined subsequently from Eq. (56) or, in particular, from Eqs. (57) and (58). We shall not consider the problem of the existence and uniqueness of the solution. We note only that if several solutions are found one must choose the solution corresponding to the smallest value of δ, since it gives the main value of V_{ij}^0 for large t.

The method that has been explained for the solution of the equations (20) can be applied to Eq. (21). This is an equation of the type of Eq. (20) for n = 1. Consequently, one can obtain its solution by iteration, taking as the initial approximation

$$W_i^0(t, \mathbf{r}, \mathbf{u}, \mathbf{v}) = c_i^3 [(e_i(u) e^{-d_i t} + e_i'(u) e^{-d_i'(u) t} + \ldots)/\pi^3 a_i^3 b_i^3 (1-k_i^2)^{3/2} (c_i t - 2l_i)^{3/2}]$$
$$\times \exp\left\{-\frac{(\mathbf{v}-k_i \mathbf{u})^2}{a_i^2(1-k_i^2)} - \frac{(c_i \mathbf{r} - l_i(\mathbf{u}+\mathbf{v}))^2}{b_i^2(c_i t - 2l_i)}\right\} (k_i = e^{-c_i t},\quad l_i = (1-e^{-c_i t})/(1+e^{-c_i t})), \tag{60}$$

with the quantities a_i, b_i, c_i, d_i, $e_i(u)$, $d_i'(u)$, $e_i'(u)$ ... determined like α, β, γ, δ, $\epsilon_i(u)$, $\delta + \delta_i'(u)$, $\epsilon_i(u)\,\epsilon_i'(u)$ for n = 1 and $P_{11} = p_1$.

We look for the solution of Eq. (22) also in the form (24). The determination of the quantities (26) is carried out in the same way. Here, using Eqs. (30) and (35), we get instead of Eq. (34)

$$\varepsilon_j = \sum_k \frac{\varepsilon_k}{\pi^{3/2}\alpha_k^3} \int_0^\infty \iiint \exp\left\{\delta\tau - \frac{w^2}{\alpha_k^2}\right\} P_{kj}(\mathbf{w}, \mathbf{v})\, W_j(\tau, \rho, \mathbf{v}, \mathbf{v})$$
$$\times \left\{1 + \frac{1}{4}\left[\frac{3}{2}\tau + \frac{(\gamma \mathbf{r} - \mathbf{u} - \mathbf{v})^2}{\beta^2\gamma} - \frac{(\gamma(\mathbf{r}-\rho) - \mathbf{u} - \mathbf{w})^2}{\beta^2\gamma}\right]\right\} d\tau\, d\rho\, d\mathbf{v}\, d\mathbf{v}\, d\mathbf{w}, \tag{61}$$

where W_j is given by the expression (60). From considerations of symmetry it follows that here, as in Eq. (34) the terms containing $\mathbf{r}$ and $\mathbf{u}$ drop out. The integration over ρ and $\mathbf{v}$ is carried out immediately. After this the integration over τ becomes elementary. The integration over $\mathbf{w}$ reduces to the substitution of the expressions (33).

After carrying out all these rather cumbersome calculations, we get instead of Eqs. (36) and (37)

$$\varepsilon_j - \sum_k \varepsilon_k \int a_{kj}(\nu)\, \alpha_j(\nu, \delta)\, d\nu = 0, \tag{62}$$

$$\sum \varepsilon_k \int a_{kj}(\nu) \left\{\frac{3}{2}\left(\frac{b_j^2}{c_j^2\beta} - \frac{\beta}{\gamma}\right)\frac{\partial \alpha_j(\nu, \delta)}{\partial \delta} + \left(\frac{3}{2}\frac{a_j^2}{\beta\gamma^2} + \frac{21}{2}\frac{a_j^2}{\beta c_j^2} - \frac{\nu^2}{\beta c_j^2} - 3\frac{b_j^2}{\beta c_j^2} - \frac{2\nu^2}{\beta\gamma c_j}\frac{b_{kj}(\nu)}{a_{kj}(\nu)} - \frac{\nu^2}{\beta\gamma^2}\frac{c_{kj}(\nu)}{a_{kj}(\nu)}\right)\alpha_j(\nu, \delta)\right.$$
$$+ 2\left(-3\frac{a_j^2}{\beta c_j^2} + \frac{\nu^2}{\beta c_j^2} + \frac{\nu^2}{\beta c_j \gamma}\frac{b_{kj}(\nu)}{a_{kj}(\nu)}\right)\alpha_j(\nu, \delta - c_j) + \left(\frac{3}{2}\frac{a_j^2}{\beta c_j^2} - \frac{3}{2}\frac{a_j^2}{\beta\gamma^2} + \frac{\nu^2}{\beta\gamma^2} - \frac{\nu^2}{\beta c_j^2}\right)\alpha_j(\nu, \delta - 2c_j)$$
$$\left. + 6\left(\frac{b_j^2}{\beta c_j^3} - 2\frac{a_j^2}{\beta c_j^3}\right)\left[e_j(\nu)\beta\left(\frac{\quad}{\quad c}\right) + e_j'(\nu)\beta\left(\frac{d_j'(\nu) - \delta}{c_j}\right) + \ldots\right]\right\} d\nu = 0, \tag{63}$$

with[19]

$$\alpha_j(\nu, x) = \frac{e_j(\nu)}{d_j - x} + \frac{e_j'(\nu)}{d_j'(\nu) - x} + \ldots, \quad \beta(x) = \int_0^\infty \frac{e^{-xt}}{1+e^{-t}}\, dt.$$

To derive the equations analogous to (47) and (53) we must first of all change the concept of the generation of a particle. We shall call a particle K a particle of the m-th generation if the particles of its chain belong to m different swarms, i.e., if among them there are m primary particles. By $V_{ij}^m(\mathbf{u}, \mathbf{v})\, d\mathbf{v}$ we shall now mean the probability of finding a particle of type A_j with velocity between v and v + dv among the primary particles of the m-th generation, if the cascade is produced from an initial particle of type A_i with velocity u. Instead of Eq. (44) we now get

$$V_{ij}^{1}(\mathbf{u}, \mathbf{v}) = \delta_{ij}\delta(\mathbf{v}-\mathbf{u}), \quad V_{ij}^{m+1}(\mathbf{u}, \mathbf{v}) = \sum_k \int\int V_{ik}^{m}(\mathbf{u}, \mathbf{w}) \frac{R_k(\mathbf{w}, \mathbf{v}) P_{kf}(\mathbf{v}, \mathbf{v})}{\sum_f \int\int R_k(\mathbf{w}, \mathbf{v}) P_{kf}(\mathbf{v}, \mathbf{v})\, d\mathbf{v}d\mathbf{v}} \, d\mathbf{w}\, d\mathbf{v}$$

with

$$R_i(\mathbf{u}, \mathbf{v}) = \int_0^\infty \int\int W_i(t, \mathbf{r}, \mathbf{u}, \mathbf{v})\, dt d\mathbf{r}.$$

The mean lifetime and mean displacement of the particles of the swarm will be $t_i(\mathbf{u})$ and $ur_i(\mathbf{u})$, where t_i and r_i are suitable functions of $\mathbf{u}$, which can be found without difficulty by means of W_i. Then Eq. (50) remains valid, with $1/p_i$ replaced by t_i, and Eqs. (46) and (52) with $1/p_i$ replaced by r_i, while instead of Eq. (51) we must write

$$\overline{r^2} = \sum_i \int_0^\infty \int\int\int\int r^2 m_i(u)\, W_i(t, \mathbf{r}, \mathbf{u}, \mathbf{v})\, dt\, d\mathbf{r}\, d\mathbf{u}\, d\mathbf{v}.$$

Equations (47) and (53) remain valid with the indicated changes of the definitions of the quantities appearing in them. As regards the definition of the functions (54), for them Eqs. (56), (57), and (58) remain valid, it being only necessary to replace the quantity P_{ij} in Eq. (58) by Q'_{ij} [Eq. (7)].

Both the proposed methods for finding the functions V_{ij} by solution of Eq. (20) or Eq. (22) are in principle equally applicable. It is clear, however, from the structure of Eqs. (36) and (37), and of (61) and (62), respectively, that if the majority of the particles arising in the collisions are particles of the same type as the incident particle, i.e., if $Q'_{ii} \gg \sum_j^{j\neq i} Q'_{ij}$, then it is more advantageous to take C_2 as the class C. Then one must use the method based on Eq. (22) with $P_{ii} = 0$. If, on the other hand, $Q'_{ii} \lesssim \sum_j^{j\neq i} Q'_{jj}$, it is better to use Eq. (20).

From the expression (59), which is a solution both of Eq. (20) and of Eq. (22), we can draw some general conclusions about the distribution of particles in first approximation. The fact that one gets for the δ values not depending on i, j, and u means that the numbers of particles of the various types A_j fall off by the same exponential laws for any i and u. The fact that the values of β and γ are independent of i, j, and u means that the ratio of the densities of particles of different types is the same at different points of space and at different times. The dependence of the quantities α_j and e_j on j (but not on i and u) means that the velocity distributions and the ratios of the densities of the various types of particles depend on the types of particles, but not on the type and velocity of the initial particle. The type and velocity of the initial particle affect the absolute values of the densities only through the common factor $\epsilon(1 + \epsilon' e^{-\delta' t} + \ldots)$. All of this is readily understandable, since for large t the distribution of the particles as to type, position, and velocity must be determined primarily by the transition probabilities p_i, P_i, and P_{ij}, and not by the choice of the initial particle.

The substitution (24) is fortunately chosen because, on one hand, it provides for a rather rapid decrease of the errors $V_{ij}^0 R_{ij}$ with increase of t, makes it possible to satisfy the equations (39), which exceed in number the disposable unknowns, and leads to values independent of r, and on the other hand the approximate solution (59) obtained on the basis of this substitution gives a qualitatively correct representation of the development of the cascade process. In this connection it must be noted that the substitution (24) is convenient practically, since it can be applied for arbitrary choice of the functions p_i, P_i, and P_{ij}, and a large part of the functions (26) turn out to be constants, not even depending on the indices i and j, which can be calculated by means of the single integrations involved in Eqs. (26), (47) and (61), (62), respectively. The method we have given for finding the functions has advantages in comparison with other methods used in such cases, based on the principle of least squares, because in the latter methods the squaring and averaging of errors involves highly multiple integrals.

An idea of the accuracy of the resulting solution can be obtained by calculations of the type of those presented in Ref. 16.

I consider it my pleasant duty to express my gratitude to Academician N. N. Bogoliubov for a valuable discussion of the results and to Professor D. D. Ivanenko for his constant interest in the work.

[1] S. Z. Belen'kii, Лавинные процессы в космических лучах (Cascade Processes in Cosmic Rays), Gostekhizdat, Moscow, 1948.

[2] B. Rossi, High Energy Particles (Russ. Transl.), Gostekhizdat, Moscow, 1955.
[3] L. Janossy, J. Exptl. Theoret. Phys. (U.S.S.R.) **26**, 386 518 (1954).
[4] N. Arley, On the Theory of Stochastic Processes and their Application to the Theory of Cosmic Radiation. New York, 1948.
[5] R. Stephenson, Introduction to Nuclear Engineering (Russ. Transl.) Moscow, 1956.
[6] A. A. Vlasov, Теория многих частиц (Theory of Many Particles), GITTL, Moscow-Leningrad, 1950.
[7] N. Bohr, Passage of Atomic Particles through Matter (Russ. Transl.) IIL, Moscow, 1950.
[8] N. S. Akulov, Теория цепных процессов (Theory of Chain Processes), GITTL, Moscow-Leningrad, 1951.
[9] A. A. Semenov, Цепные реакции (Chain Reactions), Goskhimizdat, Leningrad, 1934.
[10] M. C. Wang and G. E. Uhlenbeck, Revs. Mod. Phys. **17**, 323 (1945).
[11] Kh. Ia. Khristov, Dokl. Akad. Nauk SSSR **111**, 981 (1956).
[12] J. Doob. Stochastic Processes (Russ. Transl.). IIL, Moscow, 1956.
[13] Kh. Ia. Khristov, Dokl. Akad. Nauk SSSR **111**, 1197 (1956).
[14] J. Keilson and J. E. Stoner, Quart. Appl. Math. **10**, 243 (1952).
[15] Ch. Christov (Khristov), Acta Physica Hung. **6**, 325 (1956).
[16] Ch. Christov (Khristov), Acta Physica Hung. **7**, 51 (1957).
[17] S. Chandrasekhar, Revs. Mod. Phys. **15**, 1 (1943).
[18] L. M. Yang, Proc. Roy. Soc. **A198**, 94 (1949).
[19] I. M. Ryshik and I. S. Gradshtein Таблицы интегралов, сумм, рядов и произведений (Tables of Integrals, Sums, Series, and Products) Moscow, 1951.

Translated by W. H. Furry
133

SOVIET PHYSICS JETP VOLUME 6 (33), NUMBER 3 MARCH, 1958

CALCULATION OF THE INTERACTION POTENTIAL OF ATOMS

O. B. FIRSOV

Submitted to JETP editor March 5, 1957

J. Exptl. Theoret. Phys. (U.S.S.R.) **33**, 696-699 (September, 1957)

The sum of the Coulomb interaction between atomic nuclei and the change in electron energy connected with the mutual approach of the nuclei is taken as the interaction potential. The electron energy is computed on the basis of the statistical model.

I. It was shown in a previous article[1] that the energy H_0 of electrons, in the approximation of the Thomas-Fermi statistical model and for the presence of two nuclei, lies between the two values H and H_1, which differ by not more than 5 per cent:

$$\frac{1}{e^2}H=\int\left\{\lambda\left[\frac{3}{5}(\rho_{01}+\rho_{02})^{5/3}-\frac{1}{2}(\rho_{01}^{5/3}+\rho_{02}^{5/3})(\rho_{01}+\rho_{02})\right]-\frac{1}{2}\left(\frac{Z_1}{r_1}+\frac{Z_2}{r_2}\right)(\rho_{01}+\rho_{02})\right\}dv,$$

$$\frac{1}{e^2}H_1=\int\left\{\lambda\left[\frac{1}{2}(\rho_{01}^{1/3}+\rho_{02}^{1/3})(\rho_{01}+\rho_{02})-\frac{2}{5}(\rho_{01}^{1/3}+\rho_{02}^{1/3})^{5/3}\right]-\frac{1}{2}\left(\frac{Z_1}{r_1}+\frac{Z_2}{r_2}\right)(\rho_{01}+\rho_{02})\right\}dv, \quad (1)$$

where $\lambda=\frac{1}{2}(3\pi^2)^{2/3}\hbar^2/me^2=2.52\times10^{-8}$ cm, Z_1e and Z_2e are the nuclear charges, $\rho_{01}(r_1)$ and $\rho_{02}(r_2)$ are the Thomas-Fermi electron densities in the atoms without consideration of the mutual interaction, r_1 is the distance to the nucleus of the first atom, r_2, to the nucleus of the second atom.

The relative difference between H and H_1 decreases montonically to zero upon increase in the distance between the nuclei from zero to infinity.

Under the condition that the electrons are always in the ground states, we have for the interaction potential between the atoms, in accord with (1), $U_1(R) < U_0(R) < U(R)$, where

$$U(R) = e^2 Z_1 Z_2/R + H - H(\infty),\ U_1(R) = e^2 Z_1 Z_2/R + H_1 - H_1(\infty). \tag{2}$$

It is evident that as $R \to 0$, $\rho_{01} \to 0$, where ρ_{02} differs from zero; conversely, for $r_1 \to \infty$, $\rho_{01}(r_1) \sim 1/r_1^6$. Therefore,

$$\begin{aligned}
\frac{1}{e^2} U(R) &= \frac{Z_1 Z_2}{R} + \int \left\{ \lambda \left[\frac{3}{5} (\rho_{01} + \rho_{02})^{5/3} - \frac{1}{2} (\rho_{01}^{5/3} + \rho_{02}^{5/3})(\rho_{01} + \rho_{02}) - \frac{1}{10} (\rho_{01}^{5/3} + \rho_{02}^{5/3}) \right] - \frac{1}{2} \left(\frac{Z_1}{r_1} \rho_{02} + \frac{Z_2}{r_1} \rho_{01} \right) \right\} dv, \\
\frac{1}{e^2} U_1(R) &= \frac{Z_1 Z_2}{R} + \int \left\{ \lambda \left[\frac{1}{2} (\rho_{01}^{5/3} + \rho_{02}^{5/3})(\rho_{01} + \rho_{02}) - \frac{2}{5} (\rho_{01}^{5/3} + \rho_{02}^{5/3})^{3/2} - \frac{1}{10} (\rho_{01}^{5/3} + \rho_{02}^{5/3}) \right] - \frac{1}{2} \left(\frac{Z_1}{r_1} \rho_{02} + \frac{Z_2}{r_2} \rho_{01} \right) \right\} dv,
\end{aligned} \tag{3}$$

$Z_2/R - \int r_1^{-1} \rho_{02}(r_2)\, dv$ is the Thomas-Fermi potential of the second atom at the distance R. Therefore, we can write (3) in the form

$$\begin{aligned}
\frac{1}{e^2} U(R) &= \frac{Z_1 Z_2}{2R} \left[\chi\left(Z_1^{1/3} \frac{R}{a} \right) + \chi\left(Z_2^{1/3} \frac{R}{a} \right) \right] + \lambda \int \left[\frac{3}{5} (\rho_{01} + \rho_{02})^{5/3} - \frac{1}{2} (\rho_{01}^{5/3} + \rho_{02}^{5/3})(\rho_{01} + \rho_{02}) - \frac{1}{10} (\rho_{01}^{5/3} + \rho_{02}^{5/3}) \right] dv, \\
\frac{1}{e^2} U_1(R) &= \frac{Z_1 Z_2}{2R} \left[\chi\left(Z_1^{1/3} \frac{R}{a} \right) + \chi\left(Z_2^{1/3} \frac{R}{a} \right) \right] + \lambda \int \left[\frac{1}{2} (\rho_{01}^{5/3} + \rho_{02}^{5/3})(\rho_{01} + \rho_{02}) - \frac{1}{2} (\rho_{01}^{5/3} + \rho_{02}^{5/3})^{3/2} - \frac{1}{10} (\rho_{01}^{5/3} + \rho_{02}^{5/3}) \right] dv,
\end{aligned} \tag{4}$$

$$a = (9\pi^2/128)^{1/3} \hbar^2/me^2 = 4.68 \cdot 10^{-9} \text{ cm},$$

where $\chi(x)$ is the Thomas-Fermi function, the tabulation of which was taken from the book of Gombas.[2] The densities $\rho_{01}(r_1)$ and $\rho_{02}(r_2)$ are expressed in terms of the Thomas-Fermi function

$$\rho_{01}(r_1) = \left(\frac{Z_1}{r_1 \lambda} \cdot \chi\left(Z_1^{1/3} \frac{r_1}{a} \right) \right)^{3/2},$$

and similarly for $\rho_{02}(r_2)$.

2. If we write the potential $U_0(R)$ in the form

$$U_0(R) = Z_1 Z_2 e^2 f_0(R)/R,$$

then for small R,

$$f_0 \approx 1 - 1.59x + \ldots,\ x = \frac{3}{7} \frac{(Z_1 + Z_2)^{7/3} - Z_1^{7/3} - Z_2^{7/3}}{Z_1 Z_2} \frac{R}{a}. \tag{5}$$

This follows from the fact that for $R \to 0$, $U(R)$ differs from the Coulomb interaction by the difference of the electron energy at $R \to \infty$ and $R = 0$, which, in accord with the Thomas-Fermi model, are respectively equal to

$$-1.59 \frac{3}{7} (Z_1 + Z_2)^{7/3} \frac{e^2}{a} \text{ and } -1.59 \frac{3}{7} (Z_1^{7/3} + Z_2^{7/3}) \frac{e^2}{a}.$$

The first two terms in (5) coincide with the expansion of the Thomas-Fermi function of argument x.

With the aid of perturbation theory, we can obtain,[3] for $Z_2/Z_1 \to 0$ or $Z_1/Z_2 \to 0$:

$$f_0(R) \to \chi\left(Z_1^{1/3} \frac{R}{a} \right) \text{ or } f_0(R) \to \chi\left(Z_2^{1/3} \frac{R}{a} \right), \tag{6}$$

which coincides with (5) for $R \to 0$ under these limiting conditions. Obviously, $f_0(R)$ ought to be a symmetric function relative to a substitution of Z_2 for Z_1.

We now consider the more general expression for the electron energy

$$\frac{1}{e^2} H(R) = \frac{3}{5} \int \lambda \rho^{5/3}\, dv - \int \left(\frac{Z_1}{r_1} + \frac{Z_2}{r_2} \right) \rho\, dv + \frac{1}{2} \iint \frac{\rho(r) \rho(r')\, dv\, dv'}{|r - r'|}$$

The density ought to be such that H is minimal. Therefore,

$$\frac{3}{5} \lambda \int \rho_0^{5/3}\, dv = \frac{\lambda}{e^2} \frac{\partial H_0}{\partial \lambda};\ -\int \left(\frac{Z_1}{r_1} + \frac{Z_2}{r_2} \right) \rho_0\, dv = \frac{Z_1}{e^2} \frac{\partial H}{\partial Z_1} + \frac{Z_2}{e^2} \frac{\partial H}{\partial Z_2}. \tag{7}$$

It was found in Ref. 1 [Eq. (7)] that

$$\frac{1}{e^2}H_0 = \frac{\lambda}{10}\int \rho_0^{5/3} dv - \frac{1}{2}\int\left(\frac{Z_1}{r_1}+\frac{Z_2}{r_2}\right)\rho_0\, dv.$$

Hence, by virtue of (7), we have

$$H_0 = \frac{1}{6}\lambda\,\partial H_0/\partial\lambda - \frac{1}{2}(Z_1\,\partial H_0/\partial Z_1 + Z_2\,\partial H_0/\partial Z_2). \tag{8}$$

From (8), H_0 can be written in the form

$$(Z_1 Z_2 e^2/R)\,\Theta(Z_1^{1/3}R/a,\ Z_2^{1/3}R/a). \tag{9}$$

Consequently, $U_0(R)$ also reduces to the same form.

3. In the table below, the screening functions $f(R)$ and $f_1(R)$ have been computed as functions of the argument x [Eq. (5)] for the ratio $\alpha = Z_2/Z_1 = 1/4,\ 2/3,\ 1$.

α	x	0.2	0.3	0.5	0.7	1	1.5	2	3	5	7	10
0	$\chi(x)$	0.79	0.72	0.61	0.52	0.425	0.315	0.242	0.158	0.079	0.046	0.0244
1/4	$f(x)$	0.80	0.73	0.61	0.52	0.42	0.31	0.23	0.14	0.063	0.026	0.013
1/4	$f_1(x)$	0.79	0.71	0.59	0.50	0.40	0.28	0.21	0.12	0.052	0.024	0.010
2/3	$f(x)$	0.80	0.73	0.61	0.52	0.42	0.31	0.23	0.14	0.056	0.026	0.011
2/3	$f_1(x)$	0.79	0.71	0.5	0.49	0.39	0.28	0.20	0.12	0.046	0.021	0.008
1	$f(x)$	0.80	0.73	0.61	0.47	0.42	0.30	0.22	0.13	0.055	0.028	0.015
1	$f_1(x)$	0.79	0.70	0.58	0.44	0.39	0.28	0.20	0.11	0.046	0.024	0.012

The integrals in Eq. (4) were computed with an accuracy ~ 2 per cent. These integrals are negative and for large values of R are close in value to the first term in Eqs. (4). Therefore, the error in computing f and f_1 amounts to about 10 per cent at $x \sim 10$. Moreover, at some points there are evidently small random errors, because the computation was carried out "by hand" by a single person. Since the statistical model is generally valid only with accuracy ~ 20 per cent, these errors have no significant importance here.

It follows from the table that the screening function $f_0(x)$, whose values lie between $f(x)$ and $f_1(x)$ for large values of x, differs appreciably from $\chi(x)$ even at $\alpha = 1/4$. This corresponds to $f_0(x)$ for $\alpha \to 0$. For $x = 10$, the ratio $f_0(x)/\chi(x)$ is $\sim 1/2$. Further change of α up to 1 does not lead to a significant change in $f_0(x)$.

We can, however, introduce another scale factor in the definition of x. This factor would coincide with Eq. (5) when Z_2/Z_1 or Z_1/Z_2 tended to zero and would reduce for this same value of R to smaller values of x in the old definition. Then $f(x')$, for the new definition of x, will differ less from $\chi(x')$ at larger x'. For example, the Bohr scale factor $(Z_1^{2/3} + Z_2^{2/3})$ gives the following changes in x for various values of α:

$$\alpha = 0,\quad 1/4,\quad 2/3,\quad 1$$
$$x'/x = 1,\quad 0.93,\quad 0.92,\quad 0.92,$$

i.e., if we introduce

$$x' = \sqrt{Z_1^{2/3} + Z_2^{2/3}}\,R/a,$$

in place of the value of x defined by Eq. (5), then at $\alpha = 0$, $x' = x$, while at $\alpha = 1$, $x' = 0.92\,x$. Then the values of $f(x')$ in the table above remain practically unchanged for $x' < 0.2$, in the interval $0.5 < x' < 3$, they increase by ~ 8 per cent, and for $x' \sim 7 - 10$, they increase by ~ 20 per cent. The difference between $f(x')$ and $\chi(x')$ will be much less. It would be even better to introduce a scale factor by the relation

$$x' = (Z_1^{1/3} + Z_2^{1/3})^{3/2} R/a.$$

Then the ratio x'/x will be

$$\alpha = 0,\quad 1/4,\quad 2/3,\quad 1,$$
$$x'/x = 1,\quad 0.84,\quad 0.82,\quad 0.82.$$

In this case, $f(x')$ differ from $\chi(x')$ by not more than 20 per cent throughout the entire range of variation of x' from 0 to 10. Since

$$R \approx 4.7 \cdot 10^{-9}\ \text{cm} \cdot x'/(\sqrt{Z_1} + \sqrt{Z_2})^{2/3},$$

then, for $x' = 10$, even for $Z_1 = Z_2 = 100$, $R = 0,64 \times 10^{-8}$ cm. However, at distances $R > 10^{-8}$ cm, the calculation of the interaction potential of atoms on the basis of a statistical model loses its meaning.

Thus, in the limits of accuracy of the Thomas-Fermi statistical model of the atom, the interaction between atoms at distances between atoms less than 10^{-8} cm can be described by the potential

$$U(R) = \frac{Z_1 Z_2 e^2}{R} \cdot \chi\left(\left|\sqrt{Z_1} + \sqrt{Z_2}\right|^{-2} \frac{R}{a}\right), \tag{10}$$

where $\chi(x)$ is the Thomas-Fermi screening function.

This fact, that the screening function can be expressed approximately as a function a single argument, allows us to compute (within a suitable interval of energy of relative motion and for suitable scattering angles) the effective differential scattering cross section at once for an arbitrary pair of colliding atoms.

In conclusion, I want to thank Academician M. A. Leontovich, Prof. A. B. Migdal and V. Galitskii for useful discussions of the research. I am very grateful to G. I. Biriuk for the computation of the integrals of Eq. (4).

[1] O. B. Firsov, J. Exptl. Theoret. Phys. (U.S.S.R.) **32**, 1464 (1957); Soviet Phys. JETP **5**, 1192 (1957).
[2] P. Gombas, Statistical Theory of the Atom and its Application, (Russ. Transl.) IIL, Moscow, 1951.
[3] O. B. Firsov, Dokl. Akad. Nauk SSSR **91**, 515 (1953).

Translated by R. T. Beyer
134

SOVIET PHYSICS JETP VOLUME 6 (33), NUMBER 3 MARCH, 1958

CYLINDRICAL SELF-SIMILAR ACOUSTICAL WAVES

IA. B. ZEL'DOVICH

Submitted to JETP editor March 6, 1957

J. Exptl. Theoret. Phys. (U.S.S.R.) **33**, 700-705 (September, 1957)

A one-parameter family of self-similar solutions for cylindrical motion is constructed in the acoustical approximation. This construction is accomplished by superposition of plane waves and is expressed in elementary form by quadratures. For motion with a finite pressure discontinuity on the wave front of a converging cylindrical wave, the results agree with those obtained previously.[1] It is found again that the pressure in the reflected wave is infinite. The maximum pressure is estimated and allowances are made for the deviations from the acoustical approximation for large amplitudes.

ZABABAKHIN and Nechaev[1] have treated the propagation of a weak cylindrical shock wave and its reflection from the axis in the acoustical approximation.* Their solution for the reflected wave has an unexpected property: the pressure on the front diverges logarithmically, and is the same before and behind the front, that is

$$p \sim \frac{a}{\sqrt{r_f}} \ln \left| \frac{b r_f}{r - r_f} \right| \quad \text{for} \quad |r - r_f| \ll r_f$$

(where p is the pressure change, and the solution is valid only for $p \ll p_0$).

No such singularity occurs when a spherical acoustical wave converges onto a center and is reflected, or for strong cylindrical and spherical shock waves.[2] It is therefore desirable to obtain the result of Zababakhin and Nechaev differently, by a method in which the necessity for their solution would become clearer.

*I take this opportunity to express my gratitude to the authors, who communicated their work to me before its publication.

It was found possible to obtain a whole family of self-similar cylindrical solutions of which, however, the most interesting is just that found by Zababakhin and Nechaev.

1. GENERAL SOLUTION OF THE CYLINDRICAL PROBLEM

The known solution of the acoustical problem for a plane wave propagating along the x axis,

$$p_{\text{pl}} = f(x - ct),\ u_x = (1/\rho c) f(x - ct),\ u_y = u_z = 0, \tag{1}$$

shall be written in cylindrical coordinates with the polar axis directed at an angle ϕ to the x axis. On the polar axis $x = r\cos\phi$ so that on this line the pressure and velocities are given by

$$p_{\text{pl}} = f(r\cos\varphi - ct),\ u_r = (1/\rho c)\cos\varphi \cdot f(r\cos\varphi - ct)\quad u_\varphi = (1/\rho c)\sin\varphi \cdot f(r\cos\varphi - ct),\ u_z = 0. \tag{2}$$

By superposing such plane waves with all possible values of ϕ we obtain the cylindrically symmetric solution depending on one arbitrary function*

$$p = p(r, t) = \frac{1}{2}\int_0^{2\pi} f(r\cos\varphi - ct)\, d\varphi; \tag{3}$$

$$u_r = u_r(r, t) = \frac{1}{2\rho c}\int_0^{2\pi} \cos\varphi \cdot f(r\cos\varphi - ct)\, d\varphi,\ u_\varphi = u_z = 0. \tag{4}$$

It is convenient to change the notation by making the substitution $k = \cos\phi$, so that

$$p = \int_{-1}^{+1} f(rk - ct)\, dk / \sqrt{1 - k^2}; \tag{5}$$

$$u_r = \frac{1}{\rho c}\int_{-1}^{+1} f(rk - ct)\, k\, dk / \sqrt{1 - k^2}. \tag{6}$$

It is easy to see by direct substitution that the function $p(r, t)$ so defined satisfies the wave equation

$$\frac{1}{c^2}\frac{\partial^2 p}{\partial t^2} = \frac{1}{r}\frac{\partial}{\partial r} r \frac{\partial p}{\partial r}, \tag{7}$$

2. SELF-SIMILAR SOLUTIONS

We shall choose the function $f(z)$, where

$$z = r\cos\varphi - ct = rk - ct,$$

in such a way that the constants entering into the definition of $f(z)$ cannot be combined to form a quantity with the dimensions of a length. Then the only quantity with these dimensions which enters into the expression for the pressure will be, with the exception of the independent variable r, the product ct. Then the solution will be self similar, i.e., of the form $t^n\psi(r/ct)$.

Specifically, let us choose $f(z)$ such that

$$f(z) = 0 \quad \text{for} \quad z > 0,\ f(z) = a(-z)^n \quad \text{for} \quad z < 0. \tag{8}$$

On inserting (8) into (5), the limits of integration depend on the ratio between r and ct, and are the k interval either from -1 to $+1$ or that given by the vanishing of $f(z)$ for $z = rk - ct = 0$.

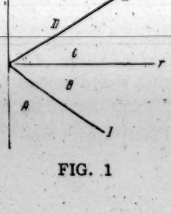

FIG. 1

It is easily seen that $t = 0$ is the time at which the wave is focused on the axis, so that t is the time calculated from the instant of focusing. The conventional rt diagram is shown in Fig. 1. Line I (or $r = -ct$) is the incident wave, and line II (or $r = +ct$) is the reflected wave. Region A (where $ct < 0$ and $r < -ct$) contains the unperturbed gas before the incident wave front. Region B (where $ct < 0$ and $r > -ct$) contains the gas behind the wave front. Region C (where $ct > 0$ and $r > ct$) contains the gas before the reflected

*The factor ½ in Eqs. (3) and (4) is introduced for convenience in writing (5) and (6) and those that follow.

wave front. Region D (where $ct > 0$ and $r < ct$) contains the gas behind the reflected wave front.

In region A, we have $z > 0$ and $f = 0$ throughout the interval $-1 < k < +1$, so that $p \equiv 0$ as is to be expected.

In region B we have $-1 < ct/r < 0$, so that

$$p = a(-ct)^n \int_{-1}^{ct/r} \left(\frac{r}{ct}k - 1\right)^n dk/\sqrt{1-k^2}. \tag{9}$$

In region C we have $0 < ct/r < 1$, so that

$$p = a(ct)^n \int_{-1}^{ct/r} \left(1 - \frac{r}{ct}k\right)^n dk/\sqrt{1-k^2}. \tag{10}$$

In region D we have $ct/r > 1$, so that

$$p = a(ct)^n \int_{-1}^{+1} \left(1 - \frac{r}{ct}k\right)^n dk/\sqrt{1-k^2}. \tag{11}$$

As follows from dimensionality considerations, in all regions the solution is of the form

$$p = a(|ct|)^n \psi(r/|ct|) = a r_f^n \psi(S),\ r_f = |ct|,\ S = r/r_f, \tag{12}$$

which means that it is self similar for arbitrary values of n. We have used simple quadratures and have not integrated the differential equation, but have been able to obtain a whole family of self similar solutions depending on an exponent n each of which build up according to different laws and have different pressure profiles determined by the dimensionless function ψ.

It should be borne in mind that the function in Eq. (12) is different in the different regions A, B, C, and D, so that it depends not only on S but also on the sign of the time. This, of course, does not destroy the self modeling property of the solution.

3. CHOICE OF THE EXPONENT FROM INITIAL CONDITIONS

Let us find the pressure profile in the incident wave. According to Eq. (9), in region B we have

$$\psi_B(S) = \int_{-1}^{-1/S} (-kS - 1)^n dk/\sqrt{1-k^2},\ S > 1. \tag{13}$$

If we let the variable of integration be $y = (-kS - 1)/(S - 1)$, we obtain

$$\psi_B(S) = (S-1)^{n+1/2}(S+1)^{-1/2} \int_0^1 y^n dy \Big/ \sqrt{(1-y)\left(1 + \frac{S-1}{S+1}y\right)}. \tag{14}$$

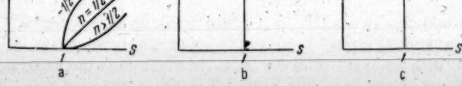

FIG. 2

In the neighborhood of the wave front with $S - 1 \ll 1$, the integral approaches a limit given by

$$\int_0^1 y^n (1-y)^{-1/2} dy,$$

so that the pressure profile is given by the factor $(S-1)^{n+1/2}$. When $n > -1/2$ we are dealing with a gradually increasing pressure (Fig. 2a), when $n = -1/2$, there is a finite discontinuity (Fig. 2b) and when $n < -1/2$ the pressure on the front is infinite (Fig. 2c).

Thus a shock wave with a steep front and a finite pressure discontinuity is described by the solution with index $n = -1/2$. As has been shown by Zababakhin and Nechaev, the amplitude increases as $r_f^{-1/2}$ as the wave converges (compare with Eq. (12)). One may have expected such a result from the fact

that the acoustical energy of a unit volume is proportional to p^2, and the area of a cylindrical wave is proportional to r_f so that when $n = -1/2$ the acoustical energy $p^2 r_f \delta$ is constant in the layer of thickness δ about the wave front.

We note that these concepts are applicable* also when there is no finite discontinuity, or when $n \neq -1/2$: the pressure is proportional to r_f^n at similar distances (for a given S), but at equal distances from the front, that is when $S = 1 + \delta/r_f$ the pressure for any n is proportional to $r_f^{-1/2}$.

Let us return to the case $n = -1/2$, for which

$$\psi = \frac{1}{\sqrt{S+1}} \int_0^1 dy \Big/ \sqrt{y(1-y)\left(1 + \frac{S-1}{S+1}\, y\right)}. \tag{15}$$

When $S = 1$ we have

$$\psi(1) = \pi/\sqrt{2}, \quad p_f = a\pi/\sqrt{2r_f}. \tag{15a}$$

It is easily seen that behind the wave front the pressure drops with a finite derivative, as shown in Fig. 2b. Far from the front we have, for large S,

$$p \sim a/\sqrt{r_f S} = a/\sqrt{r}.$$

As one may have expected, the pressure far from the front is independent of the location of the front.

4. THE REFLECTED DIVERGING WAVE

By treating a cylindrical wave as a superposition of plane waves we can clarify the question of the uniqueness of the solution after reflection. This follows from the fact that none of the plane waves have singularities on crossing the axis at time $t = 0$.

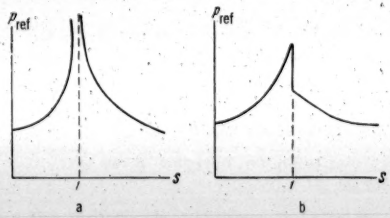

FIG. 3

Let us write the expressions in regions C and D for $n = -1/2$, namely

$$p = a r_f^{-1/2} \psi_C(S), \quad \psi_C = \int_{-1}^{1/S} dk \Big/ \sqrt{(1-k^2)(1-Sk)}, \quad S > 1; \tag{16}$$

$$p = a r_f^{-1/2} \psi_D(S), \quad \psi_D = \int_{-1}^{+1} dk \Big/ \sqrt{(1-k^2)(1-Sk)}, \quad S < 1. \tag{17}$$

When $S = 1$ both integrals approach

$$\int_{-1}^{+1} dk/(1-k)\sqrt{1+k},$$

and diverge logarithmically at the upper limit.

It is easily shown that when $|S - 1| = \epsilon \ll 1$ both expressions (16) and (17) give (up to terms which vanish as ϵ approaches zero and may be different for ψ_C and ψ_D)†

$$\psi_C = \psi_D = \frac{1}{\sqrt{2}} \ln \frac{32}{\epsilon}. \tag{18}$$

* The elementary concepts of geometric acoustics are applicable for the following reason. Close to a wave front on which the pressure or its derivatives undergo a discontinuity, harmonic analysis gives the pressure increase in terms of the asymptotic values of the short waves for which $\lambda \to 0$. Thus the condition $\lambda/r_f \ll 1$ for the applicability of geometric acoustics is fulfilled.

† To show this, let us set $S = (1-\epsilon)^{-1}$ in (16) and $S = (1+\epsilon)^{-n}$ in (17) and break up each integral in (16) and (17) into two parts J_1 from -1 to $1-a$ and J_2 from $1-a$ to the upper limit, where a is chosen such that $1 \gg a \gg \epsilon$. In J_1 we set $\epsilon = 0$ with an error of order ϵ/a, in which case the integral is elementary and equal to $2^{-1/2} \ln(8/a)$. In J_2 we may replace $\sqrt{1+k}$ by $\sqrt{2}$ with an error of the order of a. Then J_2 is elementary and given by (up to small terms of the order of ϵ and $\epsilon \ln \epsilon$) $J_2 = 2^{-1/2} \cosh^{-1}(2a/\epsilon)$ both for (16) and (17).

When $a \gg \epsilon$

$$J_2 = 2^{-1/2} \ln(4a/\epsilon), \quad \psi = J_1 + J_2 = 2^{-1/2} \ln(32/\epsilon),$$

so that a drops out of the expression for ψ.

This verifies the logarithmic divergence of the pressure in the reflected wave as found previously by Zababakhin and Nechaev.

If on the incident wave the pressure is p_{inc} on the wave front at a given distance r_f from the axis, then on the reflected wave

$$p_{ref} = \frac{p_{inc}}{\pi} \ln \frac{32 r_f}{|r - r_f|} \tag{19}$$

becomes infinite symmetrically before and behind the front $r_f = ct$ (see Fig. 3a).

This result, which has been obtained in the acoustical approximation, is known to be invalid if the pressure according to (19) is of the order of p_0, the absolute pressure of the gas in which the wave is propagating. A better evaluation can be obtained by finding the radius at which the incident plane wave can no longer be described by acoustical laws, that is

$$r_0 \sim a^2 / p_0^2, \tag{20}$$

where a is the constant in Eq. (15a).

In the region of applicability of the acoustical approximation, however, that is if $r_f \gg r_0$, the acoustical expression (19) is applicable only when $|r - r_f| > r_0$. From this some simple operations give the maximum pressure in the reflected wave of the order of

$$p_{ref}^{max} = (2 p_{inc} / \pi) \ln (p_0 / p_{inc}). \tag{21}$$

Here as in (19) p_{ref} and p_{inc} refer to the same distance from the axis.

Accounting for the deviation from the acoustical approximation also destroys the equality of the pressure at equal distances before and behind the wave front. Figure 3a gives a schematic diagram of the pressure profile when nonlinearity is not accounted for, and Fig. 3b gives the pressure profile with the deviations from the acoustical approximation.

When the reflected wave is sufficiently far from the center, $r_f \gg r_0$ and the pressure at the center can be calculated by the acoustical theory. It is clear that a perturbation in the entropy will not interfere with a smoothing out of the pressure over a region of the order of r_f. One then obtains

$$p(0, t) = a\pi / \sqrt{ct} = \sqrt{2}\, p_{inc}(-t). \tag{22}$$

We note finally that a similar method for constructing self similar solutions can be used for the spherical problem. In this case, however, when the pressure undergoes a finite discontinuity in the incident wave there will be only a finite discontinuity in the wave reflected from the center.

The difference between the cylindrical and spherical cases in the acoustical approximation is clearly related to the difference in wave propagation in spaces with even and odd numbers of dimensions, as has been mentioned by Courant.[3]

I take this opportunity to express my gratitude to E. I. Zababakhin and V. A. Aleksandrov.

[1] E. I. Zababakhin and M. N. Nechaev, J. Exptl. Theoret. Phys. (U.S.S.R.) **33**, 442 (1957), Soviet Phys. JETP **6**, 345 (1958).

[2] G. Guderlye, Luftfahrtforschung **19**, 3 (1943). Cited by Courant and Friedrichs, Supersonic Flow and Shock Waves (Russ. Transl.), IIL.

[3] R. Courant, D. Hilbert, Methods of Mathematical Physics (Russ. Transl.), Gostekhizdat, 1954, vol. II.

Translated by E. J. Saletan
135

BOUND STATES IN POSITRONIUM

IU. A. TARASOV

Moscow State University

Submitted to JETP editor March 7, 1957

J. Exptl. Theoret. Phys. (U.S.S.R.) 33, 706-709 (September, 1957)

It is shown that the bound states of an electron and positron may be studied by examining the poles of the photon propagator.

We consider the bound states of an electron and a positron. Starting from the Bethe-Salpeter equation in the ladder approximation, and taking Fourier transforms of the wave-function $\psi_{\alpha\beta}(1, 2)$ and of the functions S_F, D_F, we obtain the momentum-space equation

$$A_{n_1n_2}(\mathbf{p}, p_0) = -\frac{ie^2}{(2\pi)^4}\int\sum_{n_1'n_2'}\left\{\frac{[\bar{u}^{n_1'}(\mathbf{p}')\gamma_\mu u^{n_1}(\mathbf{p})][\bar{u}^{n_2}(\mathbf{p})\gamma_\mu u^{n_2'}(\mathbf{p}')]D_F(p-p')}{(\delta_{n_1}E_p+W/2-p_0)(\delta_{n_2}E_p-W/2-p_0)}\right. \tag{1}$$

$$\left.-\frac{[\bar{u}^{n_2}(\mathbf{p})\gamma_\mu u^{n_1}(\mathbf{p})][\bar{u}^{n_1'}(\mathbf{p}')\gamma_\mu u^{n_2'}(\mathbf{p}')]D_F(W)]}{(\delta_{n_1}E_p+W/2-p_0)(\delta_{n_2}E_p-W/2-p_0)}\right\}A_{n_1'n_2'}(\mathbf{p}', p_0').$$

Here $n = 1, 2$ denote solutions of the Dirac equation with positive energy, $n = 3, 4$ those with negative energy, and $\delta_1 = \delta_2 = 1$, $\delta_3 = \delta_4 = -1$. The second term in Eq. (1) is the exchange term. We define the three-dimensional amplitude by

$$a_{n_1n_2}(\mathbf{p}) = \int A_{n_1n_2}(p)\,dp_0.$$

We obtain the adiabatic approximation[1] from Eq. (1) if we replace D_F by $\int D_F(p)\delta(p_0)\,dp_0$. The first non-adiabatic approximation is obtained by substituting the adiabatic expression for $A_{n_1n_2}(p)$ on the right of Eq. (1) and integrating with respect to p_0 and p_0'. Neglecting the minus particles, we have the old Tamm-Dancoff equation for positronium. We are interested in the contribution of the exchange term. After dropping tensor terms and integrating over angles, we obtain the equations for the triplet s-state ($\sigma_1\sigma_2 = 1$),

$$a^\epsilon(p) = \lambda\int\left\{\frac{K_1(p, p', \varepsilon W)a^\epsilon(p')}{2E_p-\varepsilon W}+\frac{K_2(p, p', \varepsilon W)a^{-\epsilon}(p')}{2E_p-\varepsilon W}-\frac{4[a^\epsilon(p')+a^{-\epsilon}(p')]}{W^2(2E_p-\varepsilon W)}\right\}p'^2\,dp', \tag{2}$$

Here $\epsilon = 1$ for the plus-component (a^{++}), and $\epsilon = -1$ for the minus-component (a^{--}); $\lambda = e^2/4\pi^2 = 1/137\pi$.

In the adiabatic approximation

$$K_1(p, p', \varepsilon W) = K_2 = \frac{1}{pp'}\ln\frac{p+p'}{|p-p'|},$$

and in the first non-adiabatic approximation

$$K_1 = \frac{1}{pp'}\ln\frac{p+p'+E_p+E_{p'}-\varepsilon W}{|p-p'|+E_p+E_{p'}-\varepsilon W},\quad K_2 = \frac{1}{pp'}\ln\frac{p+p'+E_p+E_{p'}}{|p-p'|+E_p+E_{p'}}.$$

We introduce the notation

$$\chi = \int 4[a^\epsilon(p')+a^{-\epsilon}(p')]\frac{p'^2dp'}{W^2}.$$

and look for a solution of Eq. (2) of the form

$$a^\epsilon(p) = \lambda\Gamma^\epsilon(p, W)\chi/(2F_0-\varepsilon W)+g^\epsilon(p).$$

Substituting this ansatz into Eq. (2), we find that Γ^ϵ satisfies

$$\Gamma^{\varepsilon}(p, W) = 1 + \lambda \int_0^{\infty} \left\{ \frac{K_1 \Gamma^{\varepsilon}(p', W)}{2E_{p'} - \varepsilon W} + \frac{K_2 \Gamma^{-\varepsilon}(p', W)}{2E_{p'} + \varepsilon W} \right\} p'^2 dp', \tag{3}$$

while g^{ϵ} satisfies the homogeneous equation with kernels K_1 and K_2. The homogeneous system of equations for a^{ϵ} has energy eigenvalues W differing from the eigenvalues of the equation for g^{ϵ}. Therefore, if W is one of the eigenvalues for a^{ϵ}, the equation for g^{ϵ} has no non-zero solution. Substituting a^{ϵ} into the expression for χ, we find

$$\chi [W^2 - \Pi(W^2)] = 0, \text{ with } \Pi(W^2) = -4\lambda \sum_{\varepsilon} \int_0^{\infty} \frac{\Gamma^{\varepsilon}(p, W)\, p^3 dp}{2E_p - \varepsilon W}.$$

Since the equation for Γ^{ϵ} is the equation for a vertex function, $\Pi(W^2)$ is the photon polarization operator. Eq. (21) will have a nontrivial solution only for values of W at which the photon propagator $D_F' = 1/(W^2 - \Pi(W^2))$ has a pole. To find the poles we must carry out a renormalization. We separate a divergent factor from the vertex function

$$\Gamma^{\varepsilon}(p, W) = Z\Gamma_c^{\varepsilon}(p, W).$$

The renormalized function Γ_c^{ϵ} is defined[2] by the condition $\Gamma_c^{\epsilon}(0, m) = 1$. Substituting $\Gamma^{\epsilon}(p, W) = Z\Gamma_c^{\epsilon}(p, W)$ into Eq. (3) and separating $\Gamma_c^{\epsilon}(p, W)$ into two parts

$$\Gamma_c^{\varepsilon}(p, W) = \Gamma_c^{\varepsilon}(p, m) + \Phi^{\varepsilon}(p, W),$$

we obtain the equations

$$\Gamma_c^{\varepsilon}(p, m) = 1 + \lambda \int_0^{\infty} \left\{ \left[\frac{K_1(p, p', \varepsilon m) - K_1(0, p', \varepsilon m)}{2E_{p'} - \varepsilon m} \right] \Gamma_c^{\varepsilon}(p', m) + \left[\frac{K_2(p, p') - K_2(0, p')}{2E_{p'} + \varepsilon m} \right] \Gamma_c^{-\varepsilon}(p', m) \right\} p'^2 dp';$$

$$\Phi^{\varepsilon}(p, W) = \lambda \int_0^{\infty} \left\{ \frac{K_1(p, p', \varepsilon W)\, \Phi^{\varepsilon}(p', W)}{2E_{p'} - \varepsilon W} + \frac{K_2(p, p')\, \Phi^{-\varepsilon}(p', W)}{2E_{p'} + \varepsilon W} \right\} p'^2 dp' + P^{\varepsilon}(p, W),$$

where

$$P^{\varepsilon}(p, W) = \lambda \int_0^{\infty} \left\{ \left[\frac{K_1(p, p', \varepsilon W)}{2E_{p'} - \varepsilon W} - \frac{K_1(p, p', \varepsilon m)}{2E_{p'} - \varepsilon m} \right] \Gamma_c^{\varepsilon}(p', m) + \left[\frac{K_2(p, p')}{2E_{p'} + \varepsilon W} - \frac{K_2(p, p')}{2E_{p'} + \varepsilon m} \right] \Gamma_c^{-\varepsilon}(p', m) \right\} p'^2 dp'.$$

After removing the overlapping divergences, the finite part of the polarization operator is separated,*

$$\Pi(W^2) = \Pi(0) + \Pi'(0)\, W^2 + \Pi_c(W^2).$$

A calculation up to terms of order λ gives the result $\Pi'(0) = -1/4$ in the adiabatic approximation and $\Pi'(0) = -1/2$ in the first non-adiabatic approximation (after dividing by Z^2). The charge-renormalization is thus finite. The quantity $\Pi(W^2) - \Pi(0)$ is obtained as an integral involving $\Gamma_c^{\epsilon}(p, m)$ and $\Phi^{\epsilon}(p, W)$. The function $\Gamma_c^{\epsilon}(p, m)$ is calculated by successive approximation. The asymptotic form of $\Gamma_c^{\epsilon}(p, m)$ is $p^{-2\lambda}$ in the adiabatic and $p^{-\lambda}$ in the first non-adiabatic approximation. In the adiabatic approximation $\Phi^{+}(p, W) = \Phi^{-}(p, W)$ and so the two equations reduce to one, giving the result

$$Z^2\Pi_c(W^2) = \Pi(W^2) - \Pi(0) - \Pi'(0)\, W^2 = Z^2 \left\{ -4\lambda \int_0^{\infty} \frac{\Phi^{+}(p, W)\Gamma_c^{+}(p, m)\, 4E_p (W^2 - m^2)\, p^2 dp}{(4E_p^2 - W^2)(4p^2 + 3m^2)} + O(\lambda) \right\}.$$

$\Phi^{+}(p, W)$ satisfies a non-homogeneous equation. A variational calculation shows that up to terms of order λ we may replace the kernel of the homogeneous integral equation corresponding to the given non-homogeneous equation by the kernel which describes the motion of an electron in a Coulomb field. We make the change of variables

$$p/m = t\sqrt{\beta},\ \beta = |E|/m,\ W = 2m - |E|$$

and replace the unknown function by

$$\varphi(t) = t\Phi^{+}(t)/\sqrt{t^2 + 1},$$

* In the old Tamm-Dancoff method it is impossible to separate Π_c covariantly, since Π depends on W and not only on W^2.

Then the equation for Φ^+ becomes symmetric, and the binding energy appears only in the coefficient of the integral,

$$\varphi(t) = \gamma \int [(t^2+1)(t'^2+1)]^{-1/2} \ln \left| \frac{t+t'}{t-t'} \right| \varphi(t')\, dt' + f(t), \quad \gamma = \frac{\lambda}{\sqrt{\beta}}. \tag{4}$$

The solution of a symmetric equation may be written

$$\varphi(t) = f(t) + \gamma \sum_{n=1}^{\infty} \frac{f_n \varphi_n(t)}{\gamma_n - \gamma}, \quad f_m = (f, \varphi_m),$$

where γ_n are the eigenvalues and φ_n the eigenfunctions of Eq. (4), namely

$$\varphi_n(t) = \frac{2}{\sqrt{\pi}} (1+t^2)^{-n-1/2} \sum_{m=0}^{n-1} (-1)^m \frac{2n(2n-1)\ldots(2n-2m)}{(2m+1)!} t^{2m+1}.$$

Since Π_c contains a factor λ, the quantity $W^2 - \Pi_c(W^2)$ can vanish only near to an eigenvalue of the equation for Φ^+. For example, suppose γ is near to γ_1; then we substitute $\varphi(t)$ into $\Pi_c(W^2)$ and obtain the result

$$W^2 - \Pi_c(W^2) = 4m^2 - 4m^2(\lambda^2\pi^2\beta_1/\Delta\beta_1) + O(\lambda) = 0,$$

where $\beta_1 = E_1/m$, $E_1 = me^4/4h^2$, and $\Delta\beta_1$ is the ground-state level-shift. Therefore $W^2 - \Pi_c(W^2)$ vanishes for $\Delta\beta_1 = \beta_1\alpha^2$ or $\Delta E_1 = E_1\alpha^2$, with $\alpha = 1/137$. This result agrees with the perturbation theory calculation of the level-shift in the ground-state of positronium.[3] For the other states, taking γ near to γ_n, we find

$$W^2 - \Pi_c(W^2) = 4m^2 - 4m^2(\beta_n^2\pi^2/\Delta\beta_n \cdot n) + O(\lambda) = 0,$$

with $\beta_n = \beta_1/n^2$. Therefore $W^2 - \Pi_c(W^2)$ vanishes when

$$\Delta\beta_n = \alpha^2\beta_1/n^3.$$

We conclude that the study of the poles of a propagator can give information about the bound states of a fermion and an anti-fermion. The results are consistent with Lehmann's theorem.[4] We are currently applying the method to a study of the bound states of nucleon and antinucleon.

I thank V. Ia. Fainberg for his constant interest and advice.

[1] M. Lévy, Phys. Rev. 88, 72 (1952).

[2] R. H. Dalitz and F. J. Dyson, Phys. Rev. 99, 301 (1955).

[3] A. I. Akhiezer and V. B. Berestetskii, Квантовая электродинамика (Quantum Electrodynamics) (Gostekhizdat, Moscow, 1953), § 38.

[4] H. Lehmann, Nuovo cimento 11, 342 (1954).

Translated by F. J. Dyson
136

ON MAGNETOHYDRODYNAMICAL EQUILIBRIUM CONFIGURATIONS

V. D. SHAFRANOV

Academy of Sciences of the U.S.S.R.

Submitted to JETP editor March 8, 1957

J. Exptl. Theoret. Phys. (U.S.S.R.) **33**, 710-722 (September, 1957)

The equilibrium conditions for bounded systems of a conducting gas in a magnetic field are investigated. We have obtained the equilibrium conditions for a thin ring with a helical current (a) taking into account gravitational forces; (b) assuming the ring to be surrounded by gas; and (c) in an external magnetic field. We have formulated a theorem about the correspondence between magnetohydrodynamical equilibrium systems and hydrodynamical vortices. Using this theorem we reduce the problem of the equilibrium conditions for magnetohydrodynamical configurations to the theory of stationary flow of an incompressible fluid. We consider, for the case of axial symmetry, general equilibrium conditions for distributed currents.

INTRODUCTION

In recent years there have appeared a number of papers [1-9] investigating the equilibrium conditions and the stability of equilibrium configurations of currents in a conducting medium. The interest in these problems is partly due to attempts to explain the existence of magnetic fields in cosmic space, the magnetism of stars, and of the earth, and partly because of experimental investigations of high-current gas discharges. The current configurations investigated in the papers mentioned had axial symmetry and were unbounded along the axis of symmetry. Such systems are idealizations of real systems, except for the case where they are bounded at the ends (for instance, by electrodes in the case of gas discharges). It is therefore undoubtedly of interest to find the equilibrium conditions of bounded configurations occurring under the influence of electrodynamic forces. Recently Bostick[10] has found experimentally plasma equilibrium configurations, which he calls plasmoids, for which magnetic fields are apparently essential. Apart from the possible applications mentioned above, an investigation of such configurations may be of interest for the theory of ball lightning. In this case one often makes the natural assumption[11] that ball lightning is a closed current produced at the moment of the thunder discharge. If we forget for a moment the problem of the source of energy of ball lightning,[12] then the question whether or not the above hypothesis is possible depends on whether such a dynamic stable configuration can exist.

In the present paper we obtain the equilibrium conditions for a few systems described by the magnetohydrodynamical equations

$$-\nabla p+\frac{1}{c}[\mathbf{j}\times\mathbf{H}]+\rho\nabla\Phi=0,\quad \operatorname{curl}\mathbf{H}=\frac{4\pi}{c}\mathbf{j},\quad \nabla^2\Phi=-4\pi G\rho,\quad \operatorname{div}\mathbf{H}=0. \tag{1}$$

In these equations ρ and p are the density and pressure of the conducting gas, Φ the gravitational potential, G the gravitational constant, and $\mathbf{j}$ and $\mathbf{H}$ the current density and the magnetic field. These equations have been investigated before by a number of authors.[4-8] Lüst and Schlüter[5] obtained a bounded configuration in weak fields ($\mathbf{j}\times\mathbf{H}=0$). Prendergast[8] found a solution for the case where the whole of the magnetic field was concentrated inside a gravitating sphere.

Some general considerations about the necessary conditions for a stable equilibrium can be obtained from the virial theorem given by Chandrasekhar and Fermi[2] for the case of a magnetohydrodynamical system. This theorem has the following form for the case of a closed system in equilibrium,

$$3(\gamma-1)U+\mathfrak{M}+\Omega=0,\quad U=\frac{1}{\gamma-1}\int_V p\,d\mathbf{r},\quad \Omega=-\frac{1}{2}\int\rho\Phi\,d\mathbf{r},\quad \mathfrak{M}=\int\frac{H^2}{8\pi}\,d\mathbf{r}. \tag{2}$$

where U is the internal energy of the gas, $\mathfrak{M}$ the energy of the magnetic field, and Ω the gravitational energy.

If $\Omega=0$ there is no equilibrium possible of a closed system. For an open system and $\Omega=0$ one can

easily obtain instead of (2)

$$\int_V \left(3p + \frac{H^2}{8\pi}\right) d\mathbf{r} = \oint \left\{ \left(p + \frac{H^2}{8\pi}\right) \mathbf{r} - \frac{1}{4\pi} (\mathbf{rH})\, \mathbf{H} \right\} d\mathbf{s}. \tag{3}$$

Let the current be concentrated in a restricted region of space. Choosing the volume of integration sufficiently large we get from (3)

$$\int_V \left(3p + \frac{H^2}{8\pi}\right) d\mathbf{r} = \oint p\mathbf{r}\, d\mathbf{s} = 3p_e V. \tag{4}$$

It is therefore obvious that an equilibrium is possible provided that the external pressure p_e exceeds the average pressure in the configuration.

For $\Omega = 0$ and $p_e = 0$ equilibrium is only possible in an external magnetic field. In that case, the surface integral in (3) does not go to zero. If, for instance, the field is uniform at infinity and equal to H_0, we have

$$\int \left(3p + \frac{H^2}{8\pi}\right) d\mathbf{r} = \frac{H_0^2}{8\pi} V. \tag{5}$$

The gas pressure and the pressure due to the magnetic field in the configuration can thus be balanced in the following three cases: (a) gravitational attraction, (b) pressure of an external gas, and (c) pressure of an external magnetic field.

Corresponding to this we shall obtain in Secs. 1 to 3 three cases of the simplest possible bounded equilibrium configurations, all of the form of a thin ring. Of special interest is the ring with a current maintained in equilibrium by the pressure of an external gas (Sec. 2) since such systems are apparently stable.

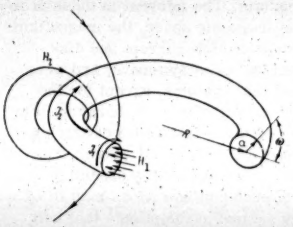

FIG. 1

In Sec. 4 it is shown that equilibrium configurations correspond to hydrodynamical vortices. Based on this analogy we give an example of a spherical configuration. In Sec. 5 we obtain the equations describing the equilibrium conditions for axially symmetric configurations.

1. GRAVITATING RING WITH CURRENT

Let us consider the equilibrium condition for a ring of a perfect gas under the following assumptions. The large radius of the ring R is considerably larger than its small radius a ($R \gg a$) (see Fig. 1). The gas density is constant along a cross section and the electric conductivity is infinite. Along the ring there is a helical surface current producing inside the ring a magnetic field,

$$\mathbf{H}_1 = \{0,\ H_\varphi,\ 0\} \tag{6}$$

and outside the ring a field

$$\mathbf{H}_2 = \{H_r,\ 0,\ H_z\}. \tag{7}$$

The field $\mathbf{H}_1$ is related to the current I_1 flowing a round the axis of the ring,

$$H_\varphi = 2I_1 / cr. \tag{8}$$

and $\mathbf{H}_2$ is related to the axial current I_2 (see Fig. 1). The fields $\mathbf{H}_1$ and $\mathbf{H}_2$ are obviously mutually orthogonal.

The equations describing the behavior of the ring can be obtained from the Lagrangian

$$L = T(R,\ a) + \mathfrak{M}(R,\ a,\ I_1,\ I_2) - \Psi(V,\ T) - \Omega(R,\ a). \tag{9}$$

where T is the kinetic energy; if the density is constant, we have

$$T = \frac{1}{2} \int_V \rho v^2 d\mathbf{r} = \frac{M}{2} \left(\dot{R}^2 + \frac{\dot{a}^2}{2}\right), \tag{10}$$

and $\mathfrak{M}$ is the potential function of the currents taken with the opposite sign and is equal to the energy of the magnetic field. Since the fields H_1 and H_2 are orthogonal, $\mathfrak{M}$ will be equal to the sum of the energies of these fields,

$$\mathfrak{M} = (1/2c^2)(L_1 I_1^2 + L_2 I_2^2), \tag{11}$$

where L_1 and L_2 are the coefficients of self-induction of the corresponding currents,

$$L_1 = 4\pi(R - \sqrt{R^2 - a^2}) \approx \frac{2\pi a^2}{R}, \quad L_2 = 4\pi R\left(\ln\frac{8R}{a} - 2\right). \tag{12}$$

The third term in the Lagrangian,

$$\Psi(V, T) = -NT \ln VT^{1/(\gamma-1)} \tag{13}$$

is the free energy of a perfect gas, N is the total number of particles, $V = 2\pi^2 R a^2$ is the volume of the ring, and T the temperature in energy units. Finally

$$\Omega(R, a) = -(GM^2/2\pi R)[\ln(8R/a) + {}^1/_4] \tag{14}$$

is the gravitational energy of the ring and M its mass. We have, corresponding to the Lagrangian (9) the generalized velocities and coordinates

$$\dot{q} = \dot{a}, \ \dot{R}, \ I_1, \ I_2, \ T; \quad q = a, \ R. \tag{15}$$

We must consider I_1, I_2, and T as cyclic velocities (see Ref. 13 for the possibility of considering T as a cyclic velocity).

The first two Lagrangian equations ($\dot{q} = \dot{a}, \dot{R}$) determine the rate of change of the two radii of the ring,

$$M\ddot{R} = F_R, \ {}^1/_2 M\ddot{a} = F_a. \tag{16}$$

The second and third equations ($\dot{q} = I_1, I_2$) give, as long as the ring is supposed to be perfectly conducting, the conservation law of the flux of magnetic induction,

$$L_1 I_1 = \text{const}, \quad L_2 I_2 = \text{const}. \tag{17}$$

The fourth equation ($\dot{q} = T$) is the adiabatic equation

$$T = \text{const}\, V^{-(\gamma-1)}. \tag{18}$$

Assuming the form of the ring to be invariant we find for the condition that the equilibrium is stable,

$$F_q = (\partial L/\partial q)_{\dot{q}} = 0, \quad \partial F_q/\partial q < 0 \quad (q = a, \ R). \tag{19}$$

The motion in the neighborhood of the equilibrium position is according to (16) and (19) determined by the formulae

$$(\ddot{\delta a}) + \omega_a^2(\delta a) = 0, \quad (\ddot{\delta R}) + \omega_R^2(\delta R) = 0, \tag{20}$$

where δa and δR are the deviations from the equilibrium values of the radii and ω_a^2 and ω_R^2 the frequencies of the radial oscillations,

$$\omega_a^2 = -\frac{2}{M}\left(\frac{\partial F_a}{\partial a}\right); \quad \omega_R^2 = -\frac{1}{M}\left(\frac{\partial F_R}{\partial R}\right). \tag{21}$$

Using (17) and (18) one can easily show that $F_q = -\partial W/\partial q$, where

$$W = \frac{NT}{\gamma - 1} + \frac{1}{2c^2}(L_1 I_1^2 + L_2 I_2^2) - \frac{GM^2}{2\pi R}\left(\ln\frac{8R}{a} + \frac{1}{4}\right) \tag{22}$$

is the total energy of the ring at rest. Thus the condition that the equilibrium be stable corresponds to asking for a minimum of the total energy W, as might have been expected.

We write down the expressions for the forces,

$$F_a = \frac{\partial L}{\partial a} = \frac{2\pi I_1^2}{c^2}\frac{a}{R} - \frac{2\pi I_2^2}{c^2}\frac{R}{a} - \frac{GM^2}{2\pi R a} + \frac{2NT}{a}, \quad F_R = \frac{\partial L}{\partial R} = -\frac{\pi I_1^2}{c^2}\frac{a^2}{R^2} + \frac{2\pi I_2^2}{c^2}\left(\ln\frac{8R}{a} - 1\right) - \frac{GM^2}{2\pi R^2}\left(\ln\frac{8R}{a} - \frac{3}{4}\right) + \frac{NT}{R}. \tag{23}$$

Assuming $F_a = F_R = 0$ we find the following relations which determine the equilibrium conditions

$$H_{10}^2 = 2H_G^2\left(\ln\frac{8R}{a} - \frac{7}{8}\right)\Big/\left(\ln\frac{8R}{a} - \frac{3}{2}\right) - 8\pi p_i\left(\ln\frac{8R}{a} - \frac{1}{2}\right)\Big/\left(\ln\frac{8R}{a} - \frac{3}{2}\right),$$

$$H_{20}^2 = H_G^2\left(\ln\frac{8R}{a} - \frac{1}{4}\right)\Big/\left(\ln\frac{8R}{a} - \frac{3}{2}\right) - 8\pi p_i\Big/\left(\ln\frac{8R}{a} - \frac{3}{2}\right). \qquad (24)$$

We have here introduced the notation

$$H_{10} = 2I_1/cR, \quad H_{20} = 2I_2/ca; \quad H_G^2 = GM^2/\pi^2R^2a^2, \quad p_i = NT/V. \qquad (25)$$

The virial theorem (2) can be obtained from (24) by multiplying the first equation of (24) by $V/8\pi$, the second by $(V/4\pi)$ $[\ln(8R/a) - 2]$, and adding them together. One can easily ascertain that the necessary conditions for the stability of the equilibrium, $\partial F_a/\partial a < 0$, $\partial F_R/\partial R < 0$ (stability of the equilibrium values of R and a under the condition that the form of the ring is kept invariant) are satisfied.

We can obtain the considerations regarding the stability of the ring form from the calculations of the stability of a straight cylinder (see Appendix). In the case where the whole of the current flows along the surface of the cylinder, an internal magnetic field, directed along the axis, will help the stabilizing action on the perturbed form of the cylinder. The most "dangerous" perturbations are of the form $\cos(2\pi z/\lambda)$ and $\cos(2\pi z/\lambda - \varphi)$, where z is the coordinate along the axis of the cylinder, φ the azimuthal angle, and λ the wave length of the perturbation. The instability of the first kind, "wriggling," is produced, on the whole, by the tendency of a gravitating mass to take on spherical form; the instability of the second kind (a winding cylinder) is connected with the instability of a straight current. If $2\pi a/\lambda \ll 1$ the stability criterion has the form (Eq. (14) of the Appendix)

$$1)\ H_{10}^2 > \frac{H_{20}^2}{2} + 2H_G^2\left(\ln\frac{\lambda}{\pi a} - C - \frac{1}{2}\right), \quad 2)\ H_{10}^2 > H_{20}^2\left(\ln\frac{\lambda}{\pi a} - C\right) - H_G^2\left(\ln\frac{\lambda}{\pi a} - C + \frac{1}{4}\right), \qquad (26)$$

with C = 0.577.

From Eq. (24) it is clear that $H_{10}^2 \lesssim 2H_G^2$, $H_{10}^2 \lesssim 2H_{20}^2$. Consequently the first inequality can not be satisfied for wavelengths $\lambda \gg 2\pi a$. A gravitating equilibrium ring is thus unstable against a perturbation of the form $\cos(2\pi z/\lambda)$ (wriggling).

2. RING WITH CURRENT IN A GAS

Let us now consider a ring with current embedded in a gaseous atmosphere, the pressure of which exceeds the gas pressure inside the ring by an amount p_e. This excess pressure together with the pressure due to the external magnetic field H_2 balances the pressure of the internal axial field H_1. As in the previous section we consider an idealized situation where the current flows in an infinitely thin surface layer of the ring. In this case the magnetic field exerts a normal pressure on the surface and the condition that the forces on the surface (s) of the ring are in equilibrium is

$$H_1^2|_s = H_2^2|_s + 8\pi p_e|_s, \qquad (27)$$

where according to (8) $H_1 = 2I_1/cr$.

Condition (27) must be used to determine the form of the cross section of the equilibrium configuration. For a thin ring this cross section is a circle with $r|_s = R + a\cos\omega$ and

$$H_1^2|_s = H_{10}^2\left(1 - 2\frac{a}{R}\cos\omega\right). \qquad (28)$$

The distribution of the magnetic field due to an axial current can be obtained from the paper by Fock[14] in which he studies the skin-effect in a torus. For $R \gg a$ the surface current density is distributed as follows

$$j_\varphi = \text{const}\left\{1 - \frac{a}{R}\left(\ln\frac{8R}{a} - \frac{1}{2}\right)\cos\omega\right\}.$$

Consequently,

$$H_2^2|_s = H_{20}^2\left\{1 - 2\frac{a}{R}\left(\ln\frac{8R}{a} - \frac{1}{2}\right)\cos\omega\right\}. \qquad (29)$$

If we now substitute (28) and (29) into (27) and compare terms independent of ω, and terms in $\cos\omega$ we obtain

$$H_{10}^2 = H_{20}^2 + 8\pi p_e, \quad H_{20}^2 = 8\pi p_e \Big/ \left(\ln\frac{8R}{a} - \frac{3}{2}\right)$$

or

$$H_{10}^2 = H_{20}^2\left(\ln\frac{8R}{a} - \frac{1}{2}\right), \quad H_{10}^2 = 8\pi p_e\left(\ln\frac{8R}{a} - \frac{1}{2}\right) \Big/ \left(\ln\frac{8R}{a} - \frac{3}{2}\right). \tag{30}$$

It is true that this equilibrium condition can also be obtained from (24) if put there G = 0 and take it into account that for p_i we must take the difference between the internal and external pressure, which now is negative, $p_i = -pe < 0$.

For p_e = constant we find from (23) and (17)

$$\frac{\partial F_a}{\partial a} = -\frac{2\pi I_2^2}{c^2 a^2} R\left[2\ln\frac{8R}{a} - 2 + \left(\ln\frac{8R}{a} - 2\right)^{-1}\right], \quad \frac{\partial F_R}{\partial R} = -\frac{2\pi I_1^2}{c^2 R}\left[2\ln\frac{8R}{a} - 1 + 2\left(\ln\frac{8R}{a} - 2\right)^{-1}\right]. \tag{31}$$

Since $\partial F_a/\partial a < 0$ and $\partial F_R/\partial R < 0$ the equilibrium is stable with respect to changes in R and a. The criterion for stability with respect to a change in form, obtained for a homogeneous cylinder, has the form (see Eq. (14) of the Appendix)

$$H_{10}^2 > H_{20}^2\left(\ln\frac{\lambda}{\pi a} - C\right).$$

According to the equilibrium condition (30)

$$H_{10}^2 = H_{20}^2\left(\ln\frac{8R}{a} - \frac{1}{2}\right).$$

Assuming that the wavelength of the perturbation has its maximum value possible in the ring, $\lambda = \pi R$, we see that the criterion for stability is satisfied.

We see thus that the configurations of magnetic fields which produce a helical current flowing along the surface of the ring and in which the external gas pressure is maintained are very probably stable configurations. This conclusion should be verified by a direct calculation of the stability of the ring. Whether such a ring could be observed in an atmosphere of a non-conducting gas under laboratory conditions is an interesting problem. The external gas can be prevented from penetrating inside the ring by the ionized envelope along which the current flows. We write down the connection between the current necessary for equilibrium and the excess of the external pressure. Expressing H_{10} in terms of I_1 and H_{20} in terms of I_2 we get from Eq. (30)

$$\frac{I_2^2}{a^2} = I_1^2 \Big/ R^2\left(\ln\frac{8R}{a} - \frac{1}{2}\right) = 2\pi p_e c^2 \Big/ \left(\ln\frac{8R}{a} - \frac{3}{2}\right). \tag{32}$$

If the currents are expressed in amperes and the pressure in atmospheres, and if to be specific we put under the logarithm sign R/a = 10, we have

$$I_2/a = I_1/2R = 15\cdot 10^3 p_e. \tag{33}$$

For instance, if a ~ 1 cm, and $p_e \sim 1$ atmos the current must be of the order of tens of thousands of amperes.

The period during which such a ring will exist unsupported from without will be determined by the time in which the originally produced current will die away due to the collisions of the electrons with ions and atoms. If collisions with ions are the determining factor, this relaxation time does not depend on the gas or its dimensions, but is determined by the magnitude of the conductivity $\sigma = e^2 n\tau/m$ [$n\tau \approx 0.1\,(mv^2/e^2)^2$] and is given by the equation

$$t_\sigma = 4\pi\sigma a^2/c^2 \approx 10\, a^2 (v/c)^3.$$

Let, for instance a ~ 1 cm and the electron velocity be $v \sim 10^{-2}$ c (such a velocity is normal for discharges with a current strength I ~ 10^4 amp); in that case $t_\sigma \sim 10\,\mu$ sec. The time of diffusion of the external gas into the current channel $t_D \sim a^2/D$ (D is the diffusion coefficient; for air under normal conditions D ~ 0.1) is larger than the relaxation time of the current right up to pressures $p \approx 0.001$ atmos and consequently can be neglected.

3. RING CURRENT IN AN EXTERNAL MAGNETIC FIELD

We shall assume that the ring with an axial current I_2 is located in a homogeneous magnetic field H_0 which is perpendicular to the plane of the ring. We can obtain expressions for the forces F_a and F_R from (23), if we assume there that $I_1 = 0$ and $G = 0$, and add in F_R the term corresponding to the Lorentz force $c^{-1} I_2 H_0 2\pi R$,

$$F_a = -\frac{2\pi I_2^2}{c^2}\frac{R}{a} + \frac{2NT}{a}, \qquad F_R = \frac{I_2^2}{2c^2}\frac{\partial L_2}{\partial R} + \frac{NT}{R} + \frac{1}{c} I_2 H_0 2\pi R. \tag{34}$$

From the condition $F_a = 0$ we get the well-known formula for the pinch effect,

$$I_2^2 = 2c^2 NT / 2\pi R. \tag{35}$$

Expressing in NT the equation $F_R = 0$ in terms of I_2^2 we find the magnitude of the magnetic field supporting the equilibrium current I_2 flowing in a ring of radius R,

$$H_0 = -\frac{I_2}{cR}\left(\frac{1}{4\pi}\frac{\partial L_2}{\partial R} + \frac{1}{2}\right). \tag{36}$$

If there is a strong skin effect, $L_2 = 4\pi R\,[\ln(8R/a) - 2]$ and consequently

$$H_0 = -\frac{I_2}{cR}\left(\ln\frac{8R}{a} - \frac{1}{2}\right). \tag{37}$$

If the current density is constant over a cross section, $L_2 = 4\pi R\,[\ln(8R/a) - 7/4]$ and

$$H_0 = -\frac{I_2}{cR}\left(\ln\frac{8R}{a} - \frac{1}{4}\right). \tag{38}$$

One can easily obtain Eq. (37) from the requirement that in equilibrium the value of the magnetic field on the surface of a perfectly conducting ring must be constant over a cross section. According to (29) the field due to the current is on the surface equal to

$$H_2 = H_{20}\left\{1 - \frac{a}{R}\left(\ln\frac{8R}{a} - \frac{1}{2}\right)\cos\omega\right\}.$$

The distribution of the external field for the case $R \gg a$ is determined in the same way as in the case of a perfectly conducting cylinder located in a homogeneous field

$$H = \nabla\varphi, \quad \varphi = aH_0\left(\frac{\rho}{a} + \frac{a}{\rho}\right)\sin\omega$$

where ρ is the polar radius and ω the azimuthal angle. Hence we have

$$H_\omega\Big|_{\rho=a} = \frac{1}{\rho}\frac{\partial\varphi}{\partial\omega}\Big|_{\rho=a} = 2H_0\cos\omega.$$

Consequently the total field on the surface of the ring is equal to

$$H_{20} + 2\left\{H_0 - \frac{H_{20}}{2}\frac{a}{R}\left(\ln\frac{8R}{a} - \frac{1}{2}\right)\right\}\cos\omega.$$

Putting the factor in front of cos ω equal to zero we obtain condition (37).

A simple calculation of the derivatives of F_a and F_R leads to

$$\frac{\partial F_a}{\partial a} = -\frac{4\pi I_2^2}{c^2}\frac{R}{a}\left(\gamma - 1 + \frac{4\pi R}{L_2}\right), \quad \frac{\partial F_R}{\partial R} = \frac{2\pi I_2 H}{c}\left\{\frac{3}{2} - \left[(5-2\gamma)\frac{2\pi R}{L_2} - 1\right]\Big/\frac{4\pi R}{L_2}\left(3 + \frac{2\pi R}{L_2}\right)\right\}. \tag{39}$$

Since both derivatives are negative the equilibrium is stable with respect to a change in R or a.

As we shall show in the next section, a ring current in a magnetic field has an interesting counterpart in hydrodynamics, namely the well known smoke rings.

4. HYDRODYNAMICAL ANALOGY OF EQUILIBRIUM CONFIGURATIONS

The theory of the equilibrium of magnetohydrodynamical systems shows an interesting analogy with the theory of hydrodynamical vortices in an incompressible fluid. This analogy can be formulated in the form of the following theorem: the magnetic field and current density in an equilibrium magnetohydrodynamical

configuration are respectively (expressed in suitably defined units) identical with the velocity field of a hydrodynamical vortex which is at rest and the vorticity in the system itself. If there are gravitational forces present the applicability of the analogy is limited by the requirement that the density in the configuration be uniform. The proof of this theorem follows from comparison of the equations describing the kinematics of a vortex with the magnetohydrostatical equations. We have written these last equations below in rationalized electro-magnetic units in order to let the analogy be more complete; one may assume that the gravitational terms are included in p:

Equations for the kinematics of a vortex	Magnetohydrostatic equations
$\operatorname{div} \mathbf{v} = 0$	$\operatorname{div} \mathbf{H} = 0$
$\operatorname{curl} \mathbf{v} = \boldsymbol{\Omega}$	$\operatorname{curl} \mathbf{H} = \mathbf{j}$
$[\boldsymbol{\Omega} \times \mathbf{v}] = -\nabla (p/\rho + v^2/2)$	$[\mathbf{j} \times \mathbf{H}] = \nabla p$

It is clear that the first two equations for $\mathbf{v}$ and $\boldsymbol{\Omega}$ on the one side, and for $\mathbf{H}$ and $\mathbf{j}$ on the other side are identical. The last equations impose on these quantities the identical conditions $\operatorname{curl} [\boldsymbol{\Omega} \times \mathbf{v}] = 0$ and $\operatorname{curl} [\mathbf{j} \times \mathbf{H}] = 0$. The boundary conditions for $\mathbf{v}$ and $\mathbf{H}$ are also identical. Consequently the distributions of $\mathbf{v}$ and $\mathbf{H}$ will be identical.

The functions $p/\rho + v^2/2$ on the one side and p on the other side, the gradients of which are determined from the last equations, may be different from zero. The analogy established a moment ago is, of course, not extended to the dynamics of a system described by equations which are no longer identical. In particular, conclusions about the stability of the one system can not be transferred to its analogue. For instance, it is well known that the plasma string with a current ("pinch effect") is unstable. The corresponding analogue — a single vortex filament in a fluid — is a stable system.

The fact that there exists this identity between the distributions of the velocity field of a vortex and of the magnetic field of a magnetohydrodynamical configuration makes it possible to transfer methods and results of investigations in the one field to the other field. For instance, from the point of view of looking for the analogue, a ring current in a magnetic field corresponds to a circular vorticity differing from zero in a ring of large radius R and small radius a. It is well known that the kinematical condition for the existence of such a vortex is the motion of the vortex ring along its axis of symmetry. According to our theorem the velocity of the current flowing along a ring, in the frame of reference in which this is at rest, corresponds to an external magnetic field maintained in equilibrium by the ring current. Knowing the magnitude of this field we can thus immediately write down also an expression for the velocity of the vortex ring motion in a non-conducting gas which will be equal to the velocity of the gas current in the ring, but with opposite sign. Introducing the intensity of vorticity $\varkappa = \int \Omega ds$ corresponding to the strength of the current, and going over to absolute rationalized electromagnetic units we obtain from (38) the velocity of the vortex ring for the case where the vorticity is constant along a cross section (see Ref. 15 p. 241)

$$v = \frac{\varkappa}{4\pi R}\left(\ln \frac{8R}{a} - \frac{1}{4}\right). \tag{41}$$

We investigated in Secs. 1 to 3 systems with a surface current; these correspond in hydrodynamics to stationary currents of an incompressible fluid with a surface where the tangential velocoty is discontinous.

Using the hydrodynamical analogy we can find a number of examples of magnetohydrodynamical equilibrium configurations with a distributed current. Thus, for instance, corresponding to the well known spherical vortex of Hill's (Ref. 15, p. 245) in hydrodynamics, we have an equilibrium configuration, which might be called a spherical plasmoid, consisting of a conducting gas inside a sphere $r \leq a$ in an external field H_0 directed along the z-axis. We give here this solution in spherical coordinates (r, ϑ, φ):

$r \leqslant a$	$r > a$
$p = \frac{45}{32\pi} H_0^2 \frac{r^2}{a^2}\left(1 - \frac{r^2}{a^2}\right)\sin^2\vartheta$	$p = 0$
$j_\varphi = \frac{15}{8}\frac{cH_0}{\pi a^2} r \sin\vartheta$	$j_\varphi = 0$
$H_r = -\frac{3}{2} H_0\left(1 - \frac{r^2}{a^2}\right)\cos\vartheta$	$H_r = H_0\left(1 - \frac{a^3}{r^3}\right)\cos\vartheta$
$H_\vartheta = -3 H_0\left(\frac{r^2}{a^2} - \frac{1}{2}\right)\sin\vartheta$	$H_\vartheta = -H_0\left(1 + \frac{a^3}{2r^3}\right)\sin\vartheta.$

(42)

One can also easily obtain the analogous spheroidal configuration. We note that Lundquist[1] and Chandrasekhar and Prendergast[7] also mentioned the analogy between a stationary flow of a fluid with a vorticity different from zero and a stationary magnetic field. However, in those papers the details of this correspondence were not established.

5. GENERAL EQUILIBRIUM CONDITIONS FOR AN AXIALLY SYMMETRIC SYSTEM

We must note that in the considerations of Secs. 2 to 4 of the simplest bounded equilibrium configurations which had the form of thin rings we assumed that they did not depend strongly on the distribution of the current over the cross section. However, they correspond to only one of the limiting cases of a more general kind of configuration which has the form of a toroid with a non-circular cross section and with arbitrary relations between the linear dimensions. Other limiting cases of such configurations are the configurations of the kind of spherical (or spheroidal) plasmoids. It is of interest to discuss general conditions for the existence of such equilibrium configurations.

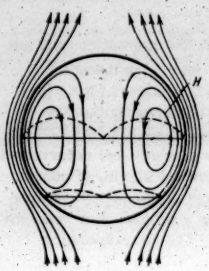

FIG. 2

We suppose that gravitational effects can be neglected (or, if it is necessary to take them into account that the gas can be considered to be incompressible). In that case we need obviously not write down the term $\rho\Phi$ and may assume it to be included in p. Using the analogy developed in the previous section we take over into the theory of equilibrium of magnetohydrodynamical configurations (magnetohydrostatics) the hydrodynamical theory of the stationary motion of an incompressible fluid. We shall consider the equilibrium conditions for axially symmetric magnetohydrodynamical configurations. In that case the set of equations describing the equilibrium conditions can be condensed into one equation according to the following scheme. We introduce the functions

$$\psi = \int_0^r H_z \cdot 2\pi r dr, \quad I = \int_0^r j_z \cdot 2\pi r dr = \frac{cr}{2} H_\varphi, \tag{43}$$

in terms of which the r- and z-components of the field and the current are expressed. The surfaces of constant ψ and of constant I are the surfaces corresponding to the magnetic lines of force and the current lines. From the equilibrium condition $-\nabla p + [\mathbf{j} \times \mathbf{H}]/c = 0$ it follows that each of these surfaces coincides with a surface of constant pressure, that is, $p = p(\psi)$, $I = I(\psi)$. From the equilibrium condition which is not used we can determine the current density component j_φ as a function of ψ and r. Finally, the equation $\partial H_r/\partial z - \partial H_z/\partial r = 4\pi j_\varphi/c$ gives us the relation we are looking for. All this can conveniently be collected in the following table,

$$\operatorname{div} \mathbf{H} = 0 \qquad \frac{1}{r}\frac{\partial (rH_r)}{\partial r} + \frac{\partial H_z}{\partial z} = 0 \qquad \begin{matrix} H_z = \frac{1}{2\pi r}\frac{\partial \psi}{\partial r} \\ H_r = -\frac{1}{2\pi r}\frac{\partial \psi}{\partial z} \end{matrix} \tag{44}$$

$$(\operatorname{curl} \mathbf{H})_{r,\,z} = \frac{4\pi}{c} j_{r,\,z} \qquad \begin{matrix} \frac{1}{r}\frac{\partial (rH_\varphi)}{\partial r} = \frac{4\pi}{c} j_z \\ -\frac{\partial H_\varphi}{\partial z} = \frac{4\pi}{c} j_r \end{matrix} \qquad \begin{matrix} j_z = \frac{1}{2\pi r}\frac{\partial I}{\partial r} \\ j_r = -\frac{1}{2\pi r}\frac{\partial I}{\partial z} \end{matrix} \tag{45}$$

$$-\nabla p + \frac{1}{c}[\mathbf{j} \times \mathbf{H}] = 0 \qquad (\mathbf{H}\nabla p) = 0, \quad (\mathbf{j}\nabla p) = 0 \qquad p = p(\psi),\ I = I(\psi) \tag{46}$$

$$-\frac{\partial p}{\partial r} + \frac{1}{c}(j_z H_z - j_z H_\varphi) = 0 \qquad r j_\varphi d\psi = \frac{1}{c} dI^2 + 2\pi c r^2 dp \tag{47}$$

$$(\operatorname{curl} \mathbf{H})_\varphi = \frac{4\pi}{c} j_\varphi \qquad \frac{\partial H_r}{\partial z} - \frac{\partial H_z}{\partial r} = \frac{4\pi}{c} j_\varphi \qquad \frac{\partial^2 \psi}{\partial z^2} + \frac{\partial^2 \psi}{\partial r^2} - \frac{1}{r}\frac{\partial \psi}{\partial r} = -\frac{8\pi^2}{c^2} r j_\varphi = -\frac{16\pi^2}{c^2} I(\psi)\frac{dI(\psi)}{d\psi} - 16\pi^2 r^2 \frac{dp(\psi)}{d\psi} \tag{48}$$

Equation (48), which contains two arbitrary functions, gives us the equilibrium condition. This equation is essentially an extension into magnetohydrostatics of the condition for a stationary flow of an incompressible fluid which has been investigated before (Lamb[15]). It was obtained, in slightly different form, by Chandrasekhar and Prendergast who instead of the functions ψ and I (the meaning of which is respectively the induction flux and the current through a circular cross section of radius r at z = constant)

introduced the functions p and T which are connected with ψ and I by relations $p = \psi/2\pi r^2$, $T = 2I/cr^2$. If these functions are introduced the meanings of the different terms of the equation are no longer clear.

Let us note a few consequences of the equations we just obtained.

From Eq. (47) for j_φ it follows that, (1) if $j_\varphi = 0$ the functions I and p do not depend on z. Consequently if there is no gravitation a bounded equilibrium configuration can exist only if there is an azimuthal current present; it also follows that, (2) if $j_\varphi = \text{const}/r$ a bounded configuration can exist only if $p = \text{const}$ (weak fields), and that, (3) if $j_\varphi = \text{const}\cdot r$ the solution depending on z exists only if $I = \text{const}$, i.e., if $H_\varphi = \text{const}/r$. In particular, solution (42) corresponding to Hill's vortex is obtained in the case where $I = 0$.

In conclusion I should like to express my gratitude to Academician M. A. Leontovich for discussing this paper with me and for a number of helpful suggestions.

APPENDIX

Criteria for the Stability of an Perfectly Conducting Cylinder with a Surface Current

We investigate the stability of a homogeneous perfectly-conducting cylinder (a) taking gravitation into account, and (b) in the presence of external pressure. The program of investigation is the same as in Ref. 9 where these effects were not taken into account. Let there be imposed on the cylinder a perturbation of the form $\exp\{i(kz + m\omega) + \Omega t)\}$. An arbitrary perturbation can be represented in the form of a superposition a such perturbations with different values of k and m ($m = 0, \pm 1, \pm 2, \ldots$). For given values of k and m the equations of motion together with the boundary conditions will determine the corresponding eigenvalue Ω^2.

If we are only interested in the stability criterion we can simplify our considerations by assuming the gas to be incompressible. Indeed, the boundary of the unstable region lies at the value $\Omega^2 = 0$. This value of Ω^2 corresponds to a stationary perturbation when the compressibility of the gas does not play a role.

(a) Gravitating cylinder. The original magnetohydrodynamical equations have the form

$$\rho \frac{d\mathbf{v}}{dt} = -\nabla\left(p - \rho\Phi + \frac{H^2}{8\pi}\right) + \frac{1}{4\pi}(\mathbf{H}\nabla)\mathbf{H}, \quad \partial\mathbf{H}/\partial t = \operatorname{curl}[\mathbf{v}\times\mathbf{H}], \quad \operatorname{div}\mathbf{v} = 0, \quad \nabla^2\Phi = -4\pi G\rho. \tag{1}$$

We give the values of the different variables in the unperturbed state:

Inside the cylinder	Outside the cylinder
$\rho = \text{const}$	$\rho = 0$
$H_\omega = 0$	$H_\omega = H_{20}a/r$
$H_z = H_{10} = \text{const}$	$H_z = 0$
$\Phi_i = -\pi G\rho r^2$	$\Phi_e = -2\pi G\rho a^2 \ln r + \text{const}$
$p = p_0 - \pi G\rho^2 r^2$	$p = 0$

(2)

After linearization equations (1) have the form

$$\rho\Omega^2\boldsymbol{\xi} = -\nabla\left(p^{(1)} + \frac{H_z^{(1)}H_{10}}{4\pi} - \rho\Phi^{(1)}\right) + \frac{1}{4\pi}(\mathbf{H}_0\nabla)\mathbf{H}^{(1)}, \quad \mathbf{H}^{(1)} = \operatorname{curl}[\boldsymbol{\xi}\times\mathbf{H}_0] = (\mathbf{H}_0\nabla)\boldsymbol{\xi} = ikH_{10}\boldsymbol{\xi}, \quad \operatorname{div}\boldsymbol{\xi} = 0, \quad \nabla^2\Phi^{(1)} = 0. \tag{3}$$

where $\boldsymbol{\xi} = \mathbf{v}/\Omega = \boldsymbol{\xi}(\mathbf{r})\exp\{i(kz + m\omega) + \Omega t\}$ is the displacement vector of the gas particles, and $p^{(1)}$ and $\mathbf{H}^{(1)}$ are the perturbation-induced deviations of the pressure and magnetic field from their equilibrium values. Eliminating $\mathbf{H}^{(1)}$ and introducing the notation $\tilde{p} = p^{(1)} + H_{10}H_z^{(1)}/4\pi$ we can write this set of equations in the following form,

$$\rho(\Omega^2 + k^2H_{10}^2/4\pi)\boldsymbol{\xi} = -\nabla(\tilde{p} - \rho\Phi^{(1)}), \tag{4}$$

$$\nabla^2\Phi^{(1)} = 0; \quad \nabla^2\tilde{p} = 0. \tag{5}$$

The solution for $\tilde{p}$ which is bounded for $r = 0$ is of the form

$$\tilde{p} = \tilde{p}(a)\frac{I_m(kr)}{I_m(ka)}e^{i(kz+m\omega)+\Omega t}. \tag{6}$$

The boundary condition for $\tilde{p}$

$$\tilde{p}(a) + \xi_r(a)\frac{\partial p_0}{\partial r} = \frac{H_\omega^0 H_\omega^{(1)}}{4\pi} + \xi_r\frac{\partial}{\partial r}\left(\frac{H_{\omega 0}^2}{8\pi}\right) \tag{7}$$

differs from the boundary condition in Ref. 9 by the term $\xi_r \partial p_0/\partial r$. Using the results of Ref. 9 we get

$$\tilde{p}(a) = -\frac{\xi_r(a)}{4\pi}\left\{H_{20}^2 - \frac{m^2 H_{20}^2}{ka\{K_{m-1}(ka)/K_m(ka)\} + m} - 2H_G^2\right\}, \tag{8}$$

where

$$2H_G^2 = -4\pi\partial p_0(a)/\partial r = 8\pi^2 G\rho^2 a^2. \tag{9}$$

The solution of the equation $\nabla^2\Phi^{(1)} = 0$ inside and outside the cylinder can therefore be expressed by

$$\Phi_i^{(1)} = C_1 I_m(kr)\, e^{i(hz+m\omega)+\Omega t}; \quad \Phi_e^{(1)} = C_2 K_m(kr)\, e^{i(hz+m\omega)+\Omega t}. \tag{10}$$

The constants C_1 and C_2 are determined by the requirement that the potential and its derivative with respect to the normal must be continuous for $r = a + \xi_r$,

$$p_i^{(1)} + \xi_r \frac{\partial\Phi_{i0}}{\partial r} = \Phi_e^{(1)} + \xi_r \frac{\partial\Phi_{e0}}{\partial r}; \quad \frac{\partial\Phi_i^{(1)}}{\partial r} + \xi_r \frac{\partial^2\Phi_{i0}}{\partial r^2} = \frac{\partial\Phi_e^{(1)}}{\partial r} + \xi_r \frac{\partial^2\Phi_{e0}}{\partial r^2}. \tag{11}$$

We find thus

$$C_1 = 4\pi G\rho a K_m(ka)\,\xi_r(a); \quad C_2 = 4\pi G\rho a I_m(ka)\,\xi_r(a). \tag{12}$$

From Eqs. (6), (8), (10), and (12) we determine $\rho\Phi^{(1)} - \tilde{p}$ and substituting this result into (4) we get

$$\Omega^2 = \left\{\frac{c^2}{a^2}\left(1 - \frac{m^2}{|kaK_{m-1}(ka)/K_m(ka)| + m}\right) + \frac{4c_G^2}{a^2}\left(K_m(ka)I_m(ka) - \frac{1}{2}\right)\right\}\left(ka\frac{I_{m-1}(ka)}{I_m(ka)} - m\right) - k^2 c_H^2, \tag{13}$$

where

$$c^2 = H_{20}^2/4\pi\rho; \; c_G^2 = H_G^2/4\pi\rho; \; c_H^2 = H_{10}^2/4\pi\rho.$$

The stability condition $\Omega^2 < 0$ is for $c_G = 0$ identical with the criterion obtained in Ref. 9 for a compressible gas; for $c = 0$ and $m = 0$ it coincides with the result of the considerations of Chandrasekhar and Fermi,[2] obtained by a different method. For an infinite cylinder the criterion for stability can not be realized for $m = 0, 1$, $ka = 2\pi a/\lambda \to 0$, when it is of the form

$$H_{10}^2 > \frac{1}{2}H_{20}^2 + 2H_G^2\left(\ln\frac{\lambda}{\pi a} - C - \frac{1}{2}\right) \quad (m=0), \quad H_{10}^2 > H_{20}^2\left(\ln\frac{\lambda}{\pi a} - C\right) - H_G^2\left(\ln\frac{\lambda}{\pi a} - C + \frac{1}{4}\right) \quad (m=-1). \tag{14}$$

(b) Cylinder with external pressure. If the external gas is non-conducting the change in the previous arguments lies in the addition to the right hand side of Eq. (7) of a correction to the external pressure, $p_e^{(1)}$, determined from the equation $\Omega^2\xi = -\nabla p_e^{(1)}$, div $\xi = 0$. When $G = 0$ the dispersion relation is

$$\left(\rho_i\frac{\Omega^2}{k^2} + \frac{H_{10}^2}{4\pi}\right)\Big/\left(\frac{I_{m-1}(ka)}{kaI_m(ka)} - \frac{m}{(ka)^2}\right) + \rho_e\frac{\Omega^2}{k^2}\Big/\left(\frac{K_{m-1}(ka)}{kaK_m(ka)} + \frac{m}{(ka)^2}\right) = \frac{H_{20}^2}{4\pi}\left[1 - m^2\Big/\left(ka\frac{K_{m-1}(ka)}{K_m(ka)} + m\right)\right]. \tag{15}$$

The absolute value of Ω is reduced, but the stability criterion remains the same as for $\rho_e = 0$.

If the gas on the outside is perfectly conducting the calculation is slightly more complicated, but one can show that the stability criterion remains the same as before.

[1] S. Lundquist, Ark. f. Fys. **5**, 297 (1952).

[2] S. Chandrasekhar and E. Fermi, Astrophys. J. **118**, 116 (1953).

[3] M. Kruskal and M. Schwarzschild, Proc. Roy. Soc. **A223**, 348 (1954).

[4] V. C. A. Ferraro, Astrophys. J. **119**, 407 (1954).

[5] R. Lüst and A. Schlüter, Z. Astrophys. **34**, 263 (1954).

[6] S. Chandrasekhar, Proc. Nat. Acad. Sci. **42**, 1 (1956).

[7] S. Chandrasekhar and K. H. Prendergast, Proc. Nat. Acad. Sci. **42**, 5 (1956).

[8] K. H. Prendergast, Astophys. J. **123**, 498 (1956).

[9] V. D. Shafranov, Атомная энергия (Atomic Energy) **5**, 38 (1956).

[10] W. H. Bostick, Phys. Rev. **104**, 292 (1956); **104**, 1191 (1956).

[11] I. S. Stekol'nikov, Физика молнии и грозозащита (The Physics of Thunder and Lightning Protection) Moscow-Leningrad, 1943.

[12] P. L. Kapitza, Dokl. Akad. Nauk SSSR **101**, 245 (1955).

[13] H. Helmholtz, Vorlesungen über die Theorie der Wärme, Leipzig, 1922.

[14] V. A. Fock, Phys. Z. USSR **1**, 215 (1932).

[15] H. Lamb, Hydrodynamics, Cambridge University Press, 1932.

Translated by D. ter Haar
137

SOVIET PHYSICS JETP VOLUME 6 (33), NUMBER 3 MARCH, 1958

COLLECTIVE EXCITATIONS OF EVEN-EVEN NUCLEI

A. S. DAVYDOV and G. F. FILIPPOV

Moscow State University

Submitted to JETP editor March 8, 1957

J. Exptl. Theoret. Phys. (U.S.S.R.) 33, 723-729 (September, 1957)

Collective excitations of axially symmetric even-even nuclei are investigated. It is shown that such excitations can be divided into two classes: those which are accompanied by appreciable changes in the nuclear quadrupole moment, and those which are not. The energy of the collective oscillations is expressed in terms of two parameters.

In a paper of Scharff-Goldhaber and Weneser[1] it was pointed out that there is a large class of even-even nuclei in the mass number region $66 < A < 150$ for which the first excited state has spin 2^+ and excitation energy of 300 kev or more, while the second excited state has spin 2^+, 4^+, 0^+. The ratio of the energy of the second excited state to that of the first had a value between 2 and 2.5. This showed that these are not purely rotational states. Apparently in such nuclei an excited state cannot be rigorously assigned to pure rotation or vibration.

In the present paper, we investigate the collective excitations of axially-symmetric even-even nuclei, using the generalized nuclear model developed by A. Bohr.[2] We shall show that the collective excited states of such nuclei can be classified into two types: excitations which do not involve an appreciable change in the nuclear quadrupole moment, and excitations in which the quadrupole moment changes considerably. Excitations of the second type may occur in nuclei which do not deviate strongly from spherical shape. In nuclei which deviate markedly from spherical shape, excitations of the second type play no part in transitions involving small changes in the energy.

1. FUNDAMENTAL EQUATIONS FOR DETERMINING COLLECTIVE NUCLEAR EXCITATIONS

In the generalized nuclear model developed by A. Bohr,[2] it is assumed that the states of nucleons outside of closed shells can be described by using the one-particle approximation, while the nucleons in filled shells (i.e., in the core) manifest themselves only through their collective properties. For collective coordinates we use the three Euler angles, characterizing the spatial orientation of the nucleus, and the parameters β and γ which determine the deviation of the nucleus from spherical shape.

In the adiabatic (strong coupling) approximation, we may treat the motion of the outer nucleons in the field of a core of fixed shape. By averaging the interaction energy of core and outer nucleons and the rotational energy of the core over a state of motion with total angular momentum J, and over all states of the outer nucleons which have quantum numbers $n_i l_i j_i m_i$ such that the projection on the nuclear symmetry axis of $J_3 = \sum_i m_i = 0$, we can find the nuclear energy as a function of the collective coordinates β, γ:

$$E = \frac{B}{2}(\dot\beta^2 + \beta^2\dot\gamma^2) + \frac{C}{2}\beta^2 + \frac{\hbar^2}{4}\left(\frac{1}{I_1} + \frac{1}{I_2}\right)[J(J+1) + D] + A\beta\cos\gamma, \qquad (1.1)$$

where the first term represents the kinetic energy of the surface oscillations, the second is the potential energy exclusive of interaction with the outer nucleons, the third is the rotational energy of the nucleus, and the fourth is the interaction of the outer nucleons with the core. The quantities A and D depend on the number of outer nucleons and their states of motion; the explicit form of the dependence can be found in a paper of Ford[3] (formula 18). The moments of inertia I_1 and I_2 with respect to axes perpendicular to the nuclear symmetry axis, are given, in the hydrodynamic approximation which is used in the model to describe the collective motion, by:

$$I_\lambda = 4B\beta^2\sin^2(\gamma - \lambda 2\pi/3),\ \lambda = 1.2. \qquad (1.2)$$

If we use the explicit form (1.2) for the dependence of the moments of inertia on β and γ, we find that the total potential energy of surface oscillation (which does not depend on J)

$$V(\beta\gamma) = \frac{C}{2}\beta^2 + A\beta\cos\gamma + \frac{\hbar^2 D}{4}\left(\frac{1}{I_1} + \frac{1}{I_2}\right) \tag{1.3}$$

has its minimum, for fixed β, at $\gamma = 0$ or $\gamma = \pi$, corresponding to nuclei with axial symmetry; the position of this minimum does not depend on the values of the parameters in (1.3). The function $V(\beta\gamma)$ becomes infinite for $\gamma = \pm\pi/3, \pm 2\pi/3$. It should be noted that (1.1) was obtained on the assumption that the nucleus has axial symmetry, so that the values $\gamma = 0, \pi$ are the "self-consistent" values.

We shall assume that the surface oscillations do not destroy the axial symmetry of the nucleus,* which is observed for the ground states of all nonspherical nuclei, and shall consider the two values $\gamma = 0$ and $\gamma = \pi$ separately.

For $\gamma = 0$, the potential energy (1.3) is given by

$$V_0(\beta) = C\beta^2/2 + A\beta + \hbar^2 D/6B\beta^2, \tag{1.4}$$

while the energy (1.1) is rewritten as

$$E = B\beta^2/2 + V_0(\beta) + M^2/6B\beta^2. \tag{1.5}$$

The potential energy (1.4) has a pole at $\beta = 0$. The presence of this pole corresponds to the fact that the moment of inertia of the nucleus tends to zero for $\beta \to 0$. If there are nucleons outside of closed shells, then even if the total angular momentum of the nucleus is zero, the angular momentum of the core and the angular momentum of the extra-core nucleons are not integrals of the motion and are not separately equal to zero. Expanding $V_0(\beta)$ in powers of the deviation from the value β_0 corresponding to the minimum of (1.4), which is given by

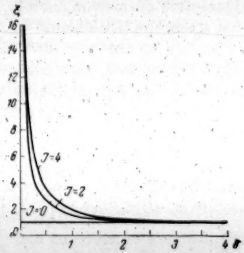

FIG. 1

$$\beta_0 = -A/C + \hbar^2 D/3CB\beta_0^3,$$

and keeping only quadratic terms, we rewrite (1.5) as

$$\varepsilon \equiv E - V_0(\beta_0) = \frac{B}{2}\dot{\beta}^2 + \frac{M^2}{6B\beta^3} + \frac{C_0}{2}(\beta - \beta_0)^2,$$

where

$$C_0 = C + \hbar^2 D/B\beta_0^4.$$

To make the transition to a quantum equation, we note that the square of the angular momentum in the coordinate system, β, θ, φ, for mass coefficient B, is

$$M^2 = B^2\beta^4(\dot{\theta}^2 + \dot{\varphi}^2\sin^2\theta).$$

If T is the kinetic energy of collective motion, then

$$2Tdt^2 = Bd\beta^2 + \frac{B}{3}\beta^2 d\theta^2 + \frac{B}{3}\beta^2\sin^2\theta\cdot d\varphi^2,$$

so that the operator for the kinetic energy of the collective motion is

$$\hat{T} = -\frac{\hbar^2}{2B\beta^2}\left\{\frac{\partial}{\partial\beta}\left(\beta^2\frac{\partial}{\partial\beta}\right) + \frac{1}{\sin\theta}\frac{\partial}{\partial\theta}\left(\sin\theta\frac{\partial}{\partial\theta}\right) + \frac{1}{\sin^2\theta}\frac{\partial^2}{\partial\varphi^2}\right\},$$

and the Schrödinger equation which determines the energy of the collective motion is

$$[\hat{T} + {}^1/_2 C_0(\beta - \beta_0)^2 - \varepsilon]\Psi(\beta\theta\varphi) = 0. \tag{1.6}$$

We shall look for a solution of (1.6) of the form

$$\Psi(\beta\theta\varphi) = \sum_J \frac{U_J(\beta)}{\beta} Y_{JM}(\theta\varphi)$$

*The question of possible deviations from axial symmetry requires investigation of the conditions for breakdown of the "self-consistent" values of γ, and cannot be solved on the basis of (1.1), which was obtained on the assumption that the nucleus has this symmetry.

where J takes on only even values, since the function should not depend on the choice of the direction of the symmetry axis. The functions $U_J(\beta)$ satisfy the equation

$$-\frac{\hbar^2}{2B}\frac{d^2U_J(\beta)}{d\beta^2}+V_J(\beta)U_J-\varepsilon U_J=0, \quad U^J(0)=0, \tag{1.7}$$

where

$$V_J(\beta)=\frac{C_0}{2}(\beta-\beta_0)^2+\frac{\hbar^2}{6B\beta^2}J(J+1)\approx V_J(\beta_J)+\frac{C_J}{2}(\beta-\beta_J)^2; \tag{1.8}$$

$$\beta_J=\beta_0+\frac{\hbar^2J(J+1)}{3BC_0\beta_0^3}, \quad C_J=C_0\left(1+\frac{\hbar^2J(J+1)}{B\beta_J^5}\right). \tag{1.9}$$

Introducing the dimensionless parameter $\delta=\beta_0(BC/\hbar^2)^{1/4}$ and $\xi=\beta_J/\beta_0\geq 1$, Eq. (1.9) becomes

$$\xi^3(\xi-1)=J(J+1)/3\delta^4. \tag{1.10}$$

The solutions of (1.10) for J = 0, 2, 4 are shown in Fig. 1.

In terms of the variables ξ, δ, and $\omega_0=\sqrt{C_0/B}$, the energy $V_J(\beta_J)$ has the form

$$V_J(\beta_J)/\hbar\omega_0=\delta^2(\xi-1)^2+J(J+1)/6\delta^2\xi^2, \tag{1.11}$$

and

$$C_J=C_0(1+J(J+1)/\delta^4\xi^4).$$

Substituting (1.8) in (1.7), we have

$$-(\hbar^2/2B)d^2U_J/d\beta^2+{}^1/_2C_J(\beta-\beta_J)^2U_J-[\varepsilon-V_J(\beta_J)]U_J=0. \tag{1.12}$$

Equation (1.12) coincides with the equation for a one-dimensional harmonic oscillator. However, because of the conditions $\beta\geq 0$ and $U_J(0)=0$, the solutions of (1.12) are not Hermite polynomials.

To determine the eigenfunctions and eigenvalues of (1.12), we introduce the new variable $\zeta=\xi\delta\times(\beta-\beta_J)/\beta_J$ which varies between the limits $-\xi\delta\leq\zeta<\infty$ and the new function $v(\zeta)$ defined by

$$U(\beta)=v(\zeta)\exp\{-\zeta^2/2\}.$$

The function $v(\zeta)$ will satisfy the differential equation

$$v''(\zeta)-2\zeta v'(\zeta)+2\nu v(\zeta)=0 \tag{1.13}$$

and the boundary conditions

$$v(-\xi\delta)=0 \text{ and } e^{-\zeta^2/2}v(\zeta)\to 0, \quad \text{for} \quad \zeta\to\infty. \tag{1.14}$$

The eigenvalue of (1.13) is related to the energy ϵ by:

$$\nu=\frac{\varepsilon-V_J(\beta_J)}{\hbar\omega_J}-\frac{1}{2}, \quad \omega_J=\sqrt{\frac{C_J}{B}}=\omega_0\sqrt{1+\frac{J(J+1)}{\delta^4\xi^4}}.$$

The general solution of (1.13) for non-integral ν is given in terms of Hermite functions[4] of the first kind:

$$v_\nu(\zeta)=aH_\nu(\zeta)+bH_\nu(\zeta),$$

which can be represented by the series

$$H_\nu(\zeta)=\frac{1}{2\Gamma(-\nu)}\sum_{k=0}^{\infty}\frac{(-1)^k}{k!}\Gamma\left(\frac{k-\nu}{2}\right)(2\zeta)^k.$$

By examining the asymptotic behavior of the Hermite functions for large ζ, we can verify that we must set b = 0 in order to satisfy the boundary condition (1.14) at $\zeta\to\infty$. Then the eigenvalues ν, and consequently the energy

$$\varepsilon-V_J(\beta_J)=\hbar\omega_J(\nu+{}^1/_2), \tag{1.15}$$

are determined by the condition

$$v(-\xi\delta)=aH_\nu(-\xi\delta)=0.$$

For $\gamma = \pi$, the potential energy (1.4) becomes

$$V_\pi(\beta) = C\beta^2/2 - A\beta + \hbar^2 D/6B\beta^2,$$

where $0 \le \beta < \infty$. It is easy to check that the replacement of β by $-\beta$ enables us to keep all the results for the previous case of $\gamma = 0$ [including Eq. (1.13)], if we merely note that now the domain of variation of β is $-\infty < \beta \le 0$, and consequently ζ varies between the limits $-\infty < \zeta \le -\xi\delta$. Then β_0, δ, and ξ will have the same meaning and values as for the case of $\gamma = 0$. The function $v(\zeta)$ must satisfy the differential equation (1.13) with the boundary conditions

$$v(\zeta)\, e^{-\zeta^2/2} \to 0 \text{ for } \zeta \to -\infty; \quad v(-\xi\delta) = 0. \tag{1.16}$$

The requirement that the boundary conditions (1.16) be satisfied gives us

$$v_\nu(\zeta) = bH_\nu(-\zeta)$$

and a transcendental equation

$$H_\nu(\delta\xi) = 0,$$

which determines the eigenvalue.

2. THE TWO CLASSES OF COLLECTIVE EXCITATIONS OF AXIALLY-SYMMETRIC NUCLEI

According to (1.15) the rotation-vibration energy of the nucleus can be written as

$$\varepsilon_J/\hbar\omega_0 = (\nu + 1/2)\sqrt{1 + J(J+1)/\delta^4\xi^4} + 1/2\,\delta^2(\xi - 1)^2 + J(J+1)/6\delta^2\xi^2, \tag{2.1}$$

where ν is determined from the transcendental equation $H_\nu(-\xi\delta) = 0$ if $\gamma = 0$ and from the equation $H_\nu(\xi\delta) = 0$ if $\gamma = \pi$. Since ξ is uniquely determined by the values of J and the parameter δ, $\varepsilon_J/\hbar\omega_0$ will be a function only of J and δ, so that the latter should be regarded as the parameter of the theory.

Figure 2 shows the dependence of (2.1) on δ as computed by Filippov[5] for nuclei having a positive quadrupole moment in the ground state. In this case, the ground state is an s-state with $\gamma = 0$. The excited states for each spin value $J = 0, 2, 4$ are shown for the case of $\gamma = 0$ by the solid lines, and for the case of $\gamma = \pi$ by the dashed lines. As we have already pointed out in a separate communication,[6] for $\delta > 0$, the case of $\gamma = 0$ corresponds to positive quadrupole moments, while for the case of $\gamma = \pi$, the quadrupole moments are small and negative. With increasing δ, the energy of excited states with positive quadrupole moment decreases, while the energy of excited states with negative quadrupole moment increases.

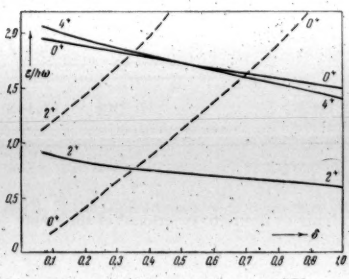

FIG. 2

A transition of the nucleus from the ground state (which has a positive quadrupole moment) to excited states corresponding to $\gamma = \pi$ (the dotted lines), is accompanied by a change in the sign as well as the absolute value of the quadrupole moment. A transition of the nucleus from the ground state to a state with $\gamma = 0$ (the solid lines) does not involve a change in the sign of the quadrupole moment. Thus the collective excitations of axially-symmetric nuclei can be of two types: (1) excitations without any essential change in the quadrupole moment; (2) excitations with a considerable change in the quadrupole moment. As we see from Fig. 2, excitations of the second type can occur in nuclei with low values of δ. We should, of course, remember that for low values of δ the adiabatic approximation is not fulfilled, and that the curves have only a qualitative meaning in this region.

Because of the small quadrupole moments in the excited states of the second type (cf. Fig. 2, dotted lines), gamma transitions between them should have very low probability.

In Table I we give experimental values (the references are given in the last column of the table) for

TABLE I

Nucleus	Level energy		Spin		δ	Literature
	exptl.	theoret	exptl.	theoret		
Sn^{116}	—	0.40	—	[0]	0.16	[7]
	1.00	1.00	2	2		
	1.65	1.65	2	[2]		
	1.86	2.28	4	4; 0		
Ba^{134}	—	0.50	—	[0]	0.2	[8]
	1.00	1.00	2	2		
	1.72	1.72	2	[2]		
	1.95	2.26	4	4; 0		
Pt^{192}	—	0.65	—	[0]	0.25	[9]
	1.00	1.00	2	2		
	1.93	1.93	2	[2]		
	2.48	2.32	4	4; 0		
Ge^{72}	0.82	0.82	0	[0]	0.29	[10]
	1.00	1.00	2	2		
	1.74	2.15	2	[2]		
Se^{76}	—	0.86	—	[0]	0.3	[11]
	1.00	1.00	2	2		
	2.18	2.2	2	[2]		
	—	2.30	—	0		
	2	2.33	—	4		
Xe^{128}	—	0.86	2	[0]	0.3	[12]
	1.00	1.00	2	2		
	2.18	2.18	2	[2]		
	—	2.30	—	0		
	—	2.33	—	4		
Cd^{114}	—	0.86	—	[0]	0.3	[13]
	1.00	1.00	2	2		
	2.17	2.18	2	[2]		
	2.30	2.30	4	0		
	2.34	2.34	0	4		
Pd^{106}	1.00	1.00	2	2	0.66	[14]
	2.2	2.35	0	[0]; 0; 4		
	3.02	4	2	[2]		

the ratio of the energy of the first few excited states to the energy of the first excited state (which has spin 2), and the spin values. We also give the corresponding values obtained from Fig. 2 with a suitably chosen value of δ (which is given in the next-to-last column). All the states given in Table I have positive parity. For levels which according to the theory are of the second type, the spin value is put in square brackets.

3. ROTATIONAL ENERGY OF NUCLEI

For large deviations from spherical symmetry, the excited states of the second type have considerable excitation energy. Thus the first few levels will all correspond to excitations of the first type and will go over into a pure rotational spectrum with increasing δ.

For $\delta > 1$, the function $\xi = F[J(J+1)/3\delta^4]$ in (1.10) is very close to unity. Expanding this function in series and stopping with the linear terms, we can rewrite (2.1) in the form

$$\varepsilon_J/\hbar\omega_0 \approx \varepsilon_0/\hbar\omega_0 + J(J+1)/6\delta^2 - aJ^2(J+1)^2/\delta^6. \quad (3.1)$$

Using the fact that $\delta = \beta_0 (BC/\hbar^2)^{1/4}$, and introducing the moment of inertia $I = 3B\beta_0^2$ we can rewrite (3.1) as

$$\varepsilon_J = \varepsilon_0 + AJ(J+1) - BJ^2(J+1)^2, \quad (3.2)$$

where

$$A = \hbar^2/2I, \quad B = a(\hbar\omega_0)^{-2}(\hbar/I)^3.$$

It is known that formula (3.2) gives good agreement with experiment if A and B are regarded as adjustable parameters. Table II gives the values of A and B obtained from the energy spectra of a few nuclei.

Using (1.16) and $I = 3B\beta_0^2$, we can express the parameter δ in terms of the moment of inertia and $\hbar\omega_0$:

$$\delta^2 = \hbar\omega_0 I/3\hbar^2 = \hbar\omega_0/6A. \quad (3.3)$$

In the third column of Table II we give the values of δ obtained from (3.3) by setting $\hbar\omega_0 \sim 1$ Mev and using the experimentally determined value of A. These are typical values of δ for nuclei having a well defined rotational spectrum.

TABLE II

Nucleus	A (kev)	B (kev)	δ
Hf^{180}	15.58	0.0703	3.3
Th^{226}	12.16	0.043	3.7
Pu^{238}	7.37	0.0033	4.7

[1] G. Scharff-Goldhaber and J. Weneser, Phys. Rev. 98, 212 (1955).
[2] A. Bohr, Dansk. Mat.-fys. Medd. 26, #14 (1952).
[3] K. Ford, Phys. Rev. 90, 29 (1953).
[4] N. N. Lebedev, Специальные функции и их приложения (Special Functions and their Application), GITTL, 1953.
[5] G. F. Filippov, Dokl. Akad. Nauk SSSR 115, 696 (1957).

[6] A. S. Davydov and G. F. Filippov, J. Exptl. Theoret. Phys. (U.S.S.R.) 32, 945 (1957), Soviet Phys. JETP 5, 773 (1957).
[7] Scharenberg, Stewart, and Wiedenbeck, Phys. Rev. 101, 689 (1956).
[8] G. Bertolini et al., Nuovo cimento 1, 746 (1955).
[9] Baggerly, Marmier, Boehm, and Du Mond, Phys. Rev. 100, 1364 (1955).
[10] Kraushaar, Brun, and Meyerhof, Phys. Rev. 101, 139 (1956).
[11] Kurbatov, Murray, and Sakai, Phys. Rev. 98, 674 (1955).
[12] Benczer, Farrelly, Koerts, and Wu, Phys. Rev. 101, 1027 (1956).
[13] H. Motz, Phys. Rev. 104, 1353 (1956).
[14] A. Alburger and B. Toppel, Phys. Rev. 100, 1357 (1955).

Translated by M. Hamermesh
138

SOVIET PHYSICS JETP VOLUME 6 (33), NUMBER 3 MARCH, 1958

ON THE THEORY OF THE INTERACTION OF "EXCESS" CHARGES IN IONIC CRYSTALS

V. L. VINETSKII and M. Sh. GITERMAN

Ural' State University

Submitted to JETP editor March 12, 1957

J. Exptl. Theoret. Phys. (U.S.S.R.) 33, 730-734 (September, 1957)

Interaction between polarons is considered. It is shown that the formation of "bipolarons," two polarons separated by a finite distance R and bound by a common polarization, is energetically feasible in crystals with parameters satisfying the condition $n^2/\epsilon \leq 0.05$.

THE interaction of an "excess" electron, introduced into an ionic dielectric, with the crystal polarization oscillations leads, as is known, to the appearance of polaron states.[1] Polarons are majority carriers in ionic crystals; they determine the electrical, photoelectrical, and optical properties of these crystals. Interaction between polarons reduces to electrostatic repulsion and attraction caused by the influence of the inertial polarizational potential well of each electron on the remaining ones (such an attraction will be called hereinafter polarizational in the interests of brevity). Interaction between polarons was not taken into account in polaron theory[1] since it was assumed that the polaron concentration was small enough. The interaction of two electrons in a common polarizational potential well was considered in Refs. 2 and 3. It has been found that such compounds (called bipolarons) do not exist independently of the crystal parameter values. Physically, this means that the Coulomb repulsion force is dominant in this case. However, the electrostatic repulsion and polarizational attraction forces depend differently on the distance between the centers of gravity of the polarizational potential wells and, in general, it cannot be stated beforehand that a stable state of a complex of polarons is impossible when this distance is not zero.

The simplest of such complexes, two interacting polarons, is considered below. The purpose of this work is to explain the possibility of the existence of such a formation. We shall henceforth call it a bipolaron, thus ascribing to this concept a more general meaning than in Refs. 2 and 3. Moreover, our analysis permits an estimate of the influence of polaron interaction on the energy of each polaron and serves therefore as a criterion of whether it is permissible to neglect this interaction for the purpose of formulating a multielectron theory.

The interaction of an "excess" electron with vacancies has also been analyzed; the interaction potential obtained can be used to analyze scattering of carriers by impurities in ionic crystals.

Using the methods developed by Pekar,[1] the Hamiltonian of a system consisting of a crystal with two

electrons introduced therein can be written as follows:

$$\hat{H} = -(\hbar^2/2\mu)\Delta_1 - (\hbar^2/2\mu)\Delta_2 + U_p(r_1, r_2) + V_p(r_1, r_2) + (e^2/n^2)r_{12}. \quad (1)$$

Here, the first two terms are the kinetic energy of the electrons, the third term is the interaction energy of the electrons with the inertially polarized crystal, the fourth is the energy of the inertially polarized crystal, and the last is the Coulomb repulsion energy; μ is the electron effective mass, n the optical refractive index of the crystal, r_{12} the distance between the electrons, and the subscripts 1 and 2 refer to the first and second electrons.

The Schrödinger equation with the Hamiltonian (1) can be replaced by an equivalent variational principle. The system energy is then determined by minimizing an appropriate functional dependent on the electron ψ functions and on the specific inertial dielectric polarization **P** created by the excess electrons, subject to the additional condition of normalization of the ψ functions. **P** is first minimized for a fixed ψ in the adiabatic approximation, after which the minimum with respect to ψ is found.

The approximating function was selected in symmetric form:

$$\psi(r_1 r_2) = A[\psi_{1a}\psi_{2b} + \psi_{1b}\psi_{2a}]; \quad \psi_{1a} = \pi^{-1/2}\alpha^{3/2}e^{-\alpha r_{1a}}; \quad \psi_{2b} = \pi^{-1/2}\alpha^{3/2}e^{-\alpha r_{2b}}; \quad (2)$$

where a, b are centers of polarization potential wells and α is the approximation parameter. The deformation of the ψ cloud of each electron is not taken into account in such a choice of the ψ function. A similar assumption is made, say, in computing the hydrogen molecule by the variational method which, as is known, does not lead to any substantial error.

A computation similar to the above was made by Deigen[4] for the F_2 center, a system consisting of two positive vacancies, separated by a distance R in the ionic crystal, and two polarons. It should be noted that the analysis carried out is not consistently quantum mechanical since the lattice ion motion was considered to be classical. The Deigen[4] results can be used if the terms giving the interaction between the vacancies and the electrons and between the vacancies themselves are cancelled in the Hamiltonian of the crystal — F_2 center system and if R is taken to be the distance between the centers of gravity of the polarized wells.

The functional defining the system energy reduces to the following by substituting (2) and minimizing over **P**:

$$I = (\hbar^2/\mu R^2) f_1(x) + (e^2 c/R) f_4(x) + (e^2/n^2 R) f_3(x), \quad (3)$$

where $x = \alpha R$, $c = 1/n^2 - 1/\epsilon$, and ϵ is the dielectric constant; the functions $f_1(x)$, $f_3(x)$, $f_4(x)$ are calculated and tabulated in Ref. 4.

A functional agreeing with (3) was also obtained by Moskalenko[5] who analyzed the problem of a bipolaron from the point of view of the second-quantization method. Moskalenko confined himself only to the tabulation of I(x, R) for certain values of the crystal parameters, which led him to conclude the impossibility of the existence of bipolarons. A more general analysis will be made below which will lead to somewhat different results than in Ref. 5.

To find the stationary states of the system, such values of R should be found for which the function I(R) would have a minimum. The condition $\partial I/\partial R = 0$ leads to the equation

$$-(2\hbar^2/\mu e^2 R^3) f_1(x) - [c f_4(x) + n^{-2} f_3(x)] R^{-2} = 0. \quad (4)$$

whose roots are

$$R_1 = R_2 = \infty; \quad R_3 = -(2\hbar^2/\mu e^2) f_1(x)/[c f_4(x) + n^{-2} f_3(x)]. \quad (5)$$

As is easy to verify, minimization of I(R) with respect to x yields the sum of the energies of two polarons in the $R = R_1 = R_2$ case. This case is trivial. Substituting R_3 from (5) into (4), we obtain

$$I(x) = -(\mu e^4 c^2/4\hbar^2)(f_4 + f_3/n^2 c)^2/f_1. \quad (6)$$

Minimizing (6) with respect to x leads to the relation

$$(f_4 + f_3/n^2 c)[2f_1 f_4' + 2f_1 f_3'/n^2 c - f_4 f_1' - f_3 f_1'/n^2 c] = 0, \quad (7)$$

from which it is not difficult to determine the value of x which yields the minimum value of I(x):

$$n^2 c = u(x); \quad u(x) = -(2f_3' f_1 - f_1' f_3)/(2f_1' f_1 - f_1' f_4). \quad (8)$$

We tabulated the first part of (8) for various x. We have $u(x) < 0$ for $x \leq 0.75$. This result is in-

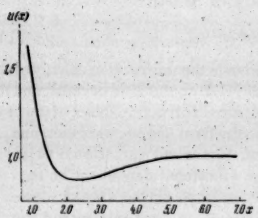

FIG. 1

agreement with the conclusion obtained in Refs. 2 and 3 that stationary states of the system do not exist independently of the crystal parameters for $R = 0$ (two electrons in a common polarization potential well). The function $u(x)$ is plotted in Fig. 1 for $x > 0.75\, u(x)$. Using the crystal parameters ϵ and n^2 and Fig. 1, the corresponding value of x_{min} can be found and I_{min} can then be determined from (6).

It follows from Fig. 1 that the solution (6) exists only if $n^2c > 0.88$ or

$$n^2/\varepsilon < 0.12. \tag{9}$$

and not for arbitrary values of the crystal parameters. The values of ϵ and n^2 for a large number of crystals are cited in Ref. 6, for example. The inequality (9) is not satisfied for all the crystals cited in Ref. 6.

As Davydov[3] and Deigen[7] have shown, the methods of polaron theory are applicable to metal-ammonia solutions. Consequently, our analysis is valid also in this case. The parameters of metal-ammonia solutions ($\epsilon = 22$, $n^2 = 1.76$) satisfy inequality (9). Figure 2 shows a plot of $I(R)$ for such solutions. As is seen from the figure, $I(R)$ has a minimum at $R \approx 4$ A and accordingly at $\alpha = 0.42 \times 10^8$ cm^{-1}. However, this minimum appears to be located somewhat higher than the sum of the energies of the two polarons. According to the variational method, a physical meaning should be ascribed to that root of (4) which gives a lower value of the functional being investigated. Consequently, the root $R = R_3$ must be discarded in this case.

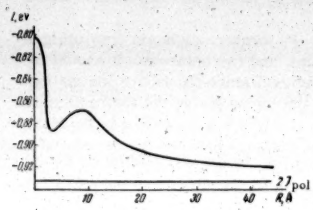

FIG. 2

Let us try to explain for which values of the crystal parameters the bipolaron energy (6) becomes less than the sum of the energies of the two polarons, i.e., the relation $I/2J_{pol} > 1$ is satisfied.

Using the value of I according to (6) and J_{pol} from Ref. 1, the criterion for the existence of bipolaron states can be represented as:

$$2{,}56\,(f_4 + f_3/n^2c)^2/f_1 > 1. \tag{10}$$

The function on the left side of (10) was tabulated for various values of n^2 and c and for the appropriate x obtained by solving (8). The ratio $I/2J_{pol}$ becomes greater than unity for

$$n^2/\varepsilon < 0.05 \tag{11}$$

and for the appropriate $x = 1.5 - 1.6$. The maximum value of this ratio for $n^2/\epsilon = 0$ is

$$(I/2I_{pol})_{max} = 1{,}08. \tag{12}$$

Hence, the transition of polarons into the bipolaron state is energetically feasible for crystals with values of the parameters ϵ and n^2 satisfying (11). This must be reflected substantially in the properties of such crystals (magnetic properties, formation of color centers, effective mass, and current carrier mobility, etc.).

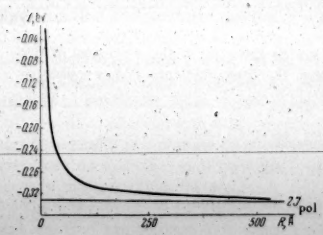

FIG. 3

The approximate wave function of the $e^{-\alpha r}$ kind used above simplifies the computations considerably but is not flexible enough. Since the energy gain calculated above for the bipolaron is small, the results of the computation made require verification by using a more flexible approximation function.

According to Pekar,[1] the best results are obtained with the variational method with one approximation parameter by using a function of the form

$$\psi = A(1 + \alpha r)\, e^{-\alpha r}, \tag{13}$$

which we have indeed used instead of the hydrogen-like functions

(2a). The functions corresponding to $f_1(x)$, $f_2(x)$, and $f_4(x)$ in (3) cannot be written in explicit form in this case because of the great complexity of the resulting integrals. However, use of the Kopineck[8] results permitted these functions to be tabulated and the solution to be found graphically. The error arising in such a solution is negligible. The numerical results obtained by using (13) are in complete agreement with those cited above [see relations (11) and (12)].

Evidently, taking the mutual deformation of the polarizing potential wells of the interacting carriers into account, as can be done by introducing an additional parameter into the approximating function, can only lead to a less stringent condition on the existence of the bipolaron than (11), since such a parameter affects the calculated bipolaron energy more than the energy of the individual polaron.

The computation carried out can be used to estimate the magnitude of the polaron interaction as a function of their concentration. As an example, we have obtained a configuration curve for KCl (Fig. 3). It is seen from the figure that the polaron interaction is still small at $R \geq 200$ A (this corresponds to an average polaron concentration of the order of 10^{16} cm^{-3}); the error in determining the polaron energy in the single electron problem is not more than 5 percent in such concentrations. This error is 5 — 20 percent for concentrations from 10^{16} — 10^{19}. The error in determining the energy becomes very substantial at concentration $n \geq 10^{19}$ ($R \approx 40$ A in Fig. 3) and the polaron interaction must be introduced into the basic Hamiltonian of the multielectron problem. Incidentally, an appropriate excess positive charge is needed in the crystal to neutralize the excess electrons at such high concentrations and other types of interaction besides the polaron one should be taken into account in the basic Hamiltonian.

ρ (Å)	$F(\rho)$ (ev)	$\lvert F(\rho) - J_{pol} \rvert$ (eV)	$\frac{e^2}{\varepsilon\rho}$ (ev)
1.64	−1.307	1.142	1.832
3.35	−0.906	0.740	0.897
5.50	−0.672	0.507	0.547
9.81	−0.462	0.297	0.307
13.6	−0.386	0.221	0.222
17.1	−0.341	0.176	0.176
34.2	−0.253	0.088	0.0879
51.4	−0.224	0.059	0.0586
68.5	−0.209	0.044	0.0440
∞	−0.165	0	0

An analysis of an electrically neutral system consisting of a crystal with a vacant lattice site and an electron introduced into the crystal is of interest. The Hamiltonian of such a system is written as

$$\hat{H} = -(\hbar^2/2\mu)\Delta + V_p(r) + U_\rho(r) - e^2/\varepsilon r. \qquad (14)$$

The first term here is the electron kinetic energy, the second is the electron interaction with the polarized crystal, the third is the polarized crystal energy and the last is the electron interaction with the vacancy. Replacing the Schrödinger equation with the Hamiltonian (14) by an equivalent variational principle, we arrive at the corresponding functional. Minimization was made with the aid of a hydrogen-like ψ function of the excess electron. Exactly the same as in the case of two excess electrons, considered above, we can arrive at a functional that is dependent on x and ρ:

$$F = (e^2/\varepsilon\rho)\,[\hbar^2\varepsilon x^2/2\mu e^2\rho - P(x)], \qquad (15)$$

where ρ is the distance between the center of gravitiy of the polarized potential well of the electron under consideration and the "vacancy;" $P(x) = 1 - e^{-2x}(1 + x) + (5\epsilon c/16)x$.

Minimization of F with respect to x was carried out for various fixed values of ρ. The results of a computation for a KCl crystal are cited as an example (see table). Values of the system energy are given in the second column; the third lists the interaction energy between the polaron and the vacancy, equal to $F(\rho) - J_{pol}$, while the fourth gives the values of the Coulomb energy for comparison.

As is seen from the table, the interaction energy between the polaron and the vacancy is notably different from the Coulomb energy only for $\rho < 10$ A.

The authors are grateful to S. I. Pekar who provided guidance and a number of valuable remarks.

[1] S. I. Pekar, Исследования по электронной теории кристаллов (Investigations in the Electron Theory of Crystals), GITTL, 1951.

[2] S. I. Pekar and O. F. Tomasevich, J. Exptl. Theoret. Phys. (U.S.S.R.) 21, 1233 (1951).

[3] A. S. Davydov, Trudy, Physics Faculty Kiev State University 5, 1952.

[4] M. F. Deigen, J. Exptl. Theoret. Phys. (U.S.S.R.) 21, 992 (1951).

[5] S. A. Moskalenko, Уч. зап. Кишиневского ун-та (Sci. Notes, Kishinev Univ.), 17, 103 (1955).

[6] N. F. Mott and R. V. Gurney, Electron Processes in Ionic Crystals, Oxford, 1948 (Russ. Transl.).

[7] M. F. Deigen, Trudy, Phys. Inst., Acad. Sci. Ukr. S.S.R. 5 (1954).
[8] H. J. Kopineck, Z. Naturforsch. 5a, 420 (1950); 6a, 177 (1951); 7a, 785 (1952).

Translated by M. D. Friedman
139

SOVIET PHYSICS JETP VOLUME 6 (33), NUMBER 3 MARCH, 1958

DE HAAS–VAN ALPHEN EFFECT IN A VARIABLE MAGNETIC FIELD

A. M. KOSEVICH

Chernovtsy State University

Submitted to JETP editor March 16, 1957

J. Exptl. Theoret. Phys. (U.S.S.R.) **33**, 735-745 (September, 1957)

A theoretical study is made of the characteristic features of the oscillations of the magnetic moment of a metallic specimen at low temperatures in a pulsed magnetic field.

In connection with the use of the pulse method for the study of the De Haas-Van Alphen effect in strong magnetic fields,[1] it is of interest to clarify the peculiarities of the oscillations of the magnetic moment of a metal at low temperatures in a variable magnetic field of a pulsed type.

In Sec. 1 of the present paper, we give qualitative consideration to this problem, and show that the oscillation properties of the magnetic moment of a metallic specimen in a pulsed field depend essentially on the ratio of the characteristic dimension in the problem of the penetration of the variable field into the metal to the dimension of the sample itself. In Sec. 2 and 3, formulas are obtained for the oscillating part of the magnetic moment for different values of this ratio, and their analysis is given.

1. OSCILLATIONS OF THE MAGNETIC MOMENT OF A METALLIC SAMPLE IN A PULSED FIELD

(Qualitative Considerations)

The oscillations of the magnetic moment of a metal are determined by the quantized motion of the conduction electrons (current carriers) in the magnetic field; their periods and amplitudes are connected with the form of the electron dispersion law near the Fermi surface.[2] There are usually some groups of electrons in the metal with different dispersion laws, and each of these makes its own contribution to the oscillations of the magnetic moment. In what follows, we shall consider the contribution to the oscillating part of the magnetic moment of only one such group of electrons with the particular dispersion law $\epsilon = \epsilon(\mathbf{p})$ (ϵ = energy, $\mathbf{p}$ = quasi-momentum of the electron).

If the homogeneous field H is constant, then the oscillating part of the magnetic moment* of the electron gas is given by the following formula:[2]

$$M_{\text{osc}} = V \sum_{n=1}^{\infty} \Psi_n(H) \cos\left(\frac{\alpha n}{H} + \gamma_n\right); \qquad (1)$$

V = volume occupied by the electron gas (the volume of the metal); $\Psi_n(H) \equiv \Psi_n(H, T)$ = some slowly changing function of H and the temperature T; $\alpha = cS_m(\zeta)/e\hbar$, where $S_m(\zeta)$ = the ex-

*We are considering the component of the magnetic moment in the direction of the magnetic field.

tremal area of the surface formed by the intersection of the Fermi surface $\epsilon(\mathbf{p}) = \zeta$ with the plane $\mathbf{p} \cdot \mathbf{H}$ = const, and the notation of the constants is standard; φ_n = some "initial" phases of the oscillations, independent of H. We recall that Eq. (1) is valid for $kT/\zeta \ll 1$ and $H/\alpha \ll 1$; we shall consider these inequalities to be satisfied.

We consider that the metallic specimen is placed in a variable homogeneous magnetic field $H_0 = f(t)$, parallel to its surface, and that $f(t)$ have the form of a pulse (see figure) of duration T [$f(t)$ differs essentially from zero only in the interval $0 < t < T$ and has a single maximum for $t = t_m$; $f(0) > 0$].

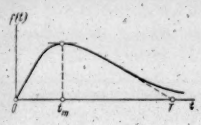

Inasmuch as the external magnetic field is variable in time, it induces eddy currents in the conductor which distort the imposed field in the body of the metal; therefore, the magnetic field inside the specimen is not homogeneous throughout its thickness.

By virtue of the inhomogeneity of the magnetic field in the metal and the large value of the ratio α/H_0, the oscillations of the magnetic moments of neighboring layers of the metal differ significantly in phase; in averaging them over the thickness, a smoothing out takes place in the oscillations of the total magnetic momentum. In this regard, the following are exceptional: (1) the layers of metal adjoining the surface of the sample, where the averaging takes place only on one side (in the depth of the metal), and (2) the layer of metal in which the magnetic field is stationary (i.e., the layer in which $\partial H/\partial x = 0$, where x is the coordinate measured along the normal to the surface, into the depth of the specimen), and there is no shift in the phase of oscillation. Only these layers of the metal make an appreciable contribution to the oscillating part of the total magnetic moment of the metal.

It is easy to estimate the thicknesses of the above-mentioned layers, and to clarify the character of the dependence of the corresponding periods of oscillation on the external field. As is seen from (1), the oscillations of the magnetic moment are produced by the change in the values of α/H in the argument of the cosine, where $H = H(x, t)$ is different in the different layers of the metal. The magnetic field at the surface of the metal coincides with the external field H_0; consequently, the period of oscillation of the magnetic moment of the given layer with change in the external field is the same as for the constant field.[2] The thickness of this layer Δx is of the order of magnitude of the distance into the body of the metal at which the phase shift is equal to the period of oscillation.

$$\Delta\left(\frac{\alpha}{H}\right) = \alpha\left|\frac{\partial}{\partial x}\,\frac{1}{H}\right|\Delta x = \frac{\alpha}{H^2}\left|\frac{\partial H}{\partial x}\right|\Delta x \sim 2\pi. \tag{2}$$

It is appropriate to estimate the order of magnitude of $\partial H/\partial x$ by starting out from the form of the differential equation which defines the penetration of the magnetic field into the metal. We can consider the equation for the magnetic field in a specimen of cylindrical form without restricting the generality of the treatment:

$$\frac{1}{\rho}\,\frac{\partial H}{\partial \rho} + \frac{\partial^2 H}{\partial \rho^2} = \frac{1}{q}\,\frac{\partial H}{\partial t}. \tag{3}$$

Here ρ = distance from the axis of the cylinder, and $q = c^2/4\pi\mu\sigma$ (μ = magnetic susceptibility, σ = specific electrical conductivity of the metal). If the pulse duration of the magnetic field is T, then the problem has as its characteristic dimension the length $l \sim \sqrt{qT}$.

In the case in which the radius of the cylinder R is much greater than the length l ($R \gg l$), the problem reduces to consideration of the penetration of the magnetic field into the semi-infinite metal, and the only characteristic length is l, so that

$$|\partial H/\partial x| = |\partial H/\partial \rho| \sim H/l. \tag{4}$$

It follows from (2) and (4) that for $R \gg l$, the thickness of the surface layer $\Delta x \sim l(H/\alpha)$, and its volume is $\Delta V \sim Gl(H/\alpha)$, where G is the surface area of the specimen. It is clear that these estimates hold also for $R \sim l$.

For the case $R \ll l$, when it is necessary to take into consideration the presence of two different characteristic dimensions (R and l), it is easiest to estimate the value of $\partial H/\partial \rho$ from Eq. (3):

$$|\partial H/\partial \rho| \sim (\rho/q)\,|\partial H/\partial t| \sim RH/qT \sim (R/l)\,H/l. \tag{5}$$

Substituting the estimate (5) in (2), we find that for $R \ll l$, the thickness of the surface layer $\Delta x \sim l(l/R)H/\alpha$ and its volume is $\Delta V \sim Gl(l/R)H/\alpha$.

The thickness of the layer in which the magnetic field is stationary in depth is determined by a relation similar to (2), namely,

$$\Delta\left(\frac{a}{H}\right)=\frac{a}{2}\left|\frac{\partial^2}{\partial x^2}\frac{1}{H}\right|\Delta x^2=\frac{a}{2H^2}\left|\frac{\partial^2 H}{\partial x^2}\right|\Delta x^2\sim 2\pi. \tag{6}$$

The order of magnitude of $\partial^2 H/\partial x^2$ does not depend on the dimensions of the specimen to such a degree as the value of $\partial H/\partial x$, and Eq. (3) always gives the expression for it:

$$|\partial^2 H/\partial x^2|=|\partial^2 H/\partial l^2|\sim H/l^2. \tag{7}$$

It follows from (6) and (7) that the thickness of the layer with stationary field is $\Delta x\sim l(H/\alpha)^{1/2}$ and consequently it exceeds the thickness of the surface layer (in the case $R\gtrsim l$) by the ratio $(\alpha/H)^{1/2}$.

It should be observed that in a cylindrical specimen one such layer corresponds to the neighborhood of the axis of the cylinder. The volume of this "layer" is $\Delta V\sim Ll^2(H/\alpha)$, where L is the length of the cylinder. If $l\ll R$, then the contribution of the region about the axis of the cylinder to the oscillating part of the total magnetic moment of the specimen gives the same order of contribution to the oscillations of the total magnetic moment as does the surface layer; however, this part has a different period (corresponding to the magnetic field on the axis of the cylinder).

So far as other layers with magnetic field stationary with respect to depth are concerned, they can exist in the metal only beyond the passage of the external field $H_0(t)$ through a maximum, i.e., for $t>t_m$. Actually, when $H_0(t)$ increases, by the law of electromagnetic induction, the rate of increase of the magnetic field inside the metal falls off with the depth; therefore, at each particular moment of time, the magnetic field decreases with depth: $\partial H/\partial x<0$. When $H_0(t)$ passes through the maximum and begins to decrease, then the opposite takes place: the drop of the magnetic field in the body of the metal does not take place at the expense of $H_0(t)$, and at a certain instant t_0 the field in the surface layer is comparable with $H_0(t)$. At this moment, $(\partial H/\partial x)_{x=0}=0$, and at the surface of the specimen, a layer arises with stationary magnetic field. Upon further lag of the drop of the field in the body of the metal behind the decrease in $H_0(t)$, the field at the surface of the specimen will increase with depth and therefore, for $t>t_0$, $(\partial H/\partial x)_{x=0}>0$. However, at a sufficient depth x, the situation undergoes no change, and, as before, $\partial H/\partial x<0$. Consequently, at the same depth $x_0>0$, the derivative $\partial H/\partial x$ passes through zero, i.e., there exists a layer with a magnetic field that is stationary with respect to depth. The function $x_0=x_0(t)$ gives the depth of this field at each moment of time $t>t_0$ [evidently, $x_0(t_0)=0$]. The period of oscillation of the magnetic moment of such a layer is determined by the magnetic field at the depth $x=x_0(t)$ and has a complicated dependence on $H_0(t)$.

Thus the oscillations of the magnetic moment of a cylindrical specimen in a pulsed field are characterized by the following peculiarities:

1. Case $l\ll R$. In the time interval $0<t<t_0$ the oscillations are completely determined by the surface layer of the specimen. The amplitude of oscillation is less, in the ratio $(l/R)(H_0/\alpha)$, than the amplitude of oscillation in a constant field, and the period of oscillation with change of the external magnetic field $\Delta(1/H_0)$ is the same as for a constant field.

At the time t_0 the amplitude of oscillation increases by a factor $(\alpha/H_0)^{1/2}$, and the oscillations of the magnetic moment begin to be determined by the layer of the metal with stationary field. For $t>t_0$, the surface layer of the specimen gives an insignificant contribution to the oscillations, and the period of the oscillation is determined by the magnetic field at the depth $x=x_0(t)$.

2. Case $l\gtrsim R$. If $1\gtrsim(R/l)^2\gg H_0/\alpha$, then in the time interval $0<t<t_0$ the oscillating part of the magnetic moment consists of two components of the same order of magnitude: the component determined by the surface layer of the metal and the component which corresponds to the region around the axis of the cylinder. The amplitudes of these components are less by a factor $(l/R)^2(H_0/\alpha)$ than the amplitudes of the oscillations in constant field. The periods of the oscillations of these two components are different, since for $l\sim R$, the magnetic field on the axis of the cylinder differs from the imposed field H_0.

At the time t_0, as in case 1, the amplitude of the oscillation increases by the factor $(R/l)(\alpha/H_0)^{1/2}$, and in what follows $(t>t_0)$ the oscillations are determined by the layer of metal with stationary field, and the period of the oscillations corresponds to the magnetic field in this layer.

It can be pointed out that at a certain moment of time t_1 $(t_0<t_1<T)$, the layer with stationary magnetic field, which "splits off" from the surface of the specimen, coincides with the region near the axis of the cylinder. Then the amplitude of the oscillation decreases and the oscillation will again be determined by the same two components as for $t<t_0$.

If $R \sim l(H_0/\alpha)^{1/2}$, then the oscillating part of the magnetic moment of the specimen is determined by its thickness, and the period of oscillation corresponds to a certain mean magnetic field over the thickness of the specimen.

If $R \ll l(H_0/\alpha)^{1/2}$, then the magnetic field inside the metal can be considered homogeneous throughout the thickness of the specimen and Eq. (1) is valid for oscillations of the magnetic moment.

Finally, one should point out the possibility of experimental observation of these oscillations, the amplitude of which is, in the most interesting cases ($l \lesssim R$), significantly less than the for constant field. The fact is that in the use of the pulse method for the investigation of the De Haas—Van Alphen effect, we measure dM_{osc}/dH, not M_{osc}.[1] But, as is evident from (1), the following relation holds:

$$dM_{osc}/dH \sim (\alpha/H) M_{osc}/H,$$

therefore, the small factor H_0/α which appears in the amplitude of the oscillation can be compensated.

Taking into consideration the qualitative difference of the effect in for different ratios of l/R, we proceed to the detailed quantitative analysis of the cases enumerated above.

2. CASE $l \ll R$. THE OSCILLATING PART OF THE MAGNETIC MOMENT OF A FLAT METALLIC SPECIMEN

Let us consider first the character of the inhomogeneity of the magnetic field inside the specimen. For $l \ll R$, the surface of the metal can be considered flat and therefore the magnetic field inside the sample, $H(x, t)$, is a function of t and the cartesian coordinate x, whose axis is perpendicular to the surface of the metal. The problem of the distortion of the given variable magnetic field $H_0 = f(t)$ inside a plane, half-bounded metal reduces to the solution of a one-dimensional thermal conductivity equation with corresponding boundary conditions:

$$H(x, t) = \frac{2}{\sqrt{\pi}} \int_{x/2\sqrt{qt}}^{\infty} f\left(t - \frac{x^2}{4q\xi^2}\right) e^{-\xi^2} d\xi. \tag{8}$$

In this case, naturally, it is assumed that q in Eq. (8) does not depend on the magnetic field.

If T is not very small (so that l is significantly larger than the mean radius of the electron orbit in the magnetic field), then the magnetic field in the metal changes so smoothly with increase in x that for the determination of the oscillating part of the magnetic moment in the variable field we can use the formula

$$M_{osc}(t) = G \sum_{n=1}^{\infty} \int_0^{\infty} \Psi_n[H(x, t)] \cos\left(\frac{an}{H(x,t)} + \varphi_n\right) dx; \tag{9}$$

G is the surface area of the metal and $H(x, t)$ is determined from (8).

Making use of the fact that $\alpha/H_0 \gg 1$, and that $\Psi_n(H)$ is a smooth function of H, we easily obtain the asymptotic expansion of (9) in powers of H/α. A similar expression for the asymptotic estimates, which is computed by the method of "critical points,"[4] is different for the interval $0 < t < t_0$ [when there is no point of stationary phase of the oscillating factor in Eq. (9)] and the interval $t > t_0$ [when there is a point of stationary phase at the depth $x = x_0(t)$]. The instant of time t_0 at which $\partial H/\partial x = 0$ for $x = +0$ can be estimated by noting that it is determined from the condition

$$\int_1^{\infty} f'\left[t_0\left(1 - \frac{1}{u^2}\right)\right] \frac{du}{u^3} = 0. \tag{10}$$

For the estimate it suffices to approximate the function $f(t)$ by means of two quadratic parabolas which have a common apex coinciding with f_{max} and which pass through zero at the points $t = 0$ and $t = T$. Then $f(t)$ is represented in the form

$$f(t) = \begin{cases} 2f_{max} t_m^{-2}(t_m - t), & 0 < t < t_m, \\ 2f_{max}(T - t_m)^{-2}(t_m - t), & t_m < t < T, \end{cases} \tag{11}$$

and for t_0 we get [from (10)] a third-degree algebraic equation. The analysis of this equation shows

that the quantity t_0 depends on the ratio of the time t_m in which the external field increases in the pulse, to the total duration of the pulse T, and increases almost linearly with T:*

$$t_0 = {}^3/_2\, t_m = {}^3/_4\, T \quad \text{for} \quad T = 2t_m,$$
$$t_0 \approx 0.6\,(1 + 0.4\, t_m/T)\, T \quad \text{for} \quad T \gg t_m. \tag{12}$$

Inasmuch as the magnetic field in real pulses does not disappear for $t > T$, but only falls off to zero asymptotically (as is shown in the drawing above), then the real value of $|f(t)|$ (for $t \approx T$) is less than assumed in (11); therefore, Eqs. (12) can give a somewhat smaller value of t_0.

As an example of a magnetic field of the pulse type $H_0 = f(t)$, we consider the pulse

$$f(t) = Ae^{-\beta_1 t}\sinh\beta_2 t, \quad \beta_1 > \beta_2 > 0. \tag{13}$$

Such a field arises in a solenoid upon passage through it of the discharge current of a condenser.

If we assume that $\beta_1 \gg \beta_2$, then $t_m \approx 1/\beta_1$, and $t_0 \approx 2.7\, t_0$. So far as the duration of the pulse (13) is concerned, it appears natural to determine it in the following way. At the point of inflection of the curve $f = f(t)$ (for the case $t = 2t_m$), we draw a tangent to it, and continue the tangent to its intersection with the abscissa. The intercept gives the duration of the pulse T. It is seen that $T \approx 4t_m$, and the value of the function $f(t)$ at this point is $f(T) \approx 0.2 f_{max}$. For comparison with (12), we note that $t_0 \approx 0.68\, T$. Although there is some arbitrariness in the determination of the length of the actual pulse, we can still assume that the estimate (11) is in excellent agreement with the value of t_0 for the pulse of form (13).

For $t > t_0$, as was noted above, the interval of integration in (9) contains a point of stationary phase of the oscillating factor, the position of which changes with time. The dependence $x_0 = x_0(t)$ is completely determined by the form of the function $f(t)$, and is found from the equation

$$\int_1^\infty f'\left[t\left(1 - \frac{1}{u^2}\right)\right]\exp\left(-\frac{x^2}{4qt}u^2\right)\frac{du}{u^2} = 0. \tag{14}$$

To solve the transcendental equation (14) in the general case is not possible; however, we can establish the dependence of $x_0 = x_0(t)$ for small $t - t_0$ and x. This dependence is linear:

$$x_0 = \frac{qd}{|df/dt_0|}(t - t_0), \quad d = (\partial^2 H/\partial x\,\partial t)_{\substack{x=+0\\ t=t_0}} > 0.$$

Taking into account the different character of the inhomogeneity $H(x, t)$ in the time intervals $0 < t < t_0$ and $t > t_0$, we can easily obtain the principal term in the asymptotic expansion of $M_{osc}(t)$ in increasing power of H/α:

1. $0 < t < t_0$

$$M_{osc}(t) = G\sum_{n=1}^{\infty}\frac{\sqrt{\pi}}{\sqrt{2anb(0)}}\Psi_n[H_0(t)]\left\{\left[\frac{1}{2} - C\left(\frac{a(0)}{2}\sqrt{\frac{an}{b(0)}}\right)\right]\cos\left(\frac{an}{H_0(t)} - \frac{an}{4}\frac{a^2(0)}{b(0)} + \varphi_n\right)\right.$$
$$\left. - \left[\frac{1}{2} - S\left(\frac{a(0)}{2}\sqrt{\frac{an}{b(0)}}\right)\right]\sin\left(\frac{an}{H_0(t)} - \frac{an}{4}\frac{a^2(0)}{b(0)} + \varphi_n\right)\right\}. \tag{15}$$

2. $t > t_0$

$$M_{osc}(t) = G\sum_{n=1}^{\infty}\frac{\sqrt{\pi}}{\sqrt{2anb(x_0)}}\Psi_n[H(x_0, t)]\left\{\left[\frac{1}{2} + C\left(\frac{qd(t-t_0)\sqrt{anb(x_0)}}{|dH_0/dt|}\right)\right]\cos\left(\frac{an}{H(x_0, t)} + \varphi_n\right)\right.$$
$$\left. - \left[\frac{1}{2} + S\left(\frac{qd(t-t_0)\sqrt{anb(x_0)}}{|dH_0/dt|}\right)\right]\sin\left(\frac{an}{H(x_0, t)} + \varphi_n\right)\right\}. \tag{16}$$

The following notation is introduced and emplyed in Eqs. (15) and (16): $C(z)$ and $S(z)$ are the Fresnel cosine and sine integrals, respectively;

$$a(x) \equiv a(x, t) = \frac{\partial}{\partial x}\left(\frac{1}{H(x, t)}\right); \quad b(x) \equiv b(x, t) = \frac{1}{2}\frac{\partial^2}{\partial x^2}\left(\frac{1}{H(x, t)}\right).$$

*For the pulses usually obtained in experiment, $T \geq 2t_m$; therefore in what follows we shall be interested only in this case.

For all time intervals which do not include the small region in the neighborhood of t_0, Eqs. (15) and (16) are considerably simplified:

1. $t > 0$, но $t_0 - t \gg H_0^2(t_0)\sqrt{b(0, t_0)}/d\sqrt{\alpha}$ $M_{osc}(t) = G\sum_{n=1}^{\infty} \frac{1}{\alpha n a(0)} \Psi_n(H_0) \cos\left(\frac{\alpha n}{H_0} + \varphi_n + \frac{\pi}{2}\right)$.

2. $t - t_0 \gg |dH_0/dt_0|/qd\sqrt{\alpha b(0, t_0)}$ $M_{osc}(t) = G\sum_{n=1}^{\infty} \frac{\sqrt{\pi}}{\sqrt{\alpha n b(x_0)}} \Psi_n[H(x_0, t)] \cos\left(\frac{\alpha n}{H(x_0, t)} + \varphi_n + \frac{\pi}{4}\right)$.

These formulas confirm the fact that: (1) In the interval of time $0 \leq t < t_0$, not including the small interval about t_0, the period of the oscillation of the magnetic moment with change in the external magnetic field $\Delta(1/H_0)$ is the same as for constant field. For $t > t_0$, the period of the oscillation is determined by the value of the magnetic field intensity at the depth $x = x_0(t)$, and consequently depends in a complicated fashion on H_0; (2) The dependence of the amplitude of the oscillation on H_0 is different than in (1); the value of the amplitude of the oscillation is considerably smaller than in a constant field, since it is proportional not to the volume of the entire metal, but to the volume of that layer which gives the fundamental contribution to the oscillation of the magnetic moment. For $t < t_0$, this layer is the surface layer, whose thickness $\sim 1/\alpha a(0) \sim l(H_0/\alpha)$, while for $t > t_0$, the layer is found at the depth $x = x_0(t)$ and has the thickness

$$\sim (\alpha b(x_0))^{-1/2} \sim l(H(x_0)/\alpha)^{1/2}.$$

3. CASE $l \lesssim R$. CYLINDRICAL SPECIMEN IN A PULSED FIELD

For the case of definite dimensions of the metal, we consider a specimen in the form of a circular cylinder of radius R, whose axis is parallel to the applied field. The variable magnetic field in such a specimen, $H(\rho, t)$, is a function of the distance ρ from the axis of the cylinder, and the solution of the differential equation (3) with boundary conditions $H(R, t) = f(t)$ leads to the following expression:*

$$H(\rho, t) \doteq f(t) - 2\sum_{k=1}^{\infty} \frac{J_0(y_k \rho/R)}{y_k J_1(y_k)} \exp\left\{-\left(y_k \frac{l}{R}\right)^2 \frac{t}{T}\right\} \int_0^{t/T} \frac{df}{d\tau} \exp\left\{\left(y_k \frac{l}{R}\right)^2 \tau\right\} d\tau, \qquad (17)$$

where $J_n(z)$ is the Bessel function of order n, and y_k is the k-th root of the equation $J_0(z) = 0$.

The oscillating part of the magnetic moment of a cylindrical specimen is determined by a formula similar to (9), namely,

$$M_{osc}(t) = 2\pi L \sum_{n=1}^{\infty} \int_0^R \Psi_n[H(\rho, t)] \cos\left(\frac{\alpha n}{H(\rho, t)} + \varphi_n\right) \rho d\rho; \qquad (18)$$

L is the length of the cylinder and $H(\rho, t)$ was defined in (17).

As we saw in Sec. 2, the result of integration in (18) depends on the position of the instant $t = t_0$ on the time axis; therefore, we shall first find (or estimate) t_0.

The instant t_0 is most simply determined in the case $l \gg R$, with the analysis of which we begin. We turn our attention to the fact that the right hand side of (17) contains (under the summation sign) integrals of the type

$$I = \int_0^z \psi(\tau) e^{w\tau} d\tau,$$

which depend on the large parameter $w = (y_k l/R)^2 \gg 1$. We can easily convince ourselves that the asymptotic value of I for $w \gg 1$ has the form:

$$I \approx \frac{1}{w} e^{wz} \left\{\psi(z) - \frac{1}{w}\psi'(z) + \ldots\right\}, \quad w \gg 1. \qquad (19)$$

*Here and in what follows, we shall consider that $l = \sqrt{qT}$.

If we make use of the asymptotic value of (19), we then obtain the expansion of $H(\rho, t)$ in increasing powers of $(R/l)^2$ from (17):

$$H(\rho, t) = f(t) + \frac{1}{4} T\dot{f}(t) \frac{\rho^2 - R^2}{l^2} + \frac{1}{64} T^2 \ddot{f}(t) \frac{\rho^4 - 4\rho^2 R^2 + 3R^4}{l^4} + \ldots \quad (20)$$

In order to put the expression for $H(\rho, t)$ in the form (20), we have introduced an obvious expansion of the functions z^{2p} in Fourier-Bessel series.

From (20) there follows the expansion of the derivative

$$\frac{\partial H}{\partial \rho} \approx \frac{\rho T}{2l^2} \left\{ \dot{f}(t) + \frac{1}{8} T\ddot{f}(t) \frac{\rho^2 - 2R^2}{l^2} \right\}.$$

The instant of time t_0 is determined by the condition $(\partial H/\partial \rho)_{\rho = R} = 0$, from which it follows that

$$\dot{f}(t_0) = {}^1/_8 (R/l)^2 T\ddot{f}(t_0); \quad (21)$$

$$|\dot{f}(t_0)| \ll T|\ddot{f}(t_0)| \sim f_{\max}/T. \quad (22)$$

The inequality (22) shows that the absolute value of the derivative $\dot{f}(t_0)$ is very small, while the latter signifies that t_0 is close to the point of the maximum of the external magnetic field t_m.

In this connection we can set

$$\dot{f}(t_0) = (t_0 - t_m)\ddot{f}(t_m), \quad \ddot{f}(t_0) \approx \ddot{f}(t_m),$$

and we then obtain the value of t_0 from (21):

$$t_0 = t_m + {}^1/_8 (R/l)^2 T. \quad (23)$$

For $t > t_0$, the range of integration in (18) contains some value $\rho = \rho_0$, which corresponds to the stationary phase of the cosine. The position of the point $\rho = \rho_0(t)$ is determined by the formula

$$\rho_0 = R\sqrt{1 - 8(l/R)^2 (t - t_0)}.$$

which comes from the condition $\partial H/\partial \rho = 0$.

But, inasmuch as in the given case, $l^2 \gg R^2$, then $\rho_0(t)$ falls off very quickly with increase in $t - t_0$, and after a short interval of time Δt, the point of stationary phase "falls back" on the axis of the cylinder. This time interval is given by

$$\Delta t = {}^1/_8 (R/l)^2 T. \quad (24)$$

We note that we can make use of Eqs. (23) and (24) over a rather wide range of values of l/R. Actually, both of these are derived under the assumption $w \gg 1$, but inasmuch as $y_1 \approx 2.4$, $y_2 \approx 5.5$, etc.; then, even for $l = 2R$ the parameter $w \gg 1$, and Eqs. (23), (24) remain in force. This allows us to think that Eqs. (23) and (24) can give the correct estimate of the order of magnitude of t_0 and Δt for all $l \gtrsim R$.

We now proceed to calculate $M_{osc}(t)$.

(a) Pulses of long duration: $l \gtrsim R(\alpha/H)^{1/2}$.

The magnetic field inside the specimen for $l \gg R$ changes little with depth, and if we leave only the first components in (20), we have the expression

$$H(\rho, t) = f(t) - {}^1/_4 (R/l)^2 T\ddot{f}(t)[1 - (\rho/R)^2]. \quad (25)$$

It is evident from (25) that the total change of the magnetic field throughout the depth of the specimen is equal to

$$H(R, t) - H(0, t) = {}^1/_4 (R/l)^2 T\ddot{f}(t) \sim (R/l)^2 H. \quad (26)$$

On the other hand, the change in the magnetic field ΔH which corresponds to the period of oscillation M_{osc} is determined by the relation

$$\Delta H = 2\pi (H/\alpha) H. \quad (27)$$

Comparing (26) and (27), we can conclude that two different cases are possible:

1) $(R/l)^2 \ll H/\alpha \ll 1$. In this case, the magnetic field changes so slightly with change of ρ from R to 0 that the phase of the oscillating factor in the integrand of (18) remains practically unchanged. Con-

sequently, in the calculation of the oscillating part of the magnetic moment of the specimen, we can make use of Eq. (1), assuming $H = H_0(t) = f(t)$.

2) $R \sim l(H/\alpha)^{1/2}$. In this case the change in phase of the cosine in (18) over the interval of integration ($0 < \rho < R$) is of the same order of magnitude as its period. It therefore follows that in the interval it is not possible to neglect the dependence of the magnetic field on ρ, but asymptotic expansion of the integral is also not possible. We can make use only of the theorem of the mean:

$$M_{osc}(t) = 2\pi L \sum_{n=1}^{\infty} \cos\left(\frac{\alpha n}{H^*(t)} + \varphi_n\right) \int_0^R \Psi_n[H(\rho, t)]\, \rho\, d\rho \approx V \sum_{n=1}^{\infty} \Psi_n[H_0(t)] \cos\left(\frac{\alpha n}{H^*(t)} + \varphi_n\right), \tag{28}$$

where $H^* = H(\rho^*, t)$ is the magnetic field at some internal point of the specimen $0 < \rho^*(t) < R$.

Inasmuch as the point of stationary phase of the cosine in (18) exists for a very short time $\Delta t = \frac{1}{8}(R/l)^2 T$, during which the magnetic field changes by the order of magnitude of a single period of oscillation, then consideration of the point of stationary phase does not change the equations (28) to any appreciable extent.

It follows from (28) that the oscillations of the magnetic moment in this case differ from the oscillations for a constant field only by some increased, complicated dependence of the argument of the oscillating factor on the applied field. As is evident from (25), the complication reduces to a shift in phase of the oscillation by an amount $\sim (R/l)^2(\alpha/H_0) \sim 1$, and to a small difference of the period from that in the constant field. If we denote the period of the oscillation of the magnetic moment with change in the external field by $\Delta(1/H_0)$, then it is determined by the expression:

$$\Delta(1/H_0) \doteq \frac{2\pi}{\alpha}\left[1 - \left(\frac{R}{l}\right)^2 \gamma(t)\left[1 - \left(\frac{\rho^*}{R}\right)^2\right]\right], \quad \gamma(t) = \frac{T}{4}\frac{d}{dt}\ln f(t); \tag{29}$$

$$2\pi/\alpha - \Delta(1/H_0) \sim (R/l)^2\, 2\pi/\alpha \sim (H_0/\alpha)\, 2\pi/\alpha. \tag{30}$$

The relations (30) indicate that the difference of $\Delta(1/H_0)$ from the period of oscillation in a constant field is very small.

(b) Short pulses: $l \lesssim R \gg l(H/\alpha)^{1/2}$.

For $l \sim R$, a change in the magnetic field over the thickness of the specimen is of the order of the magnetic field itself; therefore, Eq. (17) is not simplified, and calculations [even with a concrete form of the the function $f(t)$] are more difficult. Significant simplification takes place only for $l^2 \gg R^2 \gg l^2(H/\alpha)$, when we can make use of the expansion (20). However, if we make asymptotic estimates of the integrals in (18) by the method of "critical points," it is not difficult to obtain general relations of types (15) and (16) for $M_{osc}(t)$.

To simplify the description, we represent the oscillating part of the magnetic moment in the form of a sum

$$M_{osc}(t) = M^1_{osc}(t) + M^2_{osc}(t), \tag{31}$$

where the first term is the contribution to the oscillations of the magnetic moment of the surface layer of the specimen and the layer with a magnetic field that is stationary in depth, and the second is the contribution of the "core" of the specimen, i.e., the vicinity of the axis of the cylinder.

The component $M^1_{osc}(t)$ is determined from (15) and (16), in which we replace x by $x = R - \rho$, and in which the area of the surface corresponding to the layer is defined by

$$1)\ 0 < t < t_0, \quad G = 2\pi LR, \qquad 2)\ t > t_0, \quad G = 2\pi L\rho_0(t) = 2\pi L[R - x_0(t)].$$

The principal part of the expansion of the second component in increasing powers of H/α is equal to

$$M^2_{osc}(t) = 2\pi L \sum_{n=1}^{\infty} \frac{1}{2\alpha n g(t)} \Psi_n[H(t)] \cos\left(\frac{\alpha n}{H(t)} + \varphi_n + \frac{\pi}{2}\right), \tag{32}$$

where

$$H(t) = H(\rho, t)|_{\rho=0}, \quad g(t) = \frac{1}{2}\left(\frac{\partial^2}{\partial\rho^2}\frac{1}{H}\right)_{\rho=0} = b(R, t).$$

In the case $R^2 \ll l^2$, we can set

$$H(t) = H_0(t)[1 - (R/l)^2 \gamma(t)], \quad g(t) = -\gamma(t)/l^2 H_0(t). \tag{33}$$

For time intervals not including the small region about the time t_0, the equations stemming from (31) become simplified:

1) $t > 0$, но $t_0 - t \gg H_0^2(t_0)\sqrt{b(0, t_0)}/d\sqrt{\alpha}$

$$M_{osc}(t) = 2\pi L \sum_{n=1}^{\infty} \frac{1}{\alpha n}\left[\frac{R}{a(0)}\Psi_n(H_0)\cos\left(\frac{\alpha n}{H_0(t)} + \varphi_n + \frac{\pi}{2}\right) + \frac{1}{2g(t)}\Psi_n[H(t)]\cos\left(\frac{\alpha n}{H(t)} + \varphi_n + \frac{\pi}{2}\right)\right]. \tag{34}$$

2) $t - t_0 \gg |dH_0/dt|/qd\sqrt{ab(0, t)}$ $M_{osc}(t) = 2\pi L \rho_0(t) \sum_{n=1}^{\infty} \frac{\sqrt{\pi}}{\sqrt{\alpha n b(x_0)}} \Psi_n[H(x_0)]\cos\left(\frac{\alpha n}{H(x_0)} + \varphi_n + \frac{\pi}{4}\right)$. (35)

It can be shown that the time interval (0, T) contains the moment t_1, in which the point with stationary phases of the oscillating factor "falls back" on the axis: $\rho_0(t_1) = 0$. Then in a small region about t_1 [where Eq. (35) is comparable in value with (32) and thereafter completely disappears] and for $t > t_1$, $M_{osc}(t)$ is again determined by the expression (34).

In the case $l \sim R$, the oscillations of the magnetic moment are connected in very complicated fashion with the direction of the applied magnetic field. As is evident from (34), M_{osc} consists of two terms of the same order of magnitude in the time ragnes $0 < t < t_0$ and $t > t_1$. These terms have different periods, with different dependences on the external field. Over a sufficiently long time interval $\Delta t = t_1 - t_0 \sim T$, the dependence of $M_{osc}(t)$ on the external magnetic field becomes even more complicated.

Some singular characteristics of the oscillations appear in the case $1 \gg (R/l)^2 \gg H/\alpha$, which probably corresponds to experimental conditions.[1] Since for $R^2 \ll l^2$, we can limit ourselves in the calculations to the approximate formulas (33); then in the duration of the total pulse, after elimination of the short time interval $\Delta t = \frac{1}{2}(R/l)^2 T$ in the vicinity of the maximum point of the external field, $M_{osc}(t)$ is determined by the expression:

$$M_{osc}(t) = 2\pi l^2 L \frac{H_0(t)}{\alpha\gamma(t)} \sum_{n=1}^{\infty} \frac{1}{n}\Psi_n[H_0(t)]\sin\left[\frac{\alpha n}{2H_0}\left(\frac{R}{l}\right)^2\gamma(t)\right]\sin\left\{\frac{\alpha n}{H_0(t)}\left[1 + \frac{1}{2}(R/l)^2\gamma(t)\right] + \varphi_n + \frac{\pi}{2}\right\}. \tag{36}$$

The oscillations of the magnetic moment in (36) have the characteristic binary form. The period of the fundamental vibration is determined by a formula of the type (29):

$$\Delta(1/H_0) = (2\pi/\alpha)\left[1 - \frac{1}{2}(R/l)^2\gamma(t)\right],$$

while the "binary period" has the following order of magnitude:

$$\Delta_6(1/H_0) \sim (2\pi/\alpha)(l/R)^2 \gg 2\pi/\alpha.$$

In the experiments of Shoenberg,[1] the oscillating binary form was actually observed.

Finally, it should be emphasized that in the analysis of experiments according to the measurement of the oscillating part of the magnetic moment of the metal, it is necessary, generally speaking, to take into account the presence of certain groups of electrons which create well known additional difficulties in the interpretation of experimental results.

In conclusion, we take this opportunity to express our gratitude to Prof. I. M. Lifshitz for his valuable advice, discussions, and interest in the work.

[1] D. Shoenberg, Physica 19, 791 (1953); D. Shoenberg, Lectures at a conference on the physics of magnetic phenomena, Moscow, 1956.

[2] I. Lifshitz and A. Kosevich, J. Exptl. Theoret. Phys. (U.S.S.R.) 29, 730 (1955); Soviet Phys. JETP 2, 636 (1956).

[3] H. Carslaw and J. Jaeger, Conduction of Heat in Solids, (Oxford, Clarendon Press, 1947).

[4] J. G. Van der Corput, Proc. Acad. Sci. (Amsterdam) 51, 650 (1948).

Translated by R. T. Beyer
140

SOVIET PHYSICS JETP VOLUME 6 (33), NUMBER 3 MARCH, 1958

THE OPTICAL MODEL OF THE NUCLEUS AND THE SHELL MODEL

P. E. NEMIROVSKII

Submitted to JETP editor March 16, 1957

J. Exptl. Theoret. Phys. (U.S.S.R.) 33, 746-749 (September, 1957)

We investigate the bound states of a neutron in a potential whose parameters are obtained from the optical model of the nucleus, plus a spin-orbit interaction. Agreement with experimental data is obtained for the ordering of single particle levels for nuclei consisting of a closed shell plus one nucleon.

IT is known that the shell model is successful only for nuclei consisting of a closed shell or of a closed shell plus one particle. For nuclei which have one particle outside of a closed shell, the excited states can be divided into two groups. Among the levels belonging to the first group are those which have a high probability of excitation in (n, γ), (p, γ), (d, p), and (d, n) reactions. Such levels are usually called single particle levels, since it is assumed that they occur when the odd nucleon occupies a level in the field of the core. Other levels are excited weakly in the reactions cited; this may be regarded as a consequence of a change of state of the core in the formation of such levels. This notion is confirmed in various cases by the values of the spin and parity of the levels (for example, for O^{17}). The latest experiments of Groshev and co-workers[1] on (n, γ) reactions and the experiments of several authors on (d, p) reactions have shown that in many other odd nuclei one group of levels is excited very strongly compared to the other levels. The data on (d, p) reactions, which refer to states with arbitrary angular momentum, are especially instructive. These experiments show that single particle levels occur quite commonly, i.e., the model using an average core field has a wide range of validity. One may raise the question whether the scheme of single-particle levels could be obtained from a potential well model. In doing this it would be desirable for the parameters of the potential well to be determined from other experiments.

There is a direct connection between the problem of single particle levels and that of the broad neutron resonances which have been explained on the basis of the optical model. The first model of Weisskopf, Feshbach, and Porter,[2] which used a square well, was crude and did not explain the large value of the reaction cross section at low energies. Later, the present author[3] improved this model by considering a nucleus with a diffuse edge. The model enables one to explain the fundamental regularities in neutron cross sections, angular distributions and polarizations for scattering by medium and heavy nuclei (excluding the case of highly deformed nuclei).

Computations of cross sections done on the "Strela" computer enabled us to obtain the most reasonable set of parameters for describing the nuclear potential.

1. CHOICE OF POTENTIAL

The potential is complex. The assumption was made that a potential with the same parameters, but omitting the imaginary part (so that there are no incoming waves), should describe the stationary single particle levels. The parameters of this potential turned out to be quite close to those used in the calculations of Ross et al.,[4] although they differed from their values in various respects. The real part of the optical potential consists of two terms:

1) the average potential, which is the same for all l and j, and is equal to

$$V_1 = V_0 \Big/ \left[1 + \exp\left(\frac{r - R_0}{a}\right)\right];$$

2) the spin-orbit interaction, which is chosen in the form

$$V_2 = \frac{\varkappa}{r} \frac{dV_1}{dr} (\mathbf{l} \cdot \boldsymbol{\sigma}).$$

The constant in the spin-orbit interaction was taken from the experiments of Levintov,[5] whom the au-

thor wishes to thank. This value, $\kappa = 3.3 \times 10^{-27}$ cm^2 is somewhat lower than that of Ross et al. A calculation of the polarization of 400 kev neutrons shows that this value of κ is in agreement with the experiments of Adair. The quantity α which characterizes the diffuseness of the boundary was taken equal to $1/k_0$, where

$$k_0 = \sqrt{2mV_0}/h$$

This value of α gives reasonable values for the neutron strength function. The values of k_0 and R_0 were selected by comparing calculated and experimental curves of total cross sections and angular distributions. The final parameter values chosen were: $V_0 = 50$ Mev, $R_0 = 1.23 \times 10^{-13}\ A^{1/3}$ cm.

With this potential, we calculated the dependence of level positions on R_0.

2. CALCULATION OF BOUND STATES

The calculation of bound states was done by hand computation. The solution of the Schrödinger equation was represented in the form

$$\psi = x^{-1/2} K_{l+1/2}(x)\, v_l(x),$$

where $x = \kappa r$ and $\kappa = \sqrt{-2mE}/h$, and E is the level energy. At infinity, $v_l(x) \to 1$. We tried to find a value of R_0 for which $v_l(x)$, for a preassigned value of E, goes to zero at $x = 0$. Then the function $\psi(x)$ satisfies the correct boundary conditions at $x = 0$ and $x = \infty$, and the corresponding value of E is the level energy for given R_0, l, and j. Level positions were calculated for energies from zero up to 8 — 9 Mev. There is no sense in computing lower levels since they are already filled and cannot appear as one-particle levels. Ross et al. computed precisely those levels whose binding energy is greater than or equal to the binding energy of the first occupied level. Thus our work fills the gap between the continuous spectrum and the first capture level. At present, the calculations have been done for 1s, $1p_{3/2}$, $1p_{1/2}$, 2s, $1d_{5/2}$, $1d_{3/2}$, $1f_{7/2}$, $2p_{3/2}$, $2p_{1/2}$, and $1f_{5/2}$, i.e., for nuclei with $A < 50$. For heavier nuclei the level positions are of less interest. The calculation is interesting once more only in the region of lead, for which we plan to do it later. The dependence of level energy on nuclear radius is shown in the figure.

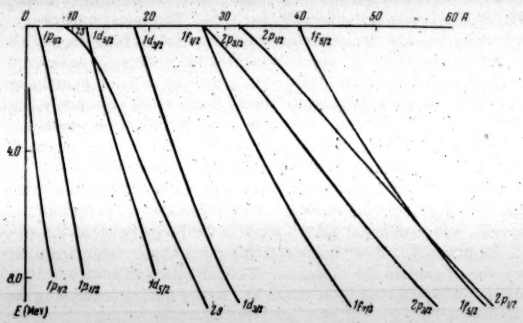

Dependence of Nuclear Energy Levels on Atomic Weight

The most important feature shown in the figure is the change in the order of levels with changing nuclear radius, i.e., the crossing of terms. When the nuclear radius is small or, what amounts to the same thing, when the term has a high excitation, the ordering is essentially different from the ordering of the ground states. Thus at high excitations the 2s level has lower energy than the $1d_{5/2}$, while the $1f_{5/2}$ lies above the $2p_{1/2}$, $2p_{3/2}$ levels. As we shift to the ground states, the $1d_{5/2}$ drops below the 2s level, while the $1f_{5/2}$ goes below the $2p_{1/2}$ level and, for large A, below the $2p_{3/2}$ level. This crossing of terms is caused by the centrifugal potential which, in nuclei of small radius, causes an appreciable increase in the energy of levels with large l, and pushes them into the continuous spectrum.

With increasing radius, the influence of the centrifugal potential diminishes, and levels with large l drop more rapidly than those with small l.

3. COMPARISON WITH EXPERIMENTAL DATA

We should like first to compare the level scheme we have obtained with the experimental data for nuclei consisting of a closed shell plus one particle. These are the nuclei O^{17} and Ca^{41}, and also those nu-

clei which correspond to a closed subshell plus one particle: C^{13}, Si^{29}, Si^{31}, and S^{33}. For the value of R_0 which we have used, the O^{16} nucleus has a radius of 3.11×10^{-13}. With this R_0, the order of the levels is the following: 1s, $1p_{3/2}$, $1p_{1/2}$, $1d_{5/2}$, 2s, $1d_{3/2}$. The 1s, $1p_{3/2}$, and $1p_{1/2}$ are filled, and the ninth neutron, in agreement with experiment, is in the $1d_{5/2}$ state, whose energy, according to the theoretical curve, is 4.1 Mev in good agreement with experiment. The first excited state is 2s. The experimental value of the excitation energy is 0.5 Mev less than calculated, but better quantitative agreement should not be expected. The $1d_{3/2}$ state lies at about 1 Mev up in the continuous spectrum, in complete agreement with experiment. Other low-lying states must be assumed to be empty.

Now we consider C^{13}. For this nucleus, the binding energy of the $1p_{1/2}$ ground state is in poor agreement with experiment (the computed value is 8 Mev). Such a deviation may be related to the inexact nature of the j-j approximation. If the coupling of orbital moment and spin is intermediate, then C^{12} does not represent a closed shell and the $1p_{1/2}$ level is not a rigorous single-particle level for C^{13}. On the other hand, the excited states have the opposite parity, and for them the field of the C^{12} nucleus may be considered to be some average field. It is therefore not surprising that better agreement with the theory is obtained for the excited 2s and $1d_{5/2}$ states. The energy of the excited state is about 1 Mev higher than the experimental value, but the order of the levels is the same as in experiment, and the splitting is $\sim$ 0.5 Mev instead of the experimental value of 0.7 Mev.

For nuclei with $A > 17$ the binding energy of the $1d_{5/2}$ state should not be compared with the theory, since there are now many particles in the $1d_{5/2}$ state, and their interaction with the last odd particle cannot be described by means of a self-consistent field. The single-particle 2s and $1d_{3/2}$ states must be assigned in each particular case. This can be done, for example, from the probability of excitation in deuteron stripping. If we assume that the ground state of Si^{29} is a single-particle 2s state, then the computed binding energy is 9.3 Mev, while experiment gives 8.5 Mev, so that the agreement is satisfactory. For S^{33} the ground state is $1d_{3/2}$, and the binding energy is also in satisfactory agreement with experiment. For nuclei with $N < 20$, the $1f_{7/2}$, $2p_{3/2}$, and $2p_{1/2}$ states should be excited. Since the parity of these states is opposite to that of the partially filled shells ($1d_{5/2}$, 2s, $1d_{3/2}$), the single-particle model can here give a satisfactory description even for incomplete shells, i.e., for any odd nucleus. Actually, the situation is made essentially more complicated by the large deformations of the nuclei in the region $20 < A < 30$. Experiments on the (n, γ) reaction indicate the presence of a bound $2p_{3/2}$ level for Mg^{25} (with a binding energy of 4 Mev). However, according to the calculation, for Mg^{25} the $1f_{7/2}$ and $2p_{3/2}$ states should still lie in the continuous spectrum. These states begin to be bound only at Si^{29}. Also the excitation energy of the $^3/_2^-$ state increases as we go to Si^{29}, which is in qualitative disagreement with the theory for spherical nuclei. For Si^{29} the $1f_{7/2}$ and $2p_{3/2}$ states have $E < 0$, but the excitation energies of these states are considerably higher than the experimental values. On the other hand, $\Delta E = E(f_{7/2}) - E(p_{3/2})$ is close to the experimental value. The agreement with experiment improves for S^{33}, although the excitation is again too high.

The level scheme for Ca^{41} is most interesting. It has been pointed out that for this nucleus, excited single-particle $2p_{3/2}$ and $2p_{1/2}$ states are observed, while the $1f_{5/2}$ state is not. According to the computation, the binding energy of the $1f_{5/2}$ state is close to zero, and one is unable to observe this state by, for example, deuteron stripping. The order of the other states and their energy differences are given more or less satisfactorily, but all the states have binding energies somewhat lower than the experimental values.

On the whole we may say that the optical model gives the correct order of excited single-particle states of light nuclei, but cannot give the position of individual levels with sufficient accuracy. This may be partially due to the fact that the $A^{1/3}$ law is not exact. A deviation of 1% from this law would be sufficient to shift a level by 0.5 Mev. In addition, the shape of the potential near the nuclear boundary is approximate. However, in some cases one may hope to go a little farther and calculate the probability of radiative transitions, starting from the singe-particle model.

[1] L. V. Groshev and A. M. Demidov, Атомная энергия (Atomic Energy) 3, 91 (1957).

[2] Feshbach, Porter, and Weisskopf, Phys. Rev. 96, 448 (1954).

[3] P. E. Nemirovskii, J. Exptl. Theoret. Phys. (U.S.S.R.) 30, 551 (1956), Soviet Phys. JETP 3, 484 (1956).

[4] Ross, Mark, and Lawson, Phys. Rev. 102, 1613 (1956).
[5] I. I. Levintov, Dokl. Akad. Nauk SSSR 107, 240 (1956), Soviet Phys. "Doklady" 1, 175 (1956).

Translated by M. Hamermesh
141

SOVIET PHYSICS JETP VOLUME 6 (33), NUMBER 3 MARCH, 1958

SCATTERING OF ELECTROMAGNETIC WAVES IN A PLASMA

A. I. AKHIEZER, I. G. PROKHODA, and A. G. SITENKO

Khar'kov State University

Submitted to JETP editor March 18, 1957

J. Exptl. Theoret. Phys. (U.S.S.R.) 33, 750-757 (September, 1957)

Combination scattering by plasma density oscillations may occur when electromagnetic waves are propagated in a plasma. The intensity of combination scattering of electromagnetic waves in a plasma is determined in the absence and in the presence of a constant uniform magnetic field.

1. It is well known that there can exist in a plasma weakly damped electromagnetic oscillations which are associated with oscillations of plasma density whose frequency (without taking dispersion into account) is given by[1] $\Omega = \sqrt{4\pi n_0 e^2/m}$. The existence of these oscillations leads to a periodic variation of the dielectric constant in the plasma. Because of this, combination scattering of electromagnetic waves propagated in the plasma becomes possible, i.e., if a wave of frequency $\omega_0 > \Omega$ is propagated in the plasma then at the same time waves with frequencies $\omega = \omega_0 \pm n\Omega$, where n is an integer, will also be propagated. The object of this paper is to determine the intensity of these waves.

Let us first determine the dielectric constant of the plasma. We start with the equation

$$\operatorname{curl} \mathbf{H} = \frac{1}{c}\frac{\partial \mathbf{D}}{\partial t} = \frac{1}{c}\frac{d\mathbf{E}}{dt} + \frac{4\pi}{c}\mathbf{j}_{\text{free}}, \tag{1}$$

where $\mathbf{j}_{\text{free}}$ is the current density associated with the motion of the plasma electrons and is equal to $\mathbf{j}_{\text{free}} = en\mathbf{v}$, n is the electron density, $\mathbf{v}$ is the electron velocity which is related to the electric field by the equation $\dot{\mathbf{v}} = e\mathbf{E}/m$. From these equations it follows that

$$\mathbf{v}(\mathbf{r}, t) = \frac{e}{m}\int^t \mathbf{E}(\mathbf{r}, t')\,dt',$$

$$\mathbf{j}_{\text{free}}(\mathbf{r}, t) = \frac{e^2}{m} n(\mathbf{r}, t)\int^t \mathbf{E}(\mathbf{r}, t')\,dt'.$$

Substituting this expression for $\mathbf{j}_{\text{free}}$ into Eq. (1), we find

$$\frac{\partial \mathbf{D}}{\partial t} = \frac{\partial \mathbf{E}}{\partial t} + \frac{4\pi e^2}{m} n(\mathbf{r}, t)\int^t \mathbf{E}(\mathbf{r}, t')\,dt'.$$

We now introduce the dielectric constant operator by $\mathbf{D} = \hat{\varepsilon}\mathbf{E}$. Then

$$\hat{\varepsilon}(\mathbf{r}, t)\,\mathbf{E}(\mathbf{r}, t) = \mathbf{E}(\mathbf{r}, t) + \frac{4\pi e^2}{m}\int^t dt' n(\mathbf{r}, t')\int^{t'} dt'' \mathbf{E}(\mathbf{r}, t''). \tag{2}$$

Let the electric field vary with time in accordance with the harmonic law $\mathbf{E}(\mathbf{r}, t) = \mathbf{E}(\mathbf{r})e^{-i\omega t}$. The result of applying the dielectric constant operator to $\mathbf{E}(\mathbf{r}, t)$ reduces in this case to multiplication by

$$\varepsilon_\omega(\mathbf{r}, t) = 1 - \frac{4\pi e^2}{im\omega} e^{i\omega t} \int^t dt' n(\mathbf{r}, t') e^{-i\omega t'}. \tag{3}$$

We now note that the plasma electron density $n(\mathbf{r}, t)$ contains the constant term n_0 plus a small additional term $\delta n(\mathbf{r}, t) = \delta n(\mathbf{r}) \cos \Omega t$, $\delta n \ll n_0$. Therefore

$$\varepsilon_\omega(\mathbf{r}, t) = \varepsilon(\omega) + \delta\varepsilon_\omega(\mathbf{r}, t), \tag{4}$$

where

$$\varepsilon(\omega) = 1 - \frac{\Omega^2}{\omega^2}, \quad \delta\varepsilon_\omega(\mathbf{r}, t) = -\frac{2\pi e^2 \delta n(\mathbf{r})}{m\omega}\left(\frac{e^{i\Omega t}}{\omega - \Omega} + \frac{e^{-i\Omega t}}{\omega + \Omega}\right).$$

If we introduce the operator for the fluctuation in the dielectric constant

$$\hat{\delta\varepsilon} = (\hat{\varepsilon} - 1)^{1/2} \frac{\delta n(\mathbf{r}, t)}{n_0} (\hat{\varepsilon} - 1)^{1/2}, \tag{5}$$

where $\hat{\varepsilon}$ is the operator for the dielectric constant of a plasma of density n_0 which is determined by means of the formula

$$\hat{\varepsilon} e^{-i\omega t} = \varepsilon(\omega) e^{-i\omega t},$$

then

$$\hat{\delta\varepsilon} e^{-i\omega t} = \delta\varepsilon_\omega(\mathbf{r}, t) e^{-i\omega t}.$$

2. Let the plane monochromatic wave $\mathbf{E}_0(\mathbf{r}, t) = \mathbf{e}_0 E_0 \exp(i\mathbf{k}_0 \cdot \mathbf{r} - i\omega_0 t)$ be propagated in the plasma. Then the electric and magnetic fields of the scattered wave may be determined by means of Maxwell's equations in which the current and charge densities have in the first approximation the form

$$\mathbf{j} = \frac{1}{4\pi} \frac{\partial}{\partial t} (\hat{\delta\varepsilon} \mathbf{E}_0), \quad \rho = -\frac{1}{4\pi} \operatorname{div} (\hat{\delta\varepsilon} \mathbf{E}_0). \tag{6}$$

Since $\delta\epsilon$ has a time dependence of the form $e^{\mp i\Omega t}$ the current $\mathbf{j}$ will excite a wave of frequency $\omega_0 \pm \Omega$. In the second approximation we would obtain the current

$$\mathbf{j}' = \frac{1}{4\pi} \frac{\partial}{\partial t} (\hat{\delta\varepsilon} \mathbf{E}),$$

where $\mathbf{E}$ is the electric field of the scattered wave. This current obviously excites a wave of frequency $\omega_0 \pm 2\Omega$, etc. Thus in a plasma when an electromagnetic wave of frequency ω_0 is being propagated combination frequencies $\omega_0 \pm n\Omega$ arise where n is an integer. In future we shall restrict ourselves to an investigation only of the combination frequencies $\omega_0 \pm \Omega$.

Introducing instead of the field instensities $\mathbf{E}$ and $\mathbf{H}$ of the scattered wave the vector and the scalar potentials $\mathbf{A}$ and φ and assuming that $\operatorname{div} \mathbf{A} = 0$ we shall start with the following basic equations:

$$\Delta\mathbf{A} - \frac{\hat{\varepsilon}}{c^2} \frac{\partial^2 \mathbf{A}}{\partial t^2} - \frac{\hat{\varepsilon}}{c} \frac{\partial}{\partial t} \operatorname{grad} \varphi = -\frac{4\pi}{c} \mathbf{j}, \tag{7}$$

$$\hat{\varepsilon}\Delta\varphi = -4\pi\rho. \tag{8}$$

The increase per unit time in the energy of the electromagnetic field is given by the expression

$$\frac{\partial W}{\partial t} = \frac{1}{8\pi} \operatorname{Re} \int \left\{ \mathbf{E} \frac{\partial \mathbf{D}^*}{\partial t} + \mathbf{H} \frac{\partial \mathbf{H}^*}{\partial t} \right\} dv = \frac{1}{2} \operatorname{Re} \frac{1}{c} \int \mathbf{j}\mathbf{A}^* dv + \frac{1}{2} \operatorname{Re} \int \rho\varphi^* dv,$$

where $\mathbf{D}$ is the electric displacement vector. Here the first term determines the increase in the energy of the transverse oscillations of the electromagnetic field, i.e., the intensity of scattering of electromagnetic waves

$$I = \frac{1}{2c} \operatorname{Re} \int \mathbf{j}\mathbf{A}^* dv, \tag{9}$$

while the second term determines the increase in the energy of the longitudinal oscillations of the plasma

$$I' = \frac{1}{2}\,\mathrm{Re}\int \rho\dot{\varphi}^{*}\,dv. \tag{10}$$

3. We seek a solution of Eq. (7) of the form

$$\mathbf{A}(\mathbf{r}, t) = \sum_{\lambda} q_{\lambda}(t)\,\mathbf{A}_{\lambda}(\mathbf{r}), \tag{11}$$

where

$$\Delta\mathbf{A}_{\lambda} + k_{\lambda}^{2}\mathbf{A}_{\lambda} = 0,\quad \mathbf{A}_{\lambda}(\mathbf{r}) = \mathbf{e}^{\lambda}\left(4\pi c^{2}/\varepsilon(\omega_{\lambda})\right)^{1/2} e^{i\mathbf{k}_{\lambda}\mathbf{r}}. \tag{12}$$

$\mathbf{e}^{\lambda}$ is the polarization unit vector ($\mathbf{e}^{\lambda}\cdot\mathbf{k}_{\lambda} = 0$); $\mathbf{k}_{\lambda}$ and ω_{λ} are related by the dispersion relation $\omega_{\lambda}^{2} = k_{\lambda}^{2}c^{2}/\epsilon(\omega_{\lambda})$, while the constant has been chosen so that the following normalization condition is satisfied

$$\int \mathbf{A}_{\lambda}\mathbf{A}_{\lambda'}^{*}\,dv = \left(4\pi c^{2}/\varepsilon(\omega_{\lambda})\right)\delta_{\lambda\lambda'}$$

(the index λ determines both $\mathbf{k}$ and the polarization).

Using (7) and noting that

$$\int \varepsilon\,\mathrm{grad}\,\dot{\varphi}\mathbf{A}_{\lambda}^{*}\,dv = 0,$$

we obtain the following equation for the determination of q_{λ}:

$$\ddot{q}_{\lambda} + \omega_{\lambda}^{2}q_{\lambda} = f_{\lambda}(t),\quad f_{\lambda}(t) = \frac{1}{c}\int \mathbf{j}\mathbf{A}_{\lambda}^{*}\,dv. \tag{13}$$

This equation has the form of the equation for the forced vibrations of an oscillator acted on by the force $f_{\lambda}(t)$.

Setting

$$f_{\lambda}(t) = \sum_{\omega} b_{\lambda}^{\omega}e^{-i\omega t},$$

we shall write the solution of (13) in the form[2,3]

$$q_{\lambda} = \frac{1}{2\omega_{\lambda}}\sum_{\omega}\left\{\frac{1}{\omega_{\lambda}-\omega} + i\pi\delta(\omega_{\lambda}-\omega)\right\}b_{\lambda}^{\omega}e^{-i\omega t}. \tag{14}$$

We substitute the expansion (11) into (9). Making use of (14) we obtain the following formula for the intensity of scattering:

$$I = \frac{\pi}{4}\sum_{\omega}\sum_{\lambda=1,2}\int |b_{\lambda}^{\omega}|^{2}\delta(\omega_{\lambda}-\omega)\,\frac{d\mathbf{k}_{\lambda}}{(2\pi)^{3}}, \tag{15}$$

where the summation is taken over the two polarization directions of the scattered wave.

Making use of the relation between the fluctuation in the dielectric constant and the deviation of the electron density from its equilibrium value we shall obtain the current that appears in (7)

$$\mathbf{j} = -\frac{i}{8\pi}\sum_{\omega-\omega_{0}\,\Omega}[1-\varepsilon(\omega)]^{1/2}[1-\varepsilon(\omega_{0})]^{1/2}\frac{\delta n(\mathbf{r})}{n_{0}}\,\omega E_{0}\mathbf{e}_{0}e^{i\mathbf{k}_{0}\mathbf{r}-i\omega t}. \tag{16}$$

Substituting this expression into (13) we obtain

$$b_{\lambda}^{\omega} = -\frac{iE_{0}\omega}{4\sqrt{\pi n_{0}}\sqrt{\varepsilon(\omega)}}[1-\varepsilon(\omega)]^{1/2}[1-\varepsilon(\omega_{0})]^{1/2}(\mathbf{e}_{0}\mathbf{e}^{\lambda})\,\delta n_{\mathbf{k}-\mathbf{k}_{0}},\qquad \delta n_{\mathbf{k}-\mathbf{k}_{0}} = \int \delta n(\mathbf{r})\,e^{-i(\mathbf{k}-\mathbf{k}_{0})\mathbf{r}}\,d\mathbf{r}.$$

From this, in accordance with (15), we obtain the following expression for the intensity of scattering of electromagnetic waves:

$$I = \sum_{\omega-\omega_{0}\in\Omega}\int I_{\omega}(\vartheta, \varphi)\,d\sigma, \tag{17}$$

$$I_\omega(\vartheta, \varphi) = \frac{2E_0^2 V\varepsilon(\omega)}{(8\pi)^3 n_0^2 c^3}\omega^4[1-\varepsilon(\omega)][1-\varepsilon(\omega_0)]\overline{|\delta n_{\mathbf{k}-\mathbf{k}_0}|^2}\{\cos^2\varphi + \sin^2\varphi\cos^2\vartheta\}, \quad (18)$$

ϑ is the angle between the propagation vector of the scattered wave $\mathbf{k}$ and the wave vector of the incident wave $\mathbf{k}_0$, while φ is the angle between the direction of polarization of the incident wave $\mathbf{e}_0$ and the normal to the plane $(\mathbf{k}_0, \mathbf{k})$. The average value of the square of the absolute value of the Fourier component of the fluctuation in the electron density which appears in (18) may be expressed in terms of the Fourier component of the correlation function

$$\overline{|\delta n_{\mathbf{k}}|^2} = n_0\{1+\nu_{\mathbf{k}}\}, \quad \nu_{\mathbf{k}} = \int \nu(\mathbf{r})\, e^{-i\mathbf{k}\mathbf{r}}dv.$$

(The correlation function is defined, as is well known, by means of the relation

$$n_0\nu(\mathbf{r}_2-\mathbf{r}_1) = \overline{\delta n(\mathbf{r}_1)\,\delta n(\mathbf{r}_2)} - n_0\delta(\mathbf{r}_2-\mathbf{r}_1).)$$

Thus

$$I_\omega(\vartheta, \varphi) = \frac{2E_0^2 V\varepsilon(\omega)\omega^4}{(8\pi)^3 n_0 c^3}[1-\varepsilon(\omega)][1-\varepsilon(\omega_0)]\,(1+\nu_{\mathbf{k}-\mathbf{k}_0})(\cos^2\varphi + \sin^2\varphi\cos^2\vartheta). \quad (18')$$

On expanding $\delta n(\mathbf{r}, t)$ into plane waves

$$\delta n(\mathbf{r}, t) = \sum_{\mathbf{k}} \delta n_{\mathbf{k}}(t)\, e^{i\mathbf{k}\mathbf{r}},$$

one may obtain the total energy of the plasma in the form

$$\int\left\{\frac{n_0 m(\delta v)^2}{2} + \frac{ms^2}{2n_0}(\delta n)^2 + \frac{(\delta E)^2}{8\pi}\right\}dv = \sum_{\mathbf{k}}{}' \frac{m}{2n_0k^2}\{|\dot{\delta n}_{\mathbf{k}}|^2 + \omega_{\mathbf{k}}^2|\delta n_{\mathbf{k}}|^2\},$$

where

$$\omega_{\mathbf{k}}^2 = \Omega^2 + k^2s^2, \quad s^2 = (\partial p/\partial\rho)_T$$

(p is the pressure, ρ is the density).

If one assumes that the equipartition law holds, then

$$\overline{(m/2n_0k^2)\{|\dot{\delta n}_{\mathbf{k}}|^2 + \omega_{\mathbf{k}}^2|\delta n_{\mathbf{k}}|^2\}} = T;$$

T is the plasma temperature in ergs. Assuming that $s^2 = T/m$ we obtain[4]

$$\overline{|\delta n_{\mathbf{k}}|^2} = n_0k^2/(4\pi n_0e^2/T + k^2).$$

For the sake of definiteness we shall henceforth use this formula for the average value of the square of the absolute value of the Fourier component of the density fluctuations.

The quantity $I_\omega(\vartheta, \varphi)$ represents the intensity of radiation of the combination frequency $\omega = \omega_0 \pm \Omega$ per unit solid angle. In the case of an unpolarized incident wave, averaging $I_\omega(\vartheta, \varphi)$ over the angle φ gives

$$I_\omega(\vartheta) = \frac{E_0^2}{(8\pi)^3 n_0^2 c^3}(1-\varepsilon)(1-\varepsilon_0)V\varepsilon\,\omega^4\frac{n_0(k^2+k_0^2-2kk_0\cos\vartheta)}{4\pi n_0e^2/T + k^2 + k_0^2 - 2kk_0\cos\vartheta}(1+\cos^2\vartheta), \quad (19)$$

$$\varepsilon_0 = \varepsilon(\omega_0), \quad \varepsilon \equiv \varepsilon(\omega), \quad k_0^2 = \omega_0^2\varepsilon_0/c^2, \quad k^2 = \omega^2\varepsilon/c^2.$$

We note that if $\vartheta = \pi/2$ then the scattered radiation will be polarized in the plane $(\mathbf{k}_0, \mathbf{k})$ irrespectively of the character of polarization of the incident wave.

We consider two limiting cases: $(\mathbf{k}-\mathbf{k}_0)^2 \ll 4\pi n_0e^2/T$ and $(\mathbf{k}-\mathbf{k}_0)^2 \gg 4\pi n_0e^2/T$. In the first case the collective oscillations of the plasma play an essential role, and the total intensity of radiation of frequency ω is equal to

$$I_\omega = \frac{e^2E_0^2T}{24\pi m^2c^3}\frac{\omega^3}{\omega_0^3}V\varepsilon(\omega^2\varepsilon + \omega_0^2\varepsilon_0), \quad \omega = \omega_0 \pm \Omega. \quad (20)$$

On dividing the total intensity of scattering $I = I_{\omega_0+\Omega} + I_{\omega_0-\Omega}$ by the energy flux density of the incident wave we obtain the scattering coefficient

$$\Sigma = \frac{e^2T}{3m^2c^4} \sum_{\omega=\omega_0\pm\Omega} \frac{\omega^2}{\omega_0^2} \sqrt{\frac{\varepsilon}{\varepsilon_0}} (\omega^2\varepsilon + \omega_0^2\varepsilon_0). \tag{21}$$

In the second limiting case the average quadratic fluctuation in the electron density is equal to n_0 and the intensity of scattering is determined by Rayleigh's formula

$$J = \frac{1}{3\cdot 16\pi^2} E_0^2 \frac{(\varepsilon_0-1)^2}{n_0 c^3} \varepsilon_0^{1/2}\omega_0^4. \tag{22}$$

In this case the scattering coefficient is

$$\Sigma = (8\pi/3)(e^2/mc^2)^2 n_0.$$

4. Let us now investigate the scattering of electromagnetic waves in a plasma in the presence of an external magnetic field H_0. In this case the plasma is an optically active anisotropic medium whose properties may be described by the dielectric constant tensor[5]

$$\varepsilon_{ik} = \begin{pmatrix} \varepsilon_1 - i\varepsilon_2 & 0 \\ i\varepsilon_2 & \varepsilon_1 & 0 \\ 0 & 0 & \varepsilon_3 \end{pmatrix},$$

where

$$\varepsilon_1 = 1 - \Omega^2/(\omega^2 - \omega_H^2), \quad \varepsilon_2 = \omega_H\Omega^2/\omega(\omega^2 - \omega_H^2), \quad \varepsilon_3 = 1 - \Omega^2/\omega^2, \quad \omega_H = eH/mc.$$

The electric and the magnetic fields of the scattered wave should be determined from the following expressions for the current density and the charge density:

$$j_i = \frac{1}{4\pi}\frac{\partial}{\partial t}(\hat{\delta\varepsilon}_{ik}E_k^0), \quad \rho = -\frac{1}{4\pi}\frac{\partial}{\partial x_i}(\hat{\delta\varepsilon}_{ik}E_k^0), \tag{23}$$

where $\hat{\delta\varepsilon}_{ik}$ is the operator for the fluctuation in the dielectric constant of the plasma in the presence of a magnetic field. Repeating the calculations which led to formula (5) one may show that this operator has the following form:*

$$\hat{\delta\varepsilon}_{ik} = (\hat{\varepsilon} - 1)^{1/2}\frac{\delta n(\mathbf{r}, t)}{n_0}(\varepsilon_{ik} - \delta_{ik})(\hat{\varepsilon} - 1)^{-1/2}. \tag{24}$$

Instead of equations (7) and (8) we must now use

$$\Delta A_i - \frac{\partial}{\partial x_i}\frac{\partial A_k}{\partial x_k} - \frac{\varepsilon_{ik}}{c^2}\frac{\partial^2 A_k}{\partial t^2} - \frac{\varepsilon_{ik}}{c}\frac{\partial}{\partial x_k}\frac{\partial\varphi}{\partial t} = -\frac{4\pi}{c}j_i, \quad \varepsilon_{ik}\partial^2\varphi/\partial x_i\partial x_k = -4\pi\rho, \tag{25}$$

and the condition[6]

$$\partial(\varepsilon_{ik}A_k)/\partial x_i = 0.$$

Choosing for the normal mode waves

$$\mathbf{A}^\lambda(\mathbf{r}) = (4\pi c^2/\varepsilon_{ik}e_i^\lambda e_k^{\lambda^*})^{1/2}\mathbf{e}^\lambda e^{i\mathbf{k}_\lambda\mathbf{r}}, \tag{26}$$

normalized in accordance with the condition

$$\int A_i^\lambda \varepsilon_{ik} A_k^{\lambda'^*} dv = 4\pi c^2 \delta_{\lambda\lambda'},$$

where $\mathbf{e}^\lambda$ is the complex polarization vector

$$\mathbf{e}^\lambda = \left\{ \frac{\varepsilon_2}{n_\lambda^2 - \varepsilon_1};\ i;\ i\frac{n_\lambda^2 \sin\vartheta\cos\vartheta}{n_\lambda^2\sin^2\vartheta - \varepsilon_3} \right\}, \quad \lambda = 1, 2$$

*In deriving this formula it should be kept in mind that the equation of motion has the form $\dot{\mathbf{v}} = e\mathbf{E}/m + (e/mc)[\mathbf{v}\times\mathbf{H}_0]$.

and n_λ is the index of refraction

$$n_{1,2}^2 = \frac{(\varepsilon_1^2 - \varepsilon_2^2)\sin^2\vartheta + \varepsilon_1\varepsilon_3(1+\cos^2\vartheta) \pm \sqrt{(\varepsilon_1^2-\varepsilon_2^2-\varepsilon_1\varepsilon_3)^2\sin^4\vartheta + 4\varepsilon_2^2\varepsilon_3^2\cos^2\vartheta}}{2(\varepsilon_1\sin^2\vartheta + \varepsilon_3\cos^2\vartheta)},$$

we obtain in this case the following expression for the driving force:

$$f_\lambda(t) = \sum_{\omega-\omega_\lambda\pm\Omega} B_\lambda^\omega e^{-i\omega t}, \quad B_\lambda^\omega = -\frac{i}{4\sqrt{\pi}}(\varepsilon_{ik}e_i^{\lambda^*}e_k^\lambda)^{-1/2}E_0(\delta n_{k_\lambda - k_\mu}/n_0)\{\delta_{ik} - \varepsilon_{ik}(\omega_0)\}e_k^\mu e_l^{\lambda^*}\omega_0,$$

where $\mathbf{k}_\mu$ and $\mathbf{e}^\mu$ are the propagation vector and the polarization vector of the incident wave.

It can be shown that the intensity of scattering at the combination frequency ω is given by the following general formula:

$$I_\omega(\vartheta,\varphi) = \frac{E_0^2\omega_0^2\omega^2}{(8\pi)^2 n_0^2 c^3}\sum_{\lambda=1,2}\frac{|e_i^\mu e_l^{\lambda^*} - \varepsilon_{ik}(\omega_0)e_k^\mu e_l^{\lambda^*}|^2}{\varepsilon_{ik}(\omega)e_l^{\lambda^*}e_k^\lambda}\, n_\lambda^3(\omega)\frac{2n_0(\mathbf{k}_\lambda - \mathbf{k}_\mu)^2}{4\pi n_0 e^2/T + (\mathbf{k}_\lambda - \mathbf{k}_\mu)^2}. \tag{27}$$

If the incident wave is travelling along the magnetic field then the intensity is given by the following expression

$$I_\omega^\pm(\vartheta) = \frac{E_0^2\omega_0^2\omega^2}{(8\pi)^2 n_0^2 c^3}\{1-\varepsilon_1(\omega_0) \pm \varepsilon_2(\omega_0)\}^2\sum_{\lambda=1,2}S_\lambda(\omega,\vartheta)\, n_\lambda^3(\omega)\frac{2n_0(\mathbf{k}_\lambda - \mathbf{k}_\mu)^2}{4\pi n_0 e^2/T + (\mathbf{k}_\lambda - \mathbf{k}_\mu)^2}, \tag{28}$$

$$S_\lambda(\omega,\vartheta) = \left(1 \pm \frac{\varepsilon_2}{n_\lambda^2 - \varepsilon_1}\right)^2 \Big/ \left[\varepsilon_1\frac{\varepsilon_2^2}{(n_\lambda^2-\varepsilon_1)^2} + \varepsilon_1 + \varepsilon_3\frac{n_\lambda^4\sin^2\vartheta\cos^2\vartheta}{(n_\lambda^2\sin^2\vartheta - \varepsilon_3)^2} + \frac{2\varepsilon_2^2}{n_\lambda^2 - \varepsilon_1}\right],$$

where the signs + and − refer respectively to right and left polarization of the incident wave.

If $(\mathbf{k}_\lambda - \mathbf{k}_\mu)^2 \ll 4\pi n_0 e^2/T$ then the scattering is due mainly to the collective oscillations of plasma density and the angular distribution of the scattering is given by the following expression

$$I_\omega^\pm(\vartheta) = \frac{2E_0^2T\Omega^2\omega^4}{(8\pi)^3 n_0 mc^5(\omega_0 \pm \omega_H)^2}\sum_{\lambda=1,2}S_\lambda(\omega,\vartheta)\, n_\lambda^5(\omega,\vartheta)\left\{1 + \frac{\omega_0^2}{\omega^2}\frac{\varepsilon_1(\omega_0) \pm \varepsilon_2(\omega_0)}{n_\lambda^2(\omega,\vartheta)} - 2\frac{\omega_0}{\omega}\frac{\sqrt{\varepsilon_1(\omega_0) \pm \varepsilon_2(\omega_0)}}{n_\lambda(\omega,\vartheta)}\cos\vartheta\right\}. \tag{29}$$

The presence of the magnetic field leads to a considerable change in the angular distribution of the scattering of electromagnetic waves.

In the limiting case of a weak magnetic field ($\epsilon_1 = \epsilon_3$, $\epsilon_2 \ll 1$) expression (24) becomes simplified

$$I_\omega^\pm(\vartheta) = \frac{2}{(8\pi)^3}\frac{E_0^2T\omega^4\omega_0^2}{n_0 m\Omega^2c^5}[\varepsilon_1(\omega_0) - 1 \pm \varepsilon_2(\omega_0)]^2\left\{\varepsilon_1^{1/2}\left(1 + \frac{\omega_0^2\varepsilon_{10}}{\omega^2\varepsilon_1} - \right.\right.$$

$$- 2\frac{\omega_0}{\omega}\sqrt{\frac{\varepsilon_{10}}{\varepsilon_1}}\cos\vartheta\Big)\left(1+\cos^2\vartheta\right) \pm \varepsilon_{20}\sqrt{\varepsilon_1}\left(\frac{\omega_0^2}{\omega^2} - \frac{\omega_0}{\omega}\sqrt{\frac{\varepsilon_1}{\varepsilon_{10}}}\cos\vartheta\right)(1+\cos^2\vartheta)$$

$$\left.\mp 2\varepsilon_2\sqrt{\varepsilon_1}\left(1 - \frac{5}{2}\cos^2\vartheta + \frac{\omega_0^2}{\omega^2}\frac{\varepsilon_{10}}{\varepsilon_1} - 2\frac{\omega_0}{\omega}\sqrt{\frac{\varepsilon_{10}}{\varepsilon_1}}\cos\vartheta - \frac{3\omega_0^2}{2\omega^2}\frac{\varepsilon_{10}}{\varepsilon_1}\cos^2\vartheta + 4\frac{\omega_0}{\omega}\sqrt{\frac{\varepsilon_{10}}{\varepsilon_1}}\cos^2\vartheta\right)\right\},$$

$$n_{1,2}^2 = \varepsilon_1 \pm \varepsilon_2|\cos\vartheta|, \quad \varepsilon_{10} \equiv \varepsilon_1(\omega_0), \quad \varepsilon_{20} \equiv \varepsilon_2(\omega_0). \tag{30}$$

In the case of a strong magnetic field ($\epsilon_2 = 0$, $\epsilon_1 \neq \epsilon_3$) we have

$$I_\omega^\pm(\vartheta) = \frac{2E_0^2T\omega^4\omega_0^2}{(8\pi)^2 n_0 m\Omega^2c^5}(\varepsilon_{10}-1)^2\left\{\varepsilon_1'\left(1 + \frac{\omega_0^2}{\omega^2}\frac{\varepsilon_{10}}{\varepsilon_1} - 2\frac{\omega_0}{\omega}\sqrt{\frac{\varepsilon_{10}}{\varepsilon_1}}\cos\vartheta\right) + \frac{n_2^7}{\varepsilon_1^2}\left(1 + \frac{\omega_0^2}{\omega^2}\frac{\varepsilon_{10}}{n_2^2} - 2\frac{\omega_0}{\omega}\sqrt{\frac{\varepsilon_{10}}{n_2^2}}\cos\vartheta\right)\cos^2\vartheta\right\},$$

$$n_1^2 = \varepsilon_1, \quad n_2^2 = \varepsilon_1\varepsilon_3/(\varepsilon_1\sin^2\vartheta + \varepsilon_3\cos^2\vartheta). \tag{31}$$

If $(\mathbf{k}_\lambda - \mathbf{k}_\mu)^2 \gg 4\pi n_0 e^2/T$ the plasma oscillations may be neglected. In this case the scattering of the electromagnetic wave is determined by the random thermal motion of the individual electrons of the plasma. The angular distribution of the scattering is given by the following formula

$$I^{\pm}(\vartheta) = \frac{2}{(8\pi)^2}\frac{E_0^2}{n_0 c^3}\{\varepsilon_1(\omega_0) - 1 \pm \varepsilon_2(\omega_0)\}^2\omega_0^4 \sum_{\lambda=1,2} S_\lambda(\omega_0, \vartheta)\, n_\lambda^2(\omega_0, \vartheta). \quad (32)$$

This expression is evidently a generalization of Rayleigh's formula for the intensity of scattering to the case of an optically active anisotropic medium.

5. Let us also determine the absorption of electromagnetic waves due to the excitation of plasma oscillations in which the energy of the incident electromagnetic wave is converted into the energy of longitudinal plasma oscillations.

The longitudinal field of the oscillations is characterized by the scalar potential φ satisfying the equation (8). We seek the solution of this equation in the form

$$\varphi(\mathbf{r}, t) = \sum_\sigma q_\sigma(t)\Phi_\sigma(\mathbf{r}), \quad \Phi_\sigma(\mathbf{r}) = \sqrt{4\pi c^2}\, e^{i\mathbf{k}_\sigma \mathbf{r}}. \quad (33)$$

The charge density ρ may be written, making use of (6), in the form

$$\rho = \frac{1}{8\pi}\sum_{\omega-\omega_*\pm\Omega} \frac{\Omega^2 E_0}{n_0\omega_0\omega}(\mathbf{e}_0 \operatorname{grad}\delta n(\mathbf{r}))\, e^{i\mathbf{k}_0\mathbf{r}-i\omega t}. \quad (34)$$

Substitution of (33) and (34) into equation (8) leads to the following expression for q_σ:

$$q_\sigma = \frac{i}{4\sqrt{\pi}}\sum_{\omega-\omega_*\pm} \frac{E_0\Omega^2}{c\omega_0\omega n_0 k_\sigma^2}(\mathbf{e}_0\mathbf{k}_\sigma)\,\delta n_{\mathbf{k}_\sigma - \mathbf{k}_0}\frac{1}{\varepsilon(\omega)}\, e^{-i\omega t}. \quad (35)$$

For $\epsilon(\omega)$ we shall take the following expression for the dielectric constant of the plasma:

$$\varepsilon(\omega) = 1 - \Omega^2/\omega(\omega + i\gamma),$$

where γ is the collision frequency of electrons in the plasma. (It is necessary to take collisions into account for otherwise at $\omega_0 = 2\Omega$ the absorption coefficient becomes infinite.)

The amount of energy absorbed per unit time per unit volume is given by formula (10) which gives after taking into account (33), (34), and (35)

$$I' = \frac{1}{2}\operatorname{Re}\sum_\sigma \dot{q}_\sigma^* \int \rho\Phi_\sigma^* dv = \frac{1}{16\pi}\sum_{\omega-\omega_*\pm} \frac{E_0^2\Omega^4}{n_0^2\omega_0^2}\int \frac{(\mathbf{e}_0\mathbf{k})^2}{k^3}\frac{\Omega^2\gamma}{(\omega^2-\Omega^2)^2+\gamma^2\omega^2}\left|\delta n_{\mathbf{k}-\mathbf{k}_0}\right|^2 \frac{d\mathbf{k}}{(2\pi)^3}. \quad (36)$$

Assuming that $(\mathbf{k}-\mathbf{k}_0)^2 \ll 4\pi n_0 e^2/T$ and carrying out in (36) integration over the angles and over $\kappa = |\mathbf{k}-\mathbf{k}_0|$ from 0 to $\kappa_m = 1/a$, where $a = \sqrt{T/4\pi n_0 e^2}$ is the Debye radius, we obtain the following expression for the absorption coefficient:

$$\Sigma' \approx \frac{1}{60\pi^2}\frac{\Omega^4}{n_0 a^3 c\varepsilon_0'^{1/2}\omega_0^2}\frac{\Omega^2\gamma}{(\omega^2-\Omega^2)^2+\gamma^2\omega^2}, \quad \omega = \omega_0 \pm \Omega. \quad (37)$$

---

[1] A. A. Vlasov, Теория вибрационных свойств электронного газа (Theory of the Vibrational Properties of an Electron Gas), Moscow (1945).

[2] A. Bohr, Det. Kgl. Danske Videnskab, Mat.-fis. Medd. 24, 19 (1948).

[3] A. I. Akhiezer and A. G. Sitenko, J. Tech. Phys. (U.S.S.R.) 23, 1217 (1953).

[4] D. Pines and D. Bohm, Phys. Rev. 85, 338 (1952).

[5] Al'pert, Ginzburg, and Feinberg, Распространение радиоволн (Propagation of Radio Waves), Moscow (1953).

[6] V. L. Ginzburg, J. Exptl. Theoret. Phys. (U.S.S.R.) 10, 601 (1940).

Translated by G. Volkoff
142

PROPAGATION OF SOUND ACROSS A BOUNDARY BETWEEN TWO SUPERFLUID PHASES

R. G. ARKHIPOV and I. M. KHALATNIKOV

Institute for Physical Problems, Academy of Sciences, U.S.S.R.

Submitted to JETP editor March 20, 1957

J. Exptl. Theoret. Phys. (U.S.S.R.) **33**, 758-764 (September, 1957)

The transmission of first and second sound across a boundary between two superfluid liquids is considered. The phenomenon of conversion of sound waves of one type into the other is revealed. Formulas are given for the energy fluxes in the reflected, refracted and converted waves. Separate consideration is given to the case in which one of the two liquids is not a superfluid.

THE hydrodynamics of concentrated solutions of He^3 in He^4 were developed in Ref. 1. In the system of equations derived there, it was assumed that all the He^3 takes part only in normal motion. This latter circumstance was proved rigorously only for the case of low concentration, and for all concentrations at absolute zero. Recently, it has been possible to carry out experiments with concentrated solutions of He^3 in He^4, which permit us to verify the validity of the hydrodynamical equations obtained in Ref. 1 by studying the propagation of sound vibrations in solutions.

As is well known, in the propagation of first sound in pure He^4, the pressure and density oscillations take place at constant entropy and temperature, while in the propagation of second sound, the temperature and entropy oscillations take place at constant pressure and density. In solutions, this is no longer the case. Propagation of first sound in solutions is accompanied by oscillations not only of pressure and density, but also of temperature and concentration. A similar picture is observed also in the propagation of second sound. The connection of the amplitudes of the vibrations of the various thermodynamical quantities can be found in the usual way[2] from the equations of hydrodynamics, taking into account the expressions for the velocities of first and second sounds in solutions (we denote by a prime the variable parts of quantities; the indices I and II refer to first and second sound, respectively: $p' = p'_I + p'_{II}$):

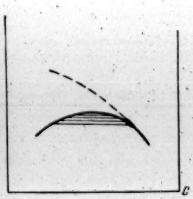

FIG. 1. Phase diagram and curve of the λ-transitions (dotted line) of the mixture of He^3 in He^4. The hypothetical region of two superfluid liquids is shaded.

$$c' = -\frac{\rho_s}{\rho_n}\frac{c^2}{\rho^2}\frac{\partial\rho}{\partial c}\frac{1}{s^2}p' + \frac{\partial c}{\partial\rho}\frac{1}{u^2}p'_{II},$$

$$T' = \left(\sigma - c\frac{\partial\sigma}{\partial c}\right)\frac{\partial T}{\partial\sigma}\frac{c'}{\varepsilon}, \quad \left(\mu - \frac{Z}{\rho}c\right)' = \frac{1}{\rho}\left(1 + \frac{c}{\rho}\frac{\partial\rho}{\partial c}\right)p'_I + \frac{1}{\rho}\left(1 - \frac{\rho_n}{\rho_s}\frac{\rho}{c}\frac{\partial c}{\partial\rho}\right)p'_{II}, \quad (1)$$

$$v_n = \frac{1}{s\rho}\left(1 - \frac{\rho_s}{\rho_n}\frac{c}{\rho}\frac{\partial\rho}{\partial c}\right)p'_I + \frac{1}{u\rho}\left(1 + \frac{\rho}{c}\frac{\partial c}{\partial\rho}\right)p'_{II}, \quad j - \rho v_n = \frac{\rho_s}{\rho_n}\frac{c}{s\rho}\frac{\partial\rho}{\partial c}p'_I + \frac{\rho}{uc}\frac{\partial c}{\partial\rho}p'_{II}.$$

Here ρ is the density of the mixture, c the weight concentration of He^3, $\mu - Zc/\rho = \mu_4$ the chemical potential of He^4 per gram, σ the entropy (per gram) of the mixture, p the pressure, T the temperature, s the velocity of first sound, u the velocity of second sound, ρ_s, ρ_n the superfluid and normal densities, v_s, v_n the superfluid and normal (particle) velocities, and $j = \rho_s v_s + \rho_n v_n$ the current density. The oscillations of the vector quantities $\mathbf{v}_n$ and $\mathbf{j} - \rho\mathbf{v}_n$ are directed along the wave vector $\mathbf{k}$. The latter two equations represent the amplitude of these vibrations.

It is evident from the formulas that the "intermeshing" of the temperature and pressure comes about through the derivative $\partial\rho/\partial c$ (and not through the very small quantity $\partial\rho/\partial T$, as in pure He^4).

New experimental possibilities for the study of sound propagation were opened up recently by Walters and Fairbank[3] with the discovery of the phenomenon of the separation of a solution of He^3 in He^4 into two phases of different concentration. The authors carried out their measurements by the method of magnetic resonance. Their results were confirmed by direct optical observations by Zinov'ev and Peshkov.[4] It

was shown that the critical point of the phase diagram lies at a temperature of about 0.85°K and a He^3 concentration of about 60% (Fig. 1). The concentration dependence of the temperature of the λ-transition is known with a very small degree of accuracy. If this curve (see Ref. 5) intersects the phase diagram to the right of the critical point, then there ought to exist two superfluid phases, which are in equilibrium with one another. Investigation of sound propagation across a boundary separating two phases should give additional information on the hydrodynamics of liquid helium.

Let us formulate the boundary conditions of the problem of the propagation of sound across a boundary separating two superfluid phases (the case of the boundary of a superfluid phase with a nonsuperfluid is obtained from the corresponding equations as the limit of $\rho_s \to 0$). We note that here, in addition to refracted and reflected waves in both phases, there arise waves which correspond to the conversion of first sound into second, and vice versa. Obviously, the excited sound will have the same values ω, k_y, k_z as the incident.[6] The case of practical interest is that in which only first or only second sound is incident on the boundary; there are then incident, reflected, refracted, and two converted waves. Because of the linearity of the problem, the general case is obtained as a superposition. As usual, we can consider that the plane of incidence of the wave is x, y; then $k_z = 0$ and the directions of the incident, reflected and the two converted waves lie in a single plane (Fig. 2). We shall consider all quantities proportional to $\exp\{i(k_x x + k_y y - \omega t)\}$. The condition $\operatorname{curl} \mathbf{v}_s = 0$ on the boundary gives $v_{sy1} = v_{sy2}$ (we shall omit the arabic numerals for the different phases). From the equation

$$\frac{\partial v_{sy}}{\partial t} + \frac{\partial}{\partial y}\left(\mu - \frac{Z}{\rho} c\right) = 0$$

we obtain

$$v_{sy} = (k_y/\omega)(\mu - Zc/\rho)'.$$

Consequently, the quantity $\mu - Zc/\rho$ must be continuous. (Here and below, we shall denote the variable part of quantities by means of a prime.) It is also evident that the pressure should be continuous at the boundary: $p_1 = p_2$.

For the derivation of two more (vector) conditions, we write down the condition of continuity of energy flow:

$$\mathbf{q} = \mathbf{j}\left(\mu - \frac{Z}{\rho} c\right) + \rho c \mathbf{v}_n \left(\frac{Z}{\rho} + \frac{\sigma}{c} T\right)$$

across the boundary $(q_{x1} = q_{x2})$ and consider that, because of the equations

$$\frac{\partial}{\partial t}(\rho\sigma) + \operatorname{div}(\rho\sigma \mathbf{v}_n) = 0, \quad \frac{\partial(\rho c)}{\partial t} + \operatorname{div}(\rho c \mathbf{v}_n) = 0$$

the quantity σ/c remains constant. Separating in each of the cofactors the part that is linear in the oscillations, we easily obtain

$$\mathbf{q} = (\mathbf{j} - \rho \mathbf{v}_n)\left(\mu - \frac{Z}{\rho} c\right)' + \mathbf{v}_n p', \tag{2}$$

from which we can conclude that $j_x - \rho v_{nx}$ and v_{nx} are also continuous; the latter is of course obvious on other grounds, since the gas excitation must be at rest relative to the boundary, while the continuity of $j_x - \rho v_{nx} = -\rho_s(v_{nx} - v_{sx})$ signifies that the superfluid part passes freely through the boundary.

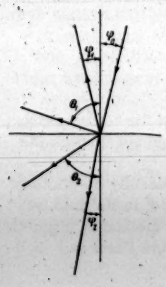

First we shall write down the set of boundary conditions for normal incidence of the sound wave, which we shall consider to be a superposition of waves of first and second sound of the same frequency

$$p' = p_I' + p_{II}', \quad p_I' = a_0 e^{i(k_I x - \omega t)}, \quad p_{II}' = b_0 e^{i(k_{II} x - \omega t)}.$$

We can easily obtain a set of equations for the reflected (a_1, b_1) and refracted (a_2, b_2) waves from the set of boundary conditions:

FIG. 2. The incident ray of second sound forms an angle φ_0 with the normal. The reflected ray of second sound makes an angle $\varphi_1 = \varphi_0$ with the normal. Moreover, the refracted ray of second sound and the converted ray of first sound in the two media make the respective angles φ_2, θ_1, θ_2 with the normal.

$$a_0+a_1+b_0+b_1=a_2+b_2,\quad \frac{1-\alpha_1}{\rho_1}(a_0+a_1)+\frac{1-\beta_1}{\rho_1}(b_0+b_1)=\frac{1-\alpha_2}{\rho_2}a_2+\frac{1-\beta_2}{\rho_2}b_2,$$
$$\frac{\beta_1-1}{s_1\rho_1\beta_1}(a_0-a_1)+\frac{\alpha_1-1}{u_1\rho_1\alpha_1}(b_0-b_1)=\frac{\beta_2-1}{\rho_2 s_2\beta_2}a_2+\frac{\alpha_2-1}{\rho_2 u_2\alpha_2}b_2,\quad \frac{1}{s_1\beta_1}(a_0-a_1)+\frac{1}{u_1\alpha_1}(b_0-b_1)=\frac{1}{s_2\beta_2}a_2+\frac{1}{u_2\alpha_2}b_2. \tag{3}$$

For brevity, we introduce the notation

$$\alpha=\rho c\frac{\partial}{\partial c}\frac{1}{\rho};\quad \beta=-\frac{\rho_n}{\rho_s\alpha}.$$

The general solution of the system (3) can be obtained by making use of the smallness of the velocity of second sound in comparison with the velocity of first sound.

We shall first assume that $a_0 = 1$, $b_0 = 0$ (only first sound is incident). As will be evident from what follows, in this case, $a_0 + a_1 \sim a_2 \sim b_1 \sim b_2 \sim u/s$, i.e., in particular, we can consider $a_1 \approx -1$ (the first sound is totally reflected from the superfluid liquid); in the last two equations of (3) we can neglect the term with a_2 on the right hand side, and also set $a_0 - a_1 \approx 2$. Solving the resultant system, we find for b_1 and b_2:

$$b_1=-2\frac{u_1\alpha_1}{s_1\beta_1}\left(\frac{1-\beta_1}{\rho_1}-\frac{1-\alpha_2}{\rho_2}\right)\Big/\Delta\left(\frac{1-\alpha}{\rho}\right),\qquad b_2=-2\frac{u_2\alpha_2}{s_2\beta_2}\frac{\beta_1-\alpha_1}{\rho_1}\Big/\Delta\left(\frac{1-\alpha}{\rho}\right), \tag{4}$$

where the symbol ΔA denotes the difference $A_2 - A_1$.

To find a_2, we eliminate $a_0 + a_1$ from the first pair of equations of (3) and substitute the above values of b_1 and b_2:

$$a_2=2\frac{\beta_1-\alpha_1}{\rho_1}\left[\frac{u_1\alpha_1}{s_1\beta_1}\left(\frac{1-\beta_1}{\rho_1}-\frac{1-\alpha_2}{\rho_2}\right)+\frac{u_2\alpha_2}{s_1\beta_1}\left(\frac{1-\beta_2}{\rho_2}+\frac{1-\alpha_1}{\rho_1}\right)\right]\left[\Delta\left(\frac{1-\alpha}{\rho}\right)\right]^{-2}. \tag{4a}$$

Now let us consider the case in which a pure second sound ($a_0 = 0$, $b_0 = 1$) is incident. Here it is seen that $b_0 - b_1 \sim b_2 \sim u/s$, i.e., the second sound is reflected almost totally. In this case we find from the first pair of equations in (3):

$$a_1=2\left(\frac{1-\beta_1}{\rho_1}-\frac{1-\alpha_2}{\beta_2}\right)\Big/\Delta\left(\frac{1-\alpha}{\rho}\right),\quad a_2=-2\frac{\beta_1-\alpha_1}{\rho_1}\Big/\Delta\left(\frac{1-\alpha}{\rho}\right). \tag{5}$$

Eliminating $b_0 - b_1$ from the second pair of equations in (3), we find b_2:

$$b_2=2\frac{\beta_1-\alpha_1}{\rho_1}\left[\frac{u_2\alpha_2}{s_1\beta_1}\left(\frac{1-\beta_1}{\rho_1}-\frac{1-\alpha_2}{\rho_2}\right)+\frac{u_2\alpha_2}{s_2\beta_2}\left(\frac{1-\beta_2}{\rho_2}-\frac{1-\alpha_1}{\rho_1}\right)\right]\left[\Delta\left(\frac{1-\alpha}{\rho}\right)\right]^{-2}. \tag{5a}$$

The resultant formulas lose their applicability whenever the concentrations (and consequently the thermodynamic functions found in the equilibrium of phases) are close to one another. By virtue of the small difference between the properties of the phases, sound is almost completely transferred from the first phase to the second ($a_2 \sim a_0$; $b_2 \sim b_0$). To find the amplitudes of the reflected and converted waves, we must expand (3) in powers of Δc. As a result of the calculation, we obtain for the case of incidence of first sound ($a_1 = 1$, $b_0 = 0$):

$$a_1=\frac{1}{2s\beta}\Delta s\beta+\frac{\rho}{2(\beta-\alpha)}\Delta\frac{2-\alpha-\beta}{\rho};\quad a_2=1-\frac{\rho s\beta}{2(\beta-\alpha)}\Delta\frac{\beta-\alpha}{\rho};$$
$$b_1=\frac{\rho}{2(\beta-\alpha)}\left[-\Delta\frac{1-\alpha}{\rho}-\frac{u\alpha}{s\beta}\Delta\frac{1-\beta}{\rho}\right];\quad b_2=\frac{\rho}{2(\beta-\alpha)}\left[\Delta\frac{1-\alpha}{\rho}-\frac{u\alpha}{s\beta}\Delta\frac{1-\beta}{\rho}\right], \tag{6}$$

and for the case of incidence of second sound ($a_0 = 0$; $b_0 = 1$):

$$b_1=\frac{1}{2u\alpha}\Delta u\alpha-\frac{\rho}{2(\beta-\alpha)}\Delta\frac{2-\alpha-\beta}{\rho};\quad b_2=1-\frac{\rho u\alpha}{2(\beta-\alpha)}\Delta\frac{\beta-\alpha}{\rho u\alpha};$$
$$a_2=\frac{\rho}{2(\beta-\alpha)}\left[\frac{s\beta}{u\alpha}\Delta\frac{1-\alpha}{\rho}+\Delta\frac{1-\beta}{\rho}\right];\quad a_2=\frac{\rho}{2(\beta-\alpha)}\left[\frac{s\beta}{u\alpha}\Delta\frac{1-\alpha}{\rho}-\Delta\frac{1-\beta}{\rho}\right]. \tag{7}$$

There still remains the case in which one of the liquids is not a superfluid. The corresponding system of equations can be obtained from (3) by passage to the limit for $\rho_s \to 0$, i.e., $\beta \to \infty$. Then the second equation of (3) yields $b = 0$, while in the remaining equations, we can set $b = 0$, $\beta = \infty$.

Thus, if the sound is propagated from the first, superfluid medium into the nonsuperfluid ($\beta_2 = \infty$), we then get the set of equations

$$a_0 + a_1 + b_0 + b_1 = a_2;\quad \frac{1-\beta_1}{\rho_1 s_1 \beta_1}(a_0 - a_1) + \frac{1-\alpha_1}{\rho_1 u_1 \alpha_1}(b_0 - b_1) = -\frac{1}{\rho_2 s_2} a_2,\quad (a_0 - a_1)/s_1\beta_1 + (b_0 - b_1)/u_1\alpha_1 = 0.$$

For incidence of pure first sound ($a_0 = 1$, $b_0 = 0$), we easily get, assuming that $u \ll s$,

$$a_1 = \left(1 - \frac{\alpha_1}{\beta_1} - \frac{\rho_1 s_1}{\rho_2 s_2}\right)\Big/\left(1 - \frac{\alpha_1}{\beta_1} + \frac{\rho_1 s_1}{\rho_2 s_2}\right);\quad a_2 = 2\left(1 - \frac{\alpha_1}{\beta_1}\right)\Big/\left(1 - \frac{\alpha_1}{\beta_1} + \frac{\rho_1 s_1}{\rho_2 s_2}\right);\quad b_1 = 2\,\frac{u_1\alpha_1}{s_1\beta_1}\,\frac{\rho_1 s_1}{\rho_2 s_2}\Big/\left(1 - \frac{\alpha_1}{\beta_1} + \frac{\rho_1 s_1}{\rho_2 s_2}\right). \quad (8)$$

If only second sound is incident ($a_0 = 0$, $b_0 = 1$)

$$a_1 = -2\Big/\left(1 + \frac{\rho_2 s_2}{\rho_1 s_1}\,\frac{\beta_1 - \alpha_1}{\beta_1}\right);\quad a_2 = 2\Big/\left(1 + \frac{\rho_1 s_1}{\rho_2 s_2}\,\frac{\beta_1}{\beta_1 - \alpha_1}\right);\quad b_1 = 1 + 2\,\frac{u_1\alpha_1}{s_1\beta_1}\Big/\left(1 + \frac{\rho_2 s_2}{\rho_1 s_1}\,\frac{\beta_1 - \alpha_1}{\beta_1}\right). \quad (9)$$

If the nonsuperfluid is the first phase ($\beta_1 = \infty$) and the sound is propagated from it, then we get a similar set of equations:

$$a_1 = -\left(1 - \frac{\rho_2 s_2}{\rho_1 s_1}\,\frac{\beta_2}{\beta_2 - \alpha_2}\right)\Big/\left(1 + \frac{\rho_2 s_2}{\rho_1 s_1}\,\frac{\beta_2}{\beta_2 - \alpha_2}\right);\quad a_2 = 2\,\frac{\rho_2 s_2}{\rho_1 s_1}\,\frac{\beta_2}{\beta_2 - \alpha_2}\Big/\left(1 + \frac{\rho_2 s_2}{\rho_1 s_1}\,\frac{\beta_2}{\beta_2 - \alpha_2}\right);\quad b_2 = -\frac{u_2\alpha_2}{s_2\beta_2}\,a_2. \quad (10)$$

With the help of Eqs. (4) – (10) and the formulas for the energy flow (2) [which it is expedient to transform in the following fashion

$$q = (j - \rho v_n)\left(\mu - \frac{Z}{\rho}c\right)' + v_n p' = \frac{\beta - \alpha}{\rho s \beta} p_I'^2 + \frac{\alpha - \beta}{\rho u \alpha} p_{II}'^2 \equiv q_a + q_b\,],$$

we can without difficulty calculate the reflection coefficients $R_I = |a_1|^2$, $R_{II} = |b_1|^2$ of the first and second sound, and also the ratio of the transmitted and converted energy fluxes to the incident. The results of the calculation are given in the Appendix.

These formulas can easily be generalized to the case of the incidence of the sound at some arbitrary angle by making the substitution $s \to s/\cos\theta$; $u \to u/\cos\varphi$ and adding to the conditions for the determination of θ_1, θ_2, φ_1, φ_2 those following from k_y = const:

$$\frac{\sin\theta_0}{s_1} = \frac{\sin\theta_1}{s_1} = \frac{\sin\theta_2}{s_2} = \frac{\sin\varphi_0}{u_1} = \frac{\sin\varphi_1}{u_1} = \frac{\sin\varphi_2}{u_2}.$$

Since $u \ll s$ always, then for incidence of the first sound at an angle $\theta_0 \sim 1$, the generated ray of second sound will make an angle $\varphi \sim u/s \ll 1$ with the normal, i.e., it will go essentially along the normal to the surface. For incidence of second sound on the boundary of separation, its conversion into first sound will take place only if $\varphi_0 < \sin^{-1}(u/s)$; in the opposite case, satisfaction of the equality $\sin\theta/s = \sin\varphi/u$ will not be possible.

The values of $\rho(c)$ and the velocities of first (s) and second (u) sound determined by experiment enter easily into these formulas. The investigation of the passage of sound across the boundary between phases permits us to resolve the problem of the validity of the equations of hydrodynamics for concentrated solutions.

I express my gratitude to Academician L. D. Landau for discussion of the work.

APPENDIX

Relation of the reflected, refracted and converted energy fluxes to the incident.

[Notation: $(1-\alpha)/\rho \equiv A$, $(1-\beta)/\rho \equiv B$]

1. Both liquids superfluid, the values of the concentrations not too close to one another [$(\Delta c)^2 s\beta/\mu\alpha \gg 1$].

(a) Incidence of first sound:

$$\frac{q_{a1}}{q_{a0}} = 1 - \frac{4}{(A_1 - A_2)^2}\left[(B_1 - A_2)^2\,\frac{u_1\alpha_1}{s_1\beta_1} + (B_1 - A_1)(B_2 - A_2)\,\frac{u_2\alpha_2}{s_1\beta_1}\right],$$

$$\frac{q_{a2}}{q_{a0}} = 4\,\frac{s_1\beta_1}{s_2\beta_2}\,\frac{(B_1 - A_1)(B_2 - A_2)}{(A_1 - A_2)^4}\left[(B_1 - A_2)\,\frac{u_1\alpha_1}{s_1\beta_1} + (B_2 - A_1)\,\frac{u_2\alpha_2}{s_1\beta_1}\right]^2,$$

$$\frac{q_{b1}}{q_{a0}} = 4\,\frac{u_1\alpha_1}{s_1\beta_1}\,\frac{(B_1 - A_2)^2}{(A_1 - A_2)^2},\quad \frac{q_{b2}}{q_{a0}} = 4\,\frac{u_2\alpha_2}{s_1\beta_1}\,\frac{(A_1 - B_1)(A_2 - B_2)}{(A_1 - A_2)^2}.$$

(b) Incidence of second sound:

$$\frac{q_{b1}}{q_{b0}} = 1 - \frac{4}{(A_1 - A_2)^2}\left[(B_1 - A_2)^2 \frac{u_1\alpha_1}{s_1\beta_1} + (A_1 - B_1)(A_2 - B_2)\frac{u_1\alpha_1}{s_2\beta_2}\right],$$

$$\frac{q_{b2}}{q_{b0}} = 4\,\frac{u_1\alpha_1}{u_2\alpha_2}\,\frac{(A_1 - B_1)(A_2 - B_2)}{(A_1 - A_2)^4}\left[(B_1 - A_2)\frac{u_2\alpha_2}{s_2\beta_1} + (B_2 - A_1)\frac{u_2\alpha_2}{s_2\beta_2}\right]^2,$$

$$\frac{q_{a1}}{q_{b0}} = 4\,\frac{u_1\alpha_1}{s_1\beta_1}\,\frac{(B_1 - A_2)^2}{(A_1 - A_2)^2};\quad \frac{q_{a2}}{q_{b0}} = 4\,\frac{u_1\alpha_1}{s_2\beta_2}\,\frac{(A_1 - B_1)(A_2 - B_2)}{(A_1 - A_2)^2}.$$

2. Both liquids superfluid, values of concentration close together $[(\Delta c)^2 s\beta/u\alpha \ll 1]$.

(a) Incidence of first sound:

$$\frac{q_{a1}}{q_{a0}} = \left[\frac{1}{2s\beta}\Delta s\beta + \frac{1}{2(A-B)}\Delta(A+B)\right]^2;\quad \frac{q_{a2}}{q_{a0}} = 1 + O[(\Delta c)^2],$$

$$\frac{q_{b1}}{q_{a0}} = \frac{s\beta}{u\alpha}\,\frac{(\Delta A)^2}{4(A-B)^2} + \frac{\Delta A\cdot\Delta B}{2(A-B)^2},$$

$$\frac{q_{b2}}{q_{a0}} = \frac{s\beta}{u\alpha}\,\frac{(\Delta A)^2}{4(A-B)^2} - \frac{\Delta A\cdot\Delta B}{2(A-B)^2}.$$

(b) Incidence of second sound:

$$\frac{q_{b1}}{q_{b0}} = \left[\frac{1}{2u\alpha}\Delta u\alpha - \frac{1}{2(A-B)}\Delta(A+B)\right]^2;\quad \frac{q_{b2}}{q_{b0}} = 1 + O[(\Delta c)^2],$$

$$\frac{q_{a1}}{q_{b0}} = \frac{s\beta}{u\alpha}\,\frac{(\Delta A)^2}{4(A-B)} + \frac{\Delta A\cdot\Delta B}{2(A-B)^2},$$

$$\frac{q_{a2}}{q_{b0}} = \frac{s\beta}{u\alpha}\,\frac{(\Delta A)^2}{4(A-B)^2} - \frac{\Delta A\cdot\Delta A}{2(A-B)^2}.$$

3. Second liquid nonsuperfluid

(a) Incidence of first sound $\left(z_1 = \left(1 - \frac{\alpha_1}{\beta_1} + \frac{\rho_1 s_1}{\rho_2 s_2}\right)^{-2}\right)$:

$$\frac{q_{a1}}{q_{a0}} = \left(1 - \frac{\alpha_1}{\beta_1} - \frac{\rho_1 s_1}{\rho_2 s_2}\right)^2 z_1,$$

$$\frac{q_{a2}}{q_{a0}} = 4\,\frac{\rho_1 s_1}{\rho_2 s_2}\left(1 - \frac{\alpha_1}{\beta_1}\right)^2 z_1,$$

$$\frac{q_{b1}}{q_{a0}} = 4\,\frac{u_1\alpha_1}{s_1\beta_1}\left(\frac{\rho_1 s_1}{\rho_2 s_2}\right)^2 z_1.$$

(b) Incidence of second sound $z_2 = \left(1 + \frac{\rho_2 s_2}{\rho_1 s_1}\,\frac{\beta_1 - \alpha_1}{\beta_1}\right)^{-1}$:

$$\frac{q_{b1}}{q_{b0}} = 1 - 4\,\frac{u_1\alpha_1}{s_1\beta_1}\,z_2,$$

$$\frac{q_{a1}}{q_{b0}} = 4\,\frac{u_1\alpha_1}{s_1\beta_1}\,z_2^2,$$

$$\frac{q_{a2}}{q_{b0}} = 4\,\frac{u_1\alpha_1}{s_2\beta_2}\left(1 + \frac{\rho_1 s_1}{\rho_2 s_2}\,\frac{\beta_1}{\beta_1 - \alpha_1}\right)^{-1} z_2.$$

4. First liquid nonsuperfluid $(\beta_1 = \infty)\ z_3 = \left(1 + \frac{\rho_2 s_2}{\rho_1 s_1}\,\frac{\beta}{\beta_2 - \alpha_2}\right)^{-2}$:

$$\frac{q_{a1}}{q_{a0}} = \left(1 - \frac{\rho_2 s_2}{\rho_1 s_1}\,\frac{\beta_2}{\beta_2 - \alpha_1}\right)^2 z_3,$$

$$\frac{q_{a2}}{q_{a0}} = 4\,\frac{\rho_2 s_2}{\rho_1 s_1}\,\frac{\beta_2}{\beta_2 - \alpha_2}\,z_3,$$

$$\frac{q_{b2}}{q_{a0}} = 4\,\frac{u_2\alpha_2\rho_2}{s_1(\beta_2 - \alpha_2)\rho_1}\,z_3.$$

[1] I. M. Khalatnikov, J. Exptl. Theoret. Phys. (U.S.S.R.) **23**, 169 (1952).
[2] E. M. Lifshitz, J. Exptl. Theoret. Phys. (U.S.S.R.) **14**, 116 (1944).
[3] G. K. Walters and W. M. Fairbank, Phys. Rev. **103**, 262 (1956).
[4] K. N. Zinov'eva and V. P. Peshkov, J. Exptl. Theoret. Phys. (U.S.S.R.) **32**, 1256 (1957), Soviet Phys. JETP **5**, 1024 (1957).
[5] Esel'son, Berezniak and Kaganov, Dokl. Akad. Nauk SSSR **111**, 568 (1956), Soviet Phys. "Doklady" **1**, 683 (1956).
[6] L. D. Landau and E. M. Lifshitz, Механика сплошных сред (Mechanics of Continuous Media), GTTI, 1954, Sec. 65.

Translated by R. T. Beyer
143

SOVIET PHYSICS JETP VOLUME 6 (33), NUMBER 3 MARCH, 1958

SCATTERING OF ELECTRONS BY PROTONS

A. I. AKHIEZER, L. N. ROZENTSVEIG, and I. M. SHMUSHKEVICH

Submitted to JETP editor March 21, 1957

J. Exptl. Theoret. Phys. (U.S.S.R.) **33**, 765-772 (September, 1957)

It is shown that under some very general assumptions, scattering of electrons by protons is determined by two real functions $a(q^2)$ and $b(q^2)$ of the invariant $q^2 = (p_1 - p_2)^2$ (p_1 and p_2 are the four-momenta of the electron before and after the collision). Experiments with polarized electrons and protons are considered which permit one in principle to determine the particular form of the functions $a(q^2)$ and $b(q^2)$.

1. In the region of not too high energies, where the proton recoil may be neglected, the scattering of electrons by protons is considered as the scattering of a Dirac particle in an external field. At high energies both particles are relativistic, which leads to a formula of the Møller type for the scattering cross section. Here, we must take account of the anomalous magnetic moment of the proton, which may be done by introducing a suitable term into the Hamiltonian of the interaction of nucleons with the electromagnetic field. But if the nucleon recoil momentum $q \gtrsim \mu c$, where μ is the mass of the π-meson, then the nucleon may not be considered to be a point, and a more detailed analysis is necessary, taking account of the interaction of the nucleon with the meson vacuum. It is clear, from semi-intuitive considerations, that this leads to the appearance of two form factors characterizing the distributions of charge and anomalous magnetic moment of the nucleon. However, a more rigorous investigation of this question is appropriate, particularly in connection with the interpretation Hofstadter's[1] experimental results.

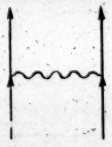

FIG. 1

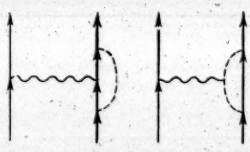

FIG. 2

2. The simplest Feynman diagram corresponding to e–p scattering is shown in Fig. 1 (the heavy line corresponds to the nucleon). The corresponding element of the S-matrix is *

$$S_{i\to f} = -i(2\pi)^4 e^2 \mathfrak{M}_{i\to f} \delta(p_1 + P_1 - p_2 - P_2), \qquad (1)$$

* We use the system of units in which $\hbar = c = 1$ and $\alpha = e^2/4\pi = 1/137$.

where

$$\mathfrak{M}_{i\to f} = q^{-2}(\overline{U}(P_2)\gamma_{i\mu}^{(p)}U(P_1))(\overline{u}(p_2)\gamma_{i\mu}^{(e)}u(p_1)); \tag{2}$$

the capital letters denote quantities referring to the nucleon, the small letters to the electron, and $q = p_1 - p_2 = P_2 - P_1$.

Limiting ourselves to the first nonvanishing approximation in e, and wishing to take account of all mesonic radiative corrections, we must, along with the diagram of Fig. 1, take into account all diagrams of the types shown in Fig. 2 (the dotted lines refer to π-mesons). Clearly, the totality of all such diagrams together with the diagram of Fig. 1 leads to a matrix element differing from Eq. (2) by the replacement of $\gamma_\mu^{(p)}$ by $\Gamma_\mu^{(p)}(P_2, P_1)$,

$$\mathfrak{M}_{i\to f} = q^{-2}(\overline{U}_2\Gamma_\mu^{(p)}(P_2, P_1)U_1)(\overline{u}_2\gamma_{i\mu}^{(e)}u_1). \tag{3}$$

$\Gamma_\mu^{(p)}(P_2, P_1)$ is the vertex operator taking account exactly of the interaction of nucleons with mesons, and to a first approximation, of nucleons with the electromagnetic field.

We will attempt to establish the most general form of the matrix element $(\overline{U}_2\Gamma_\mu^{(p)}(P_2, P_1)U_1)$. The operator Γ_μ is a vector, and must therefore be a sum of expressions containing the vectors $P_{1\mu}$, $P_{2\mu}$ (or, which is the same $q_\mu = P_{2\mu} - P_{1\mu}$) and γ_μ as factors, since there are no other vectors. In addition to the vector factor, each such expression, generally speaking, contains a function of the invariants P_1^2, P_2^2 and $P_1 \cdot P_2$ as a factor, and also the factors $\hat{P}_1$, $\hat{P}_2$ (or $\hat{q}$), arranged in a different order. But for real states of the nucleon, $P_1^2 = P_2^2 = -M^2$, and $P_1 \cdot P_2 = q^2/2 + M^2$, i.e., the above-mentioned functions depend only on the invariant q^2. Taking the identity $P_{1\mu} = 1/2(\hat{P}_1\gamma_\mu + \gamma_\mu\hat{P}_1)$ and a similar identity for P_2 into account we may limit ourselves to the consideration of only those terms in the expression for Γ_μ which contain the vector factor γ_μ. These terms may still contain some number of factors $\hat{P}_1$ and $\hat{P}_2$ in various orders.

Using the commutation relations, and also the fact that the operator $\hat{P}_2$ in the extreme left position, and $\hat{P}_1$ at the extreme right are equivalent to numerical factors iM, we conclude that effectively [in Eq. (3)] Γ_μ reduces to the sum of four terms, each of which is a product of functions of q^2 and one of the following operators $\hat{P}_1\gamma_\mu$, $\gamma_\mu\hat{P}_2$, $\hat{P}_1\gamma_\mu\hat{P}_2$ and γ_μ. But

$$\hat{P}_1\gamma_{i\mu} = -\hat{q}\gamma_{i\mu} + \hat{P}_2\gamma_{i\mu} \to (-\hat{q} + iM)\gamma_{i\mu}.$$

In the very same way we obtain

$$\gamma_{i\mu}\hat{P}_2 \to \gamma_{i\mu}(\hat{q} + iM), \quad \hat{P}_1\gamma_{i\mu}\hat{P}_2 = q^2\gamma_{i\mu} - 2q_\mu\hat{q} - \hat{q}\gamma_{i\mu}\hat{P}_1 + \hat{P}_2\gamma_{i\mu}\hat{q} + \hat{P}_2\gamma_{i\mu}\hat{P}_1 \to (-M^2 + q^2)\gamma_{i\mu} - iM(\hat{q}\gamma_{i\mu} - \gamma_{i\mu}\hat{q}),$$

since in view of the equation of continuity

$$(\overline{U}_2 q_\mu \hat{q} U_1) = q_\mu(\overline{U}_2\hat{q}U_1) = 0.$$

Consequently, the operator Γ_μ in Eq. (3) may be represented in the following form:

$$\Gamma_\mu(P_2, P_1) = a(q^2)\gamma_{i\mu} + (i/4M)[b_1(q^2)\gamma_{i\mu}\hat{q} - b_2(q^2)\hat{q}\gamma_{i\mu}]. \tag{4}$$

From the invariance of the theory with respect to charge conjugation, we have[2]

$$\Gamma_\mu(P_2, P_1) = -C\Gamma_\mu^T(-P_1, -P_2)C^{-1}.$$

Hence, it is not difficult to find that $b_1(q^2) = b_2(q^2)$. Taking into account further that $\hat{q}\gamma_\mu = -\gamma_\mu\hat{q} + 2q_\mu$ and that terms containing the factor q_μ do not contribute to the matrix element (3) [since in view of the equation of continuity for the electron flux $q_\mu(\overline{u}_2\gamma_\mu^{(e)}u_1) = (\overline{u}_2\hat{q}u_1) = 0$], we finally obtain* for Γ_μ

$$\Gamma_\mu(P_2, P_1) = a(q^2)\gamma_{i\mu} + (ib(q^2)/2M)\gamma_{i\mu}\hat{q}. \tag{5}$$

The quantities $a(q^2)$ and $b(q^2)$ may be considered as the form factors of the electric charge and the anomalous magnetic moment of the proton. For $q \ll \mu$ the quantity $a(q^2)$ is practically equal to unity,

*After completing the present work, we learned that Salzman[3] arrived at the same result using the gauge invariance of the theory. The authors thank Dr. G. Salzman for sending them a prepublication copy of his work, "Nucleon Structure in Statistical Theory," which contains a refreference to the above mentioned article.

and $b(q^2)$ to the anomalous magnetic moment of the proton, expressed in nuclear magnetons. Eq. (5) refers as well to the neutron (of course, with other functions $a(q^2)$ and $b(q^2)$: for the neutron, as $q^2 \to 0$, $a(q^2)$ approaches zero, and $b(q^2)$ approaches the anomalous magnetic moment of the neutron).

3. We will prove that the quantities $a(q^2)$ and $b(q^2)$ are real. For this purpose, we will consider the scattering of a proton in an external, infinitely weak electromagnetic field δA_μ. In this case, the S-matrix may be written in the form

$$S = S_0 + S_1, \tag{6}$$

where S_0 is the scattering matrix in the absence of an external field, and S_1 is linear in $\delta A\mu$. From the unitarity of S_0 and S_1, we have

$$S_1 = -S_0 S_1^+ S_0. \tag{7}$$

For the matrix element between states in which there is only one proton with momentum $\mathbf{P}_1$ or $\mathbf{P}_2$, respectively we obtain from,

$$(1\mathbf{P}_2 | S_1 | 1\mathbf{P}_1) = -\sum_{m,\, n} (1\mathbf{P}_2 | S_0 | m)(m | S_1^+ | n)(n | S_0 | 1\mathbf{P}_1), \tag{8}$$

where m and n are sets occupation numbers, characterizing the specified states. Clearly, the element $(n|S_0|1\mathbf{P}_1)$ differs from zero only if the state n is a state with only one proton* with momentum $\mathbf{P}_1$

$$(1\mathbf{P}_1 | S_0 | 1\mathbf{P}_1) = 1. \tag{9}$$

Therefore,

$$(1\mathbf{P}_2 | S_1 | 1\mathbf{P}_1) = -(1\mathbf{P}_2 | S_1^+ | 1\mathbf{P}_1) = -(1\mathbf{P}_1 | S_1 | 1\mathbf{P}_2)^*. \tag{10}$$

On the other hand, the same matrix element may be calculated directly, To the first approximation in e, and without taking account of mesonic-radiative corrections, we have

$$(1\mathbf{P}_2 | S_1 | 1\mathbf{P}_1) = -e(\overline{U}_2 \gamma_\mu U_1)\, \delta A_\mu(q), \quad \delta A_\mu(q) = \int \delta A_\mu(x)\, e^{-iqx} dx. \tag{11}$$

Taking account of all mesonic-radiative corrections reduces to the replacement of γ_μ by $\Gamma_\mu(P_2, P_1)$, U_2 by $Z_2^{1/2} U_2$ and U_1 by $Z_2^{1/2} U_1$ in Eq. (11).† Equation (10) now gives

$$(\overline{U}_2 \Gamma_\mu(P_2, P_1) U_1)\, \delta A_\mu(P_2 - P_1) = -\{(\overline{U}_1 \Gamma_\mu(P_1, P_2) U_2)\, \delta A_\mu(P_1 - P_2)\}^*. \tag{12}$$

Taking into account the relations

$$\delta A_\mu(q) = \{\delta A_\mu(-q)\}^* \text{ for } \mu = 1, 2, 3, \quad \delta A_4(q) = -\{\delta A_4(-q)\}^* \tag{13}$$

and the transversality of $\delta A\mu$

$$q_\mu\, \delta A_\mu(q) = 0, \tag{14}$$

we obtain for the transverse part of $\Gamma_\mu(\mathbf{P}_2, \mathbf{P}_1)$, which is the only significant part,

$$(\overline{U}_2 \Gamma_\mu(P_2, P_1) U_1) = -(\overline{U}_1 \Gamma_\mu(P_1, P_2) U_2)^* \text{ for } \mu = 1,2,3 \quad (\overline{U}_2 \Gamma_4(P_2, P_1) U_1) = (\overline{U}_1 \Gamma_4(P_1, P_2) U_2)^*. \tag{15}$$

---

*Eq. (9) is valid if mass renormalization is performed.

†We do not make the transition from $\delta A_\mu(q)$ to $\delta A'_\mu(q)$ since we are considering the electromagnetic interaction only to the first approximation, and the interaction of the electromagnetic field with π-mesons does not contribute to $\delta A'_\mu(q)$ because of the even charge parity of π^0. If neutral mesons, interacting strongly with nucleons and decaying into an odd number of photons, existed, then instead of $\Gamma_\mu(\mathbf{P}_2, \mathbf{P}_1)$ in Eq. (3), we would have the operator $V_\mu(\mathbf{P}_2, \mathbf{P}_1)$ which differs from Γ_μ by a contribution from graphs of the type shown in Fig. 3 (page 591; the double dotted line refers to a meson of odd charge parity). In this connection, Eq. (5) would hold for the operator V_μ, and all the equations obtained below would remain unchanged.

Now substituting Eq. (5) for Γ_μ, we finally obtain

$$a^*(q^2) = a(q^2), \quad b^*(q^2) = b(q^2). \tag{16}$$

That the functions $a(q^2)$ and $b(q^2)$ are real may also be proved without introducing an external field, by considering directly the scattering of electrons by protons to the first novanishing approximation in e. For this purpose, we must expand the S-matrix in a series of powers of e, and limiting ourselves to three terms of the series, $S = S_0 + S_1 + S_2$ (S_0, S_1 and S_2 are the terms of zero, first and second order in e, respectively), we must use the unitarity of S and S_0 on the one hand, and Eq. (3) on the other.

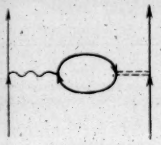

FIG. 3.

4. In the present state of theory, the form factors $a(q^2)$ and $b(q^2)$ cannot be calculated. Their determination from experiments on the scattering of electrons by protons could yield important information about the structure of the nucleon. In principle, knowing the elastic scattering cross section $d\sigma_0$ as a function of the scattering angle ϑ and the electron energy ϵ_1, each of the form factors a and b may be found separately, since one and the same value of q^2 is obtained for various ϑ and ϵ_1, and in the expression for $d\sigma_0$, the varaibles ϑ and ϵ_1 enter not only in the combination in which they are contained in q^2 [see Eq. (28)]. But the unique determination of the quantities a and b is made difficult by the unavoidable errors in the experimental values of $d\sigma_0$.

The problem would be simplified considerably, given an additional relation between a and b, which could possibly be obtained from experiments with polarized particles. However, as will be shown below, the simplest experiments of this kind (for example, investigations of the azimuthal asymmetry arising in the scattering of a polarized beam on an unpolarized target, or the polarization of particles obtained by the scattering of an unpolarized beam on an unpolarized target) cannot accomplish our purpose, since the corresponding polarization effects are proportional to the quantity $\mathrm{Im}(ab^*)$, which vanishes in view of conditions (16).

Before going on to the consideration of more complicated polarization experiments, we will introduce some equations, with the aid of which the state of polarization of a beam of relativistic particles with spin 1/2 may be described.[4] The corresponding density matrix for particles with mass m and momentum p is

$$\rho = {}^1/_2 (1 + i\gamma_5 \hat{\zeta}) \eta^{(+)}(p), \tag{17}$$

where $\eta^{(+)}(p) = (1/2\epsilon)(m - i\hat{p})\gamma_4$ is a projection operator onto states of positive energy $\epsilon = +\sqrt{m^2 + p^2}$. The four-vector $\zeta = (\boldsymbol{\zeta}, \zeta_4)$ describes the polarization of the beam. In a coordinate system in which $p = 0$, the fourth component of the vector ζ vanishes: $\zeta = (\boldsymbol{\zeta}^0, 0)$; in an arbitrary coordinate system,

$$\boldsymbol{\zeta} = \boldsymbol{\zeta}_t^0 + \frac{\epsilon}{m}\boldsymbol{\zeta}_l^0, \quad \zeta_4 = \frac{i}{m}\mathbf{p}\boldsymbol{\zeta}^0. \tag{18}$$

$\boldsymbol{\zeta}_t^0$ and $\boldsymbol{\zeta}_l^0$ are the transverse and longitudinal components of the vector $\boldsymbol{\zeta}_0$ (we note that $\zeta \cdot p = \sum_{\mu=1}^{4} \zeta_\mu p_\mu = 0$). The three-vector $\boldsymbol{\zeta}$ is determined through the known density matrix ρ by the relation $\boldsymbol{\zeta} = (\epsilon/m)\,\mathrm{Sp}\,(i\gamma\gamma_4\gamma_5\rho)$. In the future, we will denote the polarization vector of electrons by $\boldsymbol{\zeta}$, and of protons by Z.

Information about the quantities a and b may be obtained from the following polarization experiments.

(a) Scattering of polarized electrons on a polarized proton target. It will be shown below that the corresponding cross section is

$$d\sigma = d\sigma_0 (1 + M_{ik}\zeta_{1i}^0 Z_{1k}^0), \tag{19}$$

where $d\sigma_0$ is the scattering cross section in the absence of polarization, and the coefficients M_{ik} contain the ratio b/a in a known form. We note that terms of the type $K_i\zeta_{1i}^0$ and $L_k Z_{ik}^0$ are absent from (19), i.e., as already noted, polarization of the target alone, or of the incident beam alone, has no effect on the scattering.

(b) The resulting polarization Z_2 of the recoil protons during the scattering of a polarized beam of electrons ($\boldsymbol{\zeta}_1$) on an unpolarized target ($Z_1 = 0$). In this case,

$$Z_{2i} = \alpha_{ik}\zeta_{1k}. \tag{20}$$

Similarly, the components of the polarization vector of the scattered electrons ζ_2 will be

$$\zeta_{2i} = \beta_{ik}\zeta_{1k}. \tag{21}$$

The coefficients α_{ik} and β_{ik} also contain the ratio b/a.

(c) Similar effects arise in an unpolarized beam of electrons is scattered on a polarized proton target (now the vectors $\mathbf{Z_2}$ and $\boldsymbol{\zeta}_2$ will be linear vector-functions of the vector $\mathbf{Z_1}$).

(d) Still more complicated experiments associated with the measurement of the polarization of the scattered electrons or the recoil protons, arising when a polarized beam falls on a polarized target.

We shall consider only the simplest cases (a) and (b), prove relations (19) and (20), and calculate the quantities M_{ik} and α_{ik}.

In the case of the scattering of a polarized beam of electrons on a polarized proton target, the scattering cross section is

$$d\sigma = \frac{e^4}{(2\pi)^2}\frac{p_2\varepsilon_2 d\Omega}{v_1\,|\,\partial W/\partial\varepsilon_2\,|}\,\mathrm{Sp}\,[\mathfrak{M}\rho_1\mathfrak{M}^+\eta_{lm}^{(+)}(p_2)\,\eta_M^{(+)}(P_2)]. \tag{22}$$

$\mathfrak{M}$ is the transition matrix element, ρ_1 is the density matrix of the initial state and is the direct product of the corresponding electron and proton matrices,

$$\rho_1 = {}^1/_2(1+\gamma_5\hat{\zeta}_1)\,\eta_{lm}^{(+)}(p_1)\times{}^1/_2(1+i\gamma_5\hat{Z}_1)\,\eta_M^{(+)}(P_1), \tag{23}$$

and $\eta_m^{(+)}$ and $\eta_M^{(+)}$ are projection operators for the electron and the proton.

Performing the calculations in the laboratory system of coordinates ($\mathbf{P_1} = 0$), we have

$$d\sigma = \left(\frac{e^2}{4\pi}\right)^2\frac{p_2 d\Omega}{p_1 E_2\,|\,\partial W/\partial\varepsilon_2\,|}\,[P_{\mu\nu}+R_{\mu\nu}(\zeta_1)]\,[Q_{\mu\nu}+S_{\mu\nu}(Z_1)]; \tag{24}$$

where

$$P_{\mu\nu} = P_{\nu\mu} = \frac{1}{4}\,\mathrm{Sp}\,[\gamma_\mu(m-i\hat{p}_1)\,\gamma_\nu(m-i\hat{p}_2)],\quad Q_{\mu\nu} = \frac{1}{4}\,\mathrm{Sp}\left[\gamma_\mu\left(a+\frac{ib}{2M}\hat{q}\right)(1+\gamma_4)\left(a^*+\frac{ib^*}{2M}\hat{q}\right)\gamma_\nu(M-i\hat{P}_2)\right],$$
$$R_{\mu\nu} = -R_{\nu\mu} = \frac{1}{4}\,\mathrm{Sp}\,[\gamma_\mu i\gamma_5\hat{\zeta}_1(m-i\hat{p}_1)\,\gamma_\nu(m-i\hat{p}_2)],\ S_{\mu\nu} = \frac{1}{4}\,\mathrm{Sp}\left[\gamma_\mu\left(a+\frac{ib}{2M}\hat{q}\right)i\gamma_5\hat{Z}_1(1+\gamma_4)\left(a^*+\frac{ib^*}{2M}\hat{q}\right)\gamma_\nu(M-i\hat{P}_2)\right]. \tag{25}$$

$Q_{\mu\nu}$ and $S_{\mu\nu}$ may be represented in the form of a sum of symmetric and antisymmetric parts with respect to the indices μ and ν. But we may convince ourselves by direct calculations that the antisymmetric part of $Q_{\mu\nu}$ and the symmetric part of $S_{\mu\nu}$ are proportional to $ab^* - a^*b$, i.e., are equal to zero in view of the reality of a and b. Consequently,

$$Q_{\mu\nu} = Q_{\nu\mu},\quad S_{\mu\nu} = -S_{\nu\mu},$$

and (24) takes the form

$$d\sigma = d\sigma_0\,[1+R_{\mu\nu}(\zeta_1)\,S_{\mu\nu}(Z_1)/P_{\varkappa\lambda}Q_{\varkappa\lambda}]_r,\quad d\sigma_0 = (e^2/4\pi)^2\,(\varepsilon_2^2 d\Omega/\varepsilon_1^2 Mq^4)\,P_{\mu\nu}Q_{\mu\nu}. \tag{26}$$

After some tedious calculations in which we everywhere neglect the mass of the electron m compared with M and ϵ_1 and assume that $\vartheta \gg m/\epsilon_1$, we obtain*

$$\frac{d\sigma}{\sigma d\Omega} = \left(\frac{d\sigma}{d\Omega}\right)_0[1+(\zeta_1^0\mathbf{k})\,(\mathbf{Z}_1^0 M_{11}\mathbf{k}+M_{13}\mathbf{l})], \tag{27}$$

$$\left(\frac{d\sigma}{d\Omega}\right)_0 = \left(\frac{e^2}{4\pi}\right)^2\frac{a^2\cos^2\dfrac{\vartheta}{2}\left[1+\eta_1\mu^2+2\eta_1(1+\mu)^2\tan^2\dfrac{\vartheta}{2}\right]}{4M^2\varepsilon_1^2\left(1+2\xi\sin^2\dfrac{\vartheta}{2}\right)\sin^4\dfrac{\vartheta}{2}}, \tag{28}$$

$$M_{11} = \rho\tan\frac{\vartheta}{2}\left[\eta_1\left(1-\mu+\frac{1}{\xi}\right)-\xi\right],\quad M_{13} = \rho\eta_1\left(\frac{1}{\xi}-\mu\right), \tag{29}$$

$$\rho = \frac{2(1+\mu)\tan(\vartheta/2)}{1+\eta_1\mu^2+2\eta_1(1+\mu)^2\tan^2(\vartheta/2)}. \tag{30}$$

*Equation 28 was obtained by Rosenbluth[5], who attempted to find an explicit form of the form factors $a(q^2)$ and $b(q^2)$, considering several of the simplest Feynman diagrams of the type shown in Fig. 2.

where ϑ is the scattering angle of the electron in the laboratory system, $\xi = \epsilon_1/M$ is the electron energy in the same system, expressed in units of M,

$$\gamma_1 = \frac{q^2}{4M^2} = \xi^2 \sin^2\frac{\vartheta}{2} \Big/ \left(1 + 2\xi \sin^2\frac{\vartheta}{2}\right), \tag{31}$$

$$\mu(\gamma_1) = b(q^2)/a(q^2), \tag{32}$$

$\mathbf{k} = \mathbf{p}_1/|\mathbf{p}_1|$ is a unit vector in the direction of the incident beam of electrons $\boldsymbol{\ell} = [\mathbf{k} \times \mathbf{n}]$, and $\mathbf{n} = [\mathbf{p}_1 \times \mathbf{p}_2]/|[\mathbf{p}_1 \times \mathbf{p}_2]|$ is a unit vector normal to the plane of scattering. We used (18) in the derivation of (27). Terms containing $\zeta_1^0 \boldsymbol{\ell}$, $\zeta_1^0 \mathbf{n}$ and $\mathbf{Z}_1^0 \mathbf{n}$ were of the order m/M, and were neglected.

Taking the axes 1, 2, 3 along the vectors $\mathbf{k}$, $\mathbf{n}$, $\boldsymbol{\ell}$ we see that (27) reduces to (19), and (29) gives those coefficients M_{ik} which differ significantly from zero. To give some idea of the orders of magnitude which may be expected, the coefficients M_{11} and M_{13} are shown in Fig. 4 as a function of energy ξ at $\vartheta = \pi/2$ for a point proton ($\mu = 1.79$).

Let us now consider case (b). The polarization of recoil protons, resulting from the scattering of a polarized beam of electrons on an unpolarized target is

$$\mathbf{Z}_2 = \frac{(E_2/M)\mathrm{Sp}[i\gamma_\nu\gamma_4\gamma_\delta\gamma_\lambda^{(+)}(P_2)\mathfrak{R}^{1/2}(1+i\gamma_5\zeta_1)\eta_m^{(+)}(p_1)^{1/2}\eta_M^{(+)}(P_1)\,\mathfrak{R}^+\eta_m^{(+)}(p_2)\eta_M^{(+)}(P_2)]}{\mathrm{Sp}\,[\mathfrak{R}^{1/2}(1+i\gamma_5\zeta_1)\eta_m^{(+)}(p_1)^{1/2}\eta_M^{(+)}(P_1)\mathfrak{R}^+\eta_m^{(+)}(p_2)\eta_M^{(+)}(P_2)]}. \tag{33}$$

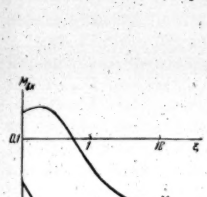

FIG. 4

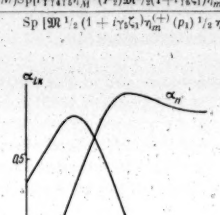

FIG. 5

Letting

$$\mathbf{B}_{\mu\nu} = -\mathbf{B}_{\nu\mu} = \frac{1}{8}\,\mathrm{Sp}\Big[i\gamma_5\hat{\gamma}(M - i\hat{P}_2) \times \gamma_\mu\Big(a + \frac{ib}{2M}\hat{q}\Big)(1+\gamma_4) \times \Big(a + \frac{ib}{2M}\hat{q}\Big)\gamma_\nu(M - i\hat{P}_2)\Big] \tag{34}$$

we obtain

$$\mathbf{Z}_2 = \mathbf{B}_{\mu\nu}\mathbf{R}_{\mu\nu}(\zeta_1)/MP_{\varkappa\lambda}Q_{\varkappa\lambda}, \tag{35}$$

where $\mathbf{P}_{\mu\nu}$, $\mathbf{Q}_{\mu\nu}$ and $\mathbf{R}_{\mu\nu}$ are determined by (25). We note that the antisymmetry of $\mathbf{B}_{\mu\nu}$ results from the reality of a and b.

Afer some tedious calculations, we find to within quantities of the order m/M, m/ϵ_1

$$\mathbf{Z}_2^0 = (\zeta_1^0\mathbf{k})(\alpha_{11}\mathbf{k} + \alpha_{31}\mathbf{l}),\ \alpha_{11} = \frac{\gamma_1\rho\,\mathrm{tg}\,(\vartheta/2)}{\gamma_1+1}\Big\{-\gamma_1\Big[\mu\Big(3+\frac{2}{\xi}\Big)+1+\frac{1}{\xi}\Big]+\mu(2\xi+1)+\xi+1-\frac{1}{\xi}\cot^2\frac{\vartheta}{2}\Big\},$$

$$\alpha_{31} = \frac{\gamma_1\rho}{\gamma_1+1}\Big\{-\gamma_1\Big[\mu\Big(1+\frac{2}{\xi}\Big)+\frac{1}{\xi}\Big]+\mu+2+\frac{1}{\xi}\Big\} \tag{36}$$

[compare with Eq. (20)]. The coefficients α_{11} and α_{31} are shown in Fig. 5 as functions of ξ at $\vartheta = \pi/2$ for a point proton.

We note in conclusion that since the quantities a and b depend on q^2, an unlimited number of independent experiments exist, through which the two quantities a and b may be determined for a definite value of q^2. Even if we limit ourselves to electrons of definite energy ϵ_1, the number of independent experiments involving polarization is greater than two. Therefore, it is possible to compare the results obtained for the quantities a and b from various experiments. If such a comparison leads to contradictions at high electron energies, it will be a significant indication of the inapplicability of the existing theory at sufficiently great electron energies, or, which is the same thing, at sufficiently small distances.

The authors thank Prof. I. Ia. Pomeranchuk for his interest in the work, and for helpful discussions.

[1] E. E. Chambers and R. Hofstadter, Phys. Rev. 103, 1454 (1956).
[2] M. Gell-Mann and M. L. Goldberger, Phys. Rev. 96, 1433 (1954).
[3] G. Salzman, Phys. Rev. 99, 973 (1955) (see the Appendix).

[4] F. W. Lipps. and H. A. Tolhoek, Physica 20, 85 (1954). L. Michel and A. S. Wightman, Phys. Rev. 98, 1190 (1955).

[5] M. N. Rosenbluth, Phys. Rev. 79, 615 (1950).

Translated by D. Lieberman
144

SOVIET PHYSICS JETP VOLUME 6 (33), NUMBER 3 MARCH, 1958

THEORY OF PARAMAGNETIC RESONANCE OF F CENTERS IN IONIC CRYSTALS

M. F. DEIGEN

Institute of Physics, Academy of Sciences, Ukrainian S.S.R.

Submitted to JETP editor March 25, 1957

J. Exptl. Theoret. Phys. (U.S.S.R.) 33, 773-779 (September, 1957)

A theory is developed for the hyperfine interaction of a localized electron with nuclear magnetic moments, displaced by a certain distance from the center of symmetry of the electron wave function. The hyperfine structure of the electron energy levels has been derived. The calculation is performed with the aid of "smoothed" and detailed F-center wave functions. The result enables one to develop a theory of paramagnetic absorption of radio-frequency waves by F-centers. As examples, the shape and width of the absorption lines in KC1 and NaC1 crystals has been obtained.

1. INTRODUCTION

THE application of the methods of radio-spectroscopy to the investigation of localized electronic centers in dielectrics and semiconductors has led to a series of important new results.[1-5] In particular, it must be pointed out, that these experiments made it possible for the first time to learn something quantitative about the distribution of the electronic ψ-function in a crystal;[4] to observe the very small effect of the g-shift[1] (spin-electron resonance); to determine the effective mass tensor[5] (cyclotron resonance), etc.

The spin-resonance absorption of radio-frequency waves by F-centers in alkali halide crystals has been subjected to a particularly thorough experimental investigation. It was shown that the half-width of the absorption line in these crystals was several tens of oersteds. The intensity curves have a nearly gaussian shape. Attempts to explain such a large half-width of the absorption line by means of the interaction of the magnetic moments of the electrons in the various F-centers were not successful, since, for the F-center concentrations attained in the experiments ($10^{17} - 10^{18}$ cm^{-3}), this interaction leads to a narrow absorption line, whose half-width is of the order of a few hundredths of an oersted. Kip, Kittel, Levy, and Portis[4] proposed that the reason for the widening of the absorption line was the interaction of the electron in the F-center with the magnetic moments of the nuclei of the metal ions which surround the missing halogen ion.

As is well known, two models are currently accepted in the theory of F-centers, i.e., the "continuum model" and the "molecular orbital."[7,8] Application of the orbital model, according to which the wave function of the electron has the form of a linear combination of the wave functions of the atoms surrounding the vacancy, led to the correct order of magnitude for the half-width of the absorption line. In contrast to this, estimates of the half-width based on the continuum model resulted in a disagreement between theory and experiment of from three to four orders of magnitude (in Ref. 4, the disagreement was somewhat less because the authors of that work used the somewhat incorrect model of Simpson,[9] instead of the results of Refs. 6 and 7). Hence, it was concluded that the continuum model was not valid. As we shall

show, this conclusion is unfounded, because two essential points have been missed in Ref. 4, as follows:

1. In the calculations, the results of Fermi[10] for the hyperfine interaction in the s-state of hydrogen were used. The coupling constant in this case is given by the equation:

$$A_H = (16\pi/3I)\,\mu\mu'\psi^2(0). \qquad \text{(A)}$$

Here μ and μ' are the magnetic moments of the electron and nucleus respectively; I is the nuclear spin; $\psi(0)$ is the value of the electron's wave function at the point where the proton is situated. Using this expression, Kip et al. substituted for $\psi(0)$ the value of the wave function at the point where the nearest metal ion is found.

However, the Fermi formula is valid only when the center of symmetry of the wave function coincides with the location of the nucleus. In the case of F-centers, the nuclei of the ions are displaced with respect to the center of symmetry of the wave function by the lattice constant. Thus, the wave function does not have spherical symmetry with respect to the ions, and Fermi's formula should not be applied. Therefore, to calculate the spin-resonance broadening correctly, one must construct a theory for the hyperfine interaction between the electron and the magnetic moments of the nuclei displaced by a certain distance from the center of symmetry of the F-center's wave function.

2. The potential for the spin-nuclear interaction is not smooth. Therefore, the calculation of physical effects from such a potential requires that one use detailed functions[7] rather than the "smoothed" functions used in Ref. 4. This point is indicated in Ref. 11, without, however, any special grounds.

In what follows, we shall develop a theory for the spin-resonance broadening of the electromagnetic emission from F-centers with the help of the observations described above. The continuum model of F-centers and the effective mass method of Pekar[12,13] are used.

In Sec. 2, the hyperfine interaction between a localized electron in an applied static magnetic field, and the magnetic moments of several nuclei, displaced with respect to the center of symmetry of the electron's wave function, is considered. For this analysis, "smoothed" electron functions are used. In Sec. 3, a similar calculation is performed for detailed wave functions, which permits one to construct a theory for the shape of the paramagnetic resonance absorption line associated with the absorption of radio-frequency waves by F-centers.

2. HYPERFINE INTERACTION OF THE S-ELECTRON WITH THE MAGNETIC MOMENTS OF DISPLACED NUCLEI ("SMOOTHED" F-CENTER FUNCTIONS)

We shall limit ourselves to the Pauli approximation to describe the behavior of the electron, as well as that of the nucleus. In Ref. 14, it is shown that a very general calculation, in which Darwin's relativistic approximation is used to describe the behavior of electrons, leads to the same results.

The energy operator for the interaction between a localized electron and the magnetic moment of the ionic nuclei can be written in the form:

$$\hat{U} = \mu \frac{\mathbf{S}}{S} \sum_j H_j, \qquad (1)$$

Here H_j is the contribution to the magnetic field from the nucleus of the j-th ion

$$H_j = (\mu_j / I_j)\,\mathrm{curl}\,\mathrm{curl}\,(\mathbf{I}_j/\rho_j), \qquad (2)$$

where μ_j and I_j are the magnetic moment and the spin of the j-th ion; ρ_j is the distance between the j-th nucleus and the electron. Expanding $1/\rho_j$ into a Fourier series

$$\frac{1}{\rho_j} = \frac{1}{2\pi^2}\int e^{i\mathbf{k}_j\rho_j}\frac{d\mathbf{k}_j}{k_j^2} \qquad (3)$$

and using (1) and (2), we find

$$\hat{U} = 4\pi\frac{\mu}{S}\,\mathbf{S}\sum_j \delta(\rho_j)\frac{\mu_j}{I_j}\mathbf{I}_j - \frac{1}{2\pi^2}\frac{\mu}{S}\sum_j \frac{\mu_j}{I_j}\int (\mathbf{I}_j\mathbf{k}_j)\,(\mathbf{S}\mathbf{k}_j)\,e^{i\mathbf{k}_j\rho_j}\frac{d\mathbf{k}_j}{k_j^2}. \qquad (4)$$

The wave function of the system, Ψ, depends on the rectilinear coordinate, r, of the electron, and on the spin coordinates of the electron, s, and of the nucleus, s_j. In the zero order approximation, when the hyperfine interaction is ignored, Ψ can be written in the form of a product:

$$\Psi(r, s, s_j) = \psi(r)\chi(s)\prod_j \chi'(s_j). \tag{5}$$

Forming the matrix of the operator of Eq. (4) with the rectilinear part of the wave function (5), we obtain the operator for the hyperfine interaction, $\hat{W}$, depending only on the spins of the electron and of the nuclei

$$\hat{W} = 4\pi\frac{\mu}{S}\mathbf{S}\sum_j \frac{\mu_j}{I_j}\mathbf{I}_j\psi^2(R_j) - \frac{1}{2\pi^2}\frac{\mu}{S}\sum_j\frac{\mu_j}{I_j}\int\{(\mathbf{I}_j\mathbf{k}_j)(\mathbf{S}\mathbf{k}_j)e^{-i\mathbf{k}_j\mathbf{R}_j}\frac{\alpha^4_j}{k_j^2}\cdot\int e^{i\mathbf{k}_j r}\psi^2(r)\,d\tau. \tag{6}$$

Here R_j is the distance from the center of symmetry of the wave function to the j-th nucleus.

The second term in (6) can be put in the form

$$\frac{1}{2\pi^2}\frac{\mu}{S}\sum_j\frac{\mu_j}{I_j}\sum_{m,n} I_{jn}S_m\frac{\partial^2}{\partial R_{jm}\partial R_{jn}}F(R_j).$$

The indices m and n signify the components x, y and z. Using as the form of the F-center wave function the expression

$$\varphi(r) = \alpha^{3/2}(1+\alpha r)e^{-\alpha r}/\sqrt{7\pi}, \tag{7}$$

we obtain

$$F(R_j) = \frac{2\pi^2}{R_j}\left[1 - e^{-2\alpha R_j}\left(1 + \frac{19}{14}\alpha R_j + \frac{5}{7}\alpha^2 R_j^2 + \frac{1}{7}\alpha^3 R_j^3\right)\right]. \tag{8}$$

In crystals in which the radius of the F-center wave function is not much greater than the lattice constant, one can sum over j in (6) by limiting oneself to the first coordination sphere. In a lattice like NaCl this means summation over six metallic ions, which are closest to the vacancy, all located at the same distance R from the center of the vacancy. In this case $\hat{W}$ simplifies to

$$\hat{W} = AS\sum_{j=1}^{6}\mathbf{I}_j + BS\sum_{j=1}^{6}R_j(\mathbf{I}_j\mathbf{R}_j), \tag{9}$$

$$\begin{gathered} A = \frac{\mu\mu'}{SIR^3}\left[-1 + e^{-q}\left(1 + q + \frac{q^2}{2} + \frac{3}{14}q^3 + \frac{5}{56}q^4 + \frac{1}{56}q^5\right)\right], \\ BR^2 = \frac{3\mu\mu'}{SIR^3}\left[1 - e^{-q}\left(1 + q + \frac{q^2}{2} + \frac{q^3}{6} + \frac{q^4}{24} + \frac{q^5}{168}\right)\right], \\ q = 2\alpha R. \end{gathered} \tag{10}$$

If the z axis coincides with the direction of an applied static magnetic field, $\hat{W}$ can be transformed into the form

$$\hat{W} = \hat{S}_z\sum_{j=1}^{6}\Delta_j(\hat{I}_{jx}\cos\alpha_j + \hat{I}_{jy}\cos\beta_j + \hat{I}_{jz}\cos\gamma_j), \tag{11}$$

$$\Delta_j = \sqrt{A^2 + B(2A + BR^2)R_{jz}^2}, \quad \cos\alpha_j = \frac{BR_{jz}R_{jx}}{\Delta_j}, \quad \cos\beta_j = \frac{BR_{jz}R_{jy}}{\Delta_j}, \quad \cos\gamma_j = \frac{A + BR_{jz}^2}{\Delta_j} \tag{12}$$

or

$$\hat{W} = \hat{S}_z\sum_{j=1}^{6}\Delta_j\hat{I}_{jn_j}, \tag{13}$$

where n_j are orthogonalized direction cosines defined by (12).

If we form the matrix of the operator $\hat{W}$ with the spin part of the same function (5), we determine the terms of the hyperfine structure

$$W = S_z\sum_{j=1}^{6}\Delta_j I_j, \tag{14}$$

where S_z has the same meaning as the spin operator of the electron and Ij is equivalent to I_{jn_j}. As seen from (14) and (15), the energy of the hyperfine interaction depends on the orientation of the magnetic field with respect to the crystal axes. To estimate the maximum width of the spin resonance broadening we apply a magnetic field along one of the crystallographic axes of the crystal and

$$W = S_z\left[A\sum_{j=1}^{6}I_j + (A + BR^2)\sum_{j=1}^{2}I_j\right]. \tag{15}$$

The effective magnetic field, corresponding to the maximum value of W_m, is found to be equal to

$$h = W_m/\mu. \tag{16}$$

Numerical calculations show that for alkali-halide crystals the maximum width $\delta = 2h$ is equal to 1 — 2 Oersted.

Thus, it has already been shown that taking into account the first of the conditions enumerated in Part 1 leads to an increase by a factor from 10 to 20 of the line width as compared to the estimates made in Ref. 4. This increase in width is not, however, sufficient to bring the theory into agreement with the experiments.

3. PARAMAGNETIC RESONANCE OF F-CENTERS (DETAILED FUNCTIONS)

Equation (6) for the operator of the hyperfine interaction also permits one to proceed with a calculation using detailed wave functions. The latter are written in the following way:

$$\psi(r) = \Omega^{1/2} \varphi u, \tag{17}$$

where φ is the smoothed F-center wave function [Eq. (7)], is the normalized Bloch wave function of the electron at the bottom of the conduction band and Ω is the volume of the fundamental cell of the crystal.

In crystals, in which $\varphi^2(r)$ decreases comparatively rapidly as the distance from the vacancy increases (alkali halides have this property), after substituting (17) into (6), the summation over j is sufficiently accurate if it is limited to the ions in the first coordination sphere (the metal ions). No essential difficulty is introduced if one does the calculation while taking into account the ions in subsequent coordination spheres.

Using the tight binding approximation, the Bloch function u can be written as a linear combination of atomic wave functions. For crystals of the type KCl, these will be, obviously, the atomic functions of potassium (ψ_s) and of the chlorine ion (ψ_q)

$$u = C\left[\sum_s \psi_s + C_1 \sum_q \psi_q\right]. \tag{18}$$

Here C is a normalization constant. The constant C_1^2, from the evaluation conducted in Ref. (4), is less than unity (in KCl it is approximately 1/6). Summation over s and q is extended over all positive and negative lattice points, respectively.

Substitution of (18) and (17) into (6) and neglecting small triple overlap integrals leads to the following result:

$$\hat{W} = \Omega\mathcal{C}\frac{\mu}{S}\hat{S}\sum_j \frac{\mu_j}{I_j}\left\{4\pi \hat{I}_j \varphi^2(R_j)\left[\sum_s \psi_s^2(R_j) + C_1^2 \sum_q \psi_q^2(R_j)\right]\right.$$
$$\left. - \frac{1}{2\pi^3}\int (\mathbf{I}_j\mathbf{k}_j)(\mathbf{S}\mathbf{k}_j) e^{-i\mathbf{k}_j\mathbf{R}_j}\frac{d\mathbf{k}_j}{k_j^2}\int e^{i\mathbf{k}_j r}\varphi^2(r)\left[\sum_s \psi_s^2 + C_1^2\sum_q \psi_q^2\right]d\tau\right\}. \tag{19}$$

In Eq. (19), in view of the rapid attenuation of $\varphi^2(r)$ the second and fourth terms are considerably smaller than the first and third. This is true also for the case of a central halogen ion, q = 0, (an ion, in an uncolored crystal, replaces the vacancy). In fact, one should substitute the value of the wave function at the point $r = R_j$ into the second term (where R_j is the point at which the metal ion is located). Nevertheless, in view of the rapid attenuation of atomic functions (e.g., the ion Cl^{--}) this term, as has been shown by calculation, at a distance equal to the lattice constant, is considerably less than the terms of the first sum. Numerical calculations show, that even in the integral the main contribution is made by the terms which depend on the wave functions of the metal atoms, and the terms containing ψ_q^2 can be neglected.

Taking all this into account, and also normalizing (18), $\hat{W}$ can be rewritten as follows:

$$\hat{W} = \frac{\mu\mu'}{SI} 4\pi\Omega_0\varphi^2(R)\,\psi^2(R)\sum_{j=1}^{6} \mathbf{S}\mathbf{I}_j = \frac{1}{2\pi^3}\frac{\mu\mu'}{SI}\Omega_0\sum_{j=1}^{6}\sum_{s=1}^{6}\int\frac{d\mathbf{k}_j}{k_j^2}(\mathbf{I}_j\mathbf{k}_j)(\mathbf{S}\mathbf{k}_j)e^{-i(\mathbf{k}_j\mathbf{R}_j)}\int e^{i\mathbf{k}_j r}\varphi^2(r)\,\psi_s^2(r)\,d\tau. \tag{20}$$

Here Ω_0 is the volume of the elementary cell of the crystal.

To perform approximate numerical calculations, one replaces $\varphi^2(r)$ in Eq. (20), by the functions of Eq. (7), and $\psi_s^2(r)$ is replaced by the Hartree free-atom wave functions for potassium in KCl and sodium in NaCl.

Performing the integration in Eq. (20) is especially convenient, if φ^2 and ψ_s^2 are approximated by sums

of gaussion exponentials:

$$\psi_s^2 = \frac{1}{4\pi}\sum_p a_p e^{-\alpha_p \rho^2}, \quad \varphi^2 = \frac{\alpha^3}{\pi}\sum b_\varkappa e^{-\beta_\varkappa r^2} \tag{21}$$

($\rho = \mathbf{r} - \mathbf{R}$). The error associated with the approximation in the integration interval does not exceed 7%, if the summation in the first sum is restricted to ten terms for KCl and seven terms for NaCl and to three terms for both crystals in the second summation.

Cumbersome, but in principle not difficult calculations, lead to the following expression for $\hat{W}$:

$$\hat{W} = (a + A_0 + A_1 + A_2)\sum_{j=1}^{6}\hat{S}_z\hat{I}_{jz} + (B_0 + B_1 + B_2)\sum_{j=1}^{6}\hat{S}_z\hat{R}_{jz}(\mathbf{I}_j\mathbf{R}_j) + \frac{1}{4}B_z\sum_{j=1}^{6}\sum_{s=1}^{4}\hat{S}_z\mathbf{R}_{jz}(\mathbf{I}_j\mathbf{R}_s). \tag{22}$$

Here

$$a = 4\pi\frac{\mu\mu'}{SI}\Omega_0\varphi^2(R)\psi^2(R), \tag{23}$$

$$A = n_i K\sum_{p,\varkappa} a_p b_\varkappa \exp\left\{-\frac{\alpha_p\beta_\varkappa R^2}{\alpha_p+\beta_\varkappa}\right\}\left[\frac{\Phi'(t_i)}{t_i^2} - \frac{\Phi(t_i)}{t_i^3}\right], \tag{24}$$

$i = 0, 1, 2$; $n_0 = n_1 = 1$; $n_2 = 4$ and $\Phi(t)$ are Kramp's functions

$$t_0 = \frac{\beta_\varkappa R}{\sqrt{\alpha_p+\beta_\varkappa}}; \quad t_1 = \frac{2\alpha_p+\beta_\varkappa}{\sqrt{\alpha_p+\beta_\varkappa}}, \quad t_2 = R\sqrt{\frac{\alpha_p^2+(\alpha_p+\beta_\varkappa)^2}{\alpha_p+\beta_\varkappa}}$$

$$B_0R^2 = K\sum_{p,\varkappa} a_p b_\varkappa \exp\left\{-\frac{\alpha_p\beta_\varkappa R^2}{\alpha_p+\beta_\varkappa}\right\}\left[\frac{\Phi''(t_0)}{t_0} - \frac{3\Phi'(t_0)}{t_0^2} + \frac{3\Phi(t_0)}{t_0^3}\right],$$

$$B_1R^2 = K\sum_{p,\varkappa} a_p b_\varkappa \exp\left\{-\frac{\alpha_p\beta_\varkappa R^2}{\alpha_p+\beta_\varkappa}\right\}\left[\frac{3\Phi(t_1)}{t_1^3} - 2\Phi'(t_1)\left(1+\frac{3}{2t_1^2}\right)\right], \tag{25}$$

$$B_2R^2 = 4K\sum_{p,\varkappa}(\alpha_p+\beta_\varkappa)R^2 a_p b_\varkappa \exp\left\{-\frac{\alpha_p\beta_\varkappa R^2}{\alpha_p+\beta_\varkappa}\right\}\left[\frac{\Phi''(t_2)}{t_2^3} - \frac{3\Phi'(t_2)}{t_2^4} + \frac{3\Phi(t_2)}{t_2^5}\right]; \quad K = \frac{\mu\mu'}{SI}\frac{\Omega_0\alpha^3}{28\sqrt{\pi}}.$$

In Eqs. (24) and (25) A_0 and B_0 are the contribution of terms corresponding to $j = s$; A_1 and B_1 are the contributions from the nucleus opposite the j-th ion and finally, A_2 and B_2 are the contributions of nuclei located in a plane perpendicular to R_j.

The operator (22) resembles the operator (9) and its eigenvalues can be determined, in the same way as in Sec. 2 (the last term in (22) does not complicate the calculation).

As has been shown by numerical calculation, the terms A_1 and B_1R^2 are smaller than a in alkali halide crystals. Furthermore, A_1 and A_2, B_1 and B_2 are considerably smaller than A_0 and B_0 respectively. Therefore for these crystals Eq. (22) simplifies as follows

$$\hat{W} = (a + A_0)\sum_{j=1}^{6}\hat{S}_z\hat{I}_{jz} + B_0\sum_{j=1}^{6}\hat{S}_z\hat{R}_{jz}(\hat{\mathbf{I}}_j\mathbf{R}_j). \tag{26}$$

In complete analogy with Eqs. (11) and (14), the eigenvalues of Eq. (26) can be written in the form

$$W = S_z\sum_{j=1}\Delta_j I_j, \tag{27}$$

$$\Delta_j = \{(a + A_0)^2 + B_0R_{jz}^2[2(a + A_0) + B_0R^2]\}^{1/2}, \tag{28}$$

S_z and I_j have the same meaning as in Eq. (14). Hence, it follows, that the hyperfine interaction energy, and therefore, the half-width of the spin-resonance absorption band, must depend on the magnitude of the angle between an externally applied static magnetic field and the crystallographic axis. The shape of the line, according to Eq. (27), differs slightly from a gaussian, since I_j contains coefficients which are functions of the size of the nucleus. Calculations show that this effect is not large in crystals of high symmetry (lattices like NaCl), but they can be, generally speaking, significant in crystals with other symmetries.

From the above it follows that, in alkali halide crystals, the shape of the paramagnetic absorption line, in agreement with experiment, is nearly gaussian. For these crystals

$$\hat{W} \approx S_z (a + A_0) \sum_{j=1}^{6} I_j. \qquad (29)$$

Using Eq. (29) it is readily shown that the effective magnetic field, h_0, corresponding to the half width of the absorption line turns out to be equal to

$$h_0 \approx 3.37\,(a + A_0)/\mu. \qquad (30)$$

Equation (30) leads to the following values: h_0 (KCl) = 8 Oersted; h_0 (NaCl) = 13 Oersted. These values are still several times smaller than the corresponding experimental ones. This difference is explained not so much by failure to include additional coordination spheres, as by failure to satisfy the criteria of the macroscopic approximation in KC1 and other alkali halide crystals. Because of this, the value of the wave function φ (r) turns out to be decreased at the point r = R.

If for purposes of evaluation, one proceeds as in Ref. 4 to make use of the value of ψ_s^2 at zero, which value is carried over from radio-frequency spectroscopic data (following this procedure, however, as is well known, causes the value of $\psi_s^2(0)$ to be underestimated with respect to its Hartree value), h_0 turns out to be 15 Oersted. The experimental value of h_0 is 52 Oersted. Similar results are also obtained for NaC1.

Thus, the continuum model of the F-center leads to theoretically values of the half-width of the absorption line which coincide with corresponding experimental values within an order of magnitude.

I wish to express my gratitude to Prof. S. I. Pekar for his interest in this work.

Note added in proof (August 26, 1957). In a recently published paper, Feher discovered experimentally a dependence of the frequency of nuclear-spin transitions of the ions, surrounding an F-center, which has been saturated by the absorption of radio-frequency waves, on the orientation of the crystal in an external magnetic field.

All the qualitative and quantitative properties of the phenomenon are described by the Hamiltonian of Eq. (22). In particular, it is readily shown, that the spin Hamiltonian can be written in the form

$$\hat{W} = A \sum_{j=1}^{6} (\mathbf{S}\mathbf{I}_j) + B \sum_{j=1}^{6} (\mathbf{S}\mathbf{R}_j)(\mathbf{I}_j\mathbf{R}_j),$$

where the second anisotropic term indeed leads to the reported angular dependence.

[1] C. A. Hutchison and J. A. Noble, Phys. Rev. 87, 1125 (1952).
[2] E. Schneider, Phys. Rev. 93, 919 (1954).
[3] Fletcher, Jager, Pearson, and Merritt, Phys. Rev. 95, 844 (1954).
[4] Kip, Kittel, Levy, and Portis, Phys. Rev. 91, 1066 (1953).
[5] Lax, Zeiger, Dexter, and Rosenblum, Phys. Rev. 93, 1418 (1954).
[6] C. Kittel and E. Abrahams, Phys. Rev. 90, 238 (1953).
[7] S. I. Pekar; J. Exptl. Theoret. Phys. (U.S.S.R.) 17, 868 (1947); S. I. Pekar and M. F. Deigen, J. Exptl. Theoret. Phys. (U.S.S.R.) 18, 481 (1948).
[8] T. Muto, Progr. Theoret. Phys. 4, 243 (1949); T. Inui and J. Uemura, Prog. Theoret. Phys. 5, 252 and 395 (1950).
[9] J. H. Simpson, Proc. Roy. Soc. A 197, 269 (1949).
[10] E. Fermi, Z. Physik 60, 320 (1930).
[11] D. N. Dexter, Phys. Rev. 93, 244 (1954); J. Krumhansl, Phys. Rev. 93, 245 (1954).
[12] S. I. Pekar, Исследования по электронной теории кристаллов (Investigations in the Electron Theory of Crystals), G.T.T.I. Moscow-Leningrad 1951.
[13] S. I. Pekar, J. Exptl. Theoret. Phys. (U.S.S.R.) 16, 933 (1946).
[14] M. F. Deigen and L. A. Shul'man, Оптика и спектроскопия (Optics and Spectroscopy) (in press).
[15] G. Feher, Phys. Rev. 105, 1122 (1957).

Translated by J. J. Loferski
145

OPTICAL PROPERTIES OF F^- CENTERS

V. L. VINETSKII

Submitted to JETP editor March 27, 1957

J. Exptl. Theoret. Phys. (U.S.S.R.) 33, 780-787 (September, 1957)

The quantum states are considered for a system consisting of a crystal with two opposite charge vacancies spaced a distance of half a lattice period from each other and of an electron which interacts with the optical vibrations of the crystal localized near this pair of vacancies (crystal with F^- center). The problem is solved in the macroscopic approximation. The parameters of the self-consistent ground state of the system are calculated. The frequencies and absorption coefficients of light are calculated in the Franck–Condon approximation for photo-transitions to the lowest excited states. The azimuthal dependence of the degree of polarization of luminescence due to irradiation with polarized light in the F^- absorption bands is also computed; this dependence may be used to identify the F^- centers. The results are carried to numerical values for the KCl crystal.

IN the present work it is shown that in the macroscopic approximation a system comprising a crystal plus a pair of opposite charge vacancies plus an electron (a crystal with an F^- center) is energetically more favorable than a system comprising a crystal plus an F^- center (Sec. 1). Although the gain is not large — on the order of hundredths of an electron volt — the result obtained furnishes the basis for assuming that under favorable conditions a sufficiently large concentration of F^- color centers can exist in a crystal. A temperature sufficiently low so that the mobility of the vacancies is small and the F^- centers are not decomposed by thermal fluctuations must be considered as a necessary condition for the presence of stable F^- centers. The formation of F^- centers can occur, for example, directly on coloration of a crystal when electrons are located at vacancy pairs, the concentration of which in a crystal can be comparable to the concentration of discrete vacancies and even significantly exceed the latter (if the crystal is maintained for a sufficient time, for example, at room temperature).[1] Another possibility of obtaining F^- centers can be connected with the decomposition of more complex color centers (for example M centers).

An examination of the properties, particularly the optical properties of a crystal containing F^- color centers thus appears desirable.

1. THE GROUND STATE OF A CRYSTAL WITH AN F^- CENTER

In the macroscopic approximation using methods developed by Pekar,[2] the energy of the system crystal + F^- center can be written in the form

$$\hat{H} = -\frac{\hbar^2}{2\mu}\Delta + e\int\frac{(\mathbf{r}_1-\mathbf{r})\,\mathbf{P}(\mathbf{r})}{|\mathbf{r}_1-\mathbf{r}|^3}\,d\tau + \frac{e^2}{\varepsilon}\left(\frac{1}{r_c}-\frac{1}{r_a}-\frac{1}{R}\right) + {}^1/_2\sum_k \hbar\omega_k\left(q_k^2-\frac{\partial^2}{\partial q_k^2}\right). \qquad (1)$$

Here the first term represents the kinetic energy of the electron, the second — the energy of interaction of the electron with the polarized surroundings, the third — the energy of electrostatic interactions of the electron with the positive (a) and negative (c) vacancies and the vacancies with one another; the fourth — the energy of normal lattice vibrations; μ is the effective mass of the electron: $\mathbf{P}(\mathbf{r})$ is the inertial part of the specific polarization of the crystal brought about by the field of the electron; ϵ is the dielectric constant of the crystal; r_a and r_c are the distances from the electron to the vanancies a and c, R is the distance between the vanancies, ω_k and q_k are the frequencies and normal coordinates of the polarization oscillations of the crystal.

Instead of solving the Schrödinger equation with the Hamiltonian (1) it is more convenient to find the minimum of the corresponding functional. If, as in Refs. 3 — 5, one disregards the dependence of R on q_k and selects an approximating function to the system in the multiplicative form

$$\Psi = \psi(r)\,\Phi(\ldots q_k\ldots), \qquad (2)$$

then as a result of minimizing over $\Phi(\ldots q_k \ldots)$ the energy of the system can be written down in the following manner:

$$\overline{H} = J[\psi(r)] + \sum_k \hbar\omega_k (n_k + {}^1/_2), \tag{3}$$

where n_k are quantum numbers of the oscillators which describe the vibrations of the lattice and J is a functional which depends only on the electronic part of the wave function of the system

$$J[\psi(r)] = \frac{\hbar^2}{2\mu}\int(\nabla\psi)^2\,d\tau - \frac{e^2}{\epsilon}\int\frac{\psi_a^2}{r_a}\,d\tau - \frac{e^2c}{2}\int\frac{\psi^2(1)\,\psi^2(2)}{r_{12}}\,d\tau_{12} + \frac{e^2}{\epsilon}\int\frac{\psi^2}{r_c}\,d\tau - \frac{e^2}{\epsilon R}. \tag{4}$$

Here c is the well-known parameter of polaron theory.[2] The first three terms in Eq. (4) represent the corresponding functional of the F center formed at the vanancy a.

Further, the variation of $J[\psi]$ with respect to $\psi(r)$ must be carried out.

The mean value of the intensity of the electric field set up by a vacancy c in the region where the electron of an F center a is localized is equal to

$$\overline{E} = \int\psi^*(r)\frac{e^2}{\epsilon r_c^2}\psi(r)\,d\tau,$$

which in real crystals, as calculation shows, is some 10 — 20 times smaller than the mean value of the intensity of the electric field produced by the vacancy a. One can assume, therefore, that the effect of the electric field of the vacancy c leads to a small change of the wave function of the ground state of the F center which has, according to Ref. 2, the following form

$$\psi_0(r) = (7\pi)^{-1/2}\alpha^{3/2}(1 + \alpha r_a)\,e^{-\alpha r_a}. \tag{5}$$

Two different approximations of the electronic part of the wave function of the ground state of the system which take into account such a change have been tested:

(a) $\psi(r)$ is approximated by a wave function of the form Eq. (5) whose maximum is located at some point b which, generally speaking, does not coincide with point a:

$$\psi_0(r) = (7\pi)^{-1/2}\alpha^{3/2}(1 + \alpha r_b)\,e^{-\alpha r_b}. \tag{6}$$

From symmetry considerations it follows that the point b must lie on the axis ac. The distance between the vacancy a and the point b (denoted by ρ) and the reciprocal radius of the state of the electron α are the parameters of the approximation. It is more convenient to use the quantities $t = \rho/R$ and $x = \alpha R$ as the independent parameters. Substituting Eq. (6) in Eq. (4) assuming $t \ll 1$ and confining ourselves to terms of second order of smallness we arrive at a functional which depends on t and x:

$$J[t, x] = \frac{\hbar^2}{2\mu R^2}\frac{3}{7}x^2 - \frac{e^2}{14\epsilon R}x\left(9 - \frac{4}{3}x^2t^2\right) + \frac{e^2}{14\epsilon R}[\varphi_0(x) + t\varphi_1(x) + t^2\varphi_2(x)] - \frac{e^2c}{2R}0.428\,x - \frac{e^2}{\epsilon R}, \tag{7}$$

where

$$\varphi_0(x) = 14 - e^{-2x}(14 + 19x + 10x^2 + 2x^3), \qquad \varphi_1(x) = -14 + e^{-2x}(14 + 28x + 28x^2 + 16x^3 + 4x^4),$$
$$\varphi_2(x) = 14 - e^{-2x}(14 + 28x + 28x^2 + 20x^3 + 12x^4 + 4x^5). \tag{7a}$$

Minimizing Eq. (7) over t permits, as a result of simple transformations, writing the functional in the form

$$J[x] = \frac{e^2}{\epsilon R}\left\{-1 + \frac{1}{14}\left[\frac{\hbar^2\epsilon}{\mu e^2 R}3x^2 - 3(\epsilon c + 3)\,x + \varphi_0(x) - \frac{3\varphi_1^2(x)}{4[3\varphi_2(x) + 4x^3]}\right]\right\}.$$

Minimizing J[x] over x permits calculation of the parameters of the self-consistent ground state of the system. Calculations carried out for a series of alkali-halide crystals show that $J(x_{min})$ is approximately 0.01 — 0.02 ev lower than the corresponding values obtained for the F center. In particular, for the KCl crystal ($\epsilon = 4.78$, $c = 0.25$, $R = 3.14$ A) the values $J = -2.19$ ev, $t = 0.043$, and $x = 4.73$ are obtained.

(b) As the approximating function we use the function proposed by Perlin[6]

$$\psi(r) = (1 - {}^1/_2\lambda^2)\psi_0(r) + \lambda\varphi(r), \tag{8}$$

where $\lambda \ll 1$; $\psi_0(r)$ is determined by Eq. (5), and

$$\varphi(r) = \pi^{-1/2}\gamma^{5/2}e^{-\gamma r}r\cos\theta. \tag{9}$$

Substitution of Eqs. (8) and (9) in Eq. (4) leads to a functional which depends on λ, x and $\omega = \gamma/\alpha$:

$$J[\lambda, x, \omega] = (e^2/\varepsilon)(a_0 + \lambda a_1 + \lambda^2 a_2 + \ldots), \tag{10}$$

$$a_0 = \frac{1}{14R}\left[\frac{3\lambda^2\varepsilon x^2}{\mu e^2 R^2} - G_0(x) - 3\varepsilon cx\right],$$

$$a_1 = \frac{1}{R}\frac{8}{\sqrt{7}}\frac{\omega^{5/2}}{(1+\omega)^6}\frac{1}{x}\{8(6+\omega) - e^{-x(1+\omega)}[x^4(1+\omega)^4$$

$$+ x^3(1+\omega)^3(7+\omega) + 4x^2(1+\omega)^2 + 8x(1+\omega)(6+\omega) + 8(6+\omega)]\},$$

$$a_2 = \frac{1}{14R}\left\{\frac{\lambda^2\varepsilon}{\mu e^2 R}x^2(7\omega^2 - 3) + G_0(x) - \frac{7}{x^2\omega^2}[\omega^3x^3 - 2\omega^2x^2 - 6 + e^{-2x\omega}(6 + 12\omega x + 14\omega^2x^2 + 11\omega^3x^3 + 6\omega^4x^4 + 2\omega^5x^5)]\right.$$

$$\left. + \varepsilon cx\left[-1 + \frac{\omega^4}{(1+\omega)^7}(66 + 84\omega + 40\omega^2 + 7\omega^3) - \frac{8}{3}\frac{\omega^5}{(1+\omega)^9}(297 + 126\omega + 14\omega^2)\right]\right\},$$

$$G_0(x) = 9x - 14 + e^{-2x}(14 + 19x + 10x^2 + 2x^3). \tag{11}$$

Disregarding terms of order λ^3 and higher, we determine λ from the condition $\partial J/\partial\lambda = 0$; substituting the value of λ obtained in this way in Eq. (10) we obtain

$$J[x, \omega] = (e^2/\varepsilon)(a_0 - a_1^2/4a_2). \tag{12}$$

Setting $x = x_0 + \zeta$ where $x_0 = \alpha_0 R$, (α_0 is the reciprocal radius of the state of the electron of the F center) assuming $\zeta \ll 1$ and varying J over ζ, it is possible to obtain a functional which depends only on ω. In view of its unwieldiness, the analytical expression for $J[\omega]$ is not quoted. Minimizing J over ω can be carried out graphically. As a result we obtain the values of J_0 and of the parameters of the approximation ω, ζ, and λ. For the KCl crystal the calculation leads to the following values of the parameters of the self-consistent ground state of the system: $J_0 = -2.21$ ev, $\lambda = -0.13$, $\zeta = -0.13$, and $\omega = 0.70$. The value of J_0 for the F center in KCl, according to Ref. 2, amounts to -2.17 ev.

The calculations carried out above show that the deformation of the wave function of the ground state of an F center which occurs under the influence of the electric field of a nearest neighbor vacancy is actually small and leads to a lowering of the energy of the system by 1–2% (hundredths of an ev).

2. EXCITED STATES OF THE F^- CENTER

The excited states of the F^- center will be examined below in the Franck-Condon approximation. The results of the preceding section permit the choice of the wave function of the F center Eq. (5) for the wave function of the ground state of the system. In this case the Schrödinger equation can be written in the form

$$E\psi = \left\{-\frac{\hbar^2}{2\mu}\Delta - \frac{e^2}{\varepsilon r_a} + \frac{e^2}{\varepsilon r_c} - \frac{e^2c}{r_a}\left[1 - e^{-2\alpha r_a}\left(1 + \frac{19}{14}\alpha r_a + \frac{5}{7}\alpha^2 r_a^2 + \frac{1}{7}\alpha^3 r_a^3\right)\right]\right\}\psi. \tag{13}$$

This equation has been solved by means of perturbation theory. The term $W = e^2/\varepsilon r_c$ was taken as a perturbation, whereby the Hamiltonian of the system in the zeroth approximation coincides with the Hamiltonian of the F center. The energy terms of the F^- center in the first approximation of perturbation theory are determined from the secular equation, taking into account four levels of the F center E_1^0, E_2^0, E_3^0 and E_4^0, which correspond to the states $2p_0$, 2s, $2p_1$ and $2p_{-1}$. We present below the values of the energies and the wave functions of the lowest excited states of the F^- center in first order perturbation theory:

$$E_1 = {}^1/_2(E_1^0 + E_2^0 + W_{11} + W_{22}) - \sqrt{{}^1/_4(E_1^0 - E_2^0 + W_{11} - W_{22})^2 + |W_{12}|^2},$$
$$\psi_1 = A(\varphi_{2p_0} + c_1\varphi_{2s}),$$
$$E_2 = {}^1/_2(E_1^0 + E_2^0 + W_{11} + W_{22}) + \sqrt{{}^1/_4(E_1^0 - E_2^0 + W_{11} - W_{22})^2 + |W_{12}|^2}, \tag{14}$$
$$\psi_2 = B(\varphi_{2p_0} + c_2\varphi_{2s}),$$
$$E_3 = E_3^0, \quad \psi_3 = \varphi_{2p_1}, \quad E_4 = E_4^0, \quad \psi_4 = \varphi_{2p_{-1}},$$

where

$$\varphi_{2p_x} = \pi^{-1/2}\beta^{3/2}e^{-\beta r}\, r\cos\vartheta, \quad \varphi_{2s} = [3\delta^5/\pi(\alpha^2+\delta^2-\alpha\delta)]^{1/2}\left(1-\frac{\alpha+\delta}{3}\right)e^{-\delta r},$$
$$\varphi_{2p_z} = \pi^{-1/2}\lambda^{5/2}e^{-\lambda r}\, r\sin\vartheta\sin\varphi, \quad \varphi_{2p_{-1}} = \pi^{-1/2}\lambda^{5/2}e^{-\lambda r}\, r\sin\vartheta\cos\varphi. \tag{15}$$

The values $E_1^0 = E_3^0 = E_4^0$ were determined by Pekar;[2] it is convenient to display them in the form

$$E_1^0 = E_3^0 = E_4^0 = -(\mu e^4/2\hbar^2\varepsilon^2)^{1/4}[1+\varepsilon c f(v)]^2, \qquad f(v) = 1 - {}^1/_7(66v^3+84v^2+40v+7)/(1+v)^7, \tag{16}$$

$v = \alpha/\beta = \alpha/\lambda$ is determined from the equation

$$v = (3+\varepsilon c)/(1+\varepsilon c f(v)). \tag{17}$$

The values of E_2^0 and δ were specially calculated:

$$E_2^0 = -\frac{\mu e^4}{2\hbar^2\varepsilon^2}\,\frac{3[^1/_2(1+\varepsilon c)(s^2-2s+3) - \varepsilon c\Phi(s)]^2}{(s^2-s+1)(s^2-s+7)}, \qquad \Phi(s) = (53s^4+164s^3+193s^2+103s+21)/14(1+s)^6, \tag{18}$$

$s = \alpha/\delta$ is determined from the equation:

$$s = (3+\varepsilon c)(s^2-s+7)/6[^1/_2(s^2-2s+3)(1+\varepsilon c) - \varepsilon c\Phi(s)].$$

The frequency of the corresponding photo-transition is determined by the formula

$$\hbar\Omega_i = |E_0 - E_i|, \tag{19}$$

where E_0 is the Schrödinger term of the ground state of the F^- center

$$E_0 = J_0 + \frac{e^2}{\varepsilon R} - \frac{e^2 c}{2}\int\frac{\psi_0^2(1)\,\psi_0^2(2)}{r_{12}}\,d\tau_{12}. \tag{20}$$

The absorption coefficients are proportional to the squares of the moduli of the matrix elements

$$z_i = \int\psi_0(r)\, r\cos\gamma\,\psi_i(r)\,d\tau, \tag{21}$$

γ is the angle between the electric field intensity vector $\mathbf{E}$ and the radius vector of the electron $\mathbf{r}$. Choosing for convenience the axis ac along the z axis, using the well-known relation

$$\cos\gamma = \cos\vartheta\cos\theta + \sin\vartheta\sin\theta\cos(\Phi-\varphi),$$

where θ and Φ are the spherical coordinates of the vector $\mathbf{E}$ and ϑ and φ of the vector $\mathbf{r}$, and substituting Eqs. (5) and (14) in Eq. (21), it is possible to compute the values of the absorption coefficient of light for photo-transitions to the states Eq. (14). It is convenient to use the ratios of the absorption coefficients for the corresponding F^- and F absorption bands which can be written in the form

$$\begin{aligned}\xi_1 &= \tau_1^{F^-}/\tau^F = 2A^2\cos^2\vartheta\,(\Omega_1^{F^-}/\Omega^F)\,N_{F^-}/N_F,\\ \xi_2 &= \tau_2^{F^-}/\tau^F = 2B^2\cos^2\vartheta\,(\Omega_2^{F^-}/\Omega^F)\,N_{F^-}/N_F,\\ \xi_3 &= \tau_{3,4}^{F^-}/\tau^F = 2\sin^2\vartheta\,(\Omega_{3,4}^{F^-}/\Omega^F)\,N_{F^-}/N_F,\end{aligned} \tag{22}$$

if the irradiation is performed with polarized light; for natural light it is necessary to average over ϑ. In the expressions Eqs. (22), $\Omega_i^{F^-}$ and Ω^F denote the absorption frequencies of F^- and F centers respectively, N_{F^-} and N_F are the concentrations of F^- and F centers.

For the KCl crystal the calculations yield:

$$\begin{aligned}&\hbar\Omega_1 = 2.2\ \text{ev}, \quad c_1 = 0.55, \quad \xi_1 = 0.85\,N_{F^-}/N_F,\\ &\hbar\Omega_2 = 2.0\ \text{ev}, \quad c_2 = 1.82, \quad \xi_2 = 0.20\,N_{F^-}/N_F,\\ &\hbar\Omega_3 = \hbar\Omega_4 = 1.9\ \text{ev}, \qquad \xi_{3,4} = 0.95N_{F^-}/N_F.\end{aligned} \tag{23}$$

An estimate indicates that the total error of the calculation brought in through the use of an inexact wave function for the ground state of the F^- center Eq. (5) and by the neglect of a second approximation in perturbation theory is of the order of hundredths of an electron volt.

Thus, two absorption bands of rather large intensity correspond to the F^- bands, situated in the immediate vicinity of the F band. It should be pointed out that the frequency of light absorbed by F centers in KCl, calculated in the Franck-Condon approximation with the use of the functions Eqs. (5) and (15) turns out equal to 2.0 ev while the experimental value is 2.2 ev.

It is interesting to note that the lowest of the excited levels of the F^- center turns out to be a $2p\pi$ level and not a $2p\sigma$, as for example in the case of the H_2^+ ion or of the F_2^+ color center.

3. POLARIZED LUMINESCENCE OF F^- CENTERS

From the results of Sec. 2 it follows that the absorption and consequently also the emission of light by each individual F^- center is proportional to $\sin^2\theta$ for the long wavelength and $\cos^2\theta$ for the short wave F^- band. In a crystal, several possible orientations of F^- centers exist, for example, six in a crystal of the KCl type according to the number of nearest different charge neighbors of each ion. The calculation shows that this circumstance leads to a depencence of the degree of polarization of the emission brought about by polarized light on the direction of the electric field intensity vector **E**, and in some cases to a dependence of the total intensity of the emission on the polarization of the excited emission and to "spontaneous" polarization of emission. These dependences can be studied by means of the experiment performed by Feofilov[1] in the investigation of F_2 centers.

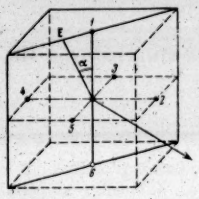

By way of example we consider one of the possible cases. From a crystal containing F^- centers let a platelet be cut having its face coincident with a 110 plane of the crystal. We shall excite F^- centers by light polarized in this plane; by rotating the crystal, one can vary the angle α between the vector **E** and the fiducial axis of the crystal (see figure). Further, the intensity of the emission in a direction perpendicular to the face of the crystal is measured as a function of the angle α and the degree of polarization of the emission is calculated.

Let us suppose for definiteness, that the excitation occurs in the long wave F^- band. Computation of the angle θ for each group of similarly orientated F^- centers permits the determination of the probability of absorption of light by each group of F^- proportional to $\sin^2\theta$:

$$W_1 = W_6 \sim \sin^2\alpha; \quad W_2 = W_3 = W_4 = W_5 \sim {}^1/_2(1+\cos^2\alpha). \tag{24}$$

Thus the number of F^- centers of each group excited by polarized light depends on α.

$$N_1 = N_6 = n\sin^2\alpha, \quad N_2 = N_3 = N_4 = N_5 = (n/2)(1+\cos^2\alpha), \quad n = \text{const}. \tag{25}$$

The probability of emission in a given direction for the i-th group of oscillators I_i^{em} is determined by means of integration of the functions Eqs. (24) over all possible directions of polarization of the emitted light; the total intensity of emission in a given direction is

$$J = \sum N_i I_i^{em} = c'[2\pi\sin^2\alpha + 3\pi(1+\cos^2\alpha)] = c(5+\cos^2\alpha) \tag{26}$$

and is in the given case a function of α.

The polarization of the emission is calculated according to the usual formula $p = \Sigma p_i I_i / \Sigma I_i$, where I_i is the intensity of light sent out in the direction of observation by each group of F^- centers and p_i are the partial polarizations determined according to $p_i = (J_{i\parallel} - J_{i\perp})/(J_{i\parallel} + J_{i\perp})$.

Below are presented the results of calculations for several cases; a crystal with the KCl type lattice is considered.

1. The face of the cut out platelet coincides with a 110 plane of the crystal.

(a) Excitation occurs in the long wave F^- absorption band. The emission occurs from this same excited level

$$J = c(5+\cos^2\alpha), \quad p = \frac{3\cos^2\alpha - 1}{\cos^2\alpha + 5}\cos 2\alpha. \tag{27}$$

It is easy to convince oneself of the existence of polarization of luminescence also for excitation with natural light ("spontaneous" polarization); calculation leads to the value

$$p_{sp} = \cos(2\alpha)/11. \tag{28}$$

(b) Excitation occurs in the short wave F^- absorption band; radiation proceeds from the same excited level

$$J = c(1+\cos^2\alpha), \qquad p = \frac{3\cos^2\alpha - 1}{1+\cos^2\alpha}\cos 2\alpha, \qquad p_{sp} = \frac{\cos 2\alpha}{3}. \tag{29}$$

(c) The excitation occurs in the short wave F^- absorption band; the emission proceeds from the lowest excited level (assuming that a non-radiative transition has taken place to the lowest excited level)

$$J = c(2 + \sin^2\alpha), \quad p = \frac{1 - 3\cos^2\alpha}{2 + \sin^2\alpha}\cos 2\alpha, \quad p_{sp} = -\frac{\cos 2\alpha}{5}. \tag{30}$$

2. The face of the cut out platelet coincides with a 100 crystal plane.

$$\text{a) } J = 6c, \quad p = \frac{\cos^2 2\alpha}{3}, \quad p_{sp} = 0, \qquad \text{b) } J = 2c, \quad p = \cos^2 2\alpha, \quad p_{sp} = 0,$$
$$\text{c) } J = 2c, \quad p = -\cos^2 2\alpha, \quad p_{sp} = 0. \tag{31}$$

For F_2 and F_2^+ centers according to references 5 and 7, cases (a) and (c) are realized.

The results Eqs. (27 – 31), generally speaking, differ from Feofilov's results[7] obtained with the hypothesis of absorption and emission of light by classical oscillators, the axes of which coincide with the axes of the F^- centers. Such a discrepancy is brought about by the unusual spacing of the excited levels of the F^- center as noted above.

4. COMPARISON OF THEORY WITH EXPERIMENT

The experimental investigations show that in the immediate neighborhood of the F absorption band under certain conditions additional bands arise situated on both the long and short wave sides of the F band. In particular, in Refs. 8 and 9 additional absorption bands were observed with a lower intensity F band. These former are masked upon increased intensity of absorption of light in the F band and apparently on this account they were not noticed by previous investigators. The frequencies of the absorption maxima of light in KCl for several of these bands are 1.76, 1.84, 1.94 and 2.03 ev, i.e., in rather good agreement with the results obtained during examination of the absorption of light by F^- centers. On the other hand, the absorption frequencies calculated in reference 5 for light in the F bands (1.91 and 2.22 ev for the intense F_2^+ band in KCl) are also very close to the experimental results of Yagi.[9]

One should note that the criterion of the macroscopic approximation used in the present work and in Refs. 3 – 5 in the alkali halide crystals for which the experimental data necessary for a comparison with theory is available, is not sufficiently well fulfilled for color centers.[2] Taking also into account the fact that in the range of frequencies in which the theory predicts the presence of the F_2^+ and F^- bands (1.8 – 2.3 ev in KCl) there is a whole series of very closely spaced bands, one must admit that a detailed comparison of experimental and theoretical results for the absorption frequency of light by the considered color centers is not possible in the given case.

The method considered in Sec. 3 of polarized luminescence of color centers, proposed by Feofilov[7] can be used for the precise identification of F^- centers.

I consider it my pleasant duty to express my appreciation to M. F. Deigen for valuable consultation.

[1] F. Seitz, Revs. Mod. Phys., **18**, 384 (1946).

[2] S. I. Pekar, Исследования по электронной теории кристаллов (Investigations in the Electron Theory of Crystals), GITTL, 1951.

[3] M. F. Deigen, J. Exptl. Theoret. Phys. (U.S.S.R.) **21**, 992 (1951); J. Exptl. Theoret. Phys. (U.S.S.R.) **24**, 631 (1953).

[4] M. F. Deigen and V. L. Vinetskii, J. Exptl. Theoret. Phys. (U.S.S.R.) **32**, 289 (1957), Soviet Phys. JETP 5, 226 (1957).

[5] V. L. Vinetskii and M. F. Deigen, Оптика и спектроскопия (Optics and Spectroscopy), (in press).

[6] Yu. E. Perlin, J. Exptl. Theoret. Phys. (U.S.S.R.) **20**, 274 (1950).

[7] P. P. Feofilov, Dokl. Akad. Nauk SSSR **92**, 545, 743 (1953); J. Exptl. Theoret. Phys. (U.S.S.R.) **26**, 607 (1954).

[8] Uchida, Ueta and Nakai, J. Phys. Soc. Jap. **6**, 107 (1951); Y. Uchida and H. Yagi, J. Phys. Soc. Jap. **7** 109 (1952).

[9] H. Yagi, J. Phys. Soc. Jap. 11, **430**, 723 (1956).

Translated by R. L. Eisner
146

LETTERS TO THE EDITOR

ON THE NUCLEAR REACTION $Li^6(n, t)He^4$

T. I. KOPALEISHVILI

Tbilisi State University

Submitted to JETP editor April 2, 1957

J. Exptl. Theoret. Phys. (U.S.S.R.) 33, 788-790 (September, 1957)

THE reaction $Li^6(n, t)He^4$ was investigated in Ref. 1 in the 1 – 14 Mev energy region on the basis of the two-particle model of the Li^6 nucleus, proposed in Ref. 2. This model assumes that the Li^6 nucleus can be considered as a system composed of a deuteron and an α-particle, the relative motion of which can be described by s-waves. It was assumed that the reaction $Li^6(n, t)He^4$ is the result of the direct interaction of the incident neutron with the deuteron of the Li^6 nucleus. In the matrix element the energy of the n-d interaction is replaced by the interaction energy of the deuteron with the α-particle. This interaction determines in addition the binding of the ground state of the nucleus $Li^6 = \alpha + d$, it being taken in the form of a potential well. On the basis of these assumptions an angular distribution was obtained in the Born approximation for the process, providing an explanation for the experimental fact that the cross section has a forward maximum.

In this work the question of the energy dependence of the total cross section of the process is investigated.

Taking into account the fact that on the basis of the assumptions in Ref. 1, the assumed analytic expression for the differential and total cross sections could not be obtained, we have changed some of the assumptions to obtain it.

First we take the interaction of the deuteron with the α-particle in the Li^6 nucleus to be not in the form of a potential well, but in the form of a potential oscillator with cut-off at a finite distance.[3] For the radial wave function corresponding to this potential, one can take to a satisfactory approximation, as has been shown in Ref. 3, the expression corresponding to a potential oscillator which extends to infinity. For an s-state this has the form

$$R(r) = \sqrt{2}\,(2\pi)^{-1/4}(r_0')^{-3/2}\exp\{-{}^1/_4(r/r_0')^2\},$$

where r_0' is the quantity connected with the nuclear radius and is introduced in the theory as a parameter.

Secondly, in the matrix element the interaction energy of the neutron with the deuteron is not replaced by the interaction energy between the deuteron and the α-particle; it is taken instead in an explicit way. Formally speaking, this interaction must consist of the two interactions between the incident neutron and each of the two nucleons that enter in the composition of the deuteron. However, instead of these two parts we take some average interaction, appearing as a function of the distance between the incident neutron and the center of the deuteron, and we assume that it has the form of a potential well of width 3×10^{-13} cm and of depth 7.81 Mev.[3]

For the wave function of the ground state of the deuteron we take the usual expression and for the triton the expression used in the work of Refs. 1 and 3. On the basis of these assumptions in the Born approximation we obtain as a result of the derivation the following expression for the total cross section of the process:

$$\sigma(E_n) = 2\pi \cdot 55.3\,(\alpha r_0')\,r_0'^2\,\Pi(E_n, \theta)\,e^{-2(a-b)}\,\frac{1-e^{-4b}}{2b}\sqrt{1+Q/E_n},\quad a = (k_t r_0')^2 + {}^4/_9(k_n r_0')^2,\quad b = 4\,(k_t r_0')\,(k_n r_0')/3,$$

$$\Pi(E_n, b) = \left\{\exp\left[-\frac{(KS_0)^2}{4.5}\right] - 0.388\,\frac{\sin KS_0}{KS_0} - 0.051\exp\left[\frac{(KS_0)^2}{4.5}\right]\right[2\cos 2KS_0 - 0.734\exp\left[\frac{(KS_0)^2}{4.5}\right]$$
$$\times\left(u_1\left(\frac{KS_0}{\sqrt{4.5}}, 1.06\right)\sin 3KS_0 + v_1\left(\frac{KS_0}{\sqrt{4.5}}, 1.06\right)\cos 3KS_0\right)\Big]\Big\}^2, \qquad (1)$$

where

$$u_1(x, y) + iv_1(x, y) = e^{-z^2} \int_0^z e^{t^2} dt, \quad z = x + iy,$$

is a tabulated function;[4] $q = k_t - 2k_n/3$ and $K = k_t/3 - k_n$, where k_t and k_n are the wave vectors of the corresponding particle in the center of mass system; $Q = 4.56$ Mev.

The energy dependence of the total cross section for $E \geq 1$ Mev, obtained from formula (1), is plotted in the figure for the parameter $r_0' = 1.5 \times 10^{-13}$ cm. The experimental results of Ref. 5 are indicated by the segments.

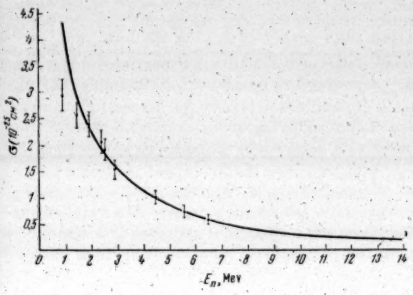

We see that in the energy region $E_n = 1 - 14$ Mev, the agreement of the theory with the experiment is satisfactory. Better results cannot be expected because of the very approximate character of the calculation. In the region of small energies the experimental cross section has a sharp maximum for $E_n = 0.25$ Mev, which is not shown on the figure and which our calculation does not give. This should have been expected, considering that an energy $E_n = 0.25$ Mev of the incident neutron corresponds to the formation of the Li^7 nucleus in one of its excited states (7.46 Mev), and consequently the process exhibits in this energy region a resonance which is not taken into account by us. The disagreement of the theory with the experiment in the region of small energies can also be ascribed to the fact that the use of the Born approximation is not permissible here.

In conclusion I thank Prof. V. I. Mamasakhlisov for his interest in this work and for many comments.

[1] J. Dabrowski and J. Sawicki, Phys. Rev. 97, 1002 (1955).

[2] I. Sh. Vashakidze and G. A. Chilashvili, J. Exptl. Theoret. Phys. (U.S.S.R.) 26, 254 (1954).

[3] T. I. Kopaleishvili, Trudy, Tbilisi State University 62, 83 (1957).

[4] K. A. Karpov, Таблицы функции $W(z) = e^{-z^2} \int_0^z e^{t^2} dt$ в комплексной области (Tables of the Functions $W(z) = e^{-z^2} \int_0^z e^{t^2} dt$ in the Complex Plane), Academy of Sciences Press (1954).

[5] F. L. Ribe, Phys. Rev. 103, 741 (1956).

Translated by Fay-Ajzenberg-Selove
147

CONCERNING SUPERPOSITIONS WITH RESPECT TO THE INTERNAL PROPERTIES OF ELEMENTARY PARTICLES

M. I. PODGORETSKII

Joint Institute for Nuclear Research

Submitted to JETP editor June 12, 1957

J. Exptl. Theoret. Phys. (U.S.S.R.) **33**, 790-791 (September, 1957)

QUITE recently facts have been found that indicate the presence of an internal structure of elementary particles. One can try making the hypothesis that this internal structure and the internal motions associated with it determine the properties of elementary particles, in analogy with the situation that exists

for atoms and nuclei. If also one assumes that the most general features of quantum mechanics are retained, one can expect the occurrence of superpositions with respect to the various internal properties of the elementary particles, i.e., the occurrence of states in which an elementary particle is not characterized by a definite value of one or another internal parameter.

A widely discussed example of superposition is that associated with the charge (or combined) parity and "strangeness" of K^0-mesons.[1] A second example relates to the spatial parity of "strange" particles.[2]* It is interesting to note that particles not having definite parity could in principle have a large electric dipole moment, of the order of 10^{-25} gm$^{-1/2}$ cm$^{5/2}$ sec^{-1}.

Nor can we exclude the possibility of the existence of particles not having a definite value of the spin. In applications to the "strange" particles such an assumption would essentially change the interpretation of many statements relating to this subject. Wide possibilities would be opened up in the discussion of various sorts of angular correlations, etc. As a consequence susceptible of direct experimental test, we suggest a change of the ratio of the numbers of long-lived and short-lived θ^0-mesons (cf. for example, Ref. 1).

If a conservation law holds for some internal property Ω (either absolutely or for strong interactions only), then in collisions of ordinary particles the particles described by superpositions with respect to Ω can be produced only in pairs or larger numbers. Similarly, if before a reaction there is one such particle, then also after the reaction there must remain at least one. For the "strange" particles we thus get conclusions that are usually connected with a law of conservation of "strangeness." This question is considered from a somewhat different point of view in Ref. 5, where the property Ω is that of spatial parity. But in general the property Ω can be of a different nature. Nor is it excluded that similar considerations can be applied not only in connection with the law of conservation of "strangeness" but also with other conservation laws.

The writer is grateful to A. Z. Dolginov, L. G. Zastavenko, L. I. Lapidus, A. L. Liubimov, V. I. Ogievetskii, and D. S. Chernavskii for participation in discussions.

*The parity nonconservation so far observed in β-decays[3,4] may have no bearing on the decays of hyperons and K-mesons into nucleon and π-mesons.

[1] Ia. B. Zel'dovich, Usp. Fiz. Nauk **59**, 377 (1956).
[2] J. Schwinger, Phys. Rev. **104**, 1164 (1956).
[3] Wu, Ambler, Hayward, Hoppes, and Hudson, Phys. Rev. **105**, 1413 (1957).
[4] Garwin, Lederman, and Weinrich, Phys. Rev. **105**, 1415 (1957).
[5] I. M. Gel'fand and M. L. Tsetlin, J. Exptl. Theoret. Phys. (U.S.S.R.) **31**, 1107 (1956); Soviet Phys. JETP **4**, 947 (1957).

Translated by W. H. Furry
148

ON THE PRINCIPLE OF LARMOR INVARIANCE

A. A. BORGARDT

Dnepropetrovsk State University

Submitted to JETP editor April 27, 1957

J. Exptl. Theoret. Phys. (U.S.S.R.) **33**, 791-792 (September, 1957)

In present day field theory relativistic invariance of the basic equations, which includes invariance under four-dimensional displacements, rotations, and reflections, is considered sufficient. The remaining transformations of the conformal group are added if the rest mass of the particle vanishes. We note that electrodynamics includes also the so-called Larmor transformation, which is not contained in the conformal group transformations and which amounts to a simultaneous change of the parities of the field quantities. Huygens' principle cannot be correctly formulated in Maxwell's electrodynamics, which, al-

though relativistically invariant, is not Larmor invariant. Such a formulation is possible only in the framework of a Larmor invariant theory which includes magnetic charges (Kottler's formulas).[1]

Recently Ohmura[2] has shown that magnetic charges must be considered to achieve stability for the classical electron.

The wave equations for a boson field, invariant under the Larmor transformation, can be written as follows[3,4]

$$\gamma_\lambda \partial\psi / \partial x_\lambda + k_0 \psi = q, \quad -\partial\psi^+\gamma_\lambda / \partial x_\lambda + k_0\psi^+ = q^+, \tag{1}$$

$$^1/_2\{\gamma_\mu\gamma_\nu\} - \delta_{\mu\nu} I = 0, \qquad \psi^+ = \psi^* R_4, \tag{2}$$

(in the general case $\psi^+ = -i\psi^* R_n$, where $R_n = n_\lambda R_\lambda$, $n_\lambda^2 = I$).

In this theory Larmor conjugation is accomplished by means of the matrix $\overline{\gamma_5} = R_5\gamma_5$:

$$\psi^L = \overline{\gamma}_5\psi, \quad q^L = \overline{\gamma}_5 q, \quad \psi^{+L} = \psi^+\overline{\gamma}_5, \quad q^{+L} = q^+\overline{\gamma}_5. \tag{3}$$

Equations (1) are Larmor invariant because $[\overline{\gamma_5}\ \gamma_\mu] = 0$ and $\overline{\gamma_5} = I$. This is not the case in Kemmer's theory where the kinematic matrices are the β_μ — the "halves" of the γ_μ:

$$\beta_\mu = {}^1/_2(\gamma_\mu + \overline{\gamma}_\mu), \quad [\overline{\gamma}_5\beta_\mu] = \overline{\gamma}_5\overline{\gamma}_\mu. \tag{4}$$

Invariance of the (1) — (2) system under the transformation (3) leads to the interesting fact, pointed out in Ref. 4, that the wave equations can be deduced from two different Larmor invariant Lagrangians, a scalar L and a pseudoscalar $\widetilde{L}$,

$$L = {}^1/_2(\varphi^+ R_5\psi + \psi^+ R_5\varphi), \quad \widetilde{L} = {}^1/_2(\varphi^+\gamma_5\psi + \psi^+\gamma_5\varphi) \quad (\varphi = \psi - q). \tag{5}$$

In actuality one apparently has to form a linear combination of the two and choose the action in the form

$$S = {}^1/_4\int(\varphi^+ R_5(I \pm \gamma_5)\psi + \psi^+ R_5(I \pm \gamma_5)\varphi)(dx). \tag{6}$$

The invariance under transformation (3) is connected with the intrinsically five-dimensional character of our space (γ_μ and γ_5 form a five dimensional representation of the Dirac algebra). Therefore it is logically unavoidable to require that both classical and quantum field theory be Larmor invariant.

The extension of these conclusions to the theory of spinor fields does not present any difficulties and requires merely a slight development of existing methods similar, for example, to those employed in Ref. 5.

[1] B. Backer and E. Copson, The Mathematical Theory of Huygens' Principle, Oxford, 1939.
[2] T. Ohmura, Progr. Theor. Phys. 16, 684, 684 (1956).
[3] A. A. Borgardt, Dokl. Akad. Nauk SSSR 78, 1113 (1951).
[4] A. A. Borgardt, J. Exptl. Theoret. Phys. (U.S.S.R.) 24, 284 (1953).
[5] Umezawa, Kamefuchi, and Tanaka, Progr. Theor. Phys. 12, 383 (1954).

Translated by A. Bincer
149

THEORY OF ELECTRON PARAMAGNETIC RESONANCE IN SUPERCONDUCTORS

M. Ia. AZBEL' and I. M. LIFSHITZ

Physico-Technical Institute, Academy of Sciences, Ukrainian S.S.R.

Submitted to JETP editor April 27, 1957

J. Exptl. Theoret. Phys. (U.S.S.R.) 33, 792-794 (September, 1957)

ELECTRON spin paramagnetic resonance has recently been observed in various metals.[1] The theory of the resonance has also been published.[2,3] The theory indicates that diffusion of conduction electrons into the depth of the metal plays an important part in the effect. The diffusion causes the attenuation of elec-

tromagnetic fields in the metal to be much less at resonance than it is away from resonance. Thin films are thus selectively transparent.

The question arises, whether paramagnetic resonance and selective transparency are possible in superconductors. Since the superconducting electrons do not diffuse, one must presumably consider only the normal electrons. Then the difference in behavior of a metal in the superconducting state will arise only from the fact that the constant magnetic field is attenuated with depth ($H = H_0 e^{-z/\delta_0}$). The electrons are consequently polarized by the constant field only for a time $(\delta_0/v) \sim 10^{-13}$ sec (v is the electron velocity), much shorter than one period of the high-frequency field. Paramagnetic resonance in bulk superconductors thus appears to be impossible. To observe resonance in a superconductor, we must make the thickness d smaller than δ_0. An experimental observation of paramagnetic resonance in a bulk superconductor would imply that the resonance is produced by the superconducting electrons.

To determine the attenuation of the high-frequency and constant fields with depth, we solve Eq. (12a) of Ref. 3. An elementary examination of the terms in Eq. (12a) shows that Eq. (15) of Ref. 3 always holds for the normal electrons. We suppose that the constant field $H_0 e^{-z/\delta_0}$ is not too strong, so that even at the surface the Larmor frequency $\Omega_0 = (2\mu H_0/\hbar)$ is small compared with the collision frequency $(1/t_0)$ of the electrons; this condition is always fulfilled in practice. Then taking the constant field along the x-axis, we obtain as in Ref. 3

$$M = -i\chi\bar{w}e^{i\omega t}; \quad M_z = \chi(B_z - \bar{w}_z); \quad \bar{\Phi} = \frac{1}{2}\int_0^\pi \Phi \sin\theta\, d\theta; \quad v\cos\theta \frac{\partial w_z}{\partial z} + \frac{\dot{w}_z}{t_0^*} = \frac{\bar{w}_z}{t_0^*} + \mathrm{Re}(\bar{w}\Omega_1^*);$$

$$v\cos\theta \frac{\partial w}{\partial z} + \frac{w}{t_0} + i(\omega - \Omega_0 e^{-z/\delta_0})w = \frac{\bar{w}}{t_0} + \omega B_1; \quad w(0; v_z) = 0; \quad w(0; -v_z) = 0 \quad (v_z > 0); \tag{1}$$

$$M = M_x + iM_y; \quad 1/t_0^* = 1/t_0 + 1/T_{sp}.$$

Here **M** is the electron spin magnetization, T_{sp} is the relaxation time for an electron spin to be flipped in a collision, v is the electron velocity, and ω the applied frequency. We find then an equation for $\bar{w}$,

$$\bar{w}(z) = \int_0^\infty K(z;\mu)\left(\frac{\bar{w}(\mu)}{t_0} + \omega H_1(\mu)\right)d\mu, \quad K(z;\mu) = \frac{1}{2v}\int_1^\infty \frac{du}{u}\exp\left\{-\frac{|z-\mu|u}{v}\left(\frac{1}{t_0^*} + i\omega\right) + \frac{i\omega\delta_0}{v}|e^{-z/\delta_0} - e^{-\mu/\delta_0}|u\right\}. \tag{2}$$

But $\omega\delta_0/v \ll 1$ for $\omega \ll 10^{13}$ sec^{-1}. Therefore

$$K(z;\mu) \approx K(|z-\mu|) = \frac{1}{2v}\int_1^\infty \frac{du}{u}\exp\left\{-\frac{|z-\mu|}{v}\left(\frac{1}{t_0^*} + i\omega\right)u\right\}. \tag{3}$$

From Eq. (2) and (3) it appears that in superconductors with $\omega\delta_0/v \ll 1$ there is never any paramagnetic resonance from the normal electrons. But even in superconductors, the spin diffusion of the normal electrons gives rise to a small deeply penetrating term in the expressions for both high-frequency and constant fields.

Using the methods which we have explained elsewhere,[3,4] we find for the constant field the expression

$$H(z) \approx H_0 e^{-z/\delta_{\mathrm{eff}}} + A\cdot 4\pi\chi\left(\frac{c^2|Z|}{2\pi v}\right)^2 |H_{\mathrm{inc}}|^2 \frac{2\mu}{\hbar\omega}\frac{3T_{sp}}{t_0}\frac{e^{-z/\delta_{\mathrm{eff}}}}{\sqrt{1+\omega^2 T_{sp}^2}}; \quad A \sim 1, \quad \delta_{\mathrm{eff}} = v\sqrt{t_0 T_{sp}/3},$$

Here we assume $\omega t_0 \ll 1$, $t_0 \ll T_{sp}$. Z is the surface impedance of the metal,[5] and H_{inc} is the strength of the incident component of the high-frequency magnetic field. Thus when $z \gg \delta_0$ the magnetic field in a superconductor is attenuated much more slowly than the usual London theory predicts.

---

[1] Griswold, Kip, and Kittel, Phys. Rev. **88**, 951 (1952); G. Feher and A. F. Kip, Phys. Rev. **95**, 1343 (1954); **98**, 337 (1955).

[2] F. J. Dyson, Phys. Rev. **98**, 349 (1955).

[3] Azbel', Gerasimenko, and Lifshitz, J. Exptl. Theoret. Phys. (U.S.S.R.) **32**, 1212 (1957), Soviet Phys. JETP **5**, 986 (1957).

[4] M. Ia. Azbel', J. Exptl. Theoret. Phys. (U.S.S.R.) 32, 1259 (1957), Soviet Phys. JETP 5, 1027 (1957).
[5] A. A. Abrikosov, Dokl. Akad. Nauk SSSR, 86, 43 (1952).

Translated by F. J. Dyson
150

ON THE THEORY OF THE NEUTRINO WITH ORIENTED SPIN

A. A. SOKOLOV

Moscow State University

Submitted to JETP editor June 5, 1957

J. Exptl. Theoret. Phys. (U.S.S.R.) 33, 794-796 (September, 1957)

LEE and Yang[1] have advanced the hypothesis of the nonconservation of parity under spatial inversion in the weak interactions. Developing this idea, Lee and Yang,[2] Salam,[3] and Landau[4] have suggested that this violation of the parity rule can in particular cases be related to special properties of the neutrino, by requiring that it satisfy an equation with the two-rowed Pauli matrices. According to this theory the spin of the neutrino is always parallel to the direction of its momentum, and the spin of the antineutrino is always antiparallel to its momentum. As has been shown by Landau and by Lee and Yang, this theory is invariant with respect to combined inversion. Combined inversion means interchange of particle and antiparticle with simultaneous spatial inversion.

We wish to show that the new theory of the neutrino can be obtained from the Dirac theory, if in the latter one carries out an explicit resolution of the functions in terms of spin states.[5] Then it is not necessary to separate the interaction energy into a sum of main quantities and their pseudo-values (for example, scalar plus pseudoscalar).

The Dirac equation for a free particle has the form

$$(\hat{E} \mp m_0 c^2)\begin{pmatrix}\psi_{1,3}\\ \psi_{2,4}\end{pmatrix} = c(\sigma'\hat{\mathbf{p}})\begin{pmatrix}\psi_{3,1}\\ \psi_{4,2}\end{pmatrix}, \tag{1}$$

where $\hat{E}$ and $\hat{\mathbf{p}}$ are the operators for energy and momentum, respectively, and σ' is the two-rowed Pauli matrices. Since the mass of the neutrino is zero ($m_0 = 0$), we get a linear relation between the functions,

$$\begin{pmatrix}\psi_1\\ \psi_2\end{pmatrix} = \varepsilon\begin{pmatrix}\psi_3\\ \psi_4\end{pmatrix}, \tag{2}$$

where $\epsilon = \pm 1$.

We can choose four values for ϵ: (a) $\epsilon = 1$ (states with $E > 0$ and $E < 0$ describe the neutrino), (b) $\epsilon = -1$ (states with $E > 0$ and $E < 0$ describe the antineutrino), (c) $\epsilon = E/|E|$ (states with $E > 0$ correspond to neutrinos and states with $E < 0$ to antineutrinos), and (d) $\epsilon = -E/|E|$ (states with $E > 0$ correspond to antineutrinos, and those with $E < 0$ to neutrinos).

We consider first of all the case $\epsilon = E/|E|$, in which the neutrino is a particle with positive energy and the antineutrino is a hole in the background of negative levels. Equation (1) takes the form

$$(\hat{E} - \varepsilon\sigma(\sigma'\hat{\mathbf{p}}))\begin{pmatrix}\psi_{1,3}\\ \psi_{2,4}\end{pmatrix} = 0. \tag{3}$$

The solution of Eq. (1) is of the form (see Ref. 5)

$$\begin{pmatrix}\psi_{1,3}\\ \psi_{2,4}\end{pmatrix} = L^{-3/2}\sum_{\mathbf{k}}\frac{1}{V2}\begin{pmatrix}\cos\frac{\theta}{2}\\ \sin\frac{\theta}{2}\,e^{i\varphi}\end{pmatrix}e^{i\mathbf{kr}}\left[C(\mathbf{k})e^{-ickt} \pm \tilde{C}^{+}(-\mathbf{k})e^{ickt}\right], \tag{4}$$

where $E = c\hbar k$ is the energy of the particle and $\mathbf{p} = \hbar\mathbf{k}$ is its momentum.

We get the following expressions for the total energy $\overline{E}$, the total momentum $\mathbf{G}$, and the total spin component $\overline{S}$ in the direction of motion:

$$\overline{E} = c\int d^3x \left[(\psi_3^+\psi_4^+)(\sigma'\hat{\mathbf{p}})\begin{pmatrix}\psi_1\\ \psi_2\end{pmatrix} + (\psi_1^+\psi_2^+)(\sigma'\hat{\mathbf{p}})\begin{pmatrix}\psi_3\\ \psi_4\end{pmatrix}\right] = \sum_{\mathbf{k}} c\hbar k\,[C^+(\mathbf{k})\,C(\mathbf{k}) - \widetilde{C}(-\mathbf{k})\,\widetilde{C}^+(-\mathbf{k})],$$

$$\overline{\mathbf{G}} = \sum_{\mathbf{k}} \hbar\mathbf{k}\,[C^+(\mathbf{k})\,C(\mathbf{k}) + \widetilde{C}(-\mathbf{k})\,\widetilde{C}^+(-\mathbf{k})],\quad \overline{S} = \sum_{\mathbf{k}} [C^+(\mathbf{k})\,C(\mathbf{k}) + \widetilde{C}(-\mathbf{k})\,\widetilde{C}^+(-\mathbf{k})]. \qquad (5)$$

If the neutrino amplitudes obey the Fermi type of commutation relations, then we have

$$C^+(\mathbf{k})\,C(\mathbf{k}) = N(\mathbf{k}),\quad \widetilde{C}(\mathbf{k})\,\widetilde{C}^+(\mathbf{k}) = 1 - \widetilde{N}(\mathbf{k}). \qquad (6)$$

It follows from Eq. (5) that neutrinos N and antineutrinos $\widetilde{N}$ have positive energies, and that the spin of the neutrino is parallel to its momentum, that of the antineutrino antiparallel to its momentum.

In this theory we have only two states (and not four as in the theory of the electron), since the neutrino has no charge. Therefore states with different charges but having the same value for the spin component are not distinguishable.

The trace with neutrino wave functions can be calculated easily from the formula for electron wave functions with fixed spin. This formula can be written in the form:[5]

$$b'^+\beta'b'b^+\beta b' = \frac{1}{16}\mathrm{Sp}\left[\beta'\left(1 + \rho_1\varepsilon'\sigma'\frac{k'}{K'} + \varepsilon'\rho_3\frac{k'_0}{K'}\right)\left(1 + s'\sigma\mathbf{k}'/k'\right)\beta\left(1 + \rho_1\varepsilon s\frac{k}{K} + \varepsilon\rho_3\frac{k_0}{K}\right)\left(1 + s\sigma\mathbf{k}/k\right)\right], \qquad (7)$$

where b and b' are the spin amplitudes of the functions and β and β' are Dirac matrices.

If one of the particles is a neutrino, the corresponding mass must be set equal to zero ($k_0 = 0$, $K = k$) and $s = 1$. Then the states with $\epsilon = 1$ correspond to neutrinos and those with $\epsilon = -1$ to antineutrinos.

From Eq. (7) it can be seen that in another variant of the theory we can put for neutrinos $\epsilon = 1$, $s = 1$, and for antineutrinos $\epsilon = 1$, $s = -1$. Therefore we can use for their description the Majorana equation with real wave functions. If we substitute into the interaction energy not the general solution for ψ_{neutrino} (as was done by Majorana himself) but the solution separated according to the spin states, then with this procedure double β-decay (i.e., emission from a nucleus of two electrons without neutrinos) will be forbidden, unlike the situation in the old variant of the Majorana theory.

[1] T. D. Lee and C. N. Yang, Phys. Rev. 104, 254 (1956).

[2] T. D. Lee and C. N. Yang, Phys. Rev. 105, 1671 (1957).

[3] A. Salam, Nuovo cimento 5, 299 (1957).

[4] L. D. Landau, Nuclear Physics 3, 127 (1957); J. Exptl. Theoret. Phys. (U.S.S.R.) 32, 405, 407 (1957), Soviet Phys. JETP 6, 336, 337 (1958).

[5] D. D. Ivanenko and A. A. Sokolov, Phys. Z. der Sowjetunion 11, 590 (1937). A. A. Sokolov, J. of Phys. (U.S.S.R.) 9, 363 (1945). A. A. Sokolov and A. Mukhtarov, Vestnik, Moscow State Univ. 8, 63 (1948). A. A. Sokolov and D. D. Ivanenko, Квантовая теория поля (Quantum Theory of Fields), Moscow-Leningrad, 1952, pp. 110-113. A. A. Sokolov and B. K. Kerimov, Nuovo cimento 5, 921 (1957).

Translated by W. H. Furry
151

LAGRANGIAN FOR THE INTERACTION OF K-MESONS AND HYPERONS

V. G. SOLOV'EV

Joint Institute for Nuclear Research

Submitted to JETP editor June 8, 1957

J. Exptl. Theoret. Phys. (U.S.S.R.) 33, 796-797 (September, 1957)

I. In a preceding note,[1] the hypothesis about the conservation of only the combination of parities IC in all interactions was introduced, and it was shown that in certain cases conservation of IC leads to conservation of spatial parity I and invariance with respect to the operation of charge conjugation C, and in other cases, I is not conserved. In the present note the consequences following from the hypothesis of conservation of only the combination of parities in all interactions are considered, with application to the interaction of K-mesons and hyperons.

2. To explain the experimental data, Schwinger[2] proposed the existence of a strong K-π interaction. He succeeded in constructing the Lagrangian of that interaction, considering that the K-mesons do not have a definite parity. The hypothesis about the conservation of only the combination of parities makes it possible to write the Lagrangian of a strong K-π interaction in the following form:

$$L_{K\pi} = ig_{K\pi}\{K^{*}K_0\Phi - KK_0^{*}\Phi^{*}\}, \tag{1}$$

where K, K_0, and Φ are the operators of the K and π-meson fields, respectively. This Lagrangian is not invariant with respect to rotations in isotropic spin space. Thus, the local Lagrangian of a direct K-π interaction, invariant with respect to the operation IC, cannot be written in an isotopic-invariant form. We note that a non-local interaction Lagrangian (for example, the Lagrangian where positive and negative frequency parts of the wave functions are separated) can be written in a charge-invariant form.

3. Salam[4] found a Lagrangian for strong interaction of nucleons and hyperons with K- and π-mesons, invariant with respect to the operations I, C, T. We construct an addition L' to this Lagrangian, invariant relative to the operation IC, but in which I and C are not separately conserved. Keeping, in the main, the notation of Ref. 3, and assuming the K-meson to be scalar, we obtain L' in the following form

$$\begin{aligned} L' = {} & ig_1'(\bar{\psi}_p\psi_n\Phi - \bar{\psi}_n\psi_p\Phi^{*}) + ig_2'(\bar{\Lambda}\Phi^{\lambda}\Sigma^{\lambda} - \bar{\Sigma}^{\lambda}\Phi^{\lambda}\Lambda) + (g_3'/2i)\,\mathrm{Sp}\,(\tau^{\lambda}\tau^{\lambda'}\tau^{\lambda''})\,\bar{\Sigma}^{\lambda}\Phi^{\lambda'}\Sigma^{\lambda''} + ig_4'(\bar{\Xi}^{+}\Xi^{0}\Phi^{*} - \bar{\Xi}^{0}\Xi^{-}\Phi), \\ & + ig_5'(\bar{N}(i\gamma_5)\Lambda\theta - \bar{\Lambda}\theta^{*}(i\gamma_5)N) + ig_6'(\bar{N}(i\gamma_5)\tau^{\lambda}\Sigma^{\lambda}\theta - \theta^{*}\bar{\Xi}^{\lambda}(i\gamma_5)\tau^{\lambda}N) \\ & + g_7'(\bar{\Xi}(i\gamma_5)\tau^{2}\theta^{*}\Lambda + \bar{\Lambda}\theta(i\gamma_5)\tau^{2}\Xi) + g_8'(\bar{\Xi}(i\gamma_5)\tau^{\lambda}\tau^{2}\Sigma^{\lambda}\theta^{*} + \theta\tau^{\lambda}\bar{\Sigma}^{\lambda}\tau^{2}(i\gamma_5)\Xi). \end{aligned} \tag{2}$$

If the K-meson has a negative internal parity (pseudoscalar), then in the terms g_5', g_6', g_7', and g_8', the matrix $i\gamma_5$ should be replaced by 1.

From Eq. (2) it can be seen that the renormalized interactions in which I and C are not separately conserved, can be written in charge-invariant form, if they contain only vertices in which the fermion changes only one of its basic characteristics — mass, charge, or strangeness. This relates to the interactions of K-mesons with baryons and π-mesons with Λ- and Σ-hyperons. Those terms in the interaction Lagrangian in which the initial and final fermions differ only by momentum cannot be described in an isotopic-invariant form. This relates to the interaction of nucleons and cascade hyperons with π-mesons.

We note that interactions invariant with respect to IC conserve the z-component of isotopic spin J_z and the relation connecting J_z, the number of nucleons n and the strangeness s with the electrical charge, i.e., $Q/e = J_z + (n + s)/2$.

4. The hypothesis of conservation of only the combination of parities leads, firstly, to a simple explanation of K-meson decays into both two and three mesons, introducing neither a particle with non-definite parity[2] nor a parity doublet[3] and, secondly, to the possibility of building a direct K-π interaction. However, a new difficulty arises: it is impossible to describe all renormalized and local interaction Lagrangians invariant with respect to IC in a charge-invariant form.

[1] V. G. Solov'ev, J. Exptl. Theoret. Phys. (U.S.S.R.) 33, 537 (1957), Soviet Phys. JETP 6, 419 (1958).

[2] J. Schwinger, Phys. Rev. 104, 1164 (1956).

[3] T. D. Lee and C. N. Yang, Phys. Rev. 102, 290; 104, 822 (1956).
[4] A. Salam, Nuclear Phys. 2, 173 (1956).

Translated by G. E. Brown
152

INTERACTION OF FERMIONS AND THE $K_{\mu 3}$-DECAY

S. G. MATINIAN

Institute of Physics, Academy of Sciences, Georgian S.S.R.

Submitted to JETP editor June 8, 1957

J. Expti. Theoret. Phys. (U.S.S.R.) 33, 797-799 (September, 1957)

THE weak interaction of four fermions plays, apparently, an important role in the decays of K-mesons into leptons ($K_{\mu 2}$, $K_{\mu 3}$, K_{e3}). An important problem is the clarification of the variants of this interaction in K_{e3}- and $K_{\mu 3}$-decays. With this in mind, the energy spectrum of the electrons and μ-mesons[1-3] and the angular correlation between the π-meson and electron (μ-meson)[4] were studied.

In the usual investigation of the energy spectrum of μ-mesons[1-3] (electrons) it is necessary, as a result of lack of information about strong interactions, to make definite assumptions about the dependence of these interactions on the particle momenta (it is easy to see[4] that in this problem there is only one independent momentum, for example, p_{π}). However, Okun'[5] proposed to study the spectrum of electrons from K_{e3}-decay, fixing the energy of the π-mesons. In this investigation definite conclusions can be drawn about the presence of this or that variant and about the conservation of parity with respect to reflection in time in the K_{e3}-decay process, independently of knowledge of strong interactions.

In this note we consider the analogous case of $K_{\mu 3}$-decay. Although here, as compared to K_{e3}, the analysis is made more difficult because it is impossible to neglect the mass of the μ-meson, some conclusions can be drawn all the same. This is of some interest also in connection with the long-standing question as to whether the μ-meson and electron are interchangeable in weak interactions of four fermions.

According to Pais and Treiman[4] the matrix element of $K_{\mu 3}$-decay of a K-meson at rest has, in the general case, the following form (without introduction of derivative lepton functions):

$$R=\left[\left(f_S-g_V\frac{m_\mu}{M}\right)\bar{\psi}_\mu\psi_\nu+f_V\bar{\psi}_\mu\gamma_4\psi_\nu+\frac{f_T}{M}\bar{\psi}_\mu\gamma_4\gamma_\pi P_\pi\psi_\nu\right](2M^3E_\pi')^{-1}. \tag{1}$$

Here $f_{S,V,T}$ and g_V are dimensionless scalar functions of the π-meson energy, expressing the contributions of strong interactions in intermediate states (at the present time they are unknown); M is the mass of the K-meson, $P_\pi=\sqrt{E_\pi^2-m_\pi^2}$; $\hbar=c=1$ everywhere.

Calculation of the probability of emission of a μ-meson with energy E_μ and a π-meson of energy E_π gives

$$\begin{aligned}w(E_\pi,\varepsilon)=\frac{(M-E_\pi)^3}{32\pi^3M^3}\Big\{&|f_S'|^2(1-\varepsilon_0^2+\mu_0^2)+|f_V|^2(\varkappa^2-(1-\varepsilon)^2)+|f_T|^2\left(1-\frac{E_\pi}{M}\right)^2[\mu_0^2(\varkappa^2+2(1-\varepsilon))\\&+(1-\varepsilon_0^2)(1-\varepsilon)^2]+4\,\mathrm{Re}(f_Sf_V^+)\mu_0(1-\varepsilon)+2\,\mathrm{Im}(f_Sf_T^+)\left(1-\frac{E_\pi}{M}\right)[\mu_0^2+(1-\varepsilon_0^2)(1-\varepsilon)]\\&+2\,\mathrm{Im}(f_Vf_T^+)\mu_0\left(1-\frac{E_\pi}{M}\right)(1+\varkappa^2-\varepsilon)\Big\};\quad \varepsilon_0=P_\pi/(M-E_\pi);\quad \varepsilon=2E_\mu/(M-E_\pi);\\ f_S'=f_S-g_V\frac{m_\mu}{M};\quad &\varkappa^2=\varepsilon_0^2+\mu_0^2;\quad \mu_0=m_\mu/(M-E_\pi);\quad 0\leqslant\varepsilon_0/\mu_0\leqslant 2.\end{aligned} \tag{2}$$

Following Okun', we consider the spectrum of μ-mesons for a fixed energy of the π-meson. Then we will have

$$w(\varepsilon) = \Phi_S + \Phi_V(x^2 - (1-\varepsilon)^2) + \Phi_T[\mu_0^2(x^2 + 2(1-\varepsilon)) + (1-\varepsilon_0^2)(1-\varepsilon)^2] + \Phi_{ST}\mu_0(1-\varepsilon) + \Phi_{ST}[\mu_0^2 + (1-\varepsilon_0^2)(1-\varepsilon)] + \Phi_{VT}\mu_0(1+x^2-\varepsilon), \quad (3)$$

where the coefficients Φ do not depend on E_μ; the first three are positive. With conservation of temporal (combined) parity we have $\Phi_{ST} = \Phi_{VT} = 0$. In this case it is possible, in general, to have interference between S- and V-variants ($\Phi_{S'}$ and Φ_{SV}). In contradistinction to the K_{e3} case, it is impossible here to say that the presence of symmetry relative to the point $\epsilon = 1$ means that the interfering terms are zero (in the T-variant we have the term with $1 - \epsilon$).

Integrating over ϵ, which can be done without any assumptions about strong interactions, does not give anything so clear as in the K_{e3} case, and we will not give the result here.

We note that, as in the K_{e3} case, the $K_{\mu 3}$ spectrum of π-mesons can, in principle, give information for determining the form of the functions Φ.

I should like to use this opportunity to express my gratitude to L. B. Okun' for sending the manuscript of his work before publication.

[1] S. Furuichi et al., Progr. Theoret. Phys. **16**, 64 (1956); **17**, 89 (1957).
[2] S. G. Matinian, J. Exptl. Theoret. Phys. (U.S.S.R.) **31**, 529 (1956), Soviet Phys. JETP **4**, 434 (1957).
[3] S. G. Matinian, J. Exptl. Theoret. Phys. (U.S.S.R.) **32**, 929 (1957), Soviet Phys. JETP **5**, 757 (1957).
[4] A. Pais and S. B. Treiman, Phys. Rev. **105**, 1616 (1957).
[5] L. B. Okun', J. Exptl. Theoret. Phys. (U.S.S.R.) (in press), Soviet Phys. JETP (in press).

Translated by G. E. Brown
153

MEASUREMENTS OF MOLECULAR ATTRACTION BETWEEN DISSIMILAR SOLIDS

I. I. ABRIKOSOVA

Institute of Physical Chemistry, Academy of Sciences, U.S.S.R.

Submitted to JETP editor June 13, 1957

J. Exptl. Theoret. Phys. (U.S.S.R.) **33**, 799-801 (September, 1957)

THE present report is a continuation of the article[1] in which the basic theory of this problem was given, the method of measurement was described in detail, and the results of measurement of molecular attraction between fused quartz plates and lenses was given.

We chose fused quartz as basic material for preparation of specimens in the first experiments for the following reasons: its transparency allows the use of the most accurate optical method for determining the size of the gap between the surfaces; its surfaces can easily be given a high polish; and, lastly, quartz surfaces are not damaged by the various cleaning methods. All the above qualities of quartz surfaces make it possible to obtain and measure small gaps between the surfaces.

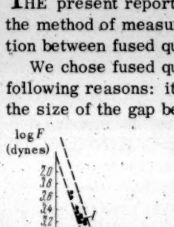

FIG. 1

The smallness of the forces of attraction between macroscopic objects makes it desirable to choose materials which, other things being equal, are characterized by large interaction forces. According to the theory of E. M. Lifshitz[2,3] the magnitude of the interaction force depends only on the electrostatic value of the dielectric constant ϵ_0 for sufficiently large distances between the bodies. The energy of attraction U, per cm^2, of two parallel plates may be written in the form

$$U = -\frac{K}{H^3}, \quad K = \frac{\hbar c}{3}\frac{\pi^2}{240}\left(\frac{\varepsilon_0 - 1}{\varepsilon_0 + 1}\right)^2 \varphi(\varepsilon_0) \quad (1)$$

(H is the magnitude of the gap between the surfaces, $\hbar$ is Planck's constant, c is the velocity of light, and $\varphi(\epsilon_0)$ is a function tabulated in Ref. 2). For the majority

of solid dielectrics the values of ϵ_0 fall in a narrow range. From among the dielectrics with a large value of ϵ_0 we found tallium halogens most convenient for our measurements.

A series of measurements was carried out on the interaction between a plate and a lens made of a mixed TlBr and TlI crystal (42.5 and 57.5% respectively). In Fig. 1 we have plotted on a log-log scale the dependence of the force of attraction F on the separation H for these samples, using a lens with a radius of 12.5 cm. In Fig. 2, where we give the dependence of the specific energy U on the separation H, the points and crosses refer to experiments with a lens of radius R = 12.5 cm and R = 5.2 cm respectively. The dashed lines in Figs. 1 and 2 are the corresponding curves obtained from formulae of Lifshitz in the limit of large separations. The theoretical curve I corresponds to assuming for the mixed tallium halogen crystal a static dielectric constant $\epsilon_0 \approx 50$ and curve II corresponds to $\epsilon = n^2 \approx 6$ (n is the index of refraction in the optical region). Here, as for quartz, the curve II is probably a more accurate approximation (see Refs. 1 and 3). The molecular attraction of these samples is approximately five times that of quartz.

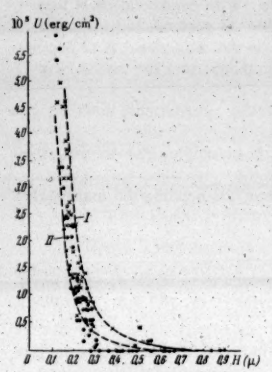

FIG. 2

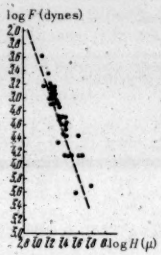

FIG. 3

The large forces of interaction and the simplicity of calculation make metals an interesting object for study; however, we must necessarily use a substantially more complicated method for measuring the gap. We had measured the gap H from the diameters of the Newton's rings seen through the upper of the studied objects. The case of a metal-transparent dielectric pair is simpler, from the point of view of procedure, since the optical method for measuring the gap can be retained. In contrast to the case of two dielectrics, it is necessary in the calculation of the gap H between the quartz and metal surfaces (from the diameters of Newton's rings) to take into account the phase shift on the reflection from the metal. In the corresponding experiments we have used a quartz-glass lens and a quartz plate coated with chromium by evaporating in vacuum. The choice of chromium was dictated by its comparatively small coefficient of reflection of light. This makes possible the observation of sufficiently contrasty interference rings in the gap between the metal and quartz surfaces. Figs. 3 and 4 give graphically the measurements for chromium.

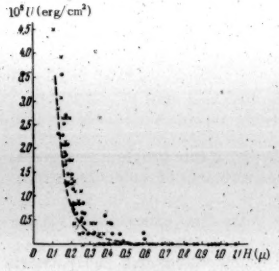

FIG. 4

According to the Lifshitz theory, the estimated interaction force f between a metal and a dielectric at sufficiently large separations is

$$f = \frac{\hbar c}{H^4} \frac{\pi^2}{240} \frac{\epsilon_0 - 1}{\epsilon_0 + 1} \varphi_1(\epsilon_0), \qquad (2)$$

where $\varphi_1(\epsilon_0)$ is the function tabulated in Ref. 3 and the remaining symbols are the same as in Eq. (1). Considering, as in the past, the transparency of quartz for wavelengths of the order of H, we have used for our calculations, the results of which are shown dashed in Figs. 3 and 4, the values ϵ_0 which also equal the squre of the index of refraction in the optical region. In the present case the measured attraction is approximately four times the interaction of quartz surfaces.

We find the agreement between experiment and theory fully satisfactory, considering the inaccuracy of the theoretical estimates and the experimental errors.

It is interesting to note that in the experiments of Prosser and Kitchener[4] precisely the same results were obtained using a method different from ours.

[1] B. V. Deriagin and I. I. Abrikosova, J. Exptl. Theoret. Phys. (U.S.S.R.) **30**, 993 (1956), **31**, 3 (1956); Soviet Phys. JETP **3**, 819 (1957), **4**, 2 (1957).

[2] E. M. Lifshitz, Dokl. Akad. Nauk SSSR **97**, 643 (1954); **100**, 879 (1955).

[3] E. M. Lifshitz, J. Exptl. Theoret. Phys. (U.S.S.R.) 29, 94 (1955), Soviet Phys. JETP 2, 73 (1956).
[4] A. P. Prosser and J. A. Kitchener, Nature 178, 1339 (1956).

Translated by A. Bincer
154

DISPERSION RELATIONS FOR S AND P WAVES FOR MESON PHOTOPRODUCTION IN FIRST ORDER OF 1/m

L. D. SOLOV'EV

Moscow State University

Submitted to JETP editor June 14, 1957

J. Exptl. Theoret. Phys. (U.S.S.R.) 33, 801-803 (September, 1957)

THE matrix element of the R-matrix for the transition corresponding to the photoproduction of a meson on a nucleon can be written in the form[1]

$$\langle \pi | R | \gamma \rangle = \frac{i(2\pi)^4}{V 4k^0 q^0} \delta(p_1 + q - p - k) \sum_{i=1}^{4} (\delta_{\rho\beta} A_i^{(1)} + \tau_\rho A_i^{(2)} + \frac{1}{2}[\tau_\rho, \tau_\beta] A_i^{(3)}) \eta_{i\beta}. \quad (1)$$

Here k, q, p, and p_1 are the momenta of the photon, meson, and nucleon in the initial and final state respectively; η_i are the spin operators which in the center of mass system have the form (e — polarization vector of the photon)

$$\eta_{i1} = i(\sigma e); \quad \eta_{i2} = k^{-1}q^{-1}(\sigma q)(\sigma[k \times e]); \eta_{i3} = ik^{-1}q^{-1}(\sigma k)(qe); \quad \eta_{i4} = iq^{-2}(\sigma q)(qe)$$

and $A_i^{(\lambda)} = A_i^{(\lambda)}(W, x)$, where W is the total energy of the system, $x = \cos\theta$ (θ — scattering angle). The quantities $A_i^{(\lambda)}$ as functions of W obey the dispersion relations[1]

$$\mathrm{Re}\, A_i^{(\lambda)}(W, x) = \overset{0}{A}{}_i^{(\lambda)}(W, x) + \frac{1}{\pi} P \int_{m+\mu}^{\infty} dW' \sum_{i'=1}^{4} f_{ii'}^{(\lambda)}(W, W', x)\, \mathrm{Im}\, A_{i'}^{(\lambda)}(W', x'), \quad (2)$$

where $\overset{0}{A}{}_i^{(\lambda)}$ and $f_{ii'}^{(\lambda)}$ are known functions, and x', the cosine of the primed angle, is connected with x, W, and W' by the relation

$$k(\omega - qx) = k'(\omega' - q'x').$$

It follows from this expression that in the c.m.s., i.e., where $\mathbf{p} + \mathbf{p}_1 = 0$, the unobservable energy range corresponds to the unobservable range of the primed angles, i.e., the range where $-\infty < x' < -1$. One therefore has to know the analytical properties of $A_i^{(\lambda)}$ as a function of x.

By means of a phase-shift analysis one can obtain expressions for the A_i in terms of Legendre polynomials; for example

$$A_1 = \sum_{l=0}^{\infty} \{[lM_{l+} + E_{l+}]P'_{l+1}(x) + [(l+1)M_{l-} + E_{l-}]P'_{l-1}(x)\} \text{ etc.}$$

(l — angular momentum of the meson; the subscript $\pm$ refers to the total angular momentum $l \pm \frac{1}{2}$ respectively; $M_{l\pm}$ corresponds to magnetic and $E_{l\pm}$ to electric multipoles). Let us assume that these infinite series can be terminated [for this to be true the integrals in (2) have to be sufficiently strongly convergent]. Then the $A_i^{(\lambda)}$ will be analytic functions of x. Further one can in (2) eliminate the angles and write down dispersion relations for $M_{l\pm}^{(\lambda)}$, $E_{l\pm}^{(\lambda)}$. We shall give these limiting ourselves to S and P waves and including recoil corrections up to the order 1/m. Introducing new variables $\epsilon = W - m$; $\epsilon' = W' - m$ we have

$$\operatorname{Re} E_{0+}^{(\lambda)}(\varepsilon) = \overset{0}{M}{}_{03}^{(\lambda)} + \frac{\varepsilon}{\pi} P\int_{\mu}^{\infty} d\varepsilon' \left\{\left(\frac{1}{\varepsilon'-\varepsilon} \pm \frac{1}{\varepsilon'+\varepsilon}\right)\frac{1}{\varepsilon'} \operatorname{Im} E_{0+}^{(\lambda)}(\varepsilon') - \left[1 \pm 1 - \frac{1}{2m}\left[\varepsilon' + \varepsilon \pm \left(\varepsilon' - \varepsilon + \frac{2(3\varepsilon^2+2q^2)}{3(\varepsilon'+\varepsilon)}\right.\right.\right.\right.$$

$$\left.\left.\left. - \frac{2\varepsilon q^2}{3(\varepsilon'+\varepsilon)^2}\right)\right]\right]\frac{1}{\varepsilon' q^3} \operatorname{Im}\left[M_{1-}^{(\lambda)}(\varepsilon') - M_{1+}^{(\lambda)}(\varepsilon')\right] + 3\left[\varepsilon' + 2\varepsilon \pm (\varepsilon' - 2\varepsilon) - \frac{1}{2m}\left[\varepsilon'(\varepsilon'+\varepsilon) + 2(\varepsilon^2+q^2)\right.\right.$$

$$\left.\left. \pm \left(\varepsilon'(\varepsilon'-\varepsilon) - \frac{2\varepsilon(\varepsilon^2+q^2)}{\varepsilon'+\varepsilon} + \frac{2\varepsilon' q^2}{3(\varepsilon'+\varepsilon)^2}\right)\right]\right]\frac{1}{\varepsilon' {}^2 q^3} \operatorname{Im} E_{1+}^{(\lambda)}(\varepsilon')\Big\}.$$

$$\operatorname{Re}\left[M_{1-}^{(\lambda)}(\varepsilon) - M_{1+}^{(\lambda)}(\varepsilon)\right] - \overset{0}{M}{}_{11}^{(\lambda)} + \frac{\varepsilon q}{\pi} P\int_{\mu}^{\infty} d\varepsilon' \left\{\mp \frac{2\varepsilon'+\varepsilon}{2m(\varepsilon'+\varepsilon)^2}\frac{1}{\varepsilon'} \operatorname{Im} E_{0+}^{(\lambda)}(\varepsilon')\right.$$

$$\left. + \left[\frac{1}{\varepsilon'-\varepsilon} \mp \frac{1}{\varepsilon'+\varepsilon}\left(1 - \frac{\varepsilon'}{m}\right)\right]\frac{1}{\varepsilon' q^3} \operatorname{Im}\left[M_{1-}^{(\lambda)}(\varepsilon') - M_{1+}^{(\lambda)}(\varepsilon')\right] + \left[1 \mp 1 - \frac{\varepsilon \pm (2\varepsilon' - 3\varepsilon)}{2m}\right]\frac{1}{\varepsilon' {}^2 q^3} \operatorname{Im} E_{1+}^{(\lambda)}(\varepsilon')\right\}.$$

$$\operatorname{Re}\left[2M_{1+}^{(\lambda)}(\varepsilon) + M_{1-}^{(\lambda)}(\varepsilon)\right] = \overset{0}{M}{}_{12}^{(\lambda)} + \frac{\varepsilon q}{\pi} P\int_{\mu}^{\infty} d\varepsilon' \left[\frac{1}{\varepsilon'-\varepsilon} \pm \frac{1}{\varepsilon'+\varepsilon}\left(1 + \frac{\varepsilon}{m}\right)\right]\frac{1}{\varepsilon' q^3} \operatorname{Im}\left[2M_{1+}^{(\lambda)}(\varepsilon') + M_{1-}^{(\lambda)}(\varepsilon')\right].$$

$$\operatorname{Re} E_{1+}^{(\lambda)}(\varepsilon) = \overset{0}{M}{}_{13}^{(\lambda)} + \frac{\varepsilon^2 q}{\pi} P\int_{\mu}^{\infty} d\varepsilon' \left\{\mp \frac{q}{6m(\varepsilon'+\varepsilon)^2}\frac{1}{\varepsilon'} \operatorname{Im} E_{0+}^{(\lambda)}(\varepsilon') + \left[\frac{1}{\varepsilon'-\varepsilon} \pm \frac{1}{\varepsilon'+\varepsilon} + \frac{1}{2m}\left(1 \mp \frac{\varepsilon'-\varepsilon}{\varepsilon'+\varepsilon}\right)\right]\frac{1}{\varepsilon' {}^2 q^3} \operatorname{Im} E_{1+}^{(\lambda)}(\varepsilon')\right\}.$$

We take here the upper sign for $\lambda = 1, 2$ and the lower sign for $\lambda = 3$. The terms $\overset{0}{M}{}_{fi}^{(\lambda)} = \overset{0}{M}{}_{fi\varepsilon}^{(\lambda)} + \overset{0}{M}{}_{fi\mu}^{(\lambda)}$ are given within the present accuracy by

$$\overset{0}{M}{}_{03\varepsilon}^{(\lambda)} = -\frac{ef}{2\mu}\left[(1 \mp 1)F_s - \frac{\omega}{2m}(1 \pm 1) \pm \frac{q^2}{3m\omega}\right];\quad \overset{0}{M}{}_{11\varepsilon}^{(\lambda)} = -\frac{ef}{2\mu}\left[(1 \mp 1)F_M - \frac{q}{2m}(1 \pm 1)\right],$$

$$\overset{0}{M}{}_{12\varepsilon}^{(\lambda)} = \frac{ef}{2\mu} \cdot \frac{q(1 \mp 1)}{2m};\quad \overset{0}{M}{}_{13\varepsilon}^{(\lambda)} = -\frac{1}{3} \cdot \frac{ef}{2\mu} \cdot (1 \pm 1)F_Q$$

($\lambda = 1, 2$ — upper sign, $\lambda = 3$ — lower sign), and

$$F_s = 1 - \frac{\omega}{2k}F;\quad F_M = \frac{4\omega}{3q}F;\quad F_Q = \frac{q}{k}\left[1 - \frac{3\omega}{4q^2}(2\omega - k)F\right]\quad F = 1 + \frac{\mu^2}{2\omega q}\ln\frac{\omega - q}{\omega + q}$$

$$\overset{0}{M}{}_{03\mu}^{(\lambda)} = \frac{f(\mu_p' \mp \mu_n)}{\mu}\left(\omega - \frac{3\omega^2 - 2q^2}{6m}\right);\quad \overset{0}{M}{}_{03\mu}^{(3)} = \frac{f(\mu_p' - \mu_n)}{\mu}\frac{q^2}{6m},\quad \overset{0}{M}{}_{11\mu}^{(\lambda)} = \frac{f(\mu_p' \mp \mu_n)}{\mu}q;\quad \overset{0}{M}{}_{11\mu}^{(3)} = 0$$

$$\overset{0}{M}{}_{12\mu}^{(\lambda)} = -\frac{f(\mu_p' \mp \mu_n)}{\mu}\,q\,\frac{\omega}{2m};\quad \overset{0}{M}{}_{12\mu}^{(3)} = \frac{f(\mu_p' - \mu_n)}{\mu}q\left(1 + \frac{\omega}{2m}\right)$$

($\lambda = 1$ — upper sign, $\lambda = 2$ — lower sign).

$$\overset{0}{M}{}_{13\mu}^{(\lambda)} = 0\ (\lambda = 1, 2, 3).$$

The equations for the P-wave are in essence similar to the corresponding expressions given by Chew and Low.[2] They differ in the meaning of the integration variable, in certain interchanges of E and M terms, and in the addition of some correction terms of the order $1/m$ [which are not important in the region of the (33) resonance]. From the equation for the S-wave we have the expression for $E_{0+}^{(3)}$ which is important in comparison with experiments:

$$-2\sqrt{2}\,E_{0+}^{(3)} = E_{0+}(\gamma p \to n\pi^+) + E_{0+}(\gamma n \to p\pi^-),$$

in which the integral converges sufficiently rapidly for large ε'.

I take the opportunity to express my gratitude to A. A. Logunov for his interest in the present work.

[1] Logunov, Tavkhelidze, and Solov'ev, Nucl. Phys. 4, 427 (1957).
[2] G. F. Chew and F. E. Low, Phys. Rev. 101, 1759 (1956).

Translated by M. Danos
155

ENERGY OF IONIZATION BY ELECTRONS IN SILICON CRYSTALS

V. M. PATSKEVICH, V. S. VAVILOV, and L. S. SMIRNOV

P. N. Lebedev Physics Institute, Academy of Sciences, U.S.S.R.

Submitted to JETP editor June 15, 1957

J. Exptl. Theoret. Phys. (U.S.S.R.) **33**, 804-805 (September, 1957)

THE mean ionization energy ϵ is one of the fundamental parameters which determines the efficiency with which the energy of nuclear radiation is transformed to electrical energy by semiconducting p-n junctions,[1] as well as the counting efficiency of crystal counters.

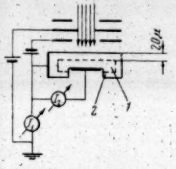

FIG. 1. Diagram of the experiment for finding ϵ in silicon. 1 — p-type silicon; 2 — n-type silicon (doped with phosphorous).

A determination of ϵ in silicon single crystals for ionization by electrons with energies between 10 and 30 kev has been performed in the same way as previously in germanium single crystals, by measuring the "multiplication" factor for current carriers.[2] We measured the ratio of the excess carrier current through the p-n junction, due to generation of electron-hole pairs by high (primary) electrons, to the primary electron current. The recombination losses were evaluated by an independent determination of the collector coefficient α, which depends on the geometry of the irradiated crystal, on the surface recombination rate of nonequilibrium carriers, and on their diffusion length.[3]

In these experiments we used p-type silicon single crystals with p-n junctions obtained by thermal diffusion of gaseous phosphorous.[4] The irradiation was performed from the direction of the n-type material, perpendicular to the crystal surface and parallel to the p-n junction (see Fig. 1).

Because of the low carrier diffusion lengths occurring in silicon after thermal diffusion of impurities to obtain a p-n junction, we used a crystal whose junction is located about 20 μ from the irradiated surface. We found that when the excess carriers are excited in these samples by monochromatic light incident on the same surface as struck by the electrons, α depends strongly on λ, and therefore also on the depth at which electron-hole pairs are produced.[4]

It was established that in contradistinction with germanium, α does not change during evacuation of the system (from atmospheric pressure to 10^{-7} mm Hg) or during electron bombardment. This is due to the occurrence of a thin, but quite firm film of quartz on the silicon surface. The thickness of this film, which lowers the initial energy of the electrons entering the silicon, was evaluated from its breakdown potential and was found to be between 0.5 and 0.7 μ. Ion bombardment led to diminution of α due to an increase in the surface recombination rate.

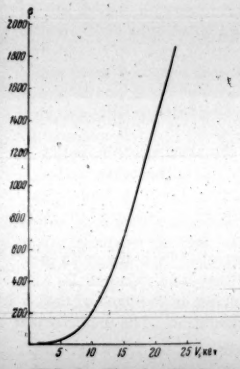

FIG. 2. The "multiplication" factor of electrons in a silicon as a function of the primary electron energy.

Figure 2 gives the experimental dependence of the "multiplication" factor β for electrons in silicon (without accounting for recombination losses) on the primary electron energy V from 1.5 to 30 kev. The shape of the curve indicates the existence of a "dead layer" on the surface. The electrons lose part of their energy in this layer, but it is transparent to light. We evaluated the distribution of ionization losses through the depth into the crystal, accounting for scattering of the primary electrons in the crystal, from the data calculated by Iurkov[5] using Spencer's method.

We evaluated ϵ for each value of V by comparing β for this energy with the value of α for light whose wavelength is such that the inverse of the linear absorption coefficient is equal to the mean free path of the electrons of given energy. The ratio α/β, which is proportional to ϵ, should not depend on the depth at which the ionization takes place in a silicon crystal. On this basis, the $\beta(V)$ curve was used to evaluate the thickness of the quartz layer. This was found to be 0.6 μ, which agrees with the data obtained from the breakdown potential.

The value of ϵ we have obtained is 4.2 ± 0.6 ev.

The authors express their gratitude to Professor B. M. Vul for many valuable remarks.

[1] Vul, Vavilov, Smirnov, Galkin, Patskevich, and Spitsyn, Атомная энергия (Atomic Energy) **2**, 533 (1957).

[2] Vavilov, Smirnov, and Patskevich, Dokl. Akad. Nauk SSSR **112**, 1020 (1957).

[3] V. S. Vavilov and L. S. Smirnov, Радиотехника и электроника (Radio Engineering and Electronics) **1**, 1147 (1956).

[4] Vavilov, Malovetskaia, Galkin, and Landsman, Usp. Fiz. Nauk (1957) (in press).

[5] B. Ia. Iurkov, J. Tech. Phys. (U.S.S.R.) (in press).

Translated by E. J. Saletan
156

FINE STRUCTURE OF ELECTRON PARAMAGNETIC RESONANCE OF THE Fe^{3+} IONS IN THE Al_2O_3 LATTICE

L. S. KORNIENKO and A. M. PROKHOROV

Moscow State University

Submitted to JETP editor June 16, 1957

J. Exptl. Theoret. Phys. (U.S.S.R.) **33**, 805-807 (September, 1957)

THE electron paramagnetic resonance spectrum of Fe^{3+} ions, introduced isomorphically into the Al_2O_3 lattice to an iron concentration of 10^{-3}, has been investigated at room temperature at three frequencies in the range from 2.5×10^{10} to 4×10^{10} cps and for magnetic fields up to 16.2 kilo-oersteds. It was found that the Fe^{3+} ions form two nonequivalent systems each of which gives a spectrum of five resonance lines. When the external magnetic field is applied parallel or perpendicular to the crystal axis, both spectra overlap. This indicates that the crystal axis fields lie in the same direction for both ion systems. The nonequivalence is due to the difference in the directions of the cubic field axes. For orientations far from the "parallel" and "perpendicular" ones, the lines of each system broaden and a weak splitting into two components is observed. This indicates that each nonequivalent ion system consists of two subsystems with somewhat differently directed cubic crystal field axes.

In order to interpret the spectrum observed, we used a Hamiltonian of the form[1]

$$\hat{H} = g\beta(H_z\hat{S}_z + H_x\hat{S}_x + H_y\hat{S}_y) + \frac{1}{6}a[\hat{S}_\xi^4 + \hat{S}_\eta^4 + \hat{S}_\zeta^4 - \frac{1}{5}S(S+1)(3S^2+3S-1)]$$
$$+ D\left[\hat{S}_z^2 - \frac{1}{3}S(S+1)\right] + \frac{1}{180}F[35\hat{S}_z^4 - 30S(S+1)\hat{S}_z^2 + 25\hat{S}_z^2 - 6S(S+1) + 3S^2(S+1)^2],$$

where g is the spectroscopic splitting factor, β is the Bohr magneton, S is the electron spin and is equal to $^5/_2$ for Fe^{3+}, $\hat{\mathbf{S}}$ is the spin operator, H is the magnetic field strength, a is the cubic lattice constant, and D and F are the second and fourth degree trigonal field constants. The $\xi\eta\zeta$ coordinate system is constructed of the cubic crystal field axes, and the Z axis lies along the direction of the trigonal axis which is also the (111) axis of the $\xi\eta\zeta$ coordinate system.

The formulas for the fields of the observed lines given by Bleaney and Trenam[1] (which are valid for strong fields when $g\beta H \gg a$, D, and F) are inapplicable because of the relatively high value of D. Therefore the energy levels were evaluated by perturbation theory, to second order in the case of the "parallel" orientation, and to first order in the case of the "perpendicular" orientation. The unperturbed Hamiltonian was taken as

$$\hat{H}_0 = g\beta(H_z\hat{S}_z + H_x\hat{S}_x + H_y\hat{S}_y) + D\left[\hat{S}_z^2 - \frac{1}{3}S(S+1)\right].$$

For the "parallel" orientation the formulas for the $\Delta M = \pm 1$ transitions are

$$M = \pm\frac{5}{2} \leftrightarrow \pm\frac{3}{2} : H_{1,5} = H_0 \pm \left\{4D - \frac{4}{3}(a-F)\right\} - \frac{20}{27}\frac{a^2}{H_{1,5} \mp 2D},$$

$$M = \pm\frac{3}{2} \leftrightarrow \pm\frac{1}{2} : H_{2,4} = H_0 \pm \left\{2D + \frac{5}{3}(a-F)\right\} + \frac{20}{27}\frac{a^2}{H_{2,4} \pm 3D},$$

$$M = +\frac{1}{2} \leftrightarrow -\frac{1}{2} : H_3 = H_0 - \frac{20}{27}a^2\left(\frac{1}{H_3 + 2D} + \frac{1}{H_3 - 2D}\right),$$

where M is the electron spin magnetic quantum number, $H_0 = h\nu/g\beta$ (ν is the frequency of the radiation field, and h is the Planck's constant), and D, a, and F are expressed in oersteds and are obtained from the corresponding constants in the expression for the Hamiltonian by dividing by $g\beta$. These formulas give good agreement with the experimental data for the following values of the constants:

$$g = 2.003 \pm 0.001, \quad |D| = (1801 \pm 3)\,\text{Oe}, \quad |a - F| = (357 \pm 2)\,\text{Oe}, \quad |a| = (280 \pm 20)\,\text{Oe}.$$

The calculated spectrum for the "perpendicular" orientation also gives good agreement between the theoretical and experimental data at the lowest of the frequencies used.

We also investigated the spectrum of a sample enriched in the isotope Fe^{57}. No line of the allowed hyperfine structure was observed, which verifies the hypothesis[1] that the nuclear magnetic moment of this iron isotope is small.

[1] B. Bleaney and R. S. Trenam, Proc. Roy. Soc. (London) **223**, 1 (1954).

Translated by E. J. Saletan
157

THE PROBLEM OF PIEZOMAGNETISM

I. E. DZIALOSHINSKII

Physical Problems Institute, Academy of Sciences, U.S.S.R.

Submitted to JETP editor June 20, 1957

J. Exptl. Theoret. Phys. (U.S.S.R.) **33**, 807-808 (September, 1957)

In the recent literature one encounters assertions that piezomagnetic bodies in general cannot exist in nature. This conclusion has been based on the invariance of the equations of mechanics with respect to a change of the sign of time when a simultaneous change is made in the signs of all magnetic fields and spins; from this the inference has been directly drawn that in the expression for the thermodynamic potential of an arbitrary substance, there can be no terms linear in the magnetic field.[1] In actuality, however, such an argument is valid only for paramagnetic bodies, whose magnetic symmetry group contains the transformation (we denote it by R) consisting of a change of sign of the magnetic field and the spin. In substances possessing, for instance, the magnetic structure of antiferromagnetics, the magnetic symmetry group does not contain the element R by itself; this element enters only in combination with other symmetry elements, or else is not present at all. Consequently such substances, in general, are capable of possessing piezomagnetic properties.[2,3] In this note several substances are pointed out that actually occur in nature and that should, on the basis of magnetic symmetry considerations be piezomagnetic.

We consider, for example, the antiferromagnetic crystals α-Fe_2O_3 and $FeCO_3$. As has been shown,[4] they have the same magnetic symmetry class, composed of the following elements:

$$2C_3,\ 3U_2,\ I,\ 2S_6,\ 3\sigma_d.$$

(This refers to that one of the two antiferromagnetic phases of α-Fe_2O_3 that exists below 250° K). Here the symbols for symmetry elements are the same as in Ref. 4; a rectangular coordinate system is chosen with the x axis along one of the twofold axes. It is easy to verify that such symmetry permits the presence, in the expression for the thermodynamic potential Φ, of two combinations linear in the components of the stress tensor σ_{ik} and of the magnetic field H:

$$\Phi = -\lambda_1\{(\sigma_{xx}-\sigma_{yy})H_x - 2\sigma_{xy}H_y\} - \lambda_2(\sigma_{xz}H_y - \sigma_{yz}H_x).$$

Hence we find at once the expressions for the magnetic moment in the absence of an external field:

$$m_x = \lambda_1(\sigma_{xx}-\sigma_{yy}) - \lambda_2\sigma_{yz}, \quad m_y = -2\lambda_1\sigma_{xy} + \lambda_2\sigma_{xz}.$$

Other examples are the antiferromagnetics MnF_2, CoF_2, and FeF_2. In accordance with Ref. 4, their magnetic symmetry class consists of

$$C_2,\ 2C_4R,\ 2U_2,\ 2U_2'R,\ I,\ \sigma_h,\ 2S_4R,\ 2\sigma_v,\ 2\sigma_v'R.$$

This symmetry group leaves invariant the following term in the expression for Φ:

$$\Phi = -\lambda(\sigma_{xz}H_y + \sigma_{yz}H_x),$$

whence we get for the magnetic moment

$$m_x = \lambda\sigma_{yz}, \quad m_y = \lambda\sigma_{xz}.$$

[1] W. Zocher and H. Török, Proc. Nat. Acad. Sci. U.S.A. **39**, 681 (1953).

[2] B. A. Tavger and V. M. Zaitsev, J. Exptl. Theoret. Phys. (U.S.S.R.) **30**, 564 (1956); Soviet Phys. JETP **3**, 430 (1956).

[3] L. D. Landau and E. M. Lifshitz, Электродинамика сплошных сред (Electrodynamics of Continous Media), Gostekhizdat, 1957.

[4] I. E. Dzialoshinskii, J. Exptl. Theoret. Phys. (U.S.S.R.) **32**, 1547 (1957); Soviet Phys. JETP **5**, 1259 (1957).

Translated by W. F. Brown, Jr.
158

THE ROLE OF NUCLEONS IN MULTIPLE PRODUCTION OF PARTICLES

A. A. EMEL'IANOV and I. L. ROZENTAL'

P. N. Lebedev Physics Institute, Academy of Sciences, U.S.S.R.

Submitted to JETP editor June 20, 1957

J. Exptl. Theoret. Phys. (U.S.S.R.) **33**, 808-809 (September, 1957)

IN the processes of multipole production of particles in collisions of high-energy nucleons with nuclei, nucleons play a special role compared to mesons.

In addition to the obvious differences caused by conservation of nuclear charge and different masses of nucleons and mesons, one should note a less obvious characteristic which is essential in a hydrodynamical description.[1] For energies of the incident nucleon $E_0 = 10^{12} - 10^{13}$ ev, the temperature of the system at the beginning of the hydrodynamical expansion is $1-2\ Mc^2$ (temperature is measured in units of energy; M is the nucleon mass). At the same time, the condition $T \gg \mu c^2$ (μ is the mass of the π-meson) is satisfied. Therefore, at the energies discussed, during the whole process the probability of production of a nucleon-antinucleon pair is very small; in this respect, nucleons and mesons differ essentially. At the present, it is not possible to unambiguously describe this difference of the nucleons in the process. Here we consider a simplified model of the hydrodynamical development of the system, taking into account the special role of the nucleons taking part in the process.[2] *

We consider a given collision of two nucleons. In the interaction between nucleons, a meson cloud is formed, which is contracted by them as if by a piston (the contraction proceeds in a non-adiabatic fashion). As a result, a system is produced in which the kinetic energy is divided between nucleons in a very small volume. It is natural, in the spirit of the whole conception, to postulate that the order of magnitude of the volume V is $(4\pi/3)(\hbar/\mu c)^3\ 2Mc^2/E'$ where E' is the energy of the nucleons in their center of

mass system, $h/\mu c$ is the radius of the meson cloud, and the factor $2Mc^2/E'$ takes into account the contraction of the cloud.

In this paper we determine the fraction of the energy carried by the fast nucleon. To obtain this, we consider the relativistic hydrodynamical equations

$$\partial T_{ik}/\partial x_k = 0, \quad T_{ik} = wu_i u_k + pg_{ik},$$

where $w = \epsilon + p$ is the enthalpy, u_i is a 4-velocity; $g_{11} = g_{22} = g_{33} = 1$, $g_{44} = -1$, $x_i = x, y, z, ict$. In the center of mass system, the system considered has the form of a flat disc at the moment of collision; therefore, in the course of the first stage, the hydrodynamical expansion can be considered as one-dimensional (for more details, see Ref. 2).

At the boundary between matter and the nucleon, the solution of Eq. (1) should satisfy the boundary condition

$$Mdu_1/dt = p\pi(h/\mu c)^2, \quad u_1 = v/\sqrt{1 - v^2/c^2},$$

where v is the nucleon velocity, p is the pressure on its 'surface,' $\pi(h/\mu c)^2$, the area of the transverse cross section of the nucleon.

A detailed consideration of the process shows that for $E_0 = 10^{11} - 10^{12}$ ev, it is sufficient to obtain a solution for simple waves in the region of nontrivial motion, bounded, on the side of the nucleon, by the region of simple waves and, on the other side, by the stationary plane of symmetry. This circumstance can be explained by the fact that the system starts to decay sooner than the wave, which is reflected by the moving nucleon, arises.

Solving the equation for the motion of the nucleon, one can obtain its energy E_k at the moment the system begins to decay (the decay of the system is characterized by a decay temperature $T_k \cong \mu c^2$). As a result of calculation, we obtained for $E_0 = 10^{11}$ and 10^{12} ev that $E_k \cong 0.3 \times 10^{11}$ and 0.2×10^{12} ev, respectively, in the laboratory system; the dependence on the energy of the fast nucleon can be written in the form

$$E_k/E_0 \sim E_0^{-1/4}.$$

It should be noted, however, that the determination of E_k is very conditional, since at an energy $E_0 \sim 10^{12}$ ev, the number of particles is small and the moment of decay cannot be determined from the local temperature near the nucleon, but from the temperature averaged over the region of space, even though there is only one nucleon. Solving, approximately, the problem for the averaged quantity, it is possible to show that $E_k \cong 0.6\, E_0$.

The energy of the fast nucleons depends appreciably also on the value of the volume V, i.e., $E_k \sim V^{-0.4}$.

*The experimental data[3,4] also shows the essential difference of the nucleons.

[1] L. D. Landau, Izv. Akad. Nauk SSSR, Ser. Fiz. 17, 51 (1953).
[2] I. L. Rozental', J. Exptl. Theoret. Phys. (U.S.S.R.) 31, 278 (1956), Soviet Phys. JETP 4, 217 (1957).
[3] I. L. Grigorov, Dissertation, Moscow, Phys. Inst. Acad. Sci. (1954).
[4] G. T. Zatsepin, Dissertation, Moscow, Phys. Inst. Acad. Sci. (1954).

Translated by G. E. Brown
159

HYDRODYNAMIC FLUCTUATIONS IN A SUPERFLUID LIQUID

I. M. KHALATNIKOV

Institute for Physical Problems, Academy of Sciences, U.S.S.R.

Submitted to JETP editor June 20, 1957

J. Exptl. Theoret. Phys. (U.S.S.R.) 33, 809-811 (September, 1957)

L. Landau and E. Lifshitz[1] have recently calculated the fluctuations of the hydrodynamical parameters in classical hydrodynamics by introducing "outside" terms in the equations of motion.[2]

We will apply the same method to a calculation of the fluctuations of the hydrodynamical parameters in a superfluid liquid. For generality we will assume that there are foreign particles dissolved in the superfluid. In view of the unusual simplicity of the method, this assumption does not complicate the calculations. We write down the hydrodynamical equations of the superfluid solution with "outside" terms

$$\partial\rho/\partial t + \operatorname{div}\mathbf{j} = 0, \quad \partial j_i/\partial t + \partial\Pi_{ik}/\partial x_k = -\partial\tau_{ik}/\partial x_k;$$

$$\partial\rho c/\partial t + \operatorname{div}\rho c\mathbf{v}_n = -\operatorname{div}\mathbf{g}, \quad \partial\mathbf{v}_s/\partial t + \nabla(\mu - cZ/\rho + v_s^2/2) = -\nabla h;$$

$$T\left(\frac{\partial S}{\partial t} + \operatorname{div}\left(S\mathbf{v}_n - \frac{Z}{\rho T}\mathbf{g}\right)\right) = -\left\{h\operatorname{div}(\mathbf{j} - \rho\mathbf{v}_n) + \frac{1}{2}\tau_{ik}\left(\frac{\partial v_{ni}}{\partial x_k} + \frac{\partial v_{nk}}{\partial x_i}\right) + \mathbf{g}T\nabla\frac{Z}{\rho T}\right\} - \operatorname{div}\mathbf{q};$$

$$\tau_{ik} = -\eta\left(\frac{\partial v_{ni}}{\partial x_k} + \frac{\partial v_{nk}}{\partial x_i} - \frac{2}{3}\delta_{ik}\frac{\partial v_{nl}}{\partial x_l}\right) - \delta_{ik}[\zeta_1\operatorname{div}(\mathbf{j} - \rho\mathbf{v}_n) + \zeta_2\operatorname{div}\mathbf{v}_n] + T_{ik},$$

$$h = -\zeta_3\operatorname{div}(\mathbf{j} - \rho\mathbf{v}_n) - \zeta_4\operatorname{div}\mathbf{v}_n + H; \quad \mathbf{g} = -\rho D\left(\nabla c + \frac{k_T}{T}\nabla T + \frac{k_p}{p}\nabla p\right) + \mathbf{G},$$

$$\mathbf{q} = -\rho DT\left(\nabla c + \frac{k_T}{T}\nabla T + \frac{k_p}{p}\nabla p\right)\left[k_T\frac{\partial}{\partial c}\left(\frac{Z}{\rho T}\right) - T\frac{\partial}{\partial T}\left(\frac{Z}{\rho T}\right)\right] - \varkappa\nabla T + \mathbf{Q}.$$

We use the same notation here as in Refs. 3 and 4.* In these equations we have introduced an "outside" momentum flow tensor T_{ik}, an "outside" potential H, and "outside" flow vector for the dissolved particles **G**, and an "outside" heat flow vector **Q**.

The rate of change of the total entropy of the liquid is, according to our earlier work,[3,4]

$$\dot{S}_{\text{tot}} = -\frac{1}{T}\int\left\{h\operatorname{div}(\mathbf{j} - \rho\mathbf{v}_n) + \frac{1}{2}\tau_{ik}\left(\frac{\partial v_{ni}}{\partial x_k} + \frac{\partial v_{nk}}{\partial x_i}\right) + \frac{\mathbf{q}\nabla T}{T} + \mathbf{g}T\nabla\frac{Z}{\rho T}\right\}dV.$$

The correspondence between the quantities figuring in the theory of fluctuations[5] (equations of motion $\dot{x}_\alpha = \gamma_{\alpha\beta}x_\beta + y_\alpha$), and the quantities in our equations are given by the following table

$\dot{x}_\alpha$	τ_{ik}	h	$\mathbf{g}$	$\mathbf{q}$
X_α	$-\frac{1}{2T}\left(\frac{\partial v_{nl}}{\partial x_i} + \frac{\partial v_{nk}}{\partial x_i}\right)\Delta V$	$-\frac{1}{T}\operatorname{div}(\mathbf{j} - \rho\mathbf{v}_n)\Delta V$	$-\nabla\frac{Z}{\rho T}\Delta V$	$-\frac{\nabla T}{T^2}\Delta V.$
y_α	T_{ik}	H	$\mathbf{G}$	$\mathbf{Q}$

Making use of the expression

$$\overline{y_\alpha(t_1)\,y_\beta(t_2)} = k(\gamma_{\alpha\beta} + \gamma_{\beta\alpha})\,\delta(t_1 - t_2),$$

we obtain the fluctuations of the "outside" terms in the hydrodynamical equations of a superfluid liquid

$$\overline{T_{ik}(\mathbf{r}_1t_1)\,T_{lm}(\mathbf{r}_2t_2)} = 2kT\left\{\eta(\delta_{il}\delta_{km} + \delta_{im}\delta_{kl}) + \left(\zeta_2 - \frac{2}{3}\eta\right)\delta_{ik}\delta_{lm}\right\}\cdot\delta(\mathbf{r}_1 - \mathbf{r}_2)\,\delta(t_1 - t_2),$$

$$\overline{T_{ik}(\mathbf{r}_1t_1)\,H(\mathbf{r}_2t_2)} = 2kT\zeta_1\delta_{ik}\,\delta(\mathbf{r}_1 - \mathbf{r}_2)\,\delta(t_1 - t_2), \quad \overline{H(\mathbf{r}_1t_1)\,H(\mathbf{r}_2t_2)} = 2kT\zeta_3\delta(\mathbf{r}_1 - \mathbf{r}_2)\,\delta(t_1 - t_2),$$

$$\overline{Q_i(\mathbf{r}_1t_1)\,Q_k(\mathbf{r}_2t_2)} = 2kT^2\left\{\varkappa + \rho D\left[\frac{\partial}{\partial c}\left(\frac{Z}{\rho T}\right)\cdot k_T - T\frac{\partial}{\partial T}\left(\frac{Z}{\rho T}\right)\right]^2\Big/\frac{\partial}{\partial c}\left(\frac{Z}{\rho T}\right)\right\}\delta(\mathbf{r}_1 - \mathbf{r}_2)\,\delta(t_1 - t_2),$$

$$\overline{G_i(\mathbf{r}_1t_1)\,G_k(\mathbf{r}_2t_2)} = \left[2k\rho D\Big/\frac{\partial}{\partial c}\left(\frac{Z}{\rho T}\right)\right]\delta_{ik}\,\delta(\mathbf{r}_1 - \mathbf{r}_2)\,\delta(t_1 - t_2),$$

$$\overline{G_i(\mathbf{r}_1 t_1)\, Q_k(\mathbf{r}_2 t_2)} = 2kT\left\{\rho D\left[\frac{\partial}{\partial c}\left(\frac{Z}{\rho T}\right) k_T - T\frac{\partial}{\partial T}\left(\frac{Z}{\rho T}\right)\right]\Big/ \frac{\partial}{\partial c}\left(\frac{Z}{\rho T}\right)\right\} \delta_{ik}\delta(\mathbf{r}_1 - \mathbf{r}_2)\,\delta(t_1 - t_2).$$

The fluctuations of the hydrodynamical parameters can be found by expressing them in terms of the "outside" quantities with the aid of the hydrodynamical equations.

In conclusion we note that the equations for fluctuations of the quantities **Q** and **g** will also apply, naturally, to solutions of ordinary (non-superfluid) liquids.

I would like to thank L. D. Landau and E. M. Lifshitz for allowing me to become acquainted with their manuscript before publication.

*The thermodynamic identity has the form

$$d\epsilon = T\,dS + \mu\,d\rho + Z\,dc + (\mathbf{v}_n - \mathbf{v}_s)\,d(\mathbf{j} - \rho\mathbf{v}_s).$$

[1] L. D. Landau and E. M. Lifshitz, J. Exptl. Theoret. Phys. (U.S.S.R.) **32**, 618 (1957), Soviet Phys. JETP **5**, 512 (1957).

[2] S. M. Rytov, Теория электрических флуктуаций и теплового излучения (Theory of Electrical Fluctuations and Heat Radiation), Academy of Sciences Press, 1953.

[3] I. M. Khalatnikov, J. Exptl. Theoret. Phys. (U.S.S.R.) **23**, 265 (1952).

[4] I. M. Khalatnikov, Usp. Fiz. Nauk **60**, 69 (1946).

[5] L. D. Landau and E. M. Lifshitz, Статистическая физика (Statistical Physics), 3rd Edition, Gostekhizdat, 1951.

Translated by W. M. Whitney
160

CAUSES OF THERMODYNAMIC IRREVERSIBILITY

B. I. DAVYDOV

Submitted to JETP editor June 20, 1957

J. Exptl. Theoret. Phys. (U.S.S.R.) **33**, 811-812 (September, 1957)

THE statistical interpretation of the second law of thermodynamics was given by Boltzmann more than eighty years ago. In spite of this long period of time, there is no clear explanation for the experimentally observed fact of macroscopic irreversibility.

The laws of elementary mechanics, both classical and quantum, are entirely reversible. This fact causes the general laws of statistical mechanics to be also reversible. Indeed, the Liouville equation is reversible just as is the equation of motion of the density matrix for a mixed state in quantum mechanics. Therefore with any mechanical process developing in time there can always be associated an analogous process moving in the opposite direction. This is accomplished by replacing all the velocities or momenta by their negatives. Thus if the entropy is increasing in time in any process, the reverse process in which the entropy decreases may always exist in principle. One cannot, therefore, assign to the second law of thermodynamics the same universal meaning as to the first law, the conservation of energy. In small-scale events, in fact, one often observes fluctuation phenomena due to the decrease of entropy with time.

It is on the basis of such concepts that Boltzmann arrived at his fluctuation hypothesis. This hypothesis, however, is of a merely speculative nature, being based on no experimental facts other than those it attempts to explain. As is known, it did not achieve recognition.

In order to find genuine reasons for thermodynamic irreversibility, one must first clarify the origin of those statistical anomalous states which approach thermal equilibrium in an irreversible way.

The sources of all the thermal energy with which we deal are nuclear processes. This is above all the energy liberated in radioactive decay; such is, for instance, the source of heat in the interior of the

earth. Further, this is the energy liberated in thermonuclear reactions; such is essentially the origin of the energy radiated by the sun and stars, and from which, in the final analysis, come all the energy resources of modern technology.

These simple considerations make it possible to give a general answer to the question of the cause of thermodynamic irreversibility. At present nuclear processes accompanied by liberation of energy very often take place in the universe surrounding us, and as far as we know reverse processes accompanied by an increase in internal nuclear energy almost never take place. A gradual dissipation of nuclear energy on a very large scale is therefore taking place around us. It is just to this quite specific process that thermodynamics refers. The law of entropy increase characterizes its directional nature.

If the general equations of mechanics are entirely reversible, irreversibility can be due only to the initial conditions. In reality such an initial condition is, on the one hand, the existence of decaying heavy nuclei and, on the other hand, the possibility of further thermonuclear synthesis. Both these phenomena lead to the continual production of particles with enormous kinetic energies which are then gradually dissipated among all the degrees of freedom of the surrounding macroscopic molecular systems. All physical kinetics is a description of various stages of this extremely complex process.

We shall not consider here the possible reasons for the fact that nuclear energy is much more often liberated around us rather than absorbed. There can be no doubt in this, of course, as an observed experimental fact. We wish only to indicate the possibility of explaining thermodynamic irreversibility by well-established experimental facts which are completely independent of thermodynamics and statistical mechanics.

Translated by E. J. Saletan
161

MAGNETIC PROPERTIES OF COBALT FLUORIDE IN THE ANTIFERROMAGNETIC STATE

D. N. ASTROV, A. S. BOROVIK-ROMANOV, and M. P. ORLOVA

All-Union Institute of Physico-Technical and Radiotechnical Measurements

Submitted to JETP editor June 20, 1957

J. Exptl. Theoret. Phys. (U.S.S.R.) **33**, 812-815 (September, 1957)

THE antiferromagnetism of cobalt fluoride was established in neutron diffraction experiments by Erickson,[1] from whose data it follows that the transition temperature of CoF_2 lies in the neighborhood of 50° K. Calorimetric measurements by Stout and Catalano[2] indicated the existence of a peak in the specific heat at a temperature of 37.7°K.

We have investigated several CoF_2 samples prepared of ChDA material which was dried in a vacuum by the method suggested by Birk and Biltz.[3] The magnetic susceptibility was measured by the Faraday method. The experimental error in the temperature was no greater than ± 0.5° at liquid hydrogen temperatures, and about ± 0.1° at higher temperatures. The error in the absolute measurements of the susceptibility was no greater than ± 5%, and in the relative ones it was no greater than ± 2%.

The results obtained are shown in Fig. 1. The inverse of the susceptibility has a minimum at T_C = 38° K, which is in good agreement with the temperature of the discontinuity in the specific heat.[2] Above 55° of the curve obeys the Curie-Weiss law $\chi_m = C_m/(T - \Theta)$ with $\Theta = -50$ and $C_m = 0.875$ (per mole). The magnetic susceptibility is field independent in the field interval we investigated (900 − 4000 oersteds).

Stout and Matarrese[4] have measured the difference between the principal molar susceptibilities ($\chi_\parallel - \chi_\perp$) in CoF_2 single crystals. It is of interest, for comparison with theory, to find the temperature dependence of the absolute values of $\chi_\parallel$ and $\chi_\perp$. Stout and Matarrese used the results of experiments with a polycrystalline sample[5] in 1939, combining them with their data to construct temperature-dependence curves for $\chi_\parallel$ and $\chi_\perp$. The curves obtained in this way are difficult to explain on the basis of existing concepts of antiferromagnetism; the value of $\chi_\perp$ increases greatly instead of remaining constant,

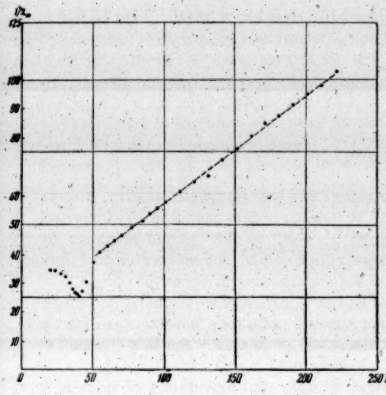

FIG. 1. The reciprocal of the molar magnetic susceptibility $1/\chi_m$ of CoF_2 as a function of temperature.

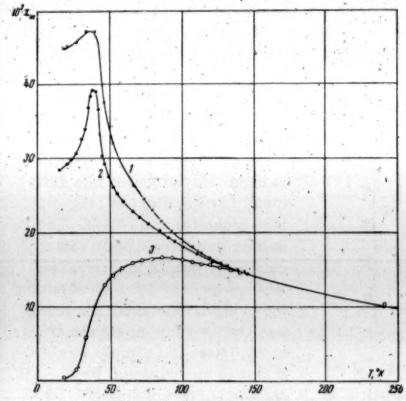

FIG. 2. The temperature dependence of the molar magnetic susceptibility of CoF_2. (1) temperature dependence of the "perpendicular" susceptibility, on the basis of our data and that of Stout and Matarrese;[4] (2) temperature dependence of the magnetic susceptibility of the powder, according to our measurements; (3) temperature dependence of the "parallel" magnetic susceptibility, based on our measurements and the data of Stout and Matarrese.[4]

Translated by E. J. Saletan
162

and after passing through a maximum at about 65° K, $\chi_\parallel$ decreases not to 0, but to 40% of its maximum value.

Entirely different but also anomalous curves were obtained by Bizett and Tsai,[6] who compared their new results for a polycrystalline sample with the data of Stout and Matarrese. According to them $\chi_\perp$ increases greatly, and $\chi_\parallel$ varies in a complex way with a maximum at 50° K, a minimum at about 23° K, and a strong increase at lower temperatures. In our opinion the low-temperature increase they obtain for the susceptibility of polycrystalline CoF_2 is due to their sample being not sufficiently baked out and containing some of the paramagnetic hydrated salt $CoF_2 \cdot 4H_2O$.

Figure 2 shows curves of the temperature dependence of $\chi_\parallel$ and $\chi_\perp$ obtained by combining our data with the anisotropy data of Stout and Matarrese. At the transition point $\chi_\perp = 4.8\ \chi_\parallel$. Below the transition point $\chi_\perp$ remains practically constant, and $\chi_\parallel$ decreases rapidly approaching 0 as $T \to 0$. The fact that no anomalies are observed on the $\chi_\parallel$ curve at the transition point may be explained by the chance coincidence of the nature of the anisotropy change in the paramagnetic and antiferromagnetic regions, as well, perhaps, by the insufficient accuracy in the measurement of $(\chi_\parallel - \chi_\perp)$ in the intermediate temperature range, when the measurements were performed while heating the apparatus.

It is thus seen that the temperature dependence of the principal magnetic moments $\chi_\parallel$ and $\chi_\perp$ of CoF_2 below the transition point is of the same general character as it is for other antiferromagnetic substances. A particular property of CoF_2 is the strong anisotropy of the Co^{++} ion in the paramagnetic state, which causes $\chi_\perp$ to be much greater than $\chi_\parallel$ at the transition point.

The authors express their deep gratitude to P. G. Strelkov for constant interest in the work.

[1] R. A. Erickson, Phys. Rev. 90, 779 (1953).
[2] I. W. Stout and E. Catalano, Phys. Rev. 92, 1575 (1953).
[3] E. Birk and W. Blitz, Z. anorg. u. allgem. Chem. 153, 121 (1926).
[4] I. W. Stout and L. M. Matarrese, Revs. Modern Phys. 25, 338 (1953).
[5] W. J. de Haas and B. H. Schultz, Physica 6, 481 (1939).
[6] H. Bizett and B. Tsai, Conference de Physique des basses temperatures, (Paris 2—8 September, 1955).

GALVANOMAGNETIC PROPERTIES OF FERROMAGNETICS NEAR ABSOLUTE ZERO

K. P. BELOV and A. V. PED'KO

Moscow State University

Submitted to JETP editor June 20, 1957

J. Exptl. Theoret. Phys. (U.S.S.R.) 33, 815-817 (September, 1957)

THE electrical resistance of ferromagnetics in fields above saturation (paramagnetic region) always diminishes; therefore $\Delta R/R$ is here a decreasing function of H (linearly decreasing in first approximation — see Fig. 1). According to the usual theory the quantity $\rho = -R^{-1}\Delta R/\Delta H$ should decrease as absolute zero is approached, owing to the decrease in the concentration of non-oriented spins in a domain as a consequence of reduced thermal motion. At 0° K absolute saturation occurs, hence $\rho = 0$.

In the work of Smith,[1] however, the 42% Ni, 58% Fe alloy is shown to behave exceptionally in this respect. The quantity ρ at liquid nitrogen and hydrogen temperatures not only does not decrease for this alloy, but even increases slightly. This interesting result is discussed by Gorter.[2] Smith's finding is explained on the assumption that the alloy in question possesses structural peculiarities; a negative exchange interaction is possible in its lattice, with the consequence that parallel orientation of spins is incomplete even at 0° K (antiferromagnetic state).

To check these conclusions we have performed more detailed measurements of the longitudinal galvanomagnetic effect, accompanying paramagnetism, in a number of ferromagnetics (including the 42% Ni, 58% Fe alloy) at low temperatures including that of liquid helium. We have use a more accurate method for determining ρ than used by Smith, who obtained this quantity graphically from the curves of $\Delta R/R$ vs. H. In our experiments ρ was determined in the following way. First the sample was subjected to a sufficiently strong field to magnetize it to technical saturation. The resulting galvanomagnetic effect, caused by motion and rotation, was compensated for by adjusting the bridge resistance; the bridge was then set for maximum sensitivity. Next the sample was subjected to an additional field $-\Delta H$ and the corresponding ΔR, due to paramagnetism, was measured. The quantity $\Delta R/\Delta H$ was referred to the resistance R at the given temperature. Our method allowed measurement of ρ with a 5% accuracy. In Fig. 2 $\Delta R/\Delta H$, R and ρ are given as functions of temperature for the 42% Ni, 58% Fe alloy. The points on the curves correspond to room and liquid nitrogen, hydrogen, and helium temperatures. One sees that $\Delta R/\Delta H$ and R are monotonic functions of the temperature, whereas ρ varies in a complicated manner. As the temperature decreases ρ first increases (this was also observed by Smith), then it reaches a maximum value and decreases. However at 0° K it does not reach zero as required by the above-mentioned theoretical considerations (i.e., at 0° K there exists a "residual" galvanomagnetic effect due to paramagnetism). The dashed lines in Fig. 2 represent the corresponding curves for the same sample after annealing. It is seen that the character of the curves, particularly of the curve $\rho(T)$,

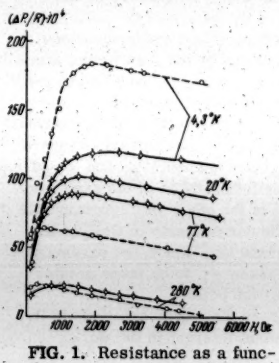

FIG. 1. Resistance as a function of magnetic field intensity for the 42% Ni, 58% Fe alloy. Solid curves refer to the unannealed sample, dashed curves refer to the sample after annealing at 800° C, 3 hours of aging.

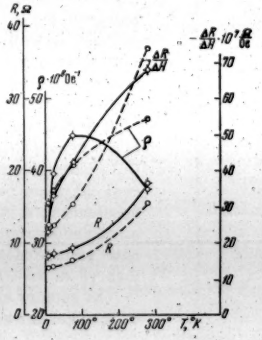

FIG. 2. $\rho = -R^{-1}\Delta R/\Delta H$ for the 42% Ni, 58% Fe alloy. Solid curves refer to the unannealed sample, dashed curves refer to the sample after annealing.

has changed substantially (the maximum has disappeared). The existence of the maximum in the curve $\rho(T)$ and its location as a function of temperature is determined by the form of the temperature dependence of $\Delta R/\Delta H$ and R; a change in the temperature dependence of $\Delta R/\Delta H$ and R shifts the maximum towards lower temperatures, or obliterates the maximum, or emphasizes it. It therefore follows that the increase in ρ with decreasing temperatures, first observed in Ref. 1, is not of great significance. The important factor in the phenomenon under discussion is the existence of a "residual" galvanomagnetic effect at 0° K due to paramagnetism.

Besides the 42% Ni, 58% Fe alloy we have investigated pure nickel, iron-nickel alloys containing 50% and 78% Ni, copper-nickel alloys containing 20% and 25% Cu, and a 23% Mn, 77% Ni alloy (in a hardened, non-ordered state). With the exception of Ni and permalloy (78% Ni, 22% Fe) in which ρ is very small at low temperatures, we have obtained for all the alloys curves very similar to those in Fig. 2. Therefore, contrary to Smith, one may conclude that the phenomenon in question is not peculiar to the 42% Ni, 58% Fe alloy; it also occurs in certain other ferromagnetic alloys. We give below values of ρ measured by us at liquid helium temperature in unannealed Ni-Fe and Cu-Ni alloys and in a hardened Mn-Ni alloy.

Alloy	$\rho \times 10^8$
42% Ni, 58% Fe	31.6
50% Ni, 50% Fe	15.6
20% Cu, 80% Ni	25.5
25% Cu, 75% Ni	11.6
23% Mn, 77% Ni	23.6

The existence of the "residual" galvanomagnetic effect due to paramagnetism at 0° K in other ferromagnetic alloys beside the 42% Ni, 58% Fe alloy raises doubts as to the validity of the explanation given in Ref. 1. We believe that the existence of this effect is connected with the influence of structure imperfections on the exchange interaction.

We take this opportunity to express appreciation to A. J. Shalnikov for his advice and interest in this work.

[1] J. Smith, Physica 17, 612 (1951).
[2] C. Gorter, J. Phys. Rad. 12, 279 (1951).

Translated by A. Bincer
163

GREEN'S FUNCTION FOR DIFFUSION OF RADIATION

B. A. VEKLENKO

Moscow Energy Institute

Submitted to JETP editor June 20, 1957

J. Exptl. Theoret. Phys. (U.S.S.R.) 33, 817-819 (September, 1957)

BIBERMAN[1] suggested a theory for the diffusion of resonance radiation, which takes account of the possibility of changing the photon frequency in each reradiation event. It was assumed that the mean free time of a photon is small compared to the duration of the excited state. The integral equation obtained was solved numerically for various stationary problems. Later a similar equation was obtained by Holstein.[2] In solving the nonstationary problem, Holstein was interested only in the first eigenfunction of the equation, and obtained it using the Rayleigh-Ritz method.

In the present note it is shown that by maintaining Biberman's assumptions and treating the diffusion of radiation in an infinite medium, one can obtain an analytic expression for the Green's function $f(\mathbf{r}, t)$ of this problem.

In this case $f(\mathbf{r}, t)\,dV$ is the probability that at time t there is an excited atom in the neighborhood of $\mathbf{r}$, if at the initial time ($t = 0$) there existed only one excited atom and it was located at $\mathbf{r} = 0$. For a homogeneous medium $f(\mathbf{r}, t) = f(r, t)$, where r is the magnitude of $\mathbf{r}$. The desired Green's function must satisfy the equation

$$\frac{\partial f(r, t)}{\partial t} = \frac{1}{4\pi\tau}\int\!\!\int \varepsilon_\nu k_\nu f(r_1, t)\frac{e^{-k_\nu|r-r_1|}}{|r-r_1|^2}\,dv\,dV_1 - \left(\frac{1}{\tau}+\sigma\right) f(r, t) \tag{1}$$

which has been investigated by Biberman and Holstein[1,2] for the initial condition $f(\mathbf{r}, t) = \delta(\mathbf{r})$ at $t = 0$. The notation in Eq. (1) is the following: τ is the mean lifetime of the excited atom, σ is the probability of a damping collision, ν is the photon frequency, and ϵ_ν and k_ν characterize the radiation and absorption line shapes, respectively.

The use of an elegant transformation suggested by Ambartsumian[3] brings Eq. (1) into the form

$$\frac{\partial A(r, t)}{\partial t} = \frac{1}{2\tau}\int_{-\infty}^{\infty}\int_0^\infty \varepsilon_\nu k_\nu \,\mathrm{Ei}\,(k_\nu|r-r_1|)\,A(r_1, t)\,dv\,dr_1 - \left(\frac{1}{\tau}+\sigma\right)A(r, t) \tag{2}$$

with the initial condition

$$A(r, t) = \delta(r)/2\pi \quad \text{for } t = 0,$$

where

$$A(r, t) = \int_r^\infty r_1 f(r_1, t)\,dr_1, f(r, t) = -\frac{1}{r}\frac{\partial A(r, t)}{\partial r}. \tag{3}$$

Here Ei is the exponential integral function.

Equation (2) can be solved by Fourier transformation. We finally obtain, using (3),

$$f(r, t) = -\frac{e^{-t(1/\tau+\sigma)}}{(2\pi)^2 r}\frac{\partial}{\partial r}\int_{-\infty}^{\infty} e^{-ipr}\left[\exp\left(\frac{t}{\tau p}\int_0^\infty \varepsilon_\nu k_\nu \tan^{-1}\frac{p}{k_\nu}\,dv\right) - 1\right]dp + 2\pi\delta(r)\Big).$$

Let $\epsilon_\nu = \delta(\nu)$, and $k_\nu = k$ be a constant, corresponding to diffusion without a frequency change. In this case

$$\int_0^\infty \varepsilon_\nu k_\nu \tan^{-1}\frac{p}{k_\nu}\,dv = k\,\tan^{-1}\frac{p}{k}.$$

Further calculation of Eq. (4) must be performed numerically, although by using known methods it is not difficult to obtain an asymptotic expression for $f(r, t)$ in the form

$$f(r, t) \cong [4\pi D t]^{-3/2} e^{-\sigma t} e^{-r^2/4Dt},\quad D = 1/3\tau k^2. \tag{5}$$

Thus in the present case of diffusion of radiation, the first approximation is similar to diffusion of particles. This similarity has already been noted by Compton.[4]

As a second example, let us consider the spectroscopically important problem of the dispersion shape of a spectral line

$$k_\nu = \frac{k_0}{1+(\nu-\nu_0)^2/\gamma^2},\quad \varepsilon_\nu = k_\nu \Big/ \int_0^\infty k_\nu\,dv,$$

where k_0 is the absorption coefficient for the frequency ν_0 corresponding to the center of the spectral line, and γ is the line half-width.

It can be shown that

$$\frac{1}{p}\int_0^\infty \varepsilon_\nu k_\nu \tan^{-1}\frac{p}{k_\nu}\,dv = 1 - \frac{1}{p}\left\{\frac{\sqrt{p}}{2}\left[\varphi_1(k_0;\ p)+\varphi_2(k_0;\ p)\right] + k_0 \tan^{-1}\frac{\varphi_1(k_0;\ p)-\sqrt{p}}{\varphi_2(k_0;\ p)-\sqrt{p}}\right\};\quad (p \geqslant 0),$$

where

$$\varphi_1(k_0;\ p)=(\sqrt{k_0^2+p^2}+k_0)^{1/2};\quad \varphi_2(k_0;\ p)=(\sqrt{k_0^2+p^2}-k_0)^{1/2}.$$

The asymptotic expression analogous to (5) now becomes

$$f(r,\ t)\cong -\frac{e^{-\alpha t}}{\pi^2 r}\frac{\partial}{\partial r}\frac{\vartheta}{r^{1/2}}\int_0^\infty \exp\left(-2\frac{\vartheta}{\sqrt{r}}x\right)\sin x^2 dx$$

$$=-\frac{e^{-\alpha t}}{2\pi r}\frac{\partial}{\partial r}\left\{\frac{1}{\vartheta}\sqrt{\frac{r}{2\pi}}\frac{\partial}{\partial r}\left(\cos\frac{\vartheta^3}{r}-\sin\frac{\vartheta^3}{r}\right)+\frac{\partial}{\partial r}\left[C^2\left(\frac{\vartheta}{\sqrt{r}}\right)+S^2\left(\frac{\vartheta}{\sqrt{r}}\right)\right]\right\}, \tag{6}$$

where

$$\vartheta=\frac{t}{3\tau\sqrt{2k_0}},\quad S(x)=\frac{2}{\sqrt{2\pi}}\int_0^x \sin t^2 dt,\ C(x)=\frac{2}{\sqrt{2\pi}}\int_0^x \cos t^2 dt$$

is the Fresnel integral. It follows from (6) that for large optical path lengths

$$f(r,\ t)\approx(4\pi)^{-1/2}(t/\tau\sqrt{k_0 r})e^{-\alpha t}/r^2. \tag{7}$$

Comparing (5) and (7) we see that the function for diffusion with redistribution of the photon frequencies decreases much slower than the other. A similar result can be obtained also for the Doppler shape of a spectral line. This is related to the slow decrease of the kernel of the integro-differential equation (1), as has been pointed out by Biberman.[1]

We note further that Ambartsumian's transformation makes it possible to obtain an analytic expression for the Green's function in the problem of diffusion of radiation if one accounts for the motion of the atoms.

In conclusion I express my gratitude to L. M. Biberman for his direction in performing the present work.

[1] L. M. Biberman, J. Exptl. Theoret. Phys. (U.S.S.R.) **17**, 416 (1947).
[2] T. Holstein, Phys. Rev. **72**, 1212 (1947).
[3] V. A. Ambartsumian, Bulletin of Erevan Astronomical Observatory, No. 6, 3 (1945).
[4] K. T. Compton, Phys. Rev. **20**, 283 (1922).

Translated by E. J. Saletan
164

EFFECT OF PROTON SIZE ON THE POSITION OF ELECTRONIC LEVELS IN HYDROGEN AND DEUTERIUM

N. N. KOLESNIKOV

Moscow State University

Submitted to JETP editor June 20, 1957

J. Exptl. Theoret. Phys. (U.S.S.R.) **33**, 819-821 (September, 1957)

RECENT experiments[1] on the scattering of electrons on protons show that the rms radius of the electric charge distribution in the proton is $(0.77 \pm 0.10) \times 10^{-13}$ cm, whereas the rms radius of the neutron is possibly smaller.[2,3] This leads to a reduction of the binding energy of the electron in atoms, i.e., to a correction to the Lamb shift. In the calculation of a similar effect, one may confine oneself to the investigation of the nonrelativistic problem, taking into account additionally the distortions of the electronic wave functions, since the corrections due to these are not large in the cases — of interest to us — of hydrogen and deuterium[4,5] for which experimental data[6] exist.

Let $e\rho(r_1)$ be the electric charge density in the proton, let $\psi_p(r)$ be the normalized wave function of the proton in the deuteron (where r is the distance of the proton center from the center of mass of the deuteron and r_1 is the distance from the center of the proton to some point within it), and let $\psi(R)$ be the wave function of an atomic s-electron (where in the case of deuterium, R is the distance from the electron to the center of mass of the deuteron, and in hydrogen, R is the distance to the proton center). The reduction, due to the finite size of the proton, of the binding energy of the electron in the hydrogen atom is given (in cm^{-1}) by

$$\Delta E_H = \frac{1}{2\pi\hbar c}\int |\psi(R)|^2 d\tau_R \left\{\frac{e^2}{R} - e^2\int\frac{\rho(r_1)\,d\tau_1}{|\mathbf{R}-\mathbf{r}_1|}\right\}. \quad (1)$$

But

$$-e^2\int\frac{\rho(r_1)\,d\tau_1}{|\mathbf{R}-\mathbf{r}_1|} = -\frac{e^2}{R} + \frac{4\pi e^2}{R}\int_R^\infty \rho(r_1)\,r_1(r_1-R)\,dr_1.$$

Moreover, if ρ falls off much more rapidly than $|\psi|^2$, then in (1), one may take $|\psi(0)|^2$ out from under the integral sign. Thus we obtain after integration by parts

$$\Delta E_H = \frac{\alpha}{3}|\psi(0)|^2\langle r^2\rangle,\ \langle r^2\rangle = 4\pi\int_0^\infty \rho(r_1)\,r_1^4\,dr_1. \quad (2)$$

This result is verified by a method employing more accurate functions in the calculations of E. V. Teodorovich.

In the case of deuterium, the volume effect is given by

$$\Delta E_D = \frac{1}{2\pi\hbar c}\int |\psi(R)|^2 d\tau_R \left\{\frac{e^2}{R} - e^2\int\int\frac{|\psi(r)|^2\rho(r_1)\,d\tau\,d\tau_1}{|\mathbf{R}-\mathbf{r}-\mathbf{r}_1|}\right\}. \quad (3)$$

Upon integration we obtain

$$\Delta E_D = \frac{\alpha}{3}|\psi(0)|^2\{\langle R^2\rangle + \langle r^2\rangle + \langle r_n^2\rangle\}, \quad (4)$$

where the additional last term takes into account the effect of the neutron volume, which has a value less than zero.

Note that if the electron is not treated as a point particle, then in (2) and (4) one should replace $\langle r^2\rangle$ with the sum $\langle r^2\rangle + \langle r_e^2\rangle$. Regardless of this, however, in the present approximation, the difference $\Delta E_D - \Delta E_H$ does not depend upon the structure of the proton and electron, but is determined only by the properties of the deuteron and by the structure of the neutron:

$$\Delta E_D - \Delta E_H = \frac{\alpha}{3}|\psi(0)|^2\{\langle R^2\rangle + \langle r_n^2\rangle\}\,cm^{-1}.$$

Regarding the computation of the magnitude of $\langle R^2\rangle$, the following remarks apply. In the first place $\langle R^2\rangle$, which is characteristic of the distribution of charge relative to the center of mass of the deuteron, is four times as small as the quantity $\langle R_1^2\rangle$, which characterizes the distribution of charge relative to the neutron. Secondly, although the wave function of the proton in the deuteron, which determines $\langle R_1^2\rangle$, depends also on the properties of the nuclear forces, which have not yet been completely explained, the various assumptions about the form of the nuclear potential give almost exactly the same results if the parameters of the potentials are chosen to fit the data on the scattering of low-energy neutrons. In particular, in the case of the square well, we obtain

$$\langle R^2\rangle = \frac{1}{8\gamma^2}\left\{1+\frac{\gamma(\beta R_0 - {}^1/_2\sin 2\beta R_0)}{\beta\sin^2\beta R_0}\right\}^{-1}\left\{1+2\gamma R_0+2\gamma^2R_0^2 + \frac{\gamma^3}{\beta^3\sin^2\beta R_0}\left(\frac{2}{3}\beta^3R_0^3 - \beta^2R_0^2\sin 2\beta R_0 - \beta R_0\cos^2\beta R_0 + \frac{1}{2}\sin 2\beta R_0\right)\right\}, \quad (5)$$

where $\gamma = (2\pi/\hbar)\sqrt{m\mathcal{E}}$; $\beta = (2\pi/\hbar)\sqrt{m(V_0-\mathcal{E})}$, m is the proton mass, $\mathcal{E} = 2.226$ Mev is the binding energy[7] of the deuteron, and V_0 and R_0 are the well depth and width, respectively, for which values[2,8] of 35.2 Mev and 2.04×10^{-13} cm were taken.

For these data the numerical values of the volume effect are: $\Delta E_H = 0.117 \pm 0.03$ Mc/sec for hydrogen,

in agreement with our previous estimate.[4] For deuterium we obtain a correction of 0.74 + 0.117 = 0.86 Mc/sec plus $\delta_n = (\alpha/3)|\psi(0)|^2\langle r_n^2\rangle$ Mc/sec, which also improves the agreement with experiment.

The isotopic volume effect, $\Delta E_D - \Delta E_H$, is equal to 0.74 Mc/sec + δ_n, i.e., together with the mass effect it amounts to 1.33 Mc/sec + δ_n, which is in good agreement with the measurements[6] of Lamb (1.23 ± 0.20 Mc/sec). Before drawing final conclusions about the magnitude of the Lamb shift, however, it would be desirable to ascertain to what extent possible corrections, e.g., higher-order quantum-electrodynamic terms, might modify these results.

The author is deeply grateful to Prof. D. D. Ivanenko and to Prof. J. P. Vigier of the Sorbonne for stimulating this work and for a discussion of the results.

[1] E. E. Chambers and R. Hofstadter, Phys. Rev. 103, 1454 (1956).
[2] Melkonian, Rustad, and Havens, Bull. Am. Phys. Soc. Ser. II, 1, 62 (1956); Hughes et al., Phys. Rev. 90, 407 (1953).
[3] J. McIntyre, Phys. Rev. 103, 1464 (1956).
[4] D. D. Ivanenko and N. N. Kolesnikov, Dokl. Akad. Nauk SSSR 91, 47 (1953).
[5] E. Salpeter, Phys. Rev. 89, 92 (1953).
[6] Triebwasser, Dayhoff, and Lamb, Phys. Rev. 89, 98 (1953).
[7] J. Blatt and V. Weisskopf, Theoretical Nuclear Physics, New York, 1952.
[8] J. Blatt and J. D. Jackson, Phys. Rev. 76, 18 (1949).

Translated by J. Heberle
165

APPLICATION OF CHARGE INVARIANCE TO POLARIZATION PHENOMENA

S. M. BILEN'KII

Joint Institute for Nuclear Research

Submitted to JETP editor June 21, 1957

J. Exptl. Theoret. Phys. (U.S.S.R.) 33, 821-822 (September, 1957)

As is well known, the hypothesis of charge invariance leads to relations between experimentally observable quantities. Up to the present time, however, the only relations that have been derived connect the cross-sections of different processes. In connection with experiments on change of polarization it is also of interest to examine the relations involving the polarization which follow from charge invariance. We shall consider an extremely simple method for finding such relations.

Suppose that the isotopic spin is conserved in the interactions that cause the process $a + A \to b + B$. Let us denote the respective isotopic spins of the particles by j_a, j_A, j_b, j_B, and the values of a particular component by m_a, m_A, m_b, m_B. The amplitude describing the transition $m_a, m_A \to m_b, m_B$ can be written in the form

$$R_{m_a m_A;\, m_b m_B} = \sum_j (j_a j_A m_a m_A \mid j_a j_A j m)\, R_j\, (j_b j_B m_b m_B \mid j_b j_B j m). \tag{1}$$

by the use of the Clebsch-Gordan coefficients. Here R_j is the amplitude in a state with a definite total isotopic spin; it depends on the angles, the spins, and the energy.

Let T_k be operators acting on the spin variables of particles b and B and forming a complete set of matrices (for example, 1 and the Pauli matrices σ_x, σ_y, σ_z in the case of a spinless particle and a particle with spin ½). The experimentally observable quantities are average values $\langle T_k \rangle$. From Eq. (1) we have:

$$(\langle T_k \rangle\, \sigma)_{m_a m_A;\, m_b m_B} = \sum_{j, j_1} (j_a j_A m_a m_A \mid j_a j_A j m)\, (j_a j_A m_a m_A \mid j_a j_A j_1 m)\, R_j^+ T_k R_{j_1} (j_b j_B m_b m_B \mid j_b j_B j m)\, (j_b j_B m_b m_B \mid j_b j_B j_1 m), \tag{2}$$

where σ is the differential cross-section. To obtain the relations we sum Eq. (2) over the isotopic spin components, keeping one of them fixed, for example m_b. Using the orthogonality and symmetry of the Clebsch-Gordan coefficients[1] we get

$$\sum_{m_a, m_A, m_B} (\langle T \rangle \sigma)_{m_a m_A; m_b m_B} = \sum_j \frac{(2j+1)}{(2I_b+1)} R_j^+ T_k R_j. \quad (3)$$

The sum on the left side does not depend on m_b. Consequently, equating the values of this sum for various values of m_b, we get relations between the observable quantities. It is obvious that any one of the components can be held fixed. It is clear from the proof that in the case in which the number of particles changes, relations between the observable quantities are obtained in just the same way. For $T_k = 1$ we get relations between the differential cross-sections, and the conclusion so obtained provides a foundation for the rule formulated by Shmushkevich.[2]

Let us consider the scattering of π-mesons by nucleons. Equating the sums (2) for π^+ and π^0-mesons we get besides Heitler's relations for the differential cross-sections, the relation

$$(P\sigma)_{\pi^+ p; \pi^+ p} + (P\sigma)_{\pi^- p; \pi^- p} = 2(P\sigma)_{\pi^0 p; \pi^0 p} + (P\sigma)_{\pi^- p; \pi^0 n}, \quad (4)$$

which involes the polarization P of the recoil nucleon.

For the production of a π-meson in collision of nucleons with formation of a deuteron we have:

$$\langle T_k \rangle_{pp; \pi^+ d} = \langle T_k \rangle_{np; \pi^0 d}. \quad (5)$$

T_k characterizes the polarization of the deuteron (3 components of a vector and 5 components of a tensor). If the nucleons in the final state are free, we get

$$(\langle T_k \rangle \sigma)_{pp; \pi^+ np} + (\langle T_k \rangle \sigma)_{pp; \pi^+ pn} + (\langle T_k \rangle \sigma)_{np; \pi^+ nn} + (\langle T_k \rangle \sigma)_{np; \pi^- pp}$$
$$= 2(\langle T_k \rangle \sigma)_{pp; \pi^0 pp} + 2(\langle T_k \rangle \sigma)_{np; \pi^0 np} + 2(\langle T_k \rangle \sigma)_{np; \pi^0 pn}.$$

In conclusion we remark that the relations (3) are very convenient for expressing the cross-sections and polarizations in states with definite total isotopic spin in terms of the experimentally observable cross-sections and polarizations.

I express my gratitude to Ia. A. Smorodinskii, L. I. Lapidus, and R. M. Ryndin for discussions of the questions considered here.

[1] J. Blatt and V. Weisskopf, Theoretical Nuclear Physics, p. 791 (New York, 1952).
[2] I. Shmushkevich, Dokl. Akad. Nauk SSSR 103, 235 (1955).

Translated by W. H. Furry
166

THERMODYNAMIC FUNCTIONS OF SUPERFLUID HELIUM FILMS

R. G. ARKHIPOV

Institute for Physical Problems, Academy of Sciences, U.S.S.R.

Submitted to JETP editor June 21, 1957

J. Exptl. Theoret. Phys. (U.S.S.R.) 33, 822-823 (September, 1957)

IT is well known that a calculation of the thermodynamic functions of superfluid helium with an excitation spectrum of the phonon-roton type proposed by Landau gives excellent agreement with experimental data.[1] In liquid helium which has a free surface, however, there exists one more branch of the energy spectrum associated with the presence of surface waves. Its contribution to the thermodynamic functions is proportional to the area of the free surface and consequently it can play a role only for very thin films.

The spectrum of the surface oscillations has the form[2]

$$\omega^2 = \left(\frac{3ak}{l^4} + \frac{\alpha k^3}{\rho}\right) \tanh kl,$$

where ω is the frequency, k the wave vector, l the film thickness, $\alpha \approx 0.35$ the surface tension, $\rho \approx 0.145$ the density, and $a \approx 8 \times 10^{-15}$ a constant connected with the van der Waals interaction between the film and the wall.

Analysis shows that for

$$l \gg a^{1/4}(\rho/\alpha)^{3/12}(\hbar/\varkappa T)^{1/6} \approx 6 \cdot 10^{-8}\ \text{cm}$$

we can use the formula $\omega^2 = \alpha k^3/\rho$, with which* we can easily find the free energy and the specific heat associated with the surface per unit area (the coefficient $1/2$ appears in the equation because the problem is two-dimensional):

$$F_{\text{surf}} = -\frac{1}{2}\int n\mathbf{k}\frac{\partial\varepsilon}{\partial k}\frac{2\pi k dk}{(2\pi)^2} = -\frac{\Gamma(7/3)\zeta(7/3)(\varkappa T)^{7/3}}{4\pi\hbar^{4/3}}\left(\frac{\rho}{\alpha}\right)^{2/3}, \qquad C_{\text{surf}} = -T\frac{\partial^2 F}{\partial T^2} = \frac{7\Gamma(7/3)\zeta(7/3)}{9\pi} \times \left(\frac{\varkappa T}{\hbar}\right)^{4/3}\left(\frac{\rho}{\alpha}\right)^{2/3}$$

$\epsilon = \hbar\omega$, n is the Planck distribution function, and κ is Boltzmann's constant.

We now ascertain when the quantity obtained above becomes equal to the phonon part of the bulk specific heat

$$C_{\text{ph}} = (2\pi^2\varkappa/15)(\varkappa T/\hbar s)^3 = C_{\text{surf}}/l$$

(where $s = 2.38 \times 10^4$ is the velocity of sound). After substituting numerical values we obtain $l \approx 0.7 \times 10^{-6} T^{-5/3}$ cm. In addition the wave length of the phonons with energy κT, which give the principal contribution to the specific heat, has to be much smaller than the film thickness

$$\hbar s/\varkappa T \sim 1.8 \cdot 10^{-7}/T \ll l \sim 7 \cdot 10^{-7} T^{-5/3}.$$

We see that the condition is satisfied, although by a narrow margin.

The surface oscillations should also make a contribution to the normal density of superfluid helium. Carrying out the calculations with the usual formulas we obtain

$$\rho_{n\,\text{surf}} = -\frac{\hbar^2}{4\pi\varkappa T}\int k^2\frac{dn}{dz}kdk = \frac{5\Gamma(5/3)\zeta(5/3)}{18\pi}\frac{(\varkappa T)^{5/3}}{\hbar^{4/3}}\left(\frac{\rho}{\alpha}\right)^{4/3}$$

($z = \hbar\omega/\kappa T$). The surface part of the normal density becomes equal to the phonon part when the following equality is satisfied:

$$\rho_{n\,\text{ph}} = 2\pi^2(\varkappa T)^4/45\hbar^3 s^5 = \rho_{n\,\text{surf}}/l,$$

which gives

$$l \approx 6 \cdot 10^{-6} T^{-7/3}.$$

The influence of film thickness on thermodynamic properties has been studied by Frederikse.[4] Unfortunately his data refer to film thicknesses of 12 atomic layers and to temperatures near the λ-point, so that it is not possible to make a quantitative comparison with our results. It can be seen from his data at lower temperatures, however, that the specific-heat curve goes above the curve corresponding to liquid helium in bulk. In these curves there can also be seen a displacement of the λ-point to lower temperatures with decreasing film thickness. One can attempt to interpret this as a result of the influence of $\rho_{n\,\text{surf}}$ on the temperature of the λ-transition.

I am grateful to Academician L. D. Landau for a discussion of this work.

*In an analogous manner Atkins[3] has found the temperature dependence of the surface tension of He^4.

[1] I. M. Khalatnikov, Usp. Fiz. Nauk 59, 673 (1956).
[2] R. G. Arkhipov, J. Exptl. Theoret. Phys. (U.S.S.R.) 33, 397 (1957), Soviet Phys. JETP 6, 307 (1958).
[3] K. R. Atkins, Canad. J. Phys. 31, 1165 (1953).
[4] H. P. R. Frederikse, Physica 15, 860 (1949).

Translated by W. M. Whitney
167

EFFECT OF PROTON STRUCTURE OF THE LAMB SHIFT

E. V. TEODOROVICH

Moscow State University

Submitted to JETP editor June 22, 1957

J. Exptl. Theoret. Phys. (U.S.S.R.) 33, 823-825 (September, 1957)

AFTER taking into account mass corrections and electromagnetic processes of the fourth and in part of the fifth order, a discrepancy of 0.6 Mc/sec remains between the experimental and theoretical values for the Lamb shift in hydrogen; it can be partially attributed to the structure of the proton (smearing of the proton charge). This has already been pointed out by several authors.[1-3] The estimates of Salpeter yield a total correction $\Delta E = 0.025$ Mc/sec; a preliminary estimate by Ivanenko and Kolesnikov[3] leads to $\Delta E = 0.11$ Mc/sec.

For computing the displacement of the levels in hydrogen, we use the method of the more accurate wave functions,[4] known from the theory of the isotope shift, in which the level shift is determined by the effective change of the principal quantum number

$$\Delta E = \alpha^2 mc^2 n^{-3} \Delta n, \quad \alpha = e^2/\hbar c, \tag{1}$$

and Δn is determined from the condition for joining the solutions for the inner and outer regions. In particular, for $S_{1/2}$ levels,

$$\Delta n = 2\alpha^4 (R/r_0)^2 (1 + 2f/\alpha g), \quad r_0 = e^2/mc^2, \tag{2}$$

where R is the radius of joining, and f and g are the components of the Dirac wave function at the point of joining. The shift $P_{1/2}$ is of order α^2 relative to the shift of the $S_{1/2}$ level and does not have to be considered now.

For determining f and g one may confine oneself to the approximation

$$g = a, \; f = \frac{a}{\hbar c} r^2 \int_0^r V(r) r^2 dr \tag{3}$$

which is correct to terms of second order in α in the region of order r_0. In the inner region, the potential of the electric field of the proton has the form

$$\varphi(r) = e\left[\int_r^R \frac{dy}{y^2}\int_0^y \rho(x)x^2dx\right]\left[\int_0^R \rho(x)x^2dx\right]^{-1} + \frac{e}{R} = e\left[\frac{1}{r}\int_0^r \rho(x)x^2dx + \int_r^R \rho(x)\,xdx\right]\left[\int_0^R \rho(x)x^2dx\right]^{-1} \tag{4}$$

Substituting in (3) and then in (2), we obtain

$$\Delta n = \frac{2}{3}\frac{\alpha^4}{r_0^2}\left[\int_0^R \rho(x)x^4dx\right]\left(\int_0^R \rho(x)x^2dx\right)^{-1}. \tag{5}$$

Having taken the radius of joining sufficiently large in comparison with the dimensions of the region of the charge distribution, we obtain a general formula for Δn which depends on the charge distribution only through the rms radius

$$\Delta n = {}^2/_3\,\alpha^4 \langle r^2\rangle / r_0^2, \tag{6}$$

$$\Delta E \text{ (Mcs)} = (\alpha^6 c/3\pi\lambda n^3)\langle r^2\rangle / r_0^2 (\lambda = \hbar/mc). \tag{7}$$

An analogous formula for the deuteron is obtained by Salpeter[1] with the aid of perturbation theory and was used recently by Kolesnikov to calculate the effect of proton structure on the energy levels of deuterium.

Using the experimental values for the rms radius of the proton $(7.7 \pm 1.0) \times 10^{-14}$ cm, obtained from scattering electrons on protons by Hofstadter's group,[5] we arrive at $\Delta E = (0.117 \pm 0.030)$ Mc/sec, which exceeds the result of Salpeter,[1] but coincides by a curious manner with a previous estimate.[3] Perturbation theory, however, does not afford a possibility of determining the correction to the energy of interaction with the vac-

uum due to the distortion of the wave function. This correction is determined by means of the formula

$$\Delta E_L = -\frac{E_{0L}\alpha^2}{3}\left[4\frac{<r^2>}{r_0^2}+\frac{(4\pi)^2}{2}\int_0^\infty \rho(y)\,dy\int_0^y \rho(x)\,x^4dx-\frac{(4\pi)^3}{12}\int_0^\infty \rho(y)\frac{dy}{y^2}\left(\int_0^y \rho(x)\,x^4\,dx\right)^2\right], \quad (8)$$

where E_{0L} is the electromagnetic part of the Lamb shift.

In formula (8) the first term takes into account the change in the normalization $\Delta N/N = -\Delta n/\alpha^2$ and yields -0.006 Mc/sec; the second and third terms take into account the distortion of the wave function. The last part depends essentially on the form of the charge distribution inside the proton; its magnitude, however, does not exceed $\Delta E = -0.012$ Mc/sec (for the charged sphere) and, consequently, lies beyond the range of the present experiment.[6]

Thus taking into account the volume of the proton reduces the Lamb-shift discrepany between theory and experiment from 0.6 to 0.5 Mc/sec. It will be possible to draw further conclusions about the effect of the structure of the elementary particles on the Lamb shift after calculating electromagnetic processes of the fifth order and improving the accuracy of experiment. We are going to apply an analogous method to the calculation of the correction to the hyperfine structure due to the volume of the proton.

In conclusion I consider it my duty to express gratitude to Professor D. D. Ivanenko for constant attention to the work and for a discussion of the results.

[1] E. Salpeter, Phys. Rev. 89, 92 (1953).
[2] Baranger, Bethe, and Feynman, Phys. Rev. 92, 482 (1953).
[3] D. D. Ivanenko and N. N. Kolesnikov, Dokl. Akad. Nauk SSSR 91, 47 (1953).
[4] A. A. Sokolov and D. D. Ivanenko, Квантовая теория поля (Quantum Theory of Fields), Part II, Chapt. III, § 7, Moscow-Leningrad (1952).
[5] E. E. Chambers and R. Hofstadter, Phys. Rev. 103, 1454 (1956).
[6] Triebwasser, Dayhoff, and Lamb, Phys. Rev. 89, 98 (1953).

Translated by J. Heberle
168

PARTICLE ANGULAR DISTRIBUTION FUNCTION AT THE CASCADE SHOWER MAXIMUM

I. P. IVANENKO

Moscow State University

Submitted to JETP editor June 25, 1957

J, Exptl. Theoret. Phys. (U.S.S.R.) 33, 825-827 (September, 1957)

BELEN'KII[1] calculated the distribution function of particles with respect to energy and angle at cascade shower maximum without assuming small deflection angles. The scattering, however, was considered to be mutliple. In the following we shall drop this limitation. We can then write the equation for $P(E, \vartheta)$, integrated over the depth of shower development with boundary conditions corresponding to a single primary electron of energy E_0 incident vertically upon the boundary of the material layer at $t = 0$, in the following form:

$$-\frac{1}{2\pi}\delta(E_0-E)\,\delta(1-\cos\vartheta)\cos\vartheta = q\frac{N(E_0,E,\vartheta)}{E}+q\frac{\partial N(E_0,E,\vartheta)}{\partial E}$$

$$+n\int_0^{\chi_{\max}}\int_0^{2\pi}P(E_0,E,\vartheta')-P(E_0,E,\vartheta)]\,f\left(2\sin\frac{\chi}{2}\right)\sin\chi\,d\chi\,d\varphi, \quad N(E_0,E,\vartheta)=\int_E^\infty P(E_0,E,\vartheta)\,dE. \quad (1)$$

Here $q = 2.29$ and $P(E, \vartheta)$ is the required distribution function of electrons with respect to energy E and angle ϑ. The angle ϑ' is determined by the equation

$$\cos\vartheta' = \cos\vartheta\cos\chi + \sin\vartheta\sin\chi\cos\varphi. \qquad (2)$$

where n is the number of scattering nuclei in 1 cm^3 of matter, $f(2\sin(\chi/2))$ is the transverse cross-section for Rutherford scattering, and χ_{max} is an angle depending on the energy and on the scattering medium. We neglect ionization losses and, therefore, our considerations are valid for energies $E > \beta$.

We shall seek the solution of Eq. (1) in the form of a series of Legendre polynomials:

$$N(E_0, E, \vartheta) = \sum_{n=0}^{\infty} \varphi_n(E_0, E)\, P_n(\cos\vartheta)\frac{2n+1}{2}. \qquad (3)$$

Substituting (3) into (1) and using the addition theorem for Legendre polynomials in transforming the integral term in (1), we obtain

$$-\delta(E_0 - E)/2\pi = q\varphi_n(E_0, E)/E + (q - K_n(E))\,\partial\varphi_n(E_0, E)/\partial E;$$

$$K_n(E) = 2\pi n \int_0^{\chi_{max}} [P_n(\cos\chi) - 1]\, f\left(2\sin\frac{\chi}{2}\right)\sin\chi\, d\chi. \qquad (4)$$

Using the explicit expression for the function f,[1] using the expansion of Legendre polynomials in terms of powers of $\sin(\chi/2)$, and taking into account screening and the finite dimensions of the nucleus[1] we obtain, finally, the following expression:

$$K_n(E) = \left(\frac{E_k}{2E}\right)^2\left\{-n(n+1) + \sum_{k=2}^{n}(-1)^k \frac{(n+k)!}{(n-k)!\,(k!)^2(2k-2)}\left(\frac{7.33}{2}10^{-3}\frac{mc^2}{E}Z^{1/3}\right)^{2k-2}\frac{1}{L_R}\left[(181Z^{-1/3})^{4k-4} - 1\right]\right\}. \qquad (5)$$

where $L_R = 2\ln(181\,Z^{-1/3})$, m is the electronic mass and Z the atomic number. The sum in Eq. (5) vanishes for $n < k$.

The solution of Eq. (4), is

$$\varphi_n(E_0, E) = \frac{1}{2\pi}(q - K_n(E_0))^{-1}\exp\left[\int_E^{E_0}\frac{q}{E'}(q - K_n(E'))^{-1}\,dE'\right]. \qquad (6)$$

Expressions (3), (5), and (6) represent the solution of our problem. They determine the energy and angular distribtuion function of electrons.

The explicit expressions for the first few functions φ_n are:

$$\varphi_0(E_0, E) = \frac{E_0}{qE}; \quad \varphi_1(E_0, E) = E_0\left(1 + \frac{2P^2}{E_0^2}\right)^{-1/2}\left(1 + \frac{2P^2}{E^2}\right)^{-1/2}/qE;$$

$$\varphi_2(E_0, E) = \frac{E_0(2 + 6P^2/E^2 - \Delta/E^2)^{1.5}P^3/\Delta}{qE\,(1 + 6P^2/E_0^2 - 3\alpha P^2/E_0^4)^{1/4}(1 + 6P^2/E^2 - 3\alpha P^2/E^4)^{1/4}(2 + 6P^2/E_0^2 - \Delta/E_0^2)^{1.5}P^3/\Delta} \cdot \frac{1}{(2 + 6P^2/E^2 + \Delta/E^2)^{1.5}P^3/\Delta}; \qquad (7)$$

$$P = \frac{E_k}{2q^{1/3}}; \quad \alpha = \left(\frac{7.33}{2}10^{-3}mc^2Z^{1/3}\right)\frac{1}{L_R}[(181Z^{-1/3})^4 - 1]; \quad \Delta^2 = \frac{3\alpha E_k^2}{q} - 3\left(\frac{E_k^2}{2q}\right)^2.$$

The functions φ_n can be calculated in an analogous way for $n > 2$. Comparison with the values φ_{nL} calculated in the Landau approximation shows that for $n = 0$ and $n = 1$ $\varphi_n = \varphi_{nL}$. For $n \geq 2$ the dependence of φ_n and φ_{nL} on E_0 and E is different. Moreover, for $n \geq 2$, φ_n depends strongly on the atomic number Z.

Using the distribution functions (3) and (7) we can find expressions for $\overline{\cos\vartheta_N}$ and $\overline{\cos^2\vartheta_N}$. In view of the orthogonality of Legendre polynomials, these are determined by the first three terms of series (3). Since $\varphi_n = \varphi_{nL}$ for $n = 0, 1$ the expressions for $\overline{\cos\vartheta_N}$ coincide with $\overline{\cos\vartheta_{NL}}$ obtained in Ref. 1. For the mean square we obtain the following expression:

$$\overline{\cos^2\vartheta_N(E_0, E)} = 1/3 + 2\varphi_2(E_0, E)/3\varphi_0(E_0, E),$$

where φ_0 and $\varphi_2(E_0, E)$ are given by Eq. (7).

For $E_0 \to \infty$ we have

$$\overline{\cos^2\vartheta_N(E)} = \frac{1}{3} + \frac{2}{3}\cdot\frac{(2 + 6P^2/E^2 - \Delta/E^2)^{1.5}P^3/\Delta}{(1 + 6P^2/E^2 - 3\alpha P^2/E^4)^{1/4}(2 + 6P^2/E^2 + \Delta/E^2)^{1.5}P^3/\Delta}.$$

In lead (Z = 82) the ratio $\overline{\cos^2\vartheta_N}/\overline{\cos^2\vartheta_{NL}}$ equals 0.99 and 0.98 for $E = 3 \times 10^7$ ev and 1.5×10^7 ev respectively.

[1] S. Z. Belen'kii, Лавинные процессы в космических лучах (Cascade Processes in Cosmic Rays), Gostekhizdat, 1948.

Translated by H. Kasha
169

EFFECT OF DAMPING ON POLARIZATION OF DIRAC PARTICLES IN SCATTERING

A. A. SOKOLOV and B. K. KERIMOV

Moscow State University

Submitted to JETP editor June 27, 1957

J. Exptl. Theoret. Phys. (U.S.S.R.) **33**, 827-829 (September, 1957)

THE elastic scattering of both Dirac and spinless particles by a fixed force center was investigated in Refs. 1 to 4 using damping theory. We calculate below, using damping theory, the polarization resulting from elastic scattering of Dirac particles.

The fundamental integral equation of damping theory which determines the scattering amplitude $f'_{s'} \equiv f'_{s'}(\mathbf{k}')$ and is relevant in a discussion of polarization phenomena has the following form (we use the notation of Ref. 3):

$$(f'_{s'} - b^+_{s'} b_s f_s) V_{\mathbf{k}'\mathbf{k}} = \frac{kK}{8\pi^2 c\hbar i} \sum_{s''} \oint d\Omega'' V_{\mathbf{k}'\mathbf{k}''} V_{\mathbf{k}''\mathbf{k}} b^+_{s'} b_{s''} f''_{s''}, \tag{1}$$

Here $E = c\hbar K$ is the total energy of the particle and $V_{\mathbf{k}'\mathbf{k}''}$ is the Fourier component of the potential $V(\mathbf{r})$.

We shall restrict ourselves to calculating the polarization resulting from elastic scattering of Dirac particles by a delta-function potential $V(\mathbf{r}) = V_0\delta(\mathbf{r})$, $V_{\mathbf{k}'\mathbf{k}''} = V_0$. In that case we have from formulas (5) of Ref. 3:

$$b^+_{s'} b_{s''} = \sum_{l=1,2} h^l_{s's''}, \tag{2}$$

where

$$h^1_{s's''} = \frac{1}{2}\left(1 + \frac{k_0}{K}\right)[\cos\theta'_{s'}\cos\theta''_{s''} + e^{i(\varphi''-\varphi')}\sin\theta'_{s'}\sin\theta''_{s''}] \qquad h^2_{s's''} = \frac{1}{2}\left(1 - \frac{k_0}{K}\right)s's''[\cos\theta'_{s'}\cos\theta''_{s''} + e^{i(\varphi''-\varphi')}\sin\theta'_{s'}\sin\theta''_{s''}].$$

We seek a solution of integral equation (1) of the form ($s' = 1, -1$):

$$f'_{s'} = \sum_{l=1,2} \varepsilon_l h^l_{s's} f_s. \tag{3}$$

Taking into account the orthogonality condition for $h^i_{s's''}$ [see Eq. (31) of Ref. 3] we obtain for ϵ_1 and ϵ_2 from Eqs. (1) – (3):

$$\varepsilon_{1,2} = \frac{1}{1 + i\delta_{1,2}}, \quad \delta_{1,2} = \frac{V_0}{4\pi c\hbar} k(K \pm k_0). \tag{4}$$

From Eqs. (3) and (4) we obtain for the amplitudes $f'_{s'}$ of the first scattering

$$f'_1 = \frac{1}{2}[a_1\varepsilon_1 + a_2\varepsilon_2]\cos\frac{\theta'}{2} f_1 - \frac{1}{2}[a_1\varepsilon_1 - a_2\varepsilon_2] e^{-i\varphi'}\sin\frac{\theta'}{2} f_{-1},$$
$$f'_{-1} = \frac{1}{2}[a_1\varepsilon_1 - a_2\varepsilon_2]\sin\frac{\theta'}{2} f_1 + \frac{1}{2}[a_1\varepsilon_1 + a_2\varepsilon_2] e^{-i\varphi'}\cos\frac{\theta'}{2} f_{-1}, \tag{5}$$

where $a_1 = 1 + k_0/K$, $a_2 = 1 - k_0/K$, and θ', φ' are the angles corresponding to the first scattering.

The expression for the second scattering amplitude $f_S''(f_1'', f_{-1}'')$ is obtained by replacing θ', φ' and f_1, f_{-1} on the right side of Eq. (5) by θ'', φ'' and f_1', f_{-1}'. The effective differential cross section for the second scattering is given in terms of f_S' and f_S'' by the relation

$$d\sigma = \frac{1}{N}\frac{\partial}{\partial t}\sum_{k'',s''} C_{s'}^{*} C_{s''}' = \frac{K^2}{4\pi^2 c^2\hbar^2}|V_{k'k'}|^2 \frac{f_1^{*}f_1' + f_{-1}^{*}f_{-1}'}{f_1^{+}f_1' + f_{-1}^{+}f_{-1}'} d\Omega'', \tag{6}$$

where

$$d\Omega'' = \sin\theta'' d\theta'' d\varphi'', \quad k' = k'' = k.$$

From here, using Eqs. (4) and (5), we obtain the following expression for the effective differential cross section for the double scattering of an initially unpolarized beam of Dirac particles ($f_1^{+}f_1 + f_{-1}^{+}f_{-1} = 1$, $f_1^{+}f_1 - f_{-1}^{+}f_{-1} = 0$, $f_1^{+}f_{-1} = f_{-1}^{+}f_1 = 0$) by a delta-function potential:

$$\sigma(\theta'', \varphi'') = \sigma_0(\theta'')[1 + \delta(\theta', \theta'')\cos\varphi''], \tag{7}$$

where

$$\delta(\theta', \theta'') = P(\theta')P(\theta'') = \left(\frac{V_0^2K^2}{4\pi^2c^2\hbar^2}\right)^2 \frac{k^4(\delta_2 - \delta_1)^2 \sin\theta' \sin\theta''}{4K^4(1+\delta_1^2)^2(1+\delta_2^2)^2\sigma_0(\theta')\sigma_0(\theta'')}, \quad \cos\varphi'' = \mathbf{n}'\mathbf{n}''. \tag{8}$$

$P(\theta')$ and $P(\theta'')$ are the polarizations acquired by an initially unpolarized beam separately in the first and second scattering, $\mathbf{n}'$ and $\mathbf{n}''$ are unit vectors in the two polarization directions, and $\sigma_0(\theta')$ is the differential scattering cross section, with damping taken into account, of an initially unpolarized beam of Dirac particles indicent on a delta-function potential

$$\sigma_0(\theta') = \frac{V_0^2K^2}{16\pi^2c^2\hbar^2}\left[\frac{a_1^2}{1+\delta_1^2} + \frac{a_2^2}{1+\delta_2^2} + 2\frac{k^2}{K^2}\cdot\frac{1+\delta_1\delta_2}{(1+\delta_1^2)(1+\delta_2^2)}\cos\theta'\right].$$

It follows from Eq. (8) that no polarization is obtained in the first approximation of perturbation theory ($\delta_1 = \delta_2 \cong 0$). In the high-energy region $k \gg (4\pi c\hbar/V_0)^{1/2}$ ($\delta_1^2 \gg 1$, $\delta_2^2 \gg 1$) we obtain for the degree of polarization in the case of two identical scatterings [$\theta'' = \theta'$, $P(\theta'') = P(\theta')$]

$$\delta(\theta', \theta') = [P(\theta')]^2 = \left(\frac{4\pi c\hbar}{V_0}\right)^2 \frac{4k_0^2}{k^6}\tan^2\frac{\theta'}{2}. \tag{9}$$

As can be seen from Eq. (7) the assymmetry in the second scattering is due only to the phase polarization ($f_1^{*}f_{-1}' \neq 0$) resulting from the first scattering. In the case when the incident beam possesses only amplitude polarization, $f_1^{+}f_1 - f_{-1}^{+}f_{-1} \neq 0$, $f_1^{+}f_{-1} = f_{-1}^{+}f_1 = 0$, the first Born approximation gives for the effective scattering cross section

$$d\sigma_{ss'} = \frac{K^2}{4\pi^2c^2\hbar^2}|V_{k'k}|^2 \frac{1}{2}\sum_{s=\pm1}\left[(1+ss')\cos^2\frac{\theta'}{2} + \frac{k_0^2}{K^2}(1-ss')\sin^2\frac{\theta'}{2}\right] f_s^{+}f_s\, d\Omega'. \tag{10}$$

Thus the ratio of the non-spin-flip cross section ($ss' = 1$) to the spin-flip cross section ($ss' = -1$) is equal to

$$\frac{d\sigma^{\uparrow\uparrow}}{d\sigma^{\uparrow\downarrow}} = \frac{K^2}{k_0^2}\cot^2\frac{\theta'}{2}.$$

[1] A. A. Sokolov and B. K. Kerimov, Dokl. Akad. Nauk SSSR 105, 961 (1955).

[2] A. A. Sokolov and B. K. Kerimov, Dokl. Akad. Nauk SSSR 106, 611 (1956), Soviet Phys. "Doklady" 1, 345 (1956).

[3] A. A. Sokolov and B. K. Kerimov, Nuovo cimento 5, 921 (1957).

[4] A. A. Sokolov, J. Phys. (U.S.S.R.) 9, 363 (1945).

Translated by A. Bincer
170

A VARIANT OF HYPERON THEORY

Ia. B. ZEL'DOVICH

Academy of Sciences, U.S.S.R.

Submitted to JETP editor July 2, 1957

J. Exptl. Theoret. Phys. (U.S.S.R.) 33, 829-831 (September, 1957)

We shall assume as the basis of our discussion the hyperon model proposed by Goldhaber[1] and D'erdi[2] representing hyperons as compound particles consisting of nucleons and $\overline{K}$-mesons, bounded together by forces dependent on the isotopic spin. Under certain assumptions given below this model yields a relation connecting the masses of the nucleon (N) and of the hyperons Λ, Σ, and Ξ.

$$2M_\Xi + 2M_N = 3M_\Lambda + M_\Sigma, \tag{1}$$

which is satisfied better (8846 and 8880) than another relation obtained by Gell-Mann[3] from different considerations:

$$2M_\Xi + 2M_N = M_\Lambda + 3M_\Sigma, \quad (8846 \text{ and } 9185). \tag{1a}$$

The model considered below permits us also to draw conclusion about hyperons with strangeness -3 and larger in the absolute value.

We shall assume the following relation for hyperons with strangeness $S = -1$

$$M = M_N + M_K + c + a(t_N t_K) = M_N + b + a(t_N t_K), \tag{2}$$

where a, b, c are constants and the parentheses contain the scalar product of isotopic spins of the bound particles. Comparing this expression with the data concerning the Λ-particle [$t = 0$ and therefore $(t_N t_K) = -3/4$, $M_\Lambda = 2182$] and the Σ-particle [$t = 1$ whence $(t_N t_K) = 1/4$, $M_\Sigma = 2334.5$] we find that $a = 152.5$, $b = 459.5$, and $c = -506$ (electron mass has been taken as 1).

For the hyperon with $S = -2$, consisting of a nucleon and two $\overline{K}$-particles, it is logical to take as a first approximation

$$M = M_N + 2b + a(t_N t_{2K}), \tag{3}$$

where a, b are identical with the constants of Eq. (2).

The following assumptions are implicit in the above: (1) the interaction between $\overline{K}$-particles is small compared with the interaction between a $\overline{K}$ and a nucleon, and (2) in a hyperon with $S = -2$ the two $\overline{K}$-particles are in the same state, identical to that of a single $\overline{K}$ in a hyperon with $S = -1$.

Since $\overline{K}$-particles are bosons it follows from the second assumption that the isotopic spin of a system consisting of two $\overline{K}$-particles can equal only 1 (and not 0). Consequently, two charge multiplets are possible in the above scheme for $S = -2$: (1) the multiplet $t = 1/2$, $(t_N t_{2K}) = -1$, representing a particle for which formula (3) yields a mass of 2603 in a good agreement* with the experimental value for the mass of equal to 2586, and (2) the multiplet (denoted by A in the following) $t = 3/2$ with an expected mass 2832.

Reaction \ Strangeness	−1 (Λ)	−2 (Ξ)	−3 (B)	−4	−2 (A)
$\pi + N = X + rK$	0.75	2.2	4.2	6.8	2.55
$N + N = X + rK + N$	1.6	3.8	6.5	9.6	4.15

D'erdi[2] predicted qualitatively, without any mass estimate, the existence of the multiplet $S = -2$, $t = 3/2$, heavier than Ξ, and analysed its properties as a function of the difference between the masses of A and Ξ. The other multiplet predicted by D'erdi, with $t = 1/2$ (beside the Ξ-particle), cannot exist since $\overline{K}$-particles are bosons.

It follows from the formula that $M_A - M_\Xi = 229 < m_\pi$. This result, however (upon which depends the possibility of detection of the tracks of A^+ and of the doubly charged A^{--}), cannot be regarded as firmly established.

If the agreement between the mass of Ξ and the value predicted by the formula is not accidental, it follows from the above considerations that the hyperon family can be extended to large (absolute) values of S, An isotopic spin $t = (r - 1)/2$ and mass $1761 + 421r$ should correspond to strangeness $S = -r$.

The hyperons Λ ($r = 1$) and Ξ ($r = 2$) belong to this group. The nucleons ($r = 0$) and the Σ-particle ($r = 1$) belong to the second group, for which $t = (r + 1)/2$ and mass equals $1837 + 497.5r$. Instability occurs soon in this group for $r = 2$ or 3, leading to fast π-meson decay.

The production thresholds in Bev (in the laboratory frame) for hyperons of the frist group with various S and for A (belonging to the second group) are given in the table. The hyperon of the first group with $S = -3$ and isotopic spin 1, denoted in the table by B, should exist in three charge states: B^0, B^-, and the doubly charged B^{--}.

If the expressions for the masses given above are at least approximately correct, then the hyperons of the first group, including B, cannot disintegrate by emission of $\overline{K}$-mesons and, therefore, are metastable cascade particles. Production of such particles is not very probable and would require great energies, but their detection does not present special difficulties.

A simple additivity of the $\overline{K}$-meson-nucleon interactions requires that the $\overline{K}$-mesons in hyperons are in the s-state in the nucleon field.

The above considerations, therefore, are correct only if the geometrical spin of all hyperons equals $\frac{1}{2}$ and if they all have even parity in a system in which nucleons and $\overline{K}$-mesons are even. It should be noted that such parity excludes the treatment of K-particles according to Fermi-Young theory as $(\Lambda + N)$.[4,5]

In the language of field theory, the proposed scheme corresponds to an interaction term in the Hamiltonian, containing the square of the absolute value of the nucleonic wave function and the square of the absolute value of the $\overline{K}$-meson wave function. It differs in this from the scheme proposed by Wentzel[6] which introduces the interaction as linear in the K-meson wave function and, therefore, has to consider the hyperon Λ, together with the nucleons and the K-meson as an elementary particle.

*This agreement is equivalent to validity of Eq. (1), since

$$M = M_N + 2b - a, \quad a = M_\Sigma - M_\Lambda, \quad b = \frac{3}{4} M_\Sigma + \frac{1}{4} M_\Lambda - M_N,$$

from which Eq. (1) follows elementarily.

[1] M. Goldhaber, Phys. Rev. **101**, 431 (1956).
[2] G. D'erdi, J. Exptl. Theoret. Phys. (U.S.S.R.) **32**, 152 (1957), Soviet Phys. JETP **5**, 152 (1957).
[3] M. Gell-Mann, Phys. Rev. (1957) (in print).
[4] M. A. Markov, О систематике элементарных частиц (Classification of Elementary Particles), Acad. Sci. Press, 1957.
[5] R. W. King and D. C. Peaslee, Phys. Rev. **106**, 360 (1957).
[6] J. Wentzel, Helvetica Physica Acta **30**, 135 (1957).

Translated by H. Kasha
171

MAGNETO-VORTEX RINGS

V. D. SHAFRANOV

Academy of Sciences, U.S.S.R.

Submitted to JETP editor May 20, 1956

J. Exptl. Theoret. Phys. (U.S.S.R.) **33**, 831-832 (September, 1957)

In Ref. 1 we considered magnetohydrodynamical equilibrium configurations. It was noted that the distribution of the field H and the current density j in those configurations is identical with the distribution of the velocity v and vorticity Ω, corresponding to the stationary flow of an incompressible fluid.

Chandrasekhar[2] paid attention to the existence and showed the stability of the simplest solution of the magnetohydrodynamical equations of an incompressible, perfectly conducting fluid, for the case where the

velocity of flow is connected to the magnetic field by the relation

$$\mathbf{v} = \mathbf{H}/\sqrt{4\pi\rho}; \quad p + \rho v^2/2 = \text{const}.$$

This solution is a generalization of the solution presenting a magnetohydrodynamical ring.[3] It is satisfied by an solenoidal vector **v**.

It is natural to generalize all these solutions even further. The magnetohydrodynamical equations of an ideal incompressible fluid of infinite conductivity can be written in the form

$$\partial \mathbf{v}/\partial t = -\nabla(p/\rho + v^2/2) + [\mathbf{j}\times\mathbf{H}]/c - [\Omega\times\mathbf{v}], \quad \partial\mathbf{H}/\partial t = \operatorname{curl}[\mathbf{v}\times\mathbf{H}], \quad \operatorname{curl}\mathbf{H} = (4\pi/c)\,\mathbf{j}, \quad \operatorname{curl}\mathbf{v} = \Omega. \tag{1}$$

Let us assume that

$$\mathbf{v} = \alpha\mathbf{H}/\sqrt{4\pi\rho}, \tag{2}$$

where α is an arbitrary constant. From the last two equations (1) it follows that

$$\Omega = (\alpha/c)\sqrt{4\pi/\rho}\,\mathbf{j}. \tag{3}$$

From the second equation of (1) we get $\partial\mathbf{H}/\partial t = 0$ and hence by virtue of Eq. (2) $\partial\mathbf{v}/\partial t = 0$. The first equation of (1) takes the form

$$-\nabla(p + \rho v^2/2) + c^{-1}(1-\alpha^2)[\mathbf{j}\times\mathbf{H}] = 0, \tag{4}$$

whence we obtain the equilibrium condition for magnethydrodynamical configurations $\operatorname{curl}[\mathbf{j}\times\mathbf{H}] = 0$, or the condition for a stationary flow of an incompressible fluid, $\operatorname{curl}[\mathbf{v}\times\Omega] = 0$. Thus any equilibrium configuration or any stationary flow of an incompressible fluid corresponds to the stationary flow of an incompressible, perfectly conducting fluid in a magnetic field **H**, in the direction of the current of the fluid, **v**.

For instance, there corresponds to a ring current in a magnetic field and a circular vortex an analogous configuration (which can be called a magneto-vortex ring) with an identical distribution of the magnetic field and the fluid velocity. Let R and a be the large and the small radius of this torus, and let $R \gg a$. If the current density j_φ and, correspondingly, the vorticity Ω_φ are constant along a cross section, then according to Ref. 1 the radii of the torus and the current through it $J = j_\varphi/\pi a^2$ are connected with the external field $H_z = H_0$, perpendiuclar to the plane of the ring, through the relation

$$H_0 = -(J/cR)[\ln(8R/a) - {}^1/_4]. \tag{5}$$

If we use Eqs. (2) and (3) to express the field and the current in formula (5) in terms of the velocity and vorticity, we find the velocity of the fluid current relative to the ring v_0, or in the frame of reference in which the fluid at infinity is at rest, the velocity of the torus $v_k = -v_0$,

$$v_k = (\varkappa/4\pi R)[\ln(8R/a) - {}^1/_4], \tag{6}$$

where $\varkappa = \pi a^2\Omega$ is the vorticity intensity. The absolute value of the velocity of the magneto-vortex ring for a given external field H_0 can be arbitrary. In the case $\alpha = 0$ the magneto-vortex ring becomes a magnetohydrodynamical equilibrium configuration at rest, while for $\alpha = \infty$ it turns into the normal vortex ring.

The distribtuion of the pressure in the ring in the case when $R \gg a$ is not essentially different from the distribution in a cylindrical magneto-vortex filament of radius a. This last distribution is easily found from Eq. (4) and has the form

$$p = p_0 - \frac{H_a^2}{8\pi}\left(1 - \frac{a^2}{2}\right)\frac{r^2}{a^2}; \quad (r<a); \qquad p = p_0 - \frac{H_a^2}{8\pi}\left(1 - \frac{a^2}{2}\right) + \frac{H_a^2}{8\pi}\frac{a^2}{2}\left(1 - \frac{a^2}{r^2}\right); \quad (r>a).$$

where p_0 is the pressure on the axis of the cylinder and $H_a = 2J/ca$.

The stability of a magneto-vortex configuration depends on the value of the parameter α. It is, for instance, well known that a cylindrical vortex is stable[4] while a straight current is not. The vortex corresponds to $\alpha = \infty$ and the current to $\alpha = 0$. Apparently the value $\alpha \sim 1$ separates the regions of stability and instability of a magneto-vortex filament.

Another kind of solution — a magneto-vortex configuration at rest — can be obtained from the equilibrium configurations which are maintained by gravitation[4] or by external pressure.[5] In those cases the magnetic lines of force, and hence also the lines of the fluid current are close (they do not go to infinity)

and the center of gravity of the magneto-vortex configuration is at rest.

In conclusion I want to express my gratitude to S. I. Braginskii for a discussion which stimulated the present paper.

[1] V. D. Shafranov, J. Exptl. Theoret. Phys. (U.S.S.R.) **32**, 1453 (1957), Soviet Phys. JETP **5**, 1183 (1957).

[2] S. Chandrasekhar, Proc. Nat. Acad. Sci. **42**, 273 (1956).

[3] H. Alfvén, Cosmical Electrodynamics, Oxford University Press, 1950.

[4] H. Lamb, Hydrodynamics, Cambridge University Press, 1932.

[5] K. H. Prendergast, Astroph. J. **123**, 498 (1956).

Translated by D. ter Haar
172

CONTENTS—continued

	Page	Russian Reference
Propagation of Sound across a Boundary between Two Superfluid Phases . . . R. G. Arkhipov and I. M. Khalatnikov	583	33, 758
Scattering of Electrons by Protons . . . A. I. Akhiezer, L. N. Rozentsveig, and I. M. Shmushkevich	588	33, 765
Theory of Paramagnetic Resonance of F Centers in Ionic Crystals . . . M. F. Deigen	594	33, 773
Optical Properties of F^- Centers . . . V. L. Vinetskii	601	33, 780
LETTERS TO THE EDITOR		
On the Nuclear Reaction $Li^6(n, t)He^4$ . . . T. I. Kopaleishvili	606	33, 788
Concerning Superpositions with Respect to the Internal Properties of Elementary Particles . . . M. I. Podgoretskii	607	33, 790
On the Principle of Larmor Invariance . . . A. A. Borgardt	608	33, 791
Theory of Electron Paramagnetic Resonance in Superconductors . . . M. Ia. Azbel' and I. M. Lifshitz	609	33, 792
On the Theory of the Neutrino with Oriented Spin . . . A. A. Sokolov	611	33, 794
Lagrangian for the Interaction of K Mesons and Hyperons . . . V. G. Solov'ev	613	33, 796
Interaction of Fermions and the $K_{\mu 3}$ Decay . . . S. G. Matinian	614	33, 797
Measurements of Molecular Attraction between Dissimilar Solids . . . I. I. Abrikosova	615	33, 799
Dispersion Relations for S and P Waves for Meson Photoproduction in First Order of 1/m . . . L. D. Solov'ev	617	33, 801
Energy of Ionization by Electrons in Silicon Crystals . . . V. M. Patskevich, V. S. Vavilov, and L. S. Smirnov	619	33, 804
Fine Structure of Electron Paramagnetic Resonance of the Fe^{3+} Ions in the Al_2O_3 Lattice. . . . L. S. Kornienko and A. M. Prokhorov	620	33, 805
The Problem of Piezomagnetism . . . I. E. Dzialoshinskii	621	33, 807
The Role of Nucleons in Multipole Production of Particles . . . A. A. Emel'ianov and I. L. Rozental'	622	33, 808
Hydrodynamic Fluctuations in a Superfluid Liquid . . . I. M. Khalatnikov	624	33, 809
Causes of Thermodynamic Irreversibility . . . B. I. Davydov	625	33, 811
Magnetic Properties of Cobalt Fluoride in the Antiferromagnetic State . . . D. N. Astrov, A. S. Borovik-Romanov, and M. P. Orlova	626	33, 812
Galvanomagnetic Properties of Ferromagnetics near Absolute Zero . . . K. P. Belov and A. V. Ped'ko	628	33, 815
Green's Function for Diffusion of Radiation . . . B. A. Veklenko	629	33, 817
Effect of Proton Size on the Position of Electronic Levels in Hydrogen and Deuterium . . . N. N. Kolesnikov	631	33, 819
Application of Charge Invariance to Polarization Phenomena . . . S. M. Bilen'kii	633	33, 821
Thermodynamic Functions of Superfluid Helium Films . . . R. G. Arkhipov	634	33, 822
Effect of Proton Structure on the Lamb Shift . . . E. V. Teodorovich	636	33, 823
Particle Angular Distribution Function at the Cascade Shower Maximum . . . I. P. Ivanenko	637	33, 825
Effect of Damping on Polarization of Dirac Particles in Scattering . . . A. A. Sokolov and B. K. Kerimov	639	33, 827
A Variant of Hyperon Theory . . . Ia. B. Zel'dovich	641	33, 829
Magneto-Vortex Rings . . . V. D. Shafranov	642	33, 831

SOVIET PHYSICS JETP VOLUME 6 (33), NUMBER 3 MARCH, 1958

CONTENTS

	Page	Russian Reference
Investigation of Nuclear Disintegration Produced by the Charged Component of Cosmic Radiation . . . T. L. Asatiani and G. V. Khrimian	437	33, 561
On the Hall Effect in Ferromagnetics . . . N. V. Bazhanova	440	33, 567
Investigation of the Characteristic Energy Losses of Electrons and the Secondary Electron Emission from GeO_2 . . . N. B. Gornyi and A. Iu. Reitsakas	443	33, 571
Change in the Isotopic Composition of Mercury by Evaporation . . . V. N. Grigor'ev, Ia. S. Kan, N. S. Rudenko, and B. G. Safronov	446	33, 576
Variations in the Isotopic Composition of Mercury in the Electric Field of a Constant Current I. V. Bogoiavlenskii, V. N. Grigor'ev, N. S. Rudenko, and D. G. Dolgopolov	450	33, 581
An Investigation of Conversion Lines in the β Spectrum of Ir^{192} . . . V. M. Kel'man, R. Ia. Metskhvarishvili, V. A. Romanov, and V. V. Tuchkevich	455	33, 588
The Stripping Process in the Interactions of Accelerated N^{14} Ions with the Nuclei of Some Elements . . . V. V. Volkov, A. S. Pasiuk, and G. N. Flerov	459	33, 595
Production of Negative π Mesons by 660 Mev Protons on Nuclei of Various Elements . . . A. G. Meshkovskii, Ia. Ia. Shalamov, and V. A. Shebanov	463	33, 602
Polarization of Protons Scattered by O^{16}. Spin and Parity of the 3.11-Mev Level of the F^{17} Nucleus . . . P. V. Sorokin, A. K. Val'ter, B. V. Gavriloskii, K. V. Karadshev, V. I. Man'ko, and A. Ia. Taranov	466	33, 606
The Phase Diagram for Cerium . . . A. I. Likhter, Iu. N. Riabinin, and L. F. Vereshchagin	469	33, 610
Photodisintegration of Deuteron at Energies from 50 to 150 Mev . . . Iu. A. Aleksandrov, N. B. Delone, L. I. Slovokhotov, G. A. Sokol, and L. N. Shtarkov	472	33, 614
The Energy Dependence of the Angular Correlation in the π^+-μ^+-e^+ Decay . . . A. O. Vaisenberg and V. A. Smirnitskii	477	33, 621
Scattering of Slow Neutrons by Diatomic Molecules . . . A. A. Ansel'm	480	33, 625
On the Scattering of Light in He^3-He^4 Mixtures . . . L. P. Gor'kov and L. P. Pitaevskii	486	33, 634
Solution of the Kinetic Equations for High-Energy Nuclear Cascade Processes . . . N. M. Gerasimova	488	33, 637
The Behavior of a Completely Ionized Plasma in a Strong Magnetic Field . . . S. I. Braginskii	494	33, 645
Resonance Scattering of γ-Rays . . . N. A. Burgov	502	33, 655
On the Theory of the Infrared Absorptivity of Metals . . . R. N. Gurzhi	506	33, 660
Correlation Theory for Rayleigh Scattering of Light. II . . . S. M. Rytov	513	33, 671
On the Green's Function of the Kinetic Equations of a Cascade . . . Kh. Ia. Khristov	524	33, 683
Calculation of the Interaction Potential of Atoms . . . O. B. Firsov	534	33, 696
Cylindrical Self Similar Acoustical Waves . . . Ia. B. Zel'dovich	537	33, 700
Bound States in Positronium . . . Iu. A. Tarasov	542	33, 706
On Magnetohydrodynamical Equilibrium Configurations . . . V. D. Shafranov	545	33, 710
Collective Excitations of Even-Even Nuclei . . . A. S. Davydov and G. P. Filippov	555	33, 723
On the Theory of the Interaction of "Excess" Charges in Ionic Crystals . . . V. L. Vinetskii and M. Sh. Giterman	560	33, 730
De Haas – Van Alphen Effect in a Variable Magnetic Field . . . A. M. Kosevich	564	33, 735
The Optical Model of the Nucleus and the Shell Model . . . P. E. Nemirovskii	573	33, 746
Scattering of Electromagnetic Waves in a Plasma . . . A. I. Akhiezer, I. G. Prokhoda, and A. G. Sitenko	576	33, 750

(Contents continued on inside back cover)